International Atomic Energy Agency

INDC(NDS)-256
Distr.: Special

INDC INTERNATIONAL NUCLEAR DATA COMMITTEE

STATUS OF THORIUM CYCLE NUCLEAR DATA EVALUATIONS: COMPARISON OF CROSS-SECTION LINE SHAPES OF JENDL-3 AND ENDF/B-VI FILES FOR ^{230}Th, ^{232}Th, ^{231}Pa, ^{233}Pa, ^{232}U, ^{233}U AND ^{234}U

S. Ganesan and P.K. McLaughlin
Nuclear Data Section
Division of Physical and Chemical Sciences
International Atomic Energy Agency
P.O. Box 100
A-1400 Vienna, Austria, Europe

February 1992

IAEA NUCLEAR DATA SECTION, WAGRAMERSTRASSE 5, A-1400 VIENNA

INDC(NDS)-256
Distr.: Special

STATUS OF THORIUM CYCLE NUCLEAR DATA EVALUATIONS: COMPARISON OF CROSS-SECTION LINE SHAPES OF JENDL-3 AND ENDF/B-VI FILES FOR ^{230}Th, ^{232}Th, ^{231}Pa, ^{233}Pa, ^{232}U, ^{233}U AND ^{234}U

S. Ganesan and P.K. McLaughlin
Nuclear Data Section
Division of Physical and Chemical Sciences
International Atomic Energy Agency
P.O. Box 100
A-1400 Vienna, Austria, Europe

February 1992

Reproduced by the IAEA in Austria
April 1992

92-01478

STATUS OF THORIUM CYCLE NUCLEAR DATA EVALUATIONS: COMPARISON OF CROSS-SECTION LINE SHAPES OF JENDL-3 AND ENDF/B-VI FILES FOR ^{230}Th, ^{232}Th, ^{231}Pa, ^{233}Pa, ^{232}U, ^{233}U AND ^{234}U

S.Ganesan and P.K. McLaughlin
NUCLEAR DATA SECTION
DIVISION OF PHYSICAL AND CHEMICAL SCIENCES
INTERNATIONAL ATOMIC ENERGY AGENCY
P.O. BOX 100
A-1400 VIENNA, AUSTRIA, EUROPE

ABSTRACT

Since 1990, one of the most interesting developments in the field of nuclear data for nuclear technology applications is that several new evaluated data files have been finalized and made available to the International Atomic Energy Agency (IAEA) for distribution to its Member States. Improved evaluated nuclear data libraries such as ENDF/B-VI from the United States and JENDL-3 from Japan were developed over a period of 10-15 years. This report is not an evaluation of the evaluations. The report as presented here gives a first look at the cross section line shapes of the isotopes that are important to the thorium fuel cycle derived from the two recently released evaluated data files: JENDL -3 and ENDF/B-VI. The basic evaluated data files JENDL-3 and ENDF/B-VI were point-processed successfully using the codes LINEAR and RECENT. The point data were multigrouped in three different group structures using the GROUPIE code. Graphs of intercomparisons of cross section line shapes of JENDL-3 and ENDF/B-VI are presented in this paper for the following isotopes of major interest to studies of the thorium fuel cycle: ^{230}Th, ^{232}Th, ^{231}Pa, ^{233}Pa, ^{232}U, ^{233}U and ^{234}U. Comparisons between JENDL-3 and ENDF/B-VI which were performed at the point and group levels show large discrepancies in various cross sections. We conclude this report with a general remark that it is necessary to perform sensitivity studies to assess the impacts of the discrepancies between the two different sets of data on calculated reactor design and safety parameters of specific reactor systems and, based on the results of such sensitivity studies, to undertake new tasks of evaluations.

I. INTRODUCTION

A look at the index of data libraries available from the IAEA Nuclear Data Section shows that three basic evaluated data libraries (JEF-1, JENDL-3 and ENDF/B-VI) provide basic data for isotopes of the thorium cycle (^{230}Th, ^{232}Th, ^{231}Pa, ^{233}Pa, ^{232}U, ^{233}U and ^{234}U) as given in Table I. For each of these libraries, a look at the comment cards of JEF-1 revealed that ENDF/B-VI has been adopted for the JEF file for each of the isotopes of interest. Thus we are left with ENDF/B-VI and JENDL-3 as sources of new data for applications to thorium fuel cycle studies. Furthermore, the comment cards of ENDF/B reveal that ENDF/B-VI evaluations for these isotopes are the same as in ENDF/B-V, which in turn have been translated into ENDF/B-VI format. It is further seen clearly from the scan of data available in the two files that for all the isotopes of interest to the thorium fuel cycle, the data in the JENDL-3 file are based on efforts of evaluation up to 1988, whereas ENDF/B-VI for these isotopes consists of evaluations made up to the 1977-78 period. It was noticed further that the resolved resonance range for ^{232}U and ^{233}Pa spans a larger energy range in the JENDL-3 file than in the ENDF/B-VI file. Concerning the relative dates of the evaluations, JENDL-3 versus ENDF/B-VI, these statements are not meant to imply that the JENDL-3 file is automatically superior to ENDF/B-VI file for all types of data (e.g., n,2n cross sections) for all the isotopes under consideration. The scope of this report is limited to an intercomparison of the two evaluated data files for the important isotopes of the thorium fuel cycle. This report does not attempt to present a recommended evaluation for use in application calculations i.e. perform an evaluation of the evaluations. Results of intercomparisons between JENDL-3 and ENDF/B-VI which were performed at the point and group levels (infinite dilution cross sections) are presented to the interested reader as a first look at the existing evaluated basic data files for the important isotopes of the thorium fuel cycle. The present comparisons do not cover several features of group constants such as self-shielding factors and transfer matrices. Hopefully the results of intercomparison of cross section data presented in this report will help those interested in the thorium fuel cycle studies to have a first look at the status of the existing data. The mammoth task of creating complete, multigroup cross section libraries from ENDF/B-VI and JENDL-3 with self-shielded, Doppler broadened cross sections and transfer matrices for elastic and inelastic processes will have to be first done to enable performing of sensitivity studies to assess the impacts of the discrepancies between the two different sets of data on calculated reactor design

and safety parameters of specific reactor systems, and, based on the results of such sensitivity studies, to undertake, if needed, new tasks of evaluations of specific nuclear data.

In this paper we shall limit our comparison studies to the following isotopes which are of major interest to studies of the thorium fuel cycle: ^{230}Th, ^{232}Th, ^{231}Pa, ^{233}Pa, ^{232}U, ^{233}U and ^{234}U.

II. MEANING OF INTERCOMPARISON OF EVALUATED DATA

If the cross section of two files completely agree with each other it does not necessarily mean that there is no error in the data or that no further evaluations or validations through integral experiments are necessary. Under ideal conditions, the data in the two evaluated data files may be considered to represent random samples from the infinite ensemble of possible evaluations. However, when the cross sections of two files agree with each other, one should keep in mind the possibility of a systematic error that may make the two files differ from the true value by the same amount. An even more likely explanation of perfect agreement is that the data files are derived from a common (evaluated) data source. Improved differential measurements should be welcome to improve the understanding of the differences in the cross sections in the two files and help eliminate them. More critical experiments to validate the cross sections are highly desirable in the case of the thorium cycle isotopes.

The magnitude of percentage differences for point cross sections and group cross sections presented in this report for various reactions should be interpreted and understood so that the real significance of differences that are seen in the comparison tables and the plots can be qualitatively appreciated with a proper perspective with regard to their possible impact on the application calculations. For instance, large differences of several tens of percent in the point cross sections in some cases can just be due to slightly different resonance energies of sharp resonances in the two files. Similarly large differences will be seen in the plots of intercomparisons if the threshold energies of a reaction for example, the inelastic level excitation cross sections are different in the two files. Many such differences essentially disappear when averaging is performed over broad energy regions to obtain multigroup constants.

III.DESCRIPTION OF PROCESSING OF BASIC EVALUATED DATA FILES

The reconstruction of cross section line shapes was carried out at the IAEA using the IBM-3081 mainframe computer using the codes LINEAR and RECENT developed by D.E. Cullen [1]. Multigrouping of data using a flat weighting spectrum for three different energy group structures was performed using GROUPIE code developed by the same author [1]. The three different group structures in the present study for the calculation of flat-weighted infinite dilution cross sections are:

a) 640 energy groups (SAND-II group structure)

b) 69 energy groups (WIMS group structure)

c) 28 energy groups (ABBN group structure)

Comparisons between JENDL-3 and ENDF/B-VI were made at the following levels, using COMPLOT code [1]:

1. Point data, i.e., the cross section line shapes at zero Kelvin as given in the resonance-reconstructed output of the RECENT code.

2. Multigroup data (flat-weighted infinite dilution cross sections) in the above mentioned three different energy group structures.

The present comparisons do not cover several features of group constants such as self-shielding factors and transfer matrices for elastic and inelastic reaction processes.

IV. RESULTS OF INTERCOMPARISON AND DISCREPANCIES

All the graphs obtained in this study are given in Figs. 1 to 245 in the Appendix to this report. The comparison graphs arranged in the following manner. The figures 1 to 35 give the comparisons for ^{232}Th, Figs. 36 to 70 for ^{233}U, Figs. 71 to 105 for ^{234}U, Figs. 106 to 140 for ^{230}Th, Figs. 141 to 175 for ^{232}U, Figs. 176 to 210 for ^{231}Pa and Figs. 211 to 245 for ^{233}Pa. The successive four graphs give respectively the comparisons for point data and multigroup data for 640, 69 and 28 groups. For example, Figs. 1 to 4 give the comparisons for total cross sections of Th-232, Fig. 1 at the point level, Fig. 2 at the 640 groups level, Fig. 3 at the 69 groups

level and Fig. 4 at the 28 group level. Although these graphs are self-explanatory, it is useful to point to some striking features. A comparison at point cross section level shows in some energy regions in some cases very large discrepancies, but the differences become generally less and less striking as we proceed through the comparisons from finer to broad groups, due to the cancellation of discrepancies which go in opposite directions within the energy group.

In Tables II to VIII, we summarize in the second column the maximum and minimum discrepancies in percentage for the point data i.e., the cross section line shapes at zero Kelvin as given in the output of the RECENT code for various important isotopes of the thorium cycle: ^{230}Th, ^{232}Th, ^{231}Pa, ^{233}Pa, ^{232}U, ^{233}U and ^{234}U. In the last three columns the maximum and the minimum discrepancies in percentage for the infinite dilution multigroup data in 28/69/640 energy groups are given. The physical implications of these numbers should be carefully understood and interpreted taking into account the specific sensitivity of the design problem to the energy regions involved (see remarks in Section II).

^{232}Th, (n,gamma) cross section:

Very large differences are generally observed (figs 32 to 35) between the two files for the (n,gamma) cross section of ^{232}Th. The capture cross sections in JENDL-3 and ENDF/B-VI show differences of -99.96 to 9999% (Fig. 32) at the level of point data, i.e., the cross section line shapes at zero Kelvin as given in the point-processed output of RECENT code. The values in ENDF/B-VI are higher than in JENDL-3. In the 640 group structure, for some groups, these discrepancies exceed a factor of 35! The differences in the 28 group capture cross section for ^{232}Th (ABBN group structure) are smaller, but range (see Fig. 35) still from -4.33 to 1401%. Again, reactor physicists would carefully note that the discrepancies in the multigroup capture cross sections in the ABBN 28 energy group structure for ^{232}Th in most of the energy regions of importance (see Fig. 35) are within 20% and that the large discrepancy over a factor of 15 is seen only in the first energy group covering the energy region above 10 MeV. Qualitatively Fig. 35 gives the impression that, relative to JENDL-3 file, the capture rate calculated using ENDF/B-VI file will be on the average about 10% higher in typical fast spectra. In particular, although the large discrepancies above 10 MeV for most of the reactions may cause concern in studies related to accelerator breeders and fission-fusion hybrids, where high energy neutrons are important, they may cause little concern to thermal and fast reactor

applications. The reactor physicists will need to perform sensitivity studies to determine which are the important energy regions in specific application. As a general remark we can say that these discrepancies seen for Th-232 in figs. 1-35 and summarized in Table III would still be generally considered as large if ^{232}Th is to be used in the ^{232}Th-^{233}U fuel cycle in the same way as ^{238}U in the ^{238}U-^{239}Pu fuel cycle.

^{232}Th, Fission cross section:

The fission cross sections of ^{232}Th in both files are generally in good agreement (see figs. 20 to 23) except for large discrepancies near the threshold. Above 2 Mev, the values of the fission cross section of JENDL-3 are higher than those in ENDF/B-VI by about 3 to 4% but the discrepancy is much higher in the threshold region 0.5 to 1.4 Mev.

^{232}Th, (n,2n) cross section:

For ^{232}Th, the (n,2n) cross sections are within 10% in most of the energy regions although beyond 14 Mev these data show larger discrepancies (see Figs. 13 to 16).

^{232}Th, Total cross section:

For the main fertile isotope ^{232}Th of the thorium fuel cycle, Table III gives the maximum and minimum percentage differences. Presented are the comparison plots in figures 1 to 35. As seen in Table III for the case of ^{232}Th, the values of multigroup <u>total</u> cross section in the ABBN 28 group structure (see Fig. 4) show more than 5% discrepancies. These discrepancies in the total cross section are to be viewed as rather large since with the existing techniques of total cross section measurements, the total cross sections can generally be measured to 1% accuracy. In Fig. 2 which gives the plot in the 640 SAND-II group structure, a difference by a factor of 2.27 is seen for the total cross section between 650 and 750 eV. Resolution of such striking discrepancies by improved measurements will be desirable.

^{233}U, Total cross sections:

The total cross sections are discrepant (Fig. 36) by -88.2% to 170% at the point level, and at the 640 group level (Fig. 37) the

difference is -36.6% to 82.5%. At the 28 group level the discrepancies in this case are -4.84 to 4.07%.

^{233}U, Fission cross sections:

For the important major fissile isotope ^{233}U, the fission cross sections are within a band of +/- 10%, except between 70 and 100 eV in the resolved resonance region, where the cross sections differ by a factor of about 6 at the point cross section level (Fig. 55) and by a factor of about 2.5 in the 640 group structure around this energy region (Fig. 56). In the 28 ABBN energy group structure, the discrepancies are -4.11 to +4.03 % which will need improvement if the reactor core is charged into the core of the reactor employing the ^{232}Th-^{233}U fuel cycle in the same way as ^{239}Pu in the ^{238}U-^{239}Pu fuel cycle.

^{233}U, (n,2n) and (n,3n) cross sections:

The (n,2n) group cross sections of ^{233}U in ENDF/B-VI are a factor of two higher than in the JENDL-3 file as seen from Figs. 49-51. Large differences of more than a factor of three are observed (Figs. 53-55) for (n,3n) cross sections.

^{233}U, (n,gamma) cross sections:

The (n,gamma) cross sections of ^{233}U show (Figs. 67-70) very large differences by a factor of over 100 at the point level and at the 640 group level at the higher energy region beyond 5 Mev. In the resolved and unresolved resonance ranges for some groups in 640 group structure, the ratio exceeds 1.5.

^{233}U, Inelastic cross sections:

Inelastic cross sections (Figs. 44-47) in both the discrete and the continuum energy ranges (Figs. 59-66) show discrepancies of more than a factor of two in many groups.

It is interesting to see that at the 28-energy group level the differences in the various reaction cross-sections are much lower: These discrepancies would still be considered as large if ^{233}U is to be exploited in the ^{232}Th-^{233}U fuel cycle in the same way as ^{239}Pu in ^{238}U-^{239}Pu fuel cycle.

^{232}U:

The (n,2n) cross sections are significantly lower in JENDL-3 as compared to those in ENDF/B-VI. (See Fig. 153)

^{234}U:

This isotope plays a similar role as ^{240}Pu in the ^{238}U-^{239}Pu fuel cycle. The various cross sections show large discrepancies as seen from the Figs. 71-105 and as summarized in Table VIII.

We have made above a few general observations only for some specific reactions. The reader is encouraged to scan the graphs (Figs. 1 to 245) which are self-explanatory to see the discrepancies in detail in various cross sections of the isotopes: ^{230}Th, ^{232}Th, ^{231}Pa, ^{233}Pa, ^{232}U, ^{233}U and ^{234}U. As already stated, the mammoth task of creating complete, multigroup cross section libraries from ENDF/B-VI and JENDL-3 with self-shielded, Doppler broadened cross sections and transfer matrices for elastic and inelastic processes will have to be first done to enable performing of sensitivity studies to assess the impacts of the discrepancies between the two different sets of data on calculated reactor design and safety parameters of specific reactor systems, and, based on the results of such sensitivity studies, to undertake, if needed, new tasks of evaluations of specific nuclear data.

V. SUMMARY

The report as presented here gives a first look at the cross section line shapes of the isotopes that are important to the thorium fuel cycle derived from the two recently released evaluated data files: JENDL -3 and ENDF/B-VI. The basic evaluated data files JENDL-3 and ENDF/B-VI were point-processed successfully using the codes LINEAR and RECENT. The point data were multigrouped in three different group structures using the GROUPIE code. Comparisons between JENDL-3 and ENDF/B-VI which were performed at the point and group levels show large discrepancies in various cross sections, as seen from the graphs (Figs 1- 245) and as summarized in Tables II to VIII.

The scope of this report is extremely limited to an intercomparison of the two evaluated data files for the important isotopes of the thorium fuel cycle. It is not the purpose of this report to

present a recommended evaluation for use in application calculations i.e. perform an evaluation of the evaluations.

The sensitivity of an integral parameter in a specific design problem to a specific cross section in a specific energy region will have to be calculated to conclude if the discrepancy is large enough to affect the integral results. Such data sensitivity studies need to be performed to focus attention on the discrepancies in various cross sections of isotopes of interest to thorium fuel cycle studies. As a first step, processing tasks should be taken up to generate complete sets of multigroup constants by processing the two files. With the multigroup sets so derived, neutronic calculations should be performed to see if there are differences in the calculated values of integral parameters. After this a detailed and formal sensitivity analysis can be attempted.

We conclude this report with a general remark that it is necessary to perform sensitivity studies to assess the impacts of the discrepancies between the two different sets of data on calculated reactor design and safety parameters of specific reactor systems.

It is sincerely hoped that the results of intercomparison of cross section data presented in this report will encourage those interested in the thorium fuel cycle studies to perform sensitivity studies to assess the impacts of the discrepancies between the two different sets of data on calculated reactor design and safety parameters of specific reactor systems, and, based on the results of such sensitivity studies, to undertake new tasks of evaluations.

VI. REFERENCES

1. D.E. Cullen and P.K. McLaughlin, "The 1989 ENDF Pre-processing Codes," IAEA-NDS-39, Revision 5, December 1989.

2. H.D. Lemmel, "Index of Data Libraries available on Magnetic Tape from the IAEA Nuclear Data Section," IAEA-NDS-7 (1990).

TABLE I

Nuclide	BROND	ENDF/B-VI	JEF-1	JENDL-3	Others
^{230}Th	--	ENDF/B-V 1977	ENDF/B-V 1977	1987	
^{231}Th	--	---	--	---	ENDL84 1978
^{232}Th	--	ENDF/B-V+ 1977	ENDF/B-IV 1974	1989	
^{233}Th	--	---	---	1983	
^{234}Th	--	---	---	1983	
^{231}Pa	--	ENDF/B-V+	ENDF/B-V 1977	1988	
^{232}Pa	--	---	----	1988	
^{233}Pa	--	ENDF/B-V+	ENDF/B-V 1978	1987	
^{232}U	--	ENDF/B-V+	ENDF/B-V 1977	1987	
^{233}U	--	ENDF/B-V+	ENDF/B-IV 1974	1987	
^{234}U	--	ENDF/B-V+	ENDF/B-V 1978	1987	

Table II

NUCLIDE: ^{230}Th

Differences in percentage: JENDL-3 versus ENDF/B-VI

Cross section	Point cross sections	Percentage differences for groups 28	69	640
Total	-100 to +9999	-45 to +50	-54 to +53	-74 to +429
Elastic	-9999 to +9999	-46 to +59	-62 to +64	-113 to +407
Capture	-100 to +9999	-88 to +9999	-88 to +4241	-99 to +9999
Fission	-69 to +300	-18 to +39	-20 to +704	-44 to +1631
n,2n	-3 to +1312	0 to +30	0 to +36	-3 to +1265
n,3n	-100 to 0	-65 to 0	*********	-94 to 0
Inelastic	-72 to +25	0 to +63	0 to +145	-72 to +2424

Table III

NUCLIDE: ^{232}Th

Differences in percentage: JENDL-3 versus ENDF/B-VI

Cross section	Point cross sections	Percentage differences for groups 28	69	640
Total	-100 to +9999	-5.4 to +8	-7.4 to +6.9	-26 to +127
Elastic	-100 to +9999	-6.8 to +12	-8 to +11	-26 to +153
Capture	-100 to +9999	-4.3 to +1401	-4.7 to +81	-26 to+3537
Fission	-100 to +5.6	-78 to 0	-100 to 0	-100 to+3.5
n,2n	-49 to +688	0 to +2802	0 to 9.4	-44 to +2647
n,3n	-23 to 512	-15 to 0	*********	-23 to +2134
Inelastic	-100 to 13	-82 to + 3.6	-82 to +4.5	-98 to +12

Table IV

NUCLIDE: ^{231}Pa

Cross section	Point cross sections	Percentage differences for groups 28	69	640
Total	-98 to +706	-31 to +38	-36 to +31	-73 to +669
Elastic	-98 to +235	-37 to +32	-38 to +35	-75 to +39
Capture	-98 to +9999	-30 to +9999	-43 to +9999	-84 to +9999
Fission	-98 to +9999	-57 to +5386	-61 to +5271	-90 to +8849
n,2n	0 to +560	0 to +63	0 to +71	0 to +555
n,3n	-66 to +101	-61 to 0	**********	-65 to +99
Inelastic	-57 to +30.1	-20 to +33	-20 to +17	-57 to +175

Table V

NUCLIDE: ^{233}Pa

Cross section	Point cross sections	Percentage differences for groups 28	69	640
Total	-87 to + 5695	-22 to +8.9	-22 to +4.3	-79 to +368
Elastic	-68 to + 2375	-32 to +18	-35 to +20	-40 to +116
Capture	-92 to +9999	-61 to +6284	-60 to +3344	-92 to +9999
Fission	0 to +118	-100 to +111	-100 to+106	-100 to +118
n,2n	-100 to +93	-66 to 0	-59 to 0	-100 to +91
n,3n	-100 to +26	-30 to 0	******	-100 to +24
Inelastic	-100 to +345	-100 to +252	-100 to+330	-100 to +344

Table VI

NUCLIDE: ^{232}U

Differences in percentage: JENDL-3 versus ENDF/B-VI

Cross section	Point cross sections	Percentage differences for groups 28	69	640
Total	-99 to +9762	-16 to +96	-16 to +94.7	-95 to +895
Elastic	-183 to +2261	-44 to +84	-44 to +76	-152 to +328
Capture	-100 to +9999	-15 to +9999	-14 to +9999	-97 to +9999
Fission	-100 to +9999	- 47 to +498	-38 to +450	-97 to +9999
n,2n	-100 to +9999	0 to +1478	0 to +1584	0 to +9999
n,3n	0 to +9999	0 to +3162	*******	0 to +9999
Inelastic	-88 to +1150	0 to +664	-46 to +531	-87 to +1071

Table VII

NUCLIDE: ^{233}U

Differences in percentage: JENDL-3 versus ENDF/B-VI

Cross section	Point cross sections	Percentage differences for groups 28	69	640
Total	-88 to +170	-4.8 to +4.1	-4.8 to +5.2	-37 to +83
Elastic	-55 to 73	-7 to +17	-8.5 to +17	-11 to +18
Capture	-95 to +9999	-79 to +9999	-78 to +2703	-81 to +9999
Fission	-90 to +496	- 4.1 to +4.	-6.8 to +4.9	-41 to +152
n,2n	-9.2 to +9999	0 to +525	0 to +814	-7 to +9999
n,3n	-100 to +18	-78 to 0	*******	-89 to +18
Inelastic	-84 to 0	-74 to 0	-66 to 0	-84 to 0

Table VIII

NUCLIDE: ^{234}U

Differences in percentage: JENDL-3 versus ENDF/B-VI

Cross section	Point cross sections	Percentage differences for groups 28	69	640
Total	-57 to +110	-24 to +17	-24 to +16	-31 to +61
Elastic	-99 to +9999	-40 to +25	-42 to +27	-63 to +34
Capture	-68 to +9999	-66 to +9999	-66 to +450	-68 to +9999
Fission	-100 to +1350	- 47 to +1314	-92 to +998	-99 to +1294
n,2n	-81 to +9999	-6.5 to 0	-7.4 to 0	-81 to +9082
n,3n	-100 to +900	0 to +27	********	-100 to +856
Inelastic	-100 to +44	-73 to +33	-58 to +33	-86 to +44

APPENDIX

COMPARISON GRAPHS OF CROSS-SECTION LINE SHAPES OF JENDL-3 AND ENDF/B-VI FILES FOR ^{230}Th, ^{232}Th, ^{231}Pa, ^{233}Pa, ^{232}U, ^{233}U AND ^{234}U

EXPLANATION OF SOME SYMBOLS IN THE COMPARISON GRAPH:

POINT-DATA:

In all the comparison graphs for ^{234}U, the symbol U234 (R) JENDL3 represents JENDL-3 based point-processed nuclear data for the nuclide ^{234}U in point-wise form, i.e., the output of the RECENT code. Similar symbols are used in the case of all other isotopes except in the case of ^{232}Th where JENDL-3 only was used inadvertently in place of THE-232 JENDL-3 (R).

INFINITE DILUTION CROSS SECTIONS IN 640 SAND-II GROUP STRUCTURE:

The symbol U 234 (G) JENDL3 represents JENDL-3 based multi-group nuclear data for the nuclide ^{234}U in the SAND-II 640 energy group structure.

INFINITE DILUTION CROSS SECTIONS IN 69 WIMS GROUP STRUCTURE:

The symbol U 234 (GW) JENDL3 represents JENDL-3 based multi-group nuclear data for the nuclide ^{234}U in the 69 WIMS energy group structure.

INFINITE DILUTION CROSS SECTIONS IN 28 ABBN GROUP STRUCTURE:

The symbol U 234 (GA) JENDL3 represents JENDL-3 based multi-group nuclear data for the nuclide ^{234}U in the 28 ABBN energy group structure.

In the case of inelastic level excitation cross-sections we have provided the graphs of inter-comparisons for only the first excited levels in order to save space.

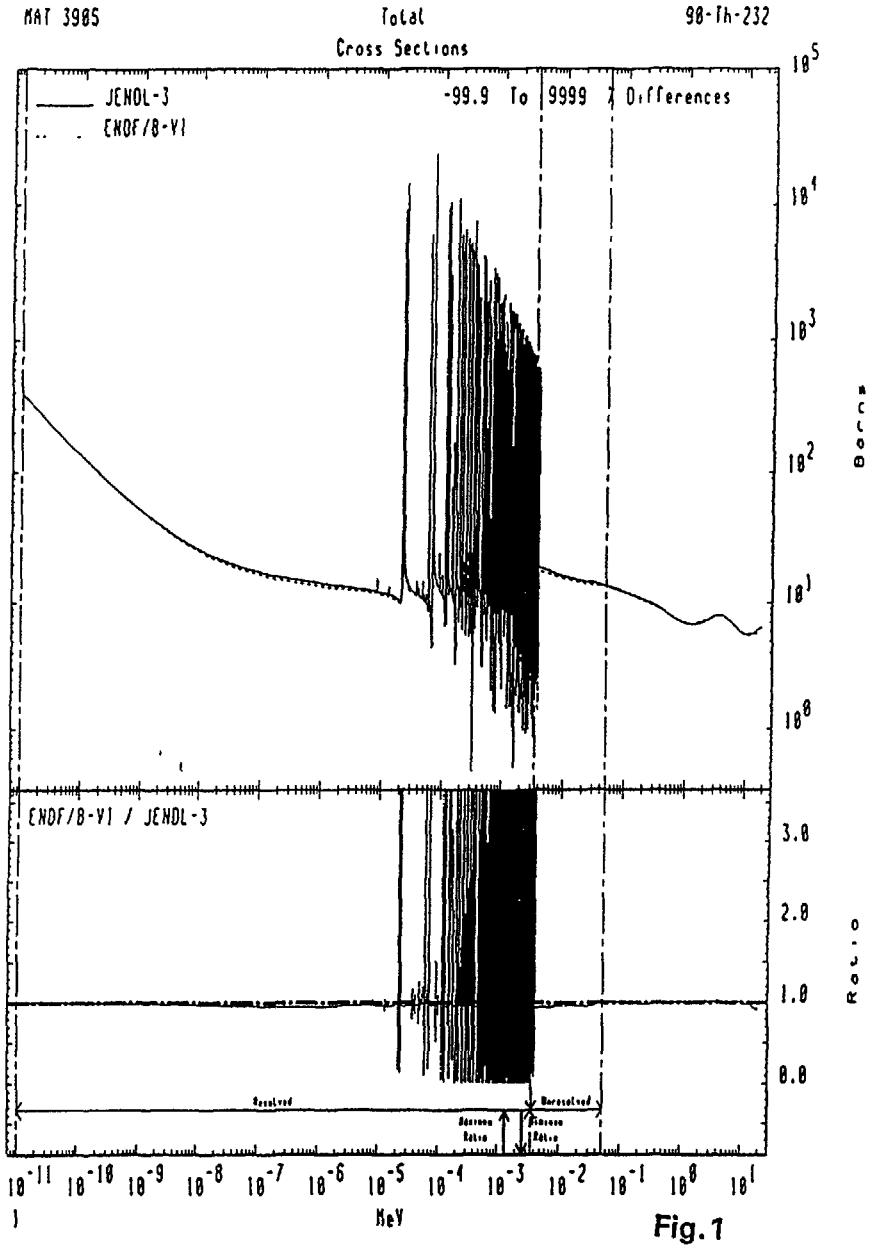
MAT 3985
Total
Cross Sections
90-Th-232
JENDL-3
ENDF/B-VI
-99.9 To 9999 % Differences
Barns
ENDF/B-VI / JENDL-3
Ratio
Resolved
Unresolved
MeV

Fig.1

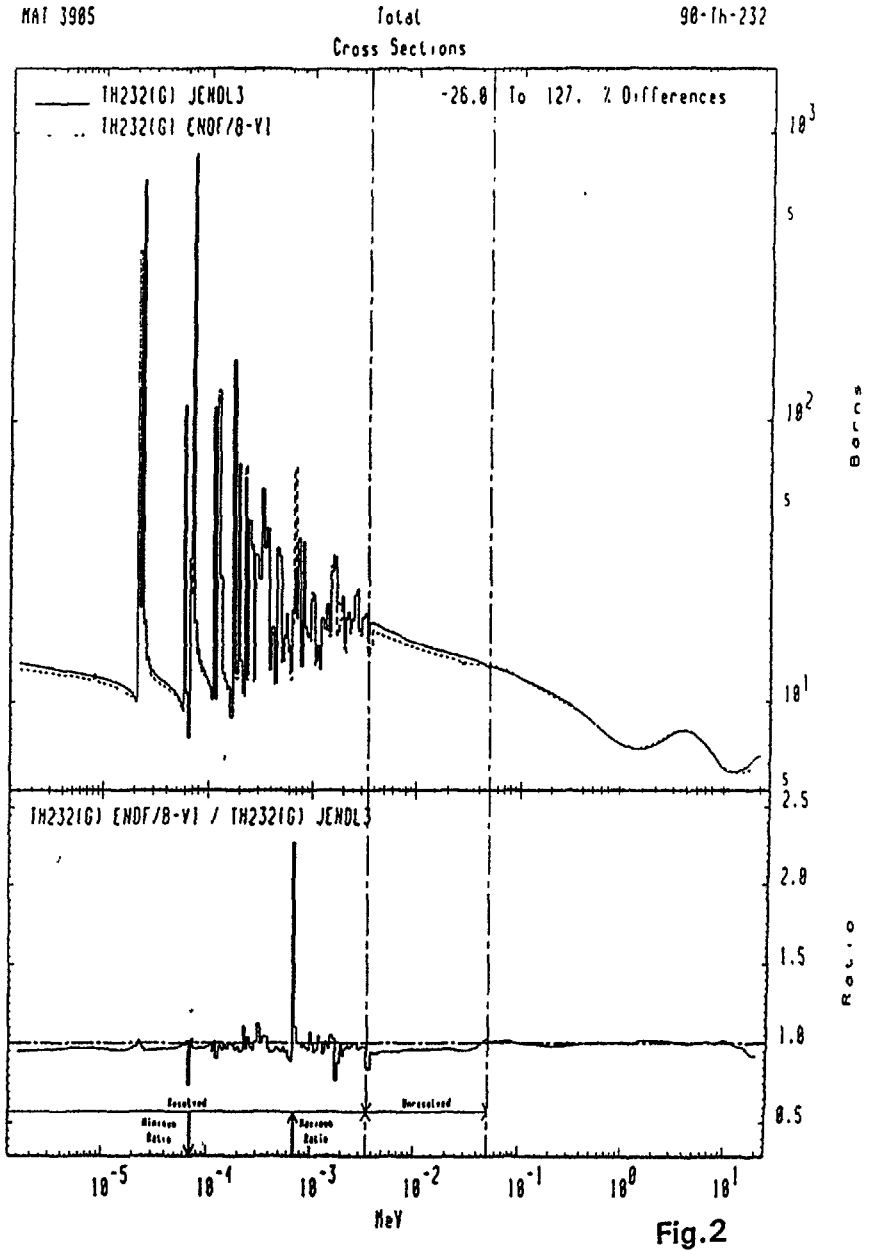
MAT 3985
Total
Cross Sections
90-Th-232
TH232(G) JENDL3
TH232(G) ENDF/B-VI
-26.8 To 127. % Differences
Barns
TH232(G) ENDF/B-VI / TH232(G) JENDL3
Ratio
Resolved
Unresolved
MeV

Fig.2

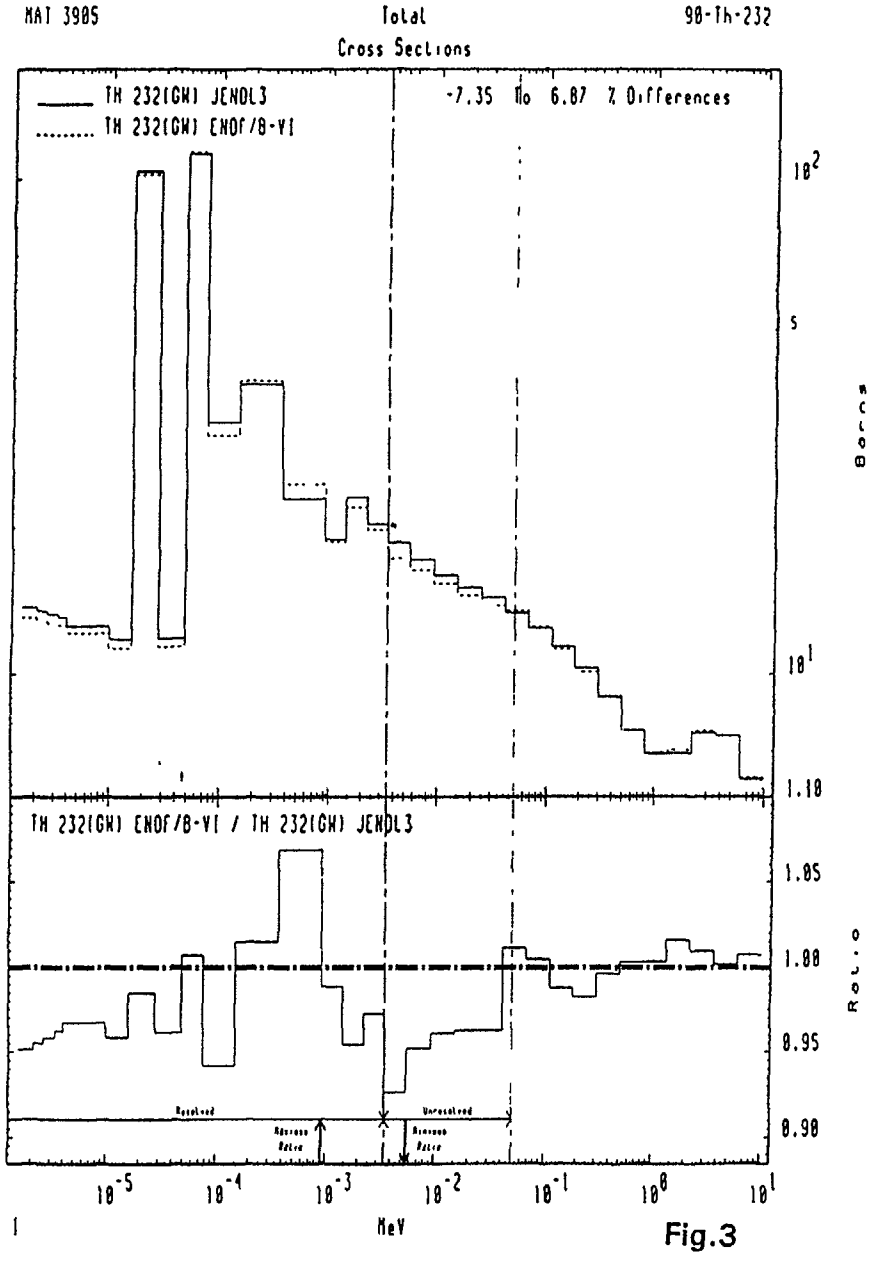
MAT 3905
Total
Cross Sections
90-Th-232
TH 232(GW) JENDL3
TH 232(GW) ENDF/B-VI
-7.35 To 6.87 % Differences
Barns
TH 232(GW) ENDF/B-VI / TH 232(GW) JENDL3
Ratio
MeV

Fig.3

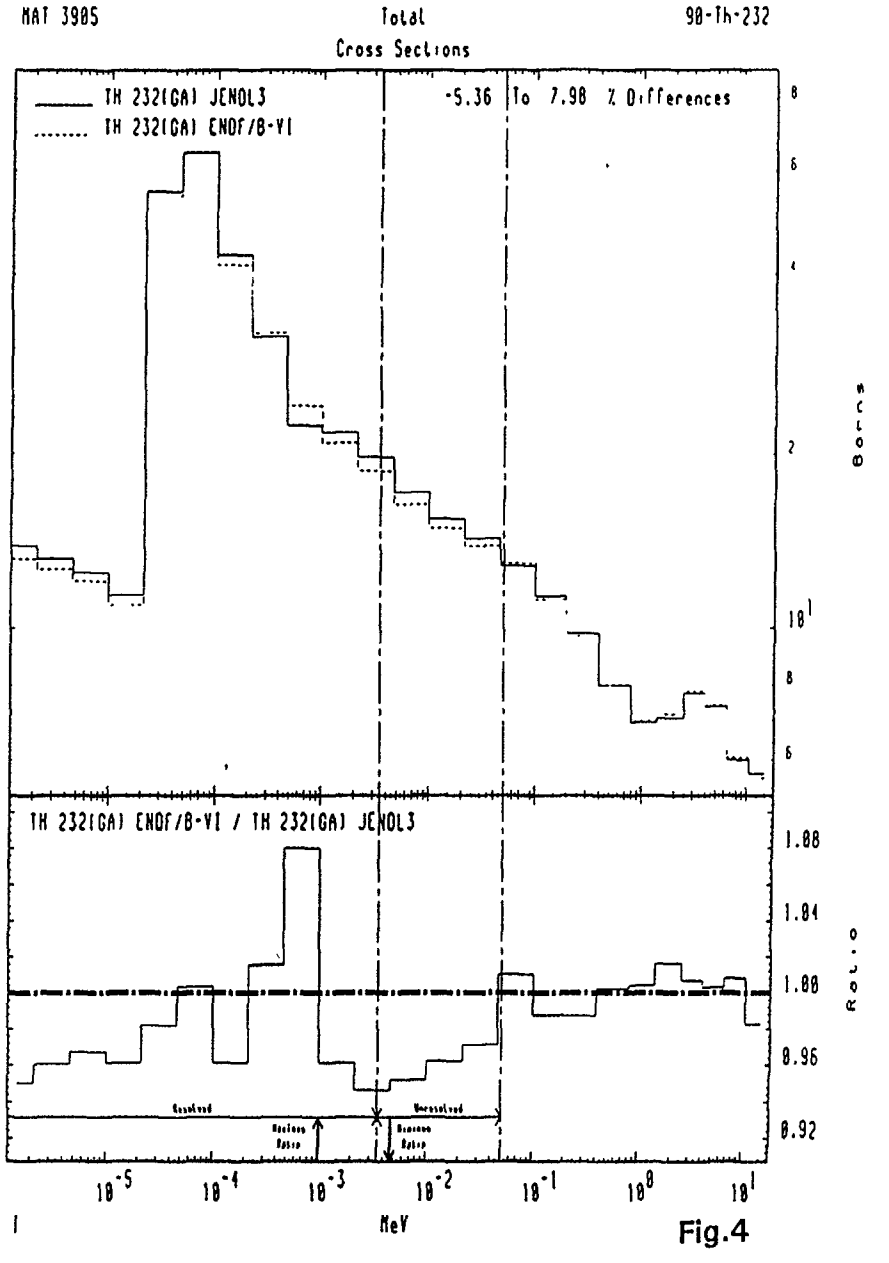
MAT 3905
Total
Cross Sections
90-Th-232
TH 232(GA) JENDL3
TH 232(GA) ENDF/B-VI
-5.36 To 7.98 % Differences
Barns
TH 232(GA) ENDF/B-VI / TH 232(GA) JENDL3
Ratio
MeV

Fig.4

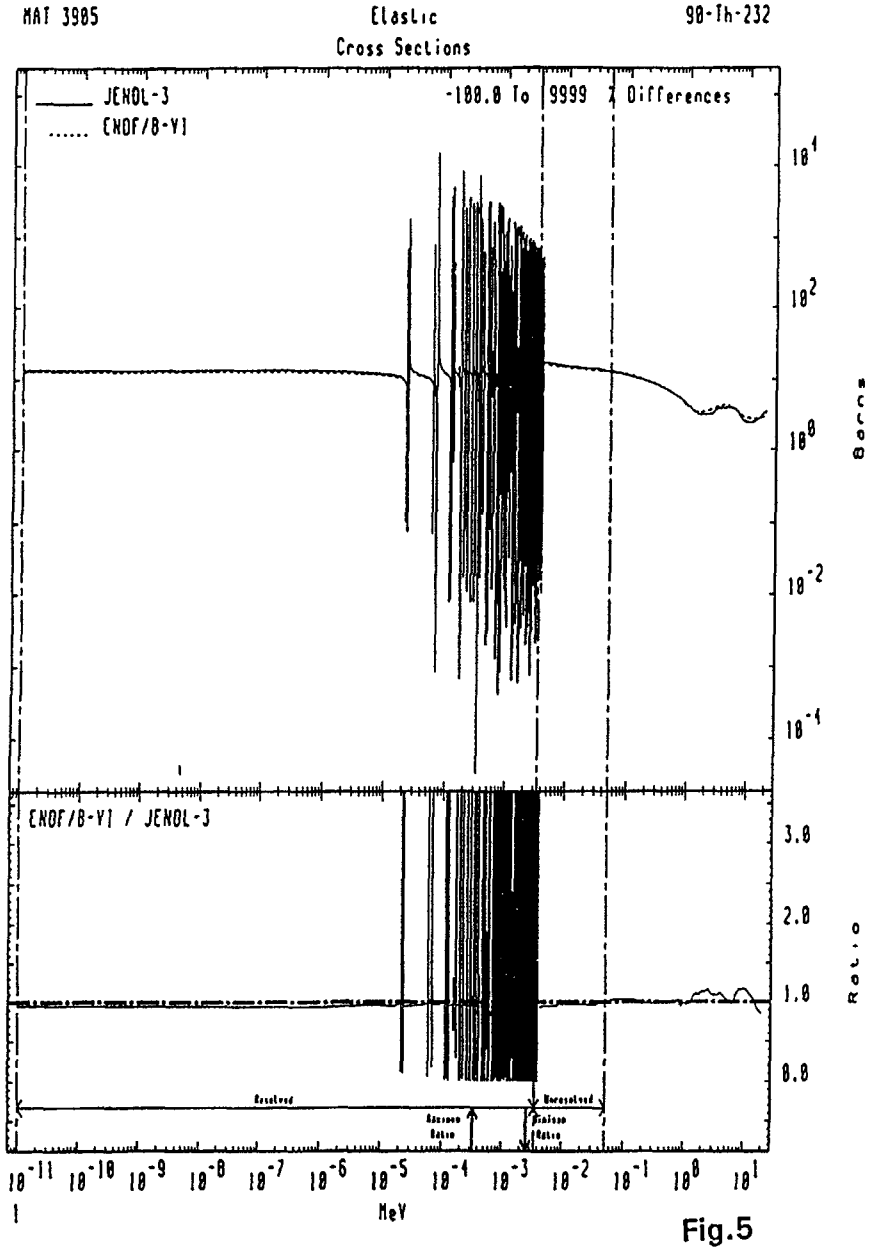
MAT 3905
Elastic
Cross Sections
90-Th-232
JENDL-3
ENDF/B-VI
-100.0 To 9999 % Differences
Barns
ENDF/B-VI / JENDL-3
Ratio
MeV

Fig.5

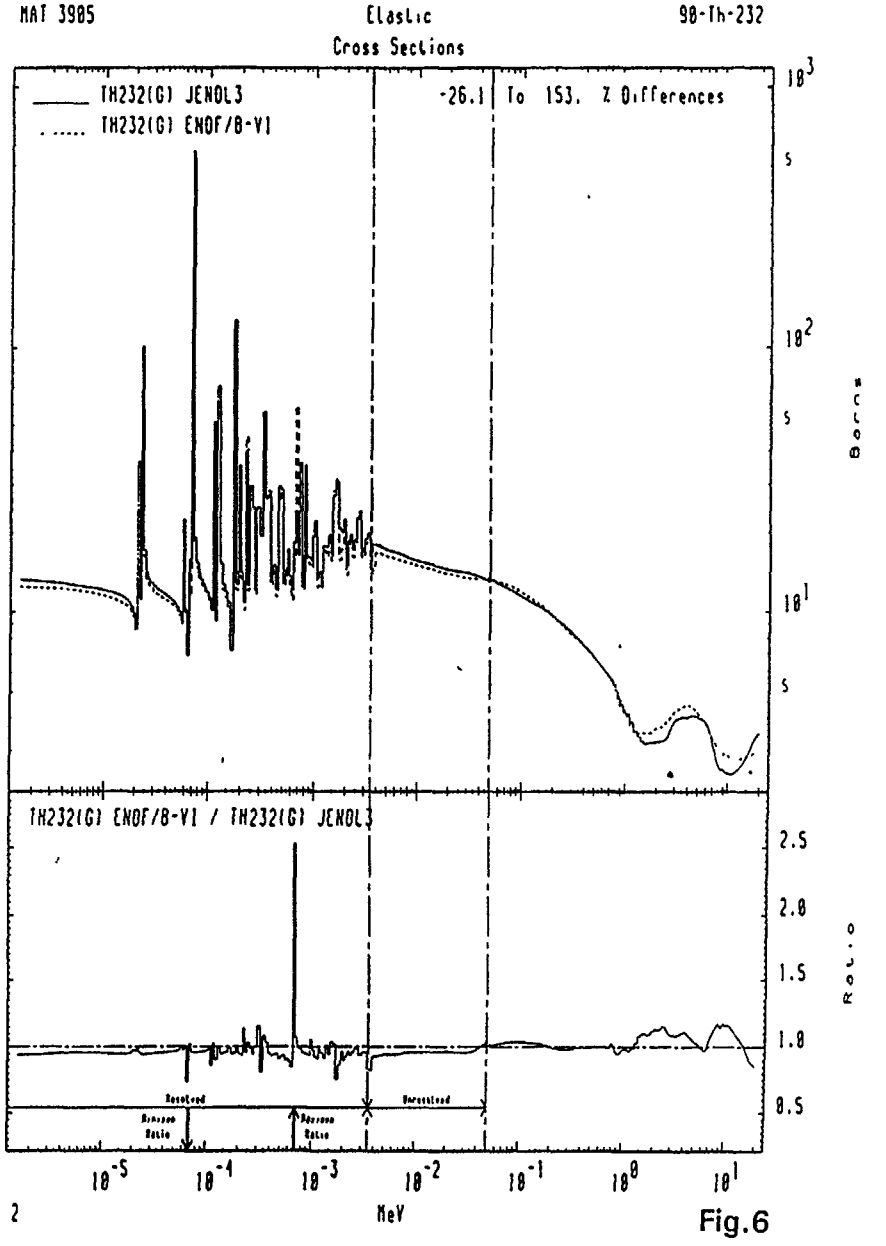
MAT 3905
Elastic
Cross Sections
90-Th-232
TH232(G) JENDL3
TH232(G) ENDF/B-VI
-26.1 To 153. % Differences
Barns
TH232(G) ENDF/B-VI / TH232(G) JENDL3
Ratio
MeV

Fig.6

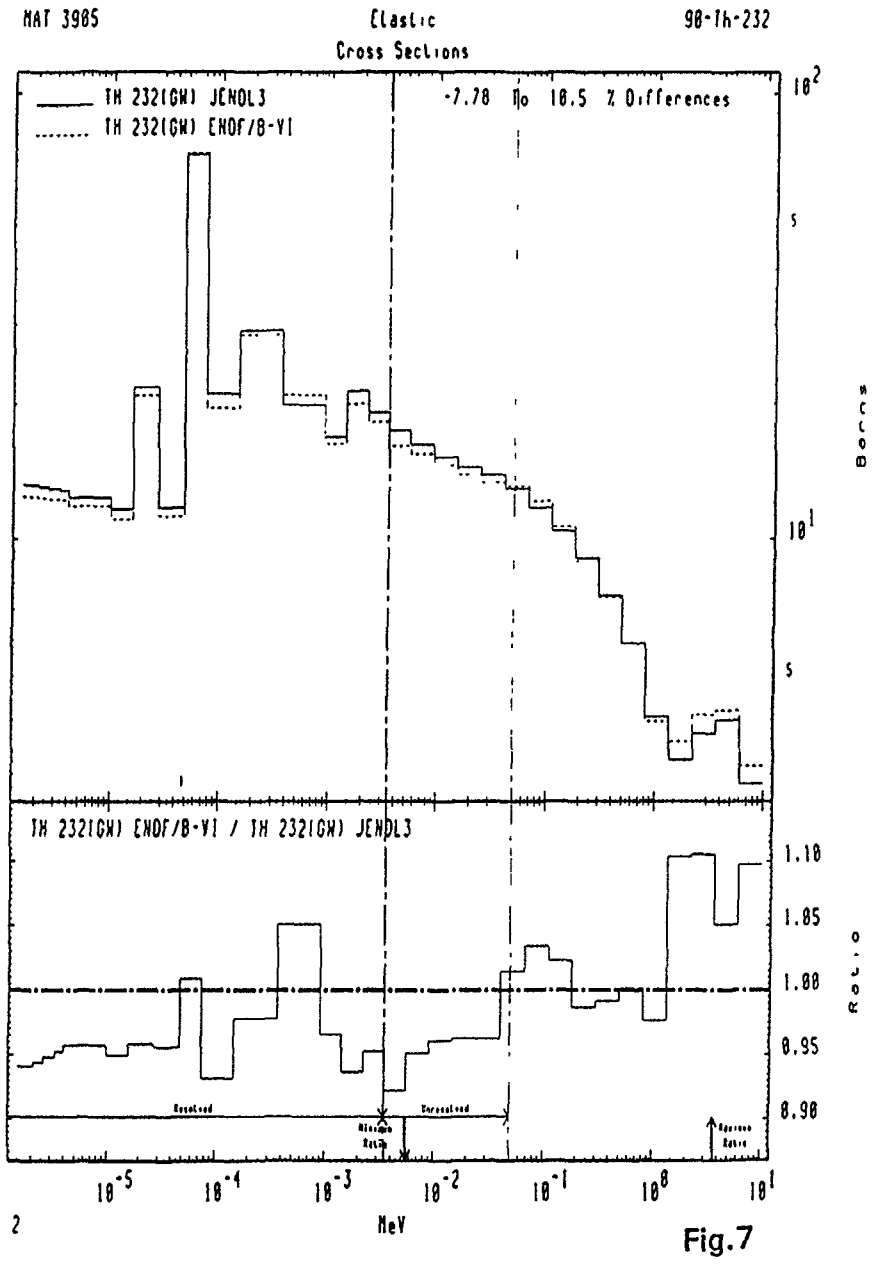
MAT 3905
Elastic
Cross Sections
90-Th-232
TH 232(GW) JENDL3
TH 232(GW) ENDF/B-VI
-7.78 To 10.5 % Differences
TH 232(GW) ENDF/B-VI / TH 232(GW) JENDL3
Barns
Ratio
MeV

Fig.7

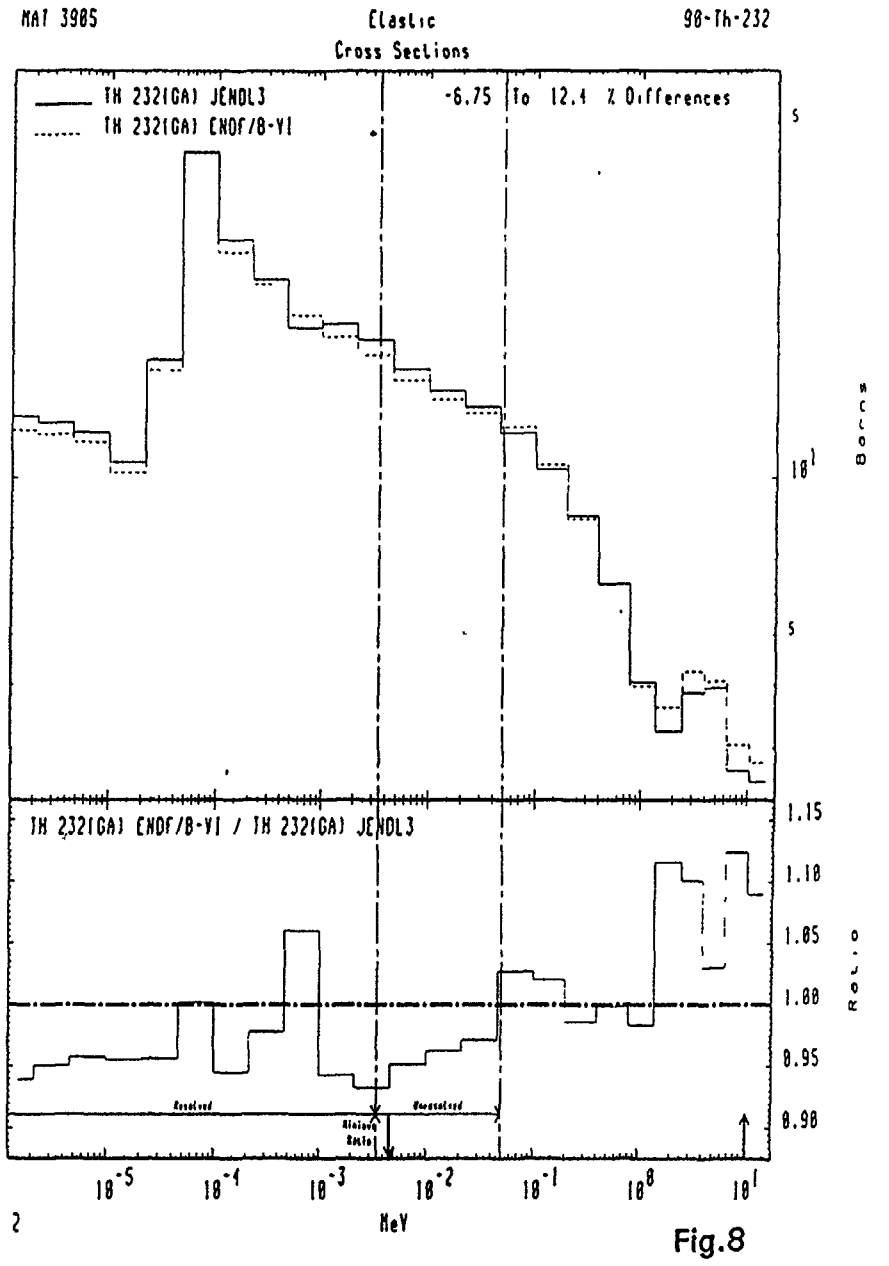
MAT 3905
Elastic
Cross Sections
90-Th-232
TH 232(GA) JENDL3
TH 232(GA) ENDF/B-VI
-6.75 To 12.4 % Differences
TH 232(GA) ENDF/B-VI / TH 232(GA) JENDL3
Barns
Ratio
MeV

Fig.8

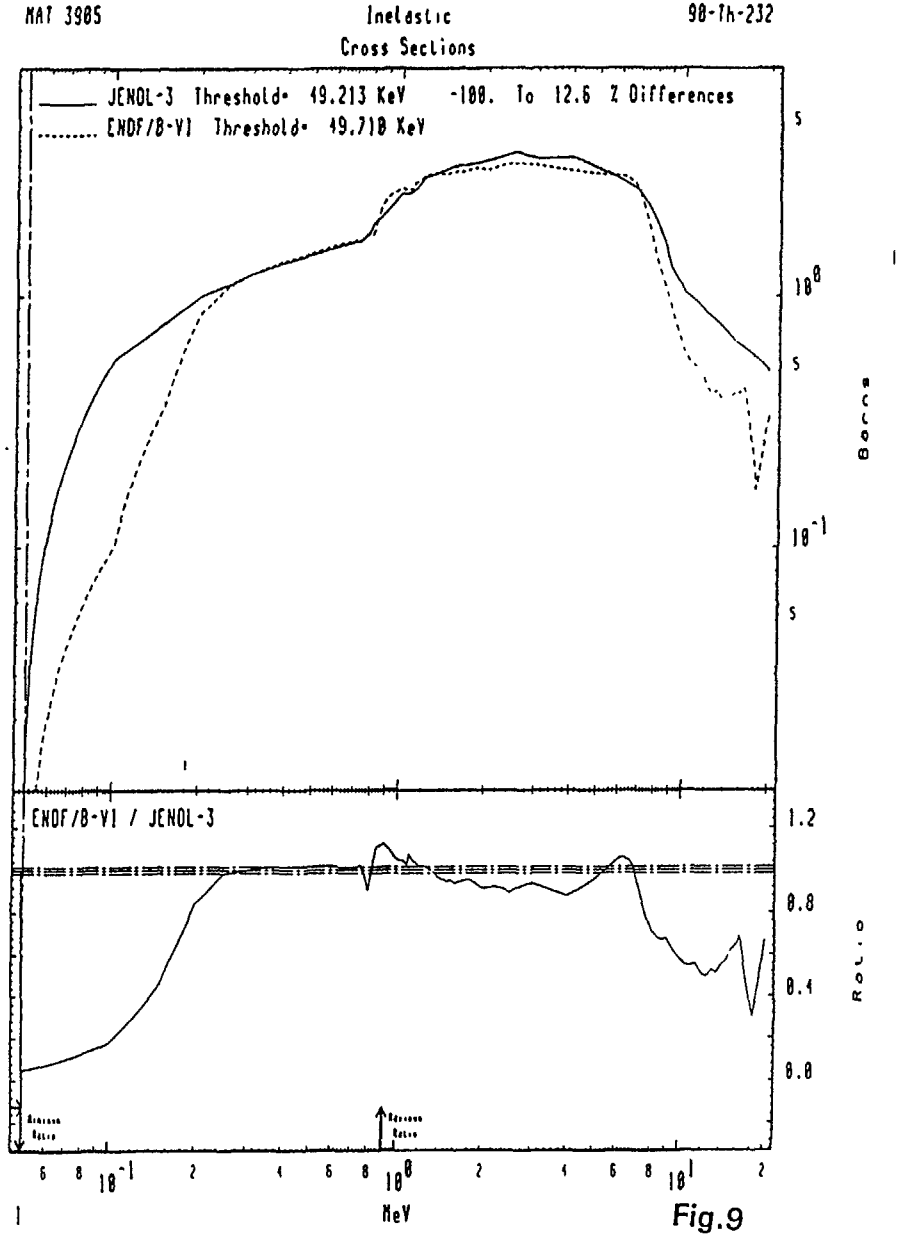
MAT 3905
Inelastic
Cross Sections
90-Th-232
JENDL-3 Threshold= 49.213 KeV -100. To 12.6 % Differences
ENDF/B-VI Threshold= 49.710 KeV
Barns
ENDF/B-VI / JENDL-3
Ratio
MeV

Fig.9

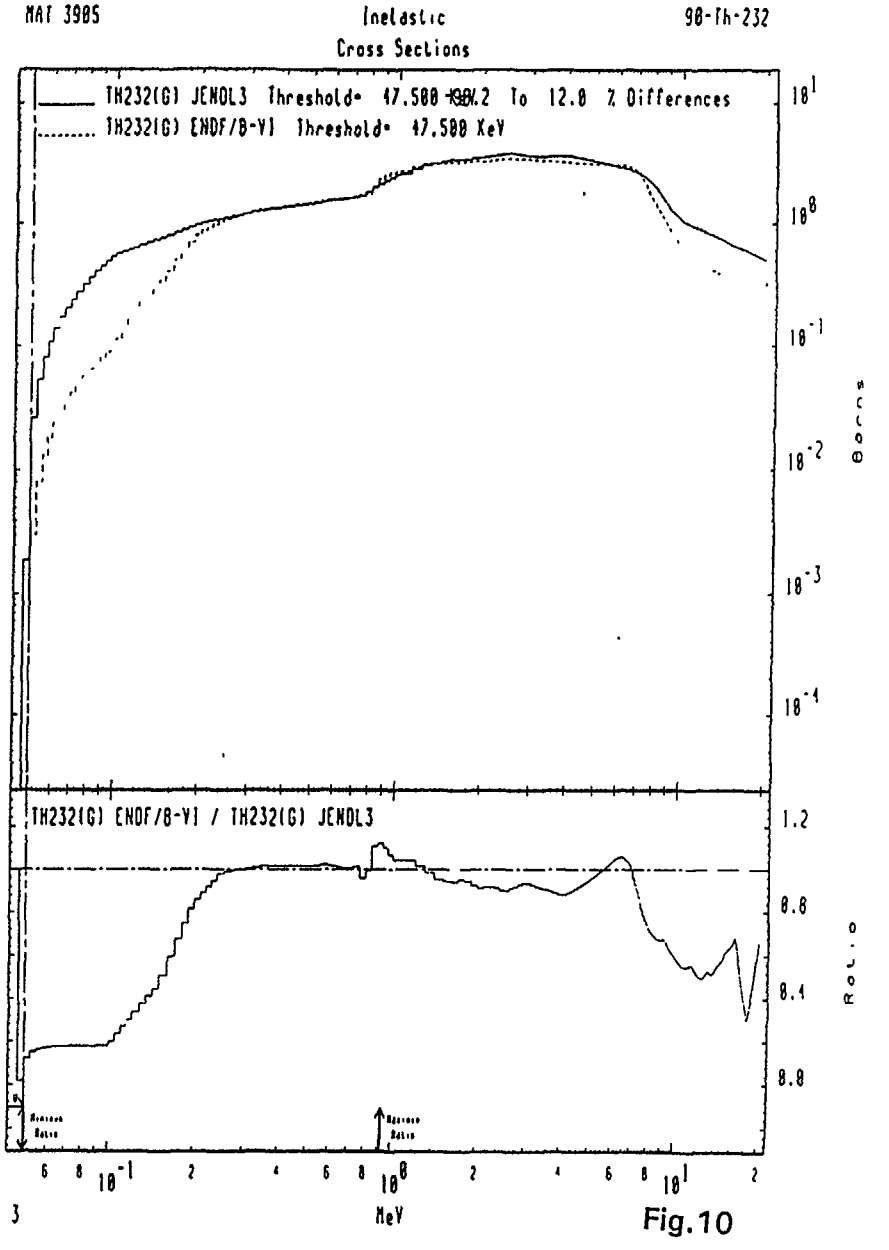
MAT 3905
Inelastic
Cross Sections
90-Th-232
TH232(G) JENDL3 Threshold= 47.500 KeV -98.2 To 12.8 % Differences
TH232(G) ENDF/B-VI Threshold= 47.500 KeV
Barns
TH232(G) ENDF/B-VI / TH232(G) JENDL3
Ratio
MeV

Fig.10

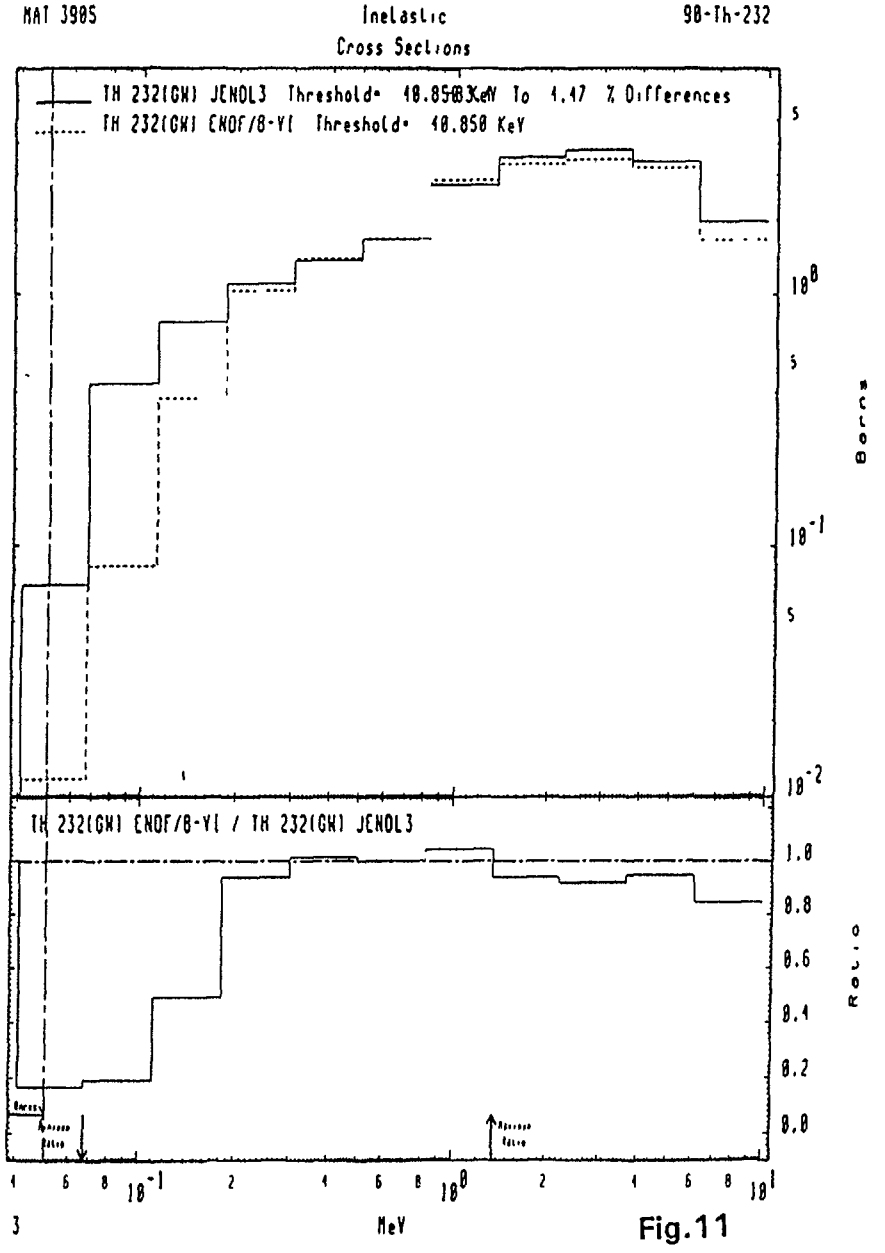
MAT 3905
Inelastic
Cross Sections
90-Th-232
TH 232(GN) JENDL3 Threshold= 48.858 KeV To 4.47 % Differences
TH 232(GN) ENDF/B-VI Threshold= 48.858 KeV
TH 232(GN) ENDF/B-VI / TH 232(GN) JENDL3
Barns
Ratio
MeV

Fig.11

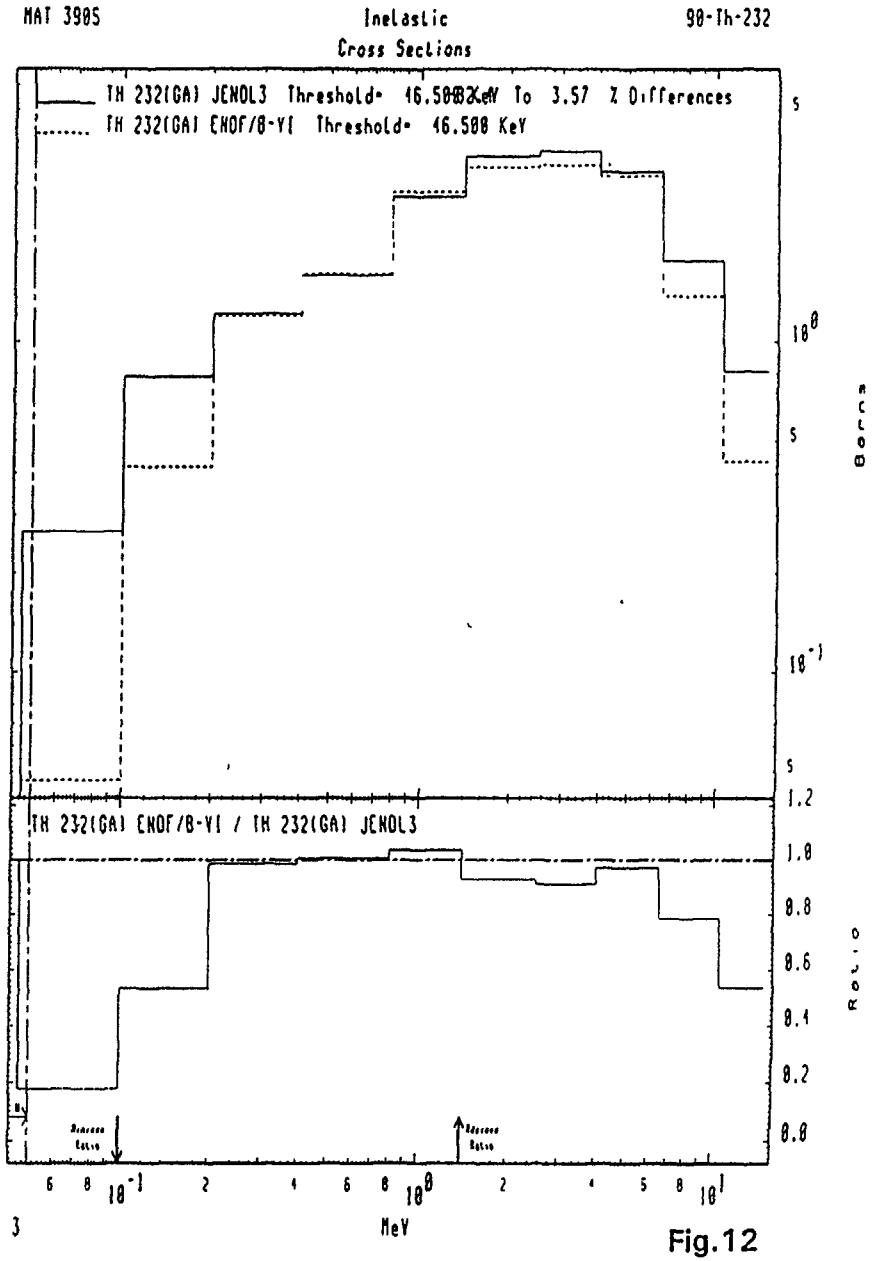
MAT 3905
Inelastic
Cross Sections
90-Th-232
TH 232(GA) JENDL3 Threshold= 46.588 KeV To 3.57 % Differences
TH 232(GA) ENDF/B-VI Threshold= 46.588 KeV
TH 232(GA) ENDF/B-VI / TH 232(GA) JENDL3
Barns
Ratio
MeV

Fig.12

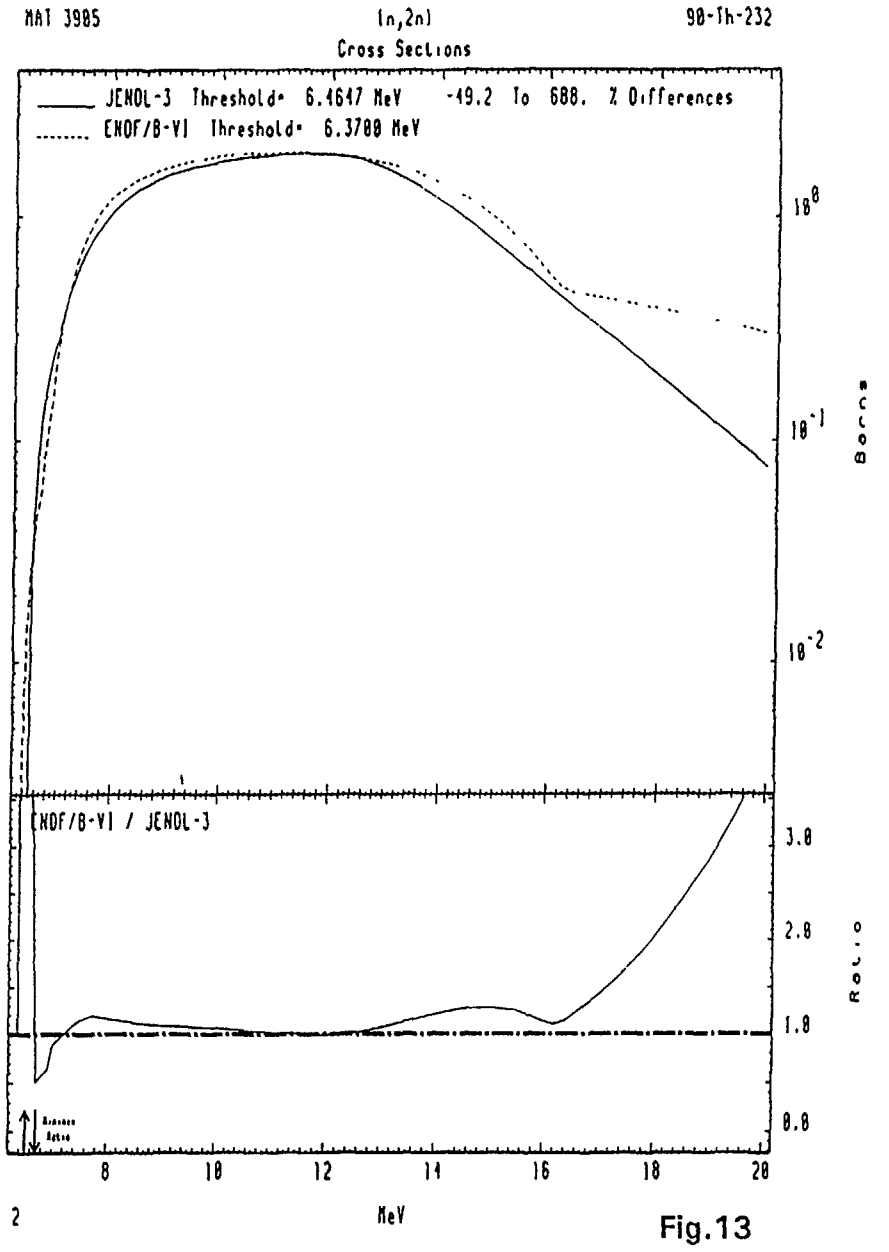
MAT 3985
(n,2n)
90-Th-232
Cross Sections
JENDL-3 Threshold= 6.4647 MeV -49.2 To 688. % Differences
ENDF/B-VI Threshold= 6.3700 MeV
Barns
ENDF/B-VI / JENDL-3
Ratio
MeV

Fig.13

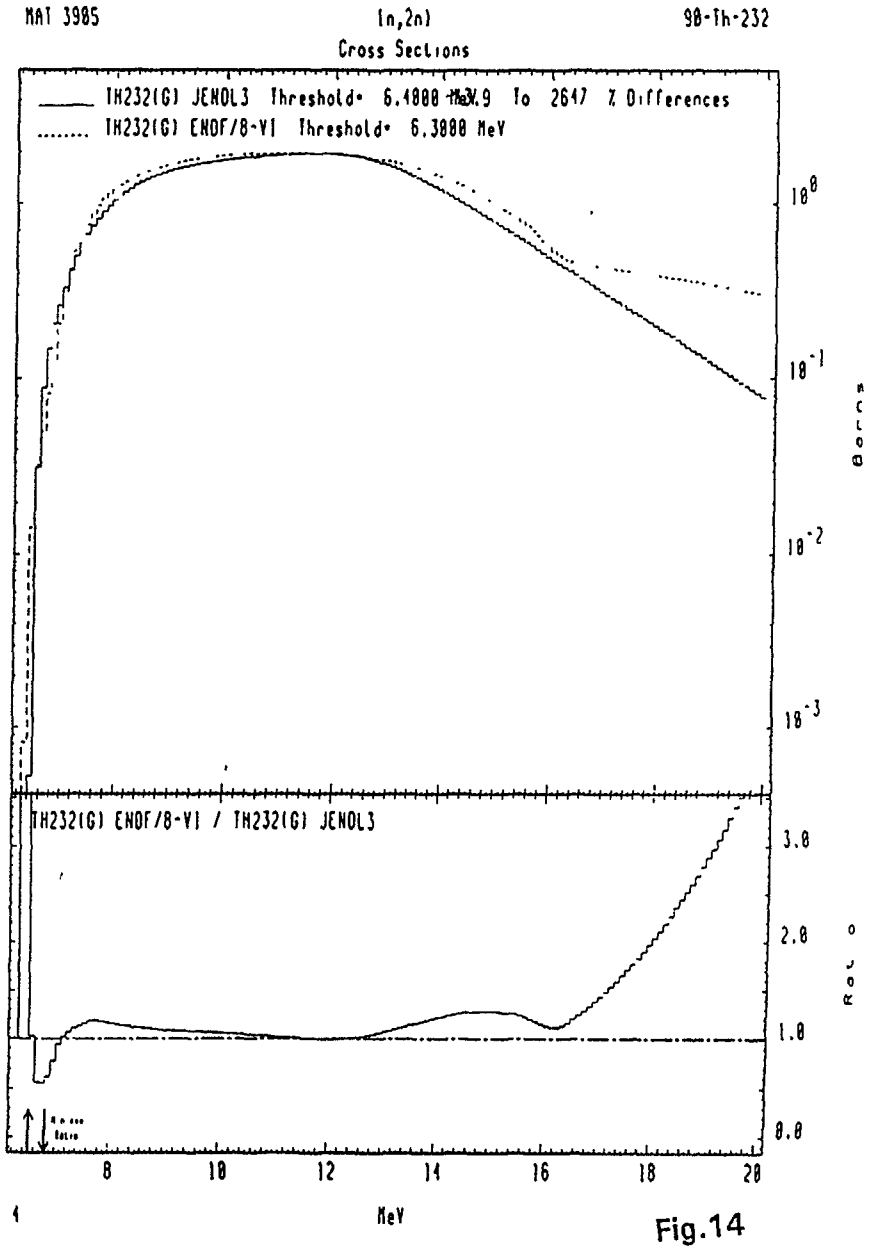
MAT 3985
(n,2n)
90-Th-232
Cross Sections
TH232(G) JENDL3 Threshold= 6.4000 MeV -3.9 To 2647 % Differences
TH232(G) ENDF/B-VI Threshold= 6.3000 MeV
Barns
TH232(G) ENDF/B-VI / TH232(G) JENDL3
Ratio
MeV

Fig.14

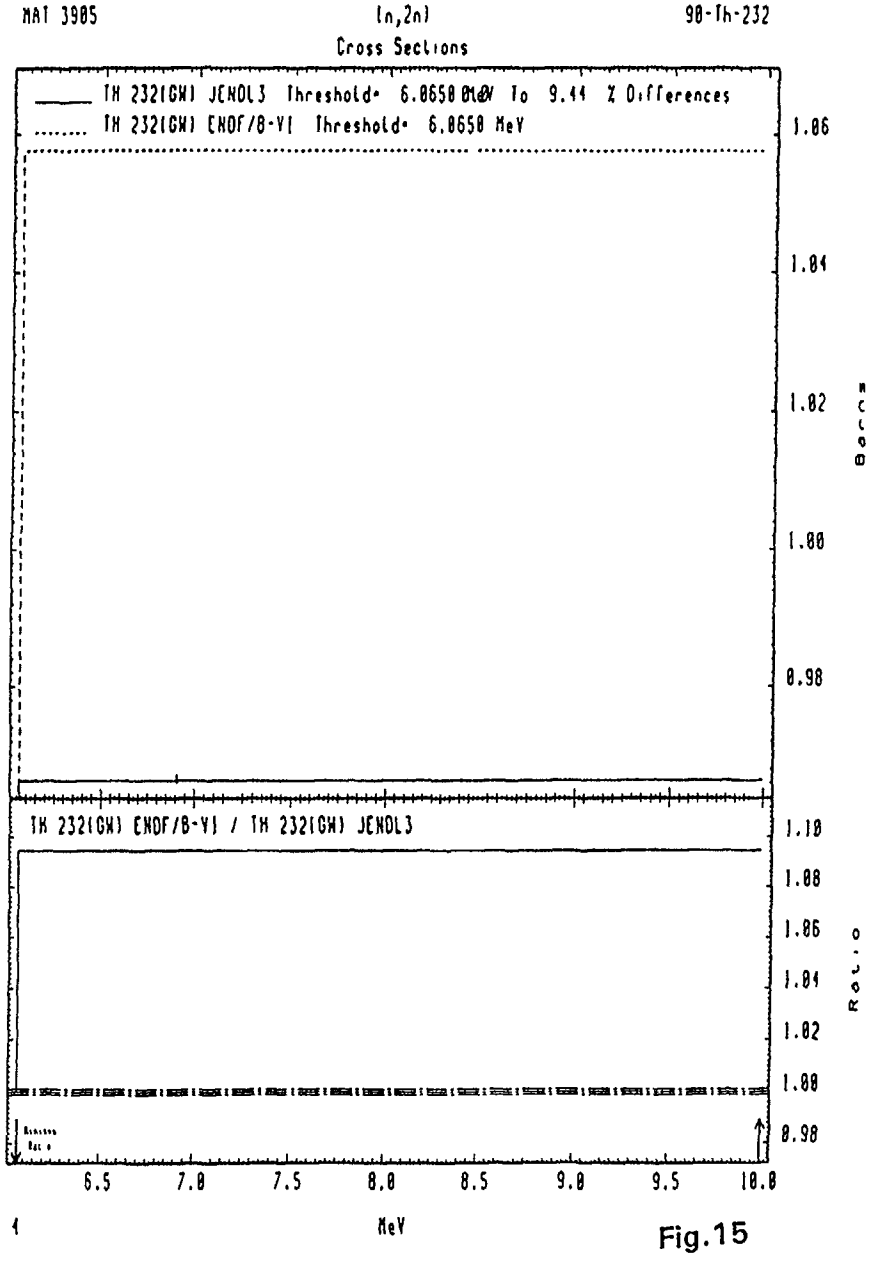
MAT 3905
(n,2n)
90-Th-232
Cross Sections
TH 232(GW) JENDL3 Threshold= 6.0650 MeV To 9.44 % Differences
TH 232(GW) ENDF/B-VI Threshold= 6.0650 MeV
TH 232(GW) ENDF/B-VI / TH 232(GW) JENDL3
Barns
Ratio
MeV

Fig.15

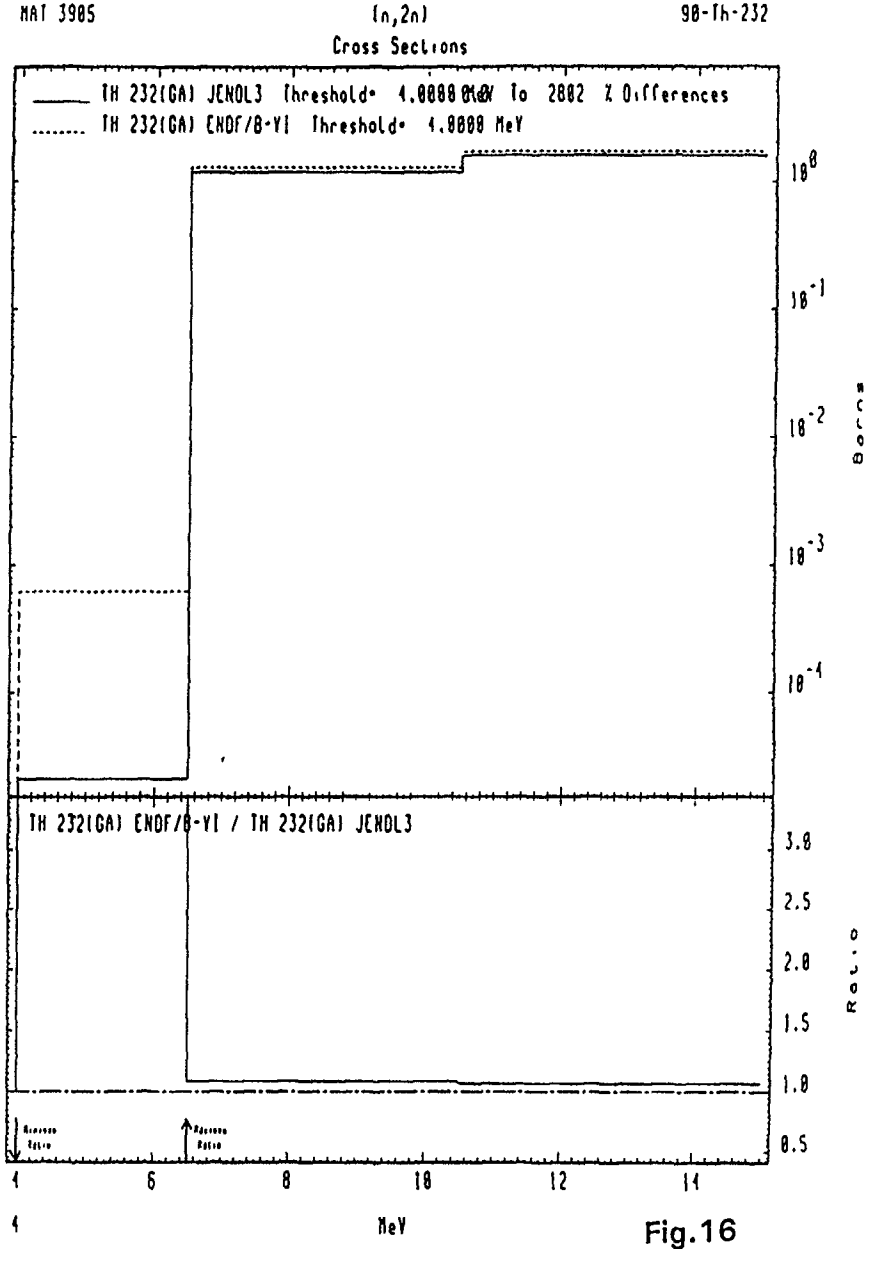
MAT 3905
(n,2n)
90-Th-232
Cross Sections
TH 232(GA) JENDL3 Threshold= 4.0000 MeV To 2802 % Differences
TH 232(GA) ENDF/B-VI Threshold= 4.0000 MeV
TH 232(GA) ENDF/B-VI / TH 232(GA) JENDL3
Barns
Ratio
MeV

Fig.16

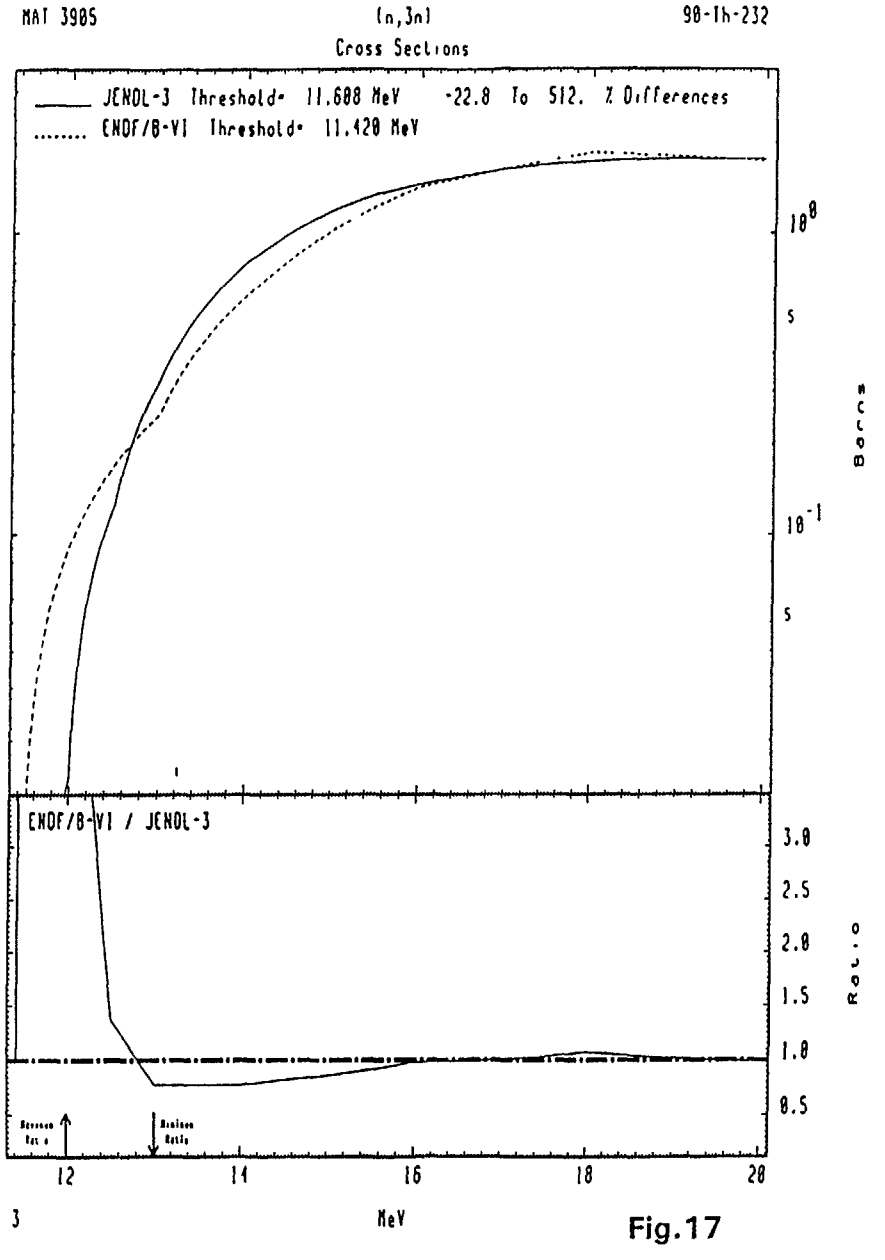
MAT 3905
(n,3n)
90-Th-232
Cross Sections
JENDL-3 Threshold= 11.600 MeV -22.8 To 512. % Differences
ENDF/B-VI Threshold= 11.420 MeV
Barns
ENDF/B-VI / JENDL-3
Ratio
MeV

Fig.17

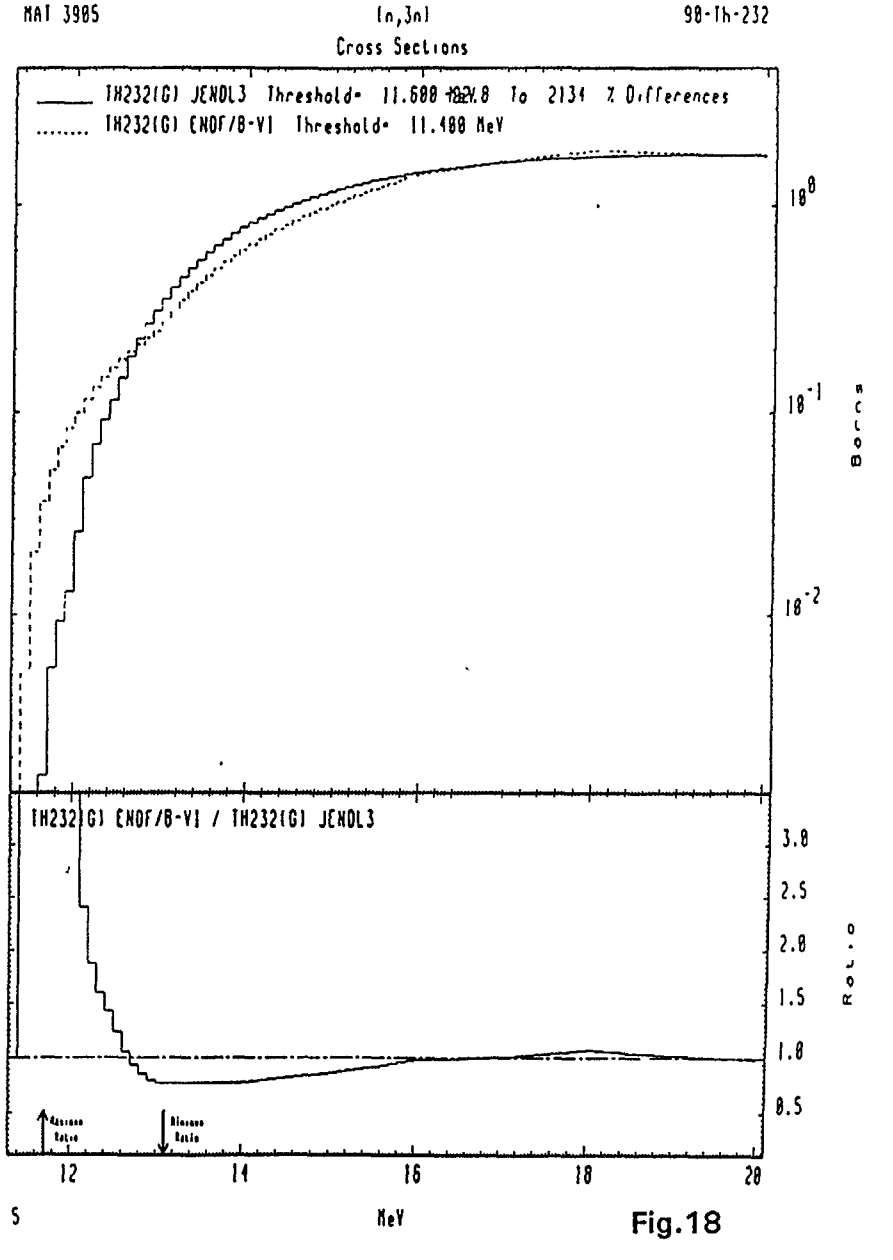
MAT 3905
(n,3n)
90-Th-232
Cross Sections
TH232(G) JENDL3 Threshold= 11.600 MeV -22.8 To 2134 % Differences
TH232(G) ENDF/B-VI Threshold= 11.400 MeV
Barns
TH232(G) ENDF/B-VI / TH232(G) JENDL3
Ratio
MeV

Fig.18

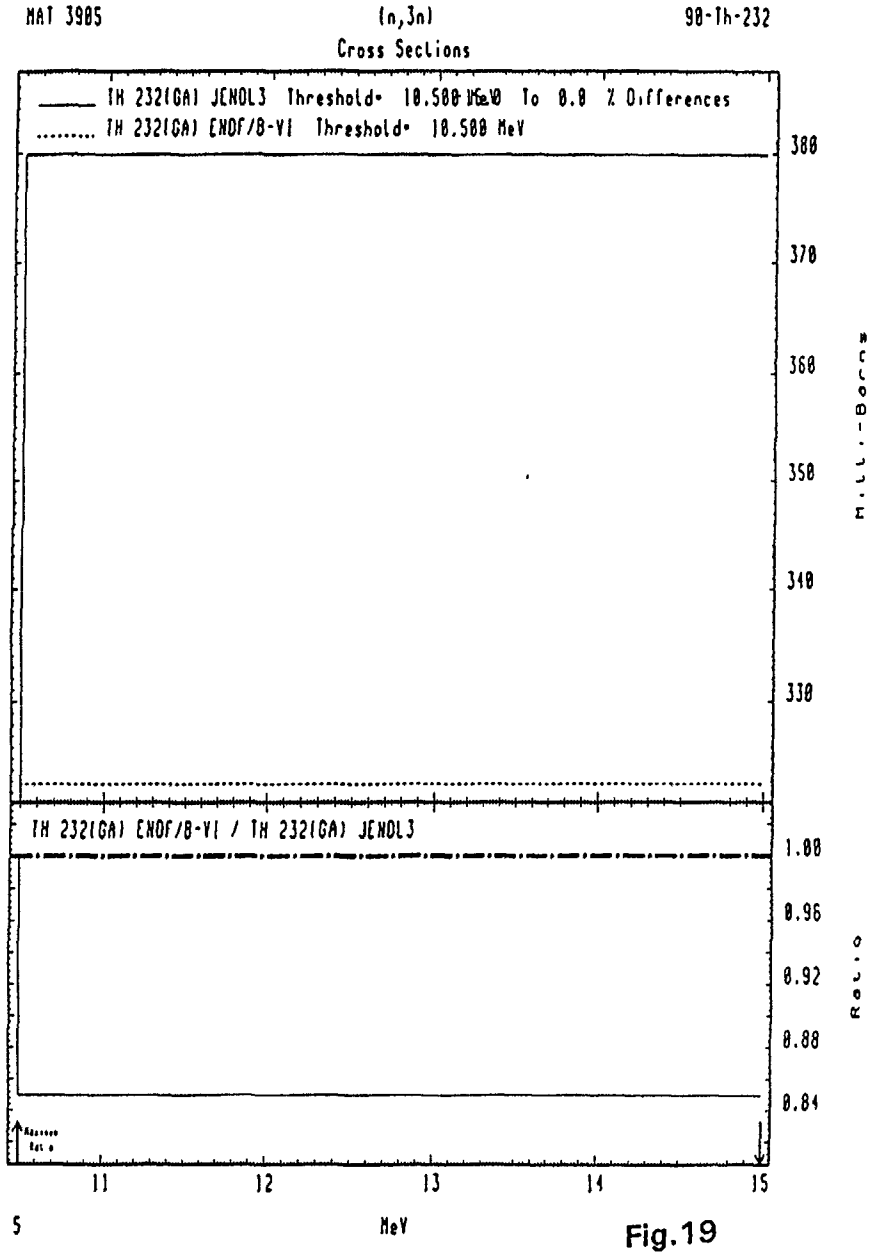
MAT 3905
(n,3n)
90-Th-232
Cross Sections
TH 232(GA) JENDL3 Threshold= 10.580 MeV 0 To 0.0 % Differences
TH 232(GA) ENDF/B-VI Threshold= 10.580 MeV
380
370
360
350
340
330
M.L.-Barns
TH 232(GA) ENDF/B-VI / TH 232(GA) JENDL3
1.00
0.96
0.92
0.88
0.84
Ratio
11
12
13
14
15
5
MeV

Fig.19

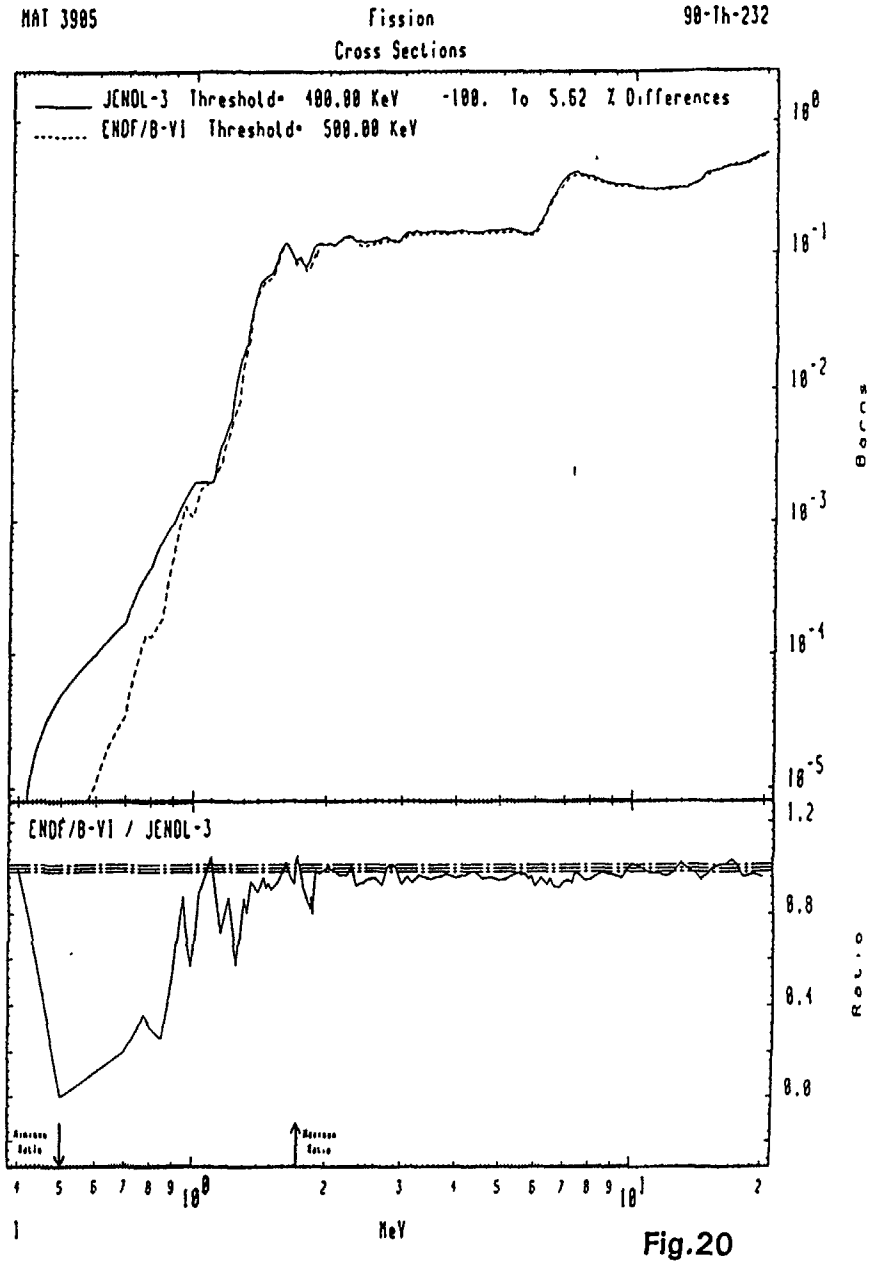
MAT 3905
Fission
90-Th-232
Cross Sections
JENDL-3 Threshold= 400.00 KeV -100. To 5.62 % Differences
ENDF/B-VI Threshold= 500.00 KeV
10^{0}
10^{-1}
10^{-2}
10^{-3}
10^{-4}
10^{-5}
Barns
ENDF/B-VI / JENDL-3
1.2
0.8
0.4
0.0
Ratio
4 5 6 7 8 9 10^{0} 2 3 4 5 6 7 8 9 10^{1} 2
1
MeV

Fig.20

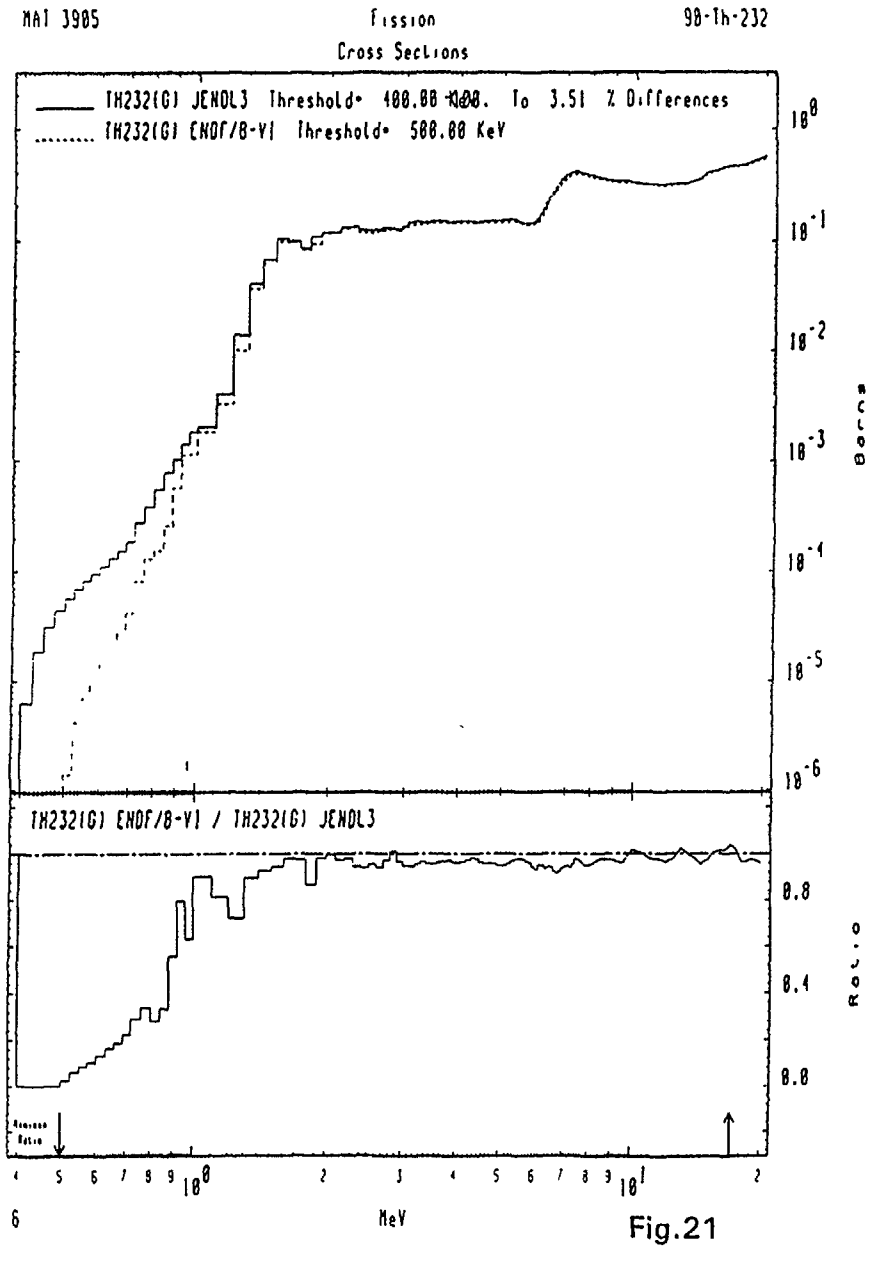
MAT 3905
Fission
Cross Sections
90-Th-232
TH232(G) JENDL3 Threshold= 400.00 KeV. To 3.51 % Differences
TH232(G) ENDF/B-VI Threshold= 500.00 KeV
TH232(G) ENDF/B-VI / TH232(G) JENDL3
Barns
Ratio
MeV

Fig.21

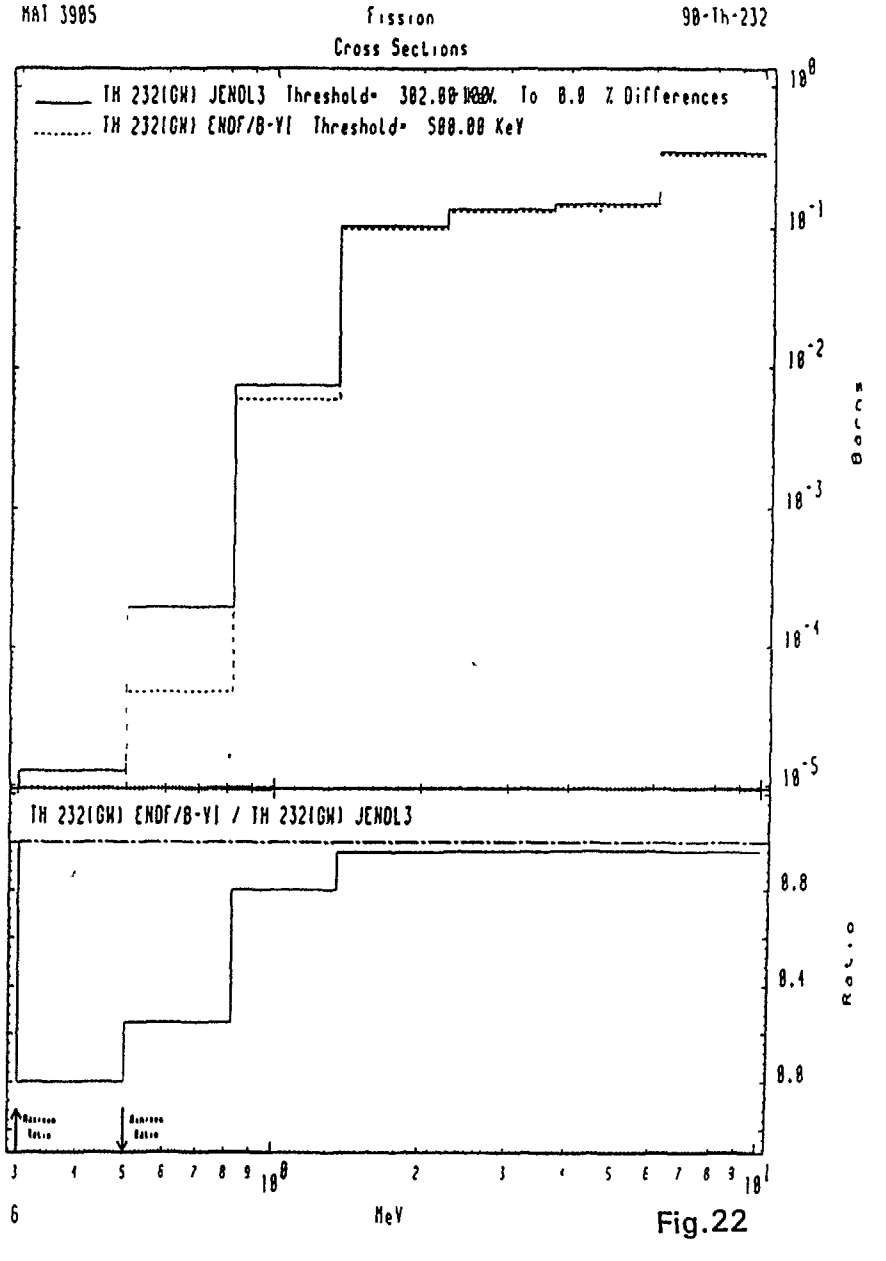
MAT 3905
Fission
Cross Sections
90-Th-232
TH 232(GW) JENDL3 Threshold= 302.00 KeV. To 0.0 % Differences
TH 232(GW) ENDF/B-VI Threshold= 500.00 KeV
TH 232(GW) ENDF/B-VI / TH 232(GW) JENDL3
Barns
Ratio
MeV

Fig.22

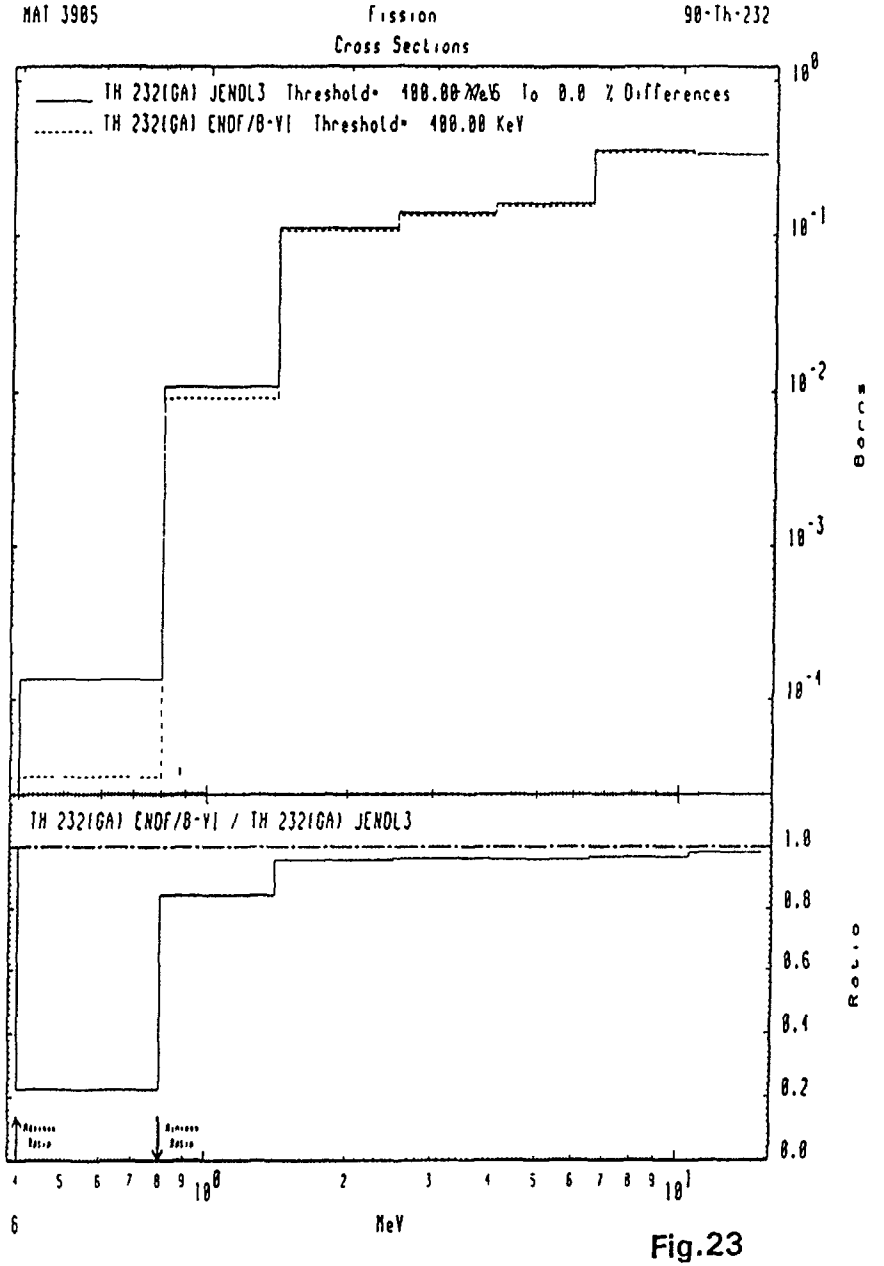
MAT 3985
Fission
90-Th-232
Cross Sections
TH 232(GA) JENDL3 Threshold= 100.00 KeV To 0.0 % Differences
TH 232(GA) ENDF/B-VI Threshold= 100.00 KeV
Barns
TH 232(GA) ENDF/B-VI / TH 232(GA) JENDL3
Ratio
MeV

Fig.23

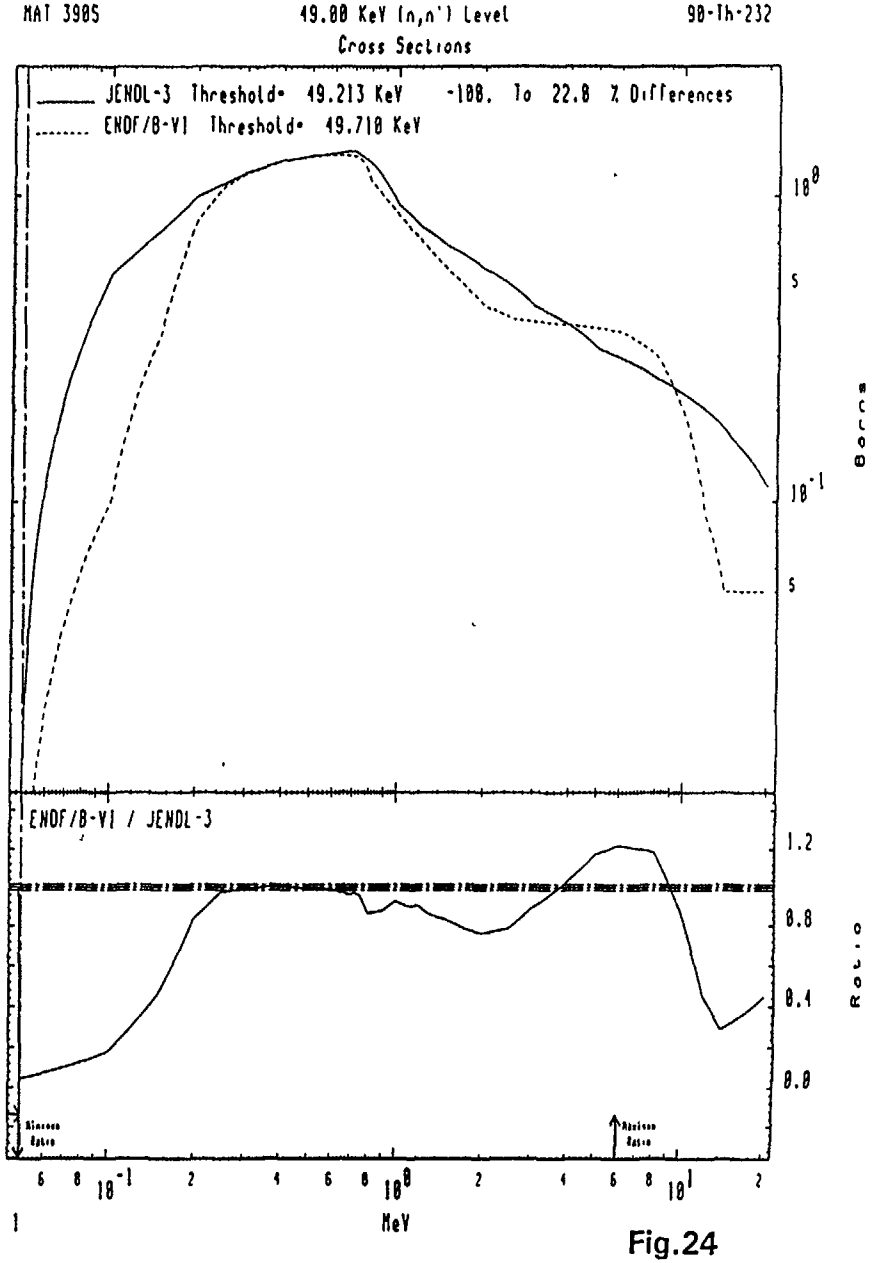
MAT 3985
49.00 KeV (n,n') Level
90-Th-232
Cross Sections
JENDL-3 Threshold= 49.213 KeV -100. To 22.8 % Differences
ENDF/B-VI Threshold= 49.710 KeV
Barns
ENDF/B-VI / JENDL-3
Ratio
MeV

Fig.24

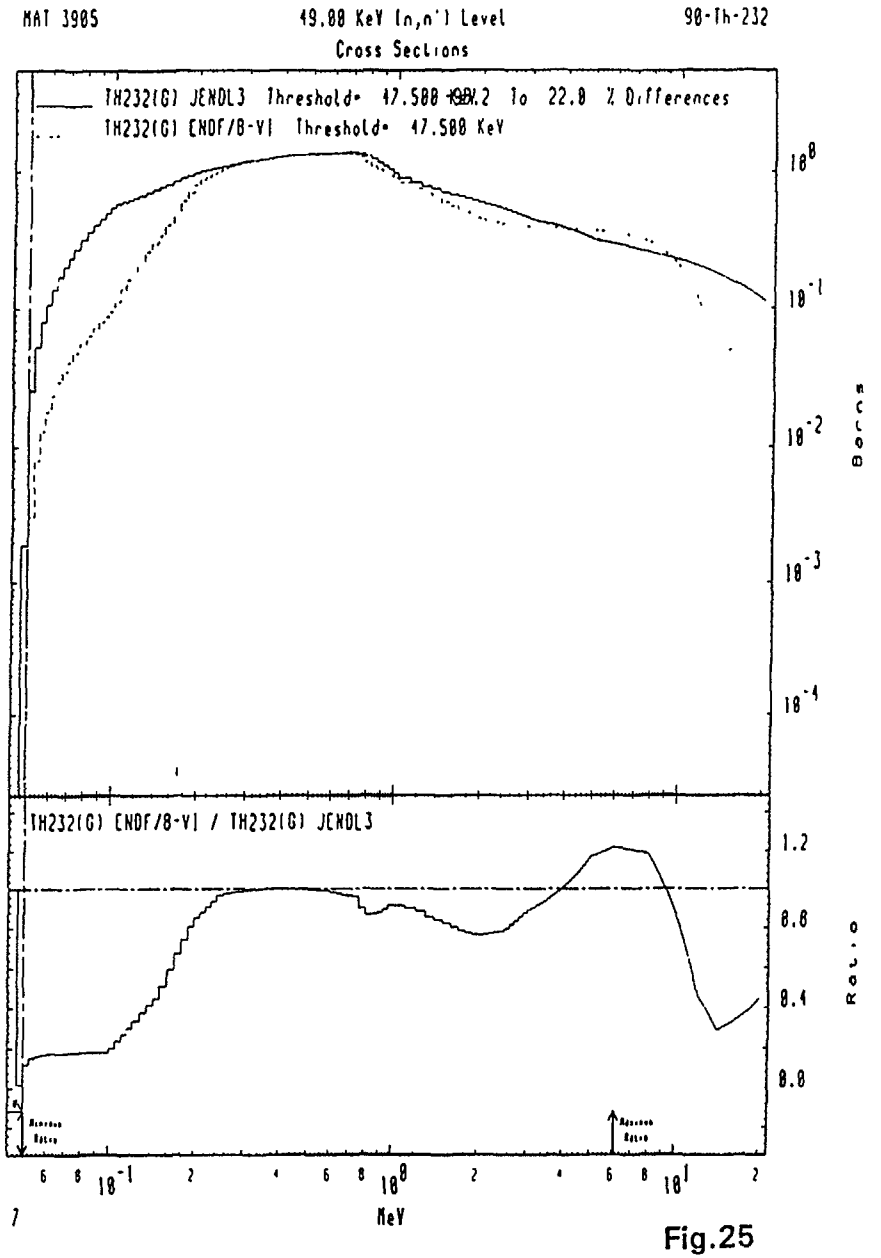
MAT 3905
49.00 KeV (n,n') Level
90-Th-232
Cross Sections
TH232(G) JENDL3 Threshold= 47.500 KeV To 22.0 % Differences
TH232(G) ENDF/B-VI Threshold= 47.500 KeV
Barns
TH232(G) ENDF/B-VI / TH232(G) JENDL3
Ratio
MeV

Fig.25

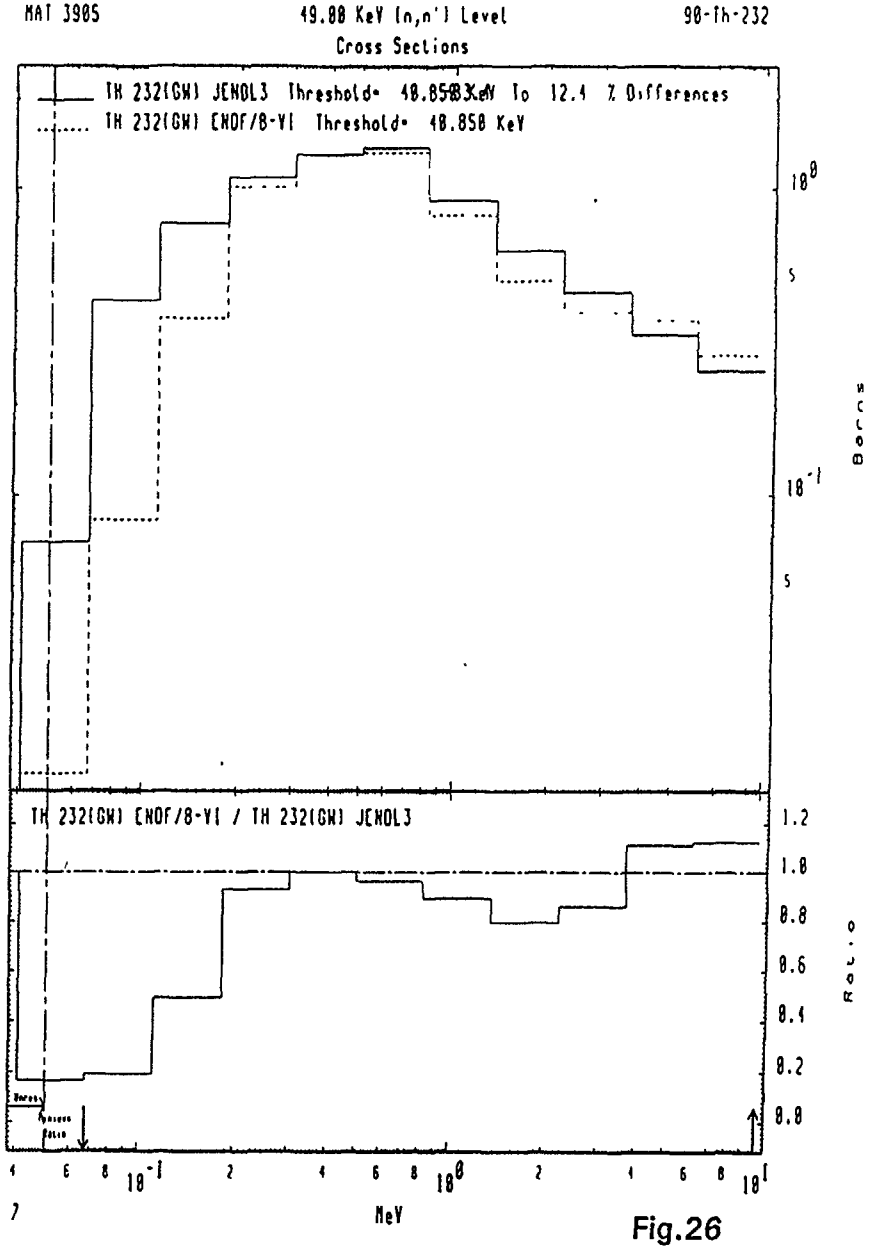
MAT 3905
49.00 KeV (n,n') Level
90-Th-232
Cross Sections
TH 232(GW) JENDL3 Threshold= 48.850 KeV To 12.4 % Differences
TH 232(GW) ENDF/B-VI Threshold= 48.850 KeV
Barns
TH 232(GW) ENDF/B-VI / TH 232(GW) JENDL3
Ratio
MeV

Fig.26

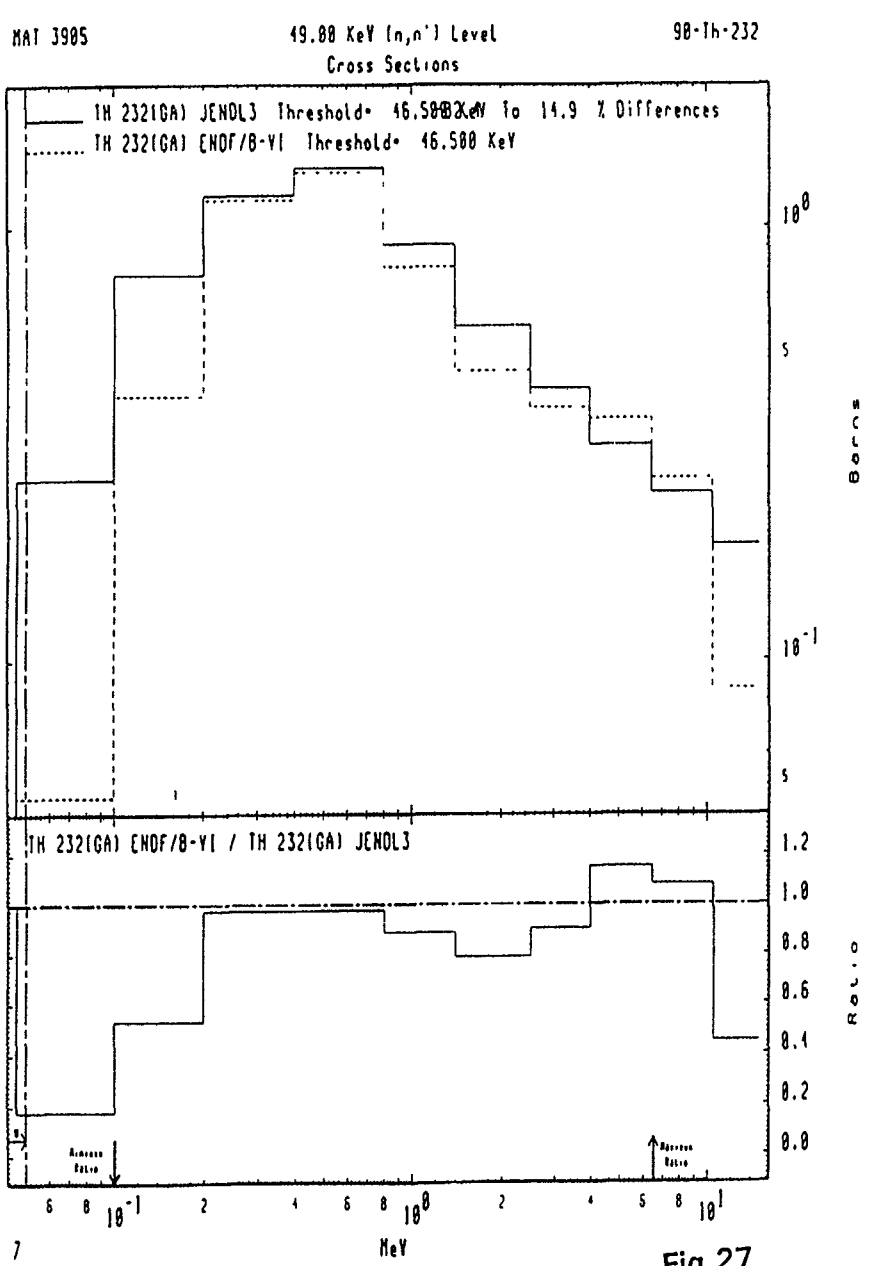
MAT 3905
49.00 KeV (n,n') Level
Cross Sections
90-Th-232
TH 232(GA) JENDL3 Threshold= 46.500 KeV To 14.9 % Differences
TH 232(GA) ENDF/B-VI Threshold= 46.500 KeV
Barns
TH 232(GA) ENDF/B-VI / TH 232(GA) JENDL3
Ratio
MeV
7

Fig.27

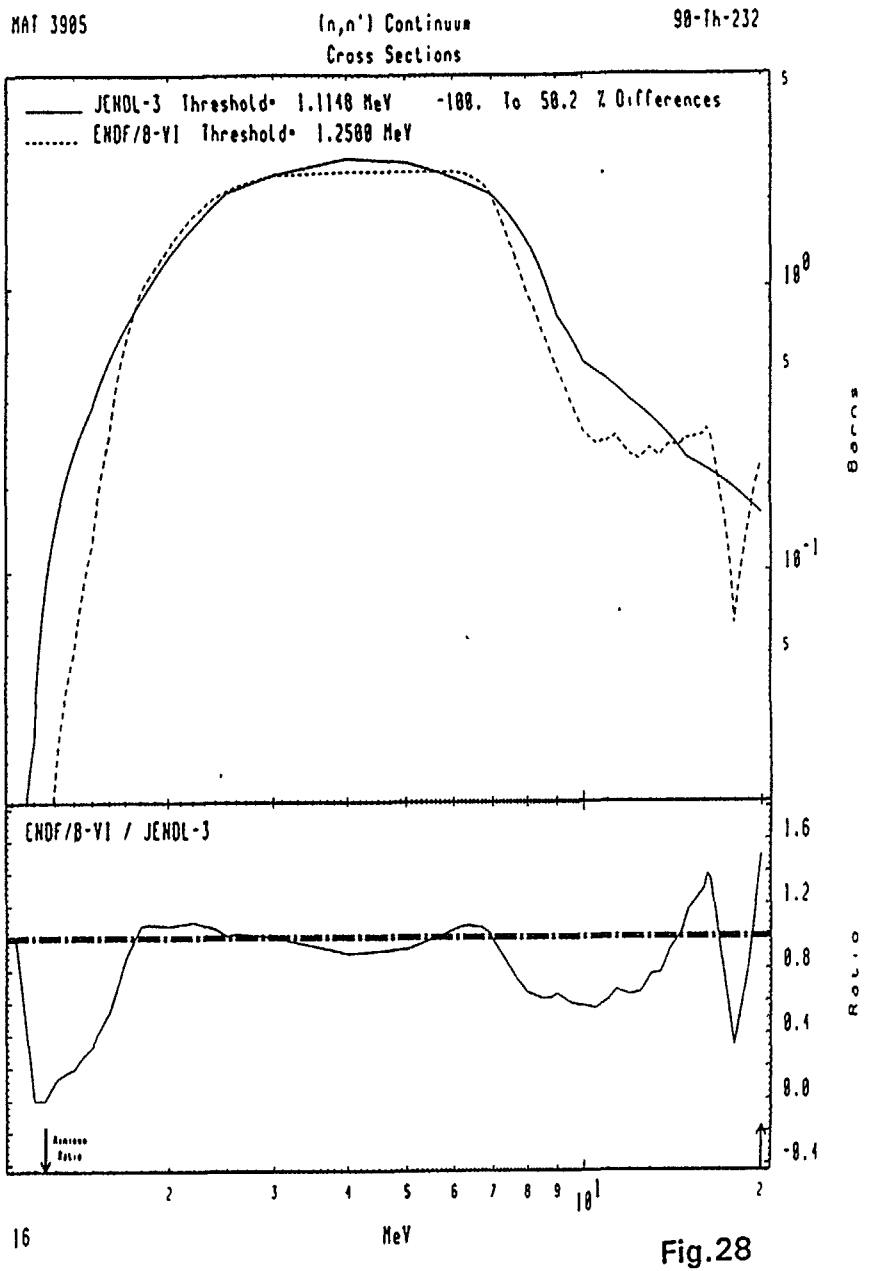
MAT 3905
(n,n') Continuum
Cross Sections
90-Th-232
JENDL-3 Threshold= 1.1140 MeV -100. To 50.2 % Differences
ENDF/B-VI Threshold= 1.2500 MeV
Barns
ENDF/B-VI / JENDL-3
Ratio
MeV
16

Fig.28

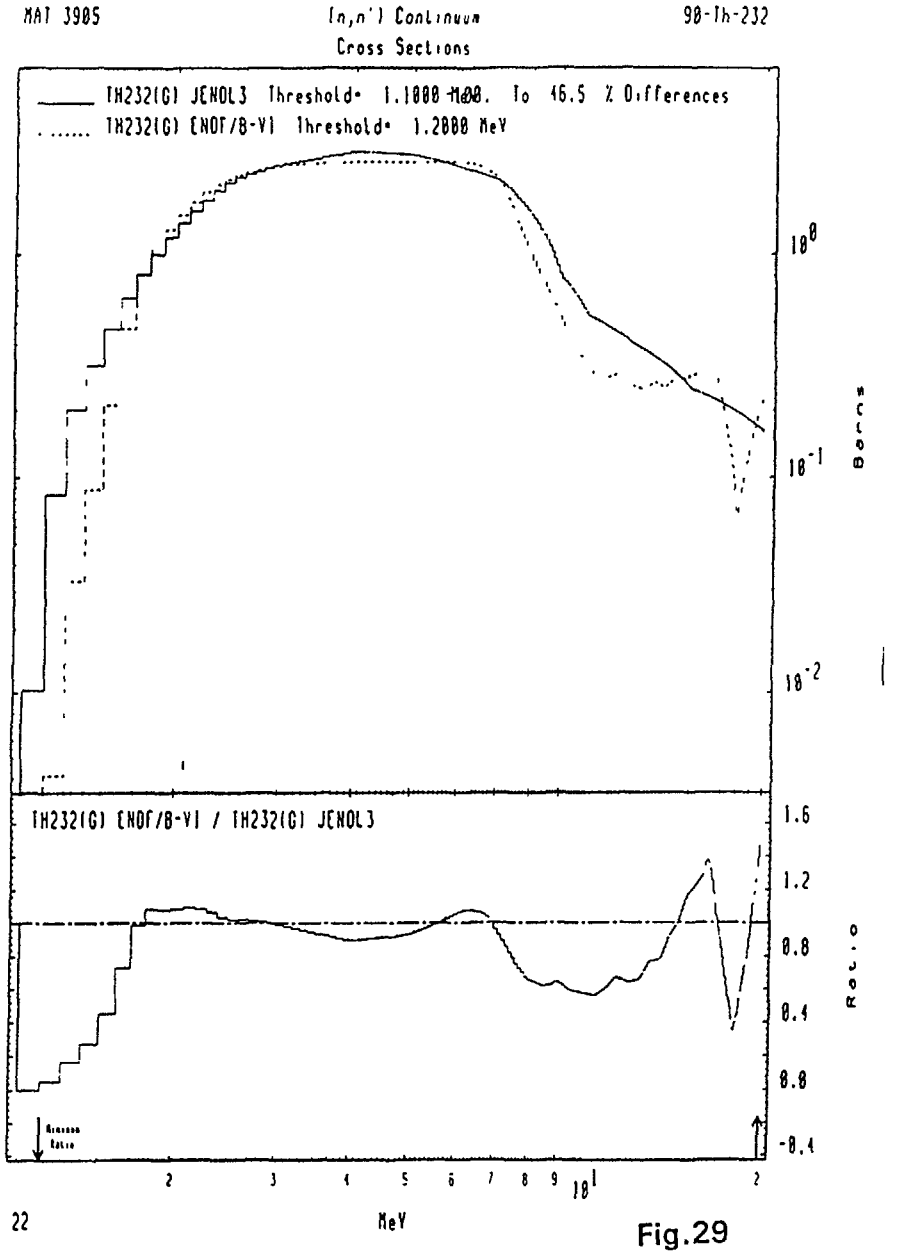
MAT 3905
(n,n') Continuum
Cross Sections
90-Th-232
TH232(G) JENDL3 Threshold= 1.1000 MeV To 46.5 % Differences
TH232(G) ENDF/B-VI Threshold= 1.2000 MeV
Barns
TH232(G) ENDF/B-VI / TH232(G) JENDL3
Ratio
MeV
22

Fig.29

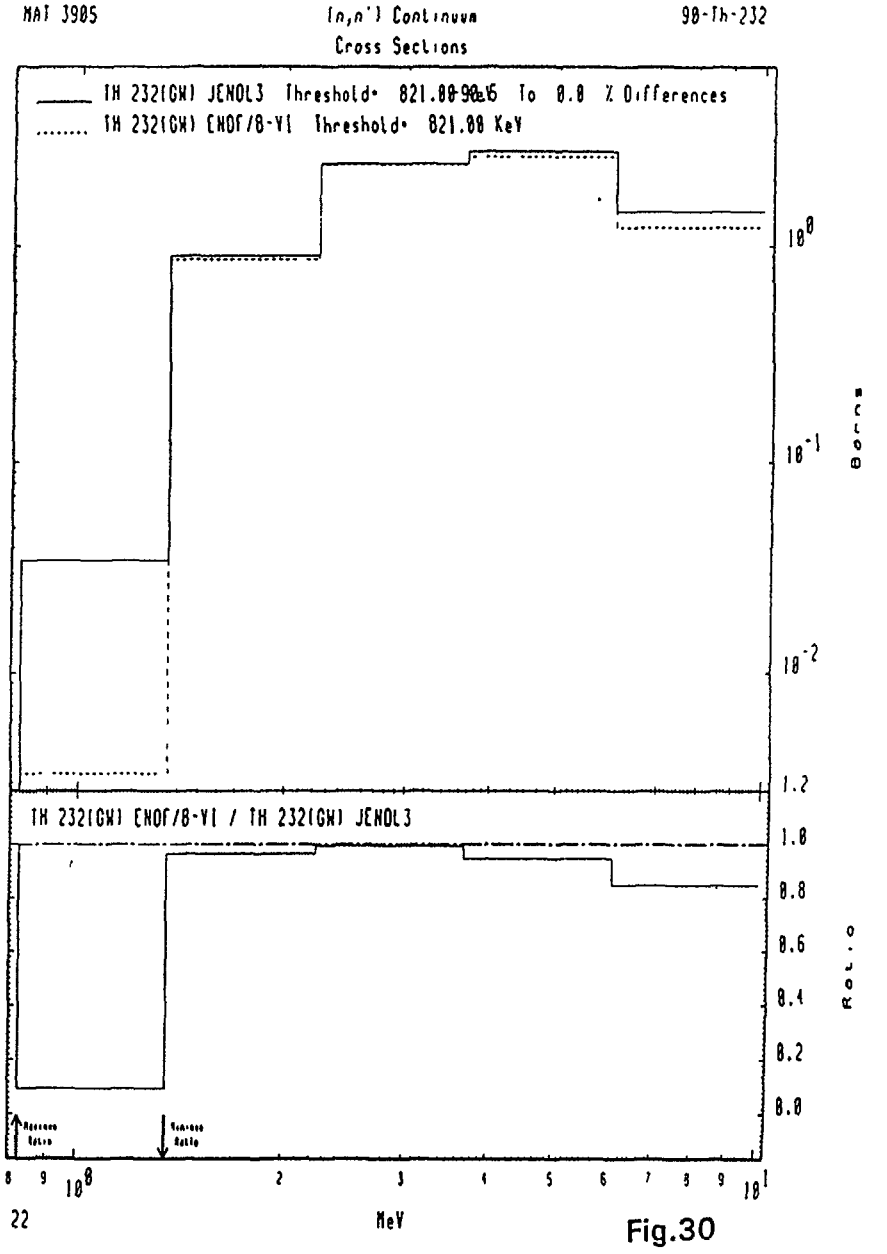
MAT 3905
(n,n') Continuum
Cross Sections
90-Th-232
TH 232(GW) JENDL3 Threshold= 821.00 KeV To 0.0 % Differences
TH 232(GW) ENDF/B-VI Threshold= 821.00 KeV
Barns
TH 232(GW) ENDF/B-VI / TH 232(GW) JENDL3
Ratio
MeV
22

Fig.30

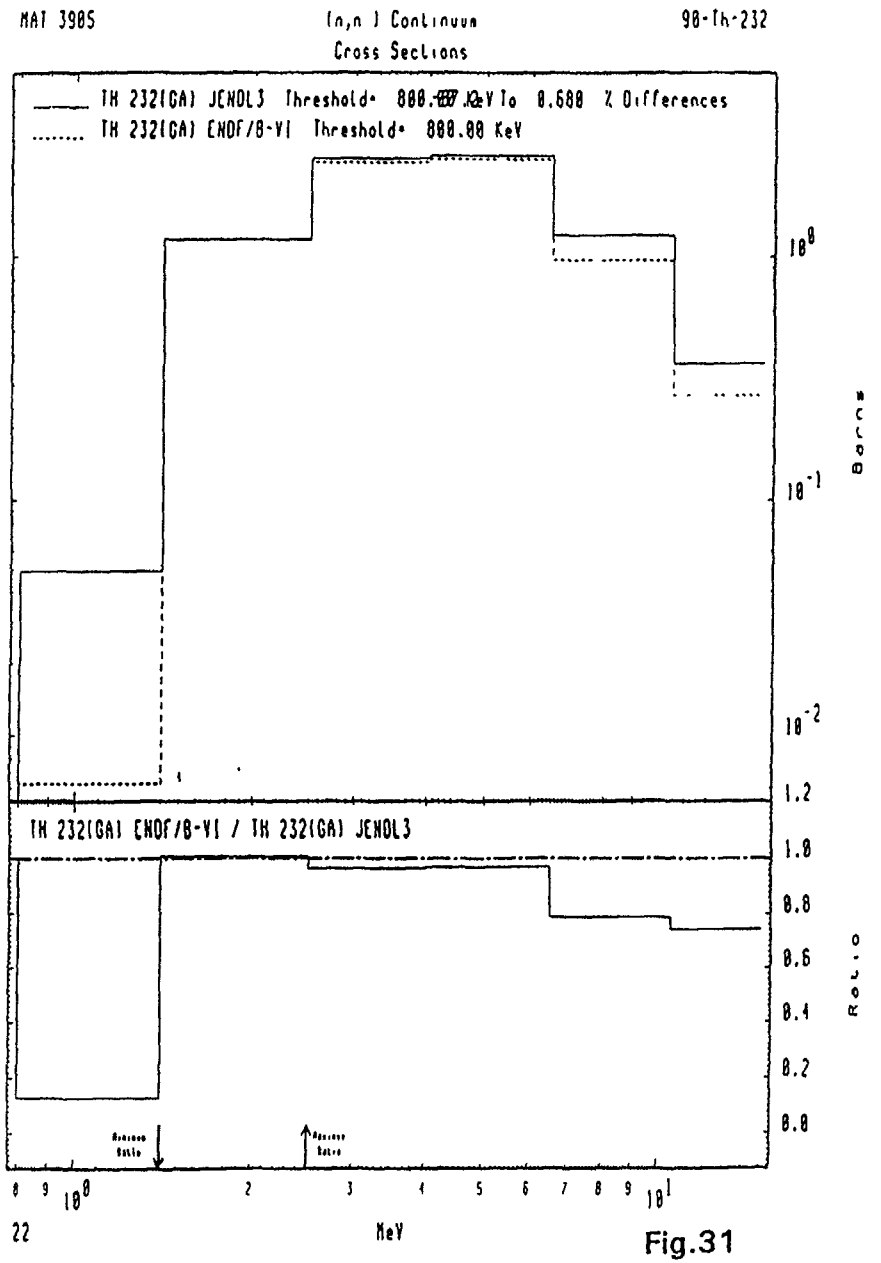
MAT 3905
(n,n') Continuum
Cross Sections
90-Th-232
TH 232(GA) JENDL3 Threshold= 800.000 KeV To 0.680 % Differences
TH 232(GA) ENDF/B-VI Threshold= 800.00 KeV
Barns
TH 232(GA) ENDF/B-VI / TH 232(GA) JENDL3
Ratio
MeV

Fig.31

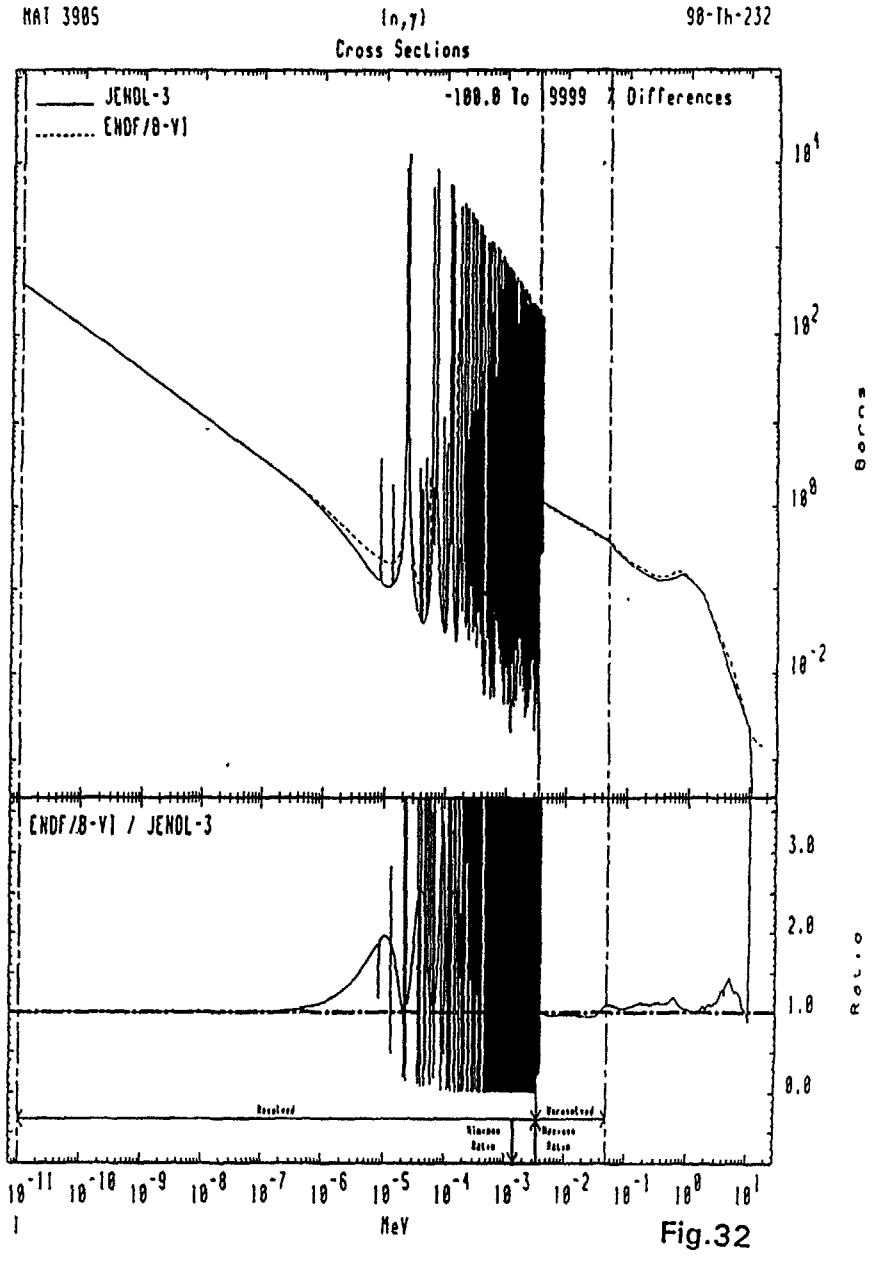
MAT 3905
(n,γ)
Cross Sections
90-Th-232
JENDL-3
ENDF/B-VI
-100.0 To 9999 % Differences
Barns
ENDF/B-VI / JENDL-3
Ratio
MeV

Fig.32

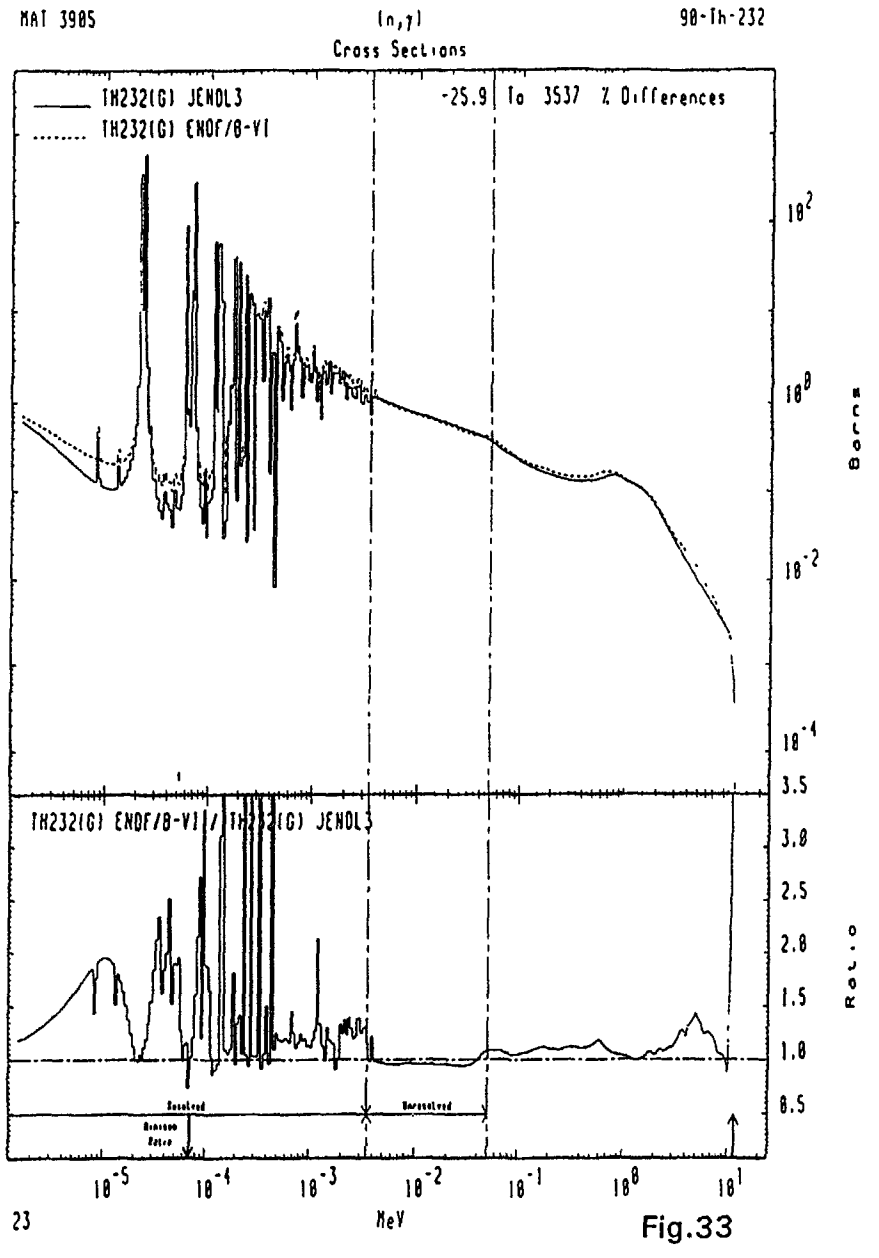
MAT 3905
(n,γ)
90-Th-232
Cross Sections
TH232(G) JENDL3
TH232(G) ENDF/B-VI
-25.9 To 3537 % Differences
Barns
TH232(G) ENDF/B-VI / TH232(G) JENDL3
Ratio
Resolved
Unresolved
MeV
23

Fig.33

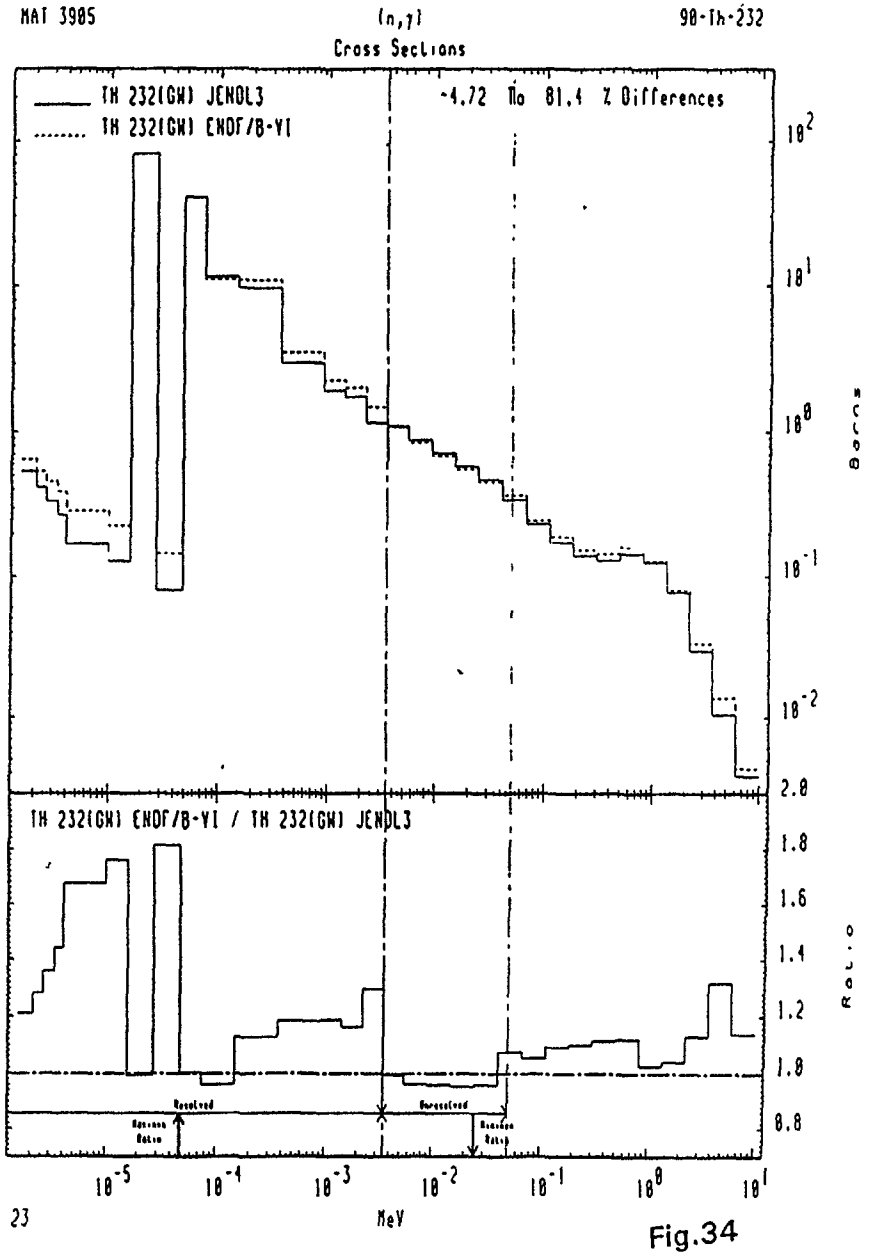
MAT 3905
(n,γ)
90-Th-232
Cross Sections
TH 232(GW) JENDL3
TH 232(GW) ENDF/B-VI
-4.72 To 81.4 % Differences
Barns
TH 232(GW) ENDF/B-VI / TH 232(GW) JENDL3
Ratio
Resolved
Unresolved
MeV
23

Fig.34

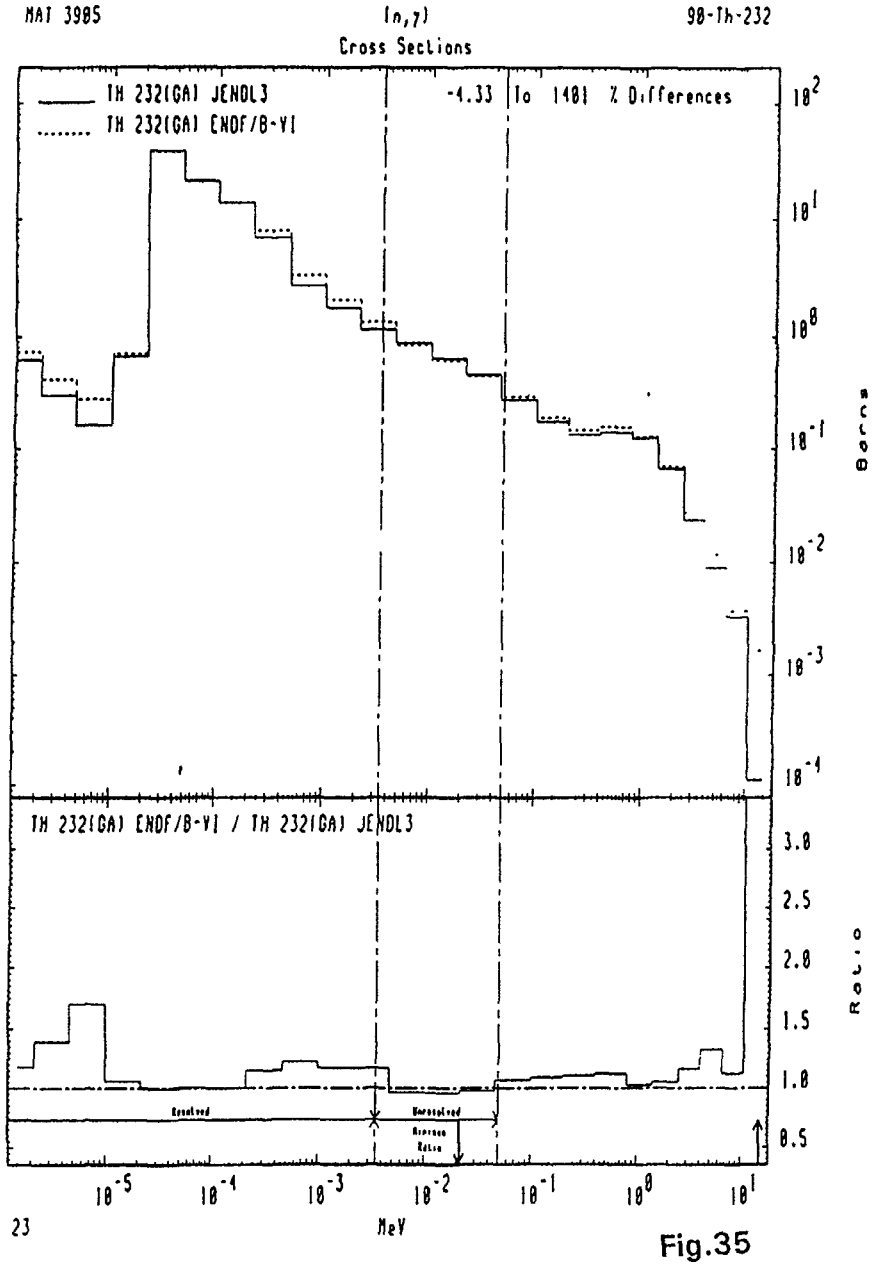
MAT 3905
(n,γ)
90-Th-232
Cross Sections
TH 232(GA) JENDL3
TH 232(GA) ENDF/B-VI
-4.33 to 140. % Differences
TH 232(GA) ENDF/B-VI / TH 232(GA) JENDL3
Barns
Ratio
MeV
23

Fig.35

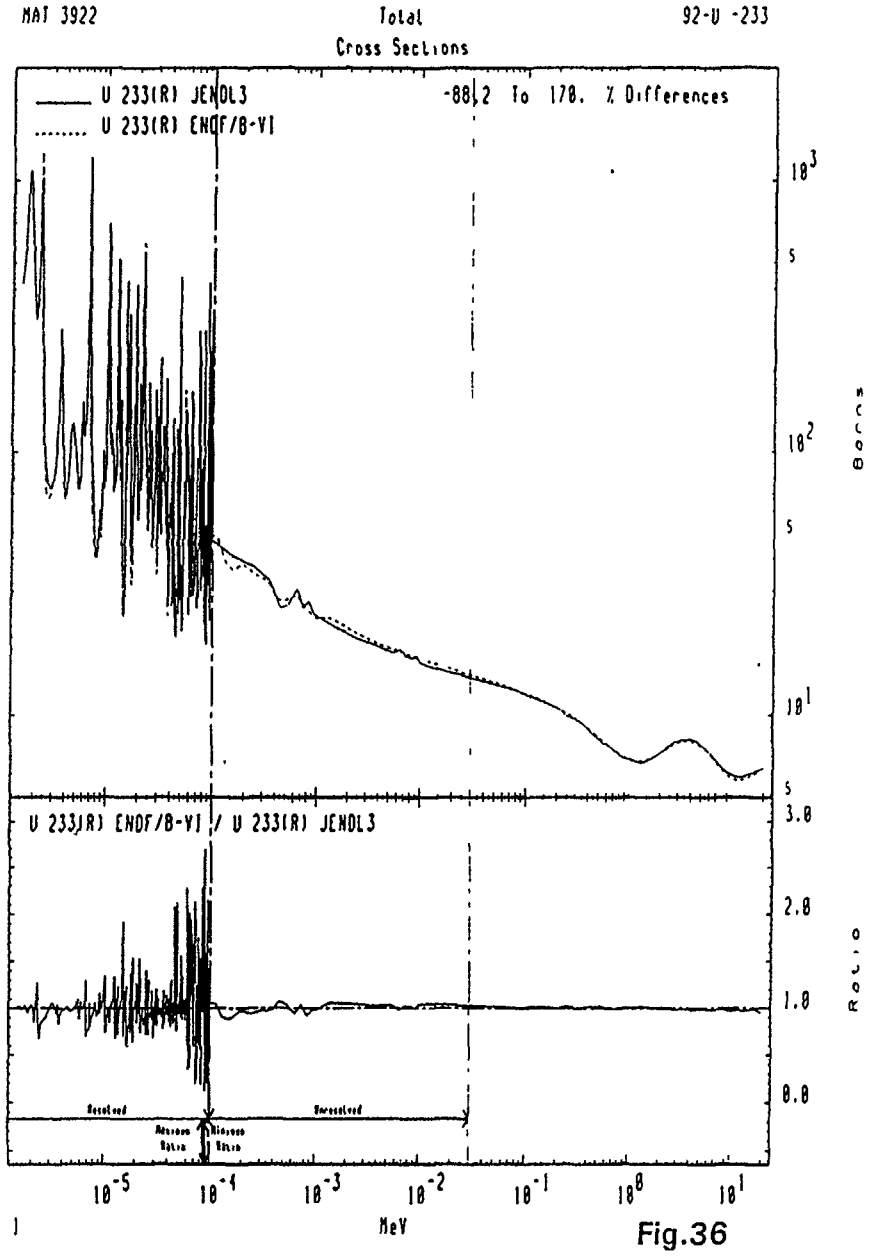
MAT 3922
Total
92-U -233
Cross Sections
U 233(R) JENDL3
U 233(R) ENDF/B-VI
-88.2 to 170. % Differences
U 233(R) ENDF/B-VI / U 233(R) JENDL3
Barns
Ratio
MeV
1

Fig.36

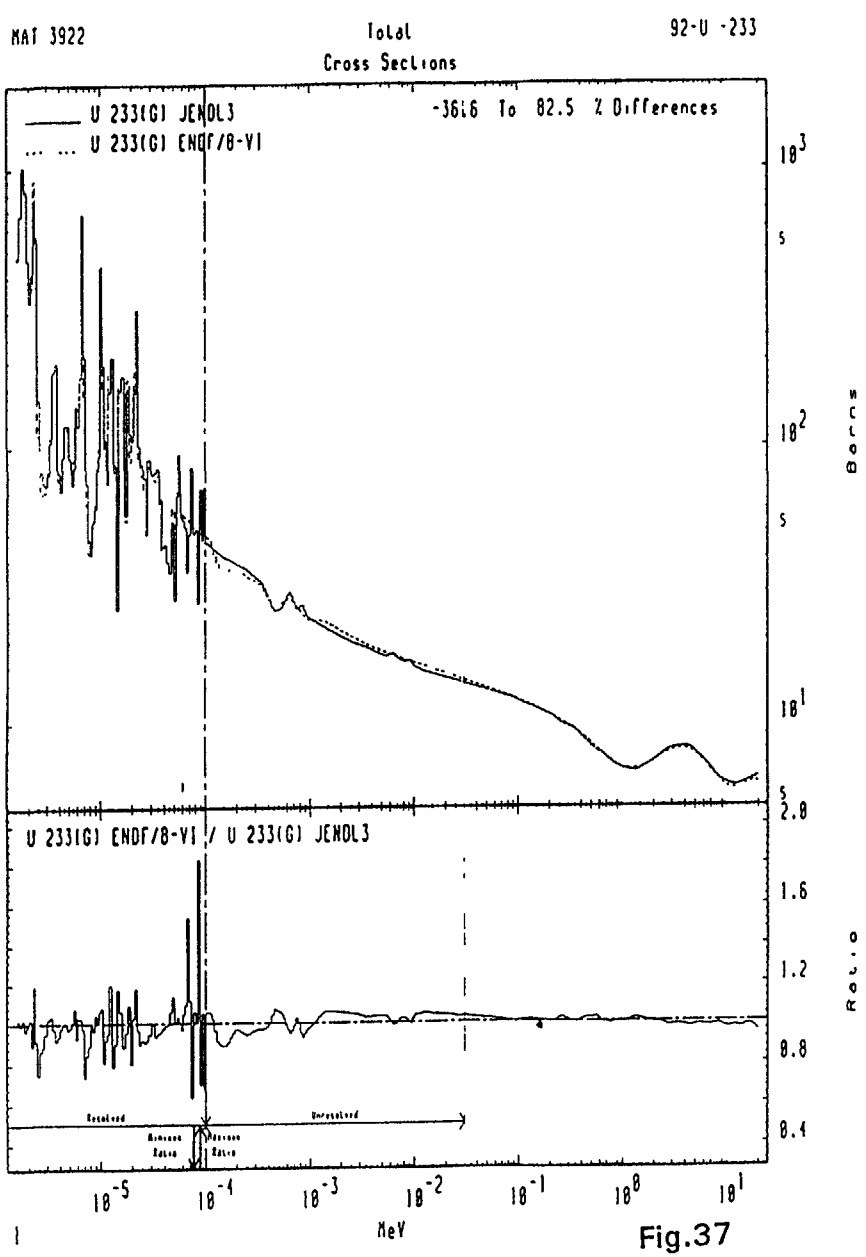
MAT 3922
Total
Cross Sections
92-U -233
U 233(G) JENDL3
U 233(G) ENDF/B-VI
-36.6 To 82.5 % Differences
U 233(G) ENDF/B-VI / U 233(G) JENDL3
Barns
Ratio
MeV

Fig.37

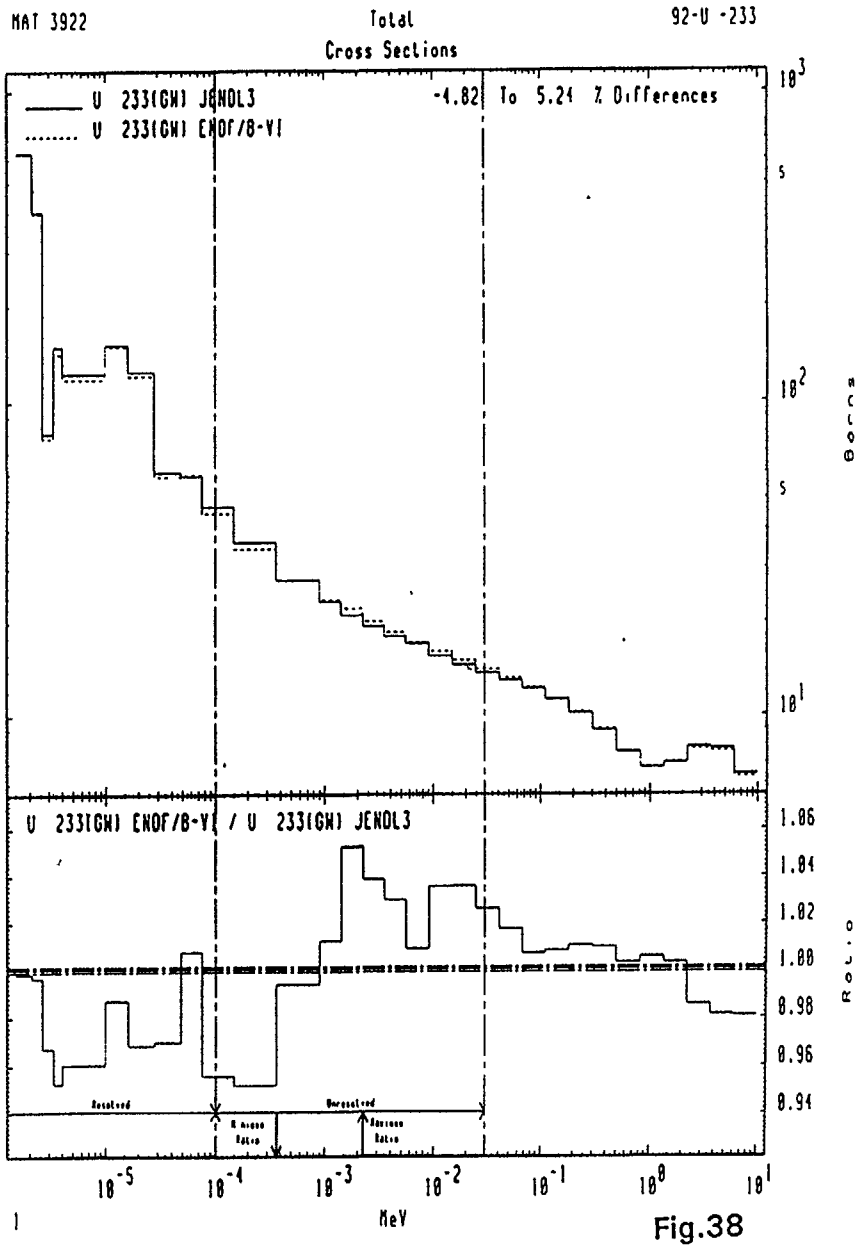
MAT 3922
Total
Cross Sections
92-U -233
U 233(GW) JENDL3
U 233(GW) ENDF/B-VI
-4.82 To 5.24 % Differences
U 233(GW) ENDF/B-VI / U 233(GW) JENDL3
Barns
Ratio
MeV

Fig.38

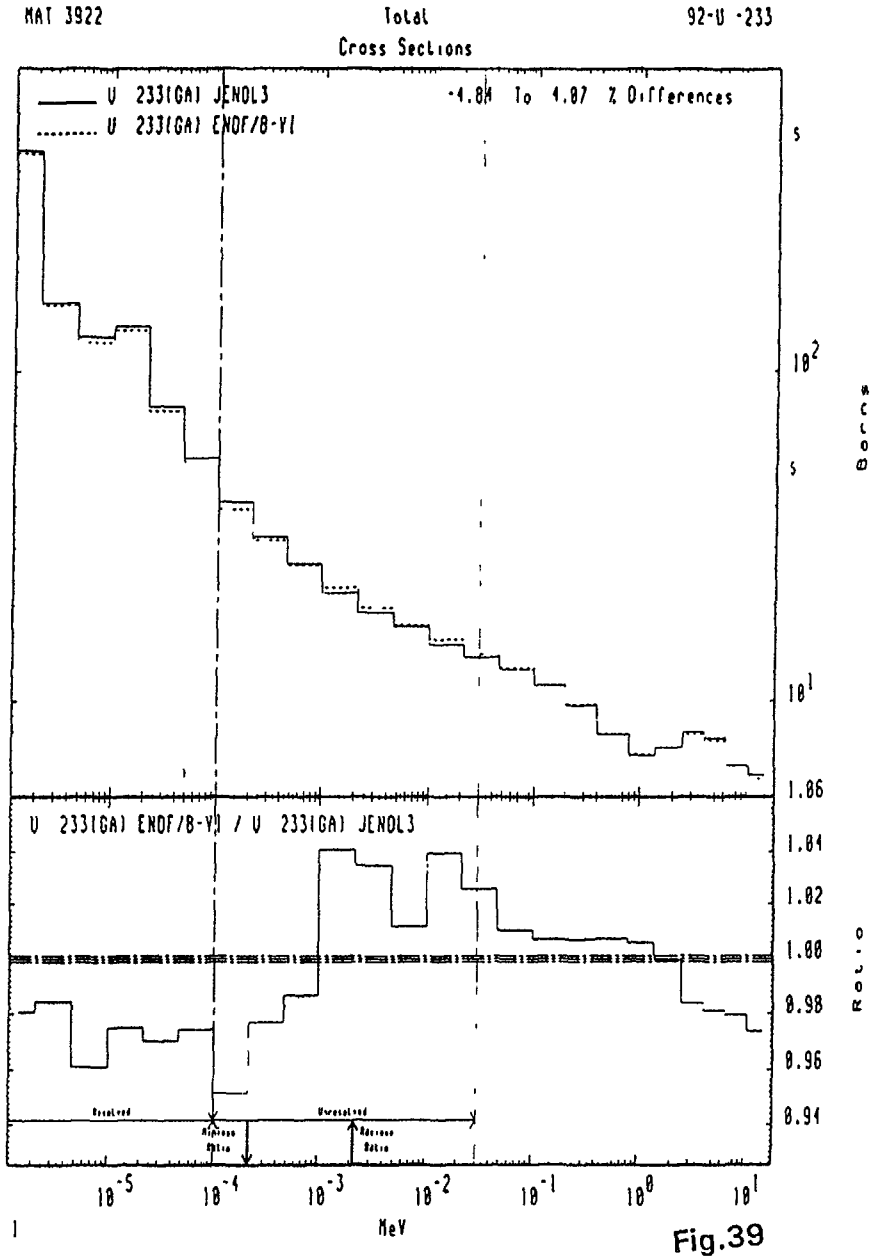
MAT 3922
Total
Cross Sections
92-U -233
U 233(GA) JENDL3
U 233(GA) ENDF/B-VI
-4.84 To 4.87 % Differences
U 233(GA) ENDF/B-VI / U 233(GA) JENDL3
Barns
Ratio
MeV
1

Fig.39

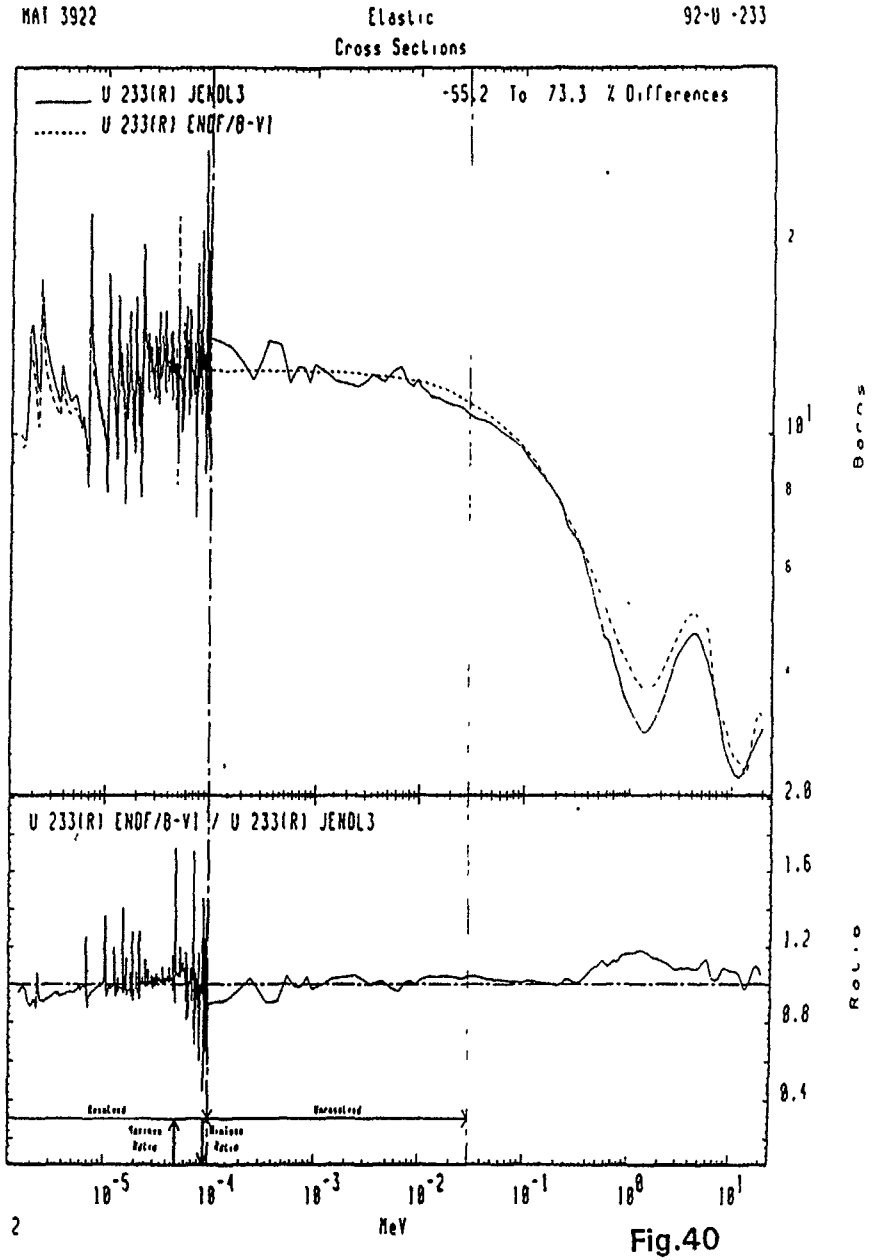
MAT 3922
Elastic
Cross Sections
92-U -233
U 233(R) JENDL3
U 233(R) ENDF/B-VI
-55.2 To 73.3 % Differences
U 233(R) ENDF/B-VI / U 233(R) JENDL3
Barns
Ratio
MeV
2

Fig.40

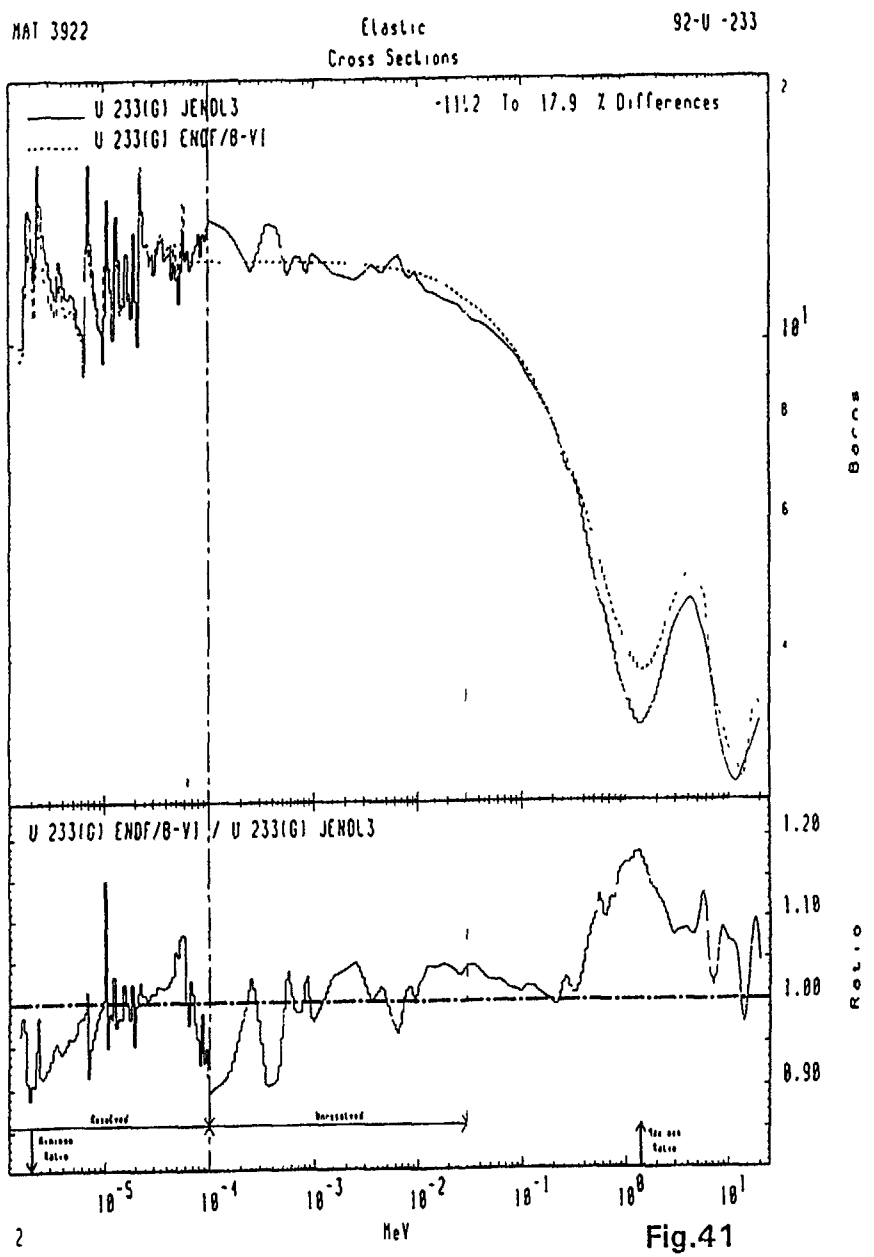
MAT 3922
Elastic
Cross Sections
92-U -233
U 233(G) JENDL3
U 233(G) ENDF/B-VI
-11.2 To 17.9 % Differences
U 233(G) ENDF/B-VI / U 233(G) JENDL3
Barns
Ratio
MeV
Fig.41

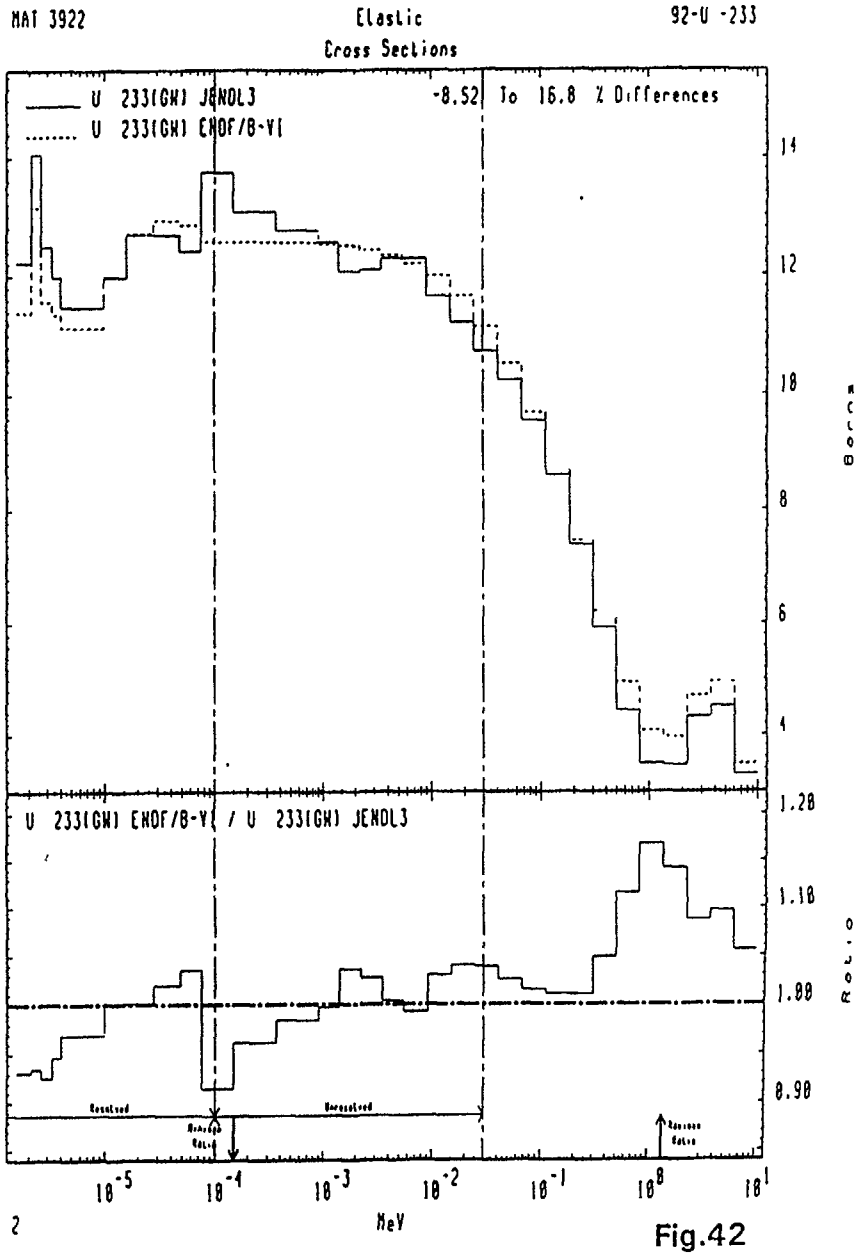
MAT 3922
Elastic
Cross Sections
92-U -233
U 233(GH) JENDL3
U 233(GH) ENDF/B-VI
-8.52 To 16.8 % Differences
U 233(GH) ENDF/B-VI / U 233(GH) JENDL3
Barns
Ratio
MeV
Fig.42

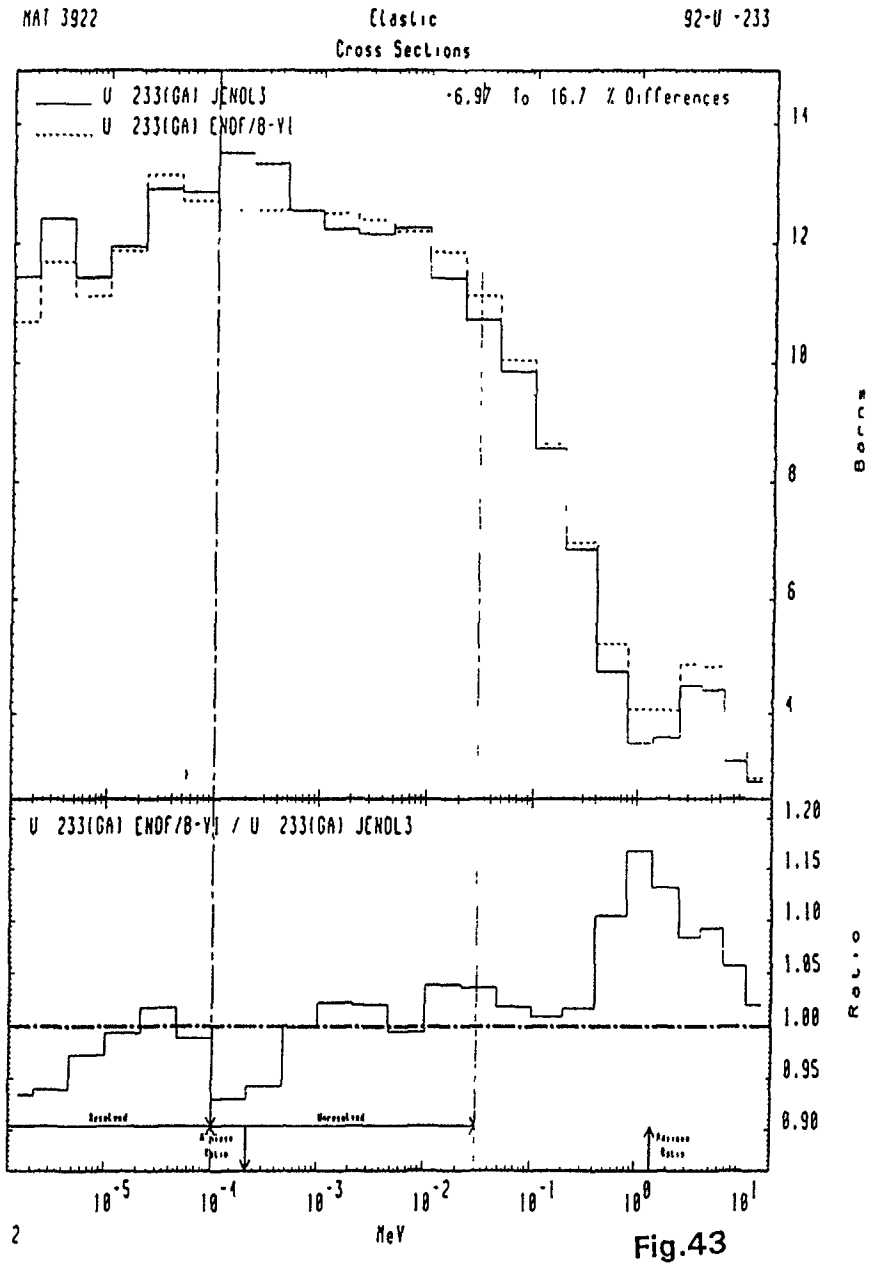
MAT 3922
Elastic
Cross Sections
92-U -233
U 233(GA) JENDL3
U 233(GA) ENDF/B-VI
-6.97 to 16.7 % Differences
Barns
U 233(GA) ENDF/B-VI / U 233(GA) JENDL3
Ratio
MeV

Fig.43

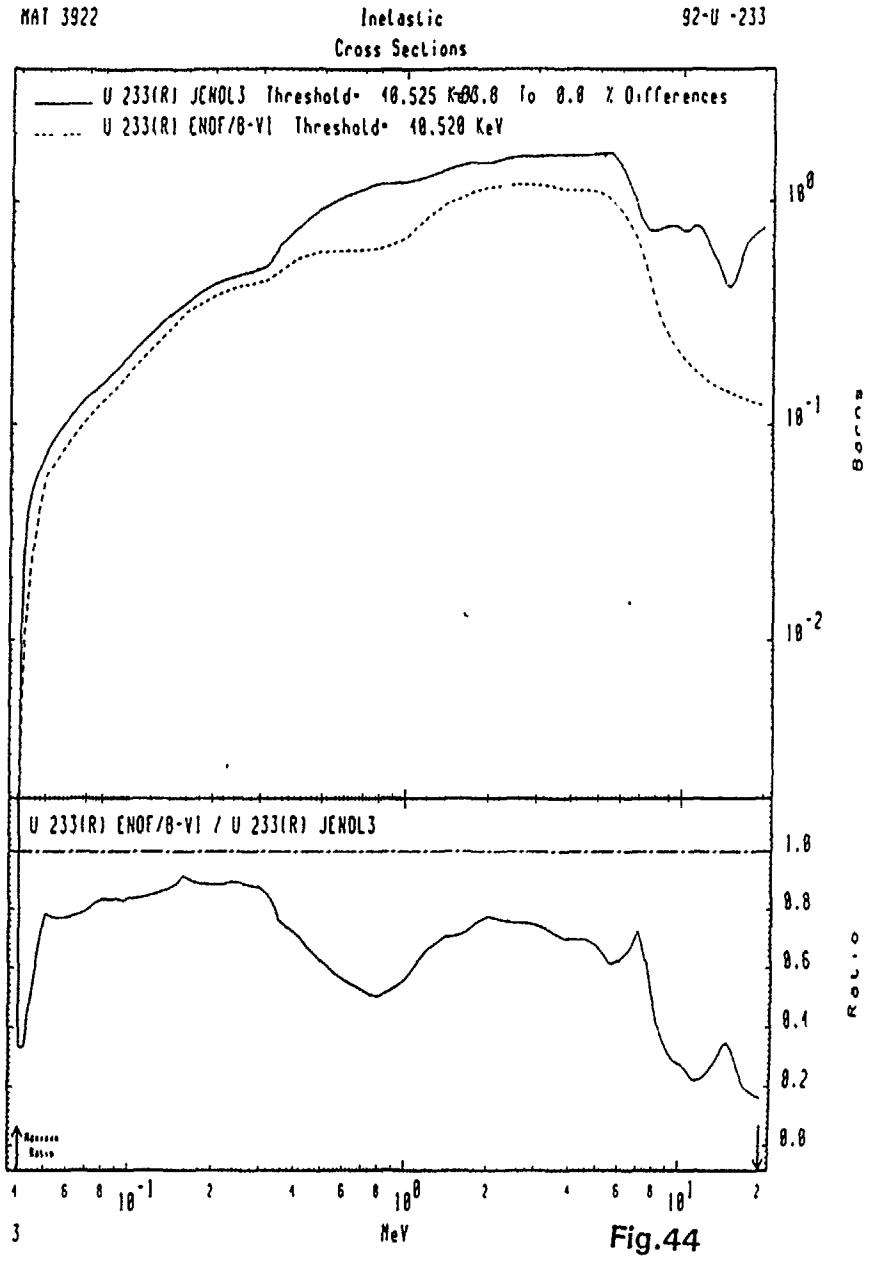
MAT 3922
Inelastic
Cross Sections
92-U -233
U 233(R) JENDL3 Threshold= 40.525 KeV
U 233(R) ENDF/B-VI Threshold= 40.520 KeV
0.0 to 0.0 % Differences
Barns
U 233(R) ENDF/B-VI / U 233(R) JENDL3
Ratio
MeV

Fig.44

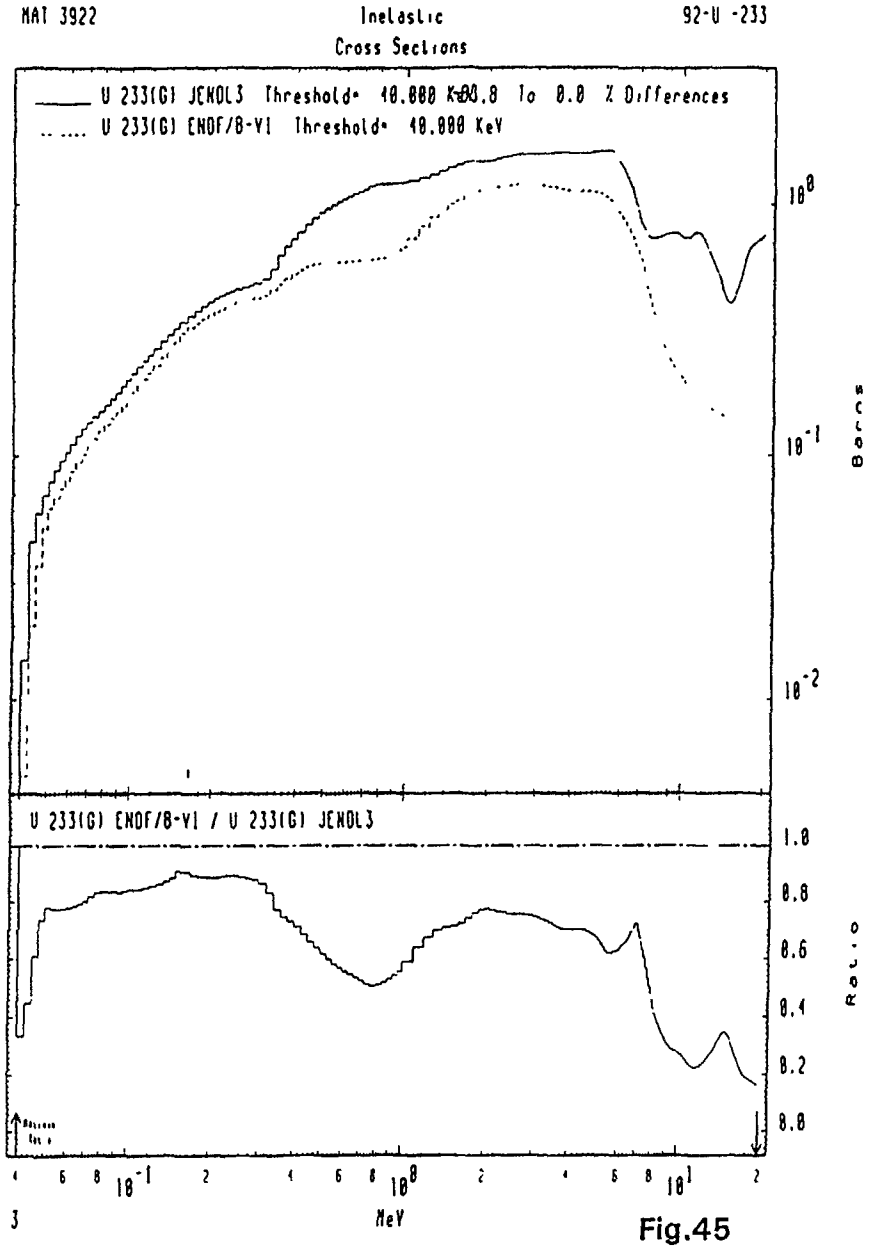
MAT 3922
Inelastic
Cross Sections
92-U -233
U 233(G) JENDL3 Threshold= 40.000 KeV to 0.0 % Differences
U 233(G) ENDF/B-VI Threshold= 40.000 KeV
U 233(G) ENDF/B-VI / U 233(G) JENDL3
Barns
Ratio
MeV

Fig.45

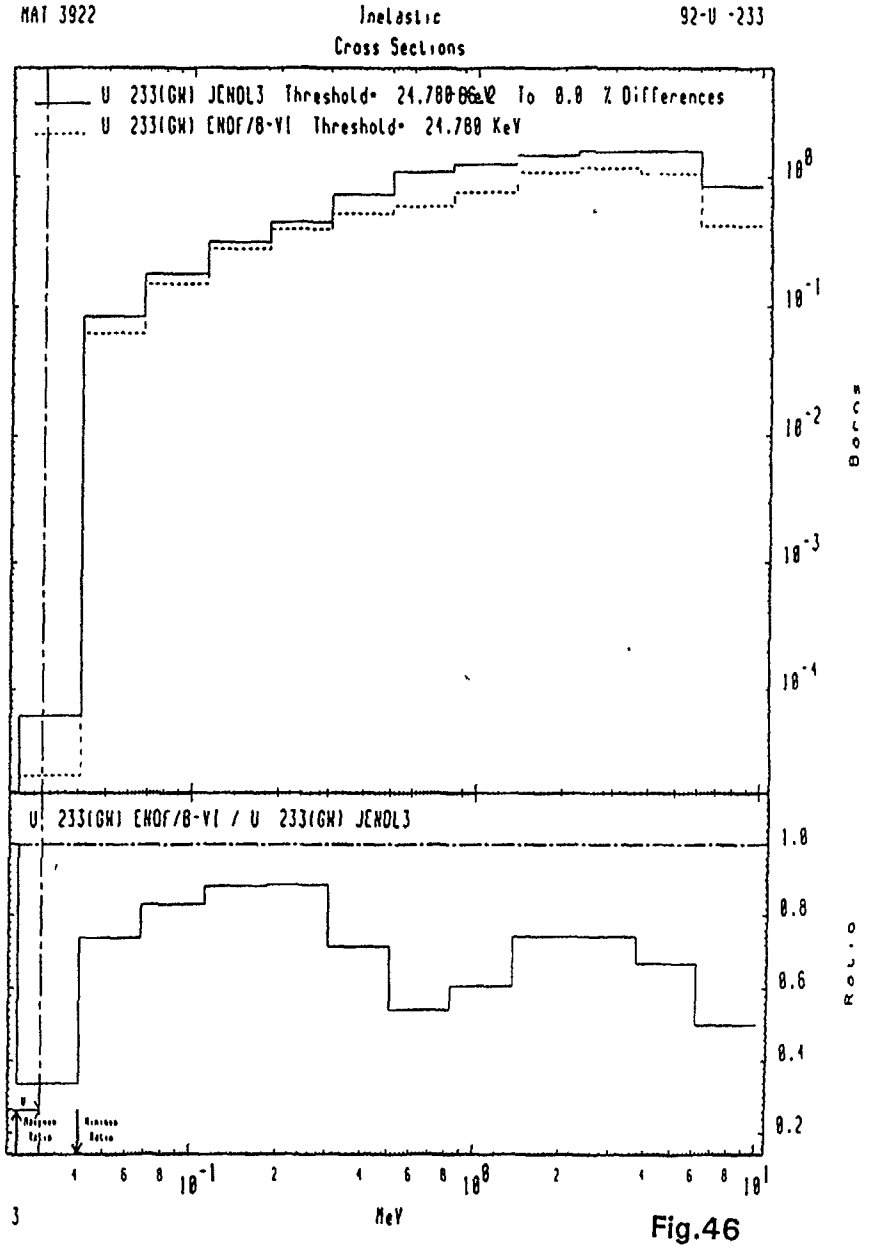
MAT 3922
Inelastic
Cross Sections
92-U -233
U 233(GW) JENDL3 Threshold= 24.780 KeV to 0.0 % Differences
U 233(GW) ENDF/B-VI Threshold= 24.780 KeV
U 233(GW) ENDF/B-VI / U 233(GW) JENDL3
Barns
Ratio
MeV

Fig.46

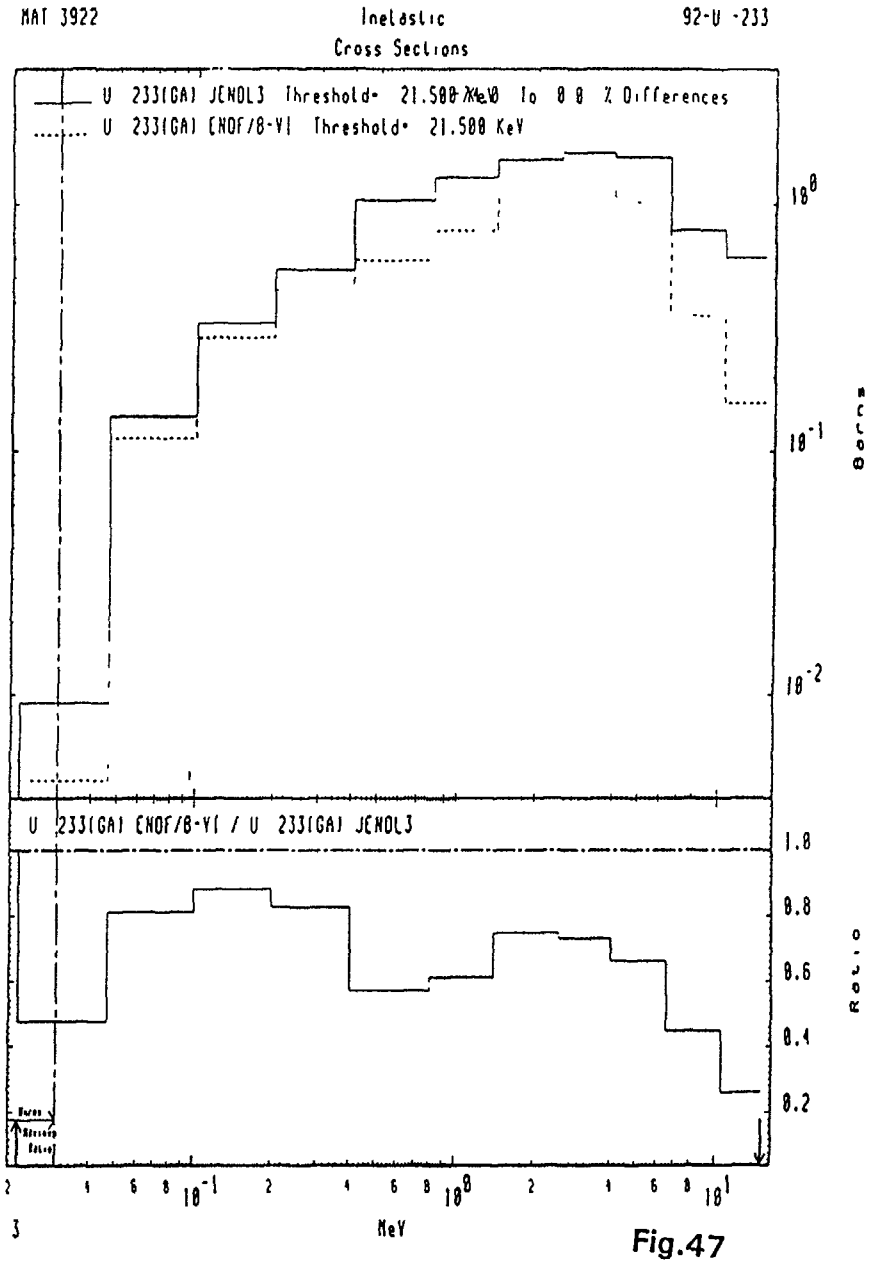
MAT 3922
Inelastic
Cross Sections
92-U -233
U 233(GA) JENDL3 Threshold= 21.500 KeV To 0.0 % Differences
U 233(GA) ENDF/B-VI Threshold= 21.500 KeV
Barns
U 233(GA) ENDF/B-VI / U 233(GA) JENDL3
Ratio
MeV

Fig.47

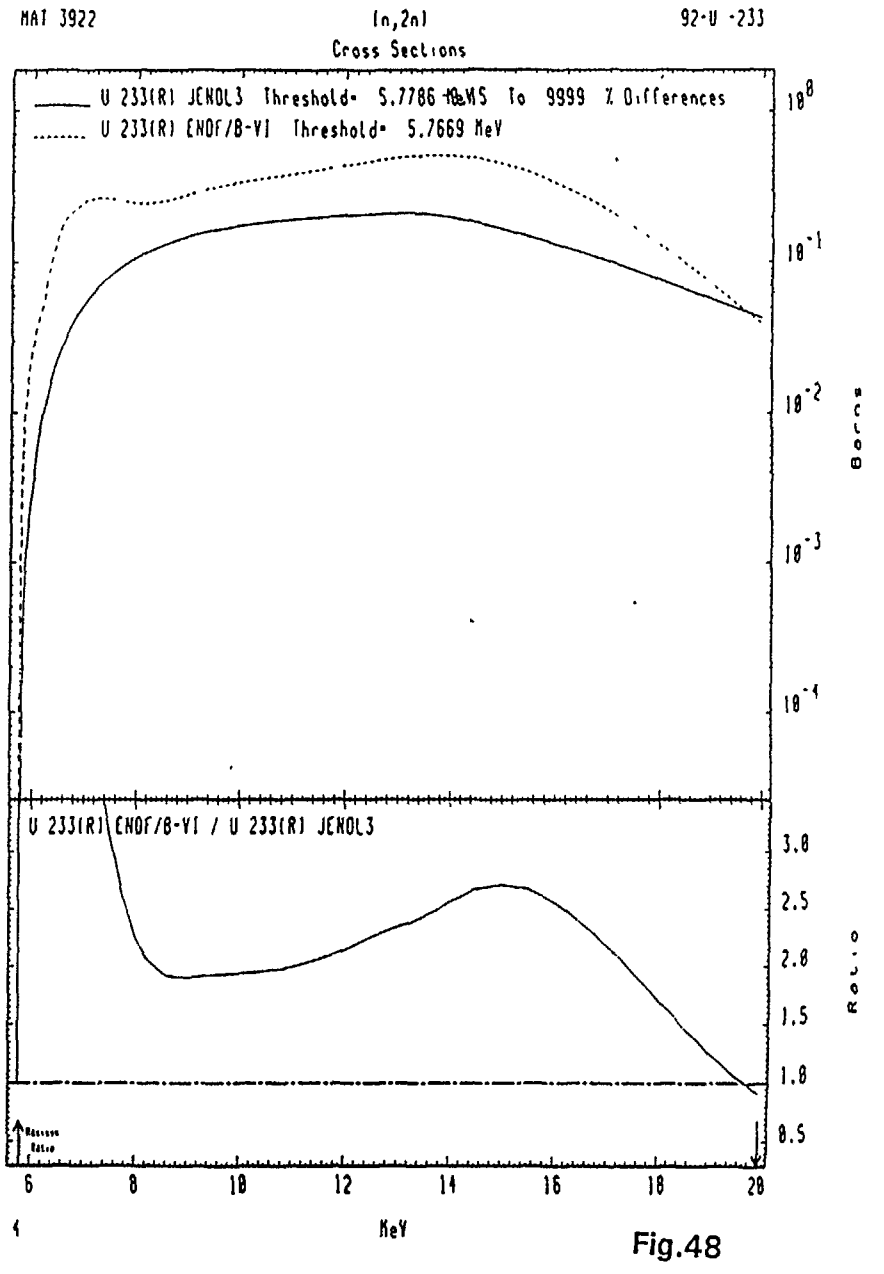
MAT 3922
(n,2n)
Cross Sections
92-U -233
U 233(R) JENDL3 Threshold= 5.7786 MeV To 9999 % Differences
U 233(R) ENDF/B-VI Threshold= 5.7669 MeV
Barns
U 233(R) ENDF/B-VI / U 233(R) JENDL3
Ratio
MeV

Fig.48

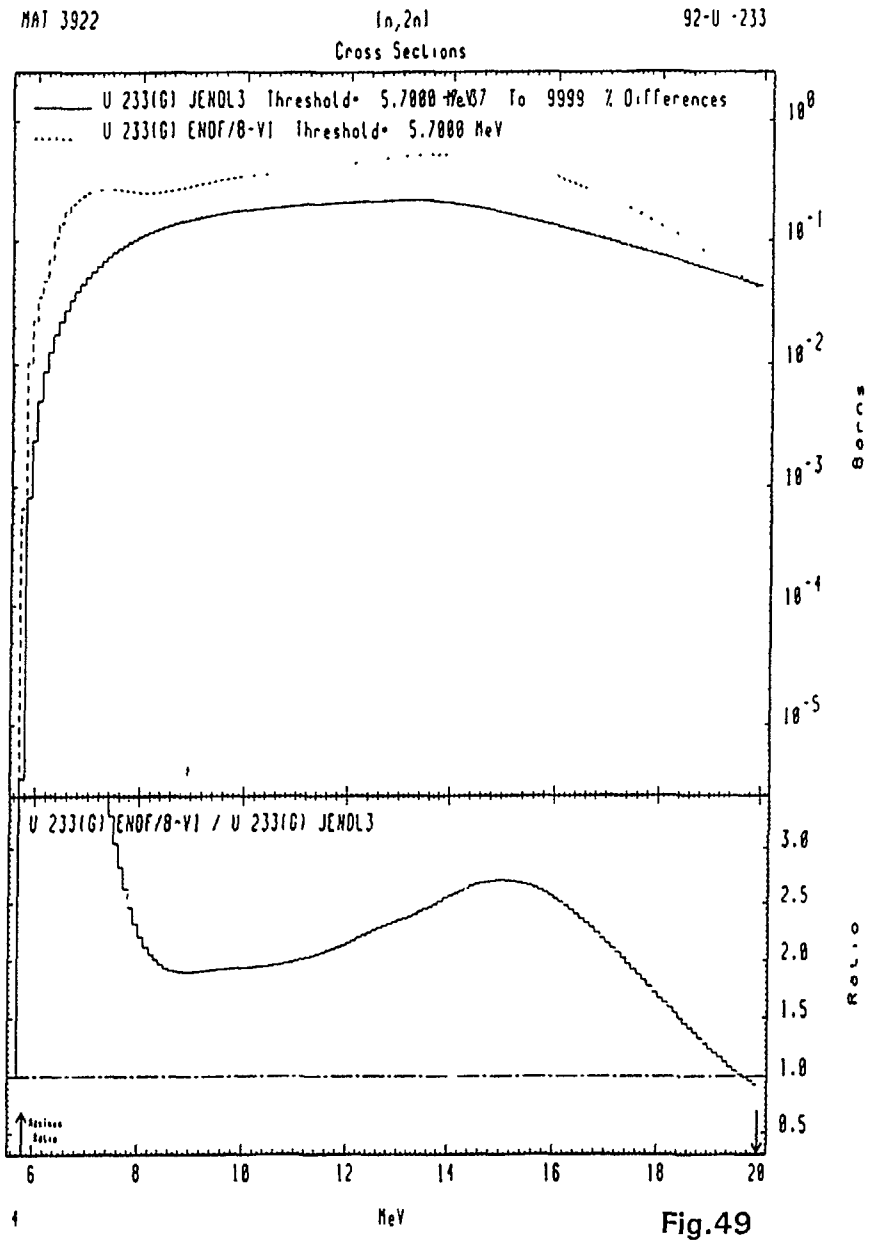
MAT 3922
(n,2n)
92-U -233
Cross Sections
U 233(G) JENDL3 Threshold= 5.7000 MeV To 9999 % Differences
U 233(G) ENDF/B-VI Threshold= 5.7000 MeV
Barns
U 233(G) ENDF/B-VI / U 233(G) JENDL3
Ratio
MeV

Fig.49

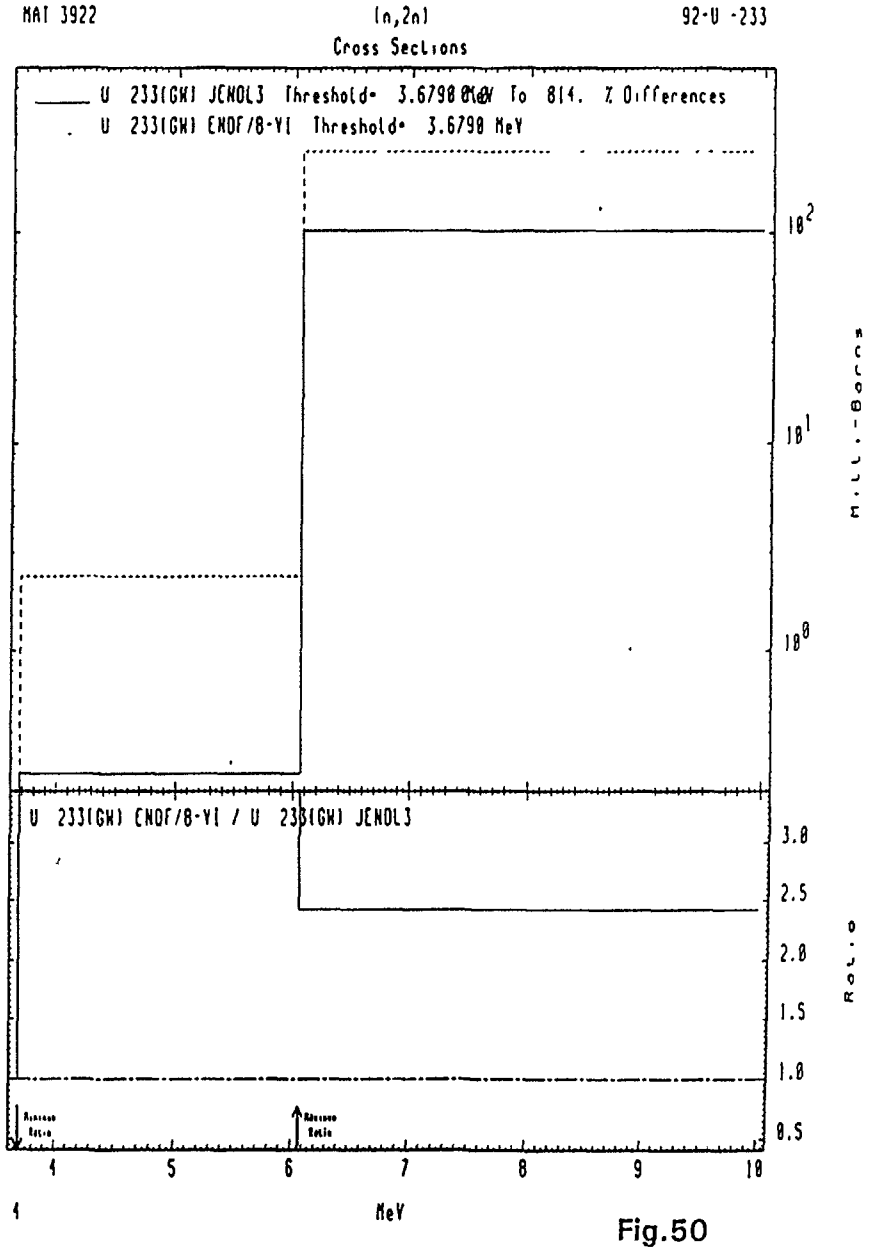
MAT 3922
(n,2n)
92-U -233
Cross Sections
U 233(GW) JENDL3 Threshold= 3.6790 MeV To 814. % Differences
U 233(GW) ENDF/B-VI Threshold= 3.6790 MeV
Milli-Barns
U 233(GW) ENDF/B-VI / U 233(GW) JENDL3
Ratio
MeV

Fig.50

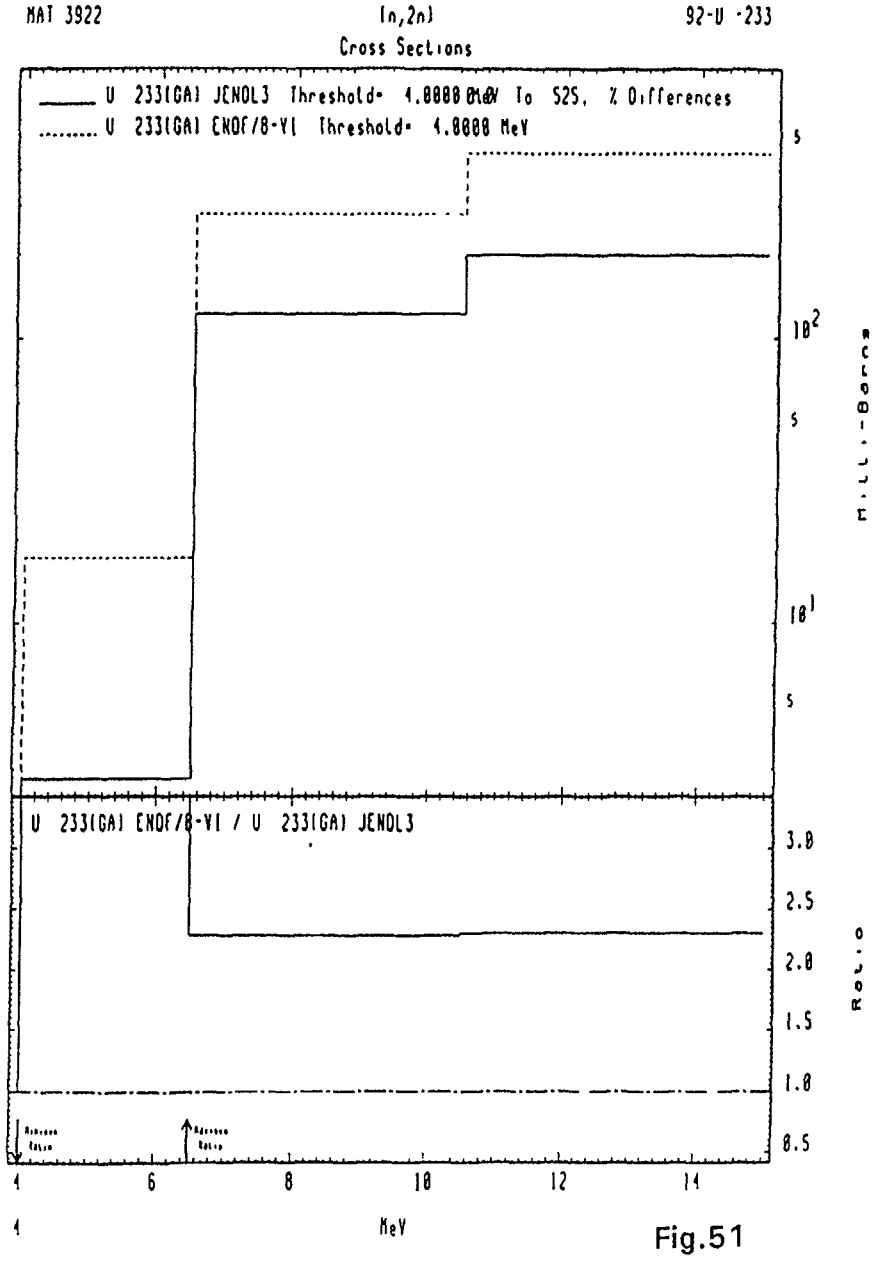
MAT 3922
(n,2n)
92-U -233
Cross Sections
U 233(GA) JENDL3 Threshold= 4.0000 MeV To 525. % Differences
U 233(GA) ENDF/B-VI Threshold= 4.0000 MeV
U 233(GA) ENDF/B-VI / U 233(GA) JENDL3
Milli-Barns
Ratio
MeV

Fig.51

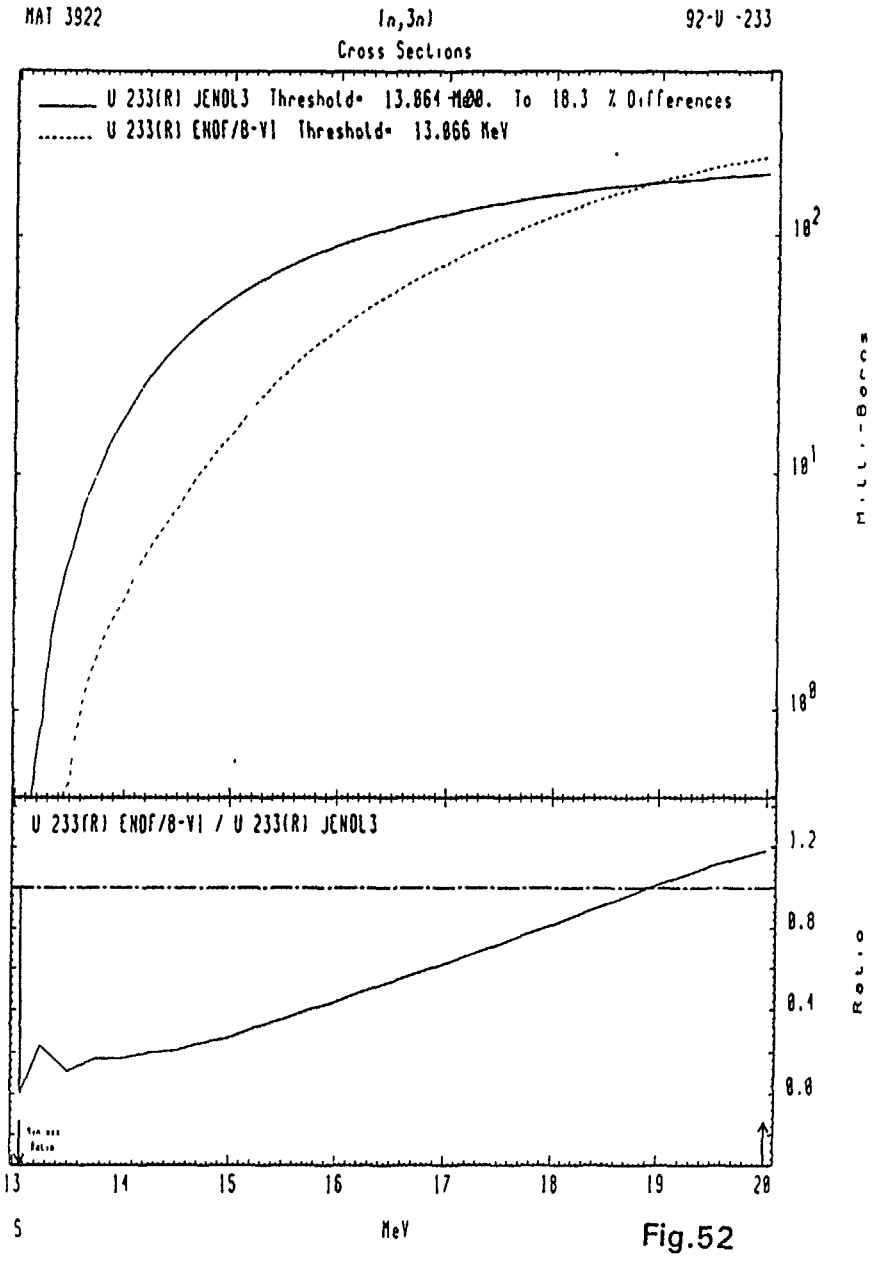
MAT 3922
(n,3n)
92-U -233
Cross Sections
U 233(R) JENDL3 Threshold= 13.864 MeV To 18.3 % Differences
U 233(R) ENDF/B-VI Threshold= 13.866 MeV
U 233(R) ENDF/B-VI / U 233(R) JENDL3
Milli-Barns
Ratio
MeV

Fig.52

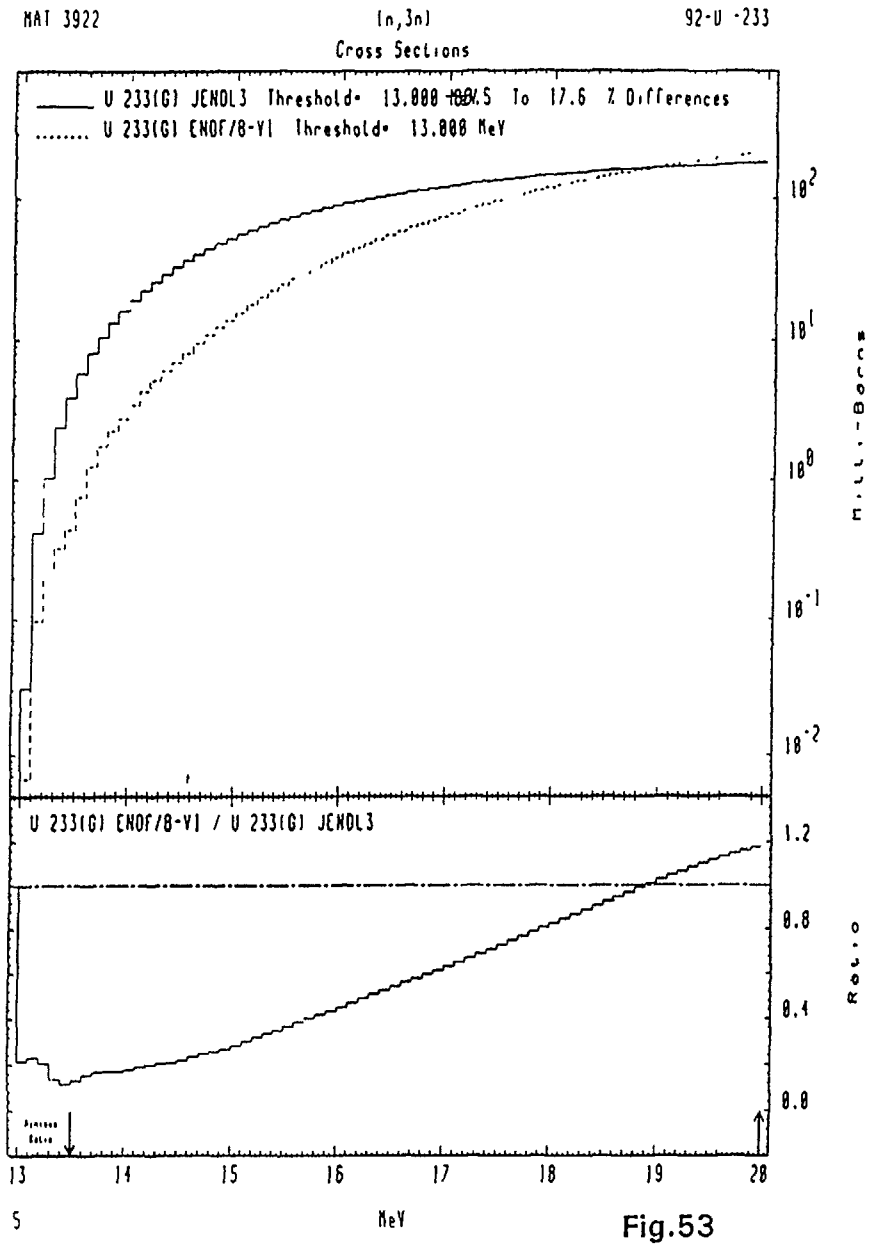
MAT 3922
(n,3n)
92-U -233
Cross Sections
U 233(G) JENDL3 Threshold= 13.000 MeV To 17.6 % Differences
U 233(G) ENDF/B-VI Threshold= 13.000 MeV
U 233(G) ENDF/B-VI / U 233(G) JENDL3
Millibarns
Ratio
MeV

Fig.53

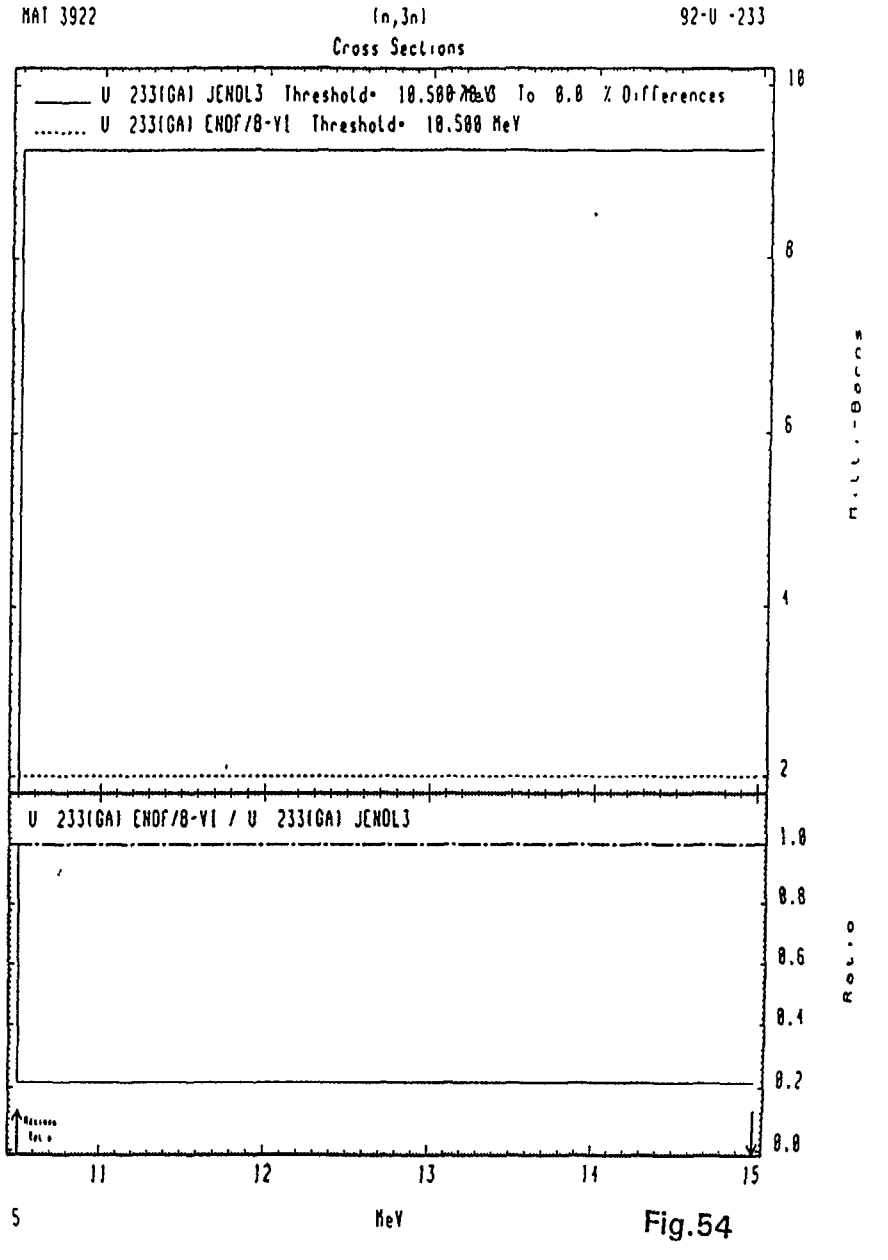
MAT 3922
(n,3n)
92-U -233
Cross Sections
U 233(GA) JENDL3 Threshold= 10.500 MeV To 0.0 % Differences
U 233(GA) ENDF/B-VI Threshold= 10.500 MeV
U 233(GA) ENDF/B-VI / U 233(GA) JENDL3
Millibarns
Ratio
MeV

Fig.54

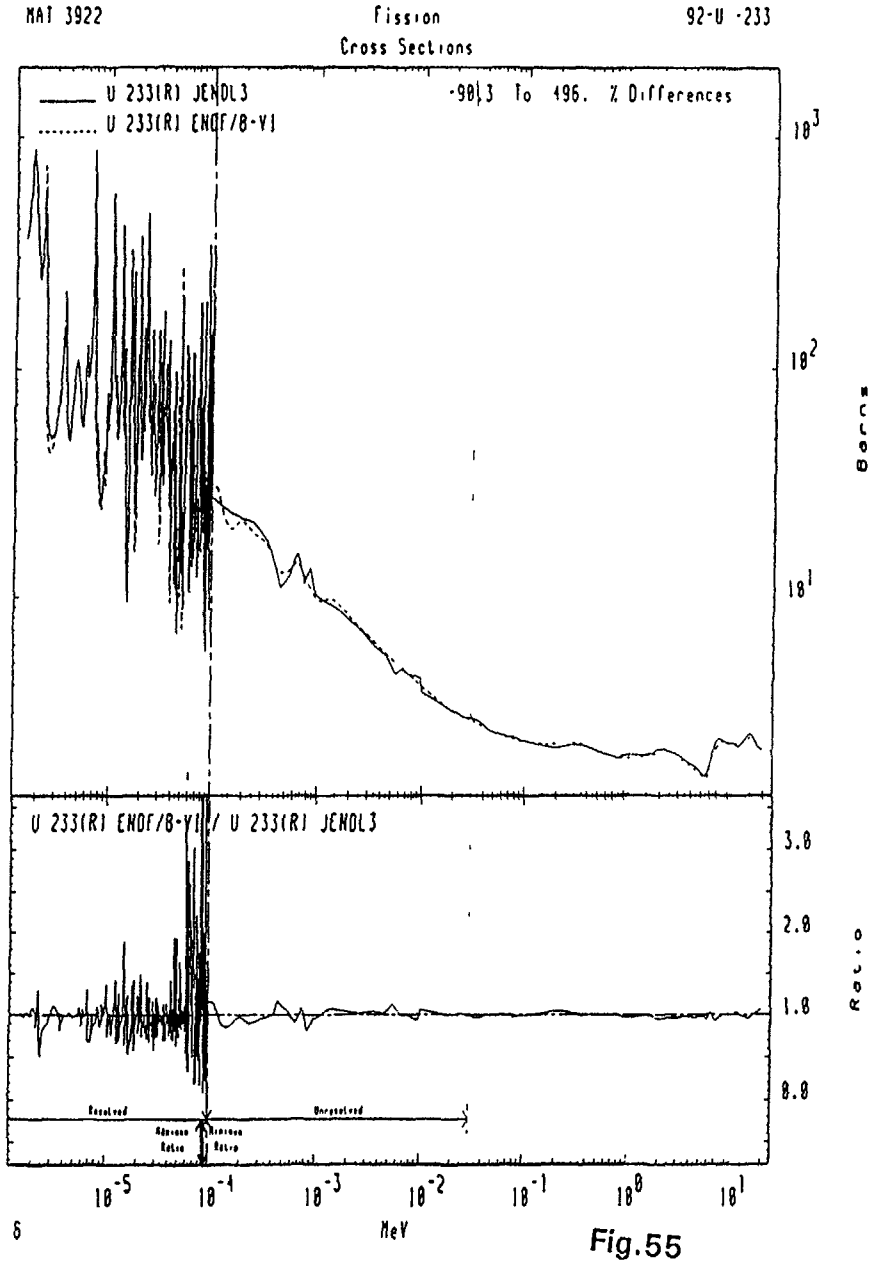
MAT 3922
Fission
Cross Sections
92-U -233
U 233(R) JENDL3
U 233(R) ENDF/B-VI
-98.3 To 496. % Differences
Barns
U 233(R) ENDF/B-VI / U 233(R) JENDL3
Ratio
Resolved
Unresolved
MeV

Fig.55

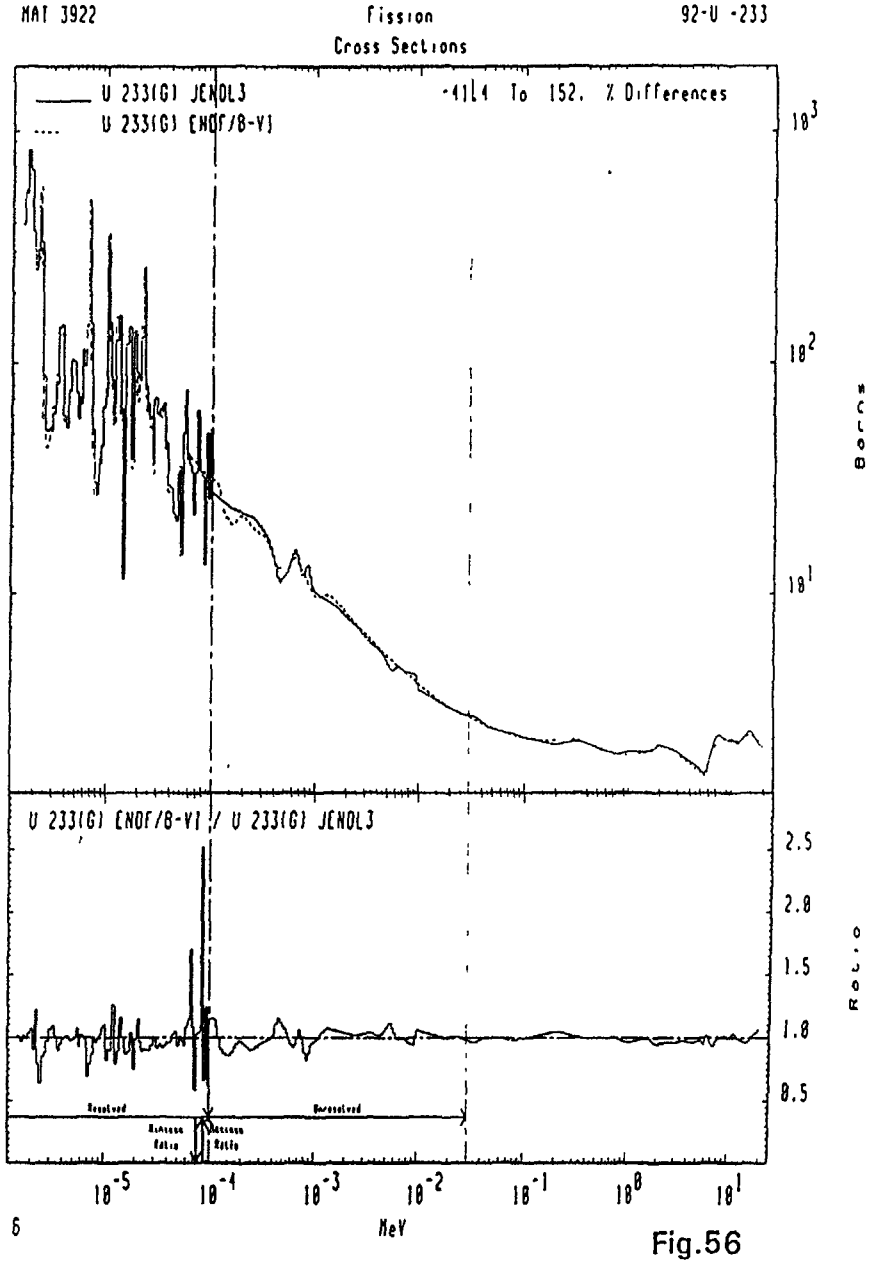
MAT 3922
Fission
Cross Sections
92-U -233
U 233(G) JENDL3
U 233(G) ENDF/B-VI
-41.4 To 152. % Differences
Barns
U 233(G) ENDF/B-VI / U 233(G) JENDL3
Ratio
Resolved
Unresolved
MeV

Fig.56

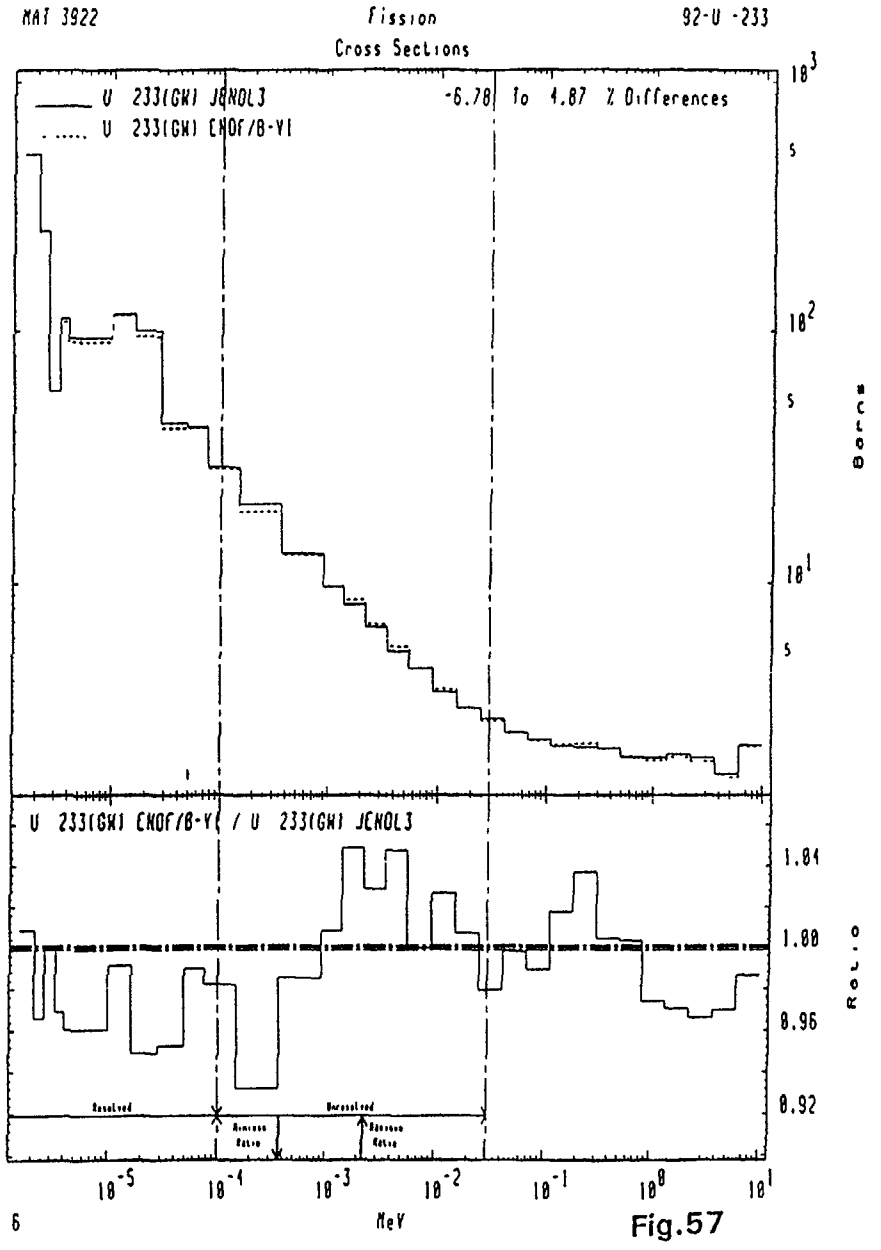
MAT 3922
Fission
Cross Sections
92-U -233
U 233(GW) JENDL3
U 233(GW) ENDF/B-VI
-6.78 To 4.87 % Differences
U 233(GW) ENDF/B-VI / U 233(GW) JENDL3
Barns
Ratio
Resolved
Unresolved
MeV

Fig.57

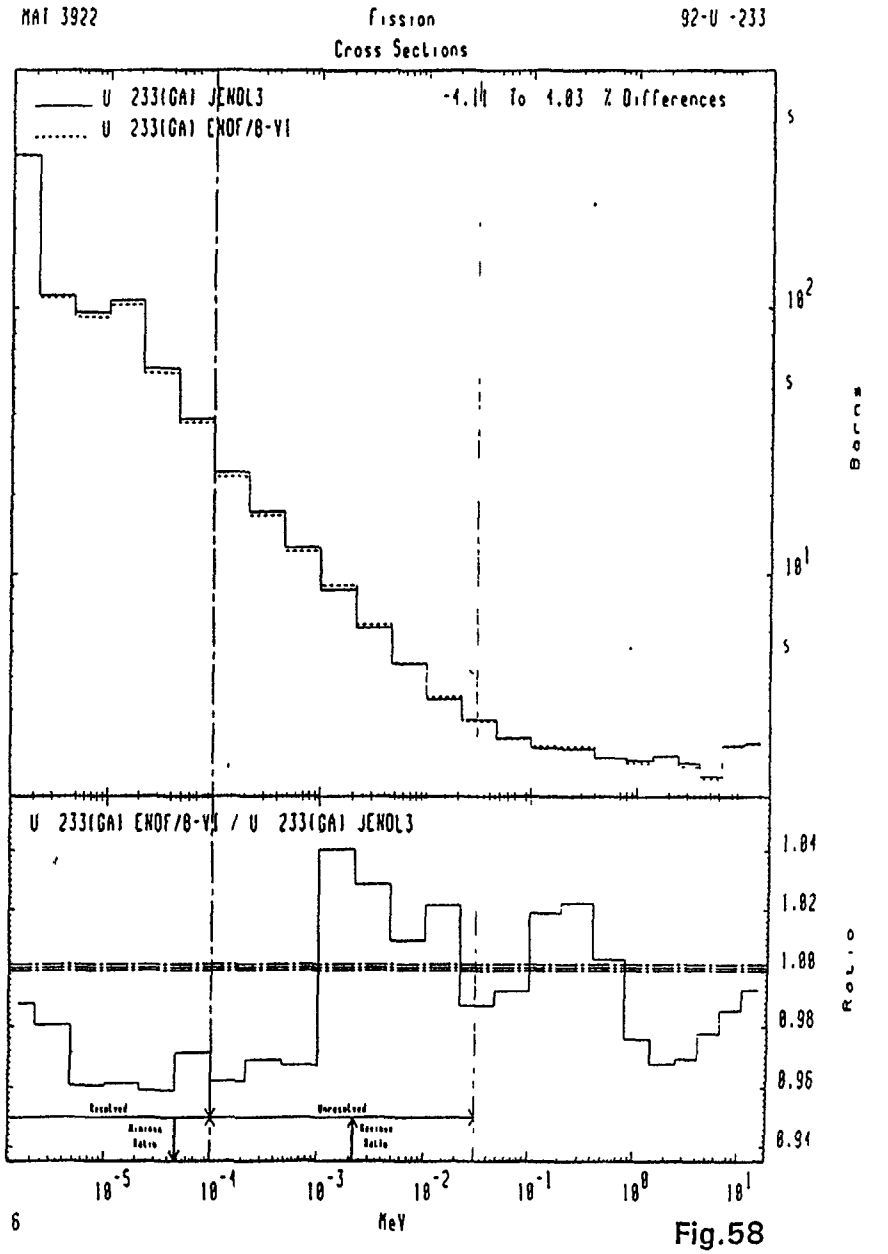
MAT 3922
Fission
Cross Sections
92-U -233
U 233(GA) JENDL3
U 233(GA) ENDF/B-VI
-4.14 To 4.83 % Differences
U 233(GA) ENDF/B-VI / U 233(GA) JENDL3
Barns
Ratio
Resolved
Unresolved
MeV

Fig.58

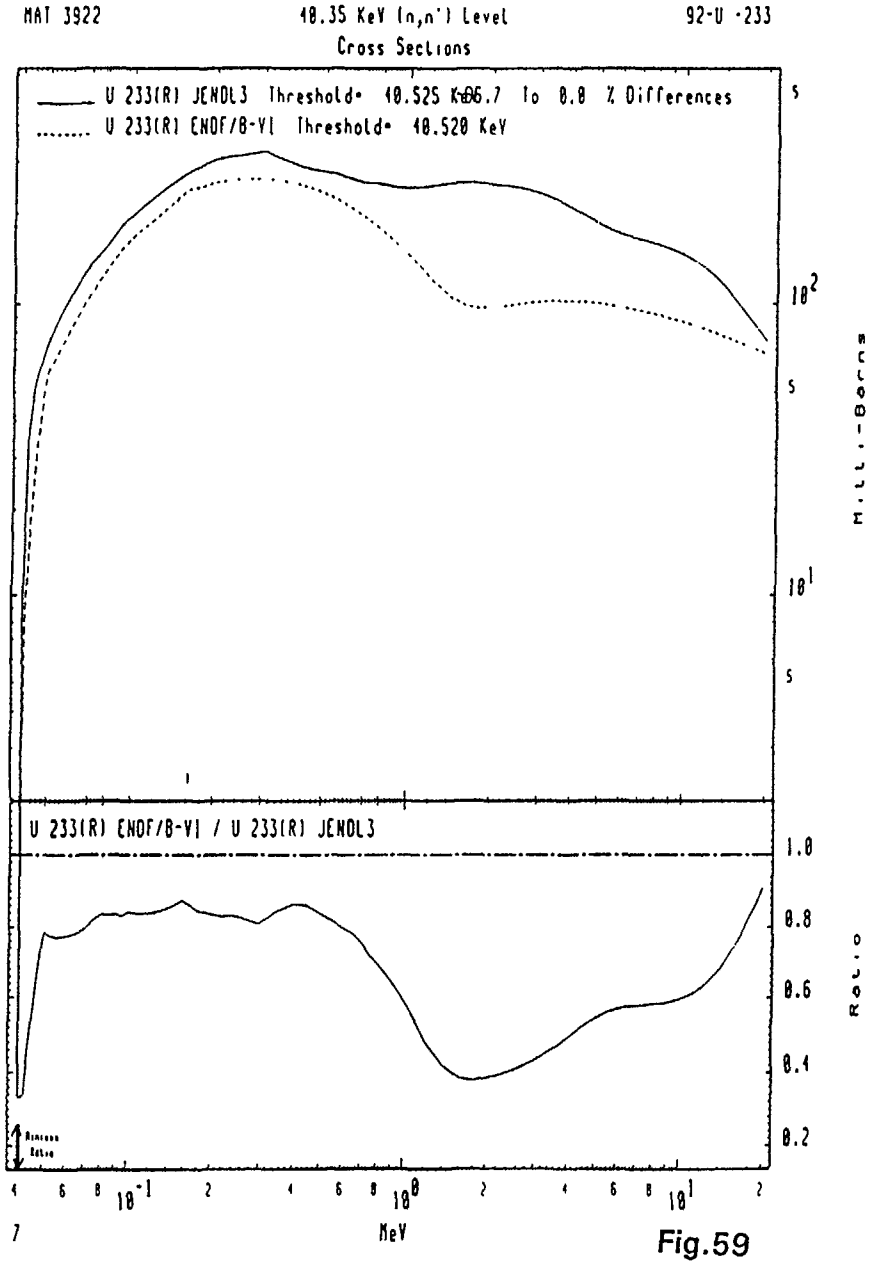
MAT 3922
10.35 KeV (n,n') Level
92-U -233
Cross Sections
U 233(R) JENDL3 Threshold= 10.525 KeV 6.7 To 0.0 % Differences
U 233(R) ENDF/B-VI Threshold= 10.520 KeV
M.L.-Barns
U 233(R) ENDF/B-VI / U 233(R) JENDL3
Ratio
MeV

Fig.59

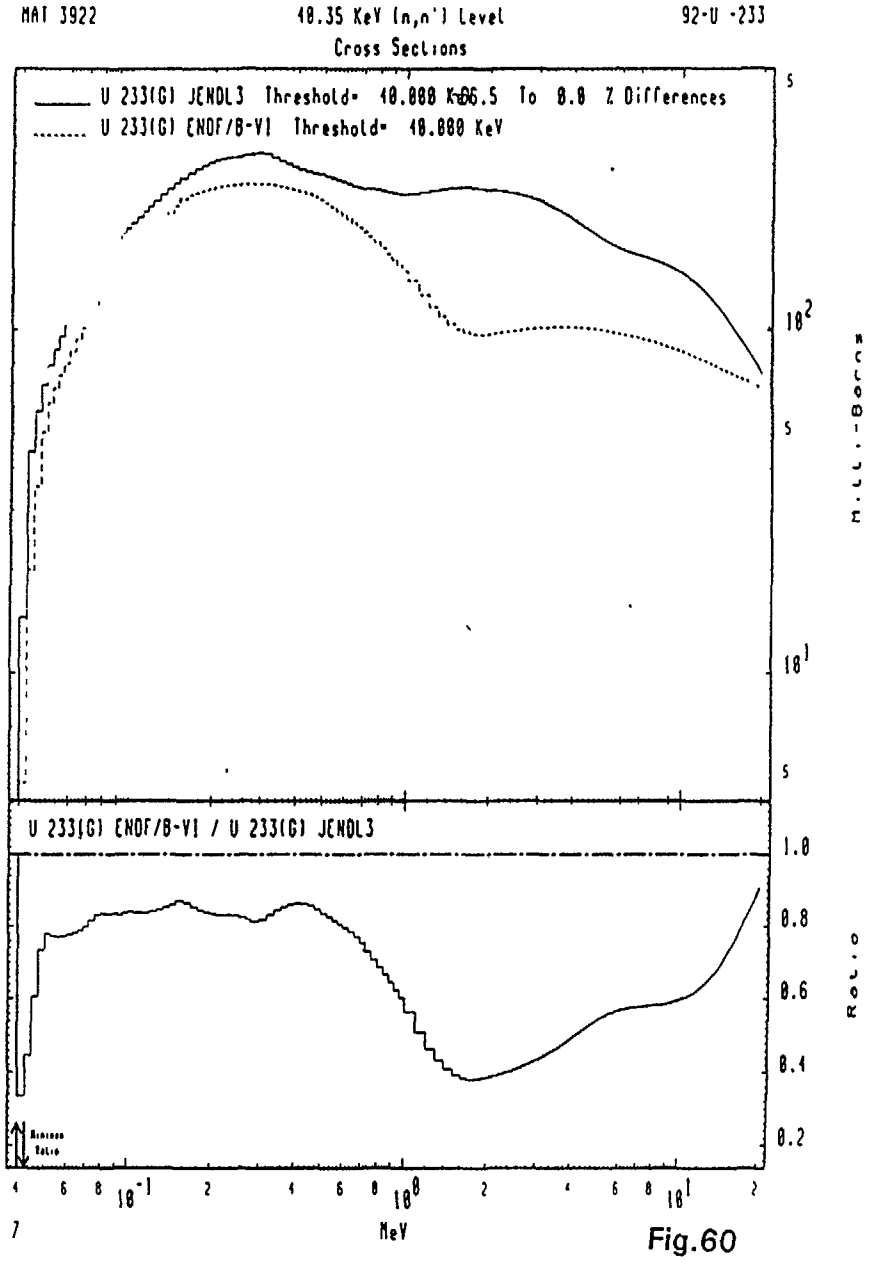
MAT 3922
10.35 KeV (n,n') Level
92-U -233
Cross Sections
U 233(G) JENDL3 Threshold= 10.000 KeV 6.5 To 0.0 % Differences
U 233(G) ENDF/B-VI Threshold= 10.000 KeV
M.L.-Barns
U 233(G) ENDF/B-VI / U 233(G) JENDL3
Ratio
MeV

Fig.60

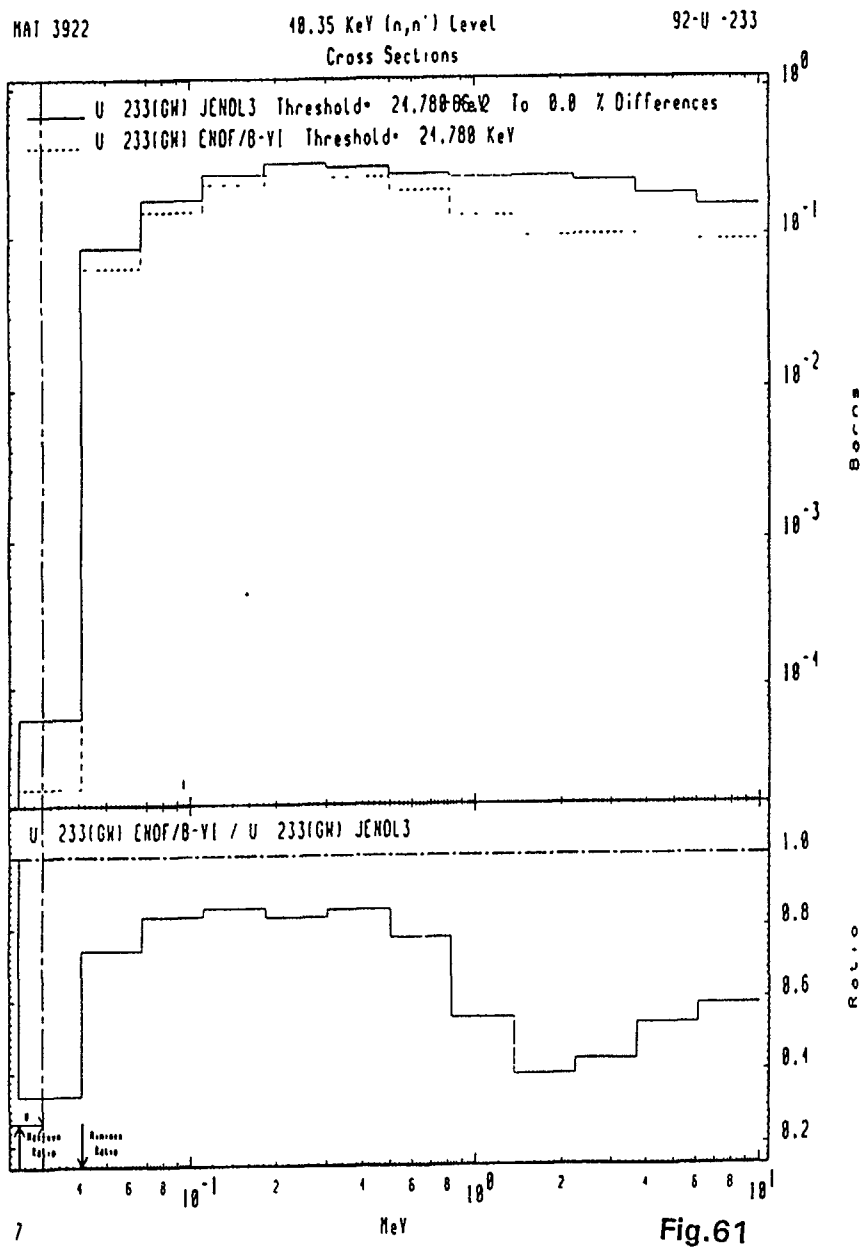
MAT 3922
48.35 KeV (n,n') Level
Cross Sections
92-U -233
U 233(GW) JENDL3 Threshold= 24.788 KeV To 0.0 % Differences
U 233(GW) ENDF/B-VI Threshold= 24.788 KeV
Barns
U 233(GW) ENDF/B-VI / U 233(GW) JENDL3
Ratio
MeV

Fig.61

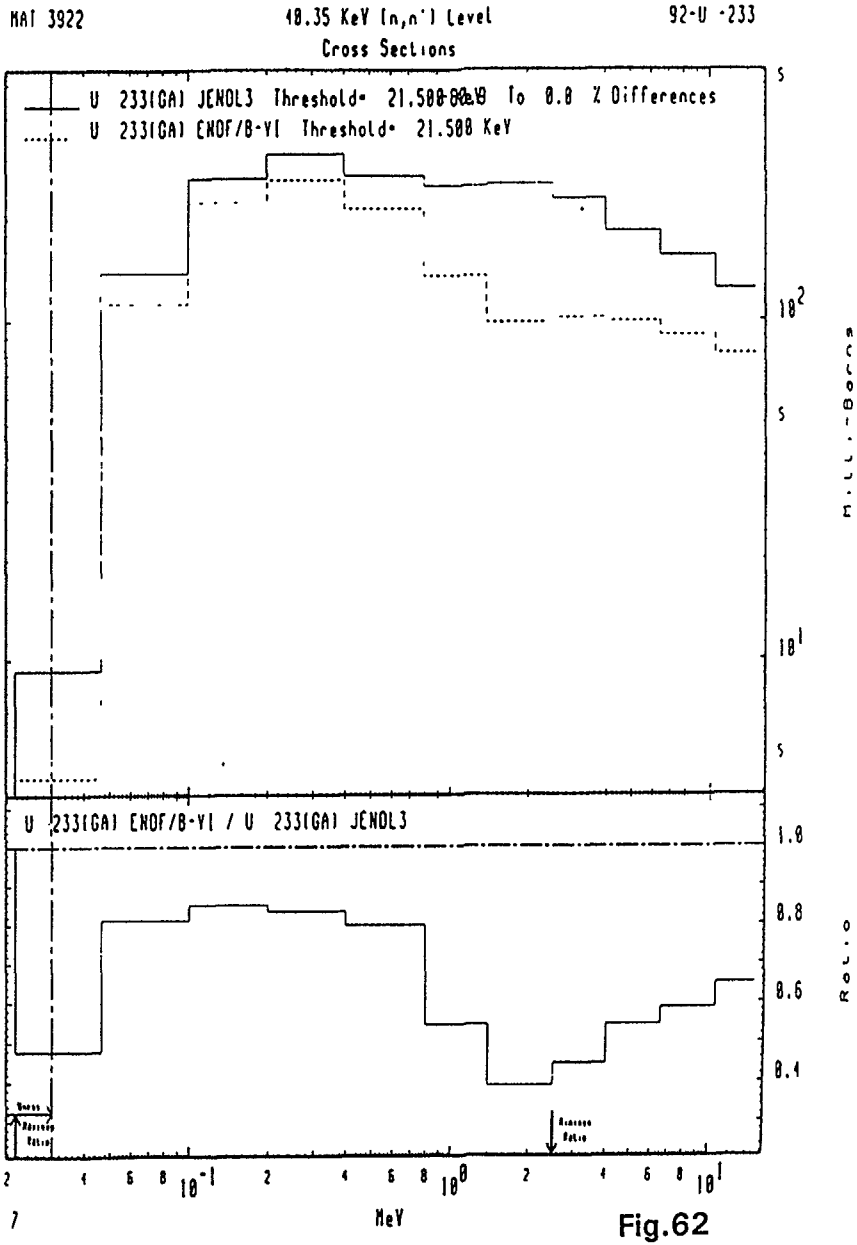
MAT 3922
48.35 KeV (n,n') Level
Cross Sections
92-U -233
U 233(GA) JENDL3 Threshold= 21.500 KeV To 0.0 % Differences
U 233(GA) ENDF/B-VI Threshold= 21.500 KeV
Milli-Barns
U 233(GA) ENDF/B-VI / U 233(GA) JENDL3
Ratio
MeV

Fig.62

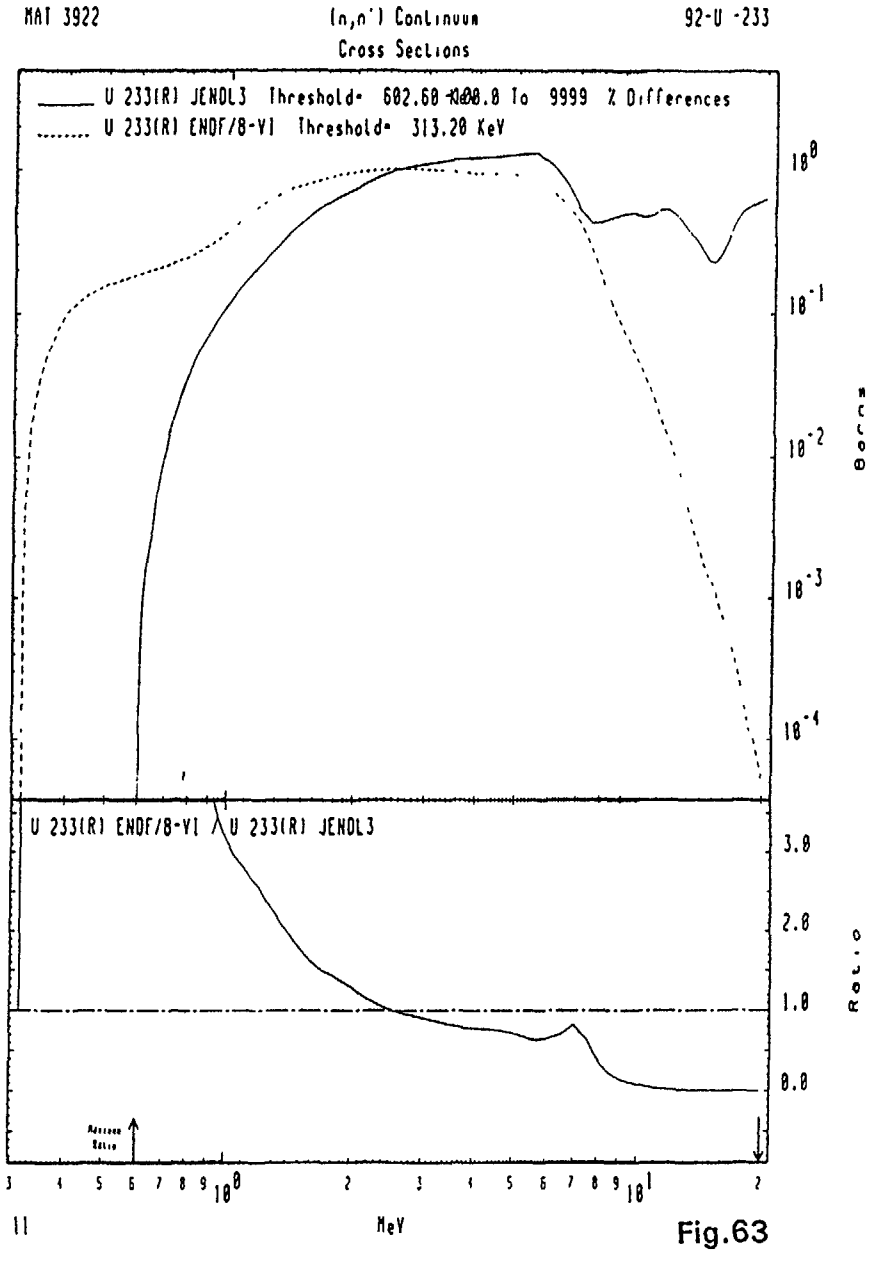
MAT 3922
(n,n') Continuum
Cross Sections
92-U -233
U 233(R) JENDL3 Threshold= 602.60 to 9999 % Differences
U 233(R) ENDF/B-VI Threshold= 313.20 KeV
Barns
U 233(R) ENDF/B-VI / U 233(R) JENDL3
Ratio
MeV

Fig.63

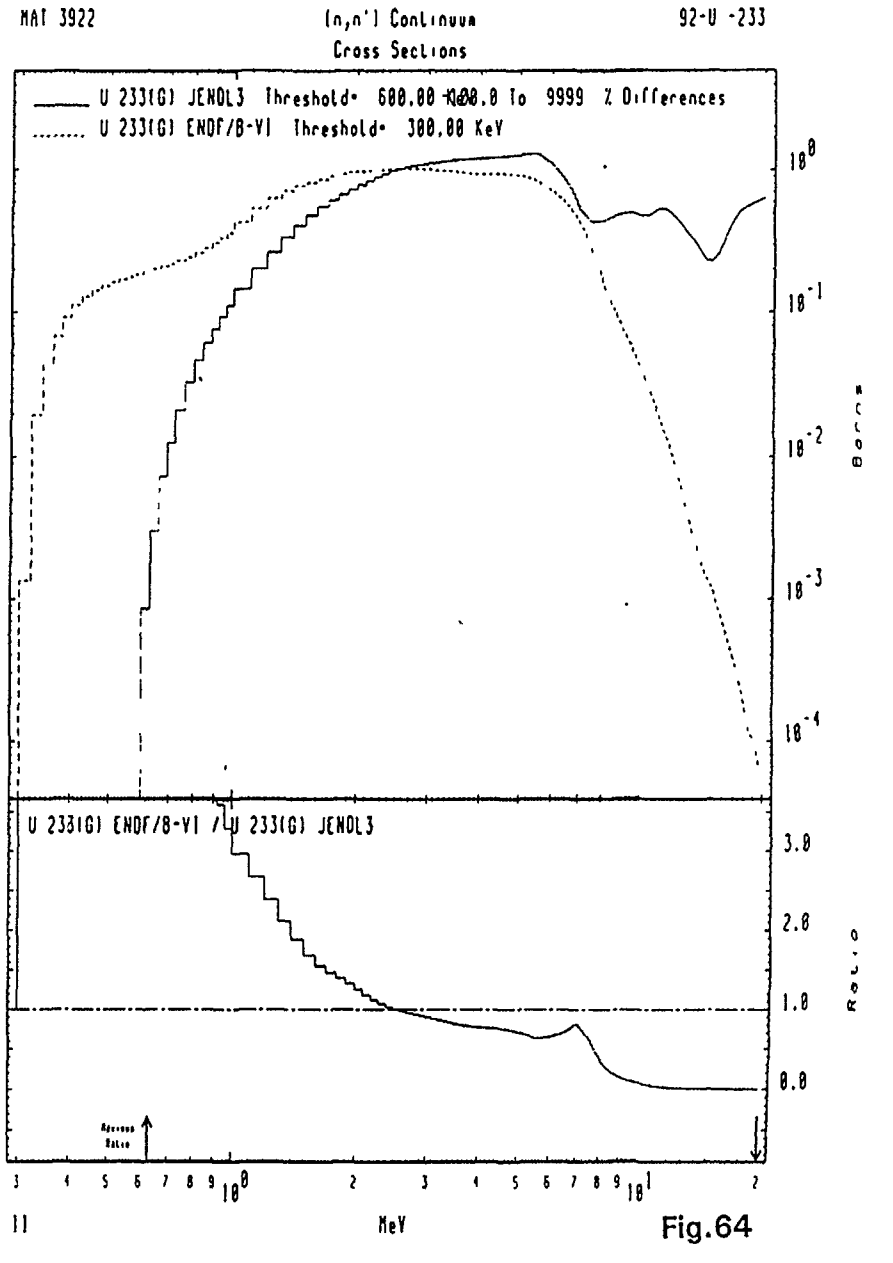
MAT 3922
(n,n') Continuum
Cross Sections
92-U -233
U 233(G) JENDL3 Threshold= 600.00 to 9999 % Differences
U 233(G) ENDF/B-VI Threshold= 300.00 KeV
Barns
U 233(G) ENDF/B-VI / U 233(G) JENDL3
Ratio
MeV

Fig.64

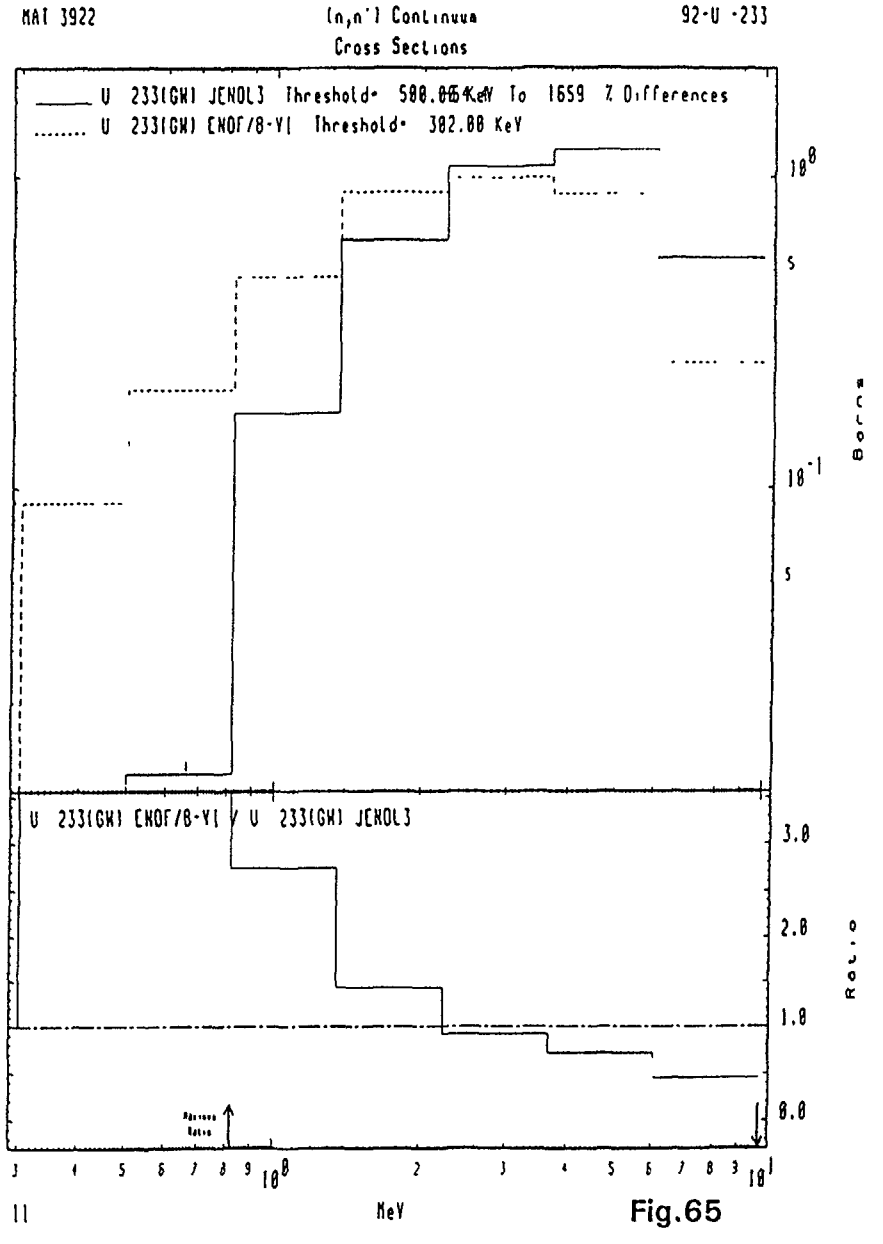
MAT 3922
(n,n') Continuum
Cross Sections
92-U -233
U 233(GW) JENDL3 Threshold= 500.00 KeV To 1659 % Differences
U 233(GW) ENDF/B-VI Threshold= 382.00 KeV
Barns
U 233(GW) ENDF/B-VI / U 233(GW) JENDL3
Ratio
MeV

Fig.65

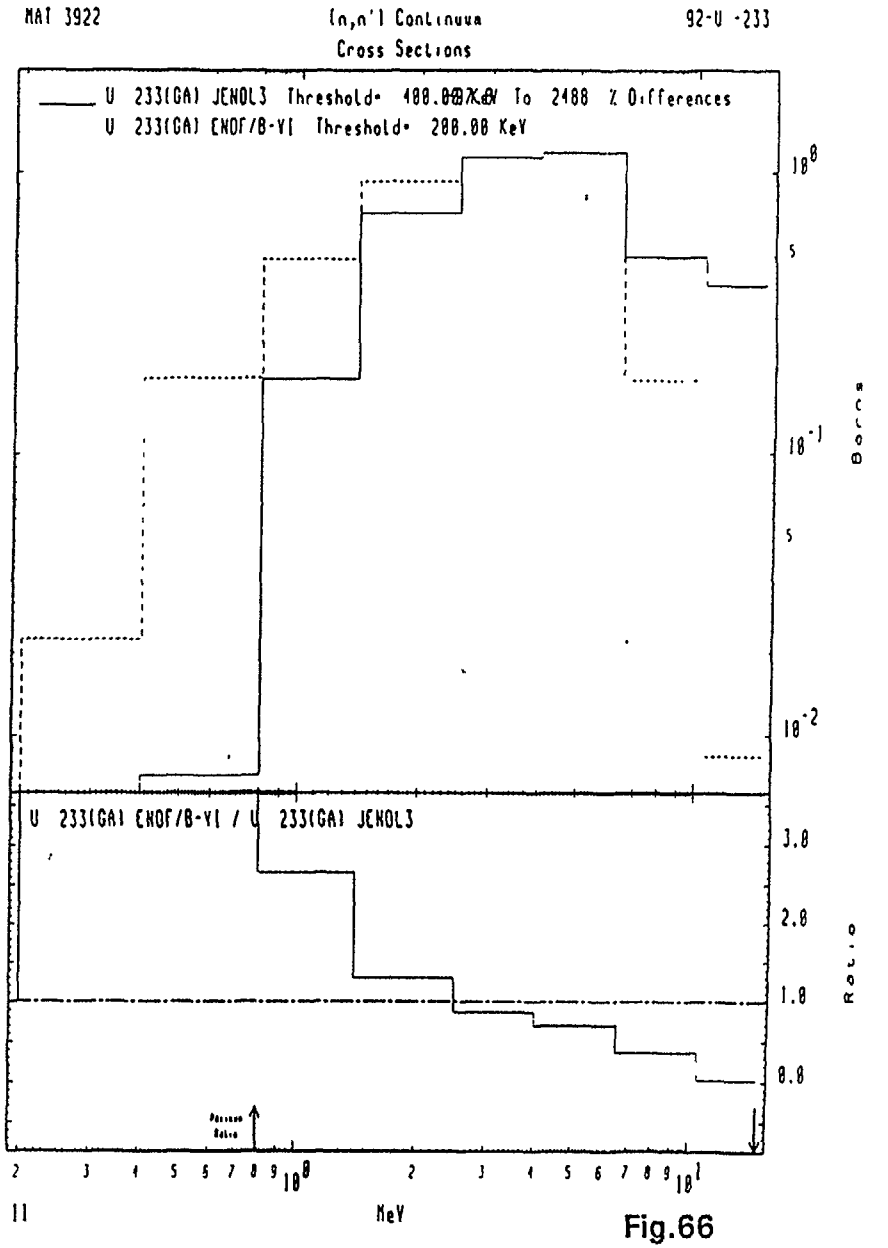
MAT 3922
(n,n') Continuum
Cross Sections
92-U -233
U 233(GA) JENDL3 Threshold= 400.00 KeV To 2488 % Differences
U 233(GA) ENDF/B-VI Threshold= 200.00 KeV
Barns
U 233(GA) ENDF/B-VI / U 233(GA) JENDL3
Ratio
MeV

Fig.66

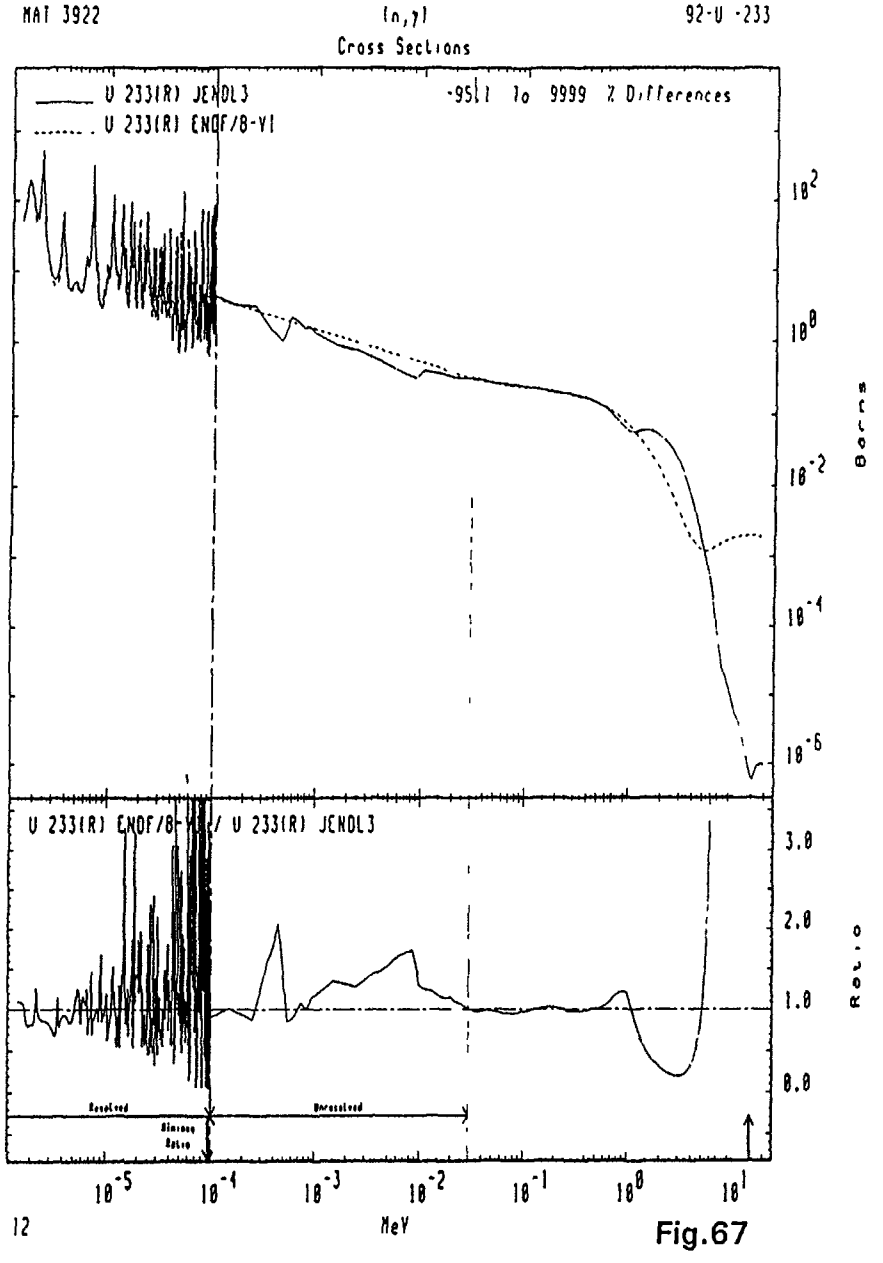
MAT 3922
(n,γ)
92-U -233
Cross Sections
U 233(R) JENDL3
U 233(R) ENDF/B-VI
-95.1 To 9999 % Differences
Barns
U 233(R) ENDF/B-VI / U 233(R) JENDL3
Ratio
Resolved
Unresolved
Fission Ratio
MeV
12

Fig.67

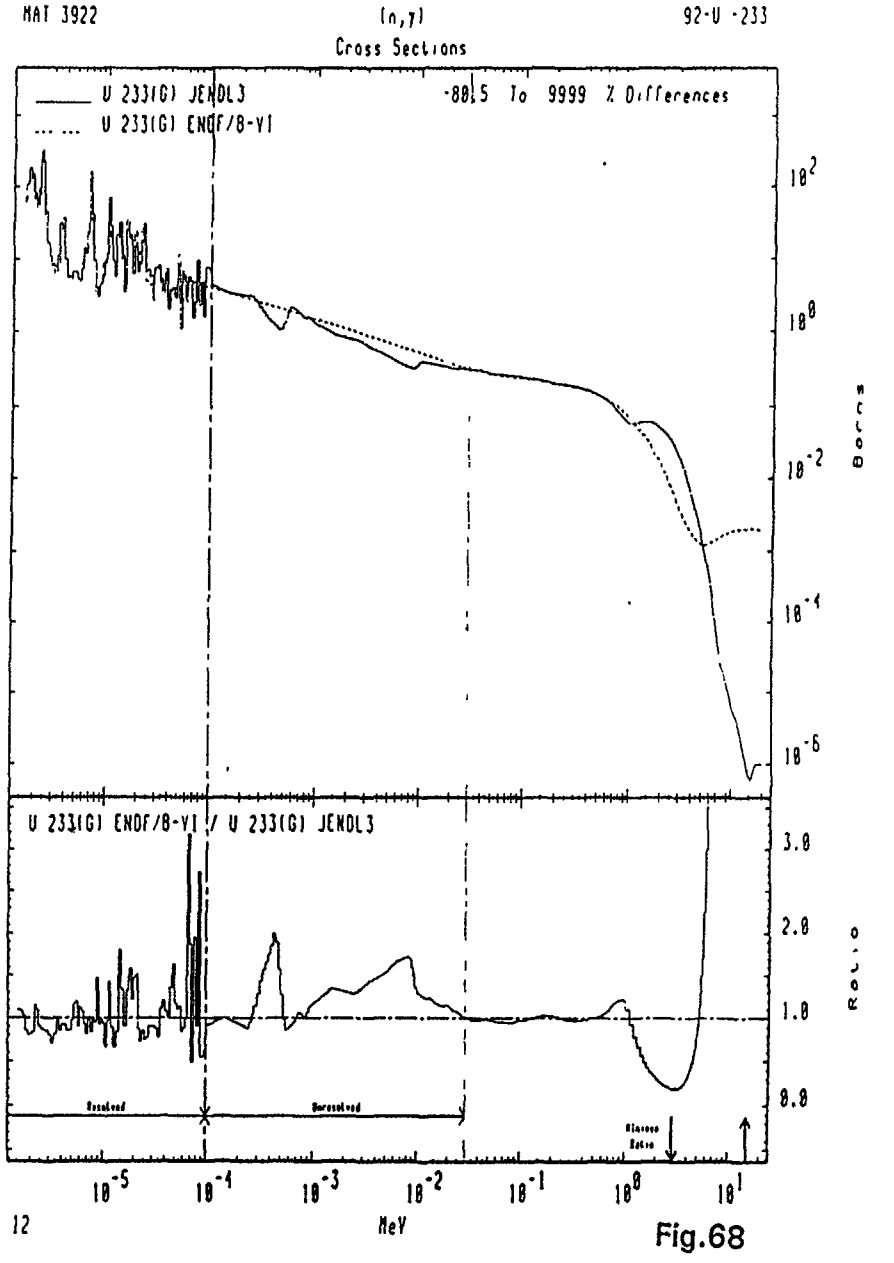
MAT 3922
(n,γ)
92-U -233
Cross Sections
U 233(G) JENDL3
U 233(G) ENDF/B-VI
-80.5 To 9999 % Differences
Barns
U 233(G) ENDF/B-VI / U 233(G) JENDL3
Ratio
Resolved
Unresolved
Fission Ratio
MeV
12

Fig.68

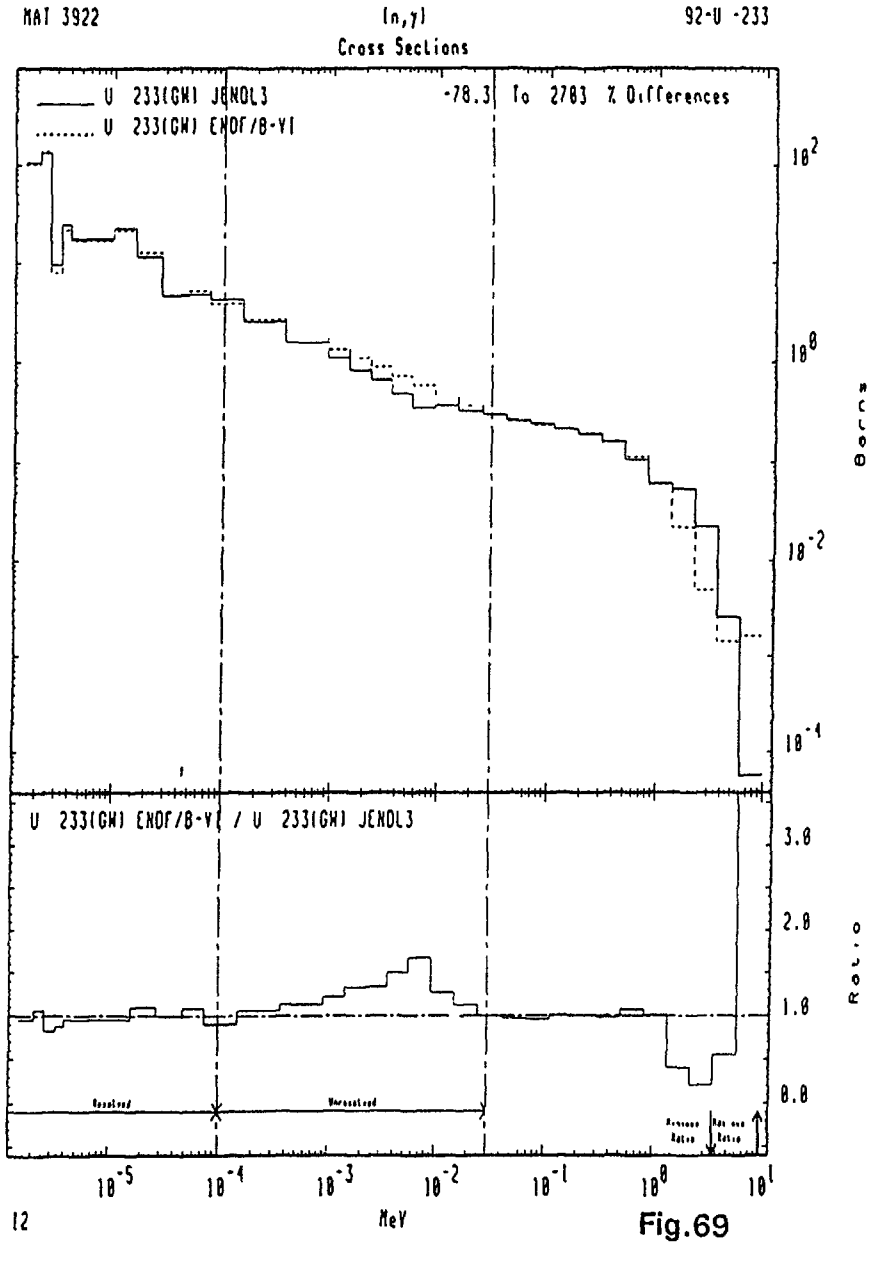
MAT 3922
(n,γ)
92-U -233
Cross Sections
U 233(GW) JENDL3
U 233(GW) ENDF/B-VI
-78.3 To 2703 % Differences
Barns
U 233(GW) ENDF/B-VI / U 233(GW) JENDL3
Ratio
Resolved
Unresolved
MeV
12

Fig.69

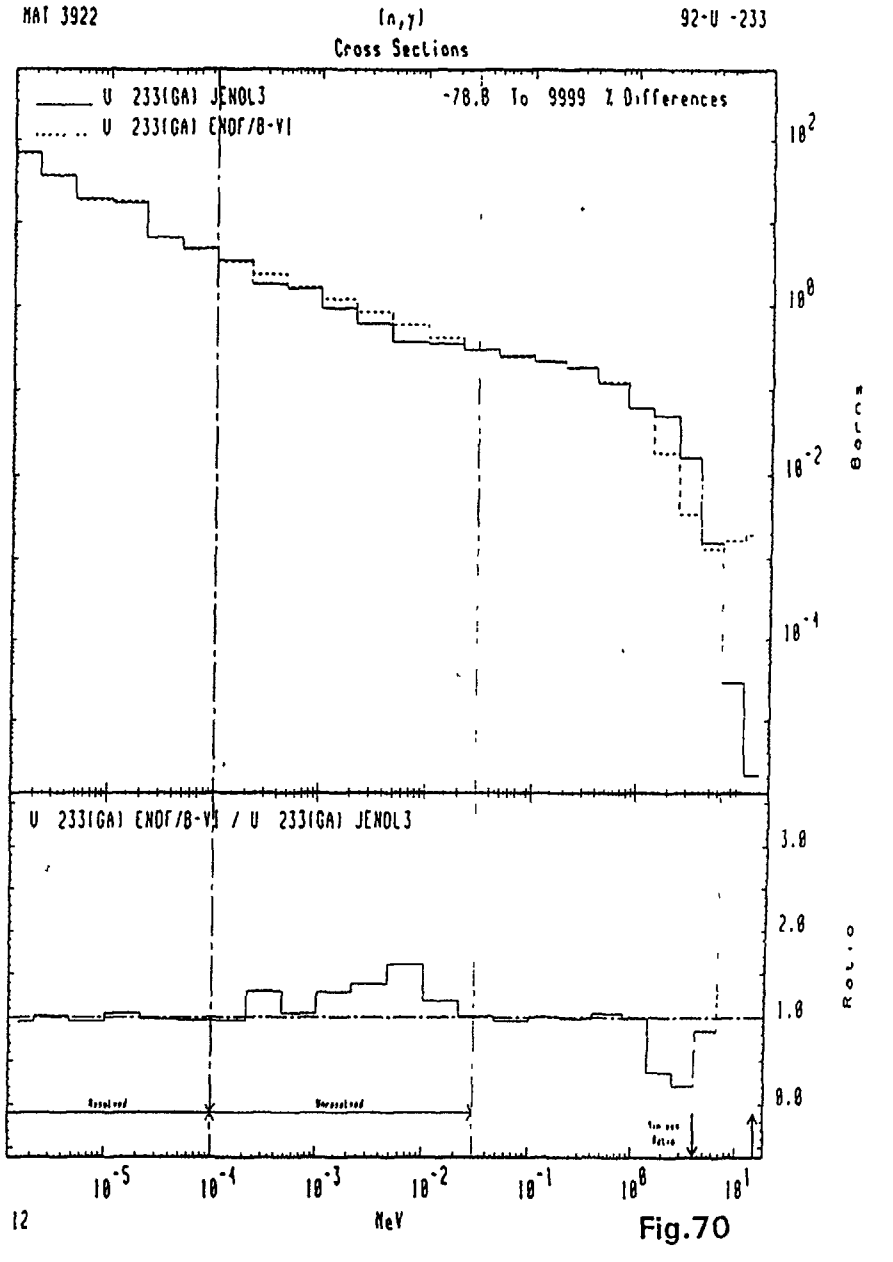
MAT 3922
(n,γ)
92-U -233
Cross Sections
U 233(GA) JENDL3
U 233(GA) ENDF/B-VI
-78.8 To 9999 % Differences
Barns
U 233(GA) ENDF/B-VI / U 233(GA) JENDL3
Ratio
Resolved
Unresolved
MeV
12

Fig.70

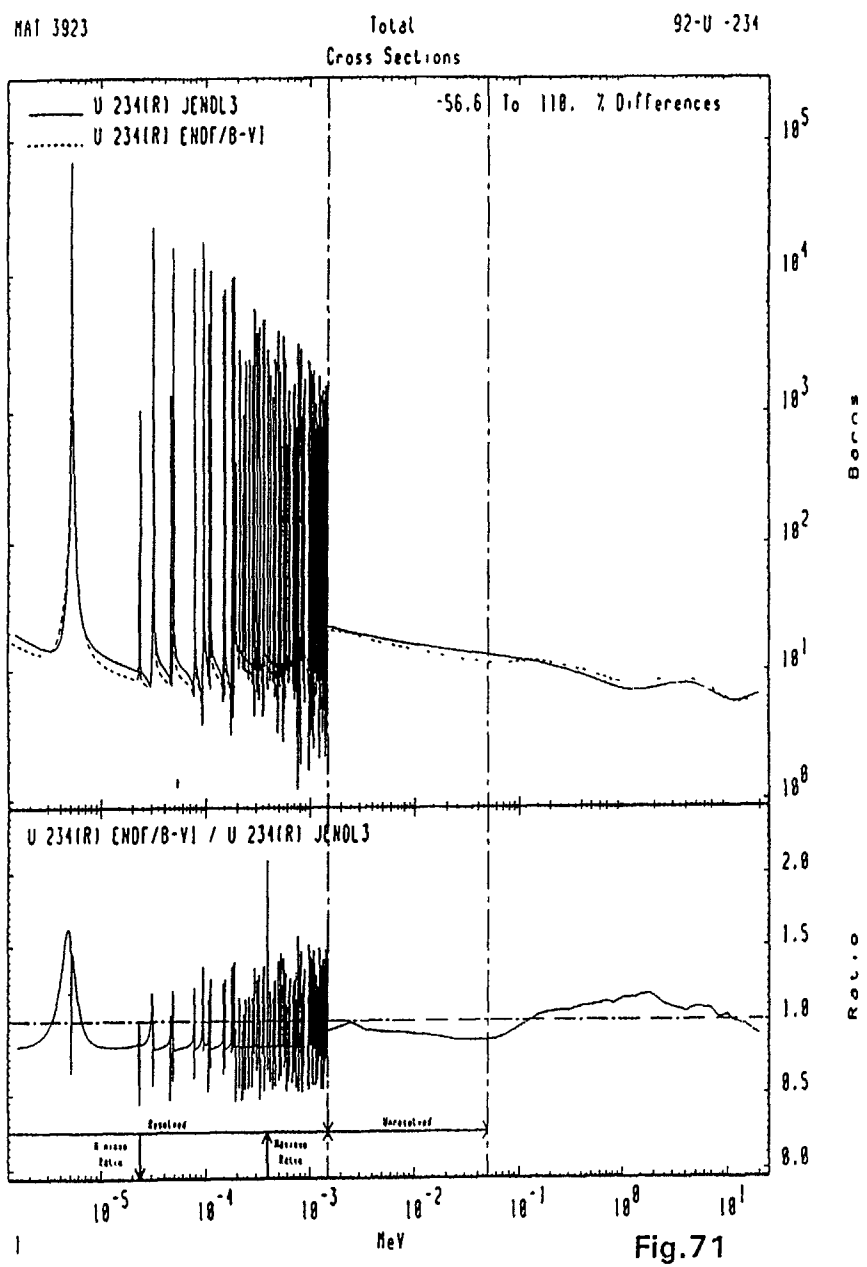
MAT 3923
Total
Cross Sections
92-U -234
U 234(R) JENDL3
U 234(R) ENDF/B-VI
-56.6 To 110. % Differences
Barns
U 234(R) ENDF/B-VI / U 234(R) JENDL3
Ratio
MeV

Fig.71

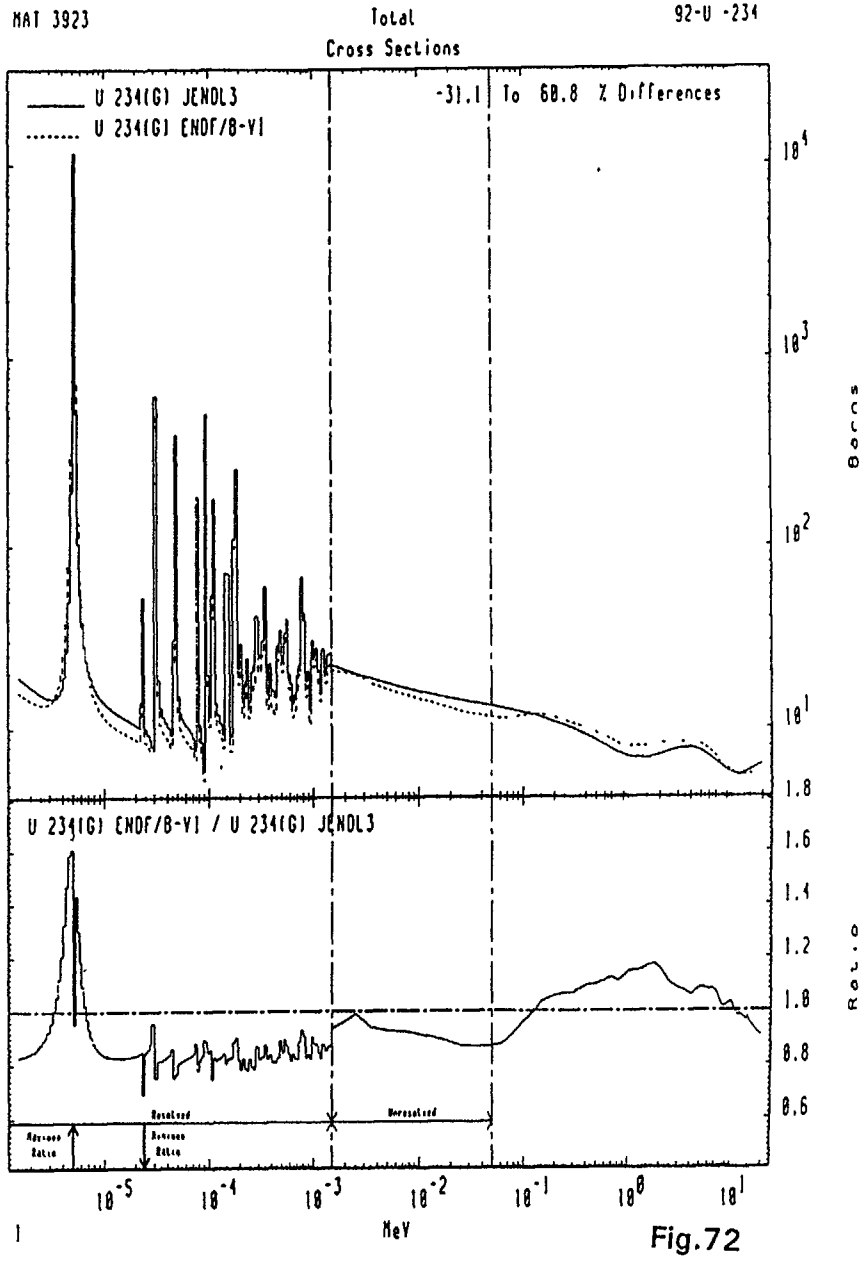
MAT 3923
Total
Cross Sections
92-U -234
U 234(G) JENDL3
U 234(G) ENDF/B-VI
-31.1 To 60.8 % Differences
Barns
U 234(G) ENDF/B-VI / U 234(G) JENDL3
Ratio
MeV

Fig.72

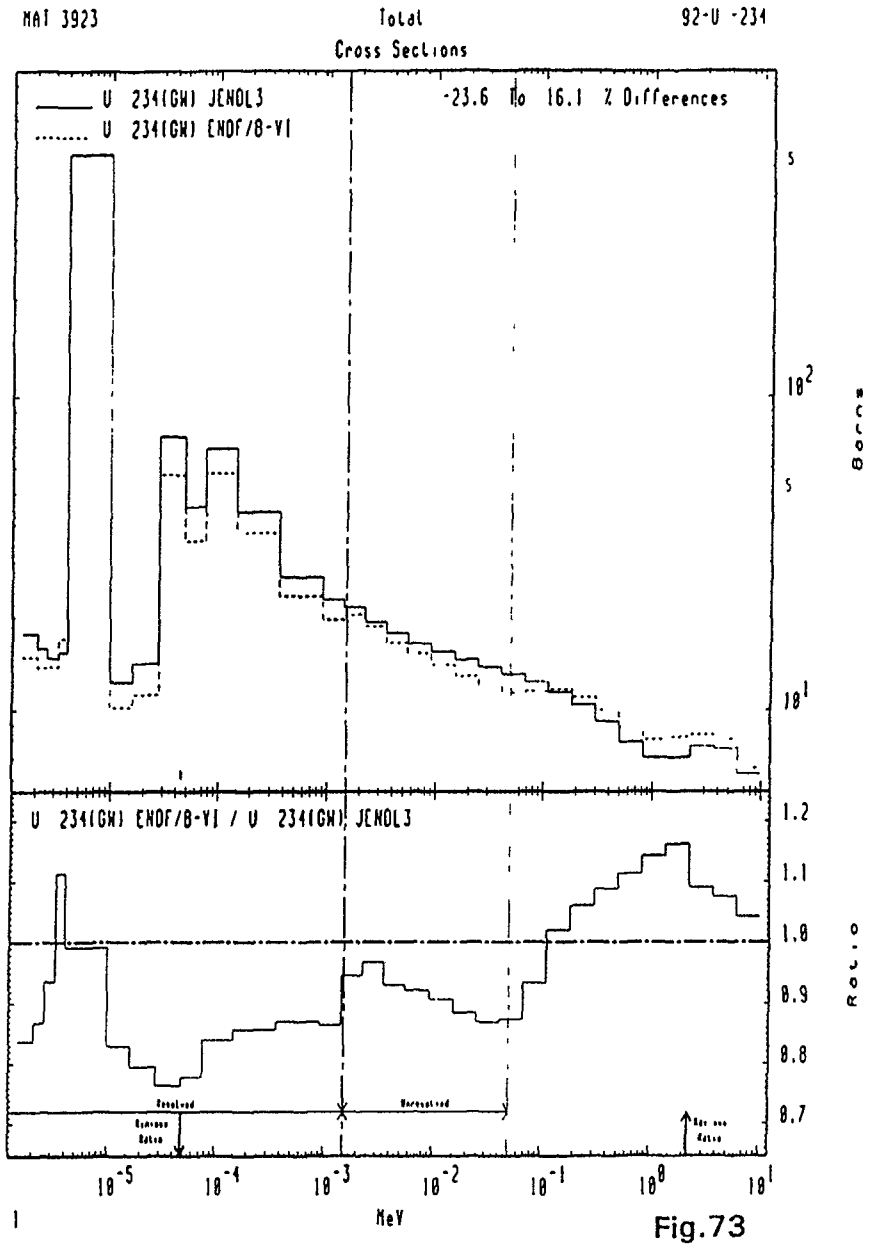
MAT 3923
Total
Cross Sections
92-U -234
U 234(GW) JENDL3
U 234(GW) ENDF/B-VI
-23.6 To 16.1 % Differences
Barns
U 234(GW) ENDF/B-VI / U 234(GW) JENDL3
Ratio
Resolved
Unresolved
MeV

Fig.73

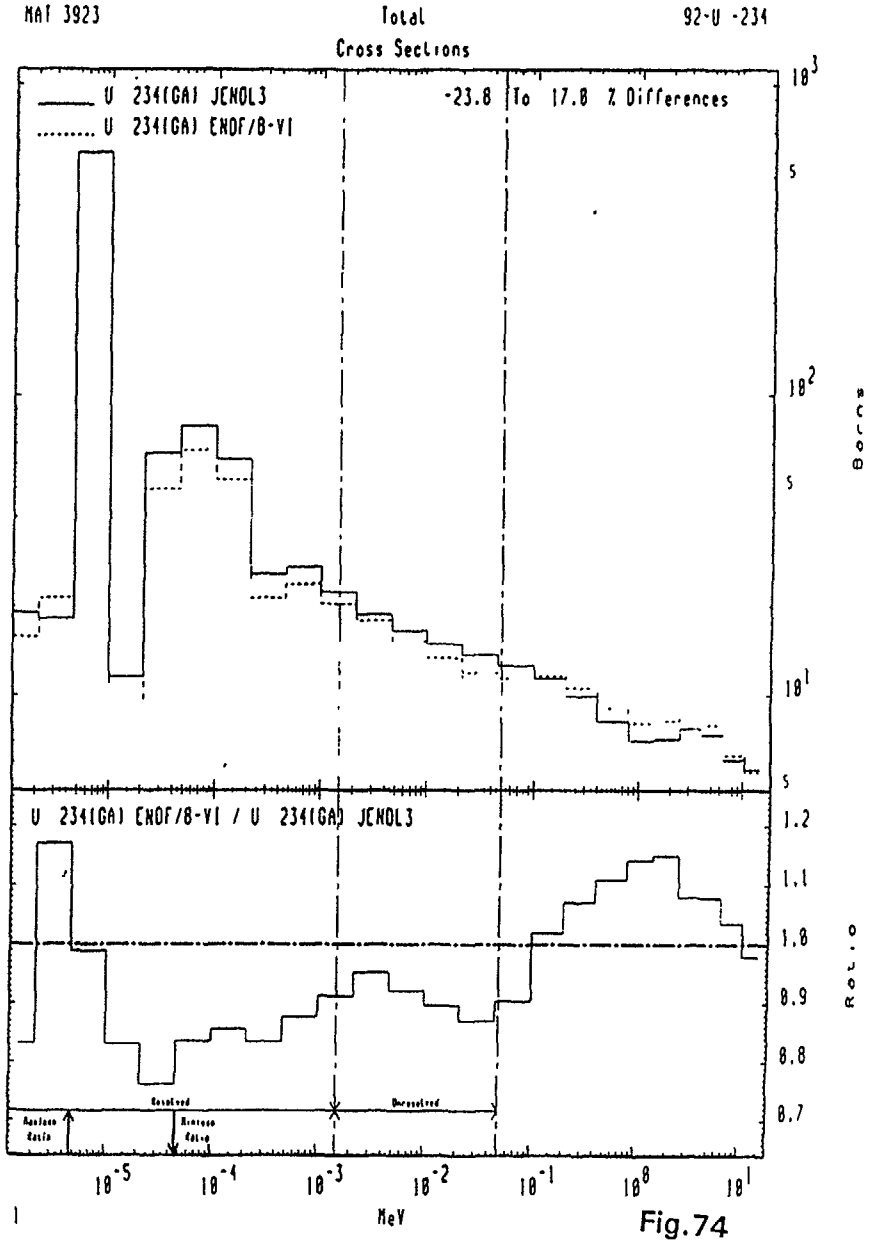
MAT 3923
Total
Cross Sections
92-U -234
U 234(GA) JENDL3
U 234(GA) ENDF/B-VI
-23.8 To 17.8 % Differences
Barns
U 234(GA) ENDF/B-VI / U 234(GA) JENDL3
Ratio
Resolved
Unresolved
MeV

Fig.74

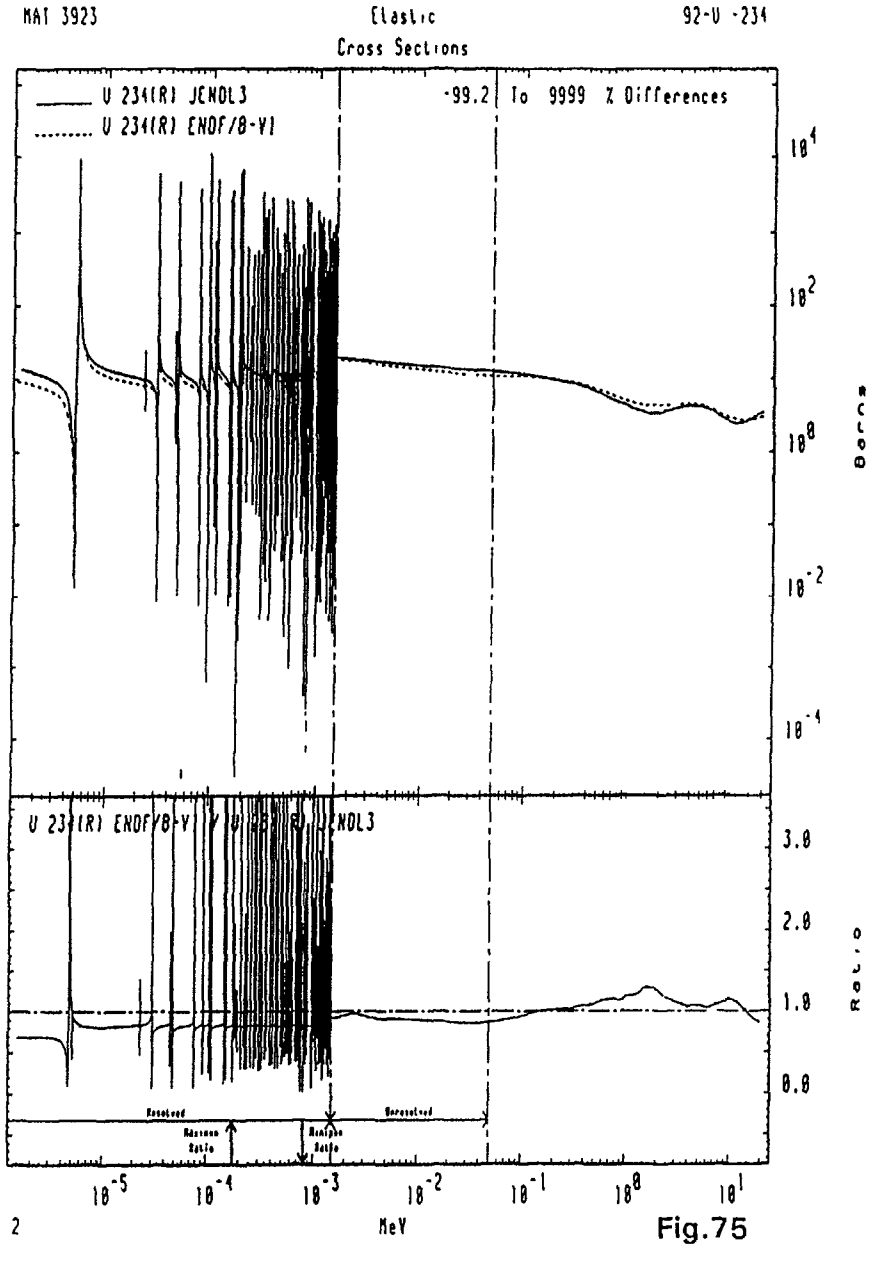
MAT 3923
Elastic
Cross Sections
92-U -234
U 234(R) JENDL3
U 234(R) ENDF/B-VI
-99.2 To 9999 % Differences
Barns
U 234(R) ENDF/B-VI / U 234(R) JENDL3
Ratio
Resolved
Unresolved
MeV

Fig.75

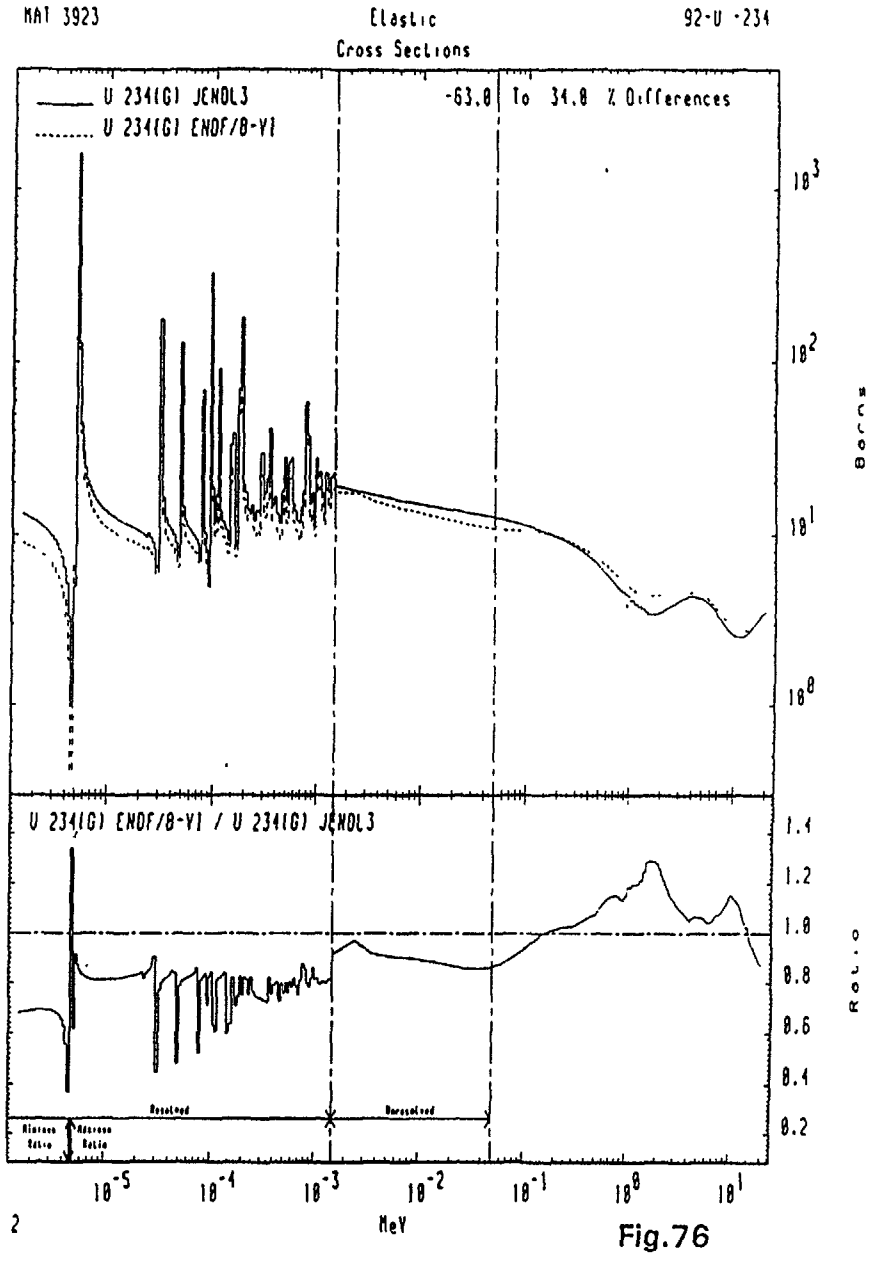
MAT 3923
Elastic
Cross Sections
92-U -234
U 234(G) JENDL3
U 234(G) ENDF/B-VI
-63.0 To 34.0 % Differences
Barns
U 234(G) ENDF/B-VI / U 234(G) JENDL3
Ratio
Resolved
Unresolved
MeV

Fig.76

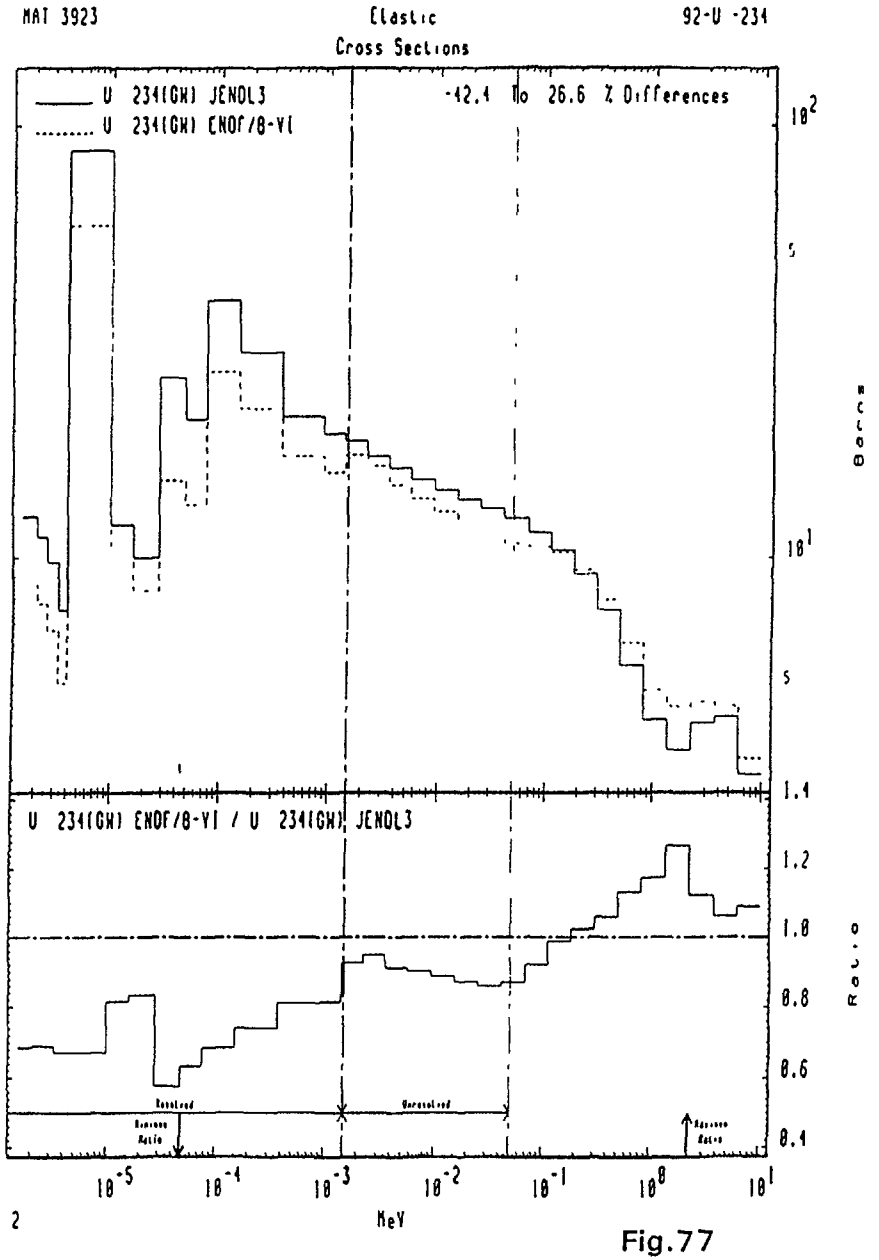
MAT 3923
Elastic
Cross Sections
92-U -234
U 234(GW) JENDL3
U 234(GW) ENDF/B-VI
-42.4 to 26.6 % Differences
U 234(GW) ENDF/B-VI / U 234(GW) JENDL3
Barns
Ratio
MeV

Fig.77

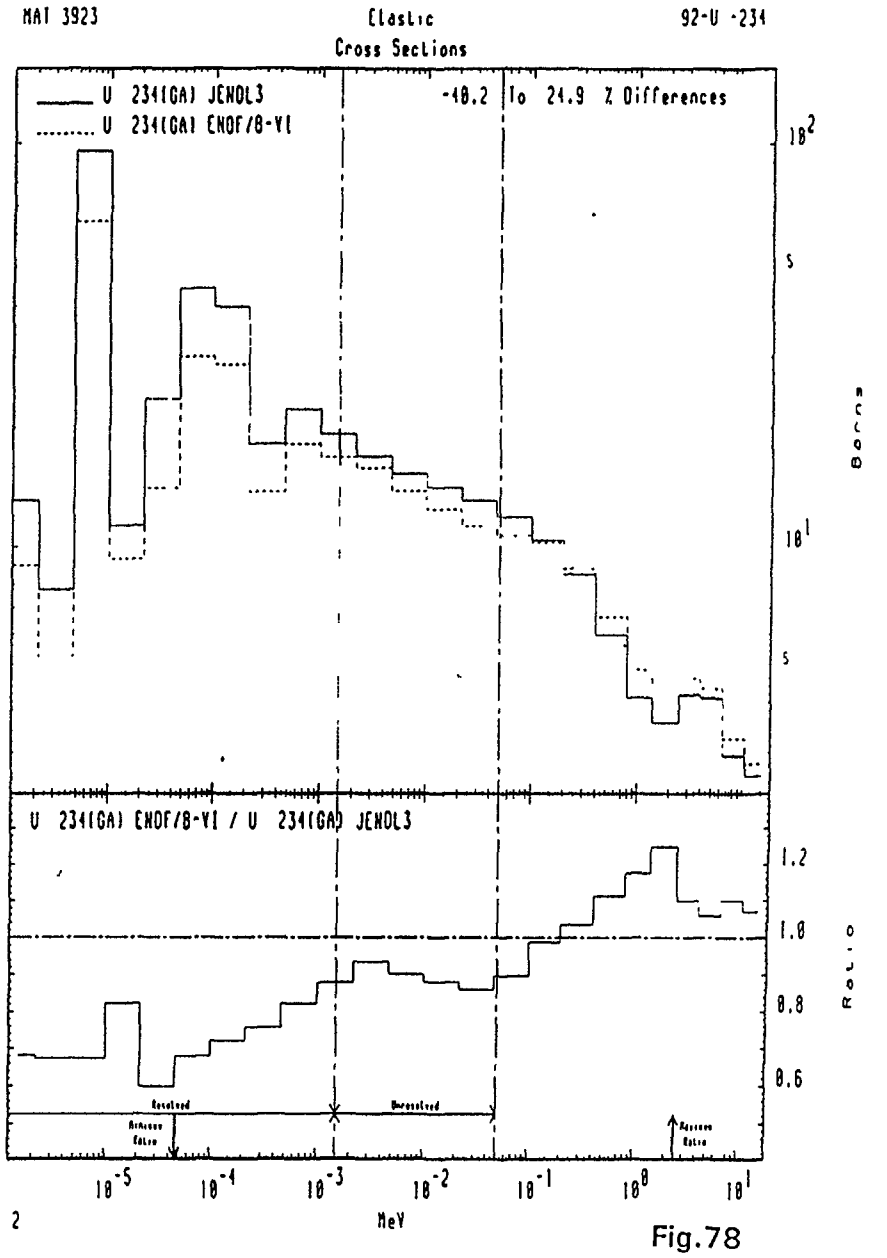
MAT 3923
Elastic
Cross Sections
92-U -234
U 234(GA) JENDL3
U 234(GA) ENDF/B-VI
-48.2 to 24.9 % Differences
U 234(GA) ENDF/B-VI / U 234(GA) JENDL3
Barns
Ratio
MeV

Fig.78

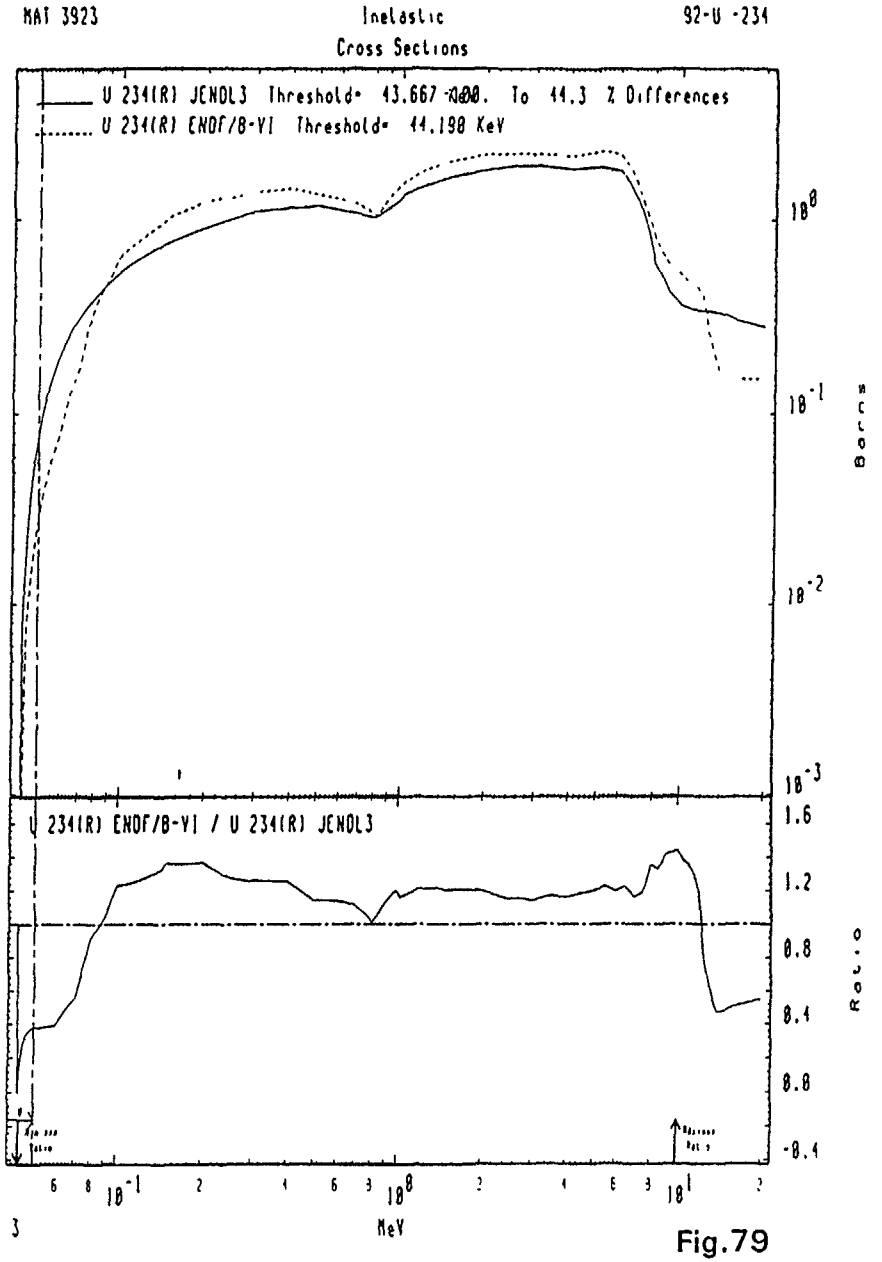
MAT 3923
Inelastic
Cross Sections
92-U -234
U 234(R) JENDL3 Threshold= 43.667 KeV To 44.3 % Differences
U 234(R) ENDF/B-VI Threshold= 44.190 KeV
Barns
U 234(R) ENDF/B-VI / U 234(R) JENDL3
Ratio
MeV

Fig.79

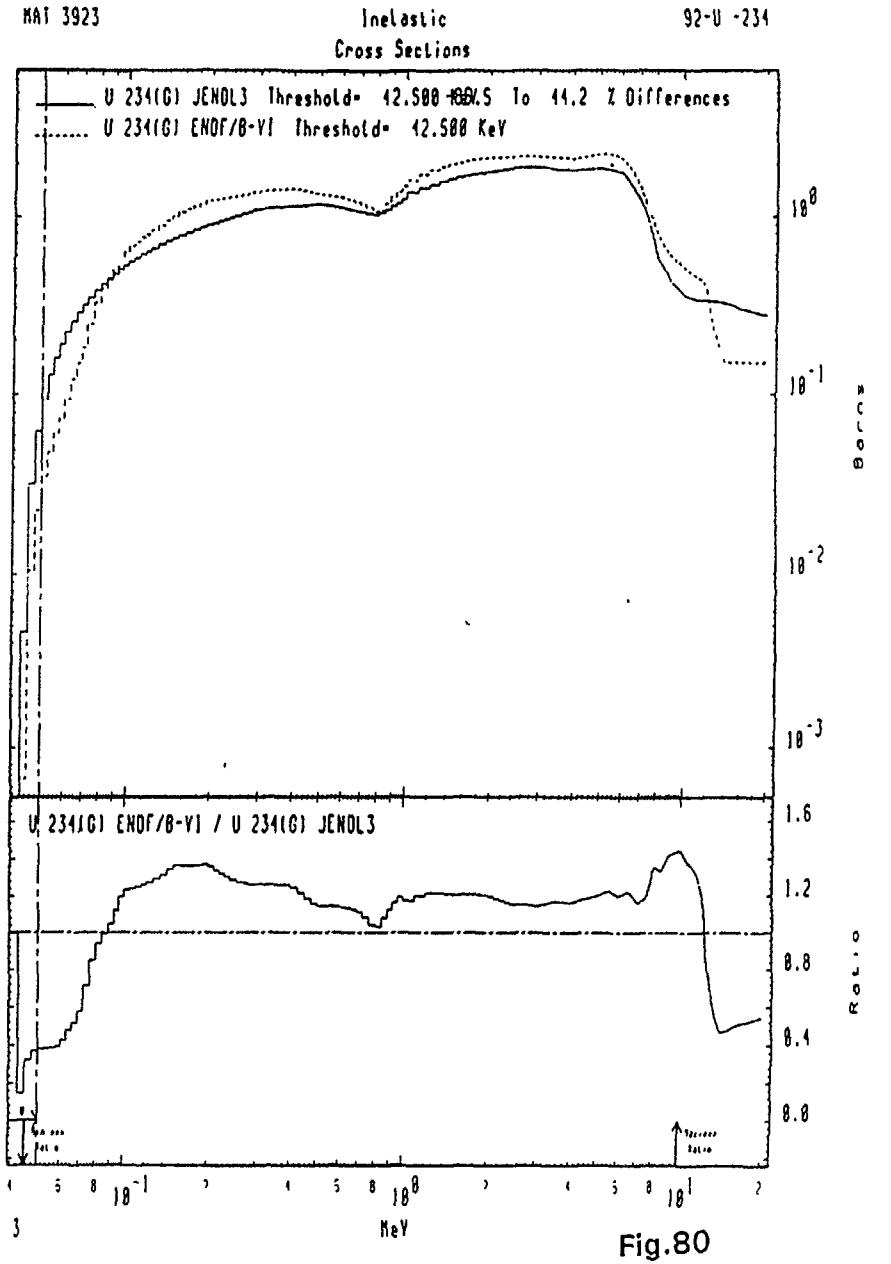
MAT 3923
Inelastic
Cross Sections
92-U -234
U 234(G) JENDL3 Threshold= 42.500 KeV To 44.2 % Differences
U 234(G) ENDF/B-VI Threshold= 42.500 KeV
Barns
U 234(G) ENDF/B-VI / U 234(G) JENDL3
Ratio
MeV

Fig.80

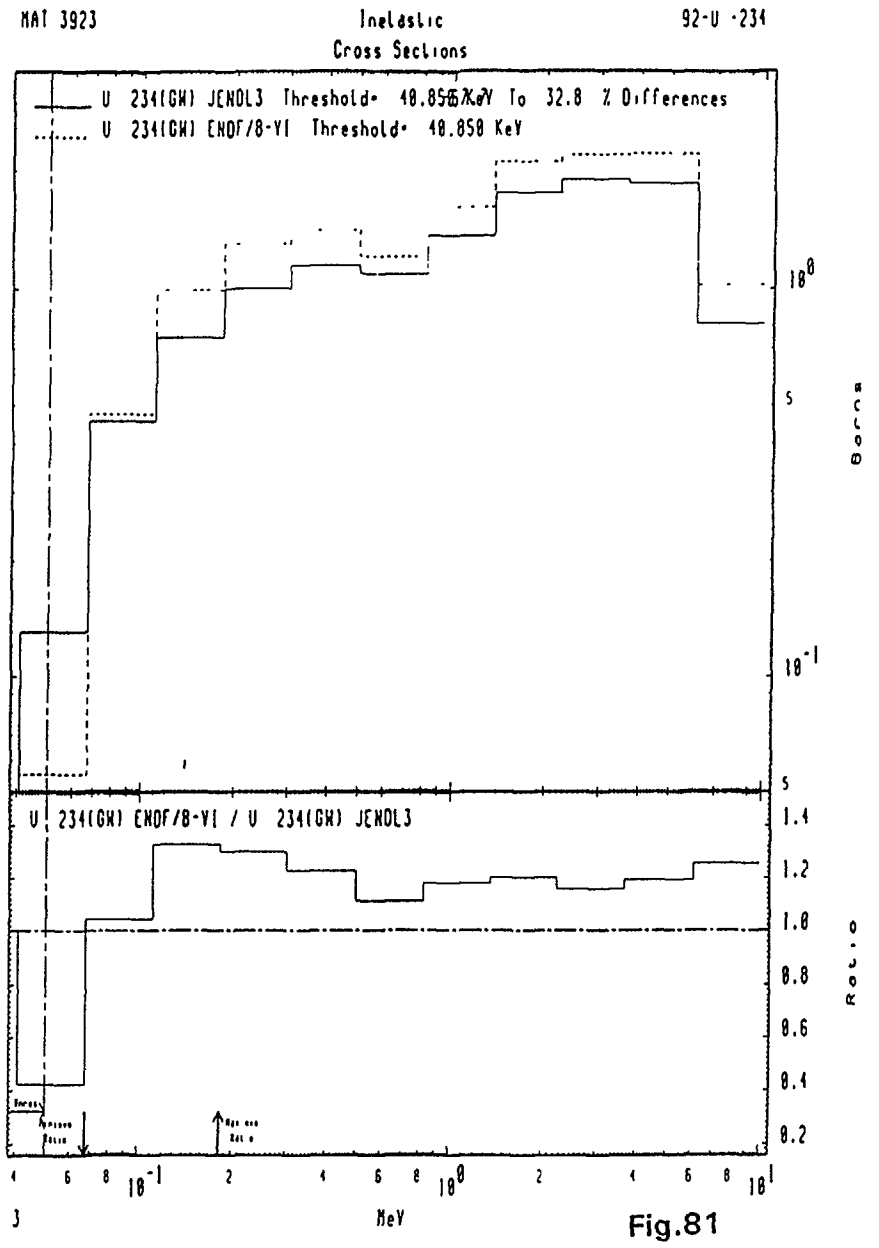
MAT 3923
Inelastic
Cross Sections
92-U -234
U 234(GW) JENDL3 Threshold= 40.850 KeV To 32.8 % Differences
U 234(GW) ENDF/B-VI Threshold= 40.850 KeV
U 234(GW) ENDF/B-VI / U 234(GW) JENDL3
Barns
Ratio
MeV

Fig.81

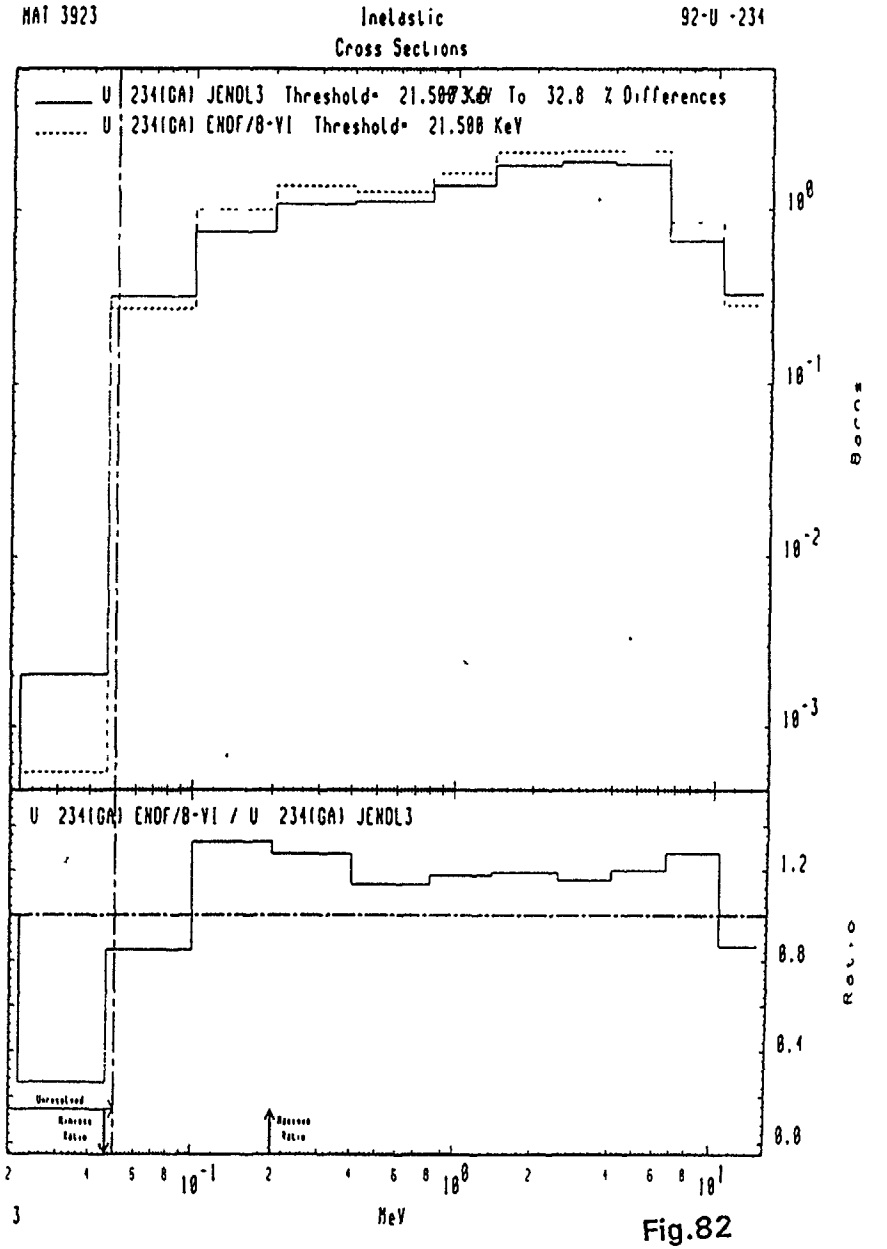
MAT 3923
Inelastic
Cross Sections
92-U -234
U 234(GA) JENDL3 Threshold= 21.508 KeV To 32.8 % Differences
U 234(GA) ENDF/B-VI Threshold= 21.508 KeV
U 234(GA) ENDF/B-VI / U 234(GA) JENDL3
Barns
Ratio
MeV

Fig.82

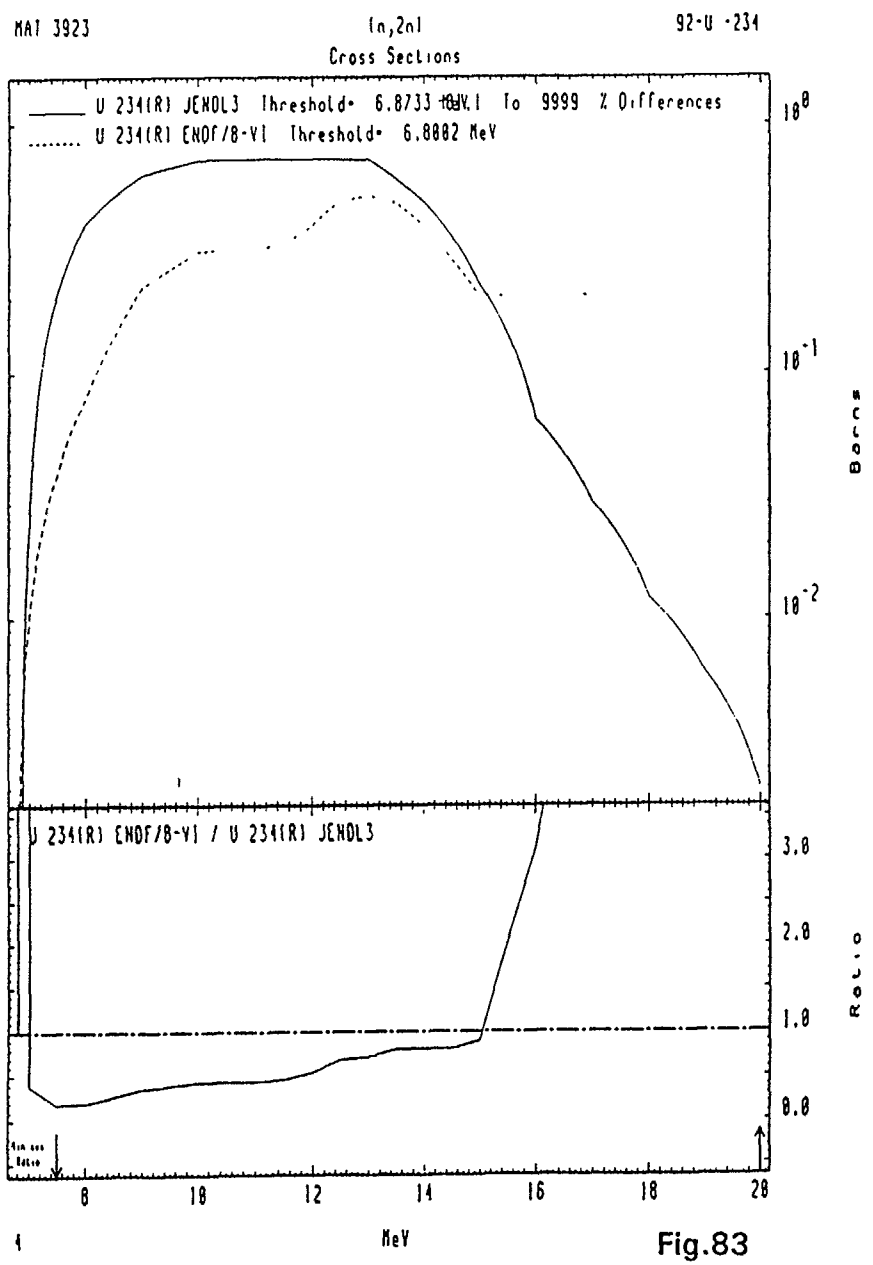
MAT 3923
(n,2n)
92-U -234
Cross Sections
U 234(R) JENDL3 Threshold= 6.8733 MeV To 9999 % Differences
U 234(R) ENDF/B-VI Threshold= 6.8802 MeV
Barns
U 234(R) ENDF/B-VI / U 234(R) JENDL3
Ratio
MeV

Fig.83

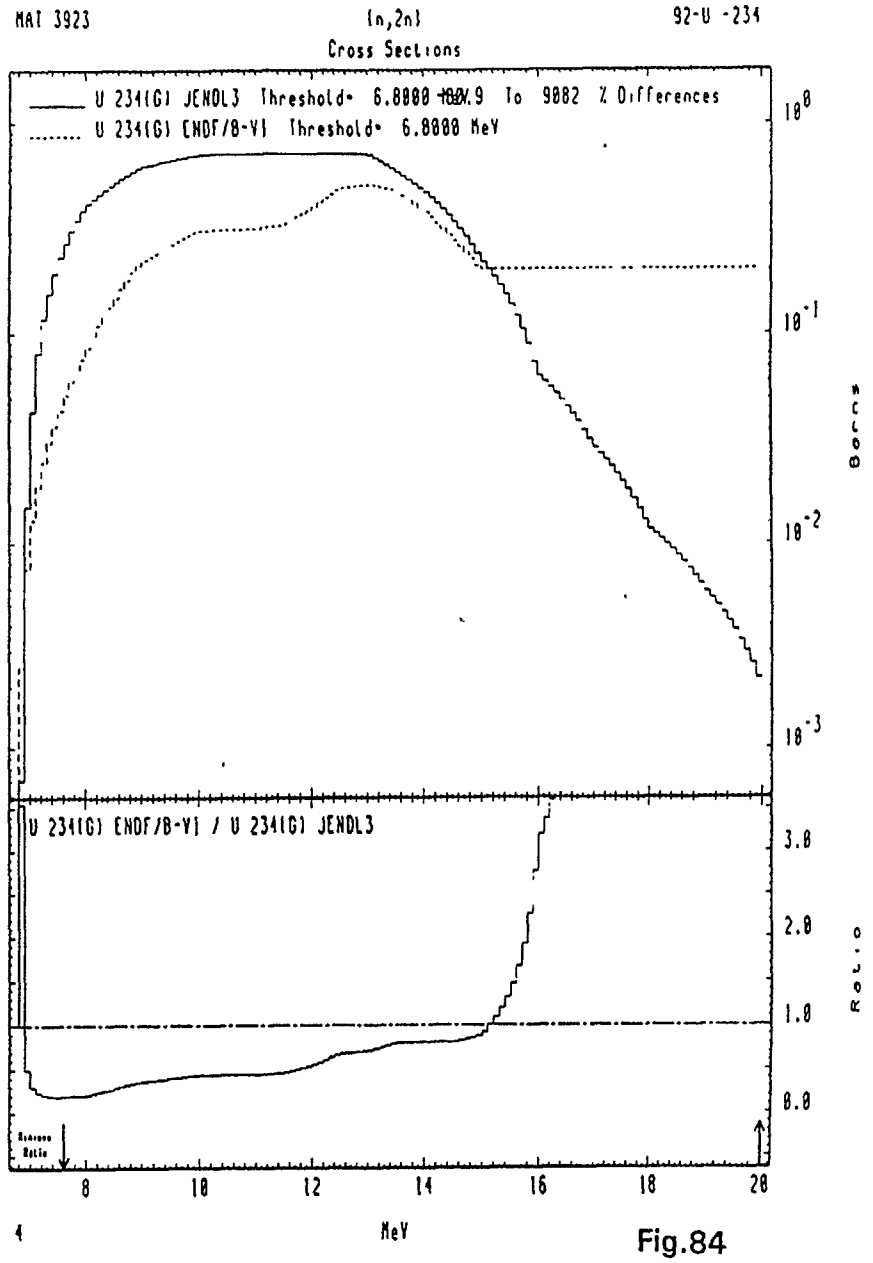
MAT 3923
(n,2n)
92-U -234
Cross Sections
U 234(G) JENDL3 Threshold= 6.8000 MeV To 9882 % Differences
U 234(G) ENDF/B-VI Threshold= 6.8000 MeV
Barns
U 234(G) ENDF/B-VI / U 234(G) JENDL3
Ratio
MeV

Fig.84

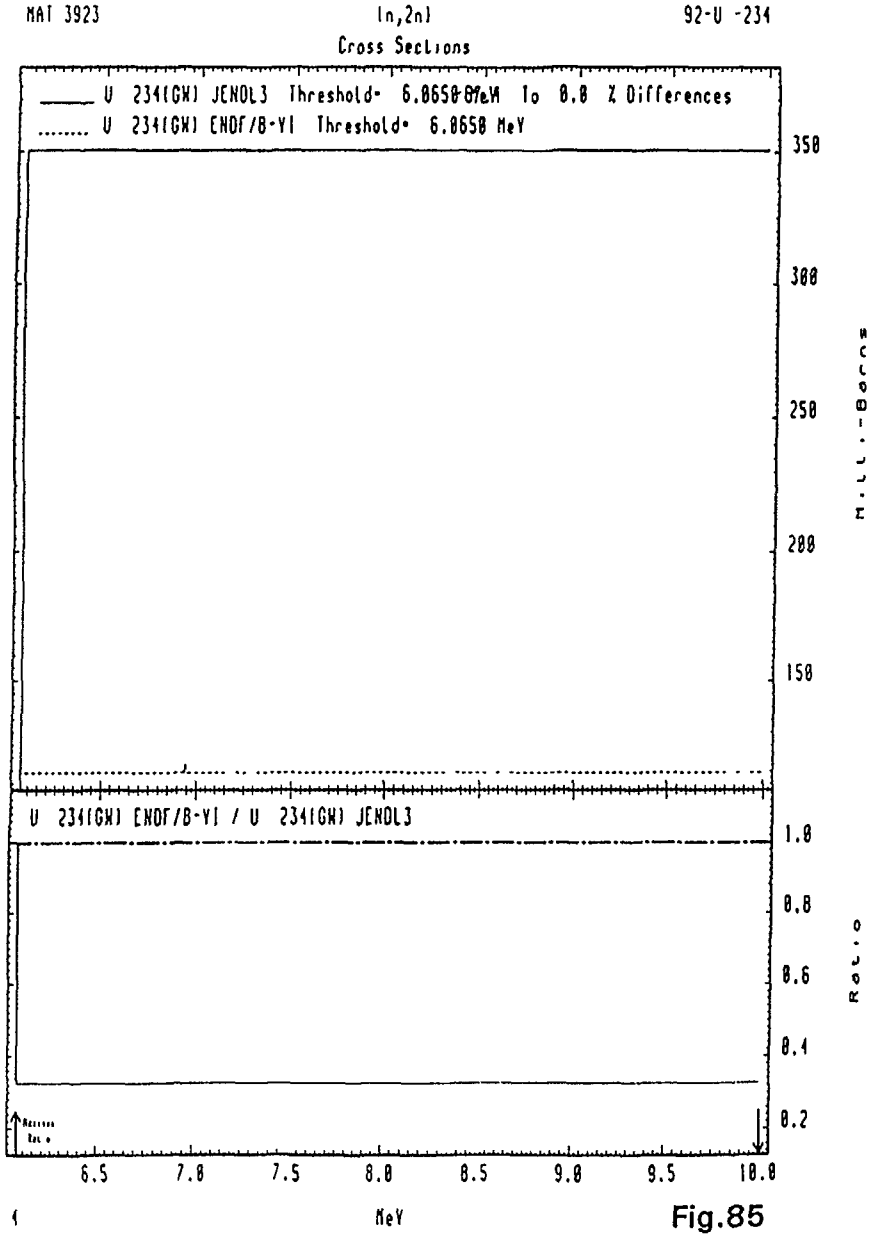
MAT 3923
(n,2n)
92-U -234
Cross Sections
U 234(GW) JENDL3 Threshold= 6.8658 MeV To 0.0 % Differences
U 234(GW) ENDF/B-VI Threshold= 6.8658 MeV
U 234(GW) ENDF/B-VI / U 234(GW) JENDL3
MILLI-Barns
Ratio
MeV

Fig.85

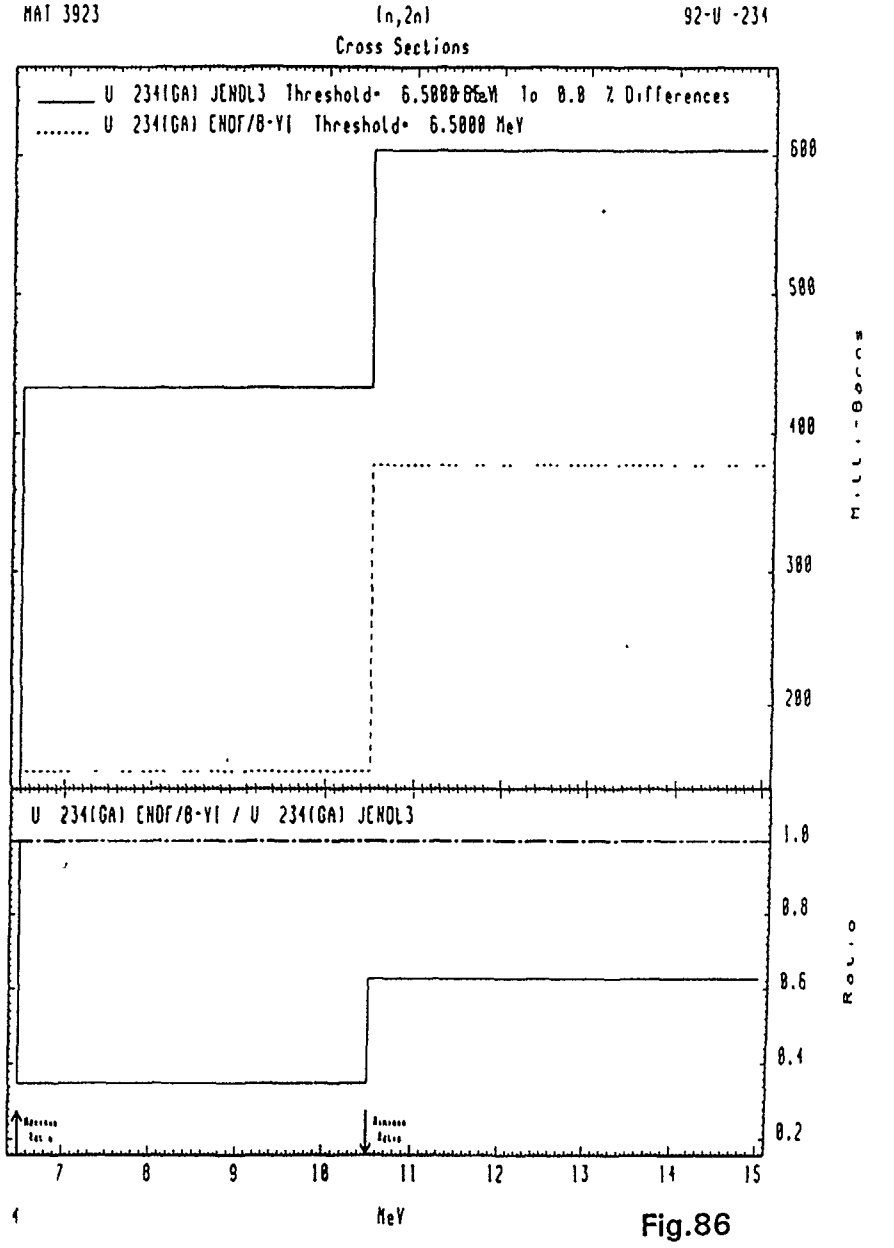
MAT 3923
(n,2n)
92-U -234
Cross Sections
U 234(GA) JENDL3 Threshold= 6.5000 MeV To 0.0 % Differences
U 234(GA) ENDF/B-VI Threshold= 6.5000 MeV
U 234(GA) ENDF/B-VI / U 234(GA) JENDL3
MILLI-Barns
Ratio
MeV

Fig.86

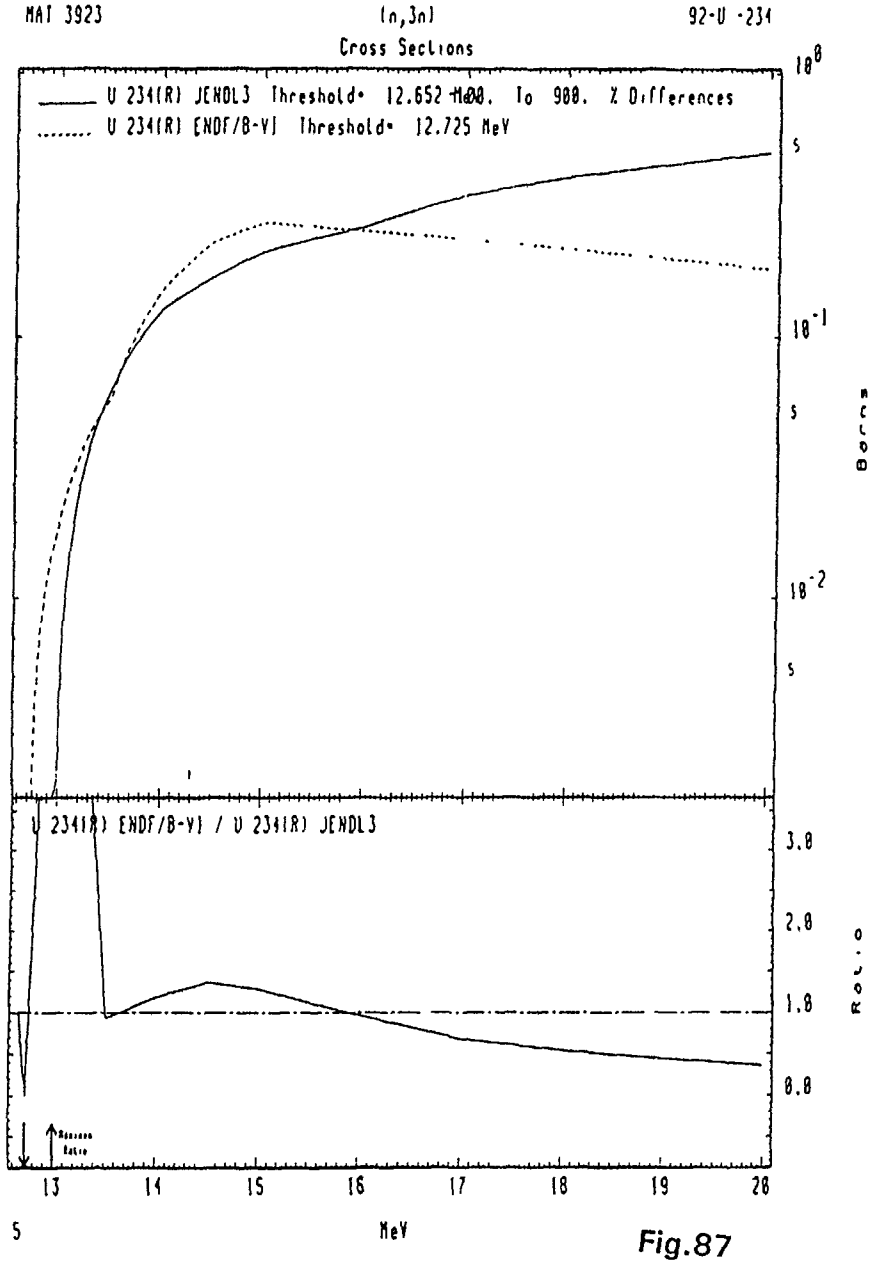
MAT 3923
(n,3n)
92-U -234
Cross Sections
U 234(R) JENDL3 Threshold= 12.652 MeV. To 900. % Differences
U 234(R) ENDF/B-VI Threshold= 12.725 MeV
U 234(R) ENDF/B-VI / U 234(R) JENDL3
Barns
Ratio
MeV

Fig.87

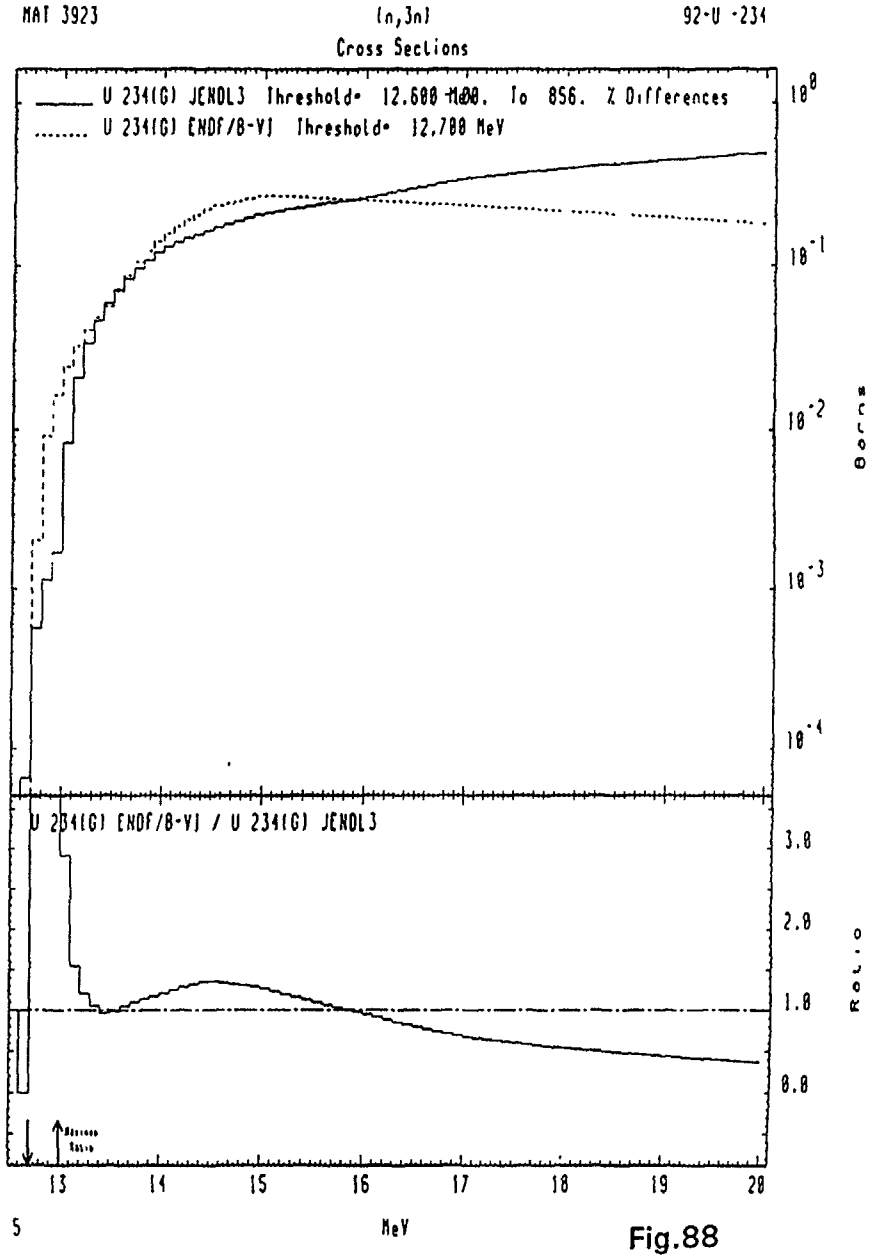
MAT 3923
(n,3n)
92-U -234
Cross Sections
U 234(G) JENDL3 Threshold= 12.600 MeV. To 856. % Differences
U 234(G) ENDF/B-VI Threshold= 12.700 MeV
U 234(G) ENDF/B-VI / U 234(G) JENDL3
Barns
Ratio
MeV

Fig.88

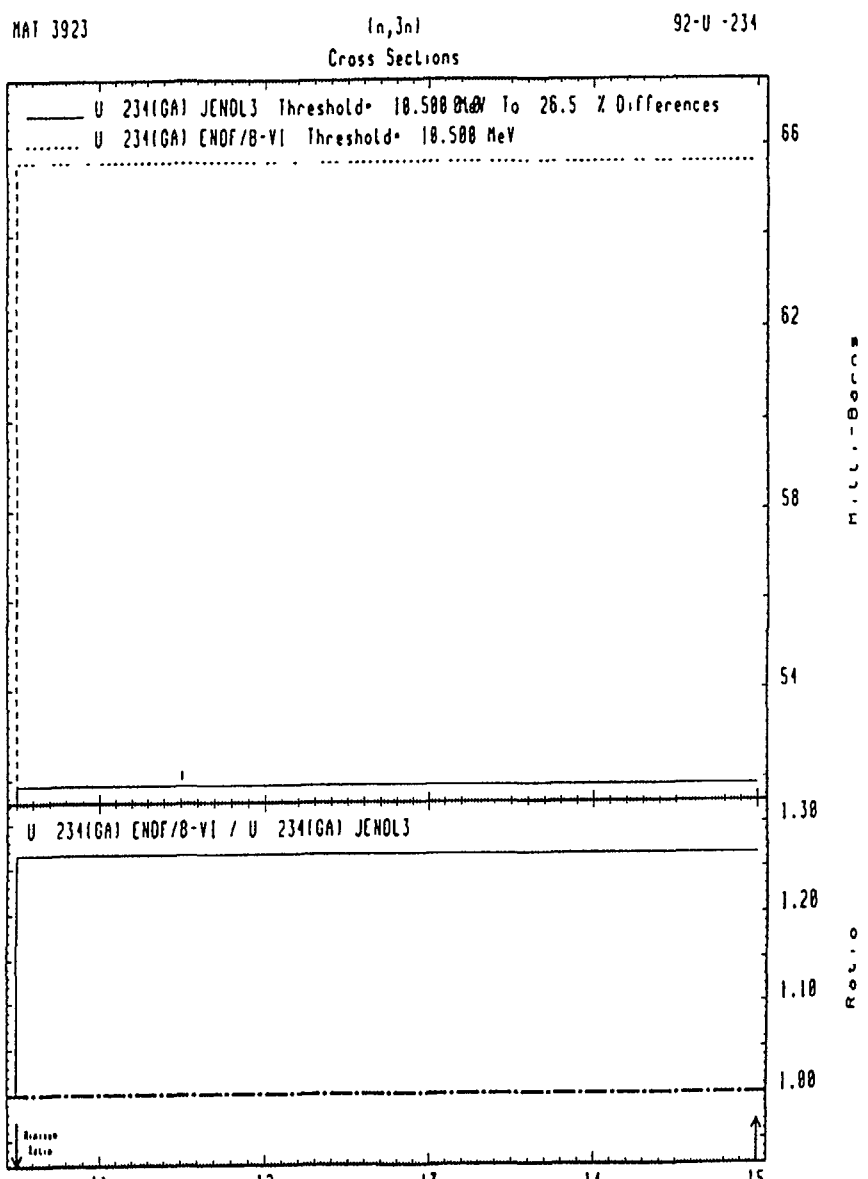
MAT 3923
(n,3n)
92-U -234
Cross Sections
U 234(GA) JENDL3 Threshold= 18.588 MeV To 26.5 % Differences
U 234(GA) ENDF/B-VI Threshold= 18.588 MeV
66
62
58
54
Milli-Barns
U 234(GA) ENDF/B-VI / U 234(GA) JENDL3
1.30
1.20
1.10
1.00
Ratio
11
12
13
14
15
MeV
5

Fig.89

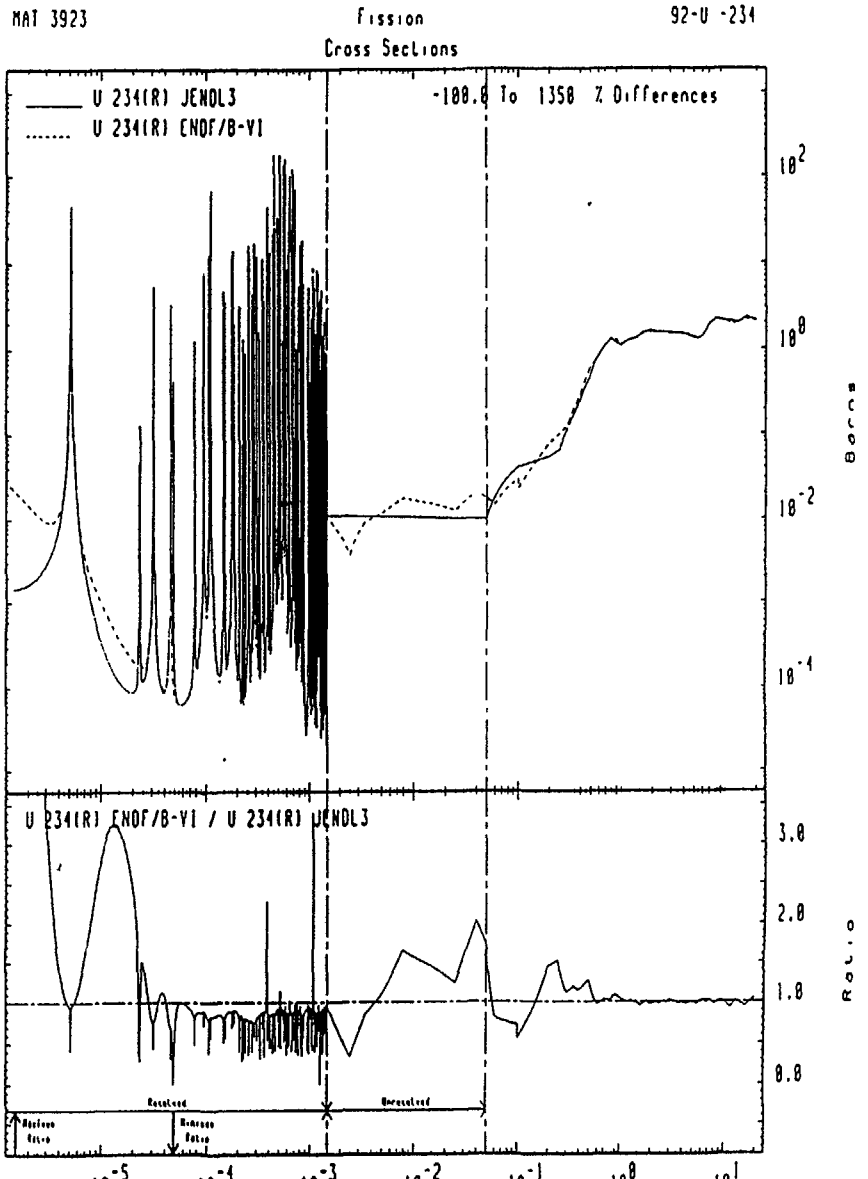
MAT 3923
Fission
92-U -234
Cross Sections
U 234(R) JENDL3
U 234(R) ENDF/B-VI
-100.0 To 1350 % Differences
10^2
10^0
10^-2
10^-4
Barns
U 234(R) ENDF/B-VI / U 234(R) JENDL3
3.0
2.0
1.0
0.0
Ratio
Resolved
Unresolved
10^-5
10^-4
10^-3
10^-2
10^-1
10^0
10^1
MeV
6

Fig.90

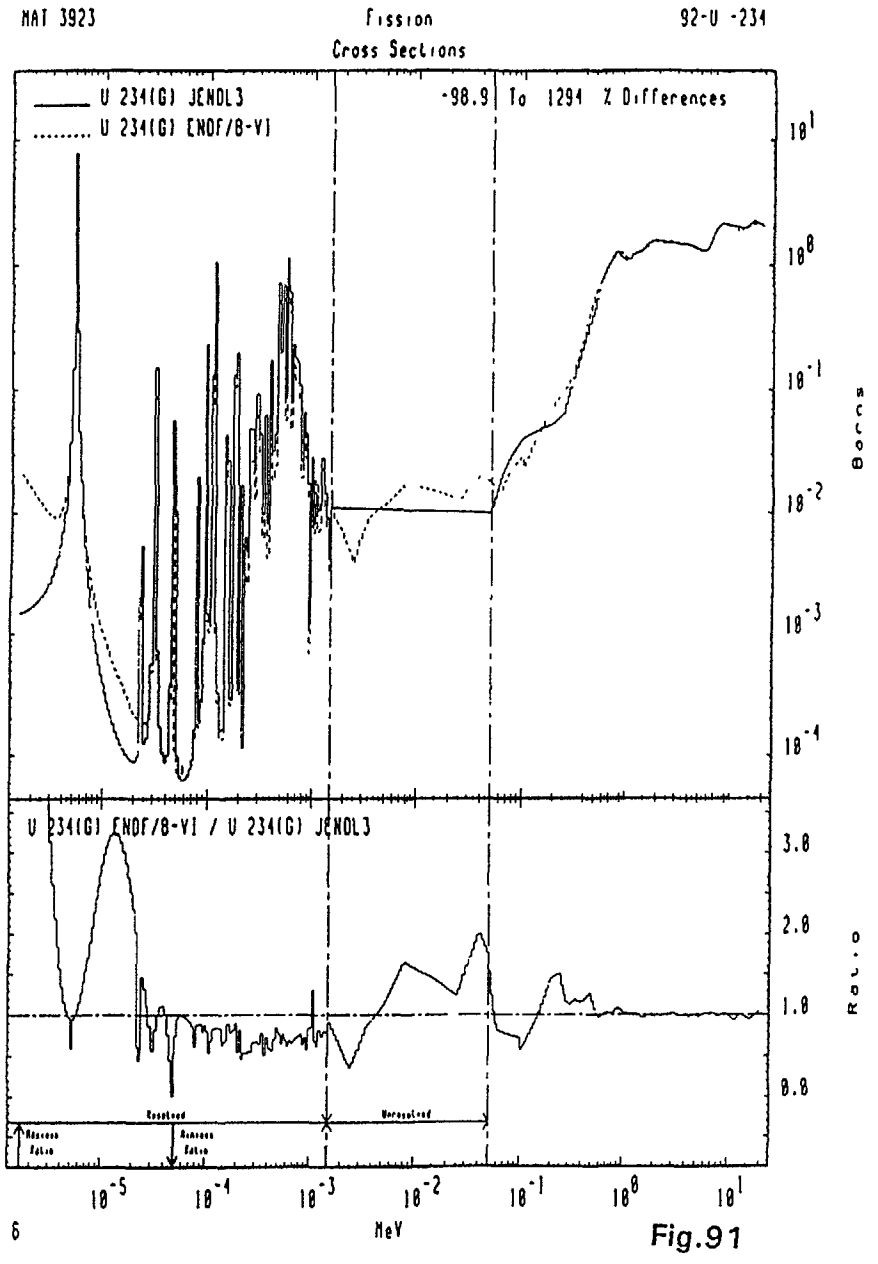
MAT 3923
Fission
Cross Sections
92-U -234
U 234(G) JENDL3
U 234(G) ENDF/B-VI
-98.9 To 1294 % Differences
U 234(G) ENDF/B-VI / U 234(G) JENDL3
Barns
Ratio
MeV

Fig.91

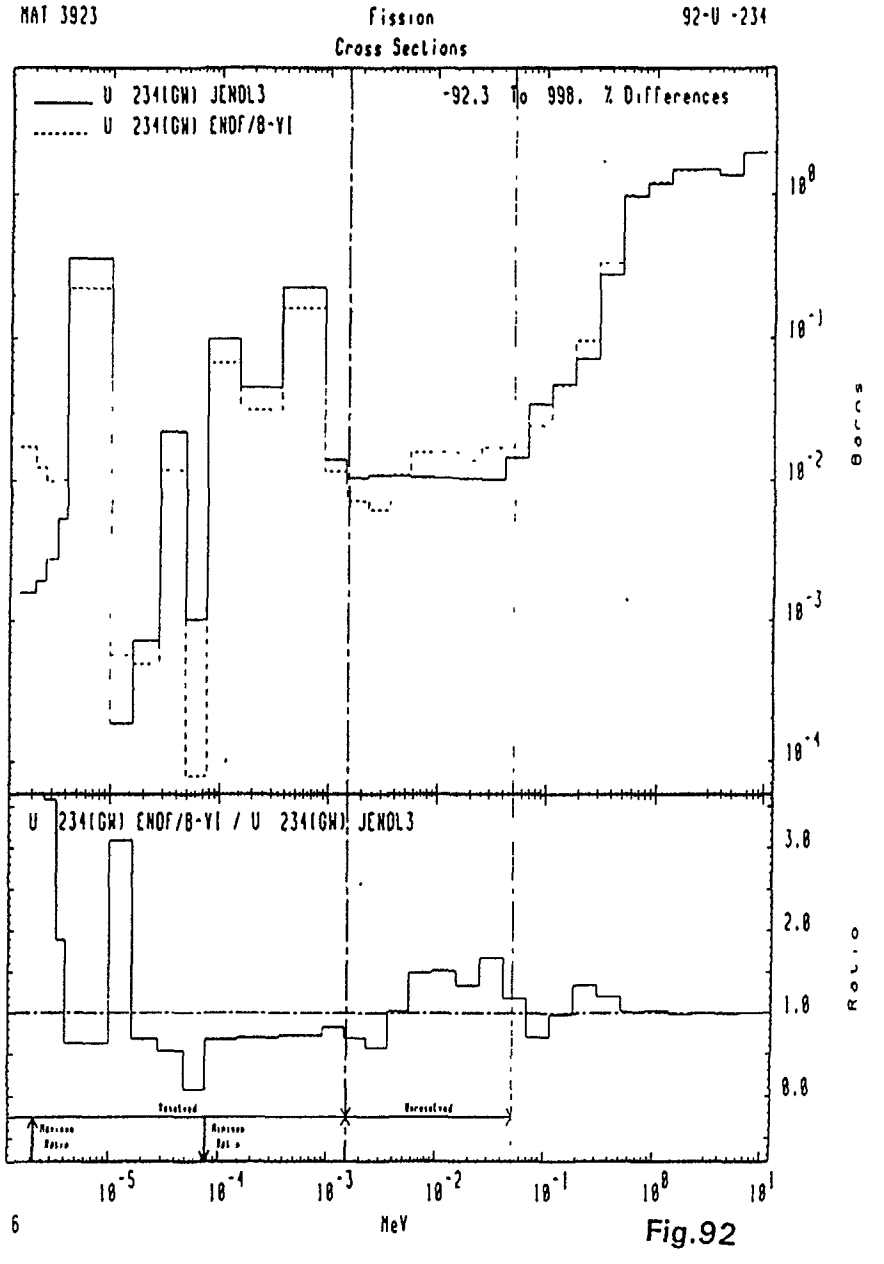
MAT 3923
Fission
Cross Sections
92-U -234
U 234(GW) JENDL3
U 234(GW) ENDF/B-VI
-92.3 To 998. % Differences
U 234(GW) ENDF/B-VI / U 234(GW) JENDL3
Barns
Ratio
MeV

Fig.92

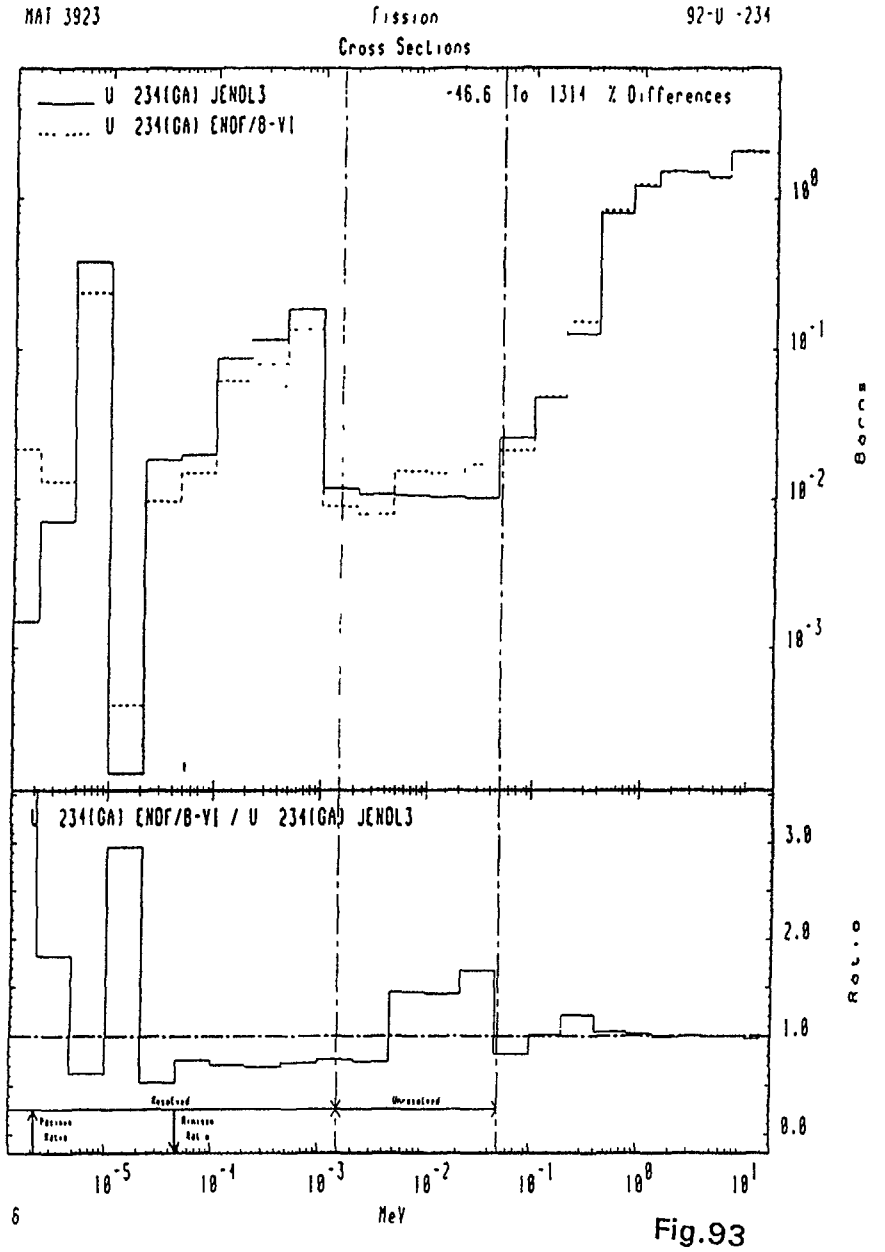
MAT 3923
Fission
Cross Sections
92-U -234
U 234(GA) JENDL3
U 234(GA) ENDF/B-VI
-46.6 To 1314 % Differences
U 234(GA) ENDF/B-VI / U 234(GA) JENDL3
Barns
Ratio
MeV
6

Fig.93

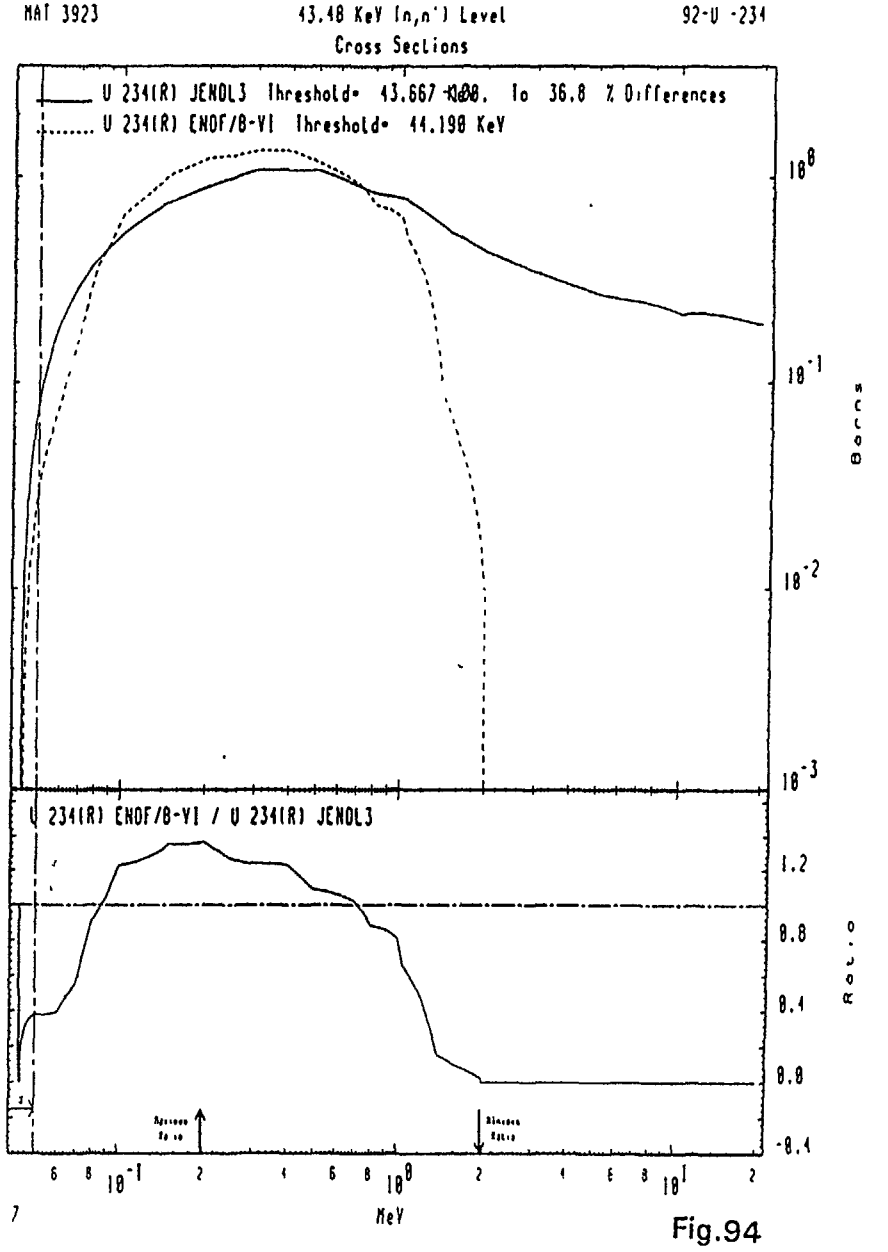
MAT 3923
43.48 KeV (n,n') Level
Cross Sections
92-U -234
U 234(R) JENDL3 Threshold= 43.667 KeV
U 234(R) ENDF/B-VI Threshold= 44.190 KeV
To 36.8 % Differences
U 234(R) ENDF/B-VI / U 234(R) JENDL3
Barns
Ratio
MeV
7

Fig.94

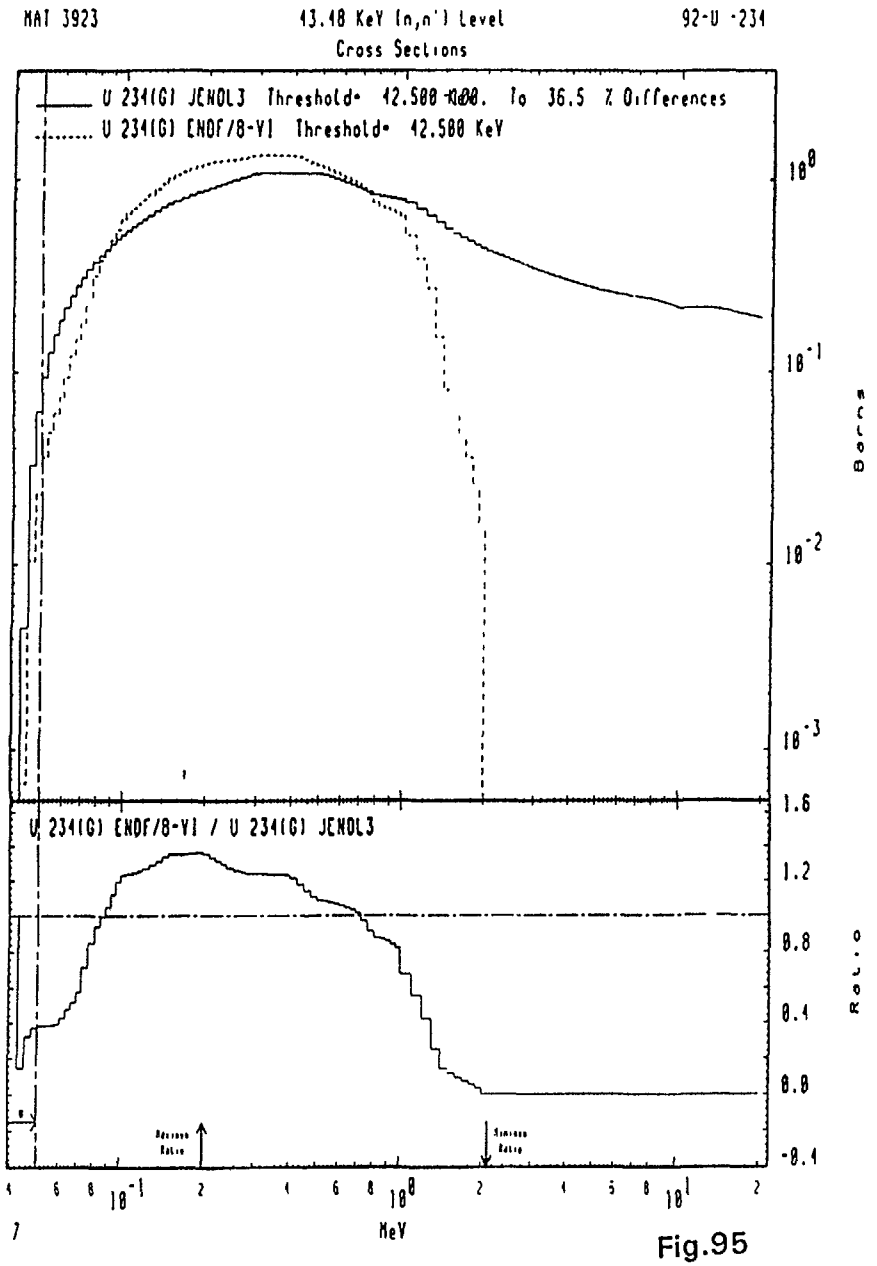
MAT 3923
13.18 KeV (n,n') Level
92-U -234
Cross Sections
U 234(G) JENDL3 Threshold= 42.500 KeV To 36.5 % Differences
U 234(G) ENDF/B-VI Threshold= 42.500 KeV
U 234(G) ENDF/B-VI / U 234(G) JENDL3
Barns
Ratio
MeV

Fig.95

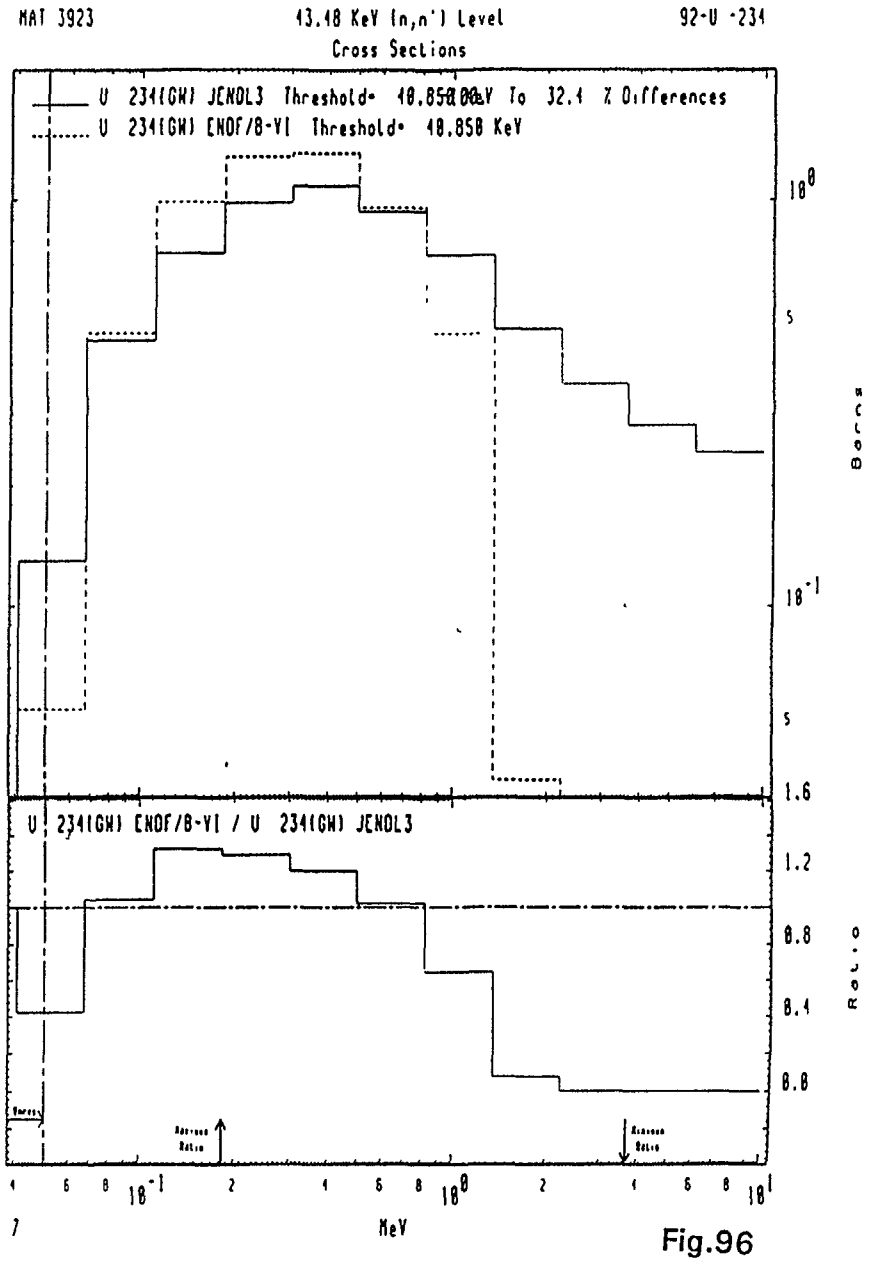
MAT 3923
13.18 KeV (n,n') Level
92-U -234
Cross Sections
U 234(GW) JENDL3 Threshold= 40.858 KeV To 32.1 % Differences
U 234(GW) ENDF/B-VI Threshold= 40.858 KeV
U 234(GW) ENDF/B-VI / U 234(GW) JENDL3
Barns
Ratio
MeV

Fig.96

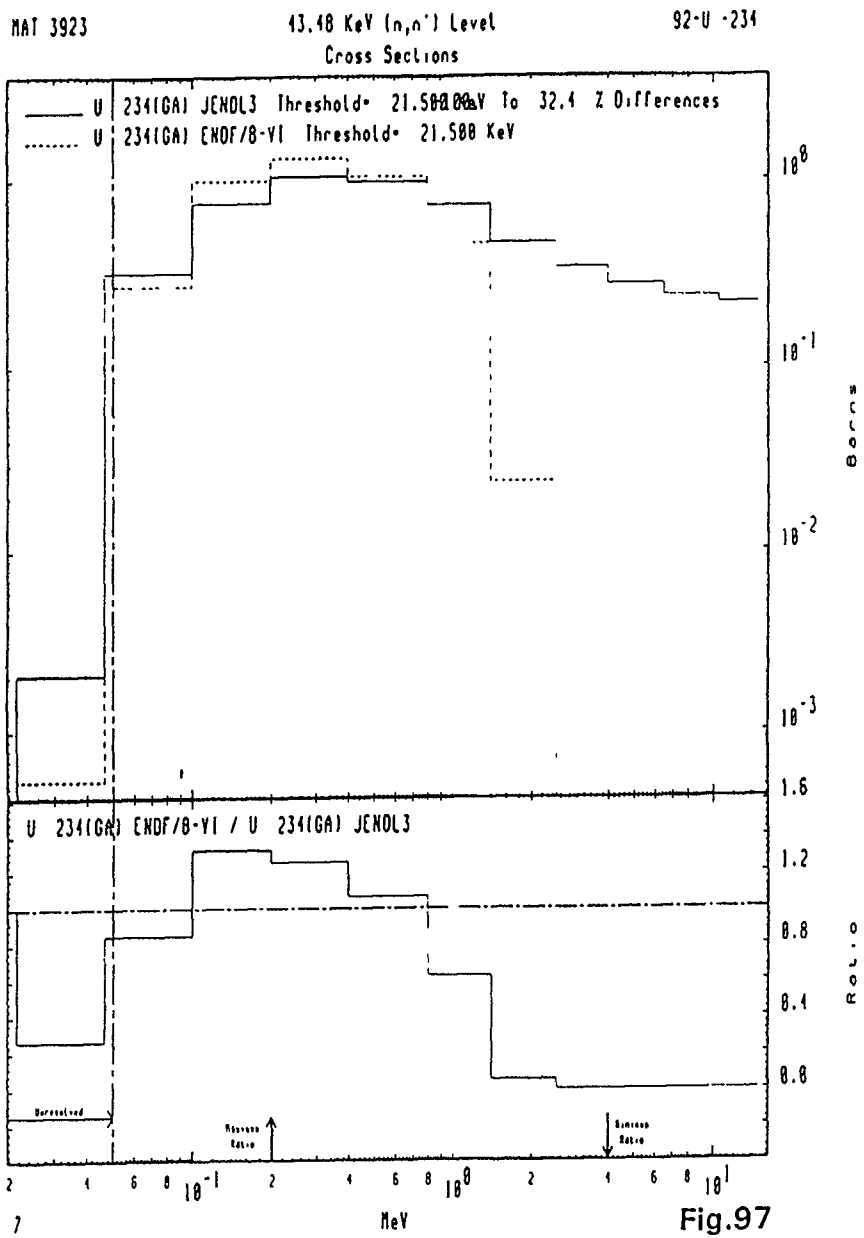
MAT 3923
43.48 KeV (n,n') Level
Cross Sections
92-U -234
U 234(GA) JENDL3 Threshold= 21.500 KeV to 32.4 % Differences
U 234(GA) ENDF/B-VI Threshold= 21.500 KeV
Barns
U 234(GA) ENDF/B-VI / U 234(GA) JENDL3
Ratio
MeV
7

Fig.97

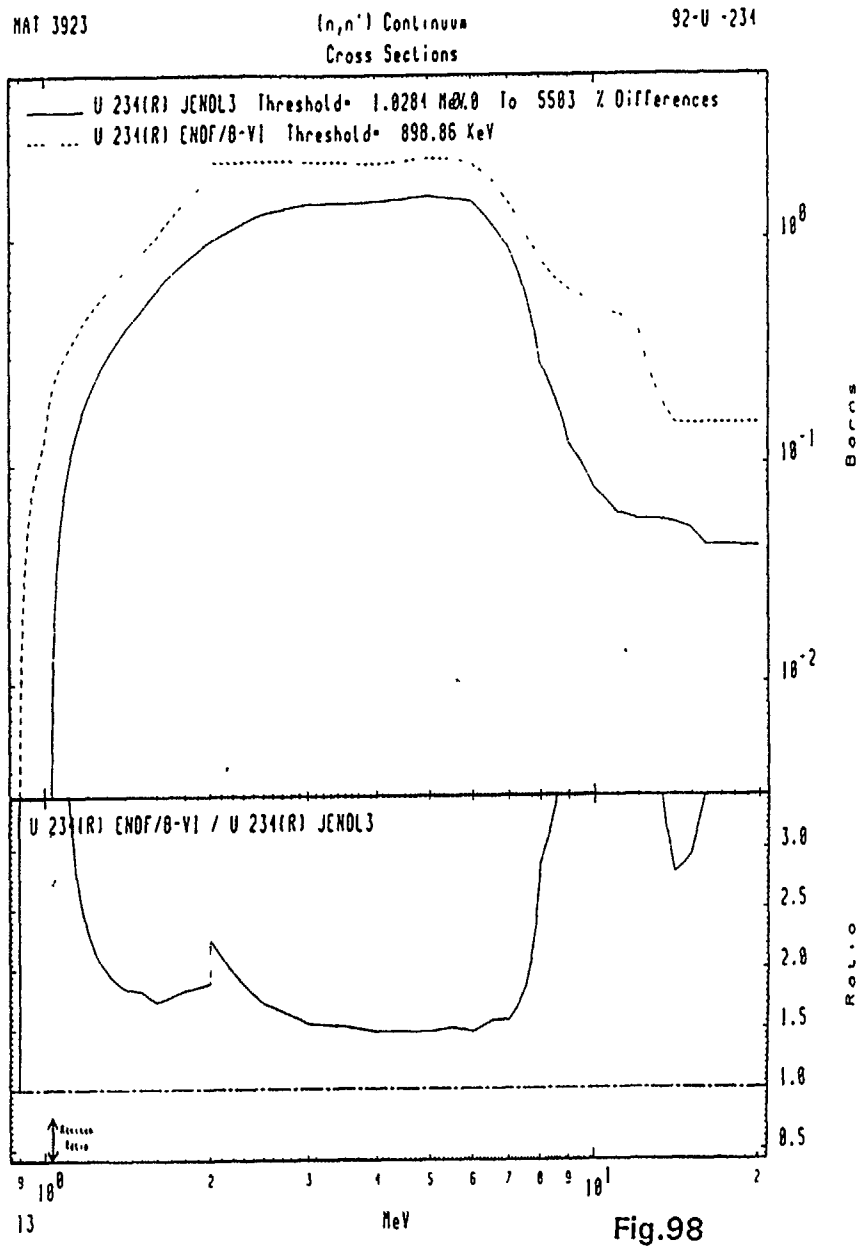
MAT 3923
(n,n') Continuum
Cross Sections
92-U -234
U 234(R) JENDL3 Threshold= 1.0284 MeV to 5503 % Differences
U 234(R) ENDF/B-VI Threshold= 898.86 KeV
Barns
U 234(R) ENDF/B-VI / U 234(R) JENDL3
Ratio
MeV
13

Fig.98

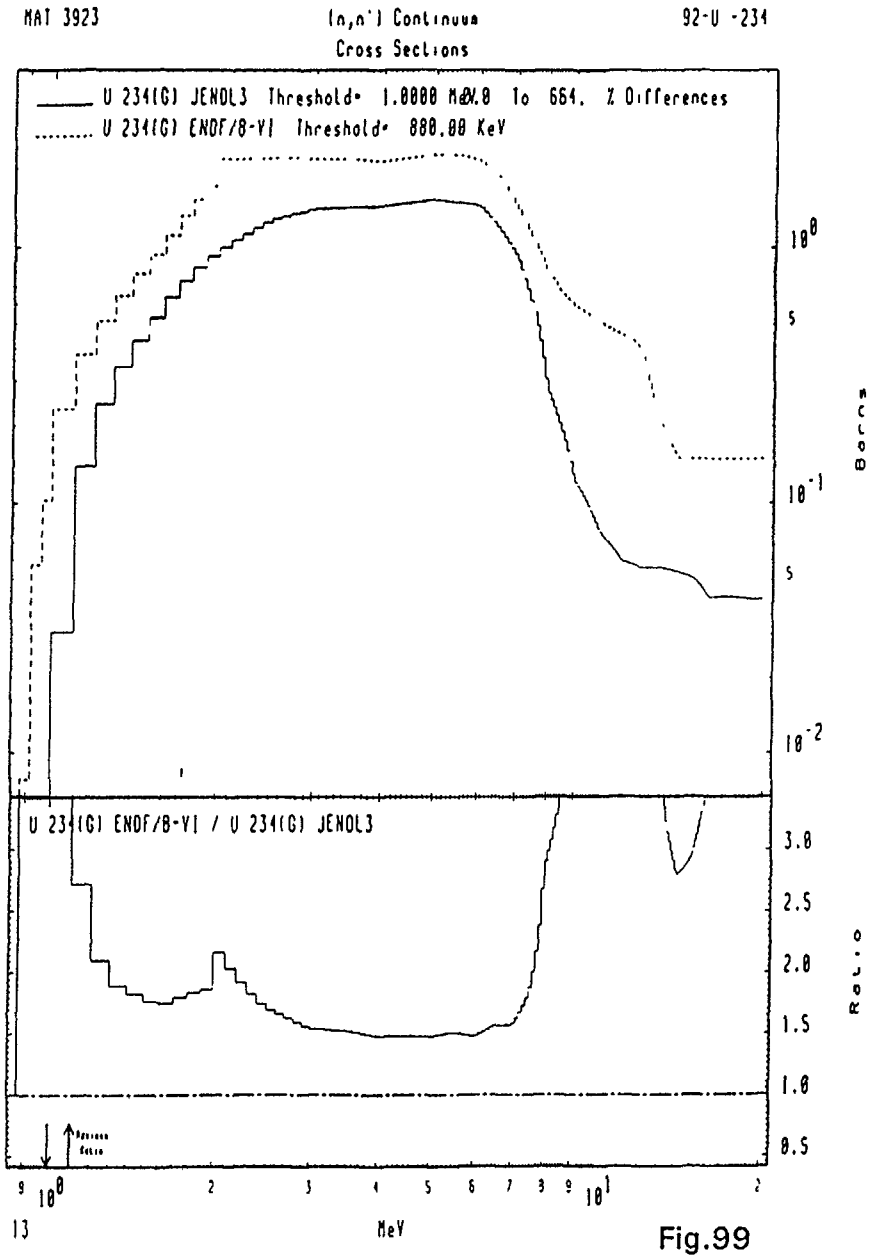

Fig.99

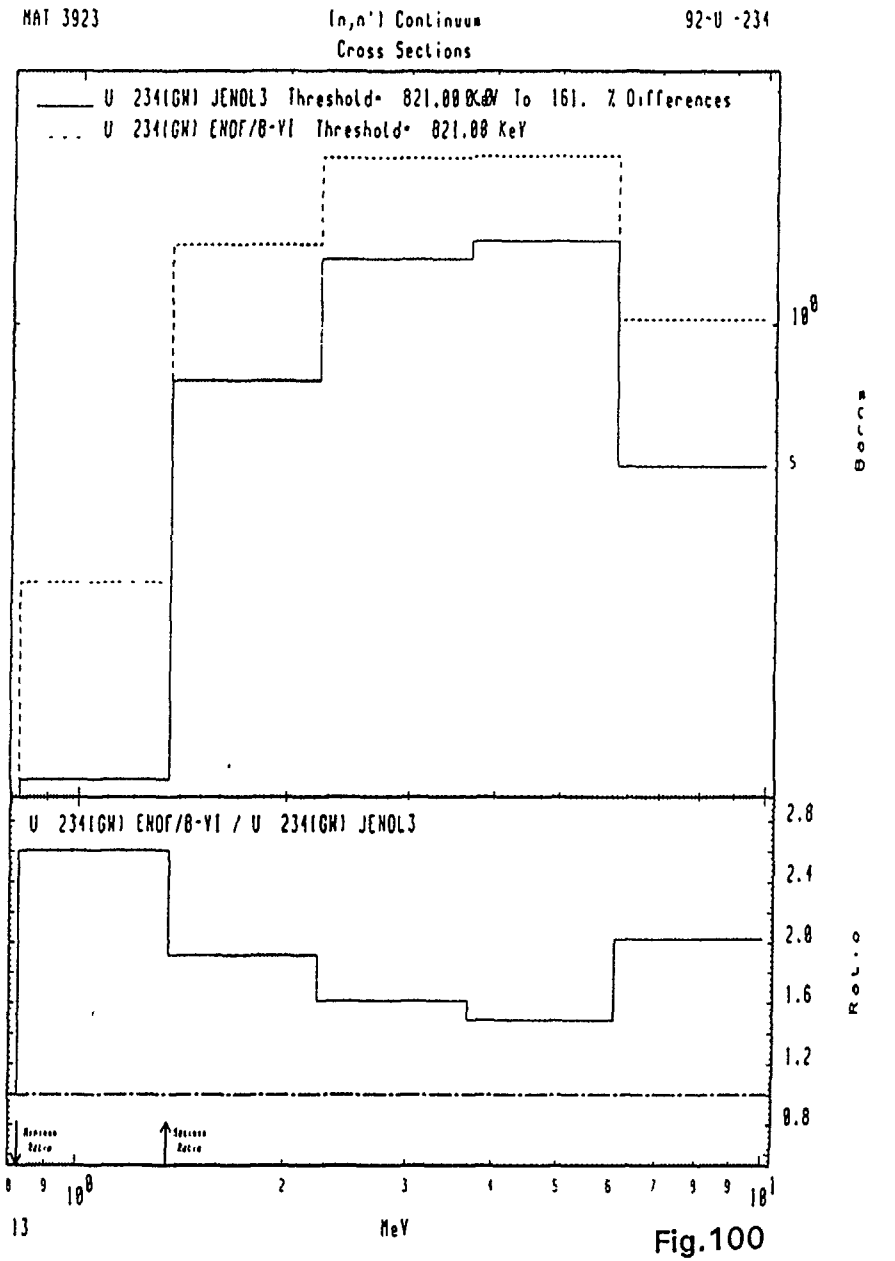

Fig.100

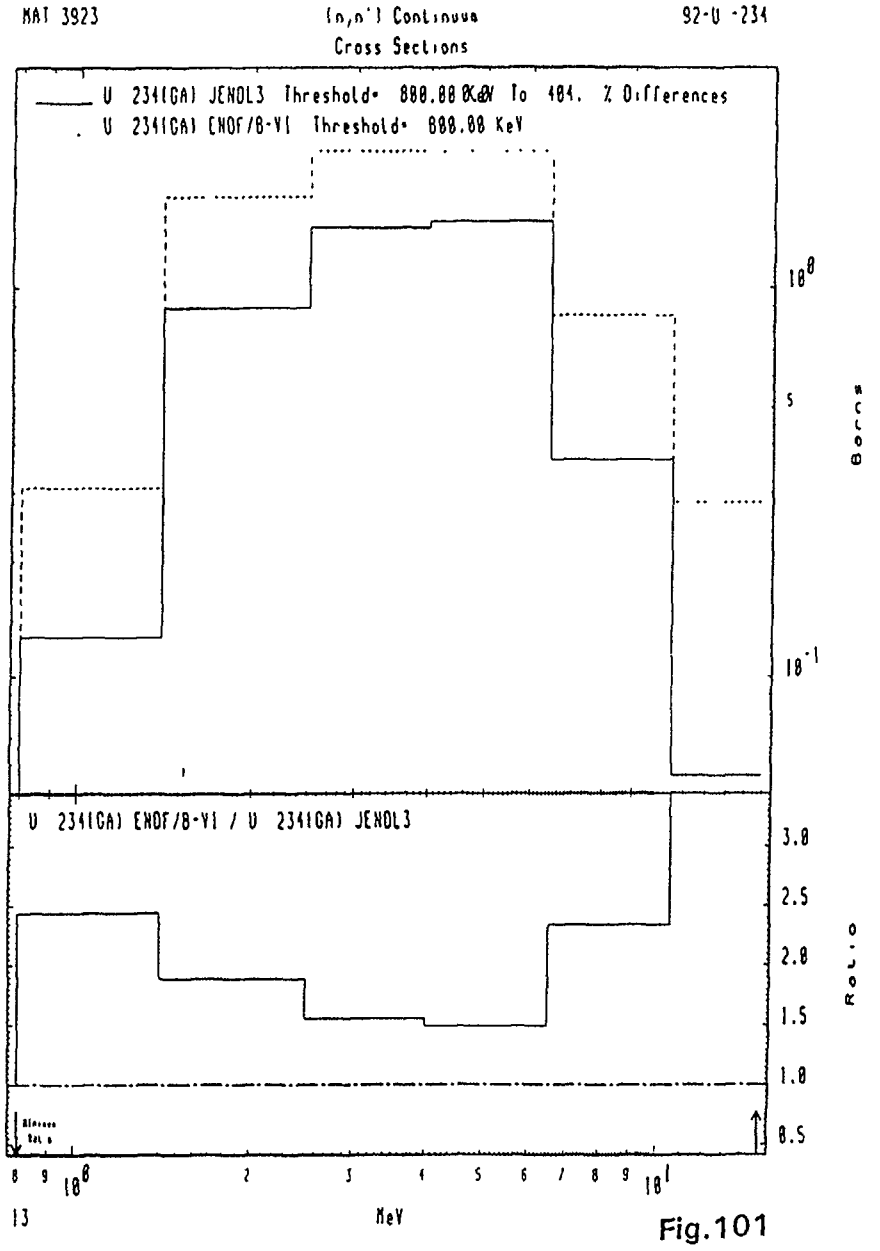

Fig.101

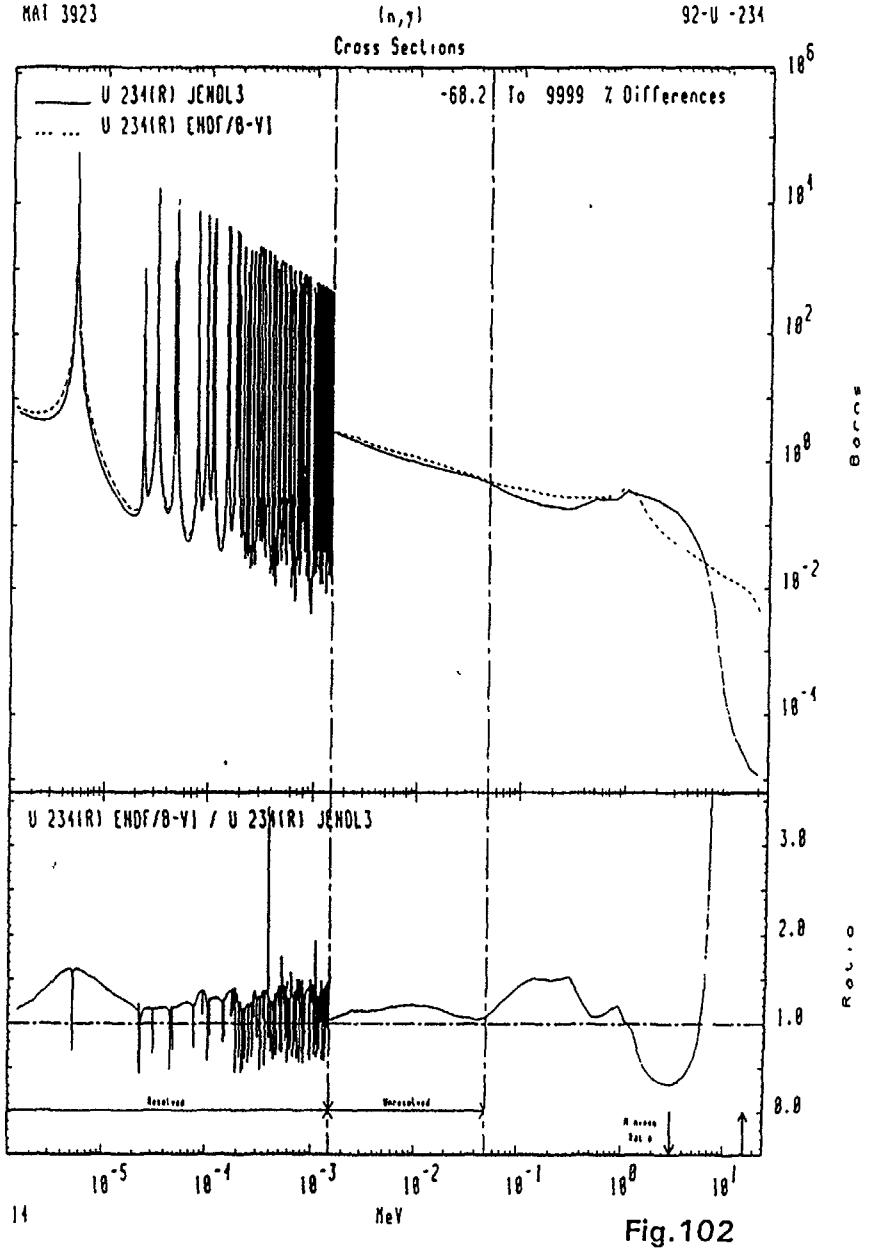

Fig.102

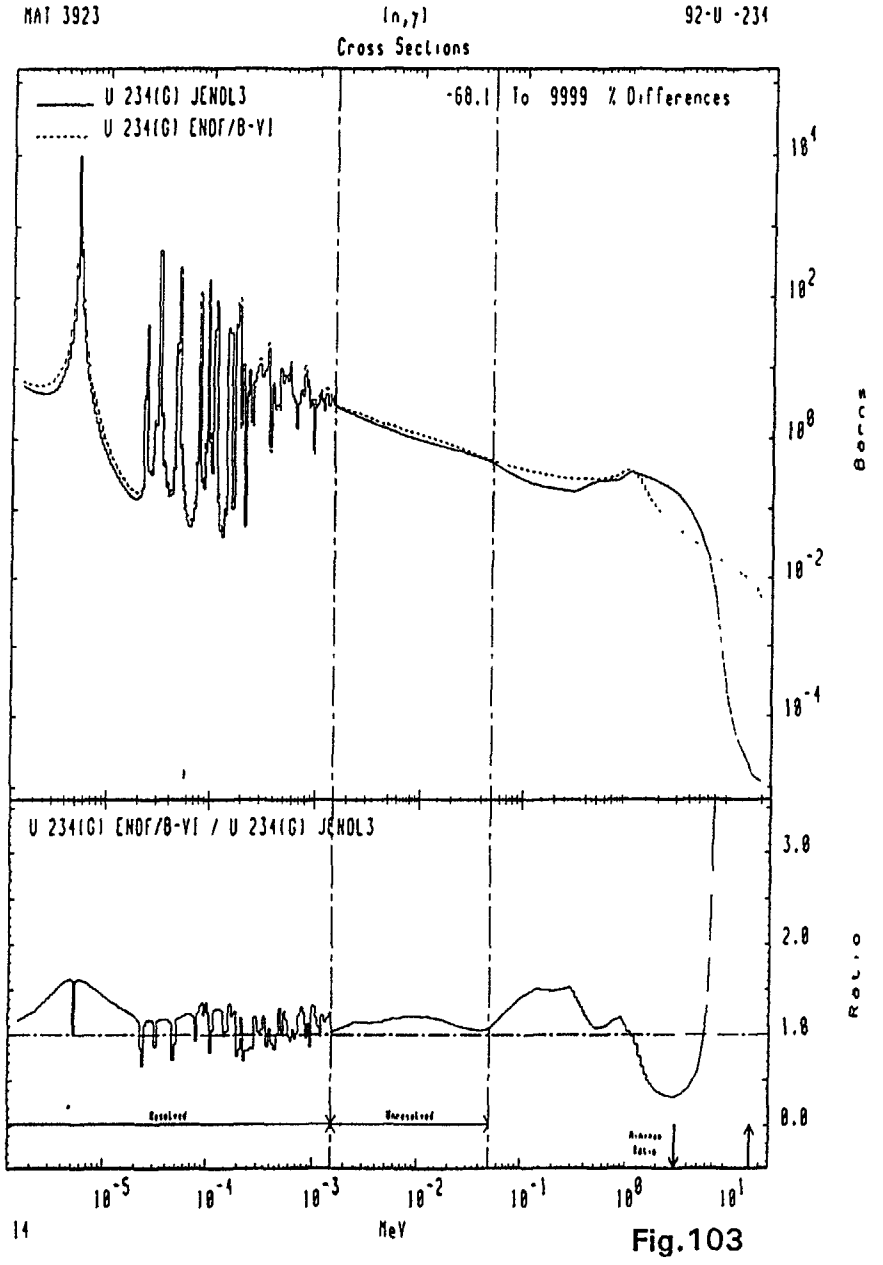

Fig.103

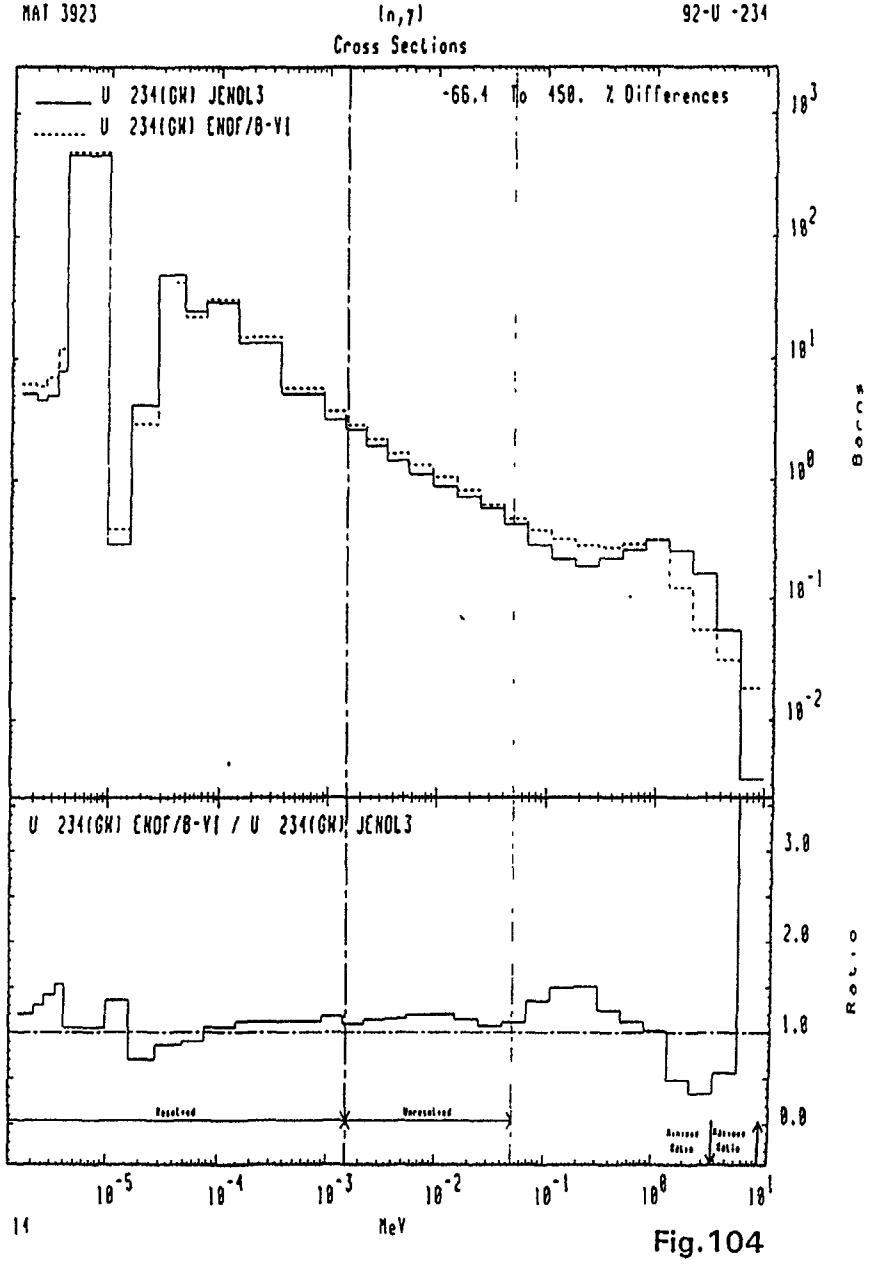

Fig.104

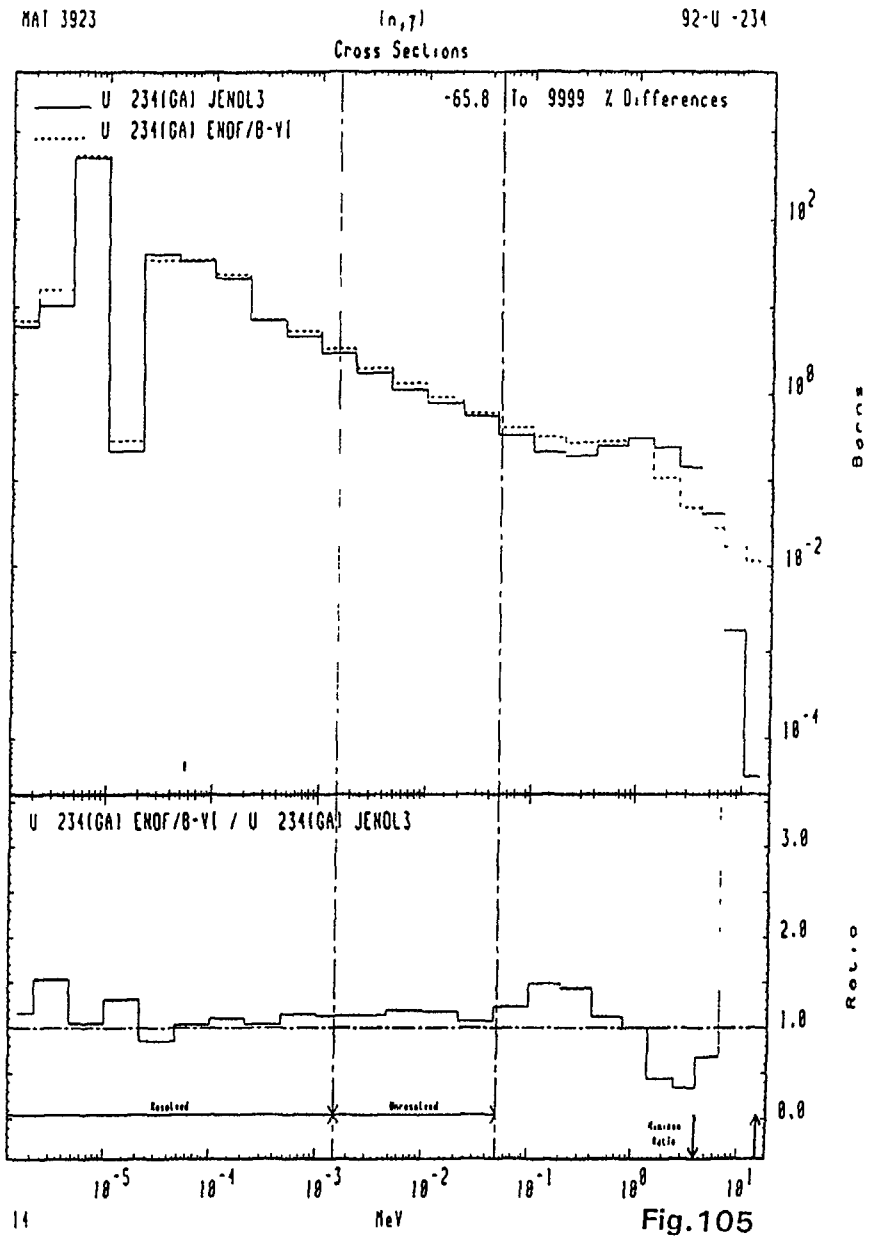

Fig.105

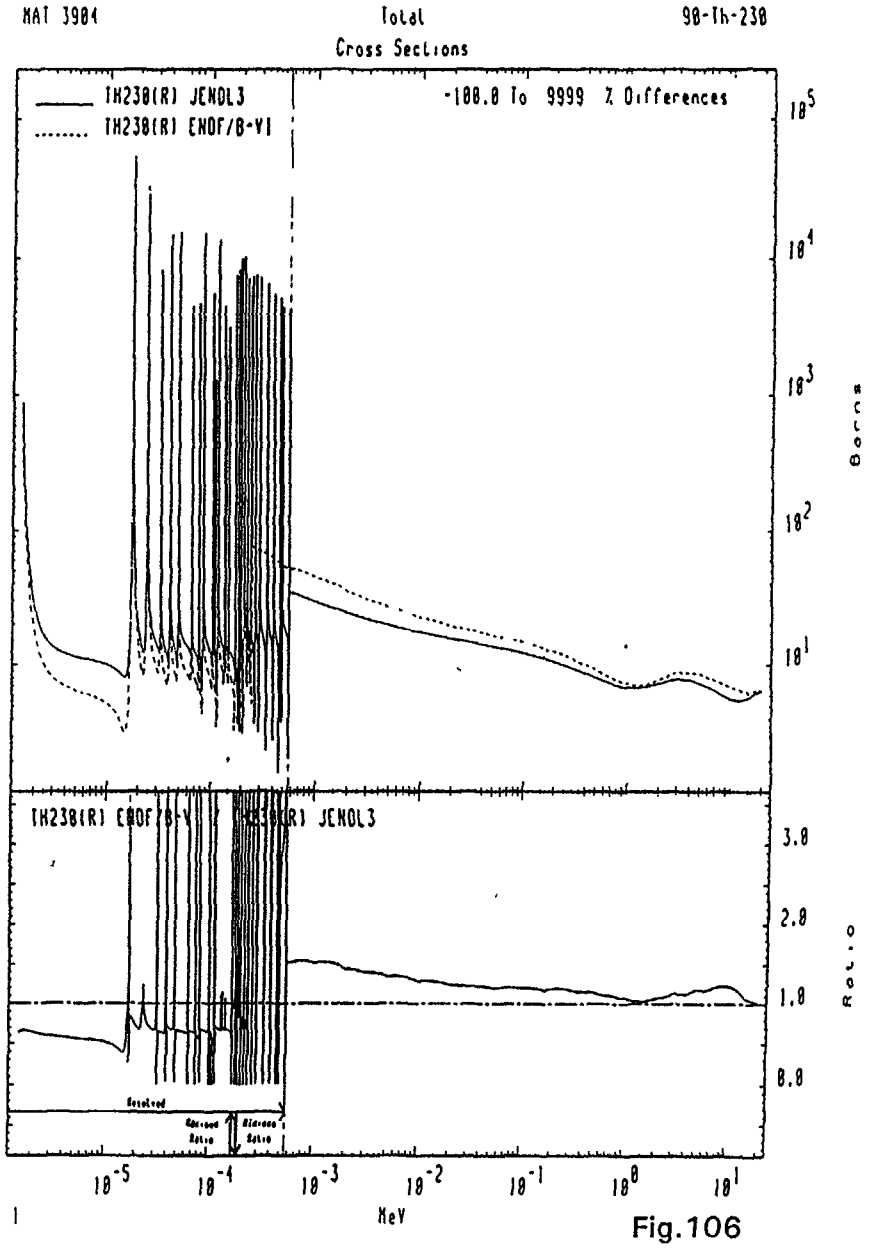

Fig.106

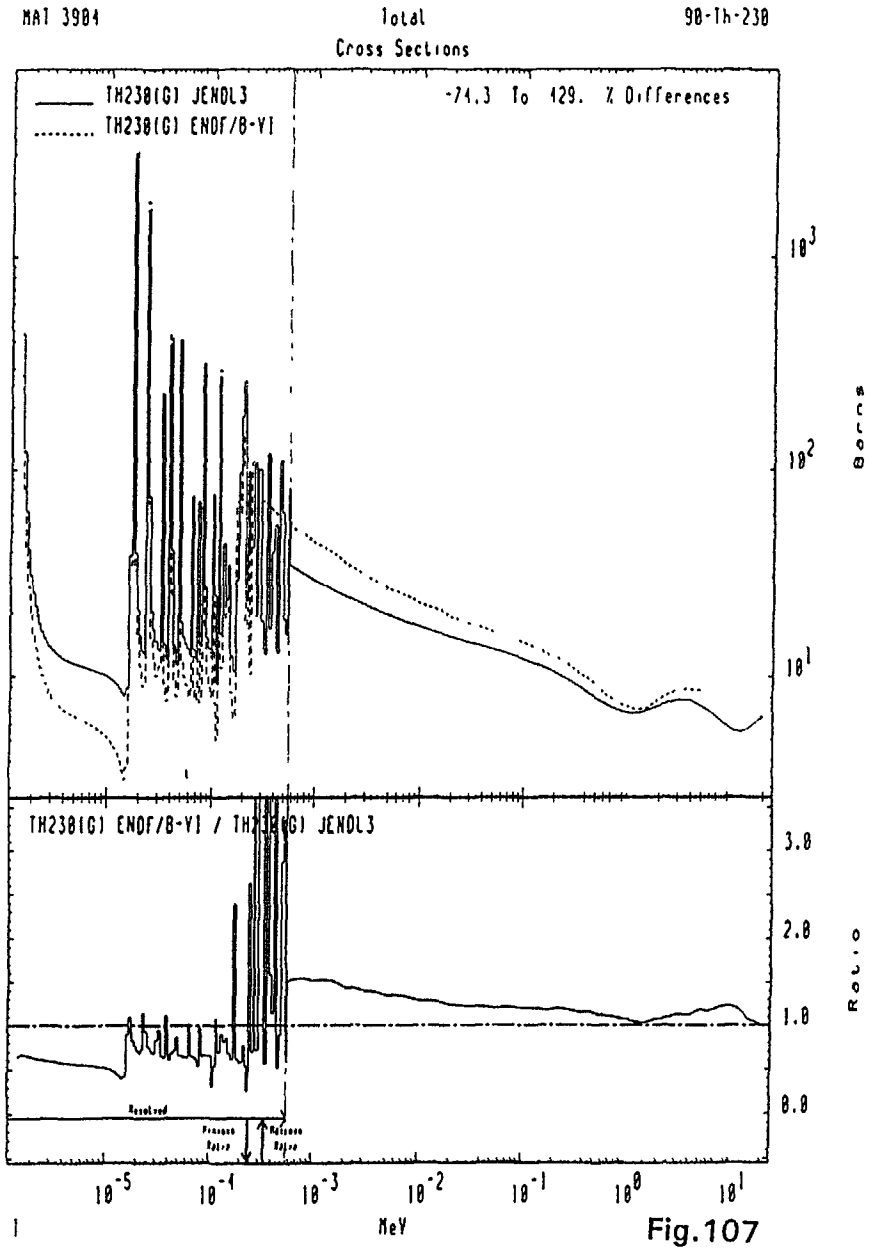

Fig.107

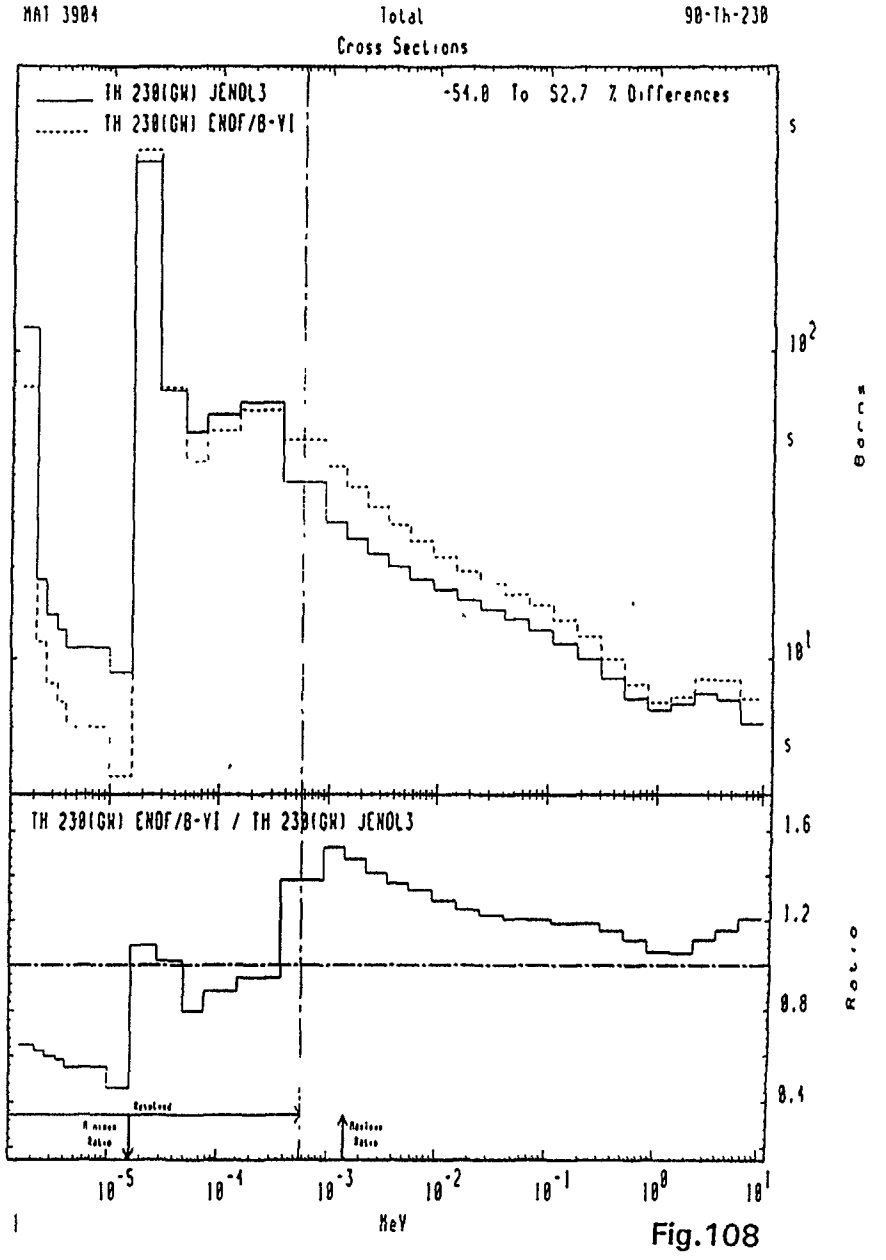

Fig.108

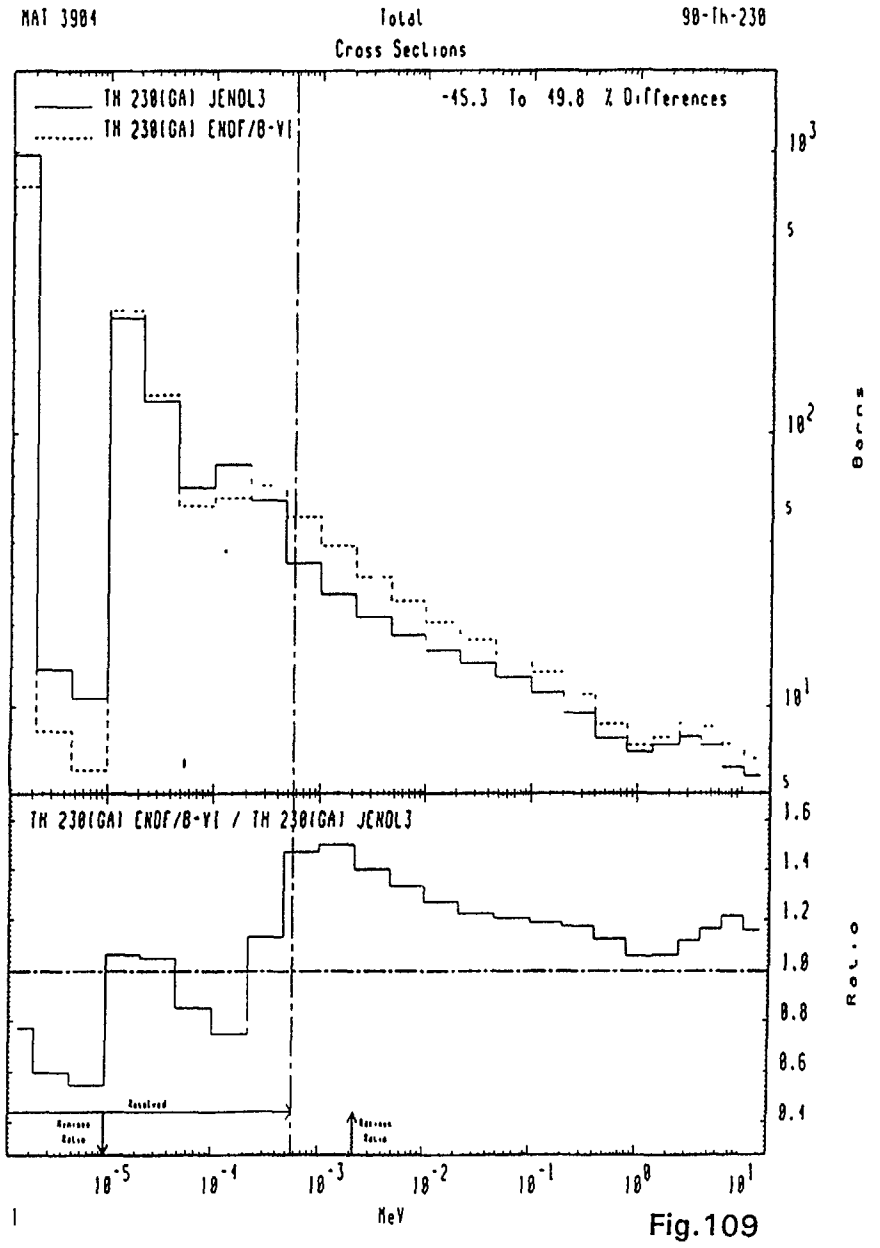

Fig.109

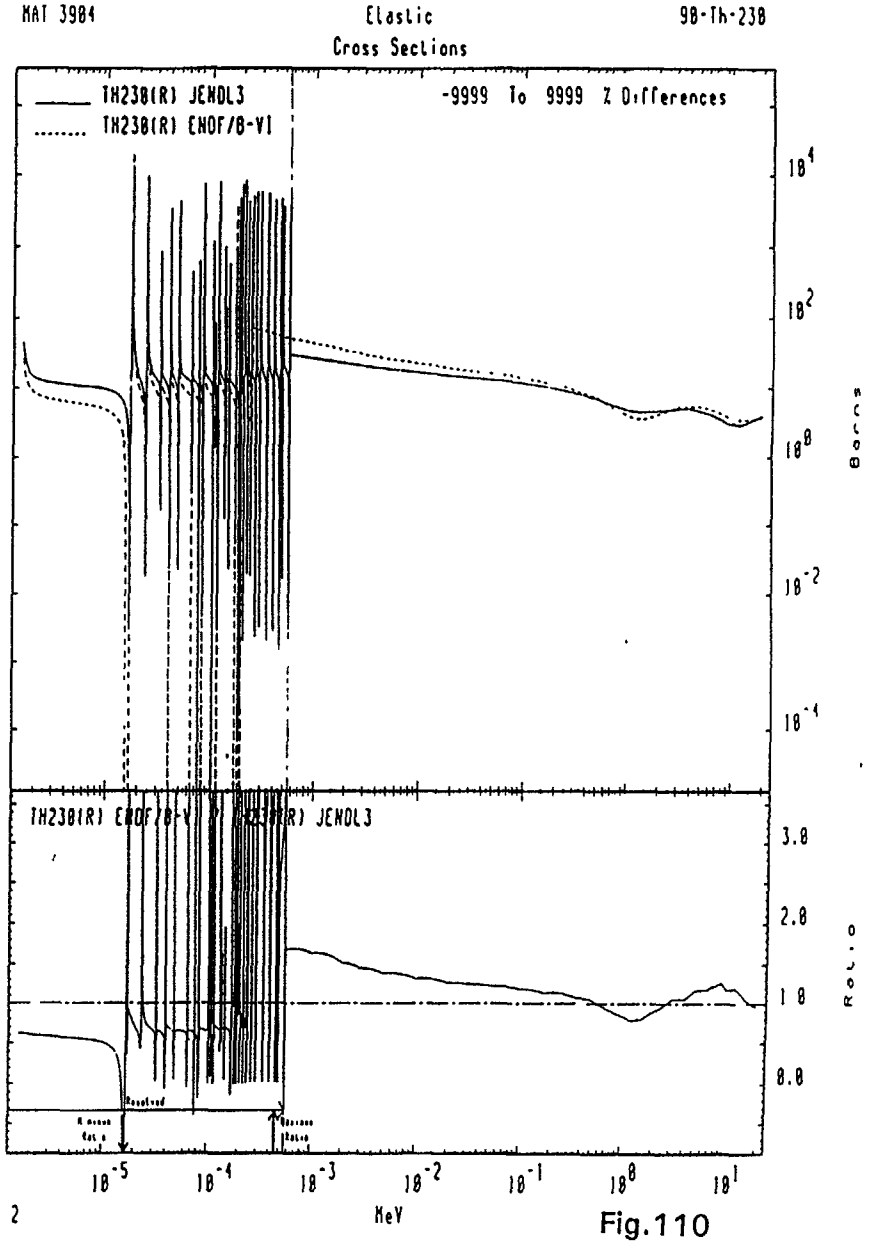

Fig.110

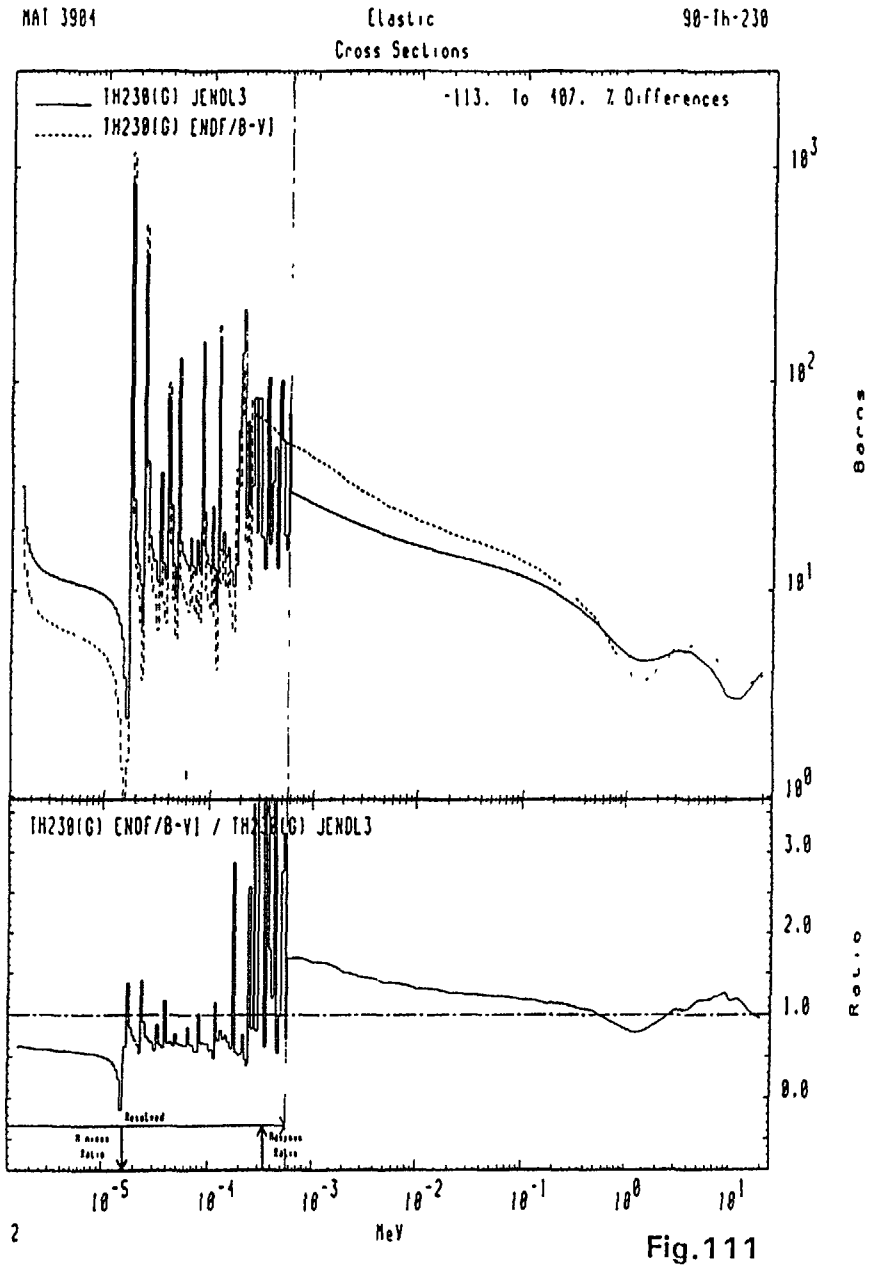

Fig.111

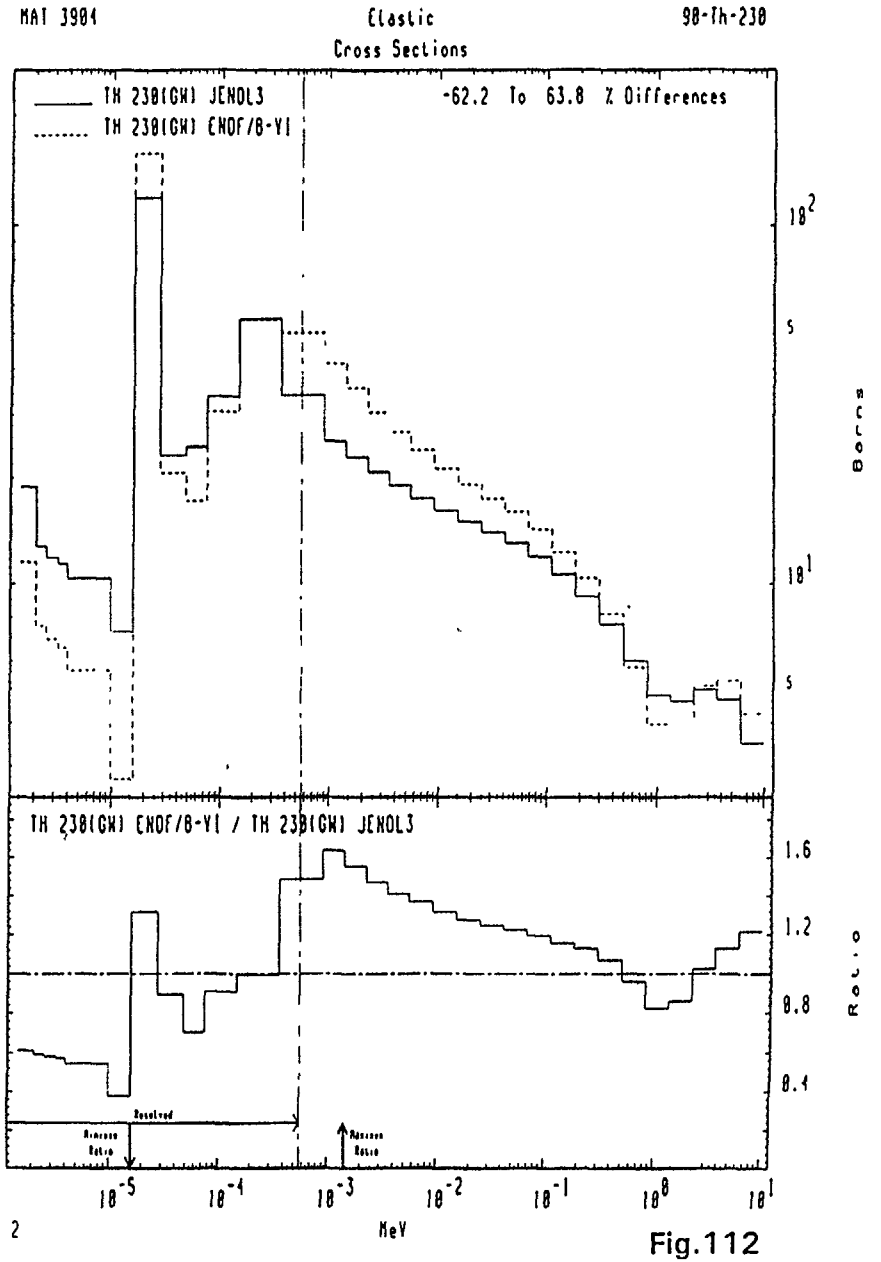

Fig.112

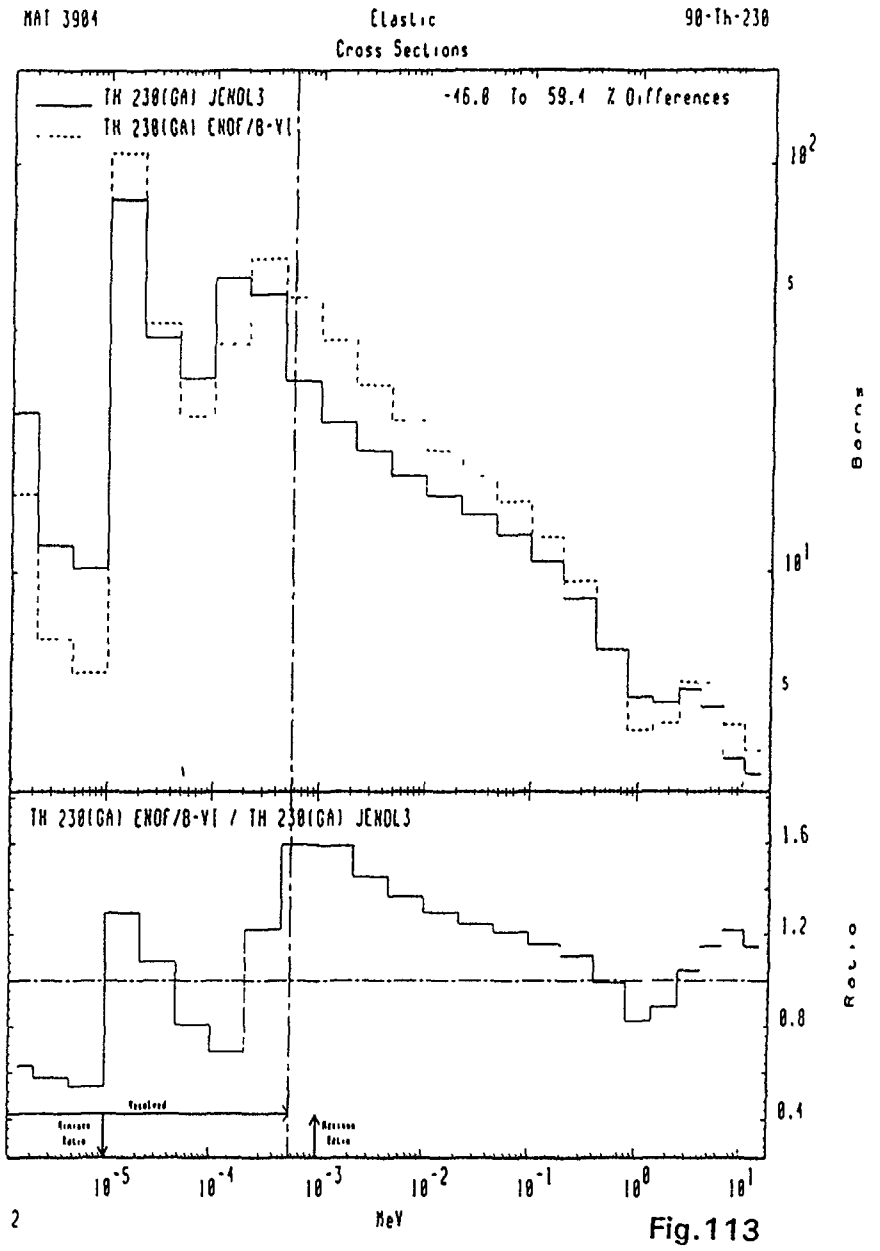

Fig.113

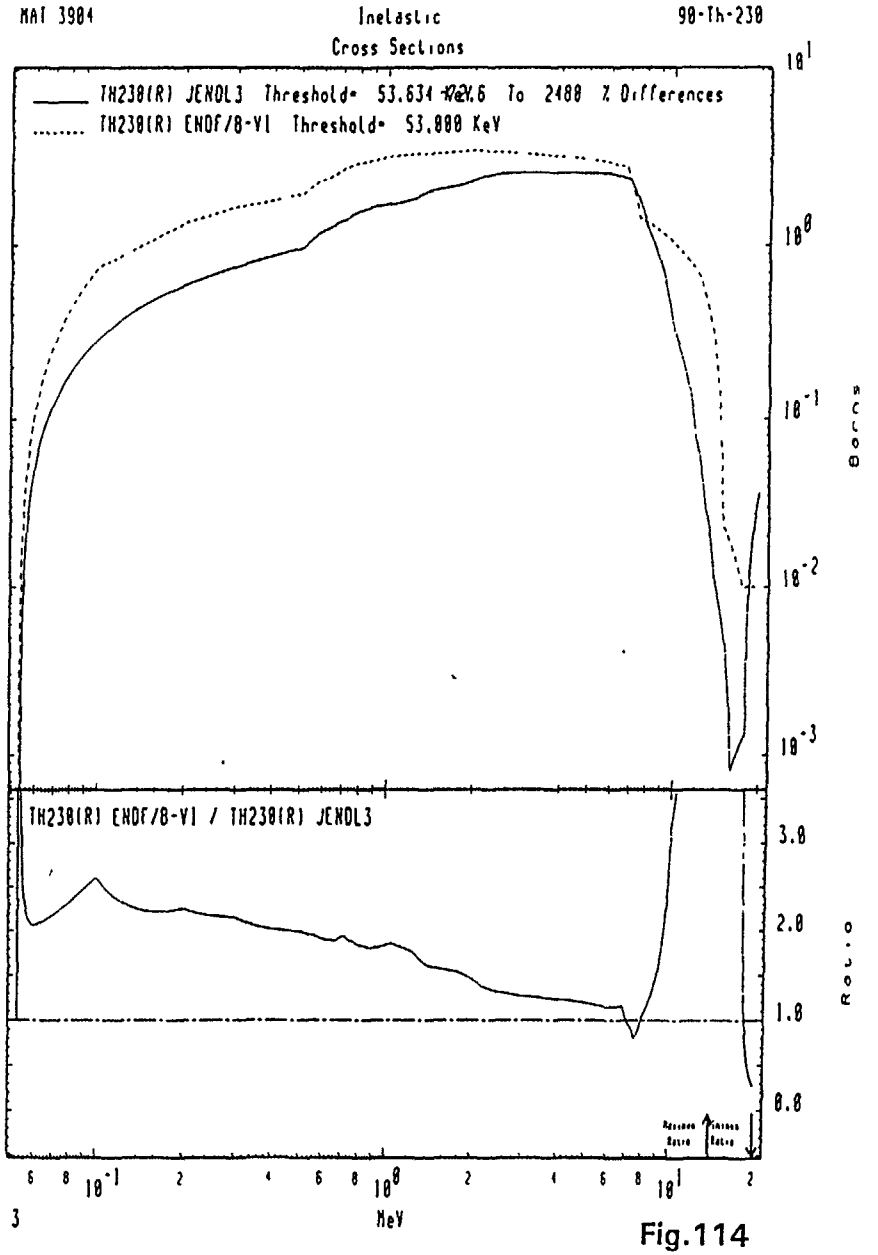

Fig.114

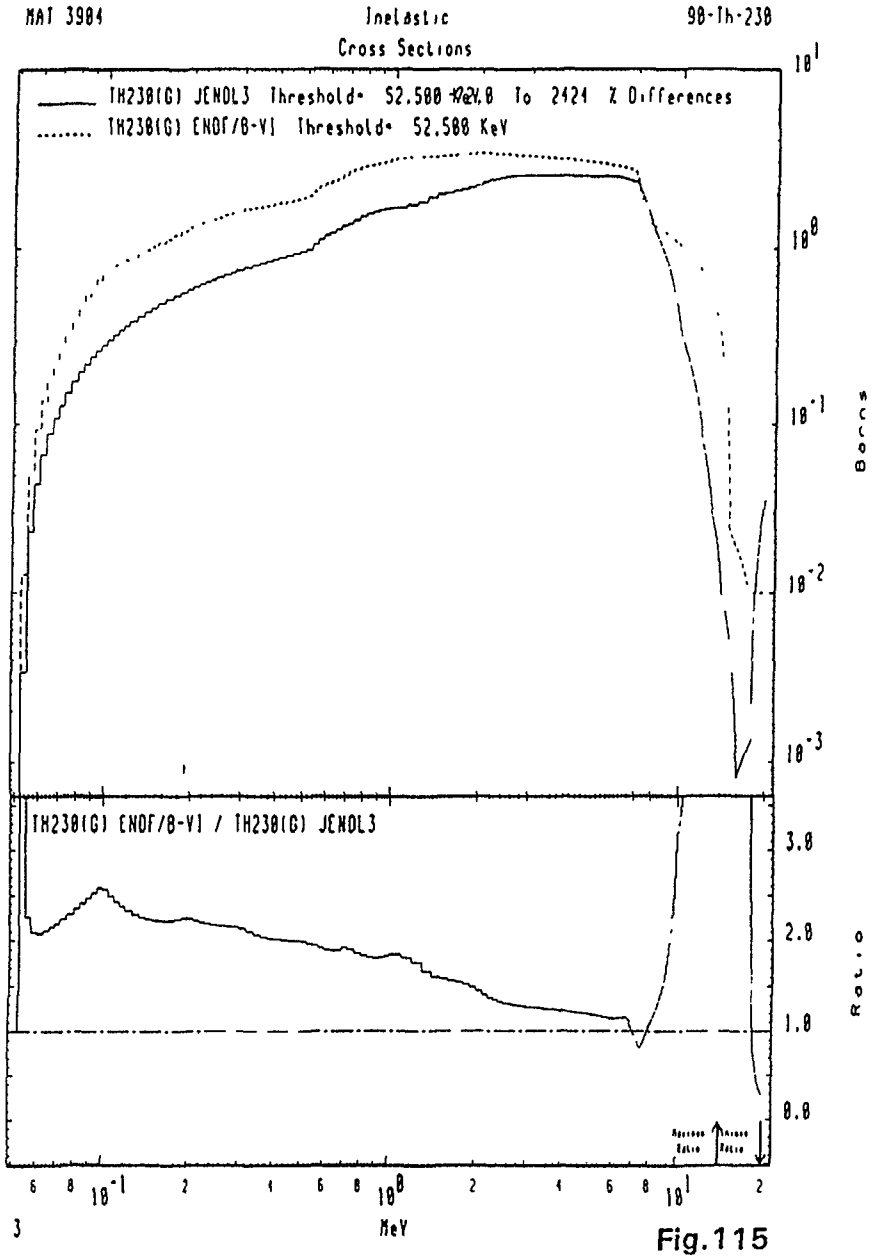

Fig.115

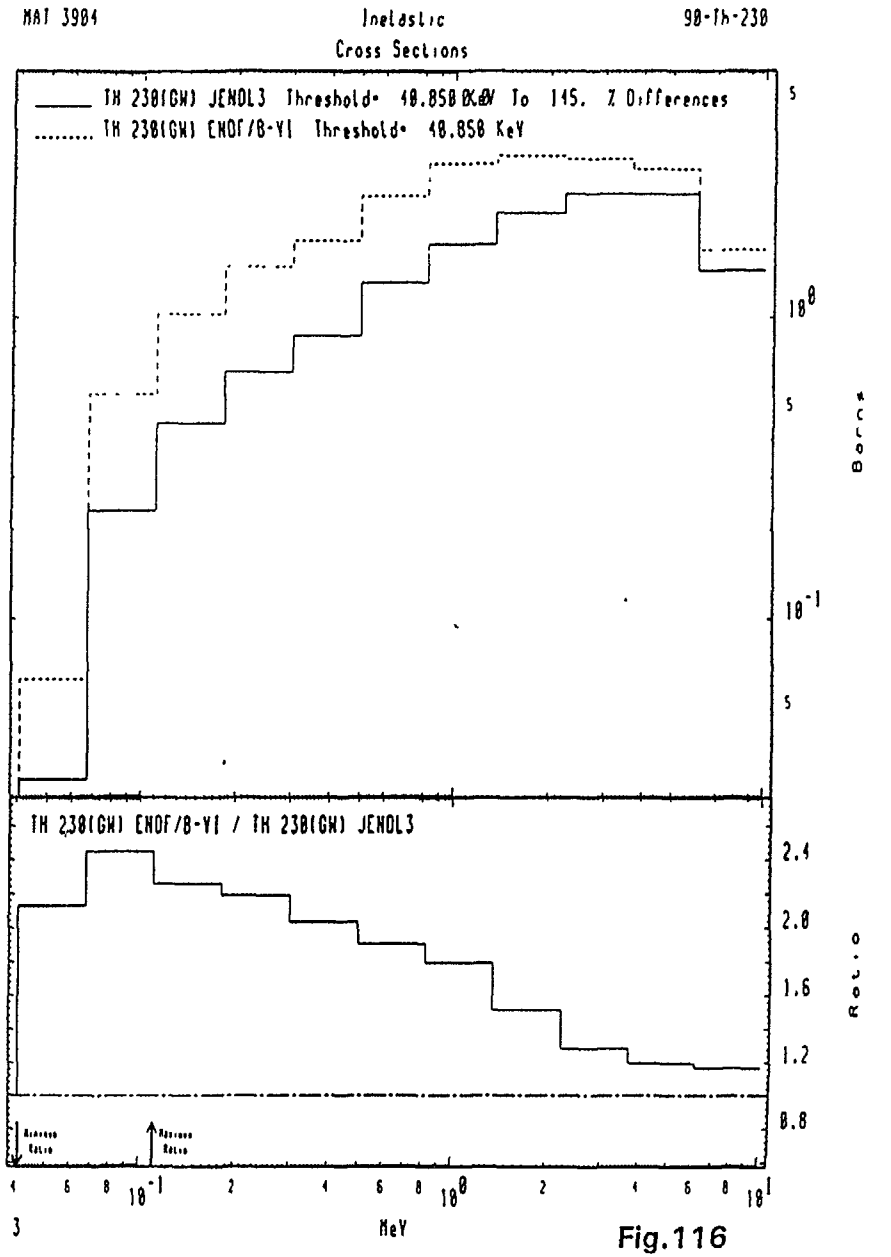

Fig.116

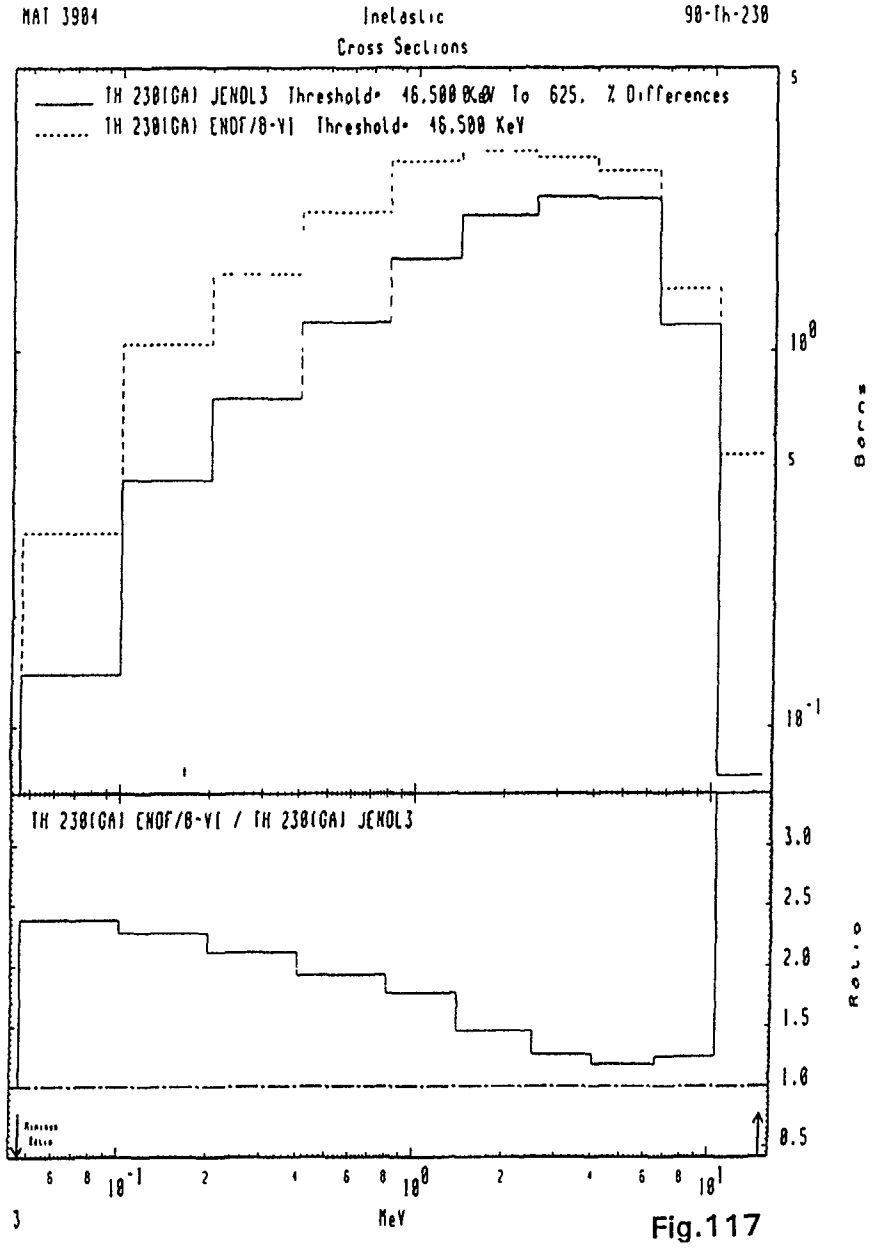

Fig.117

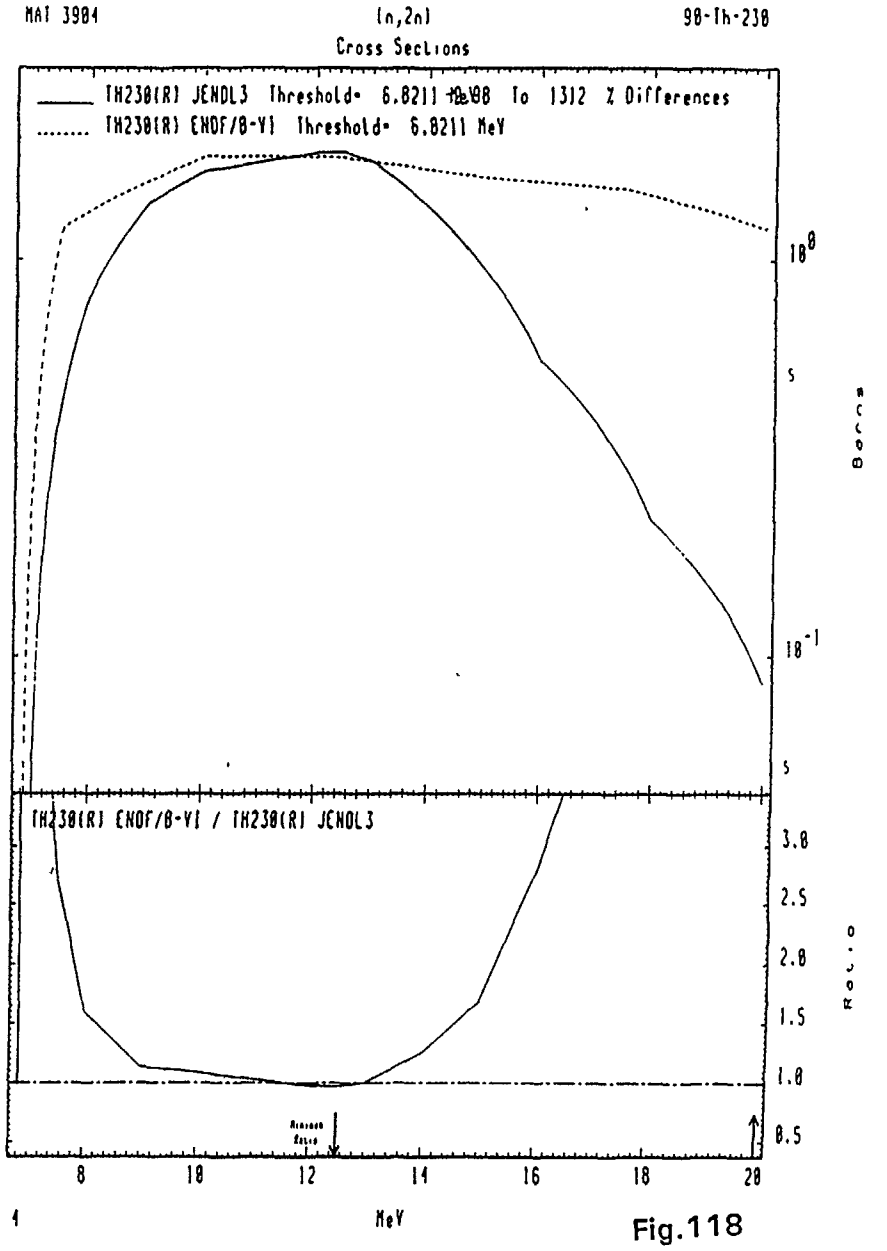

Fig.118

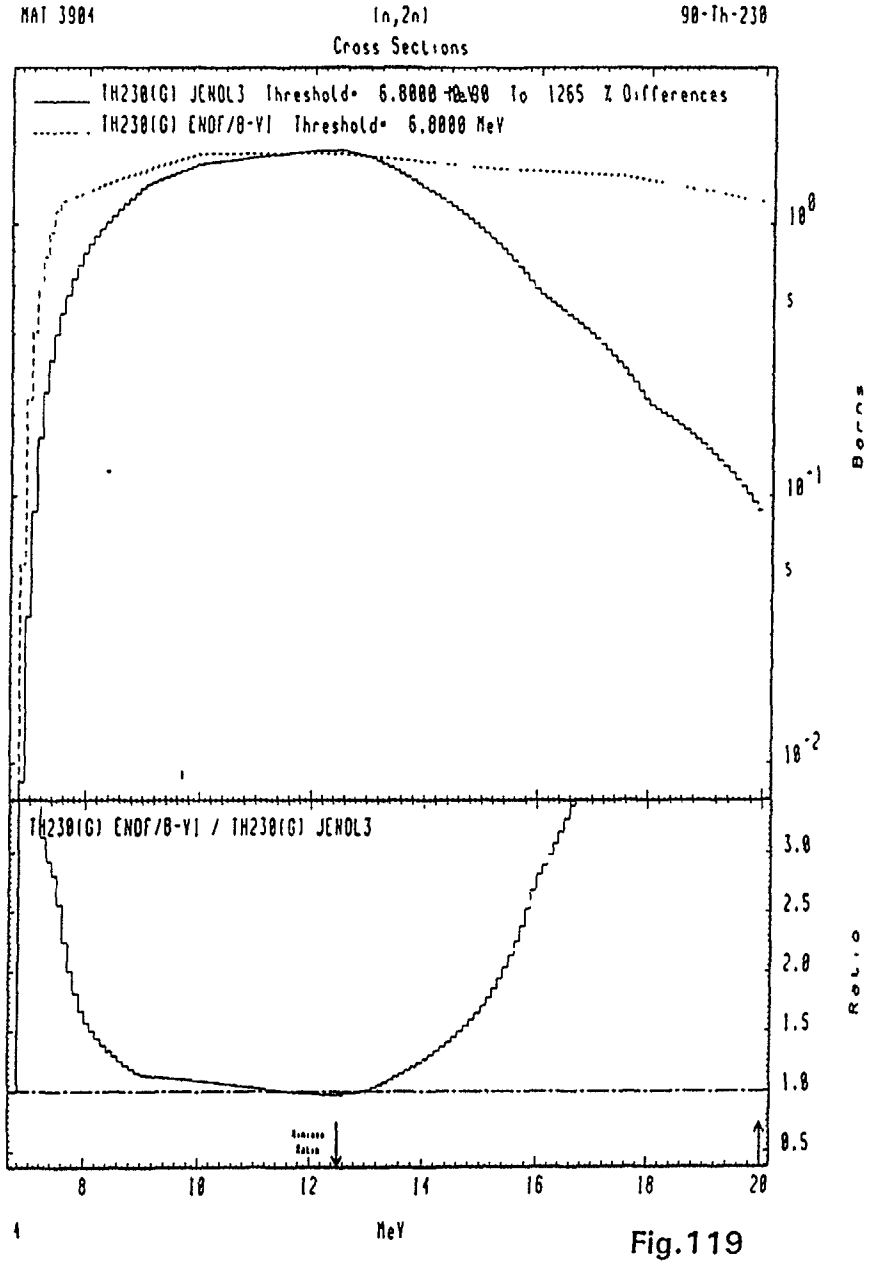

Fig.119

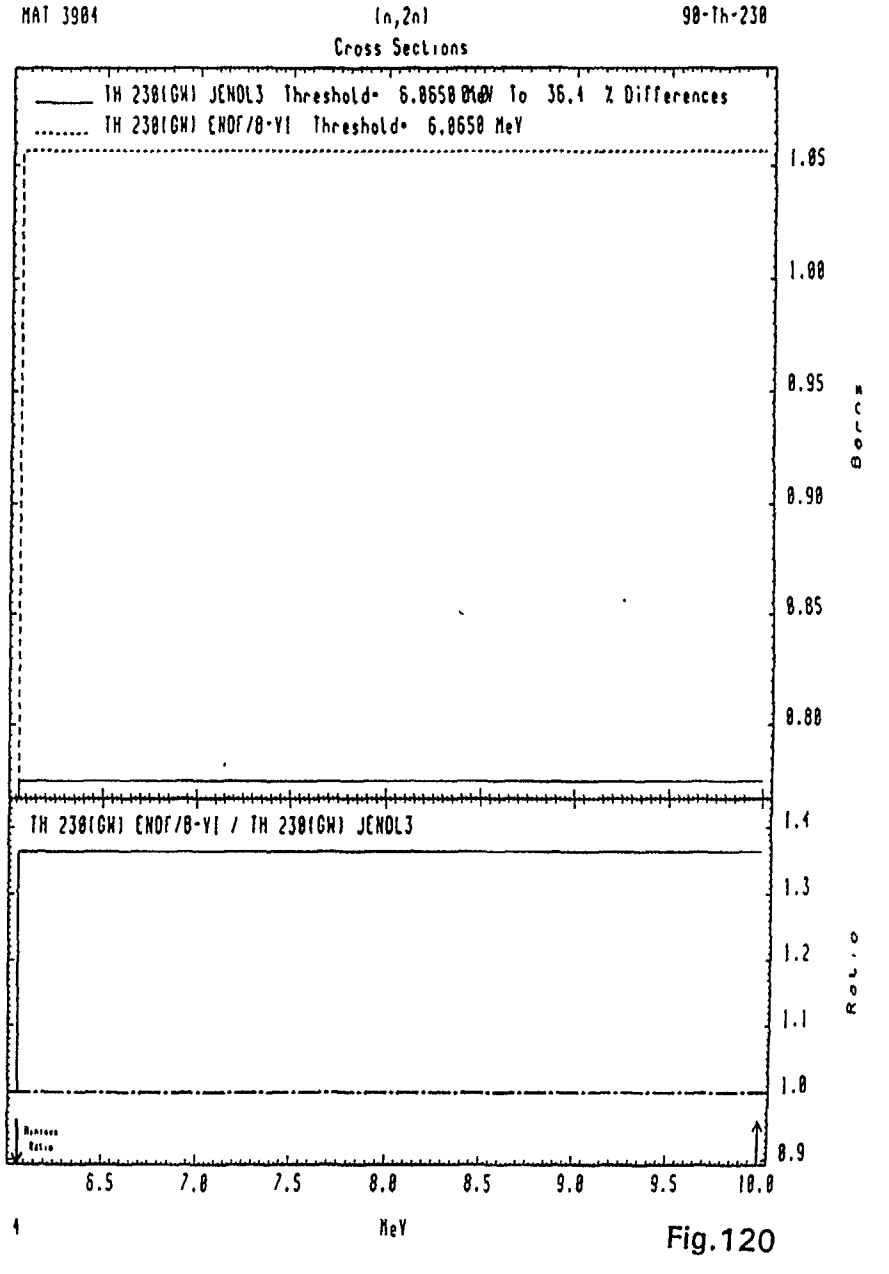

Fig.120

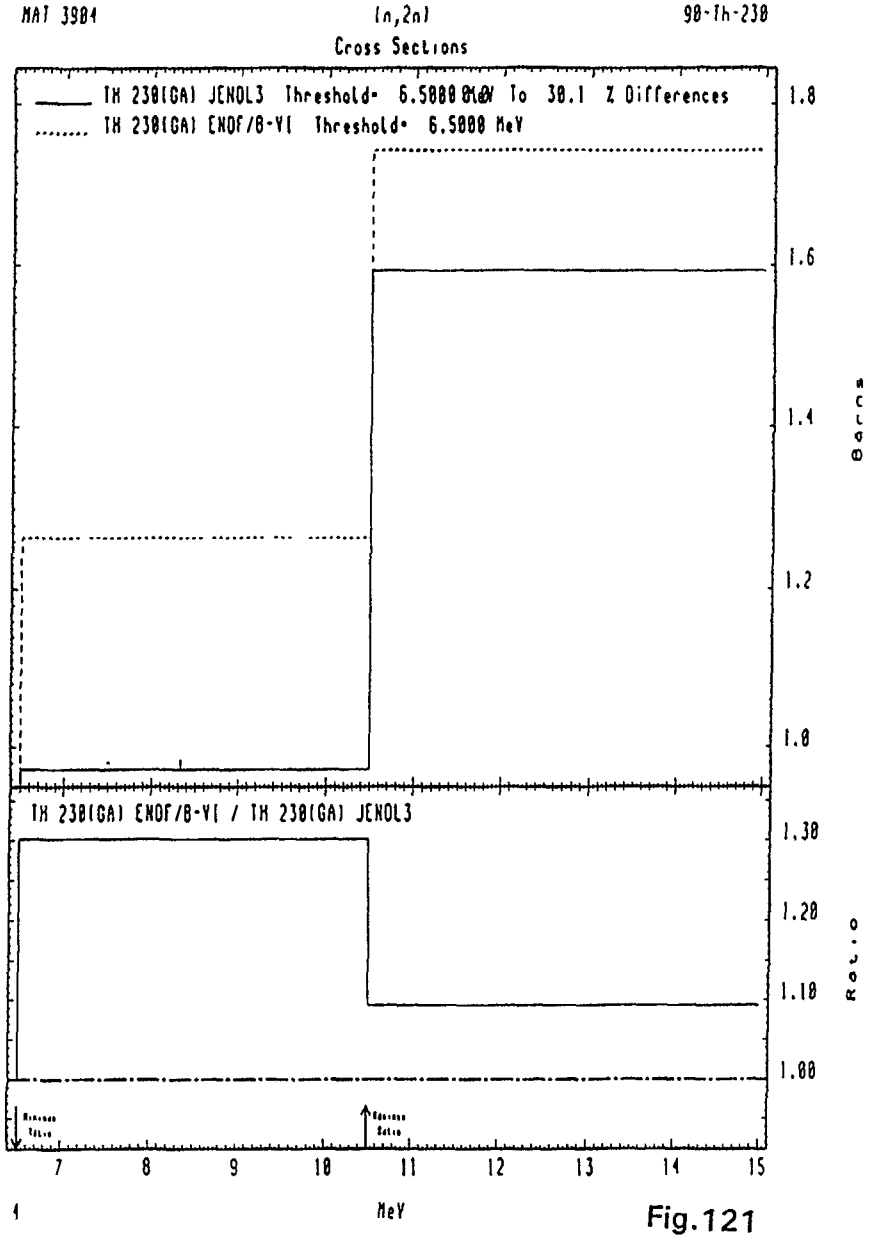

Fig.121

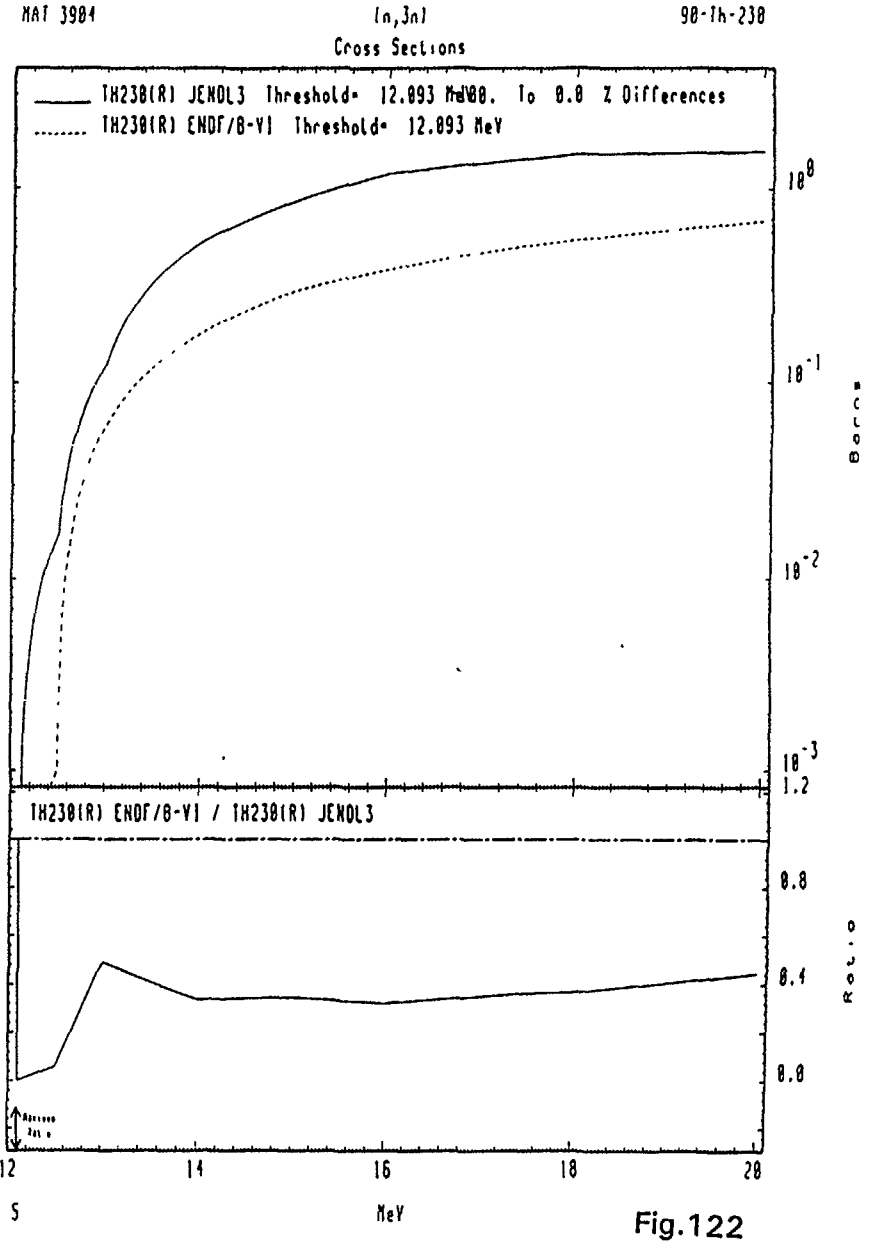

Fig.122

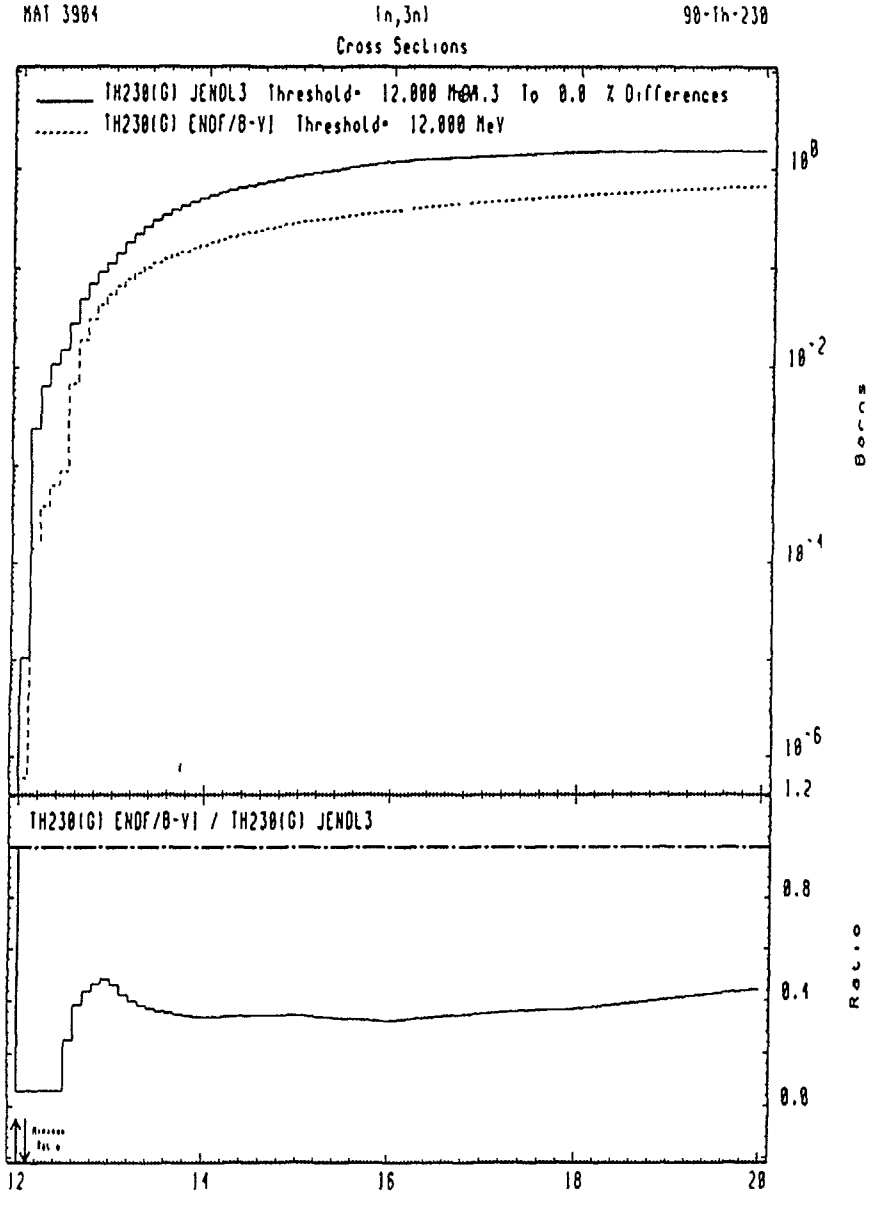

Fig.123

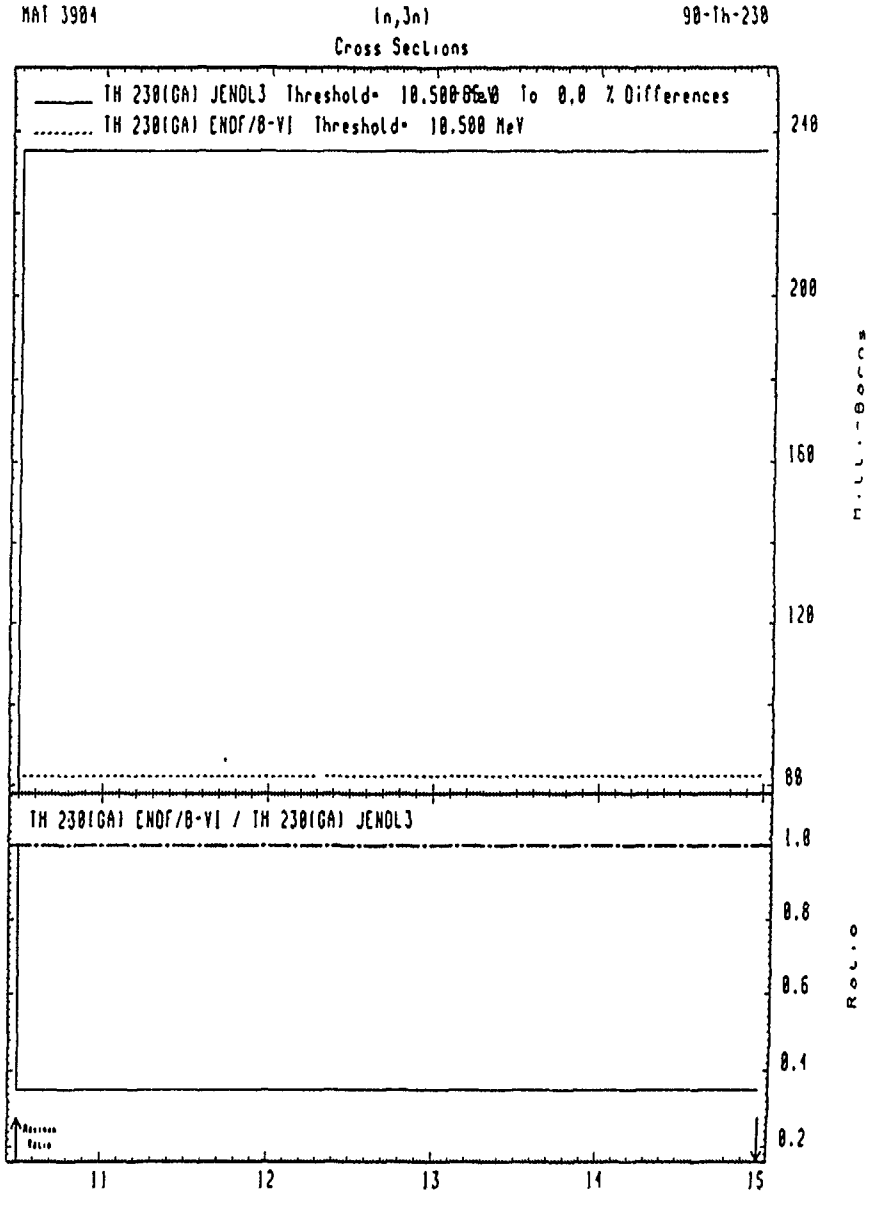

Fig.124

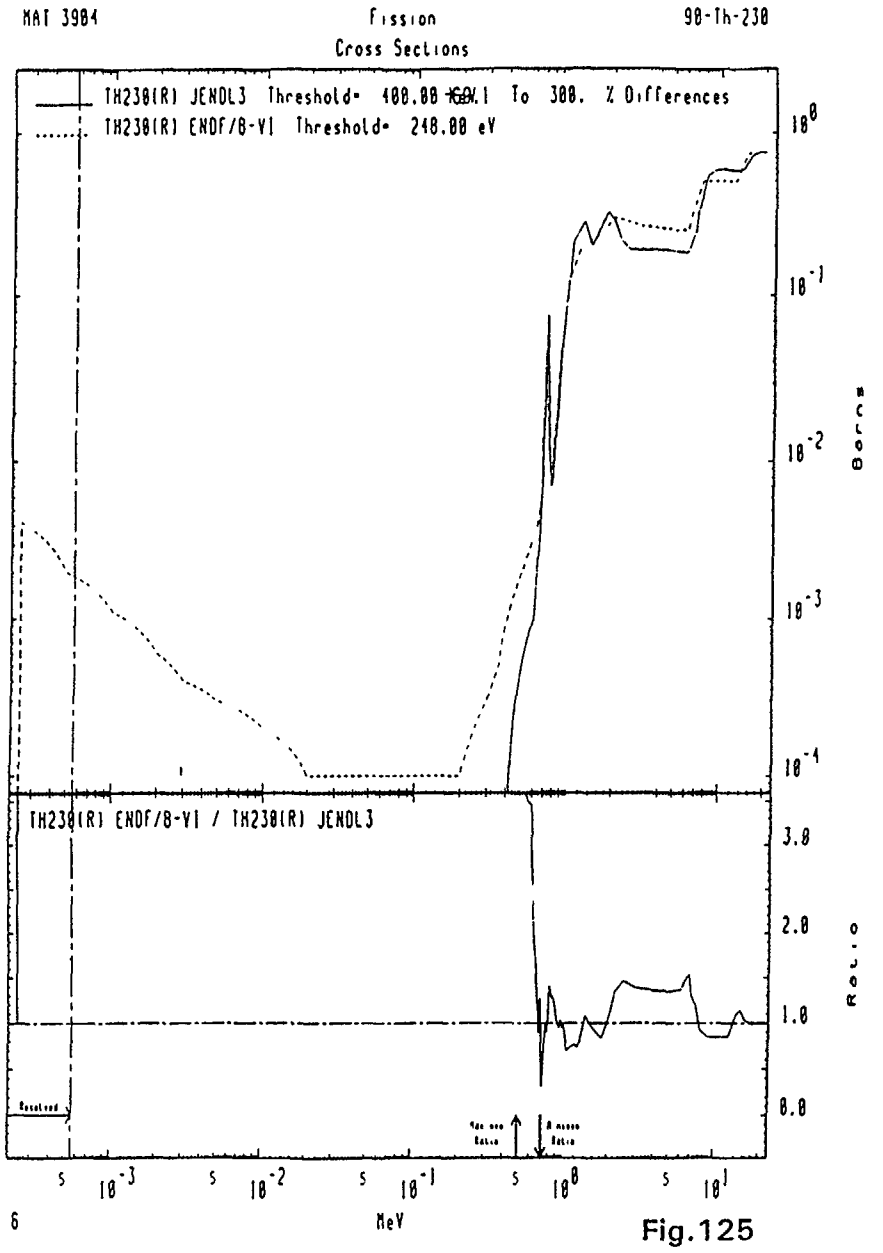

Fig.125

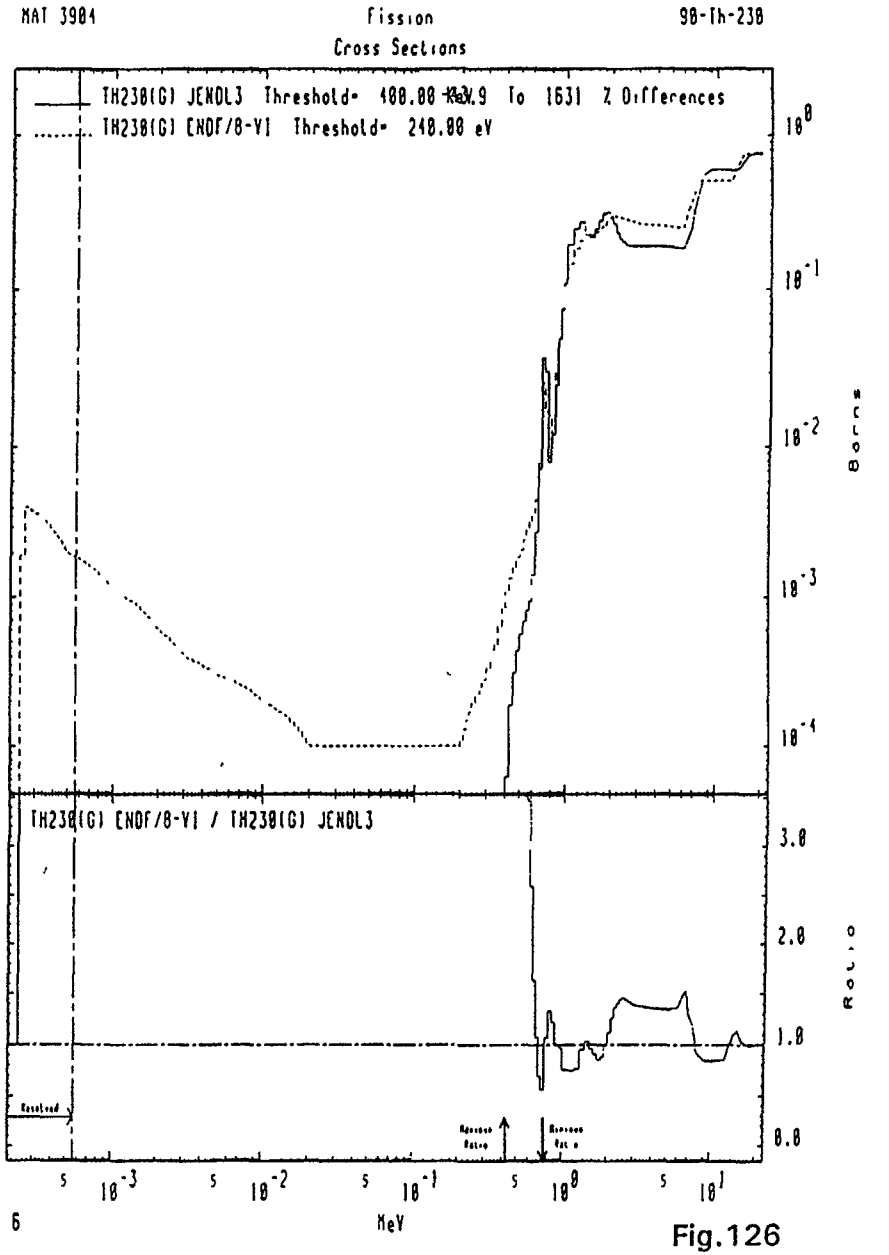

Fig.126

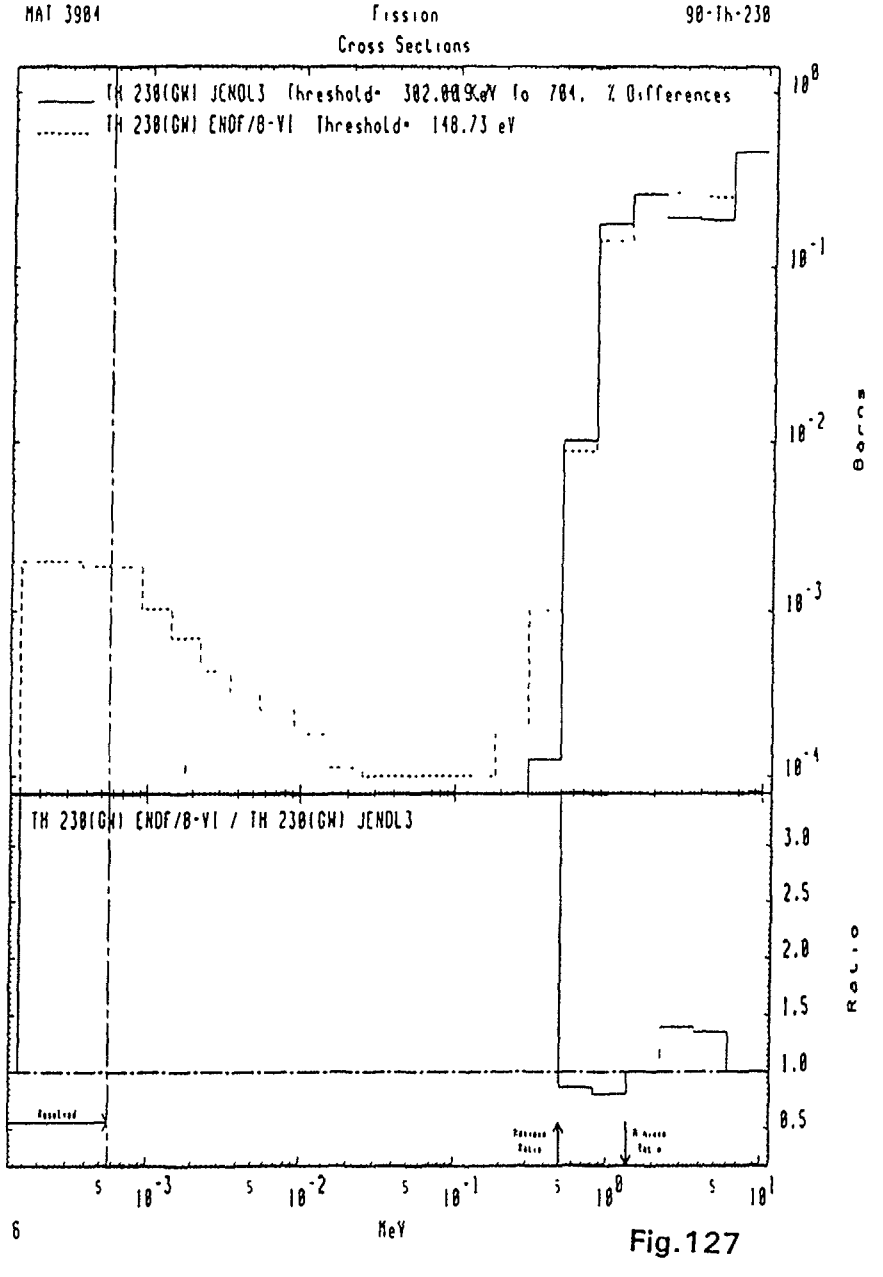

Fig.127

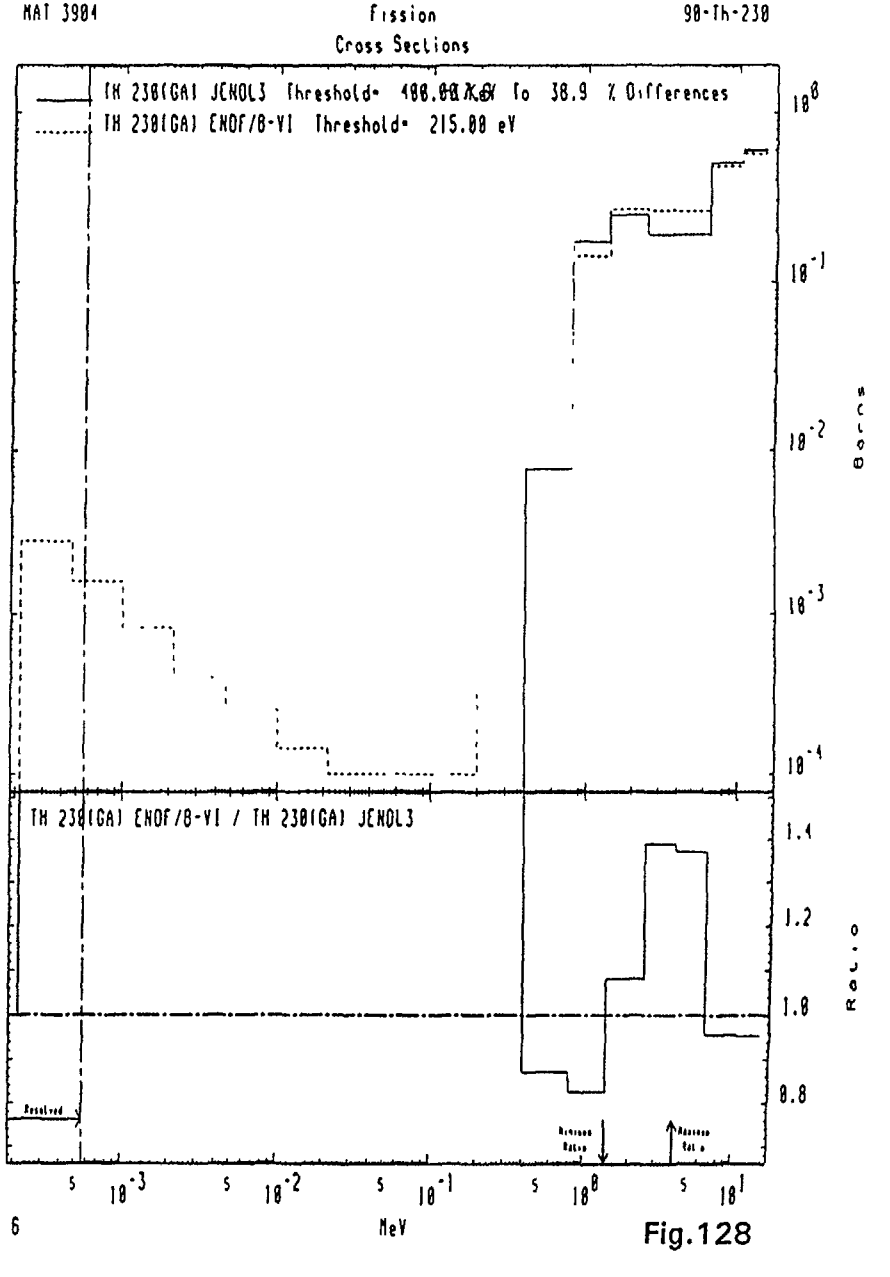

Fig.128

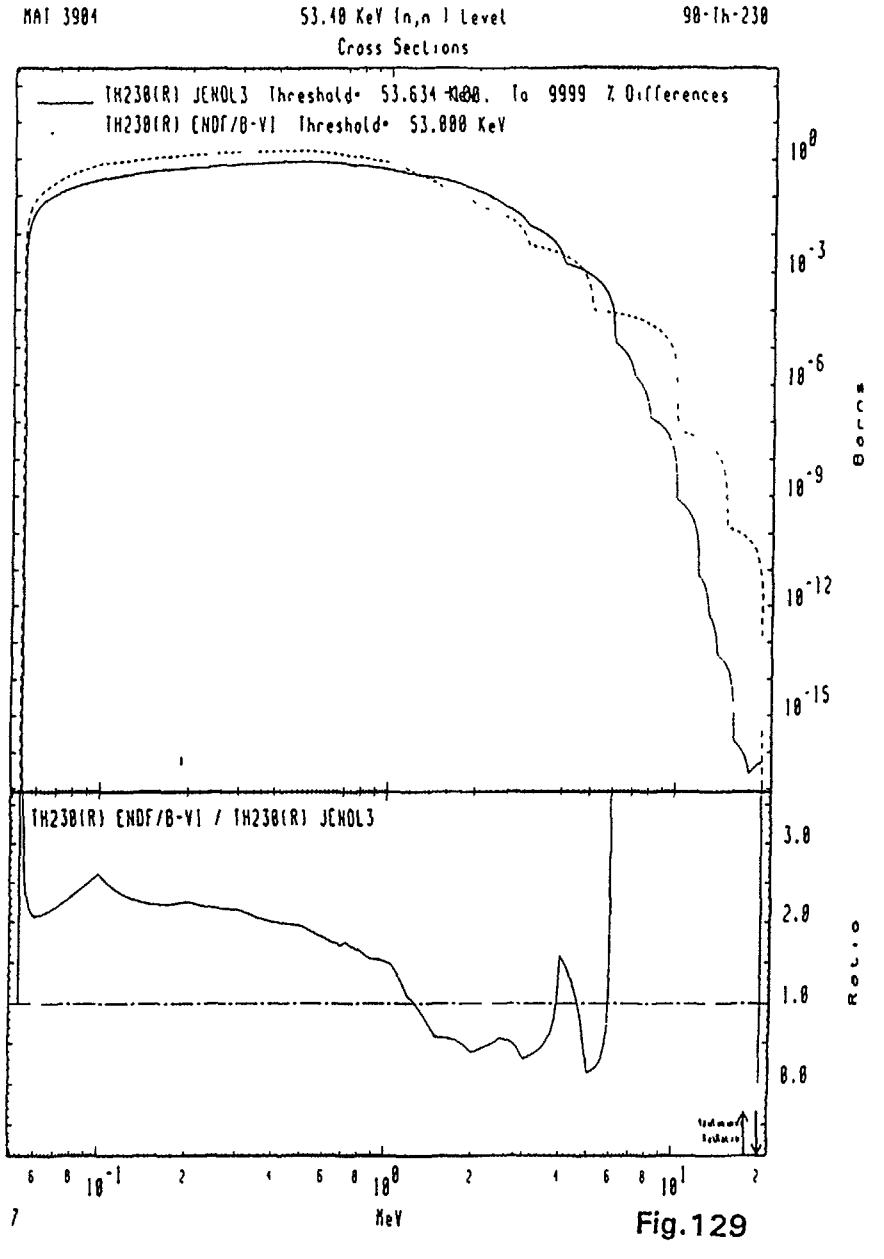

Fig.129

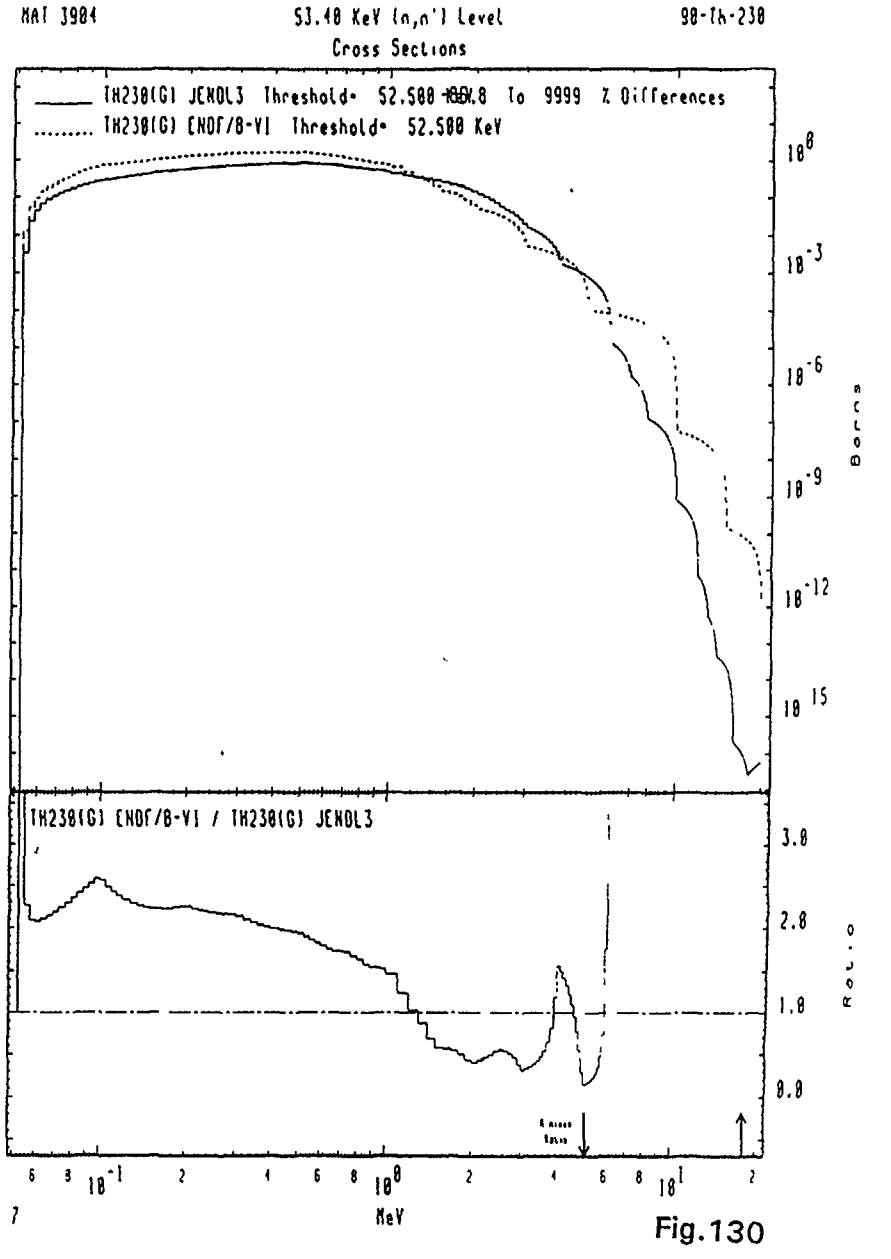

Fig.130

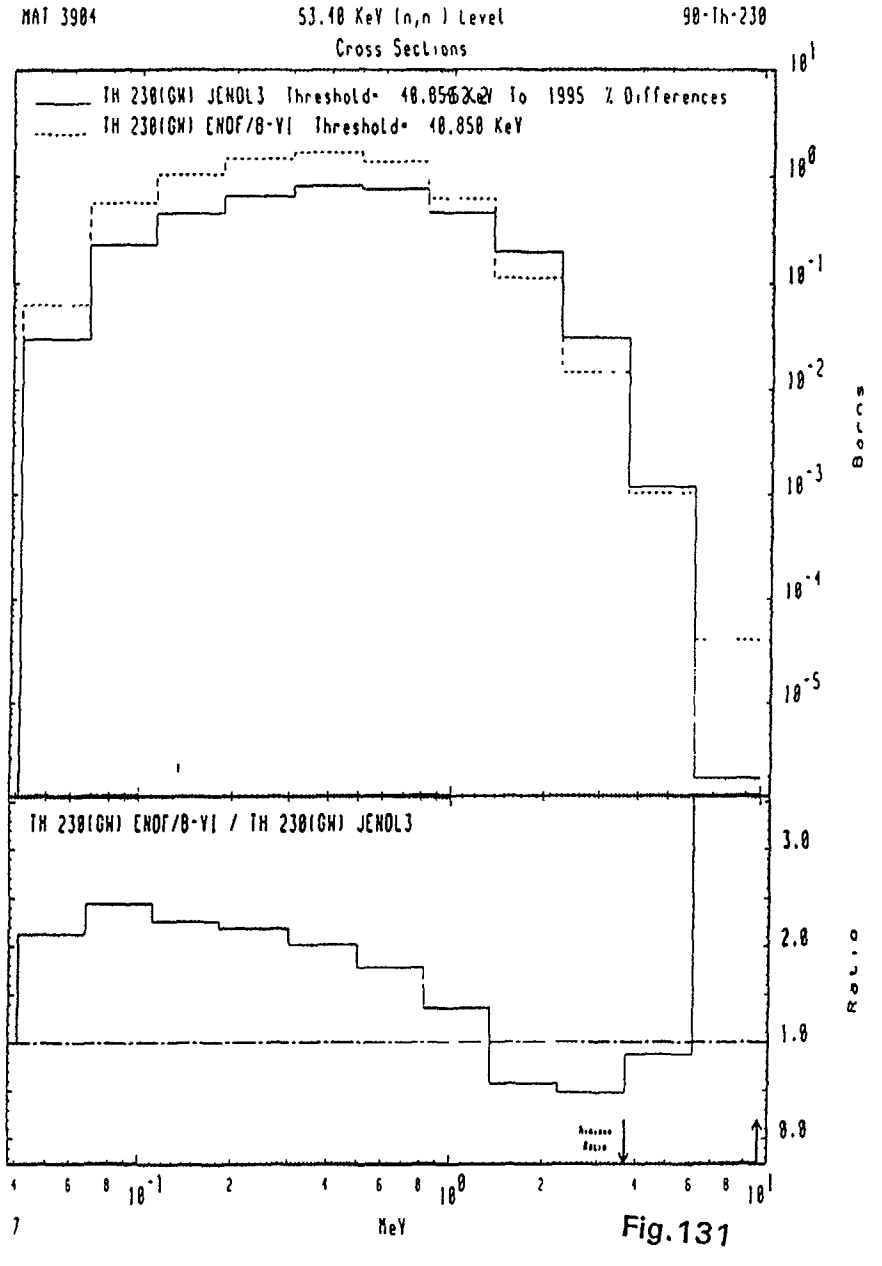

Fig.131

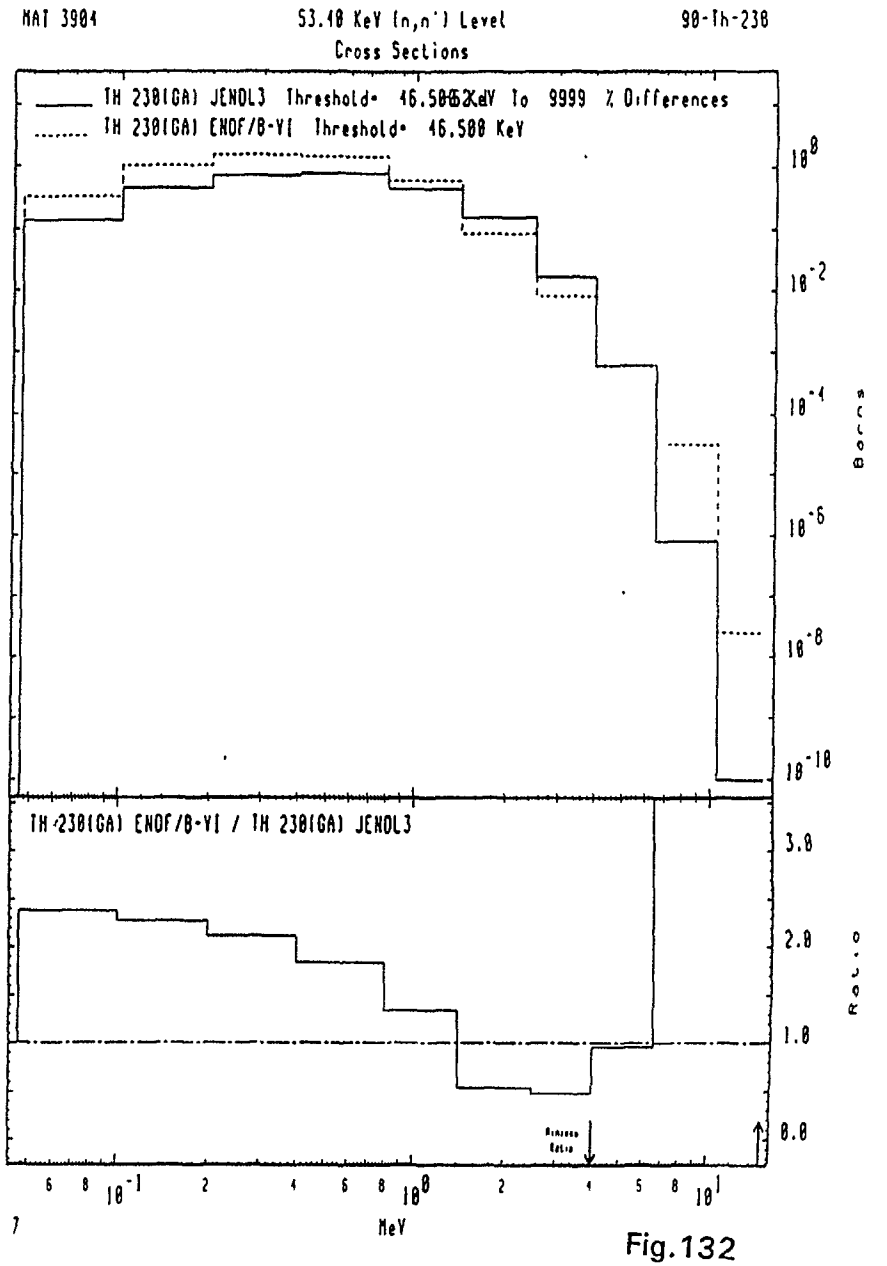

Fig.132

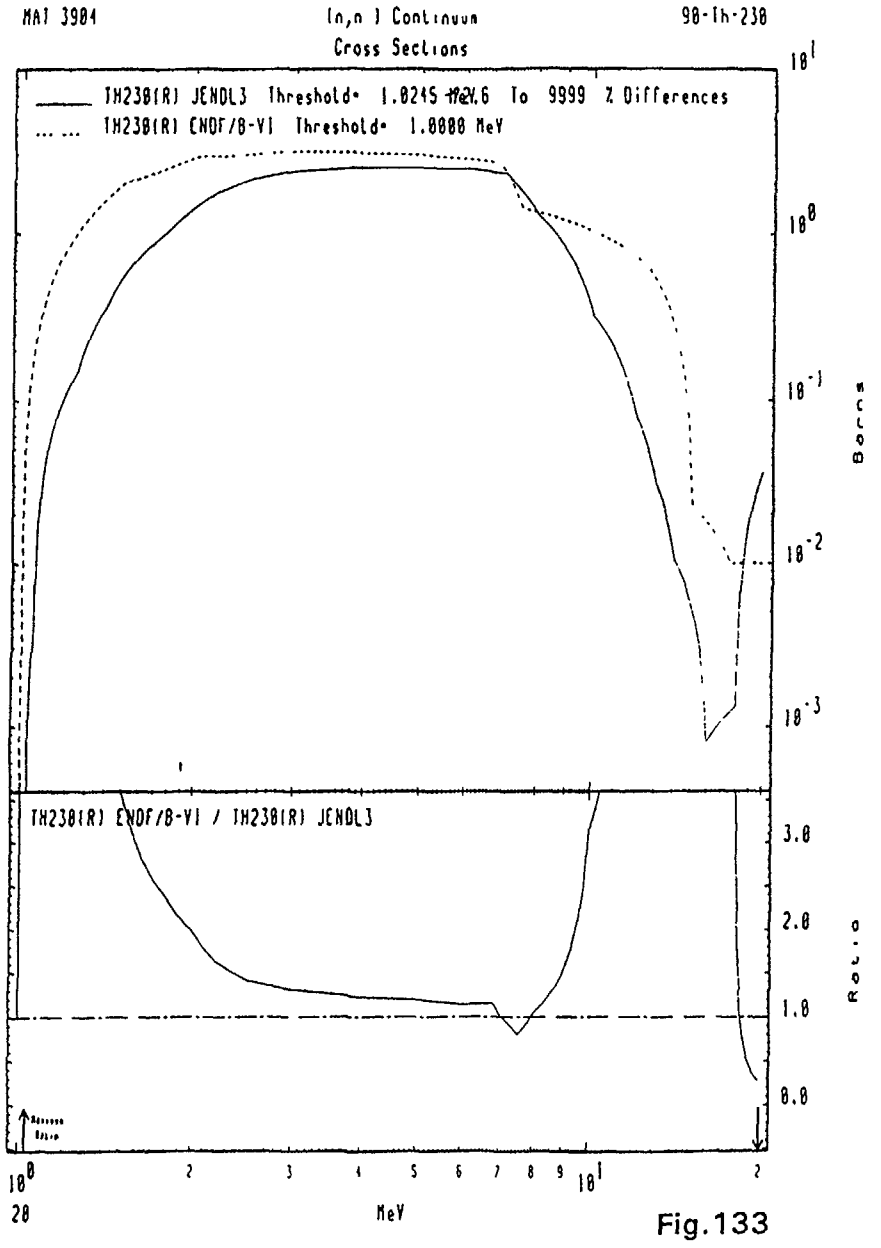

Fig.133

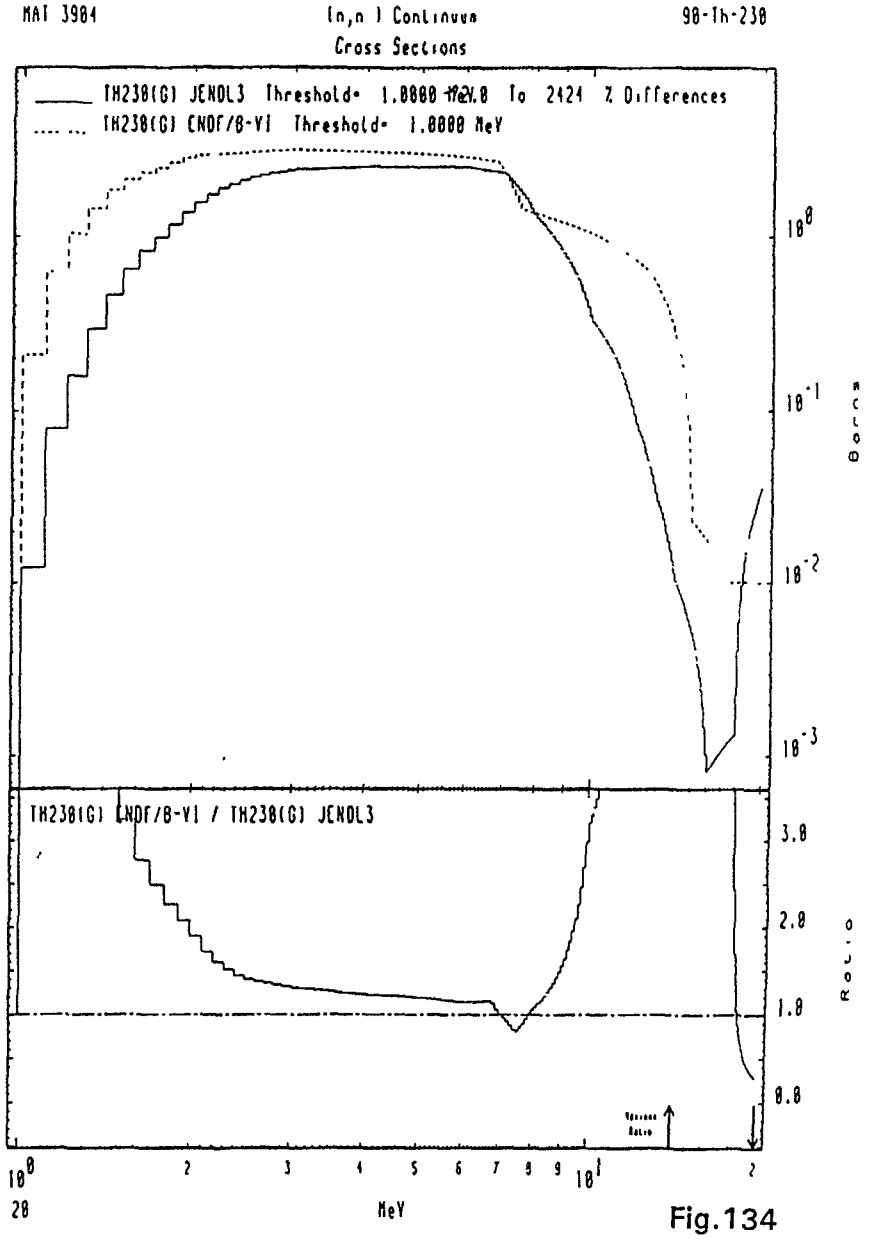

Fig.134

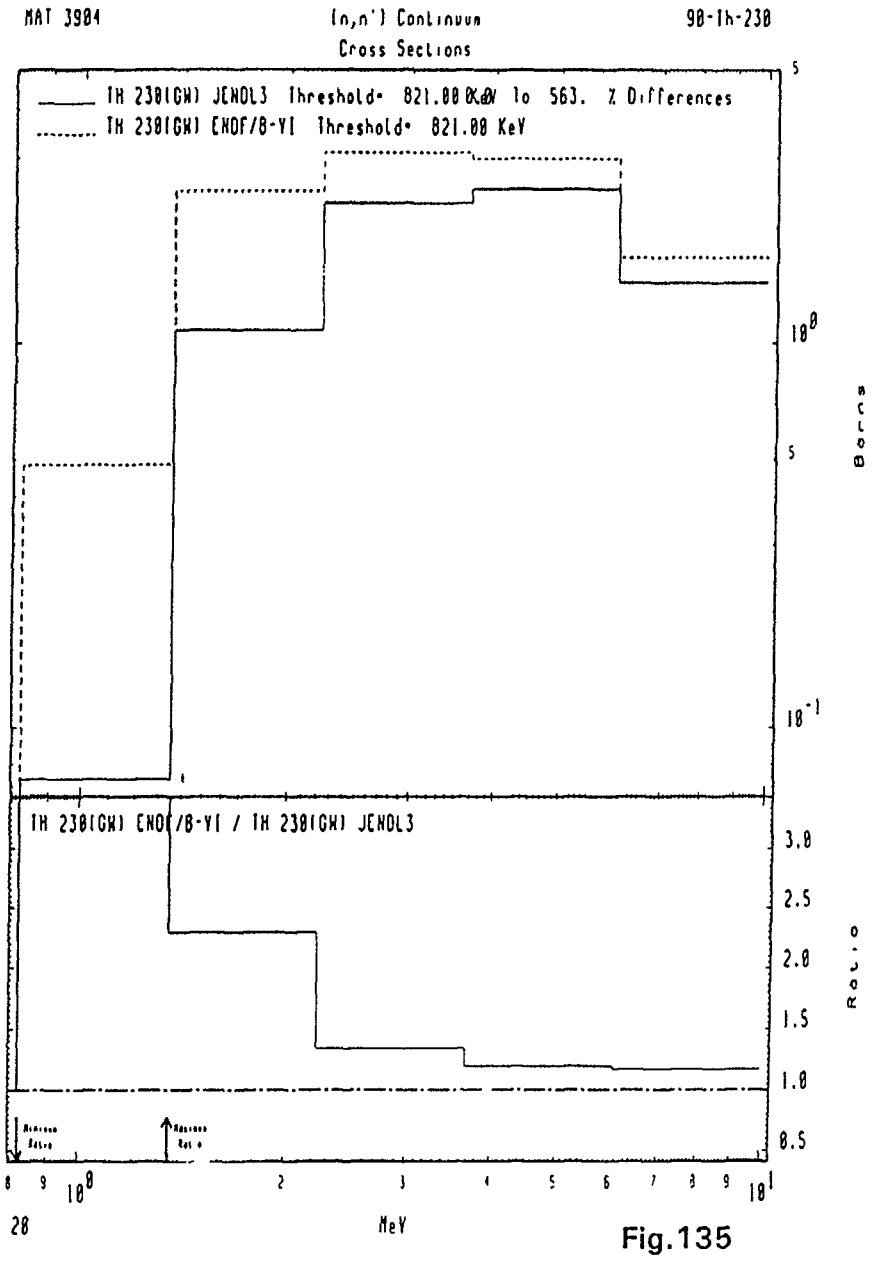

Fig.135

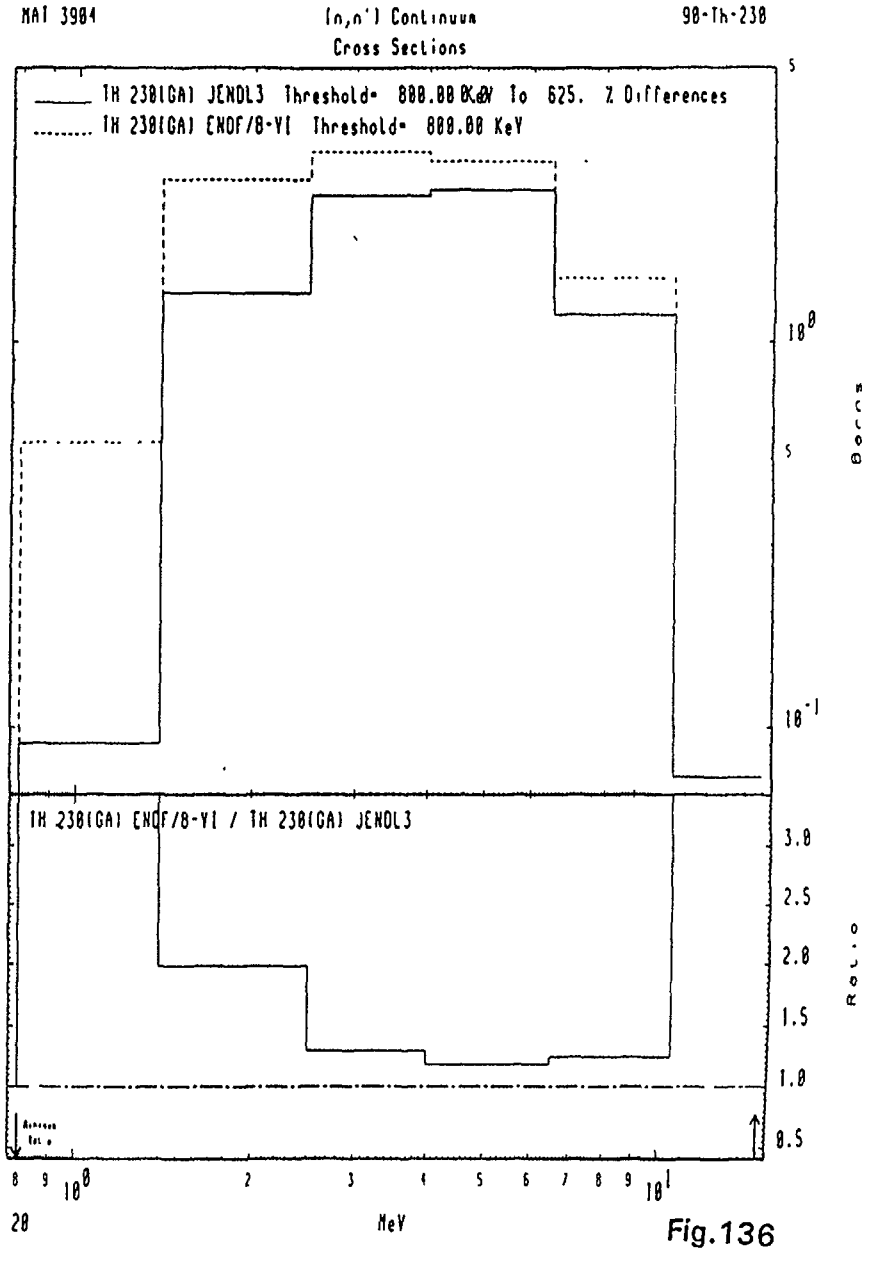

Fig.136

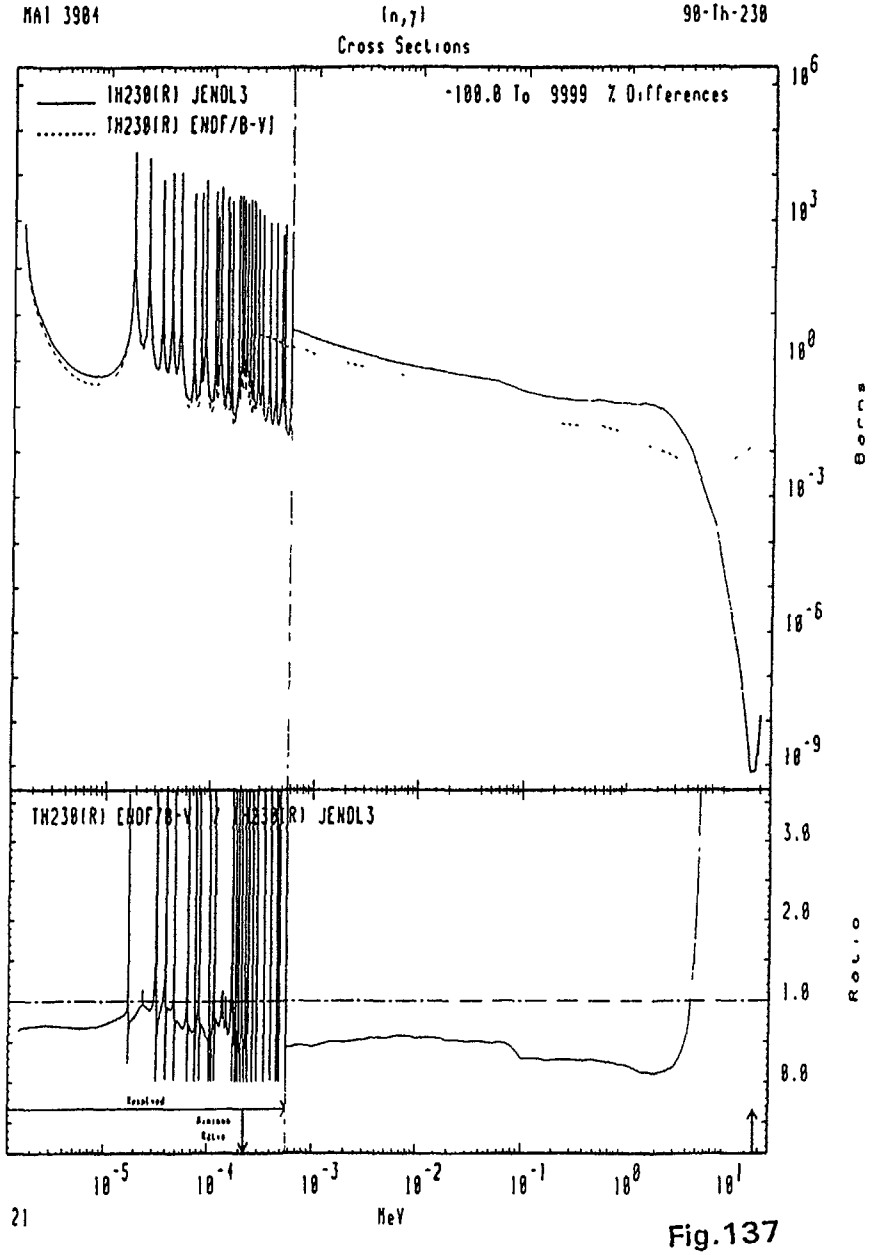

Fig.137

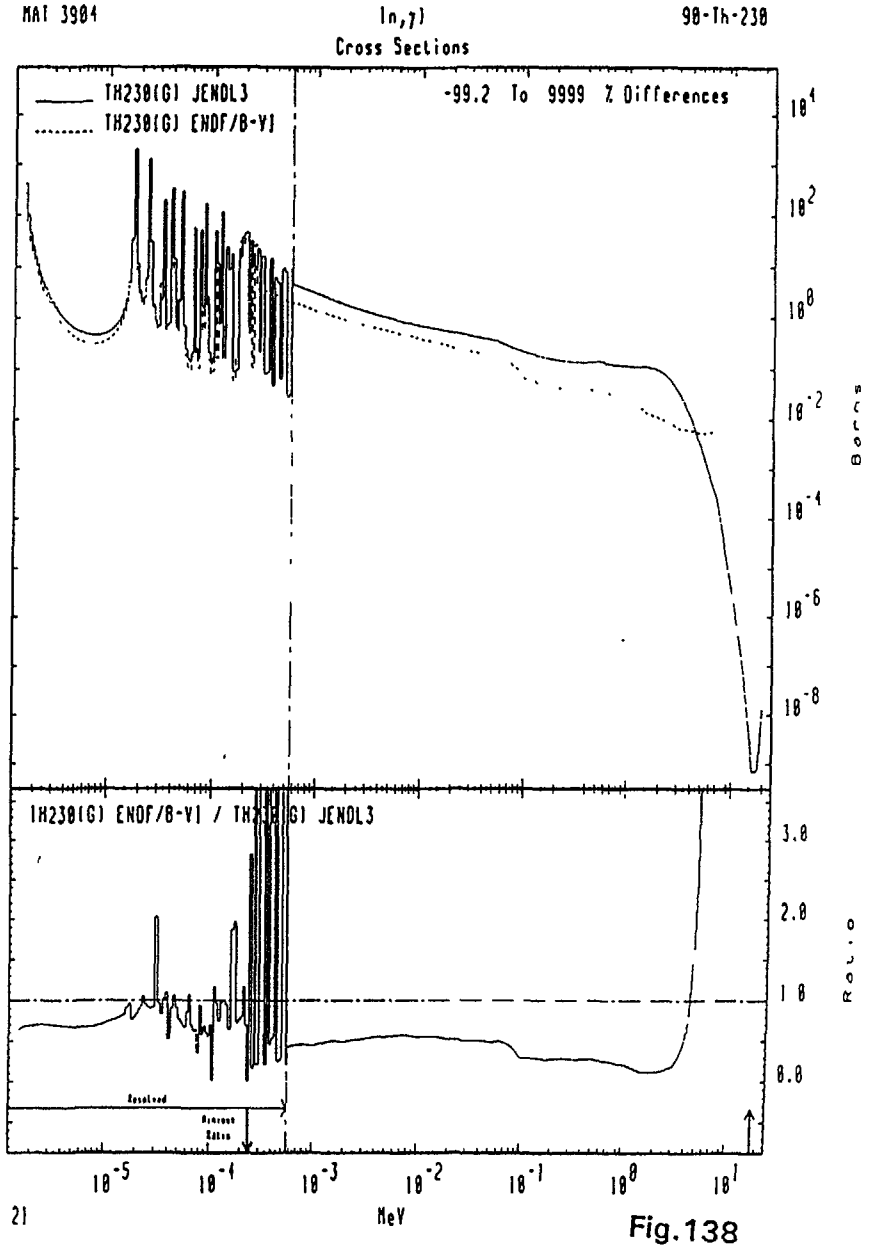

Fig.138

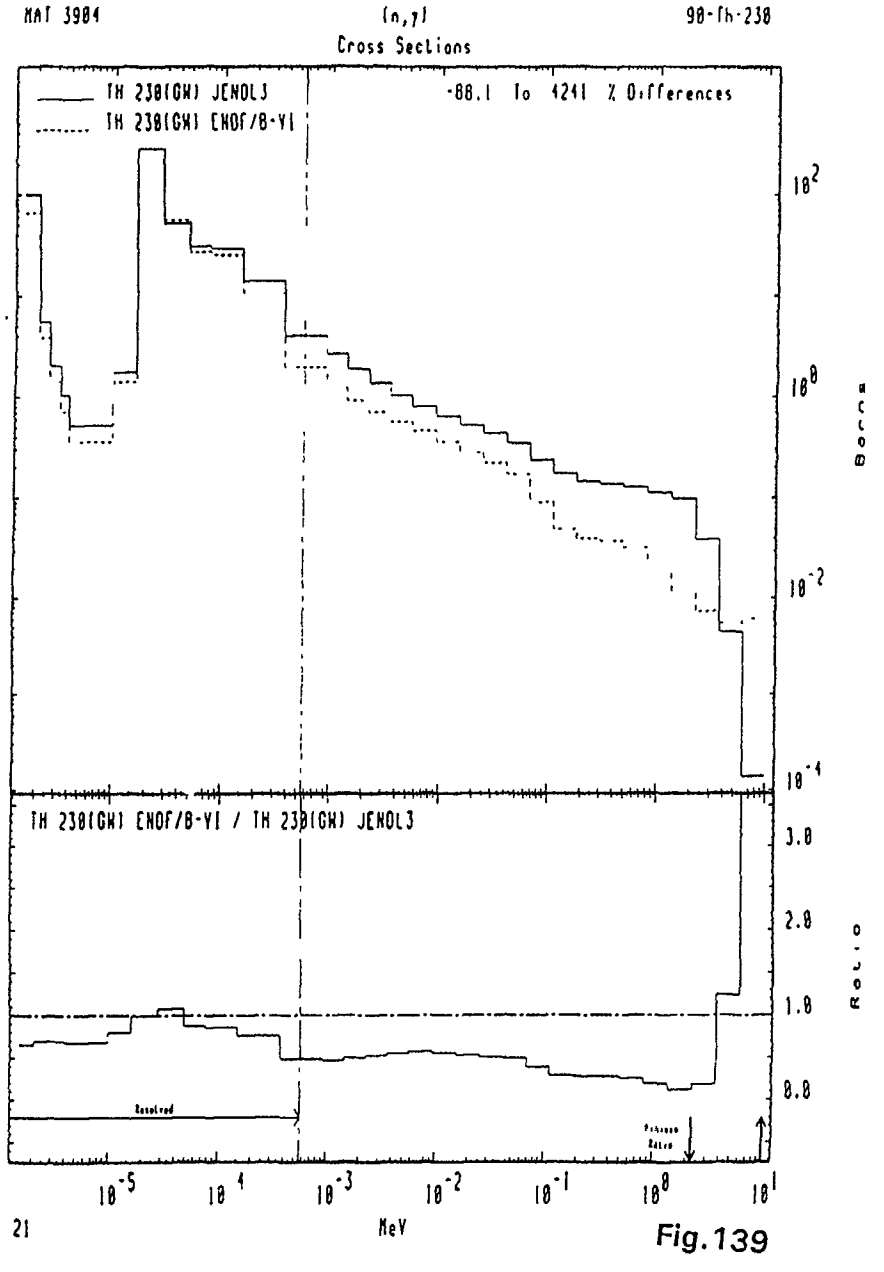

Fig.139

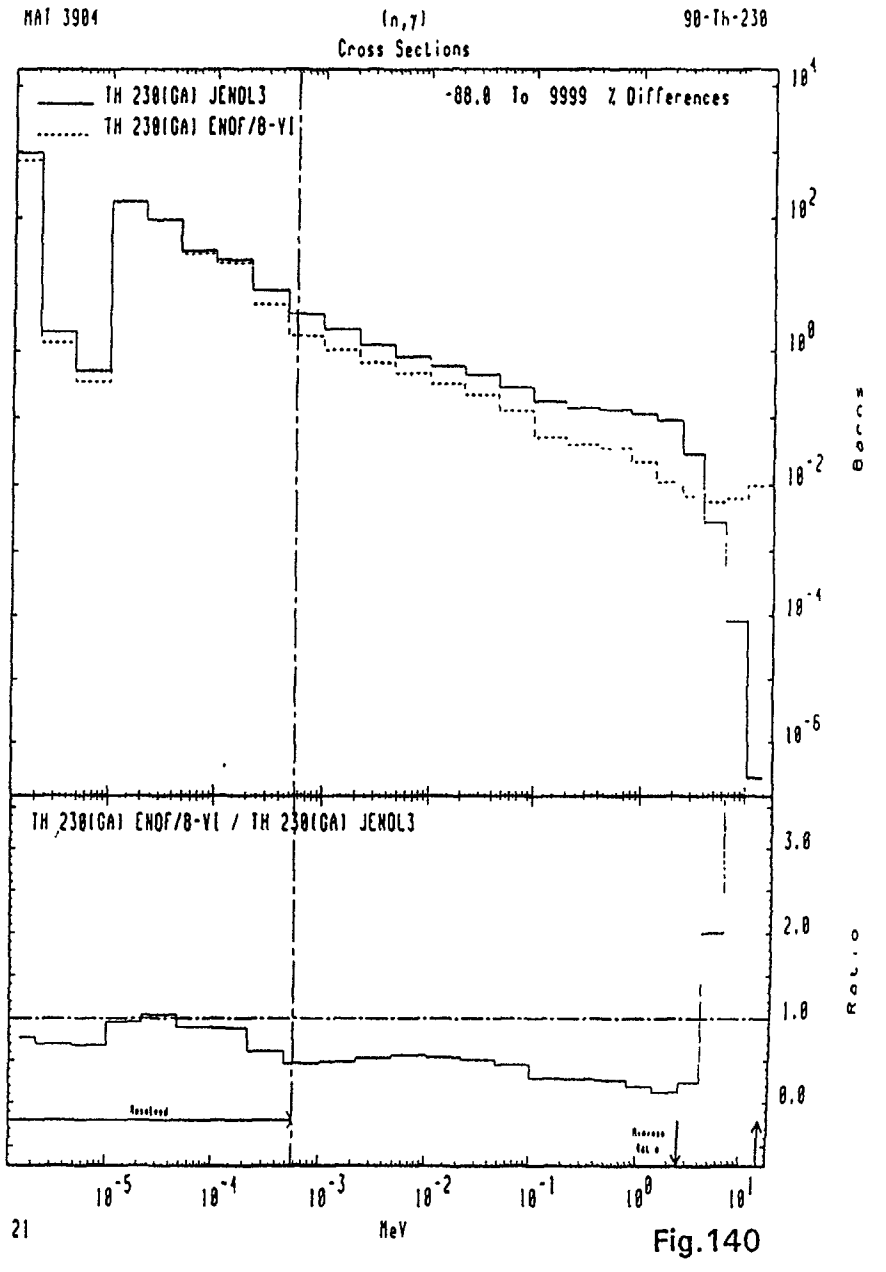

Fig.140

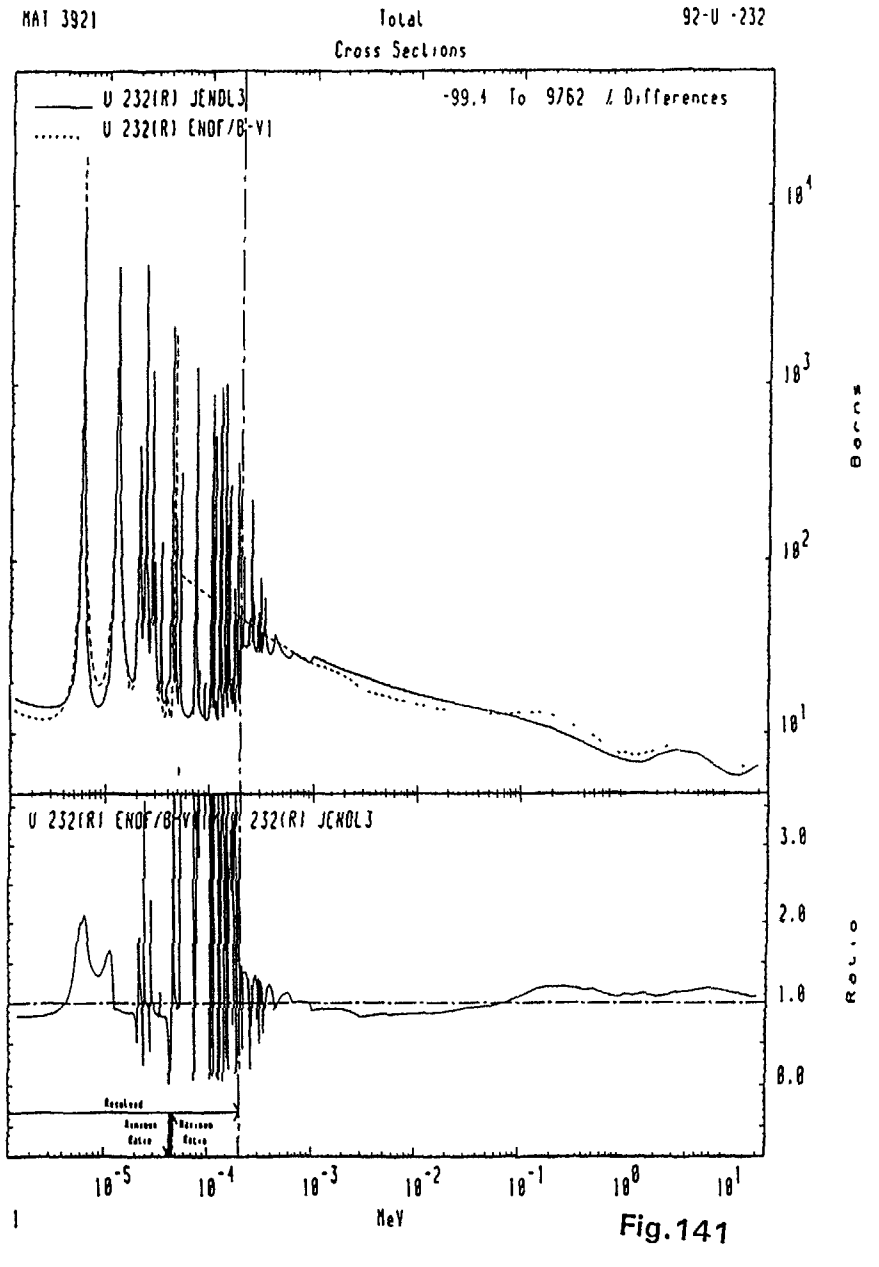

Fig.141

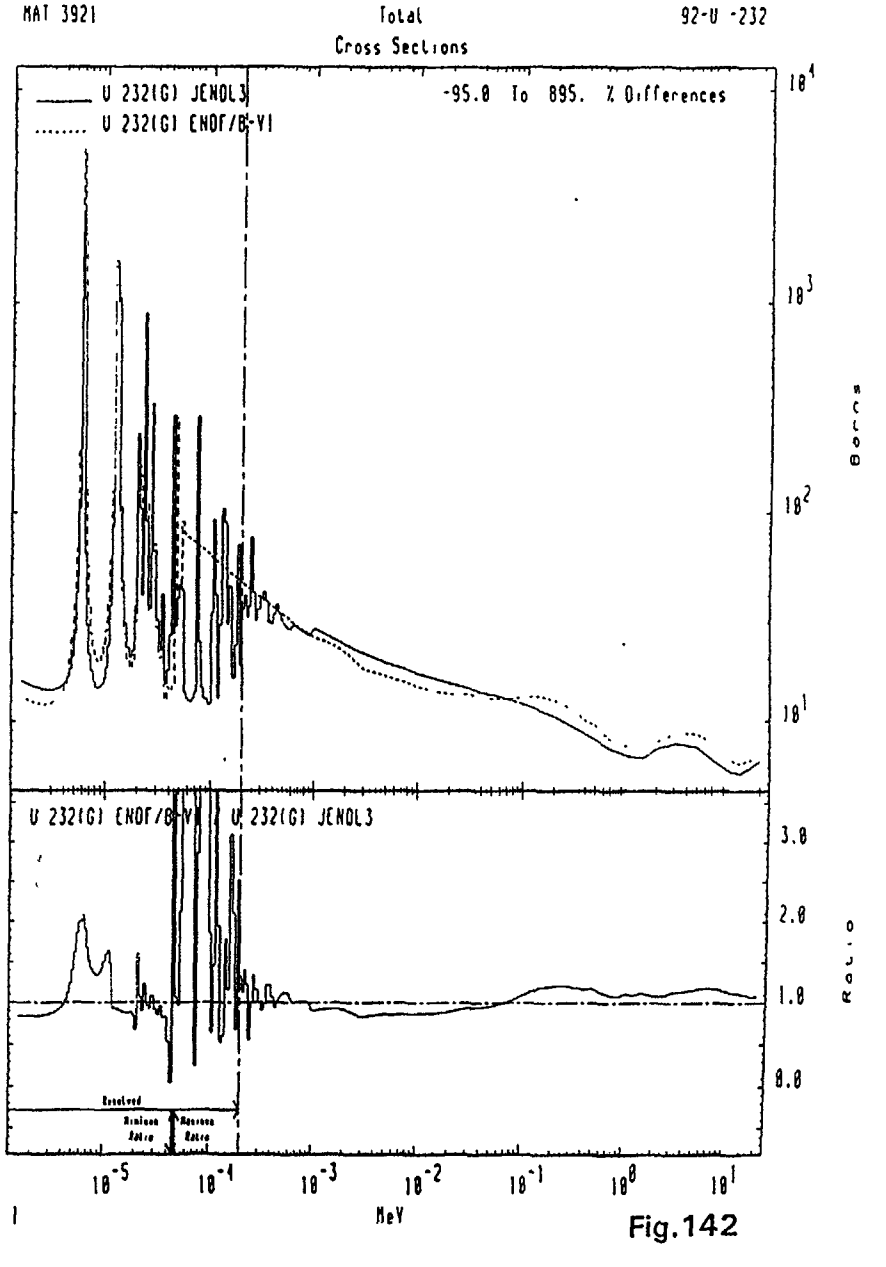

Fig.142

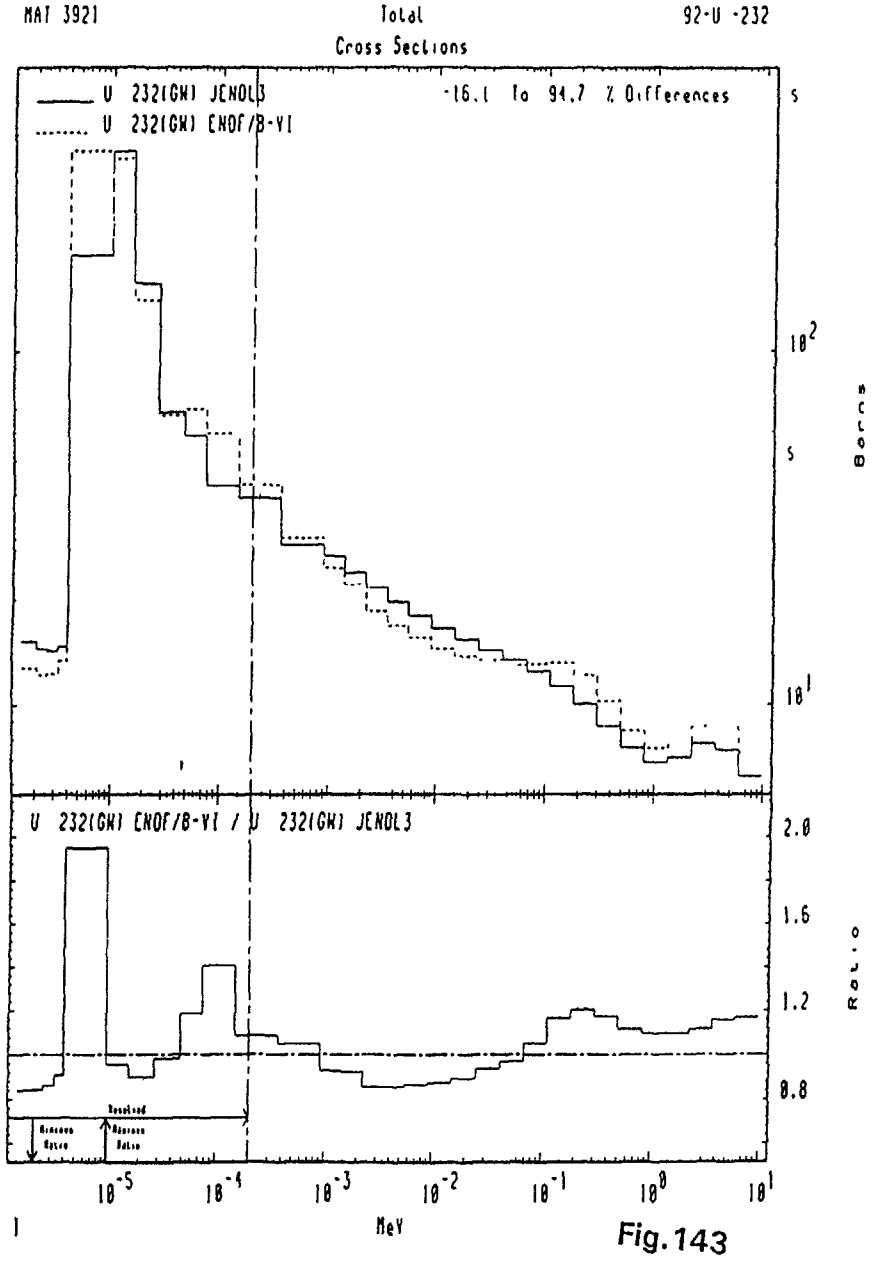

Fig.143

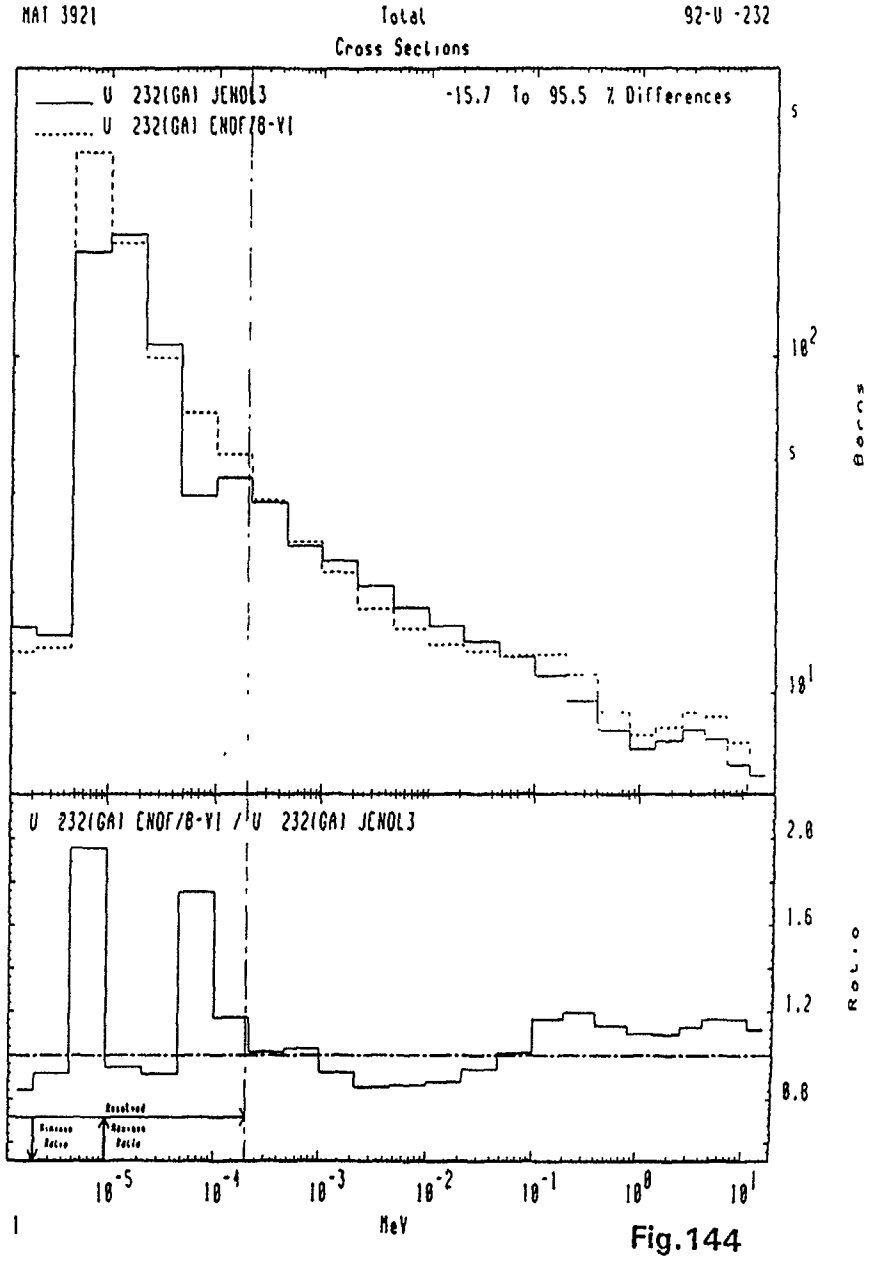

Fig.144

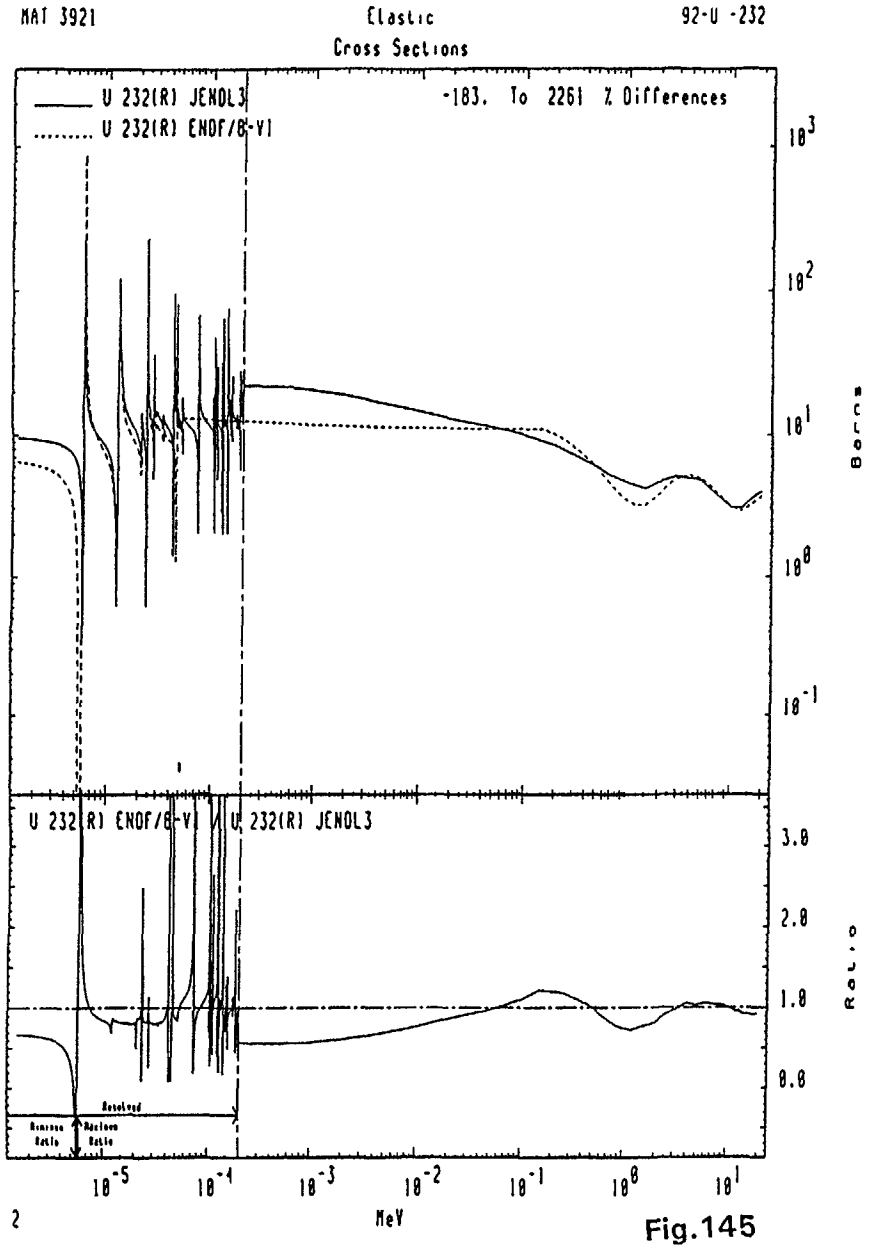

Fig.145

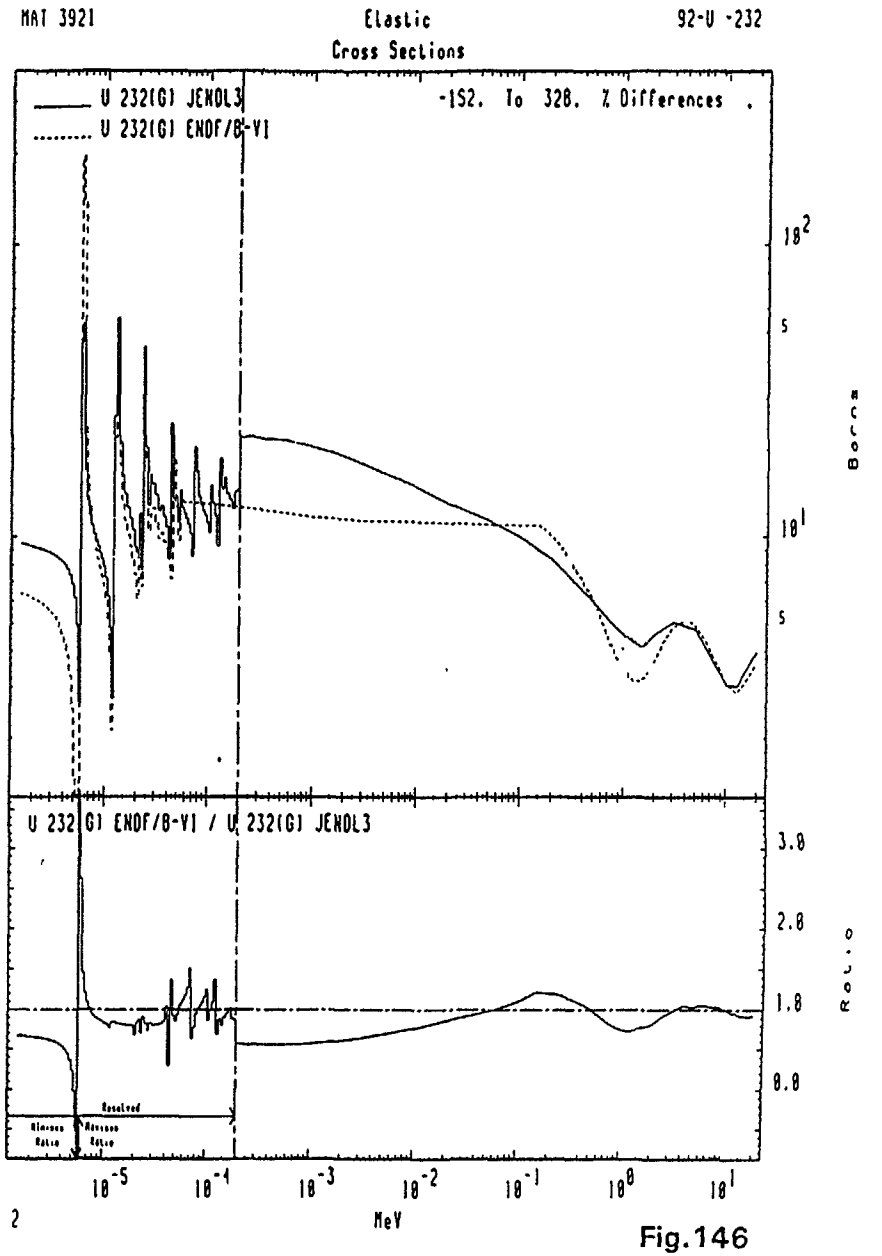

Fig.146

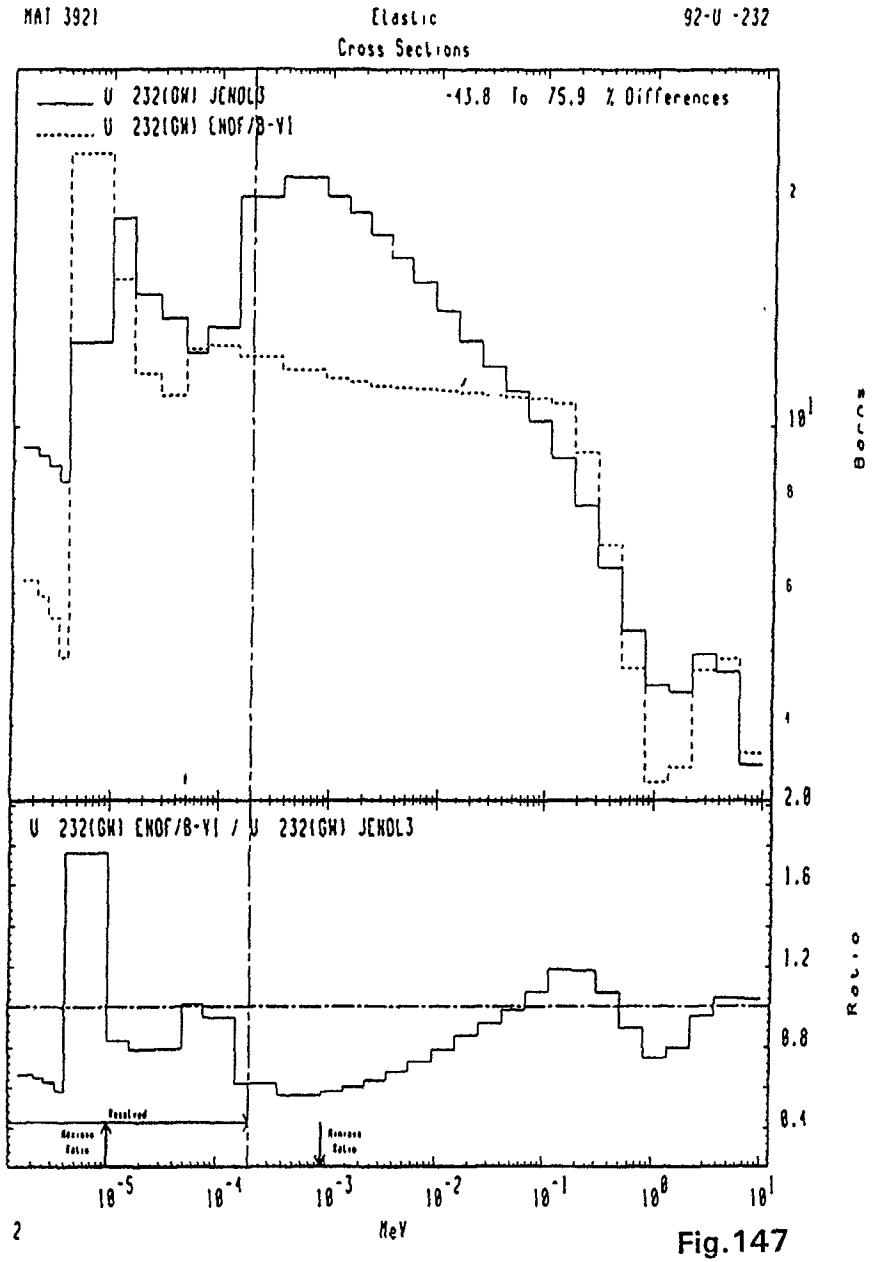

Fig.147

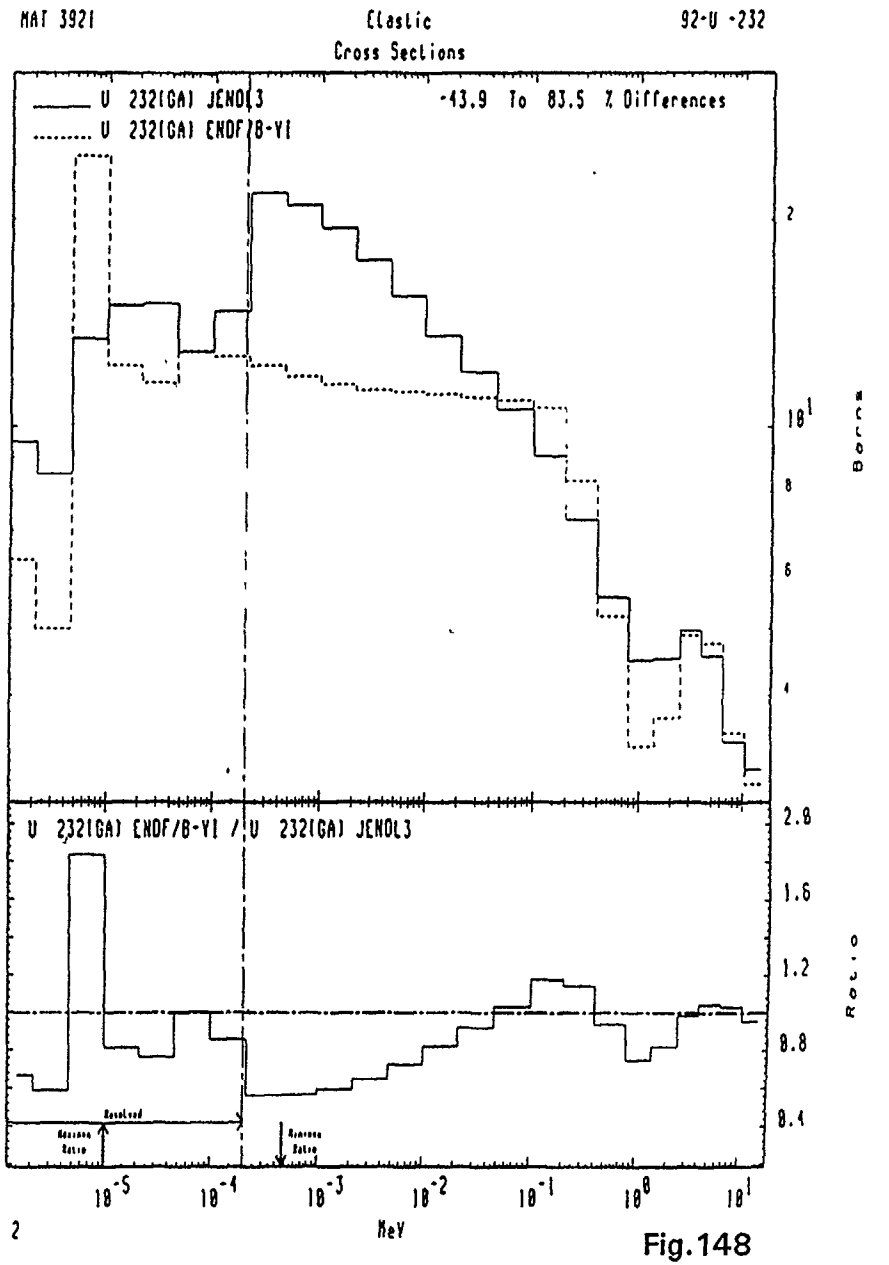

Fig.148

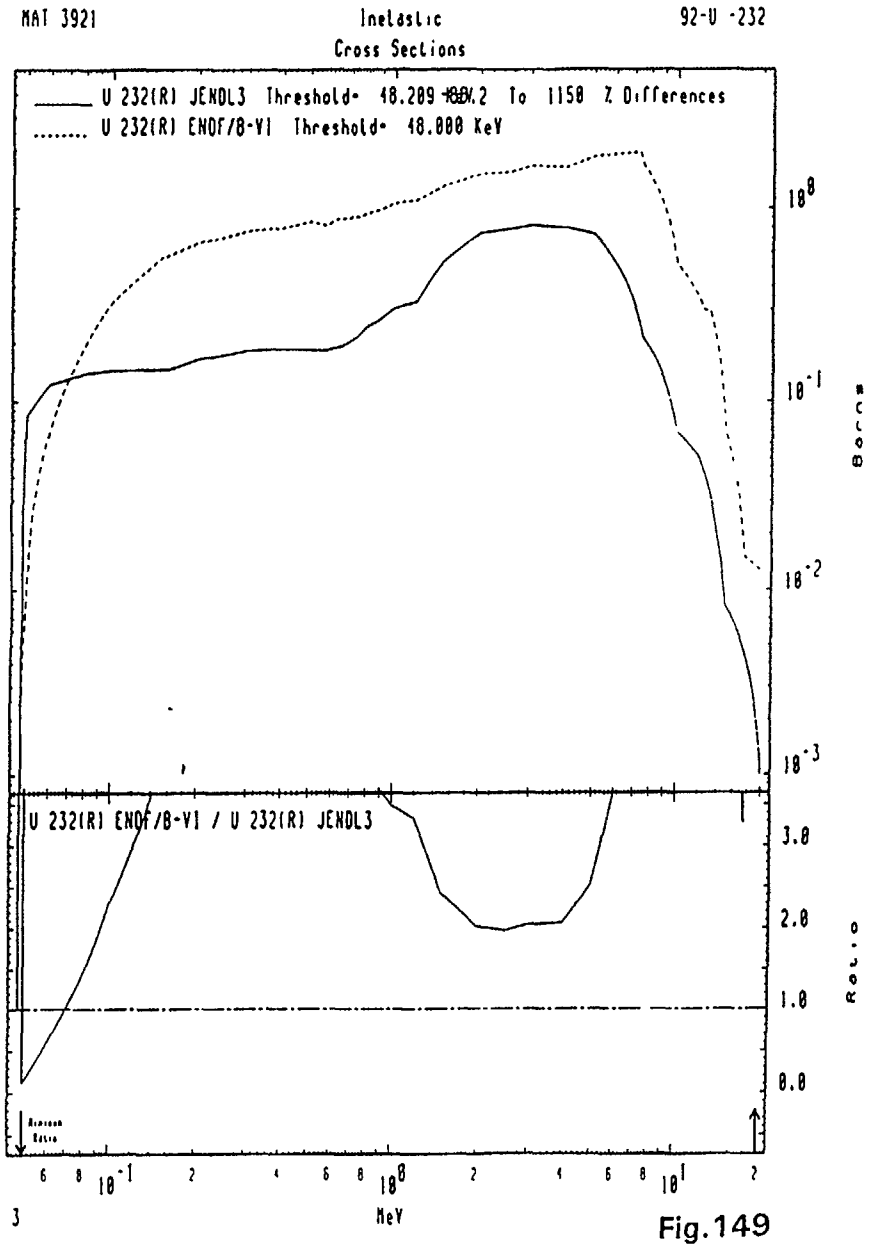

Fig.149

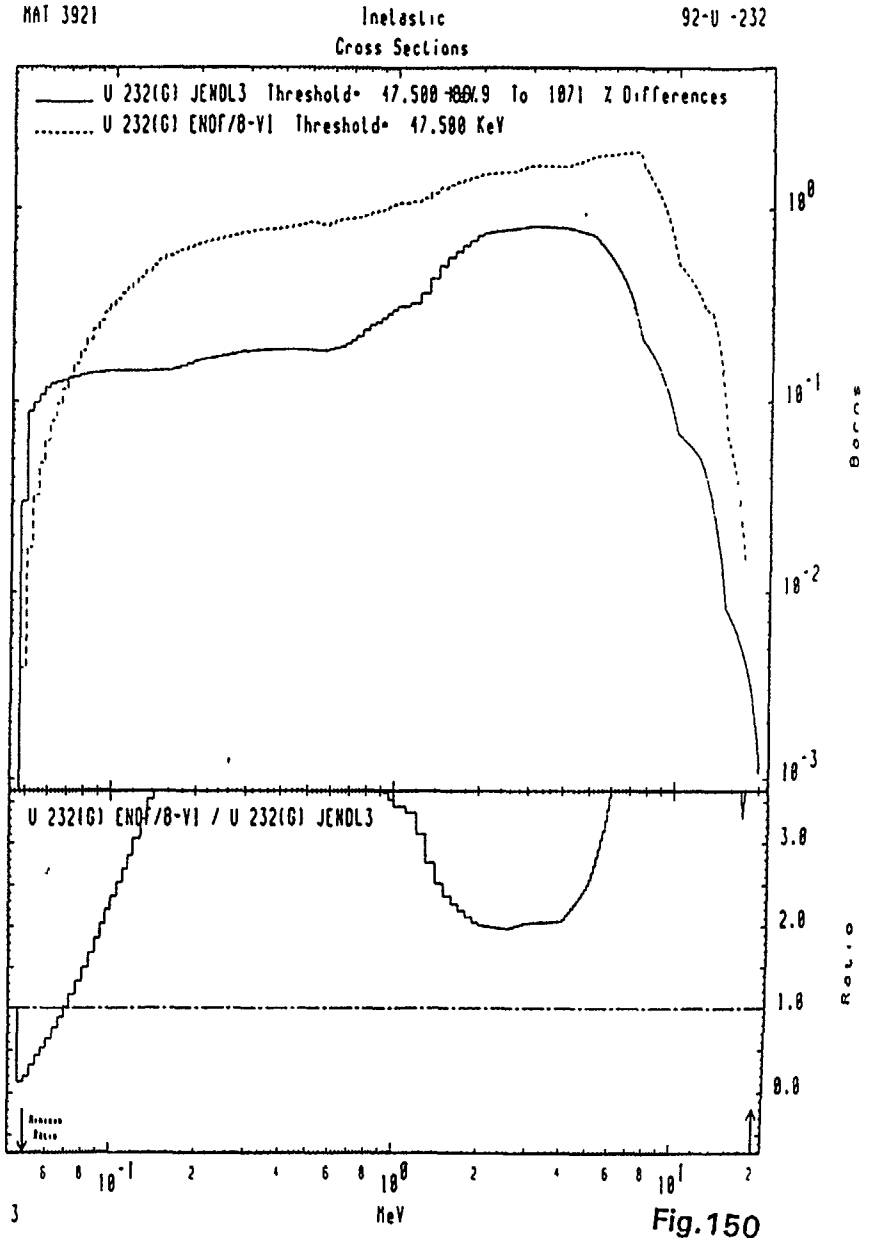

Fig.150

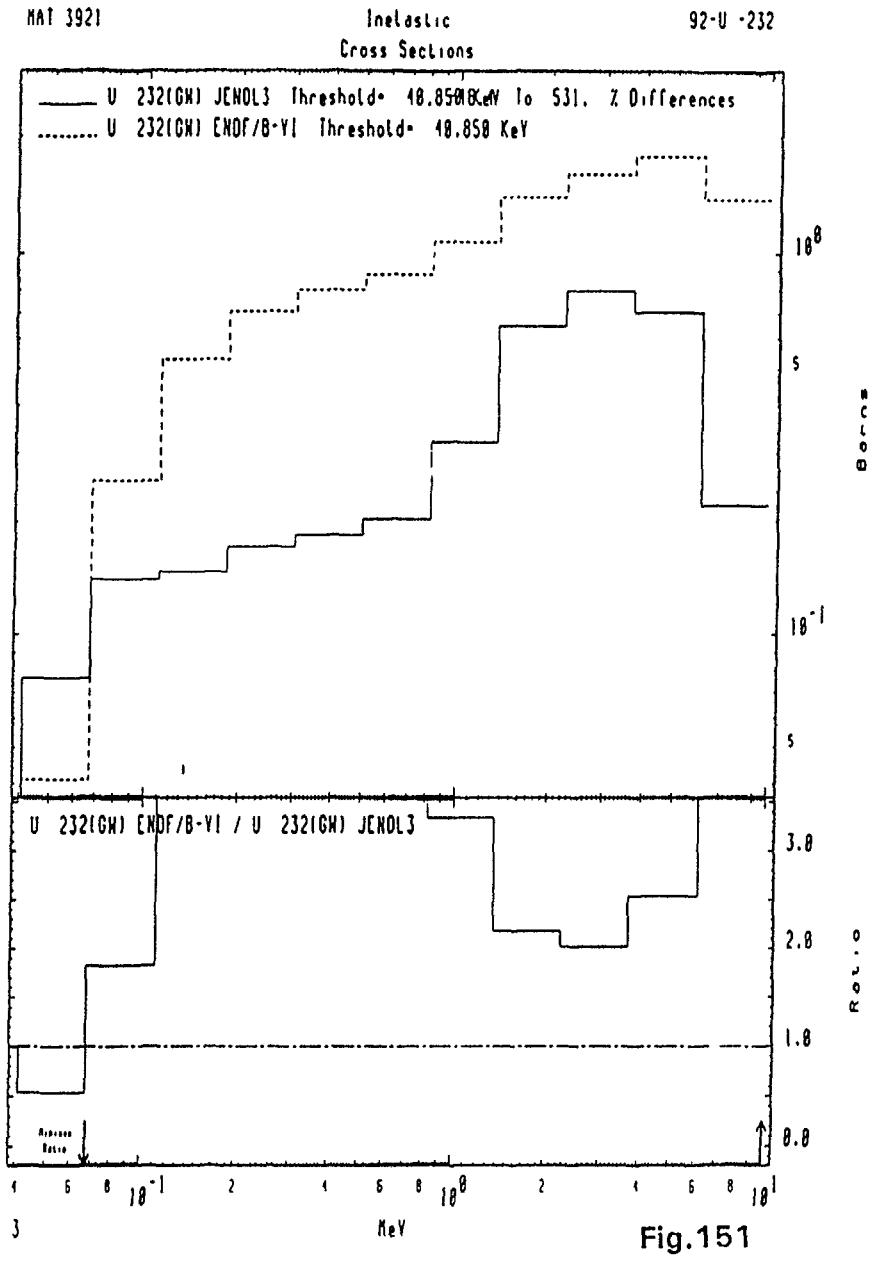

Fig.151

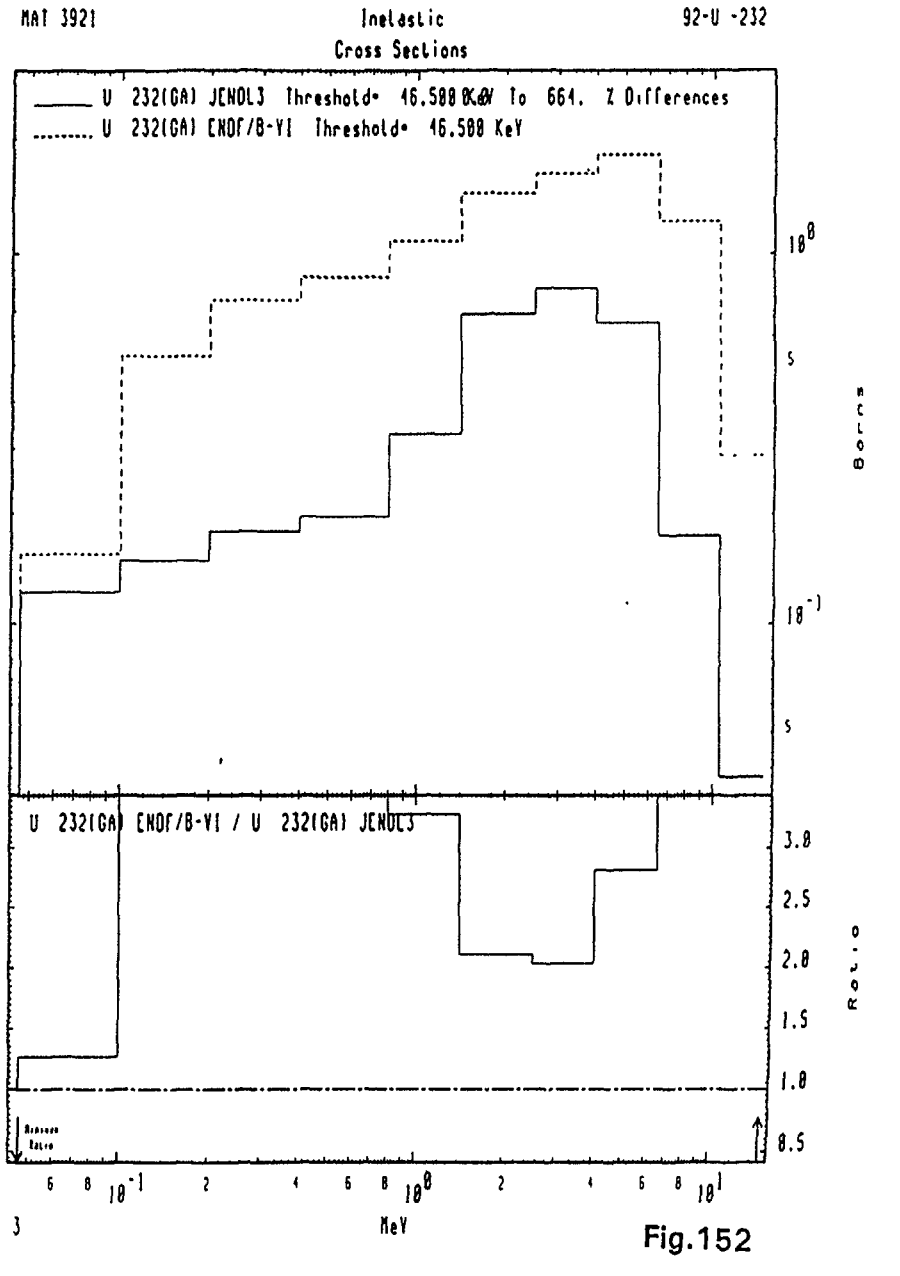

Fig.152

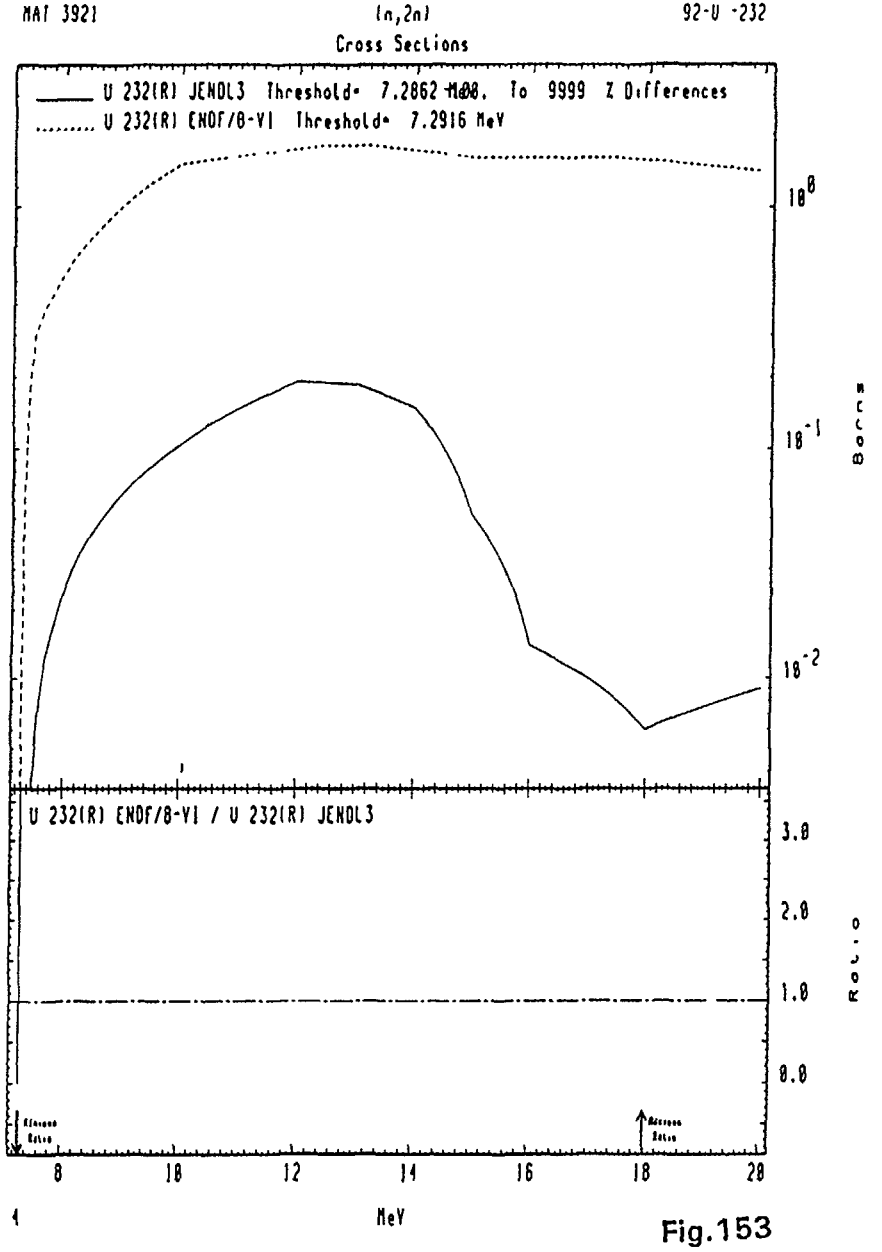

Fig.153

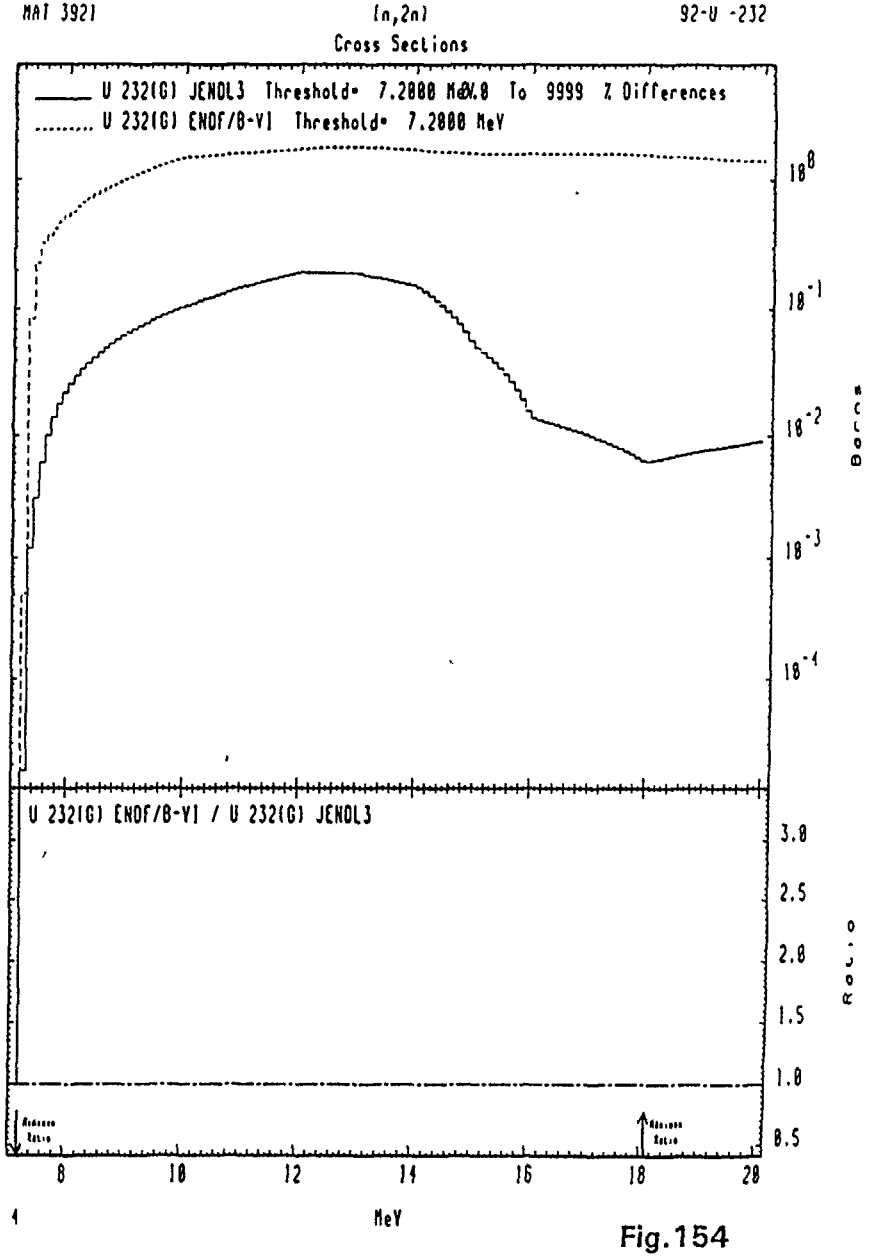

Fig.154

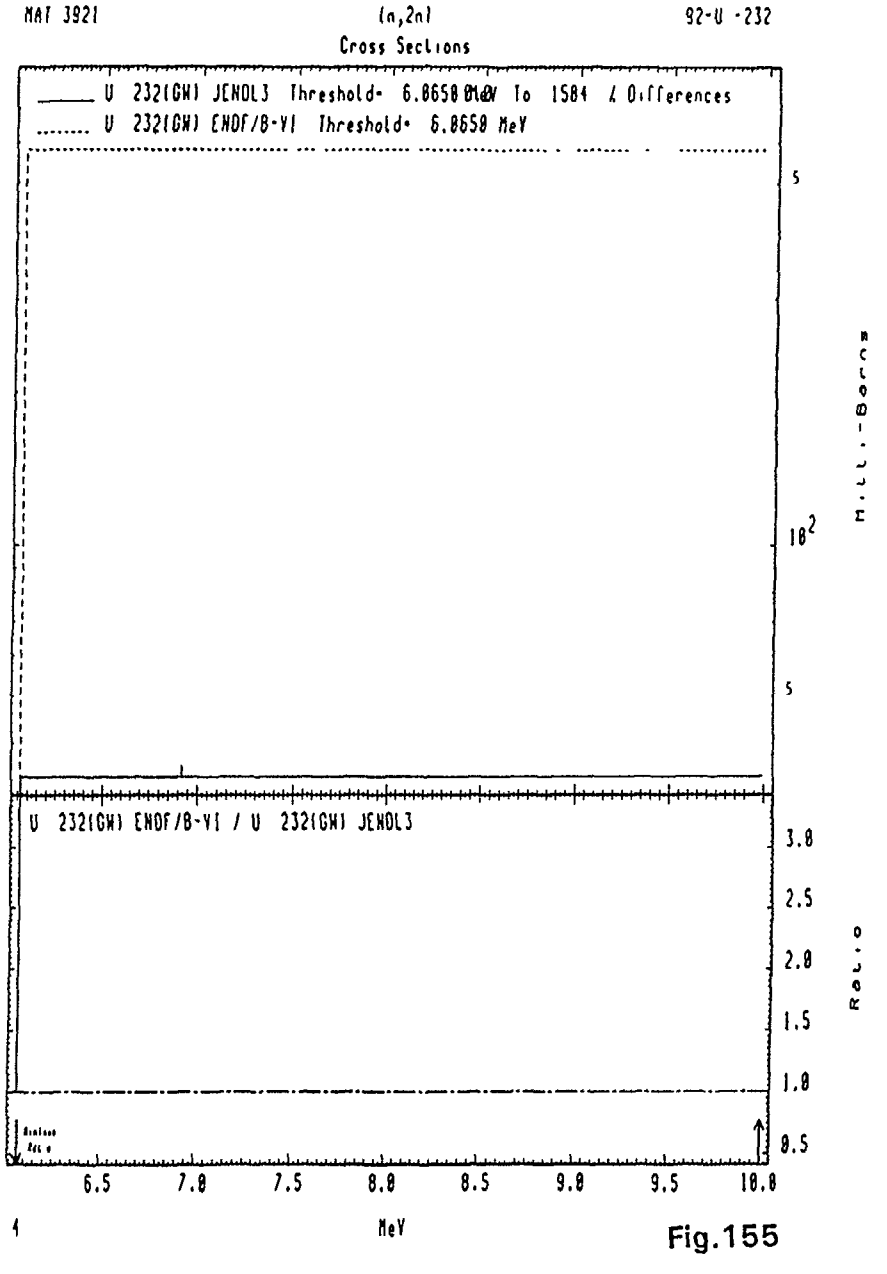

Fig.155

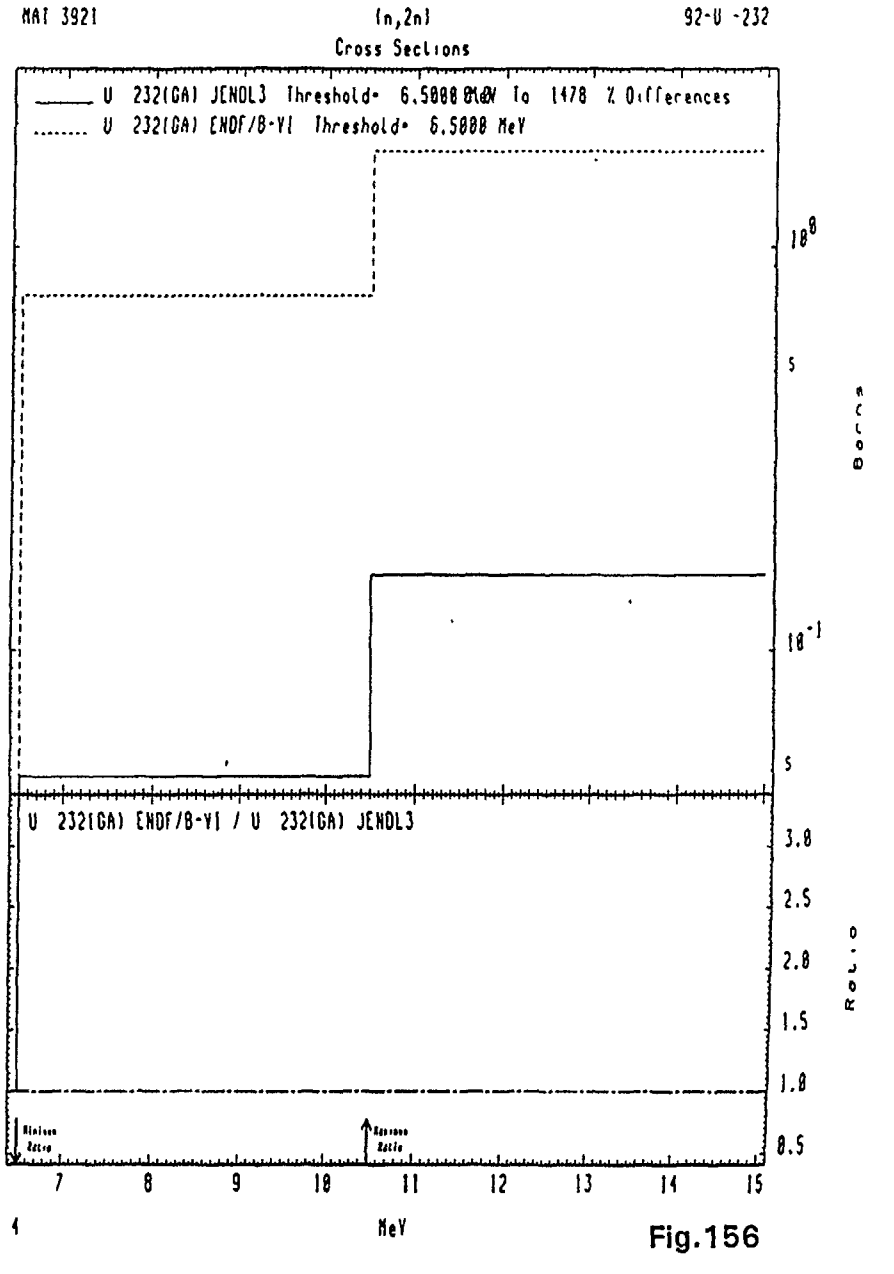

Fig.156

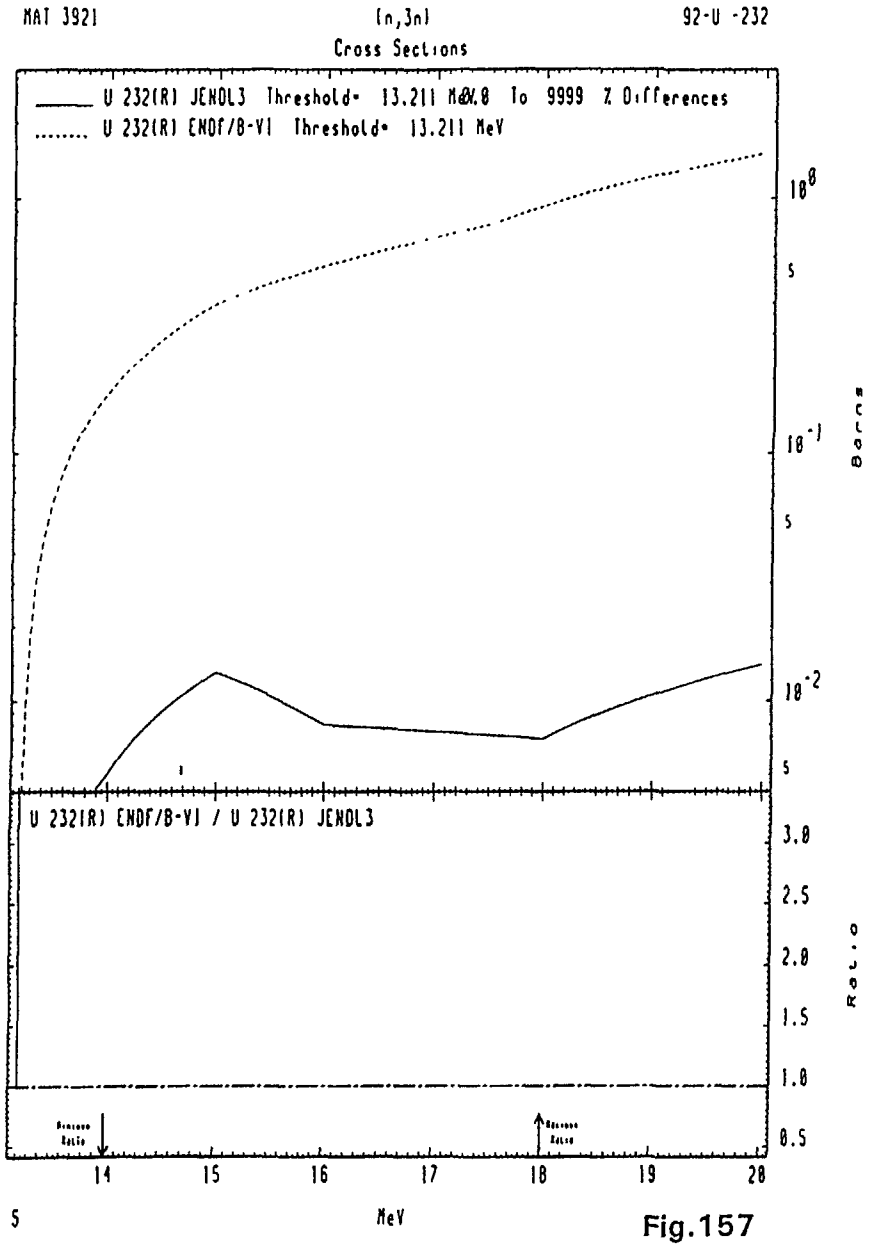

Fig.157

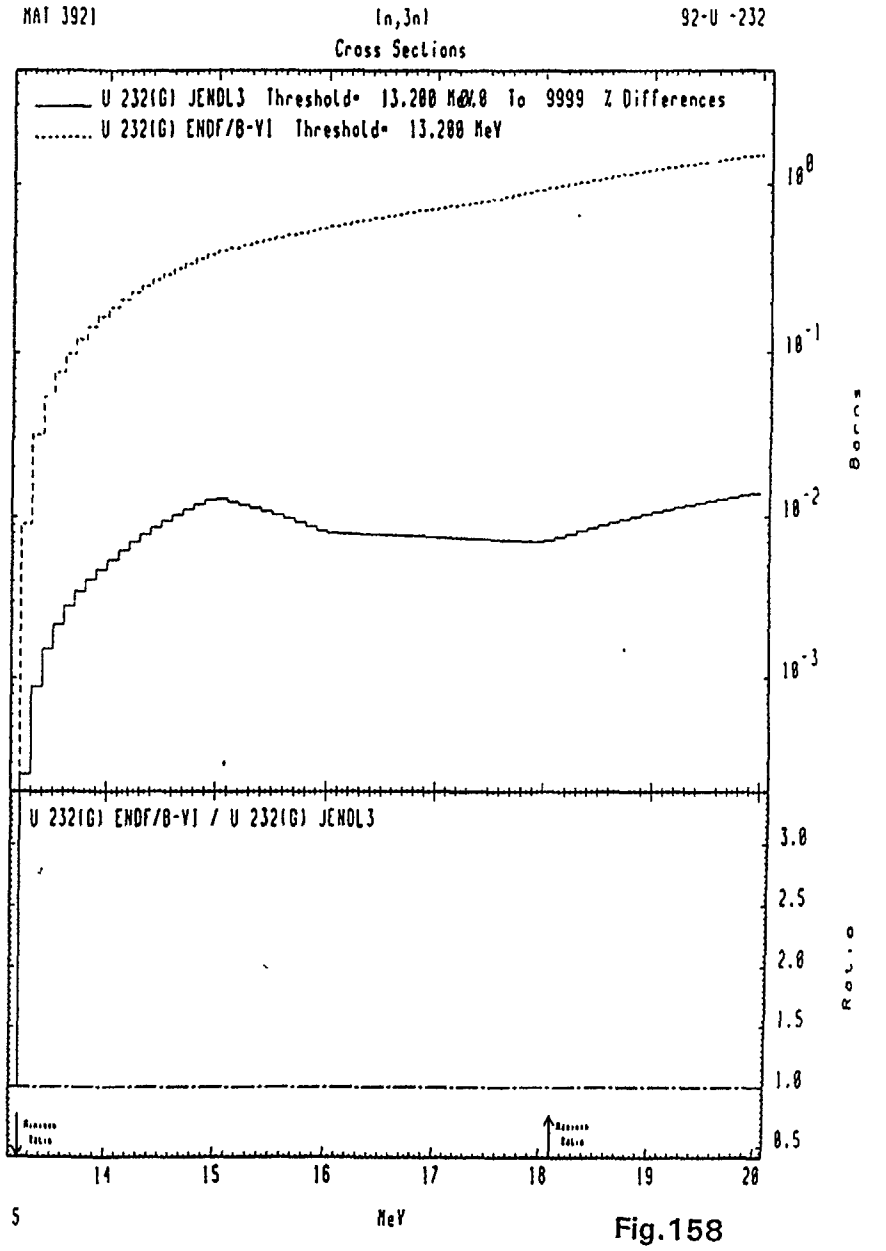

Fig.158

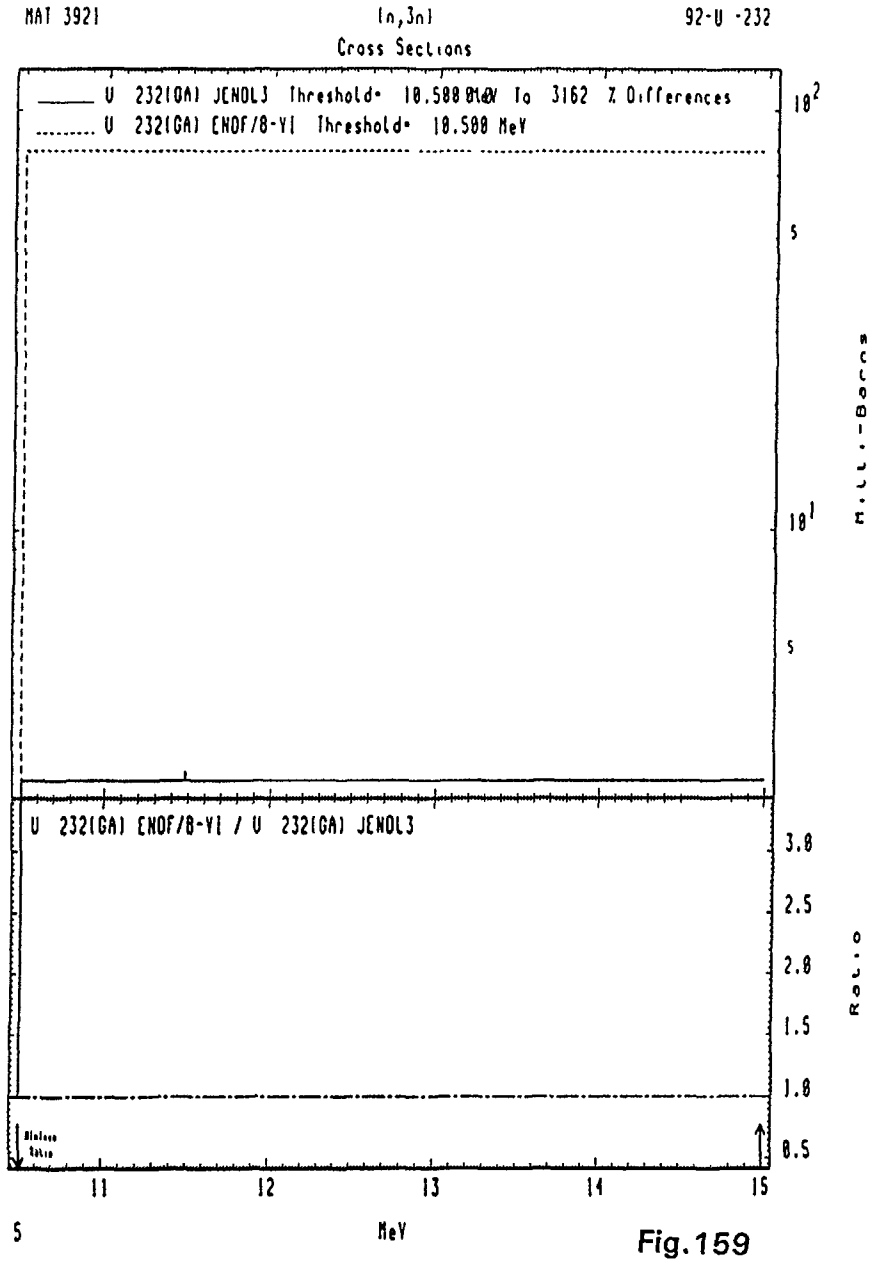

Fig.159

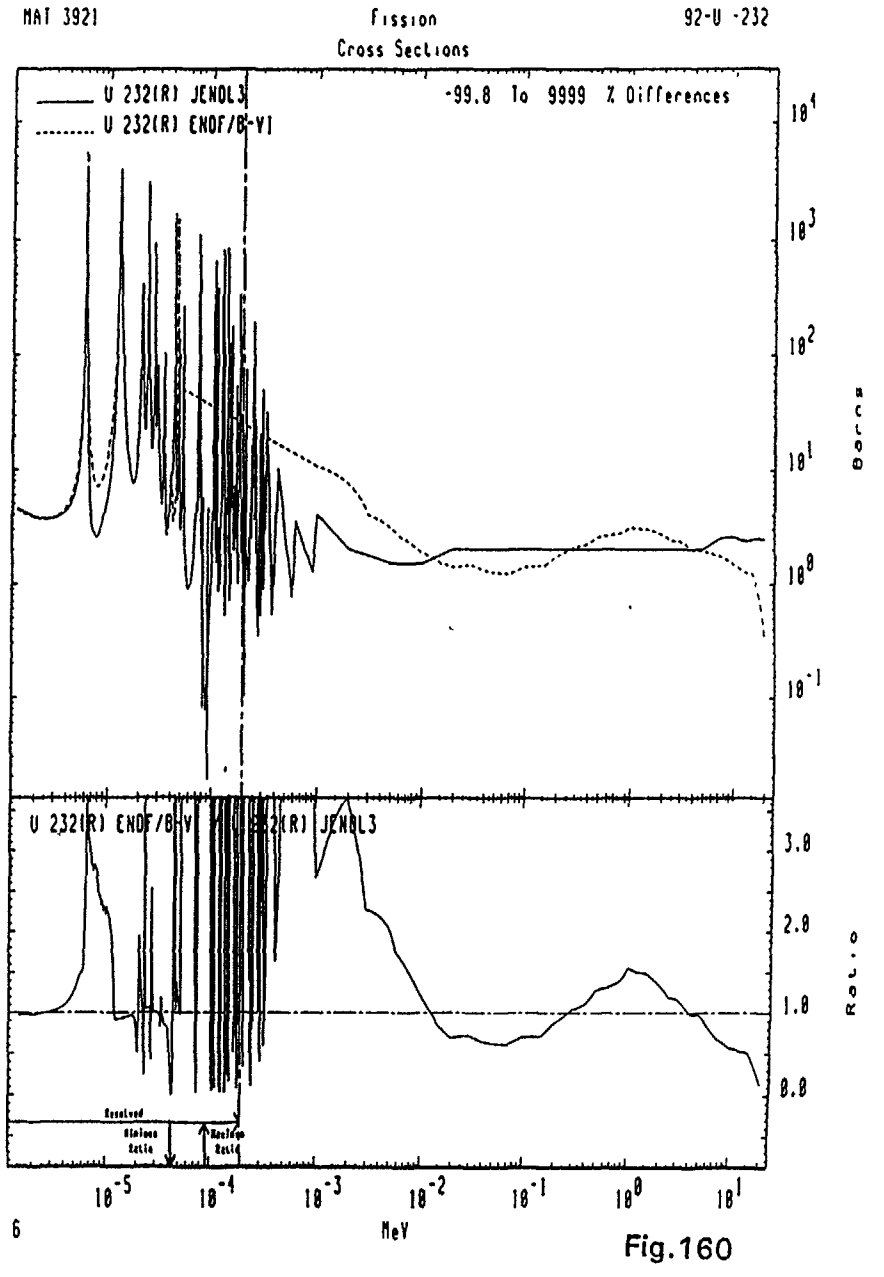

Fig.160

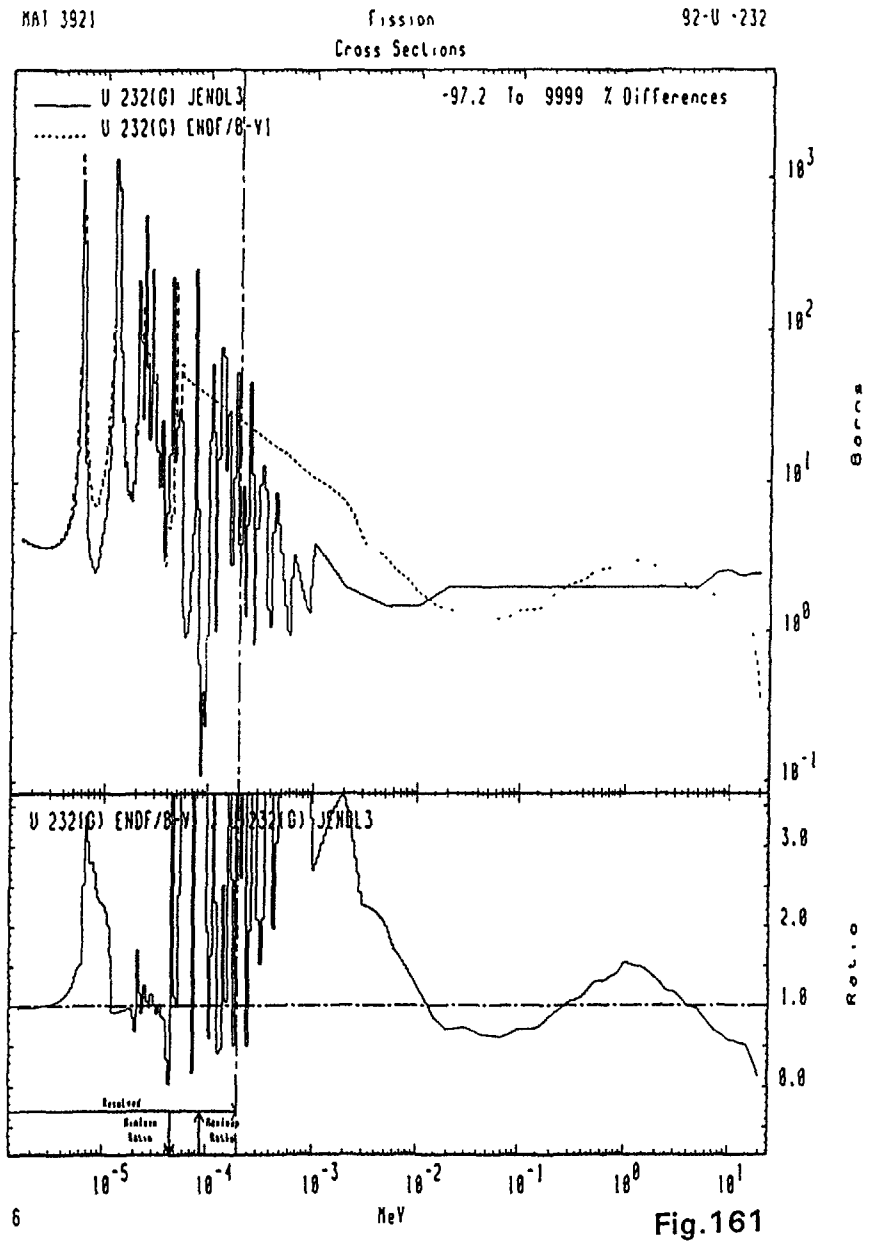

Fig.161

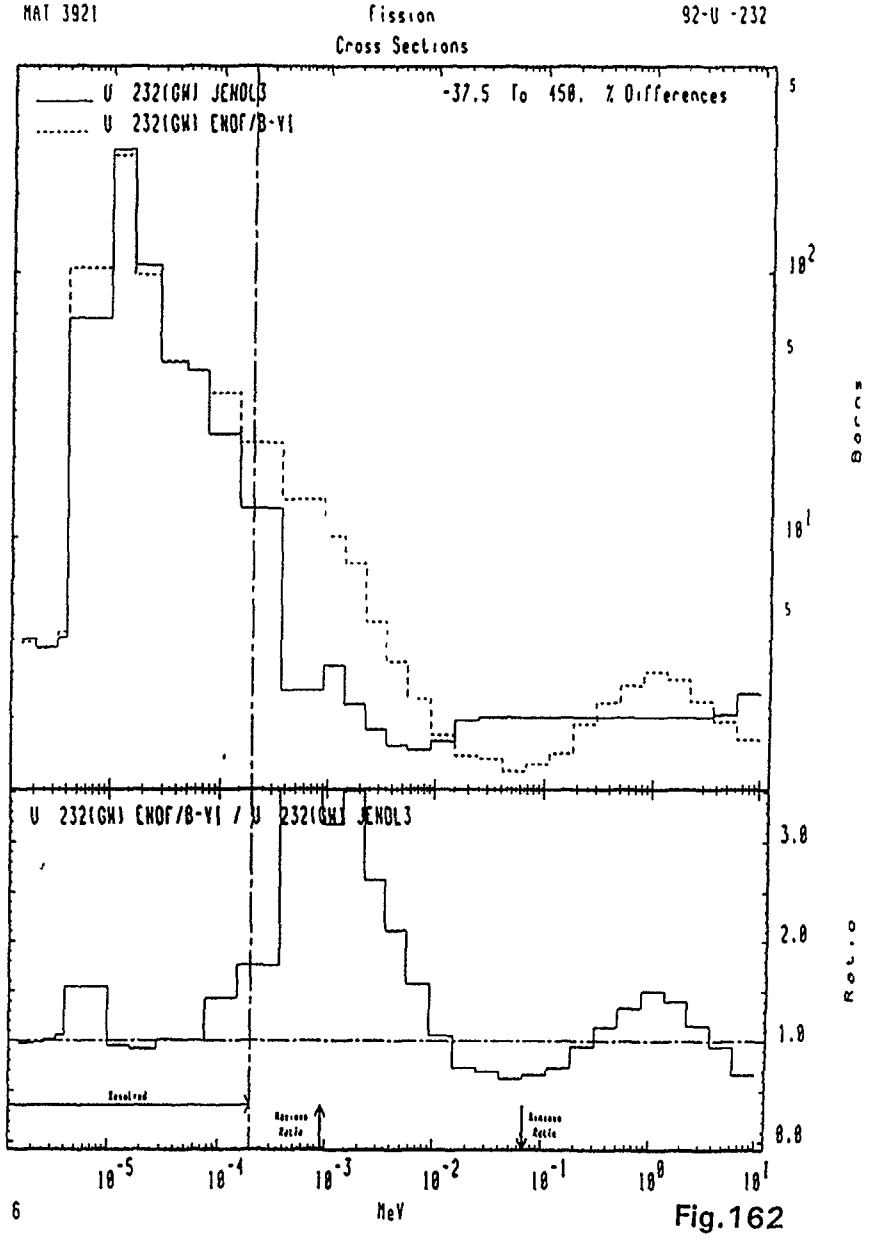

Fig.162

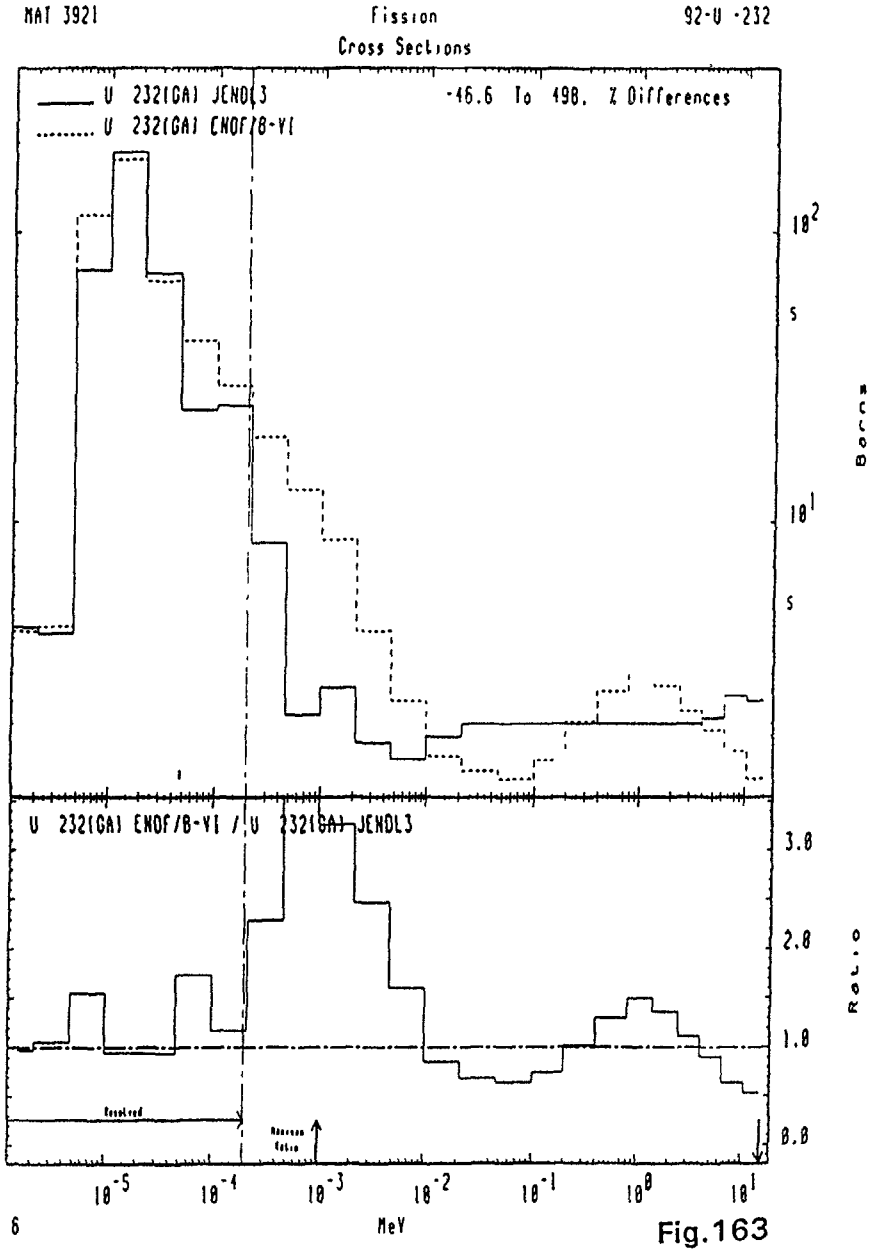

Fig.163

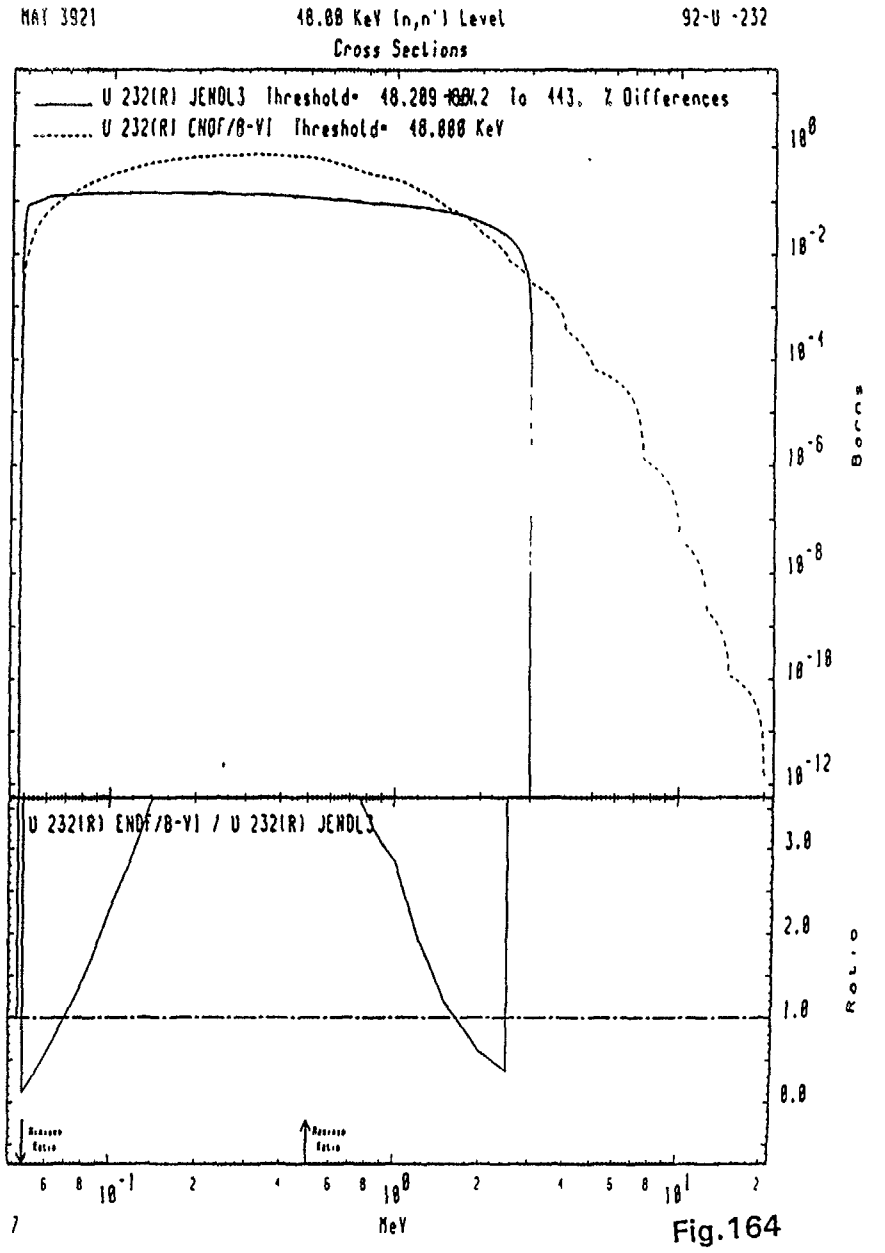

Fig.164

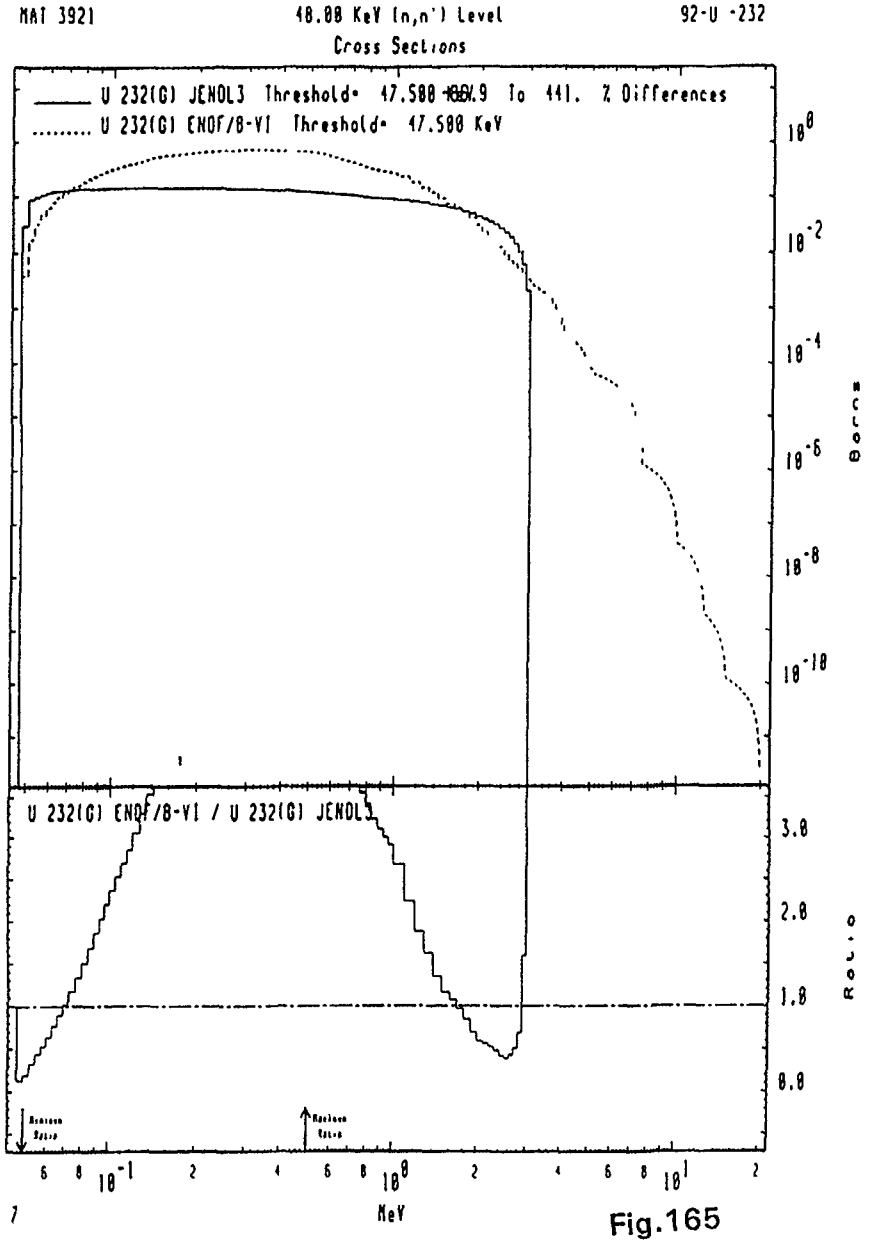

Fig.165

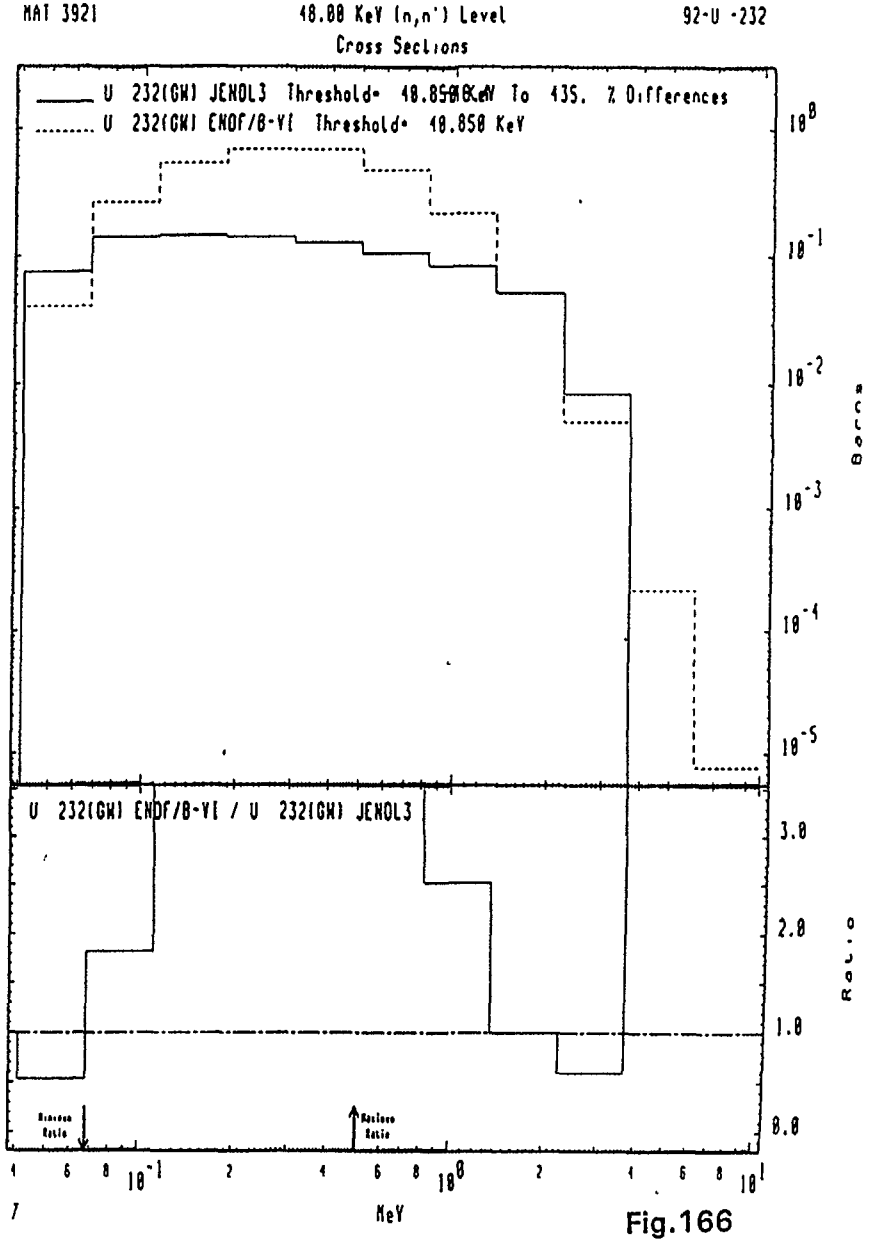

Fig.166

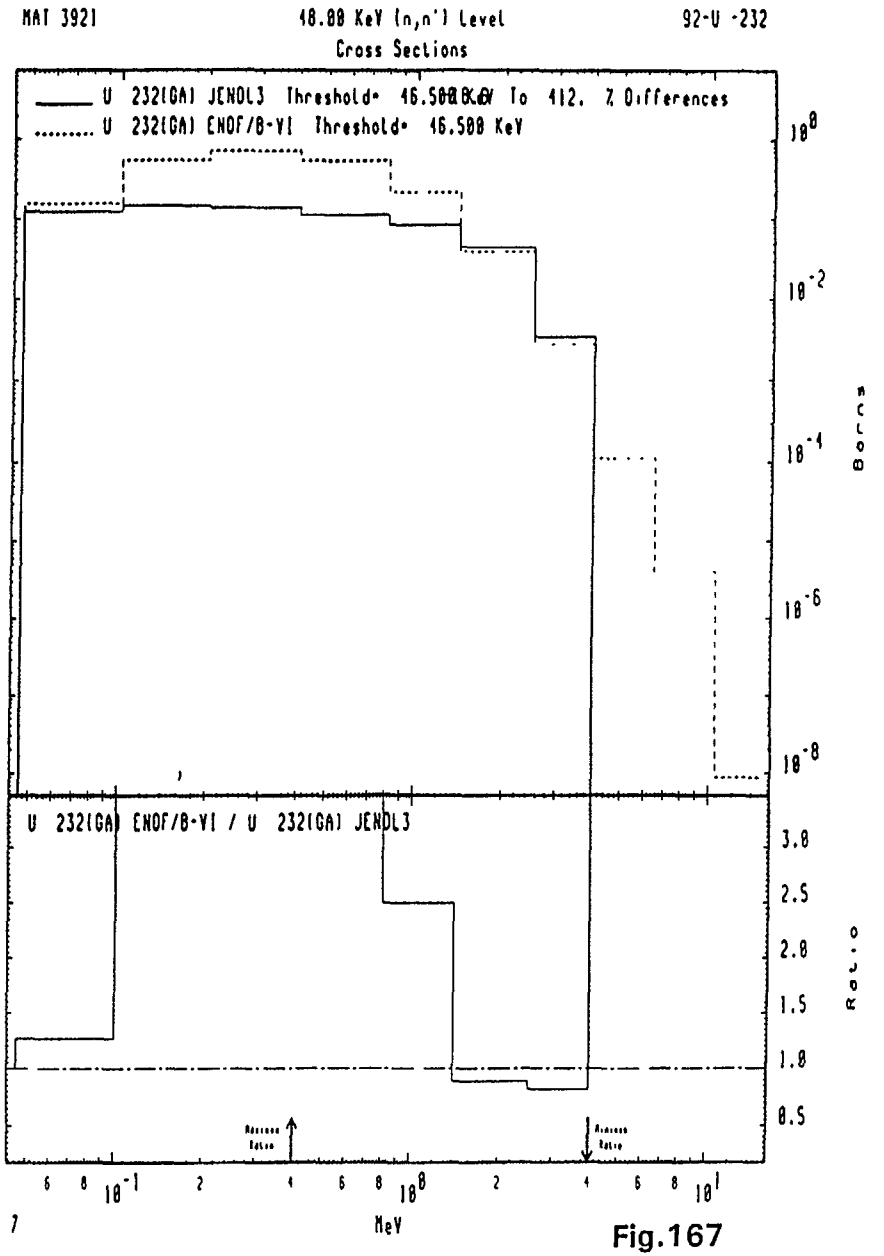

Fig.167

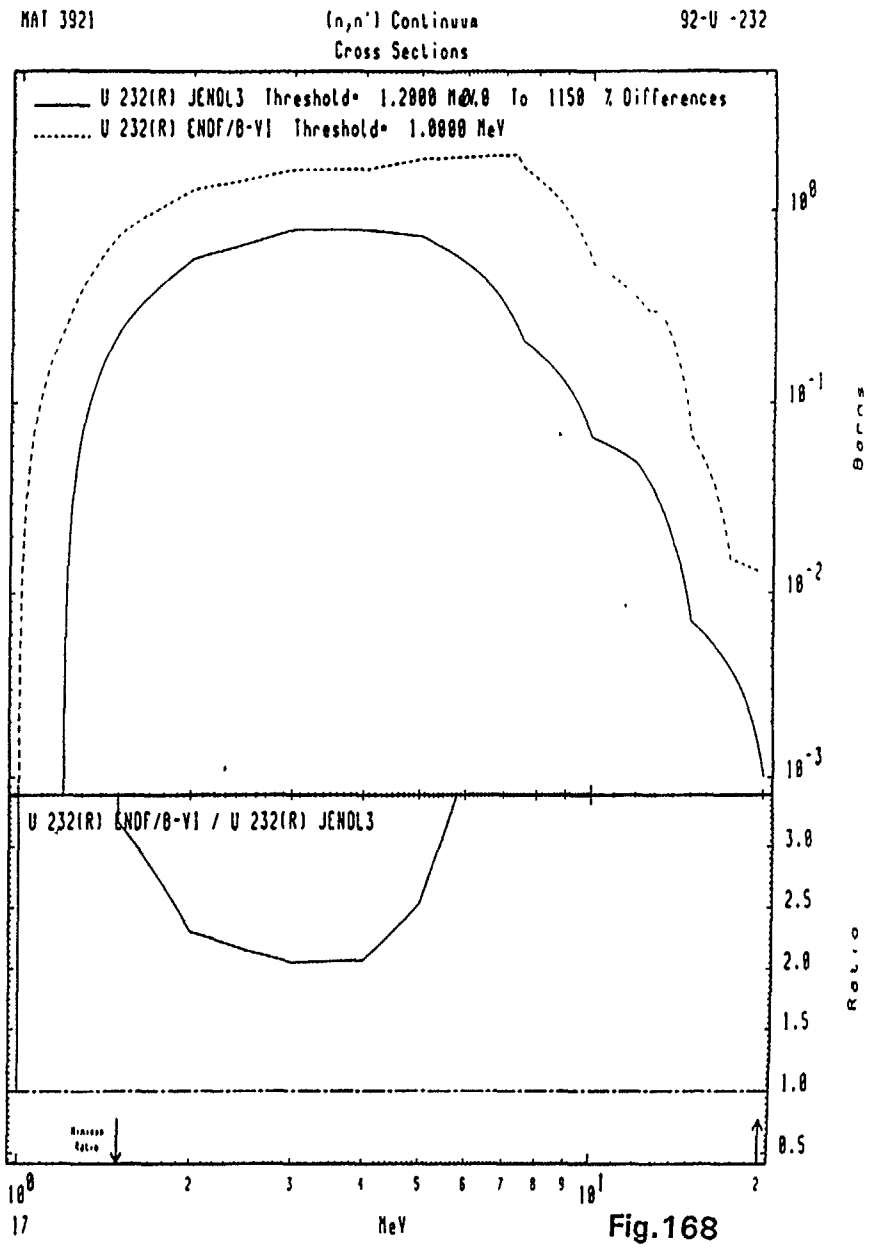

Fig.168

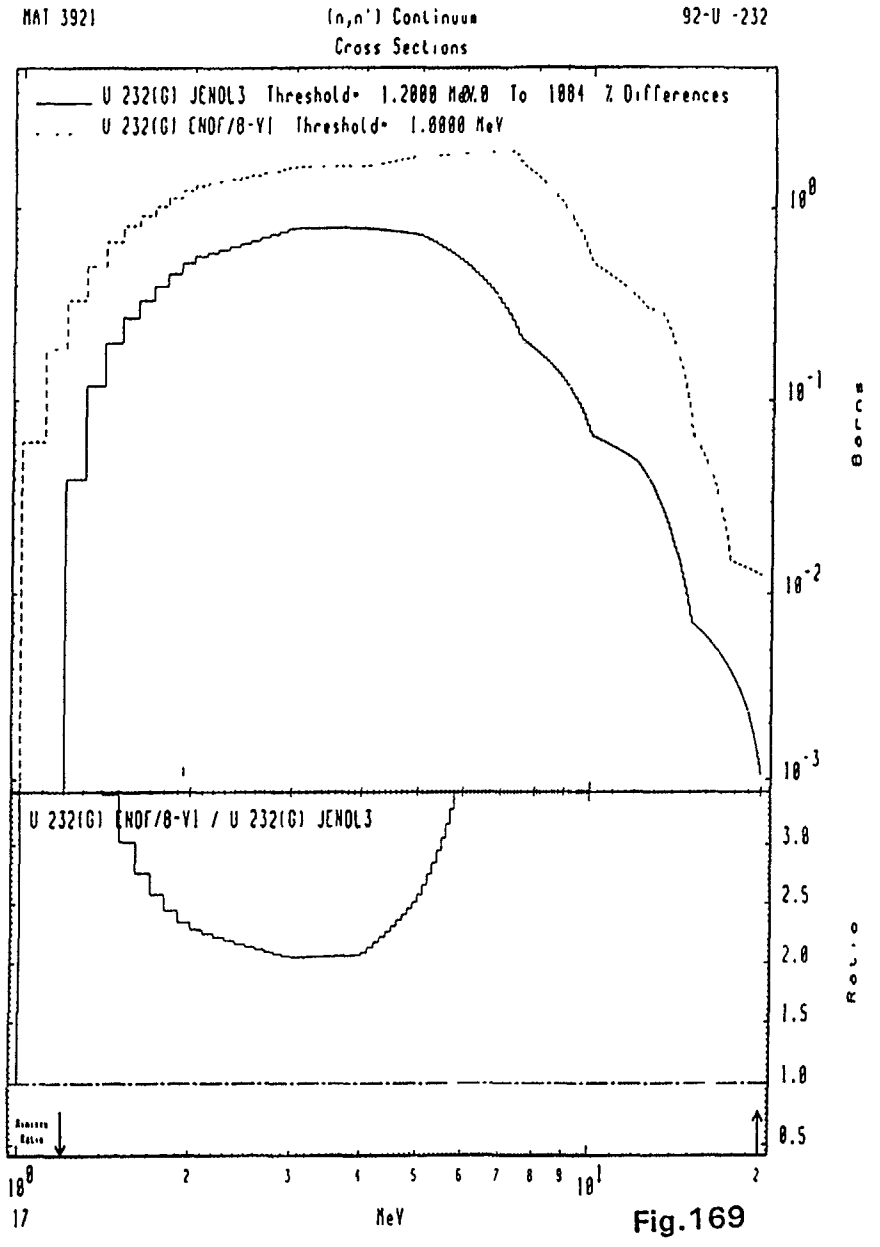

Fig.169

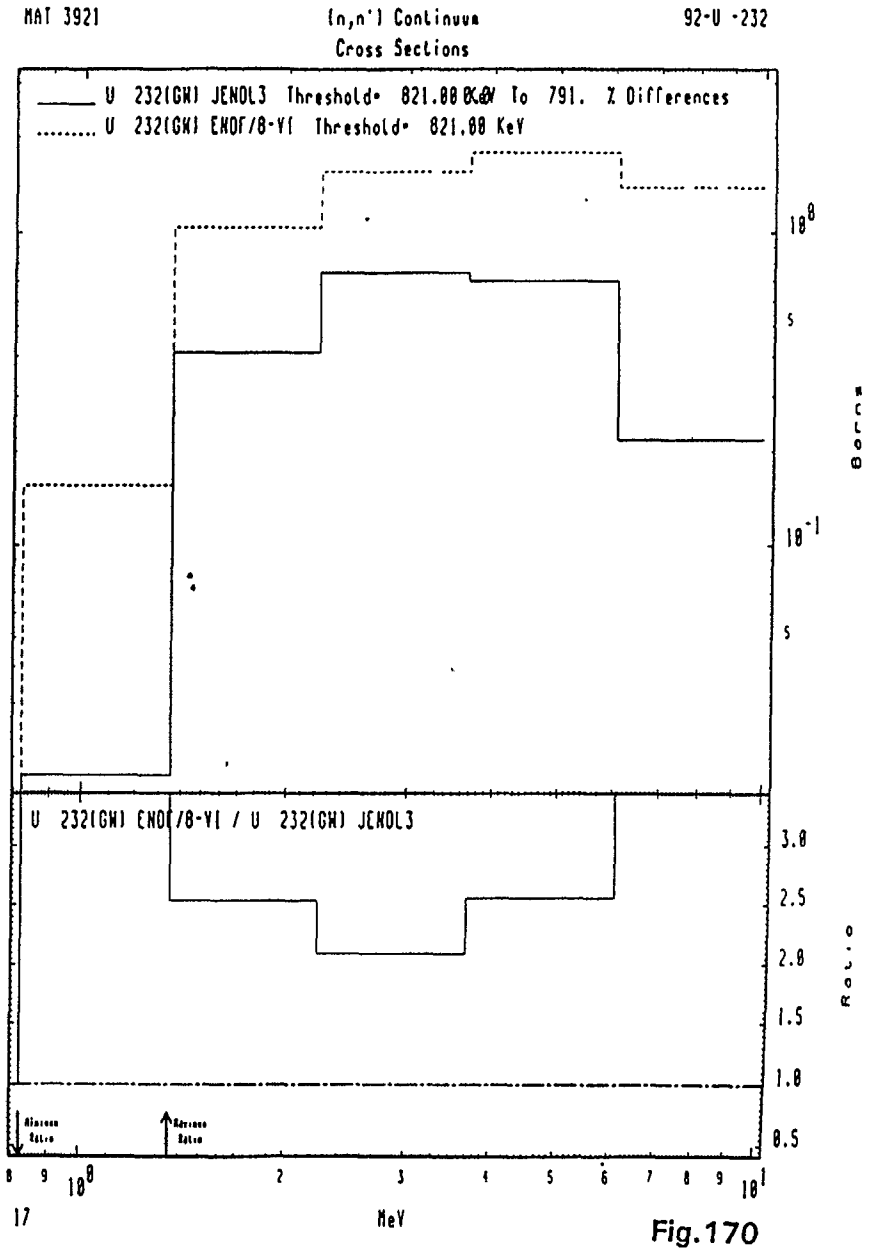

Fig.170

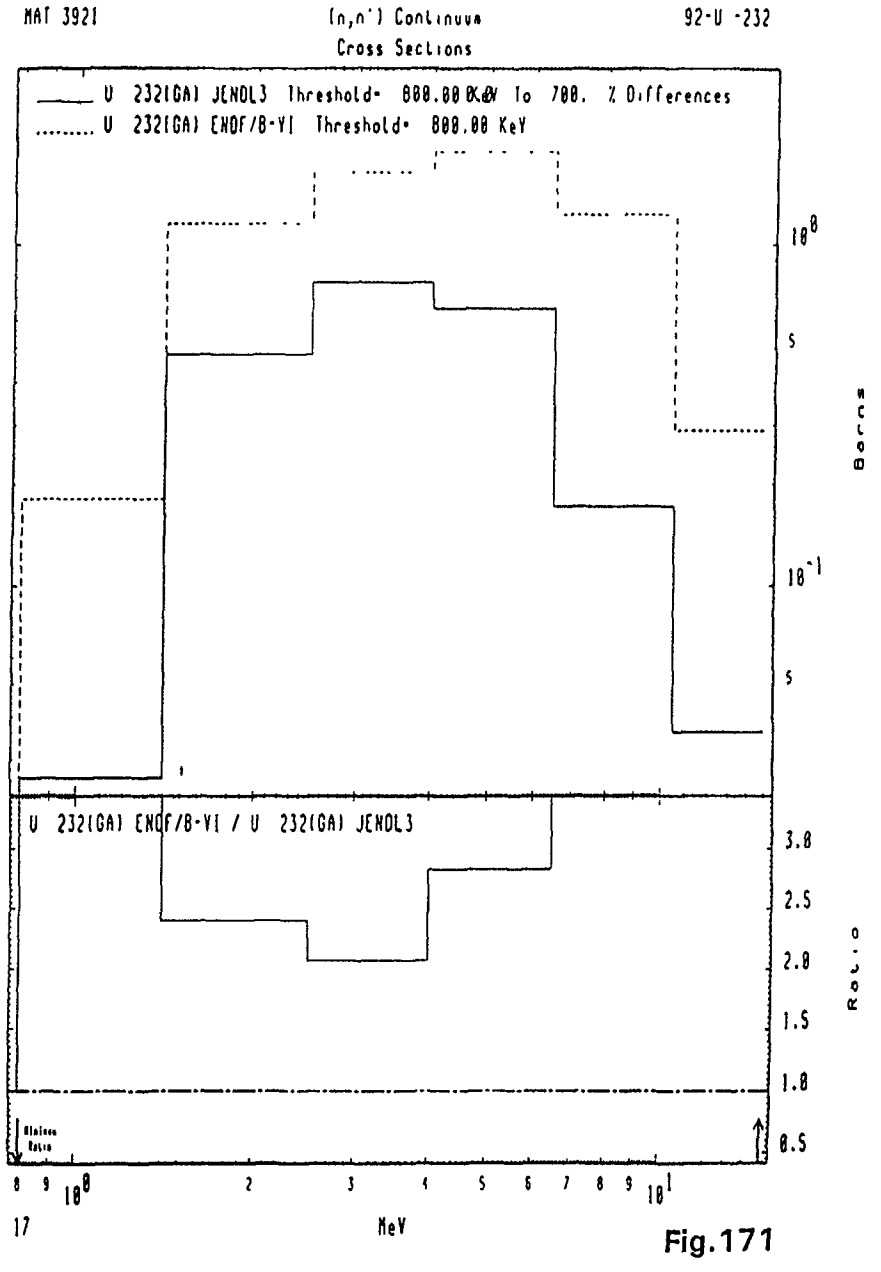

Fig.171

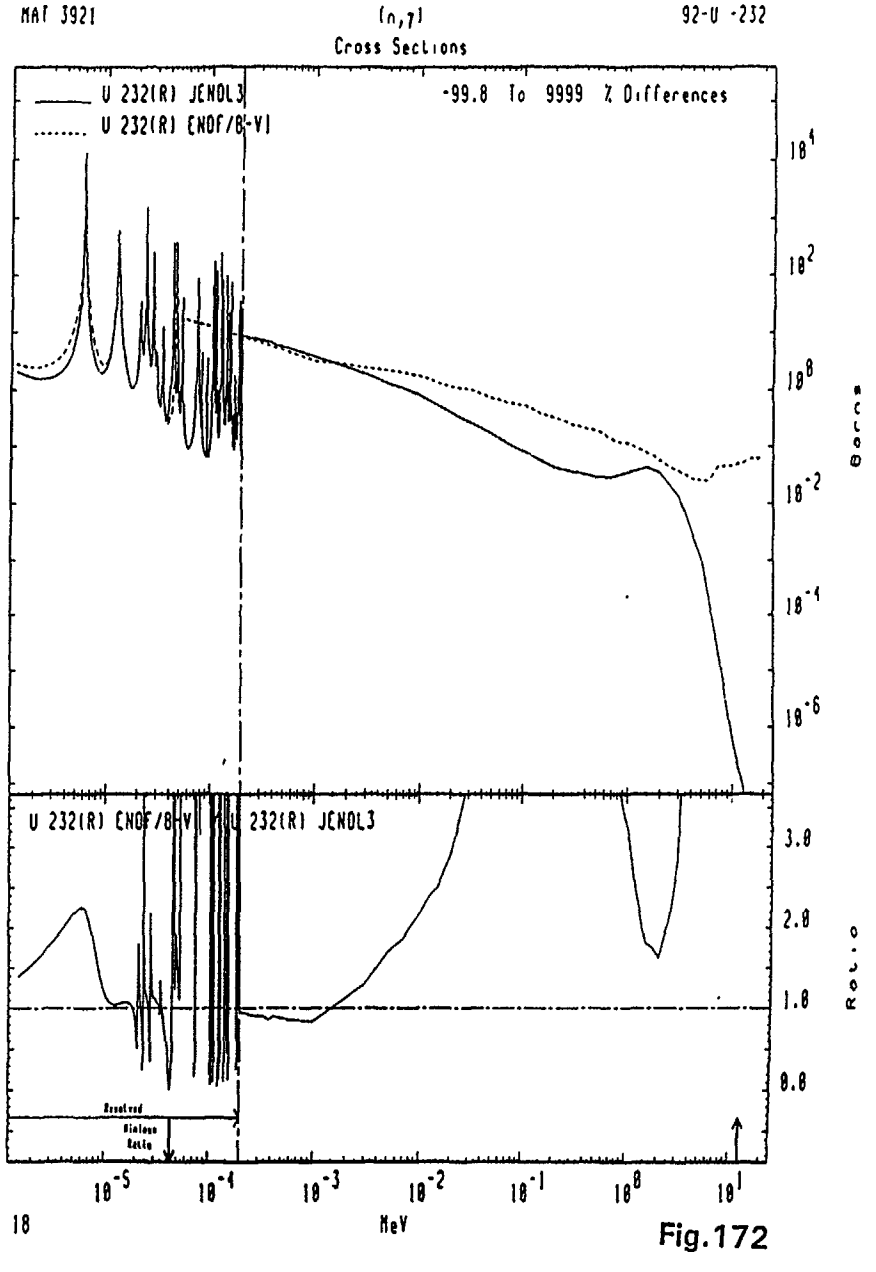

Fig.172

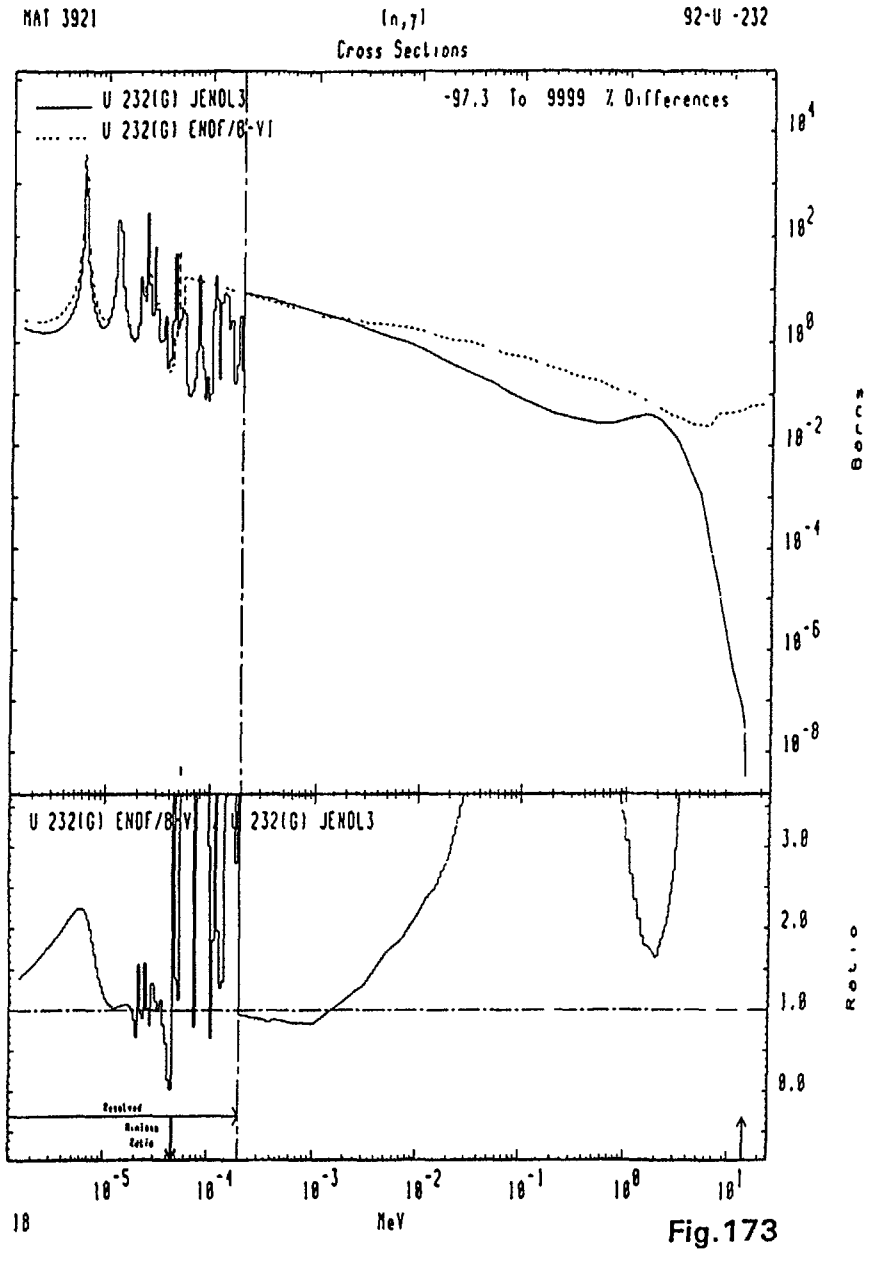

Fig.173

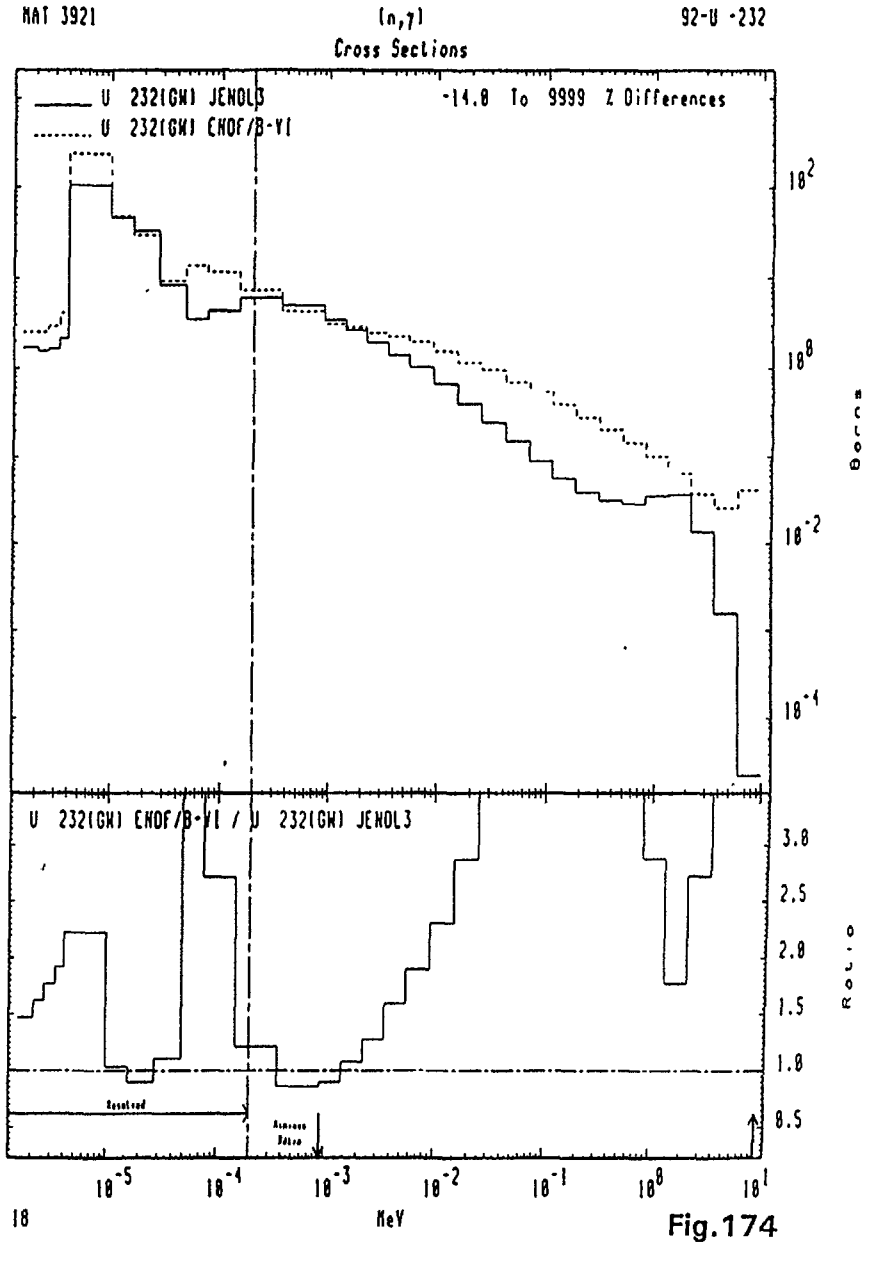

Fig.174

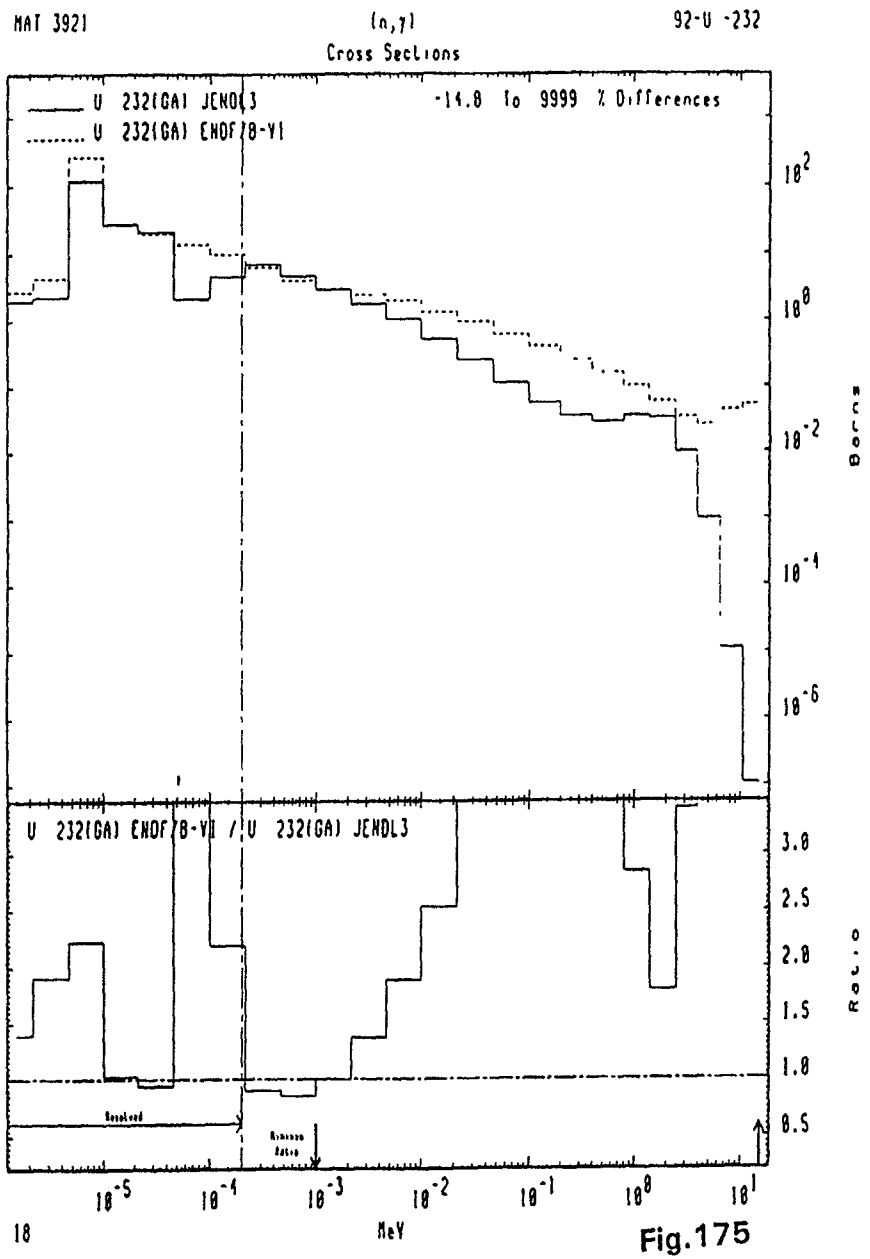

Fig.175

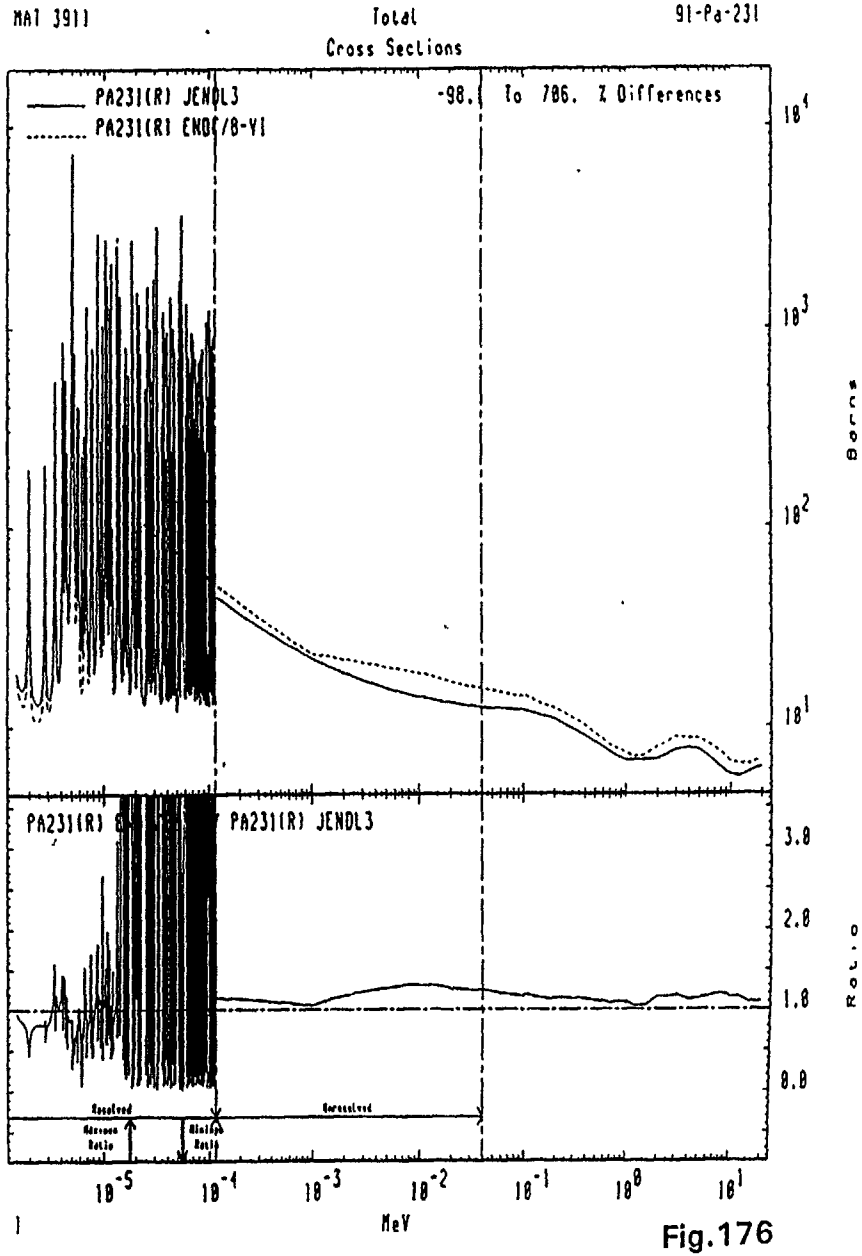

Fig.176

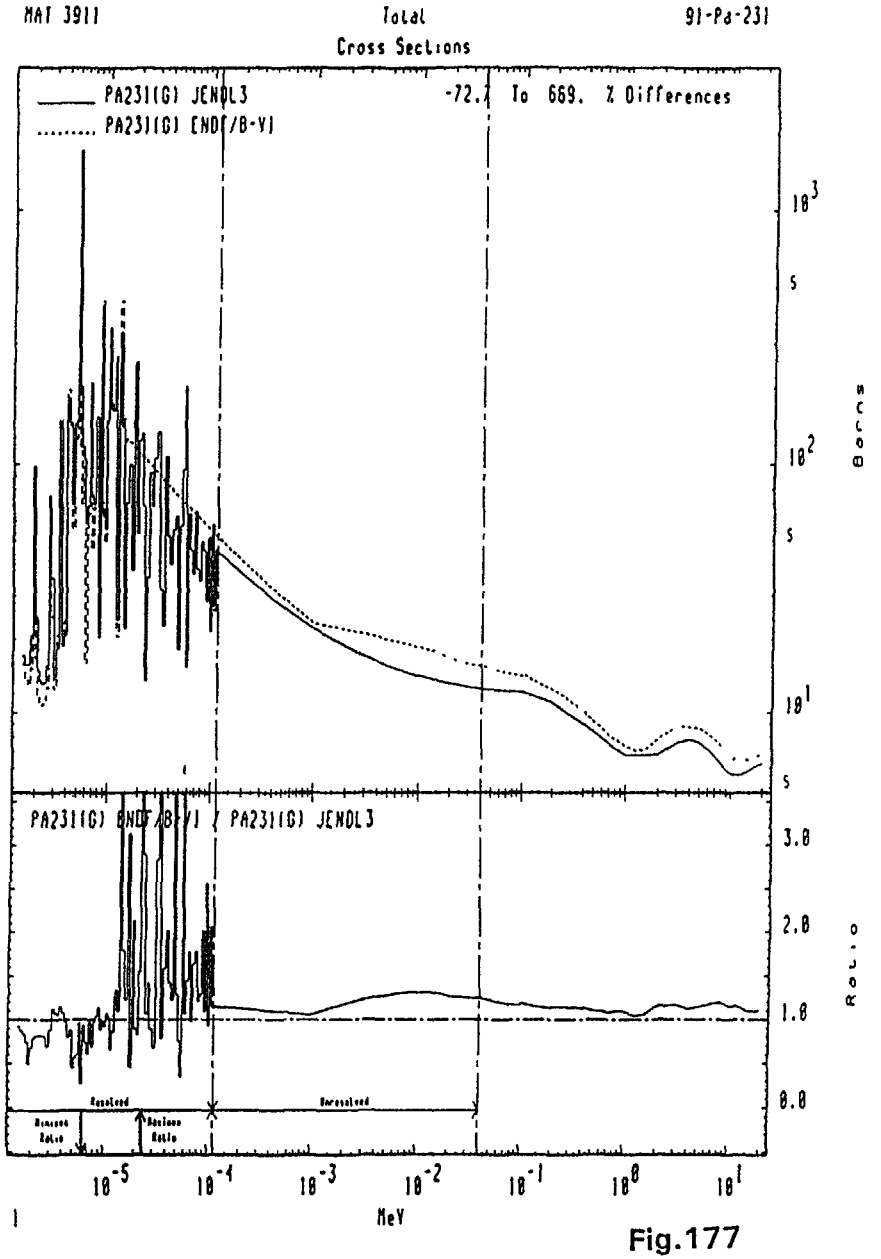

Fig.177

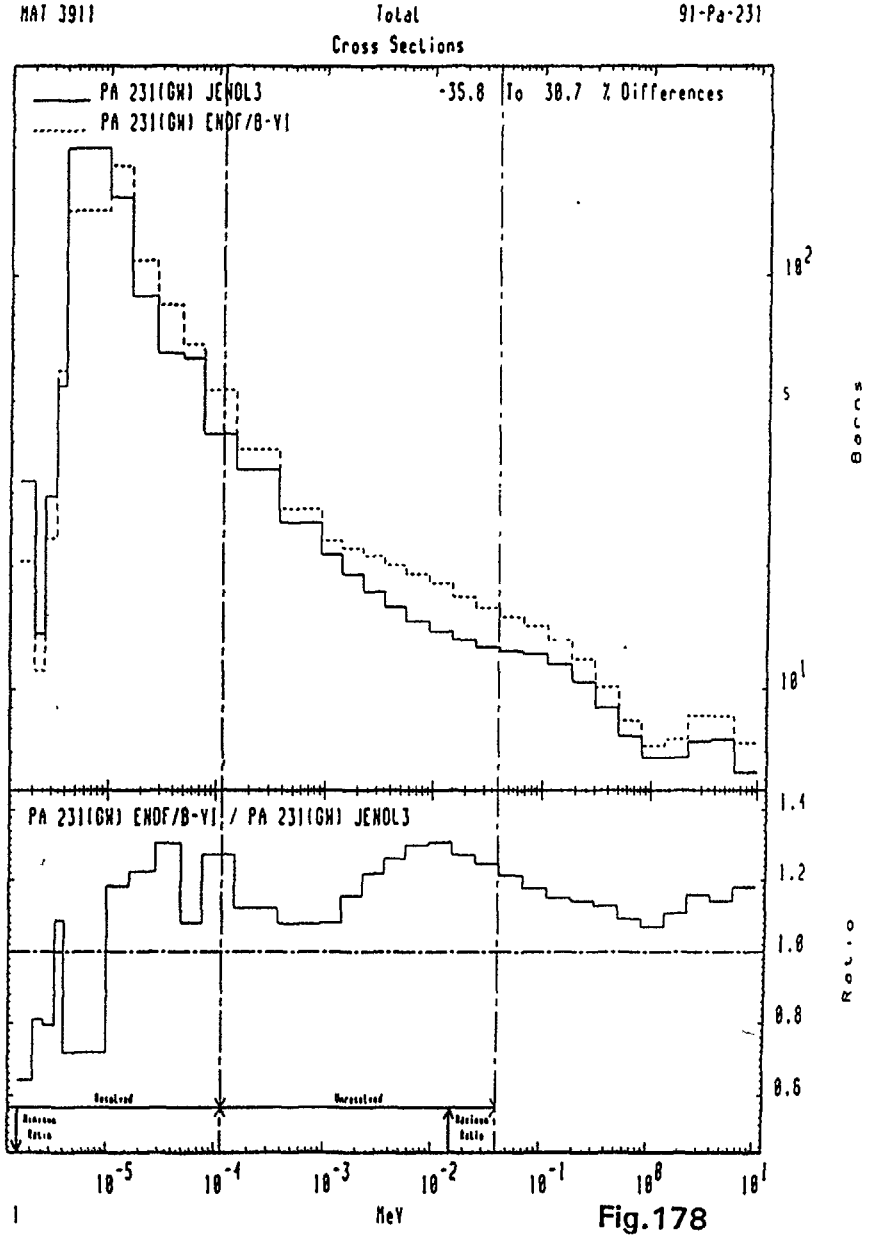

Fig.178

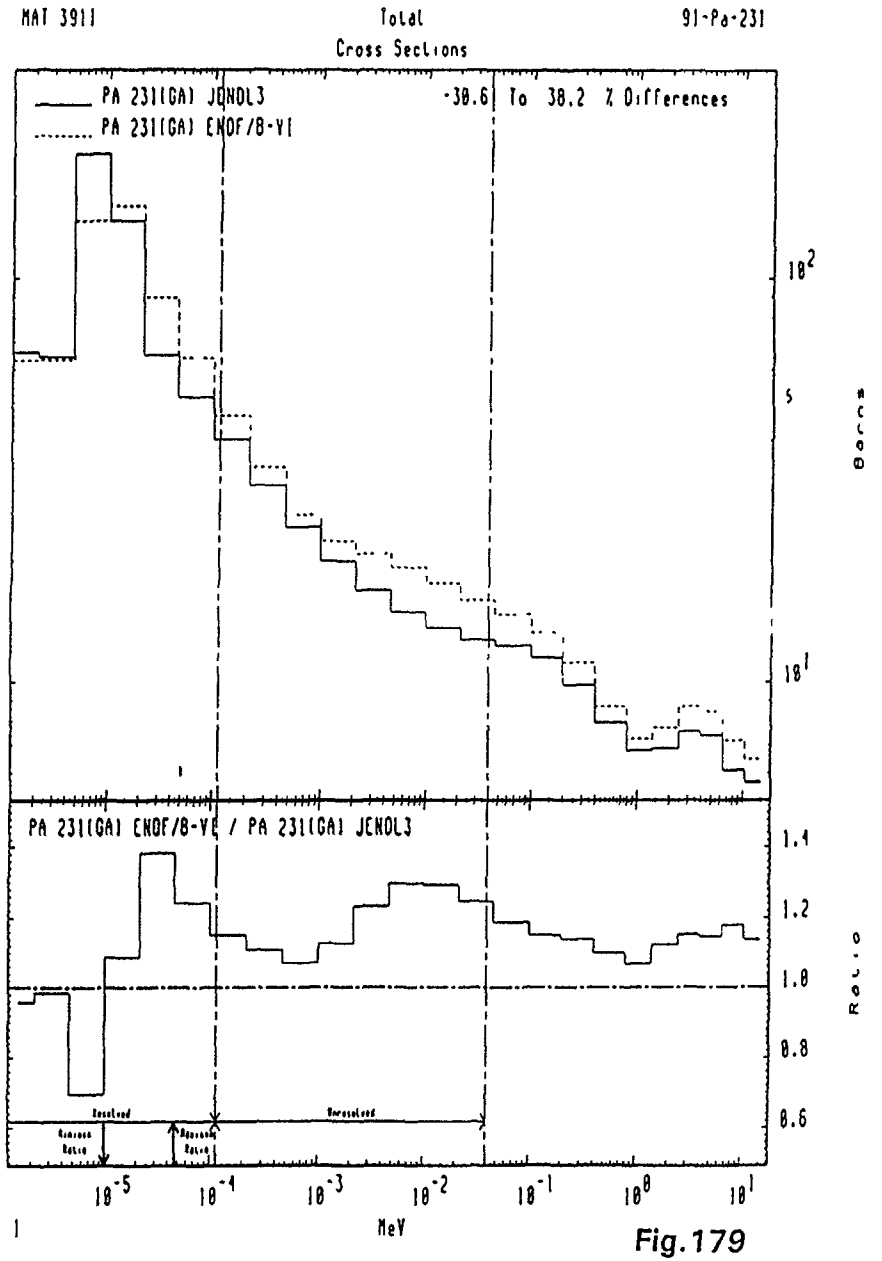

Fig.179

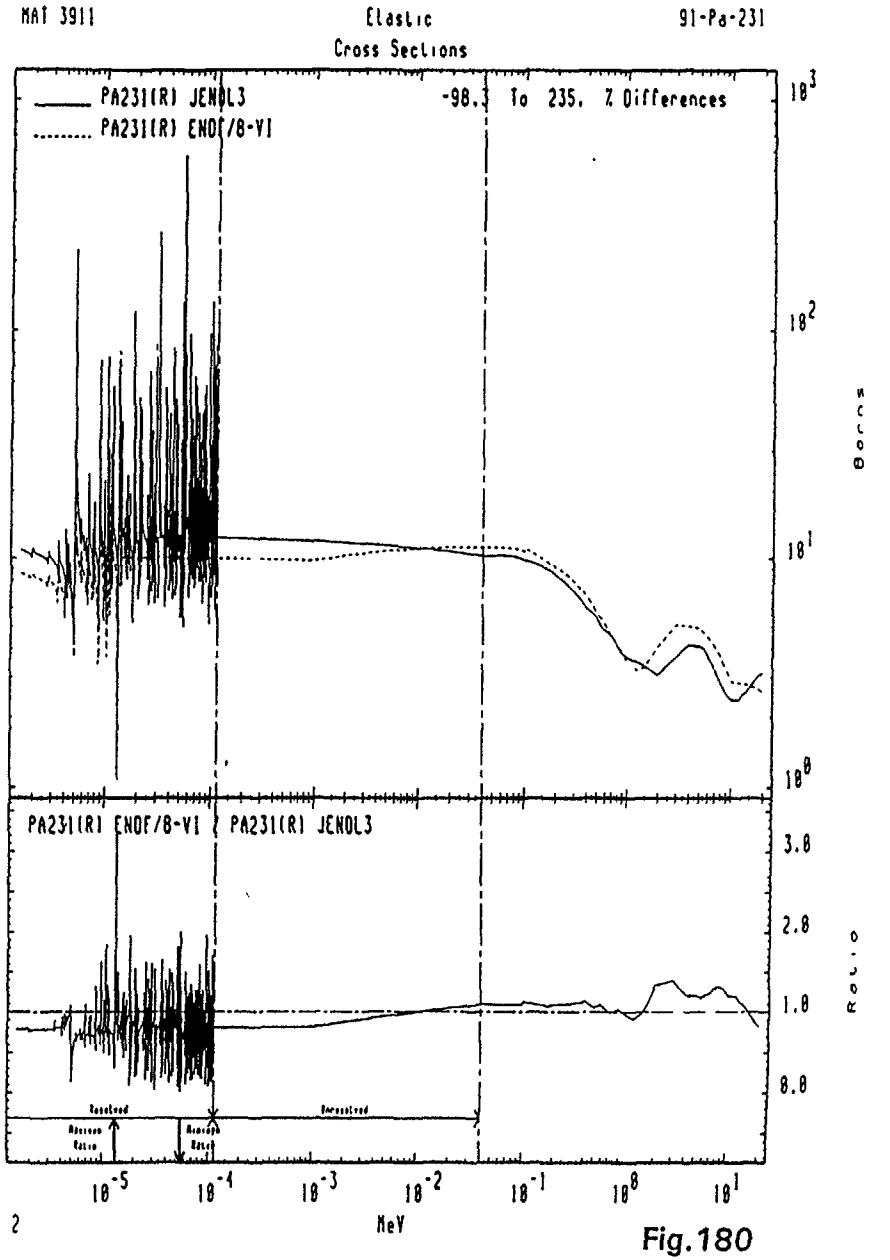

Fig.180

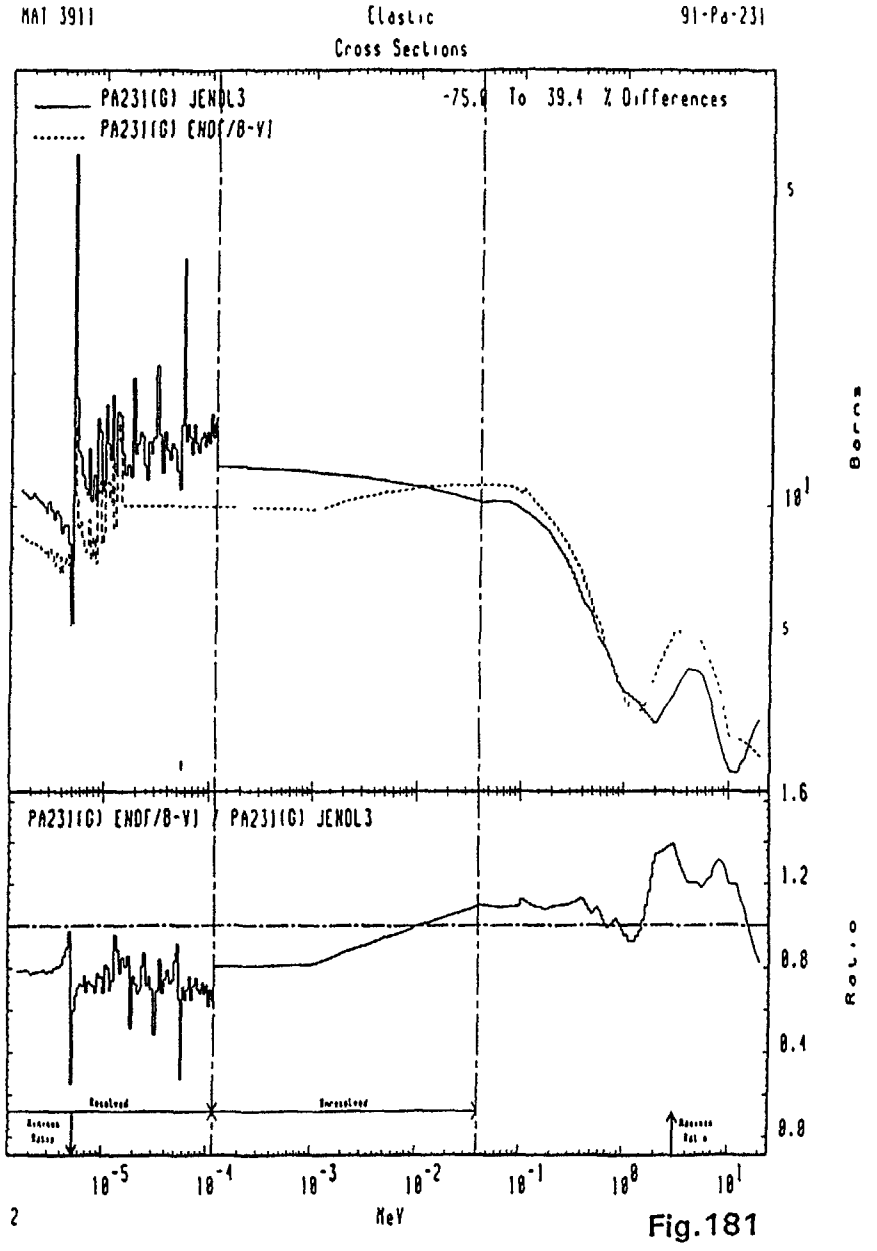

Fig.181

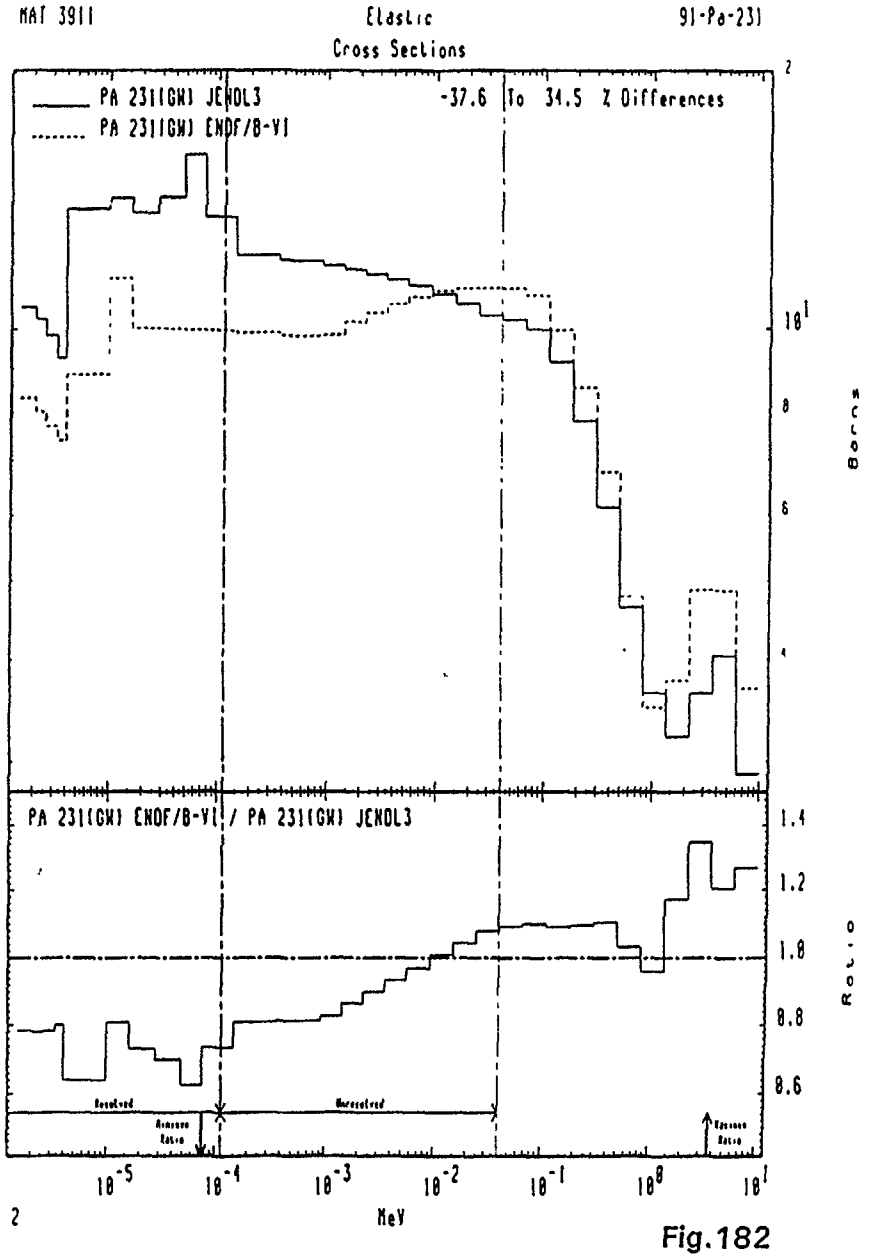

Fig.182

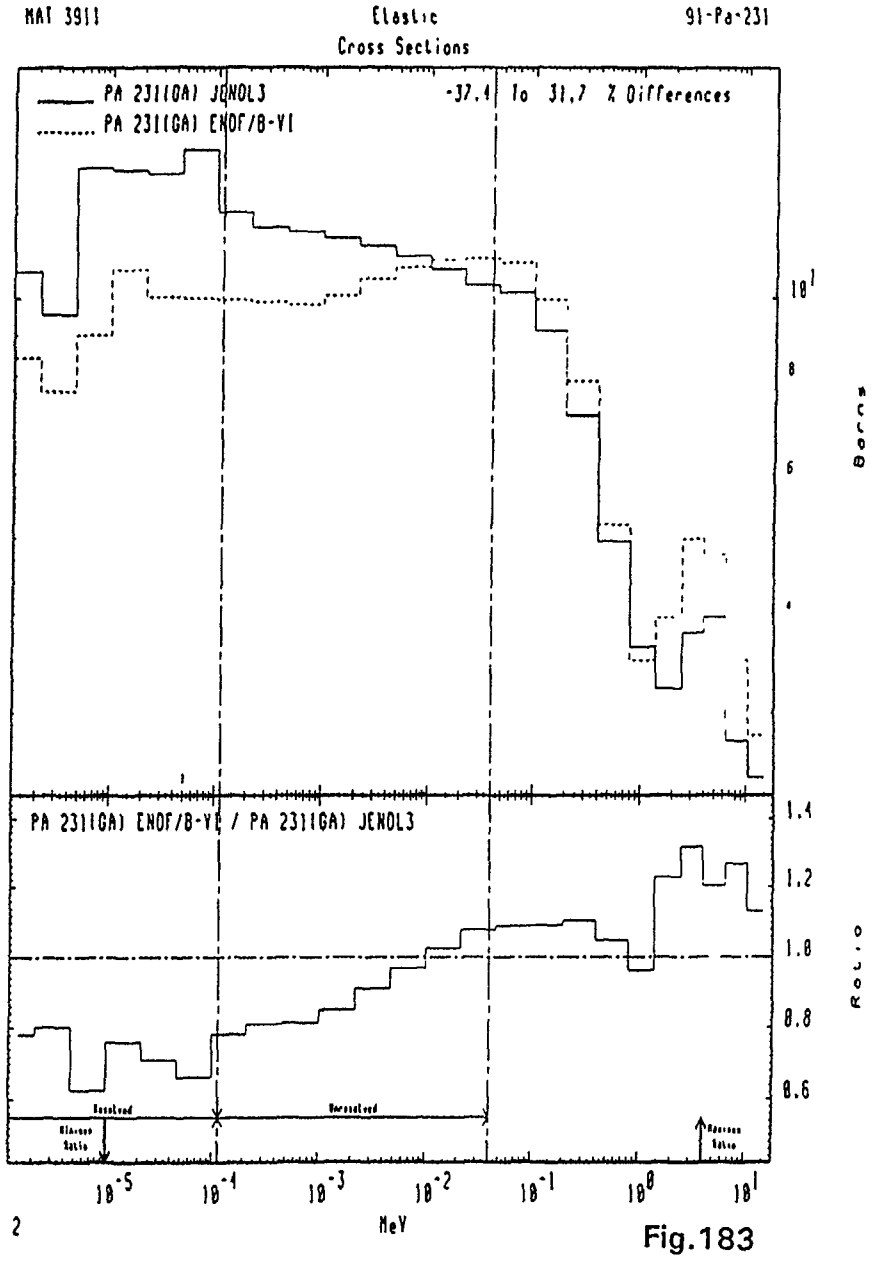

Fig.183

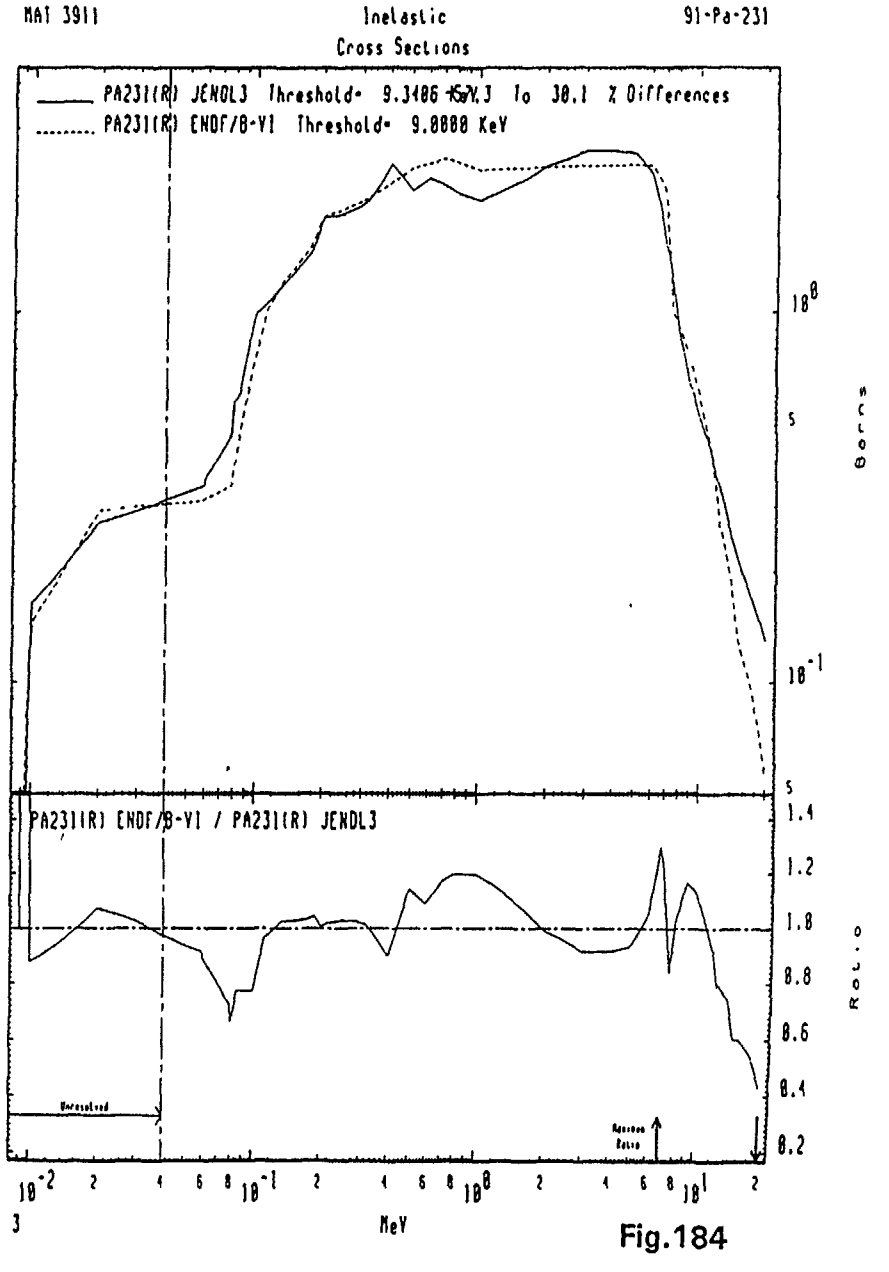

Fig.184

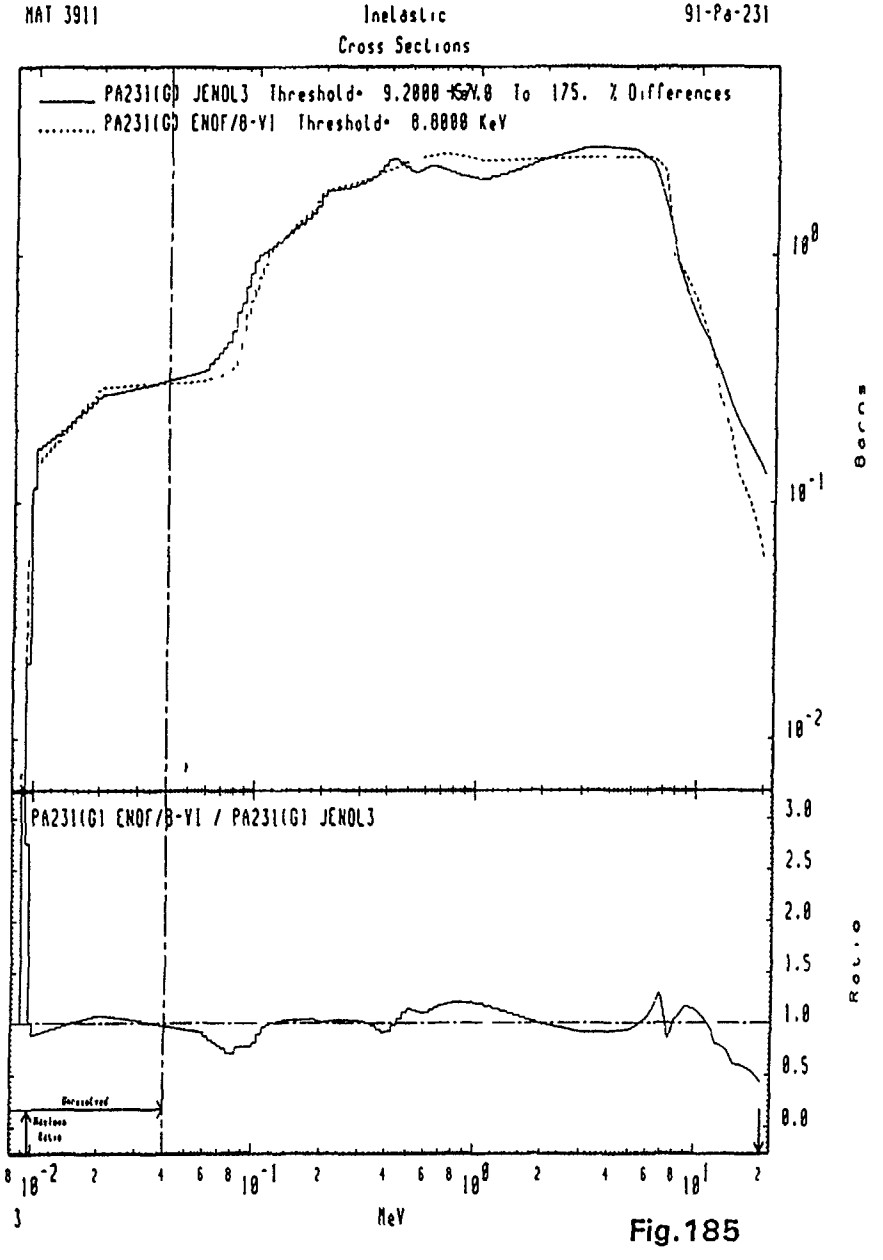

Fig.185

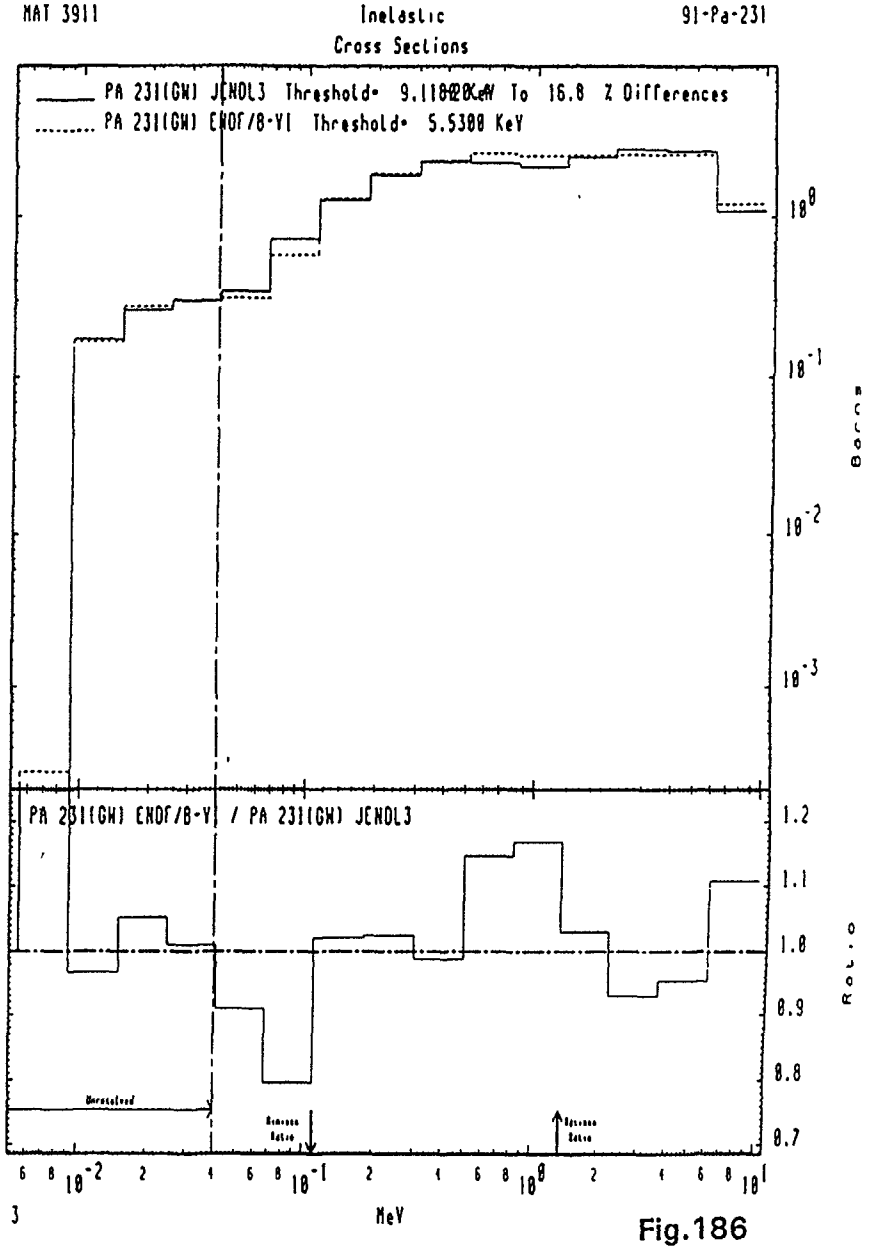

Fig.186

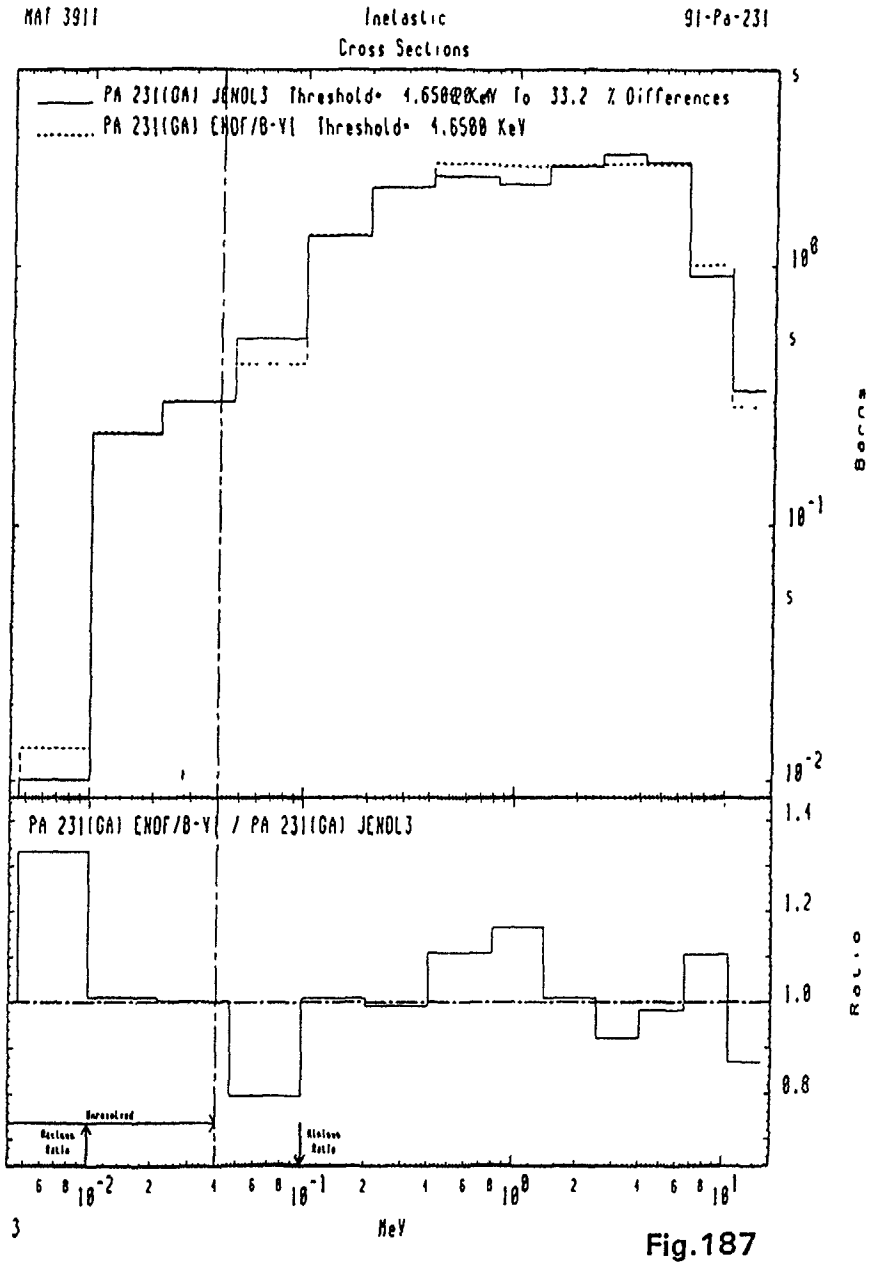

Fig.187

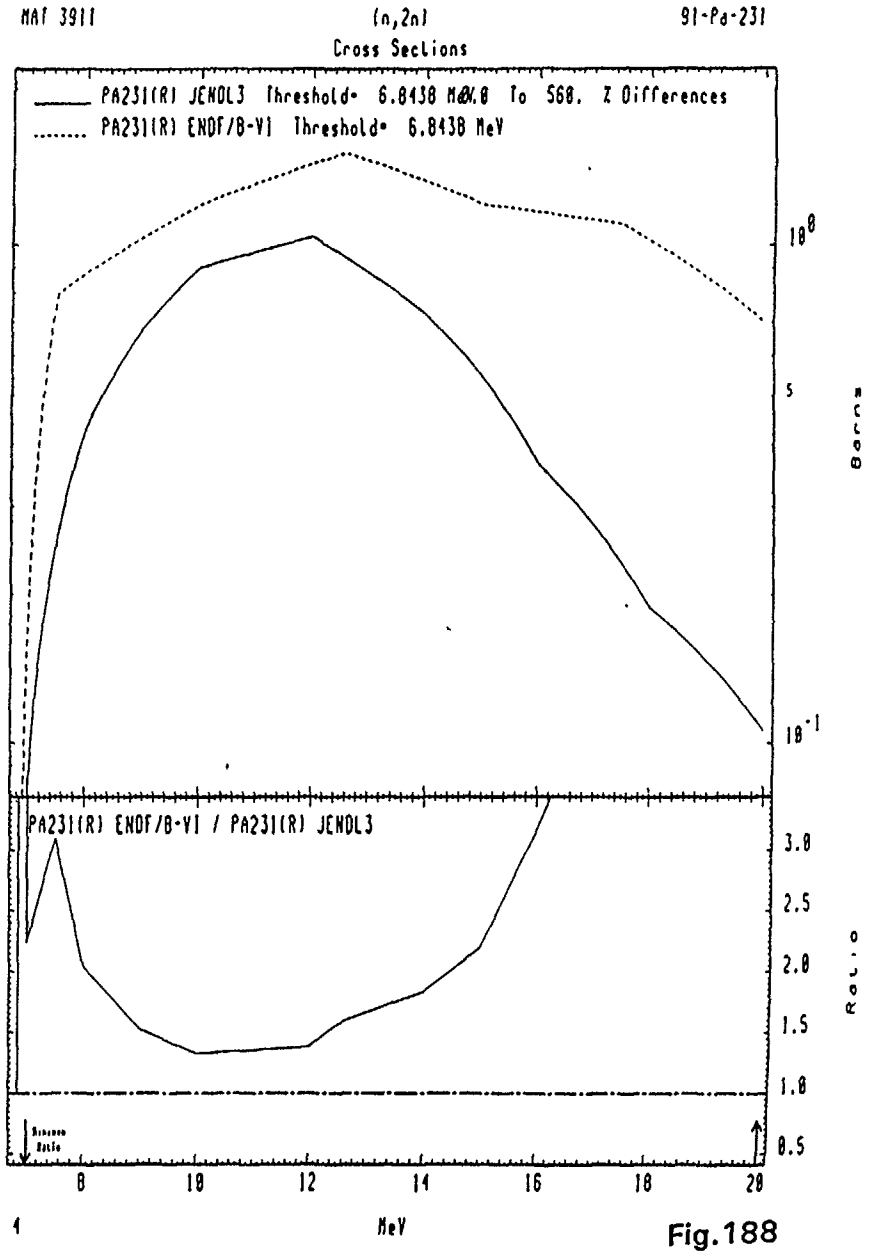

Fig.188

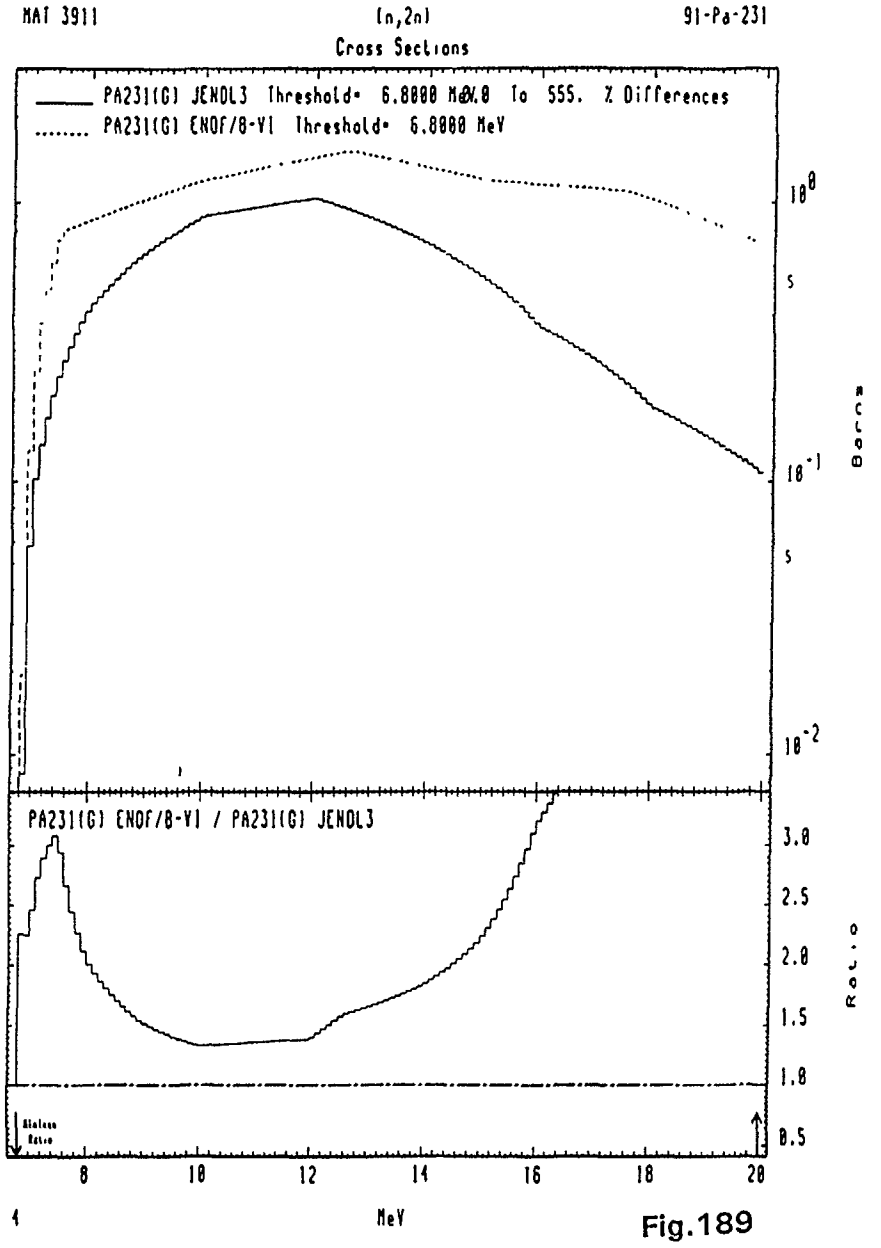

Fig.189

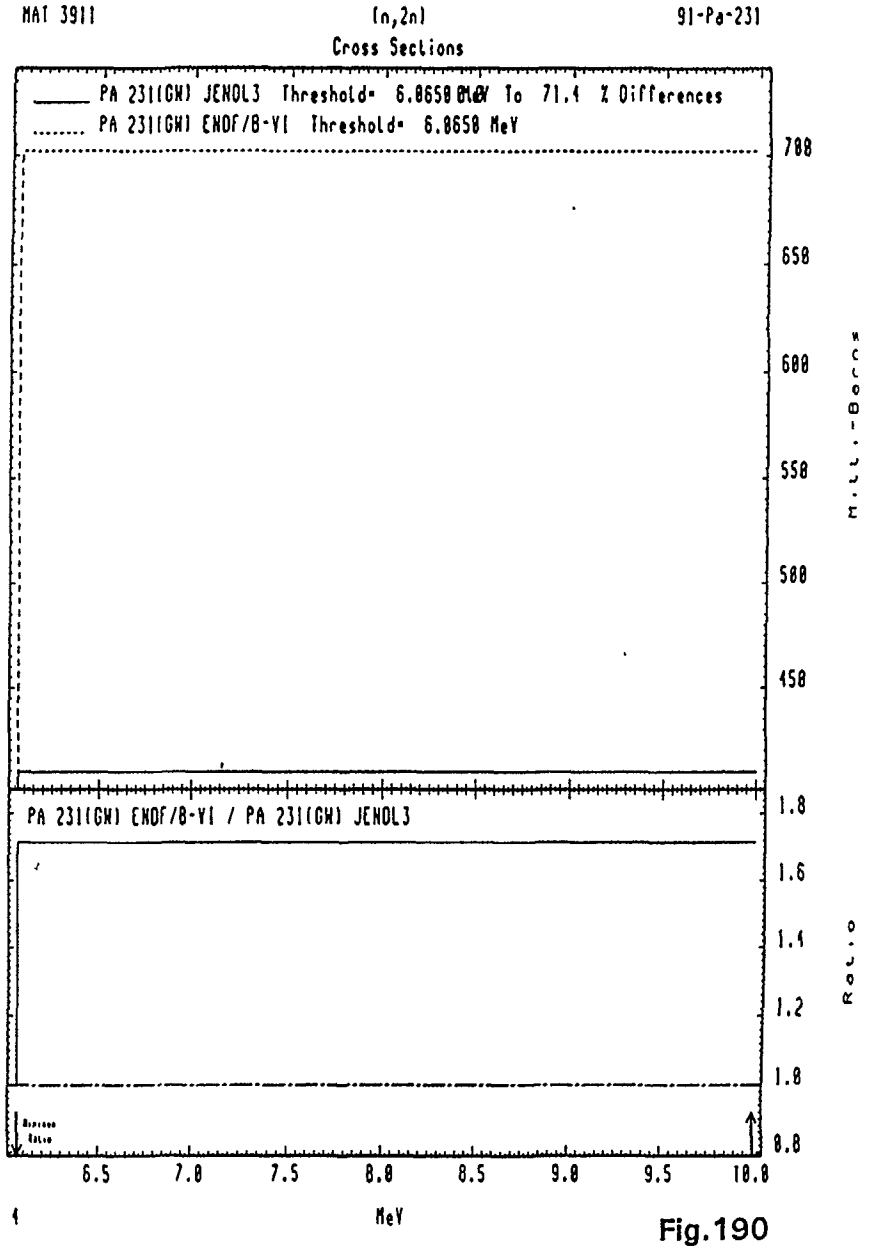

Fig.190

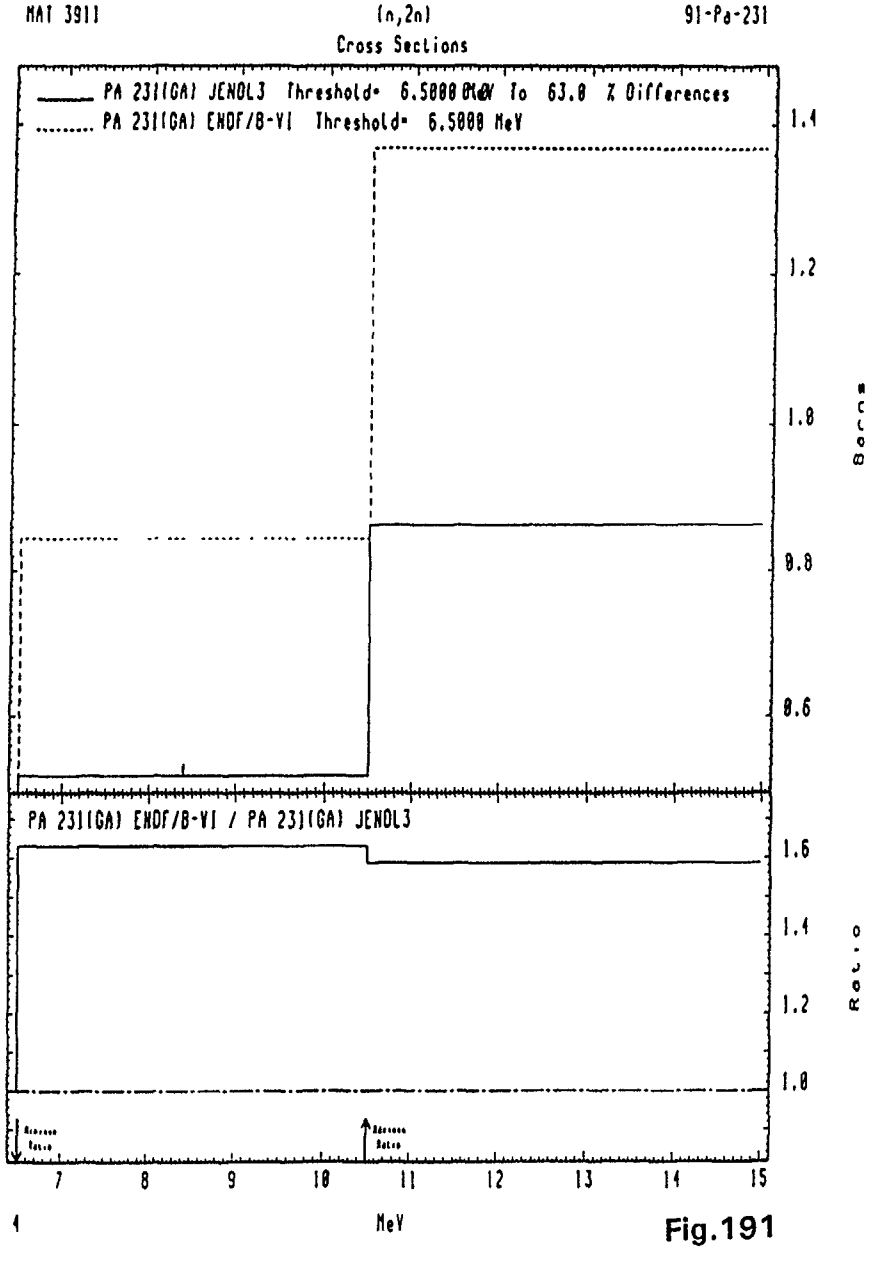

Fig.191

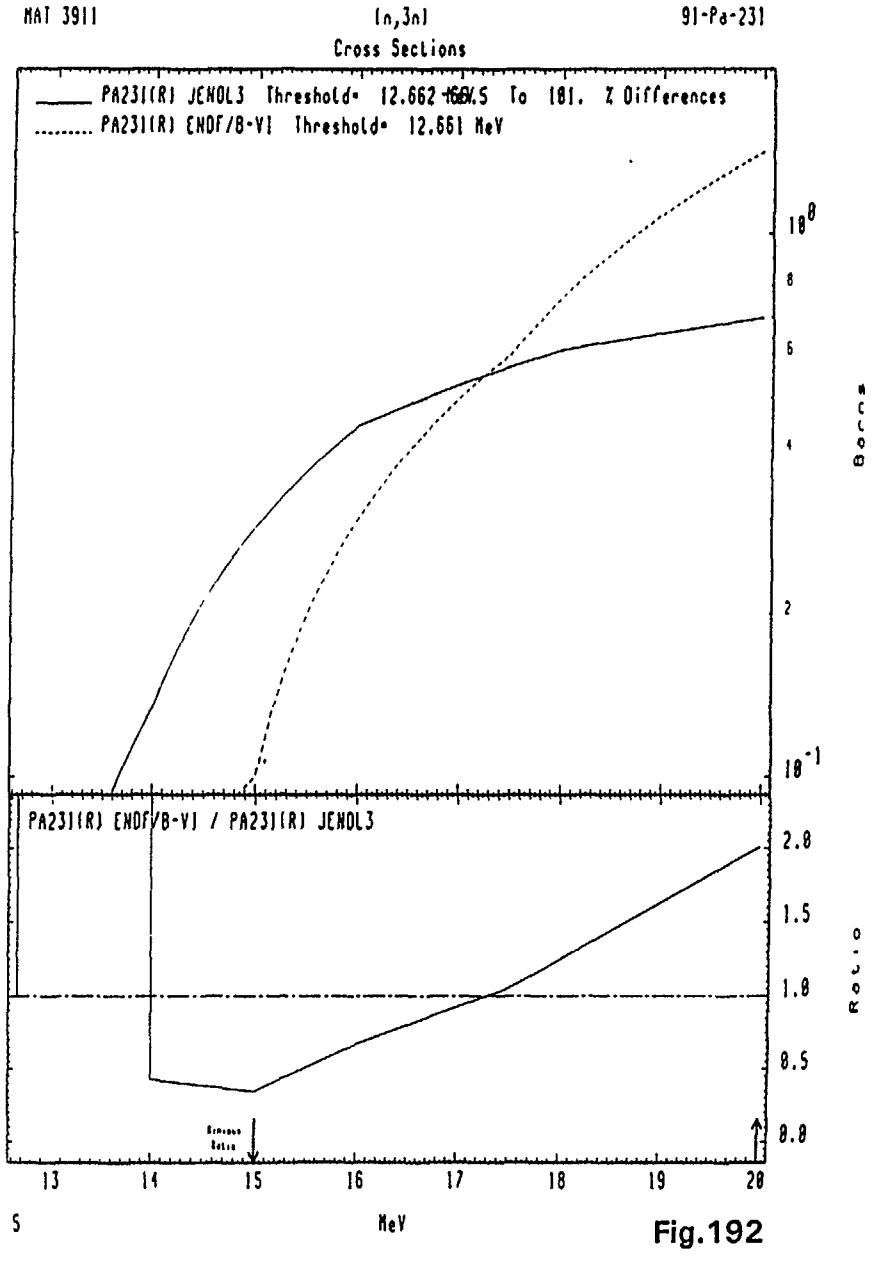

Fig.192

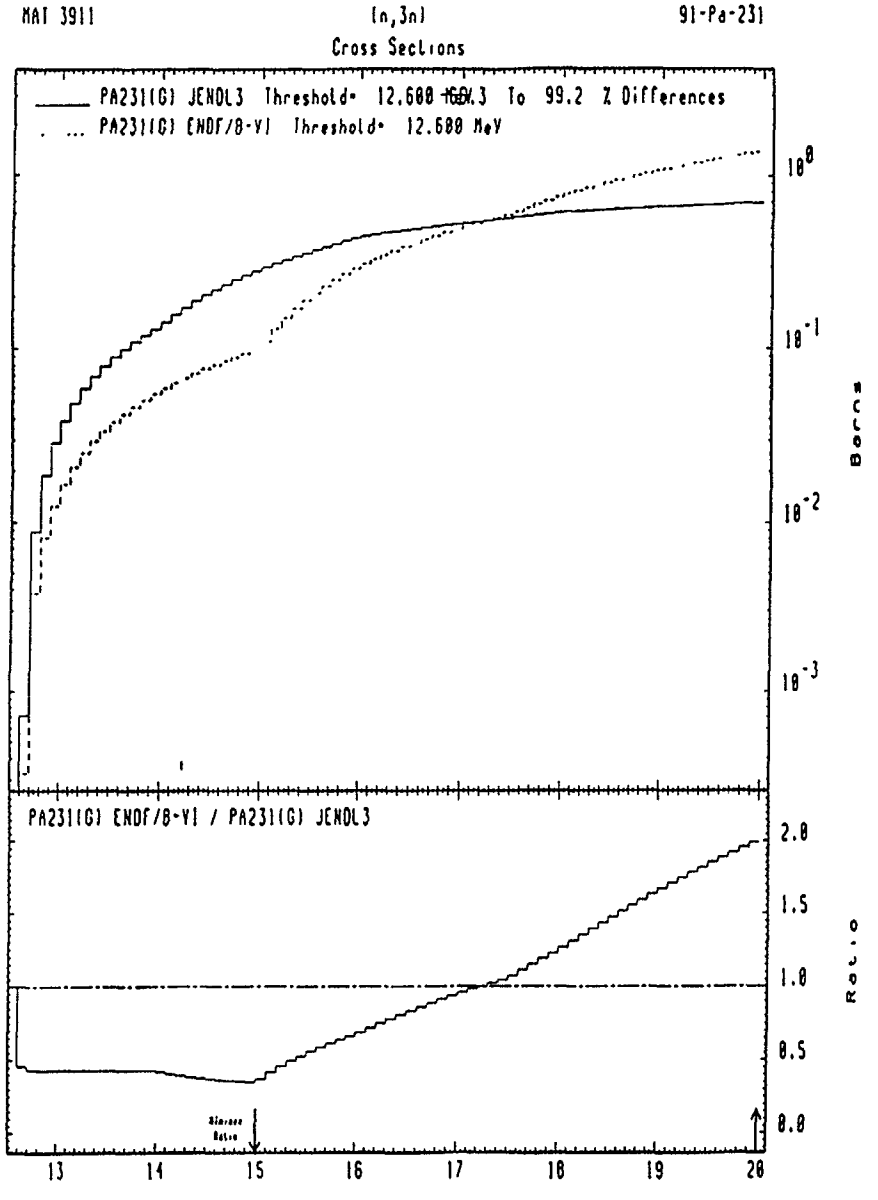

Fig.193

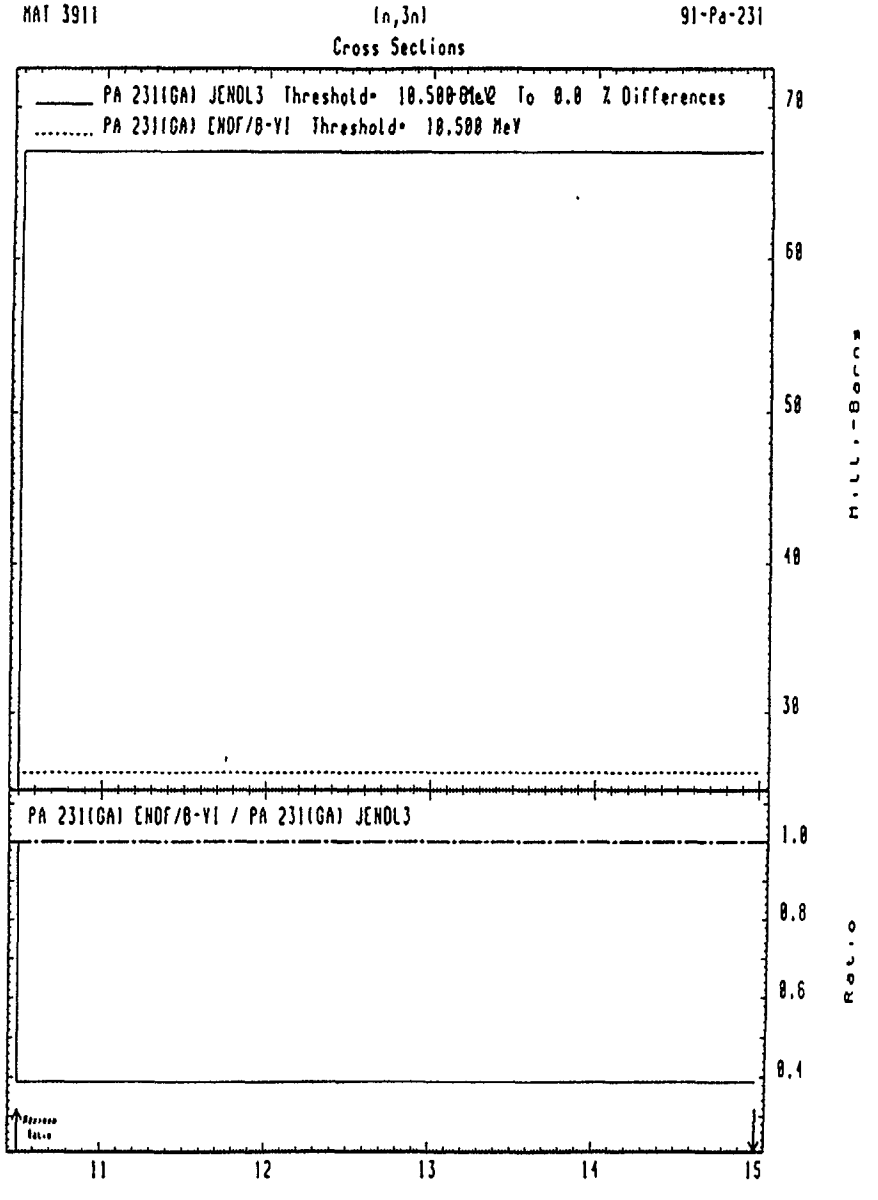

Fig.194

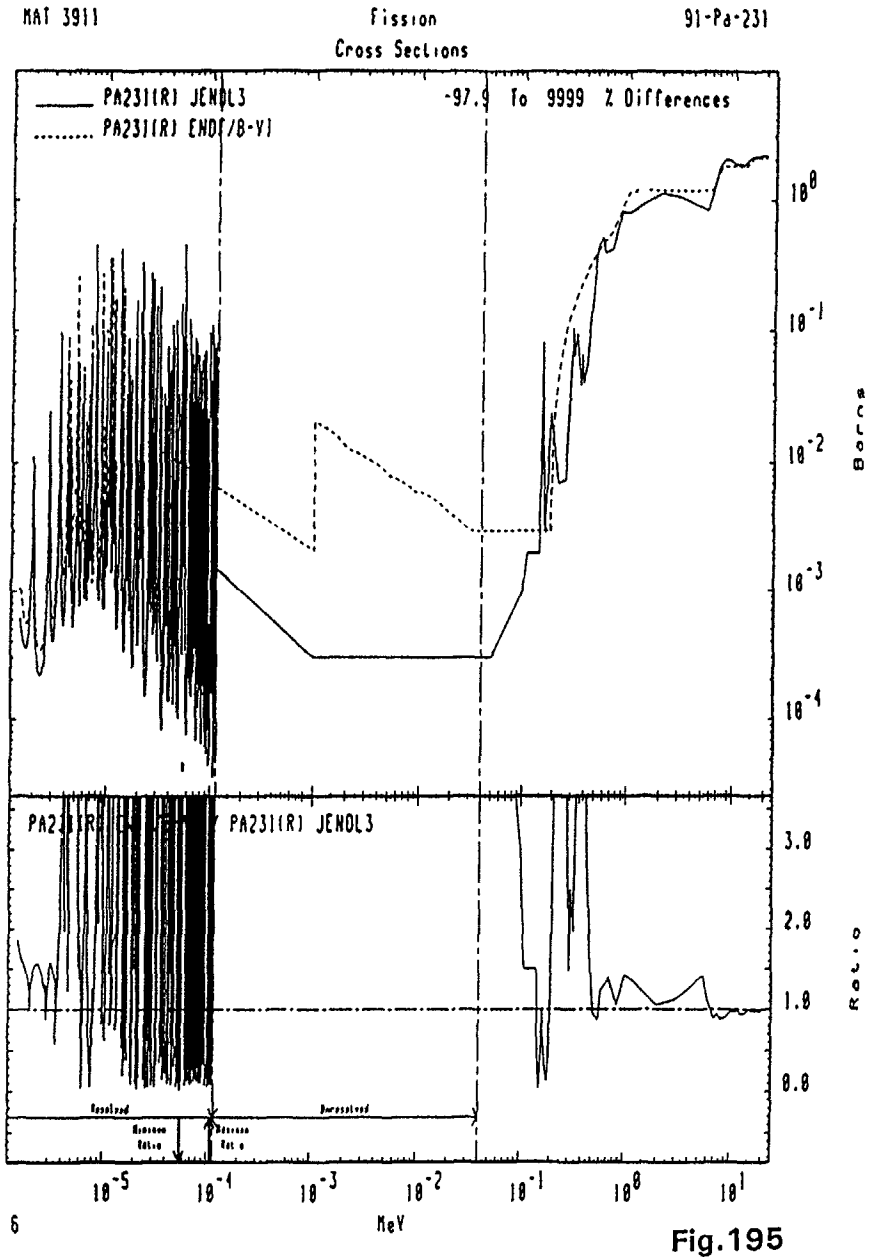

Fig.195

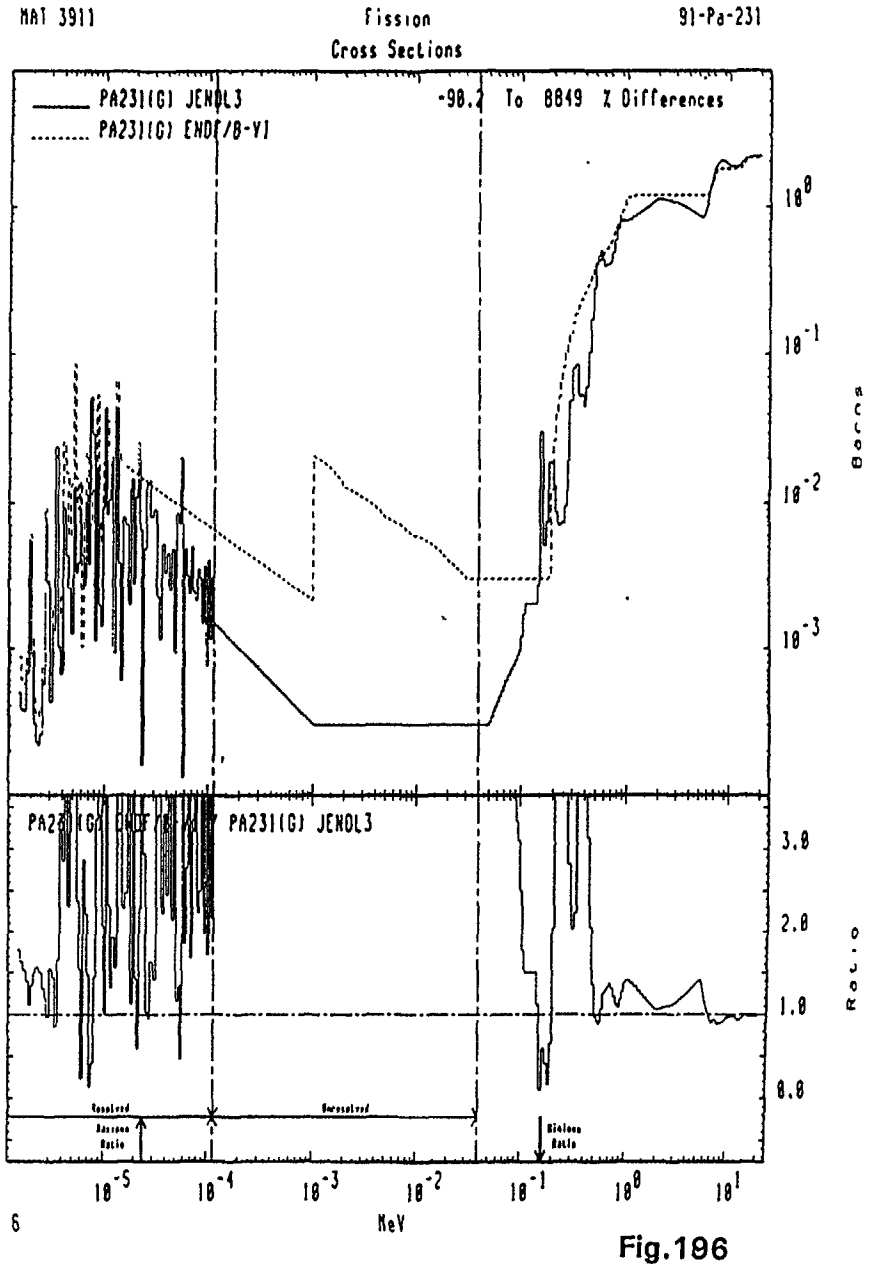

Fig.196

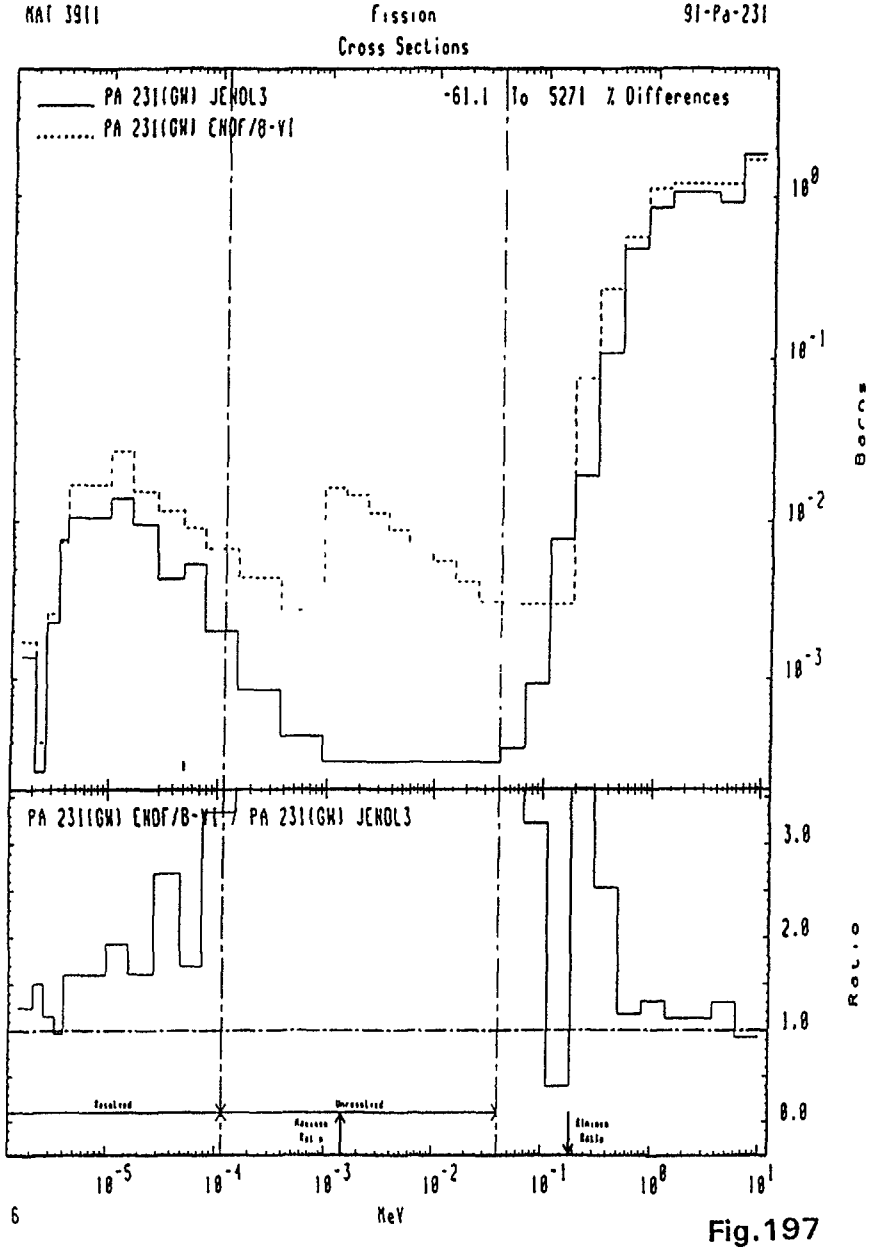

Fig.197

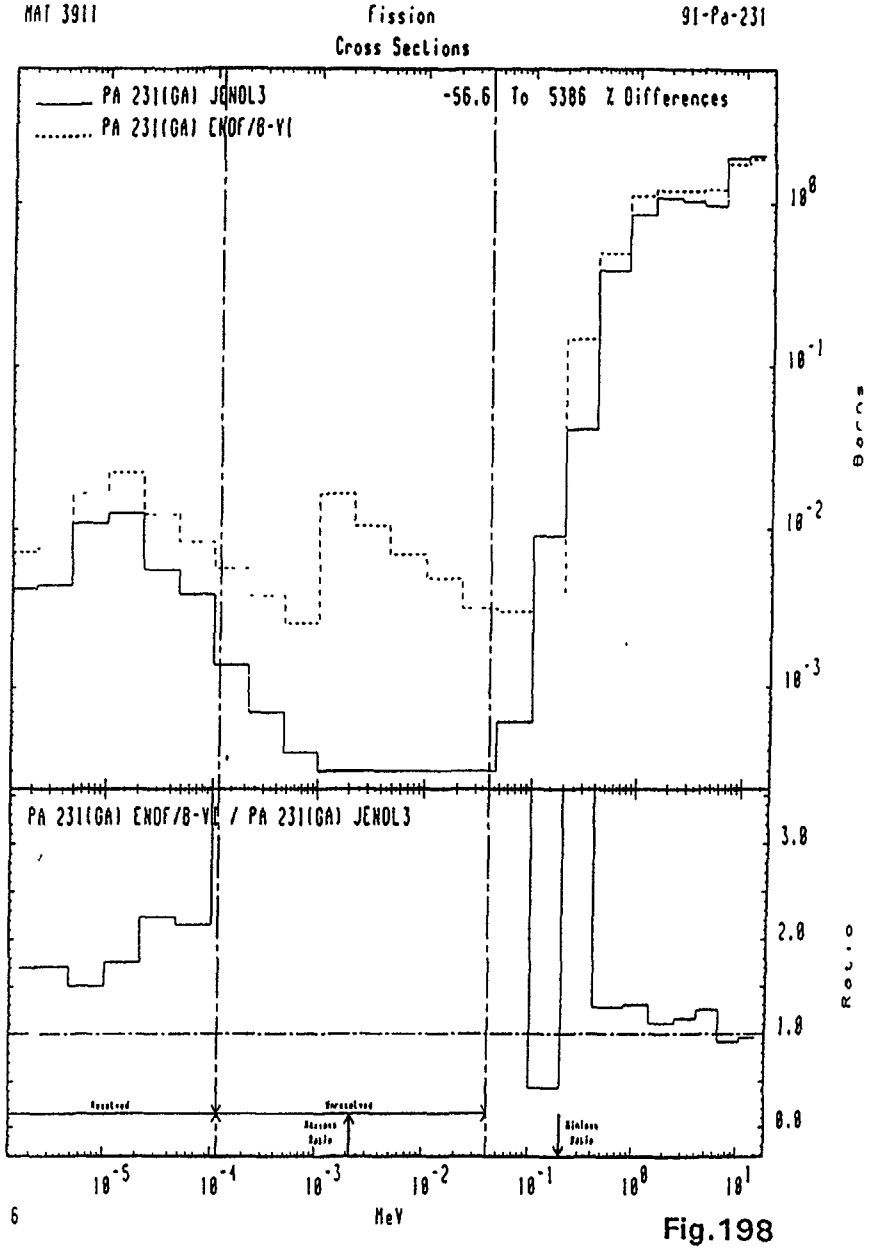

Fig.198

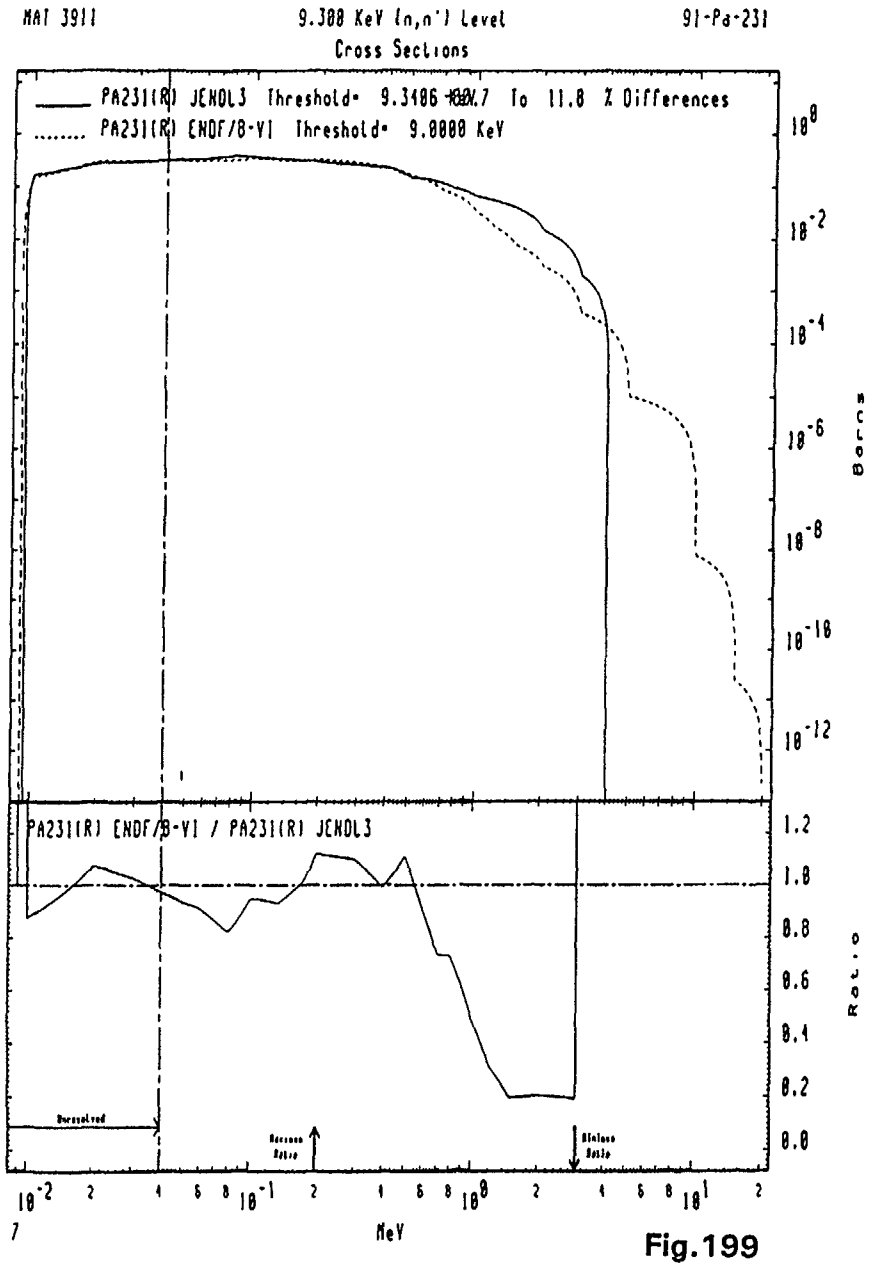

Fig.199

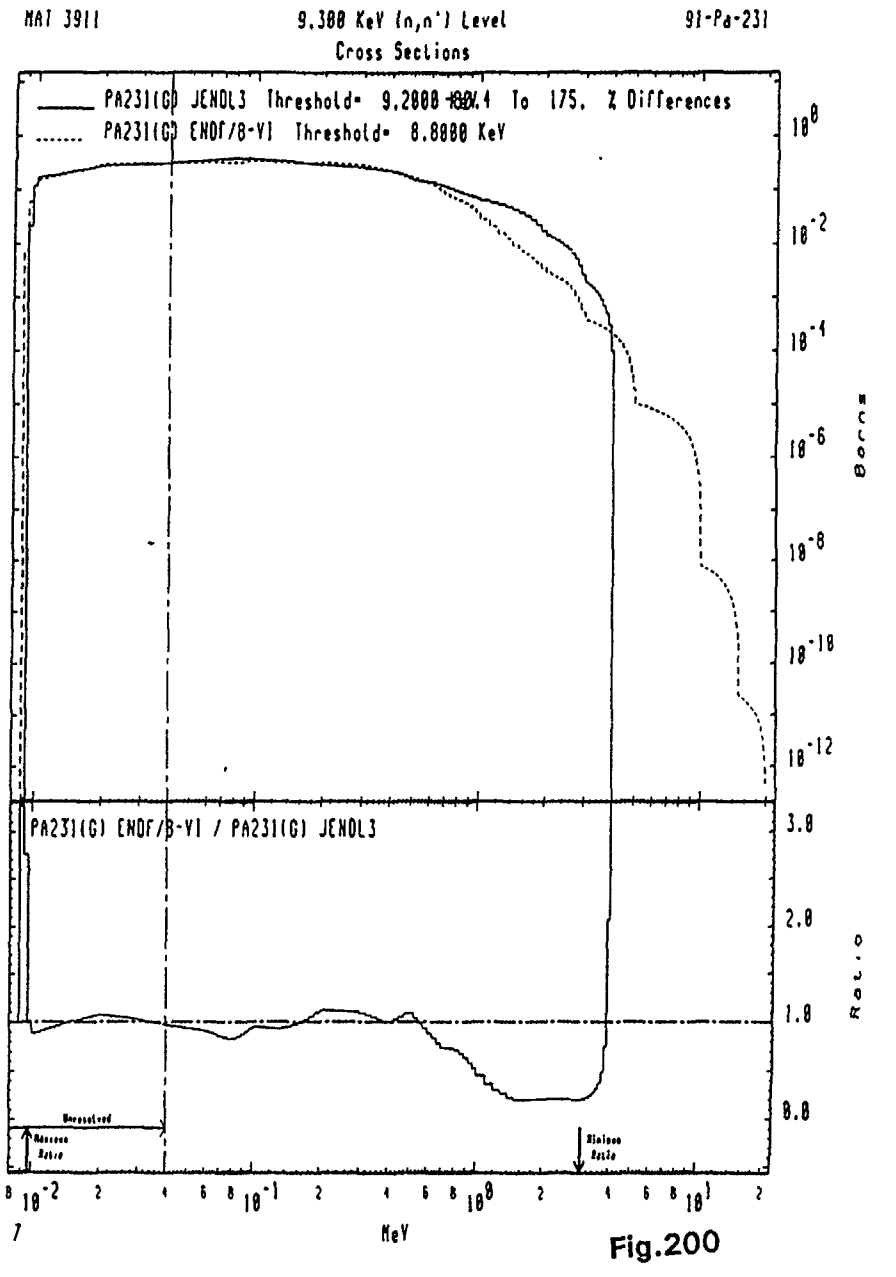

Fig.200

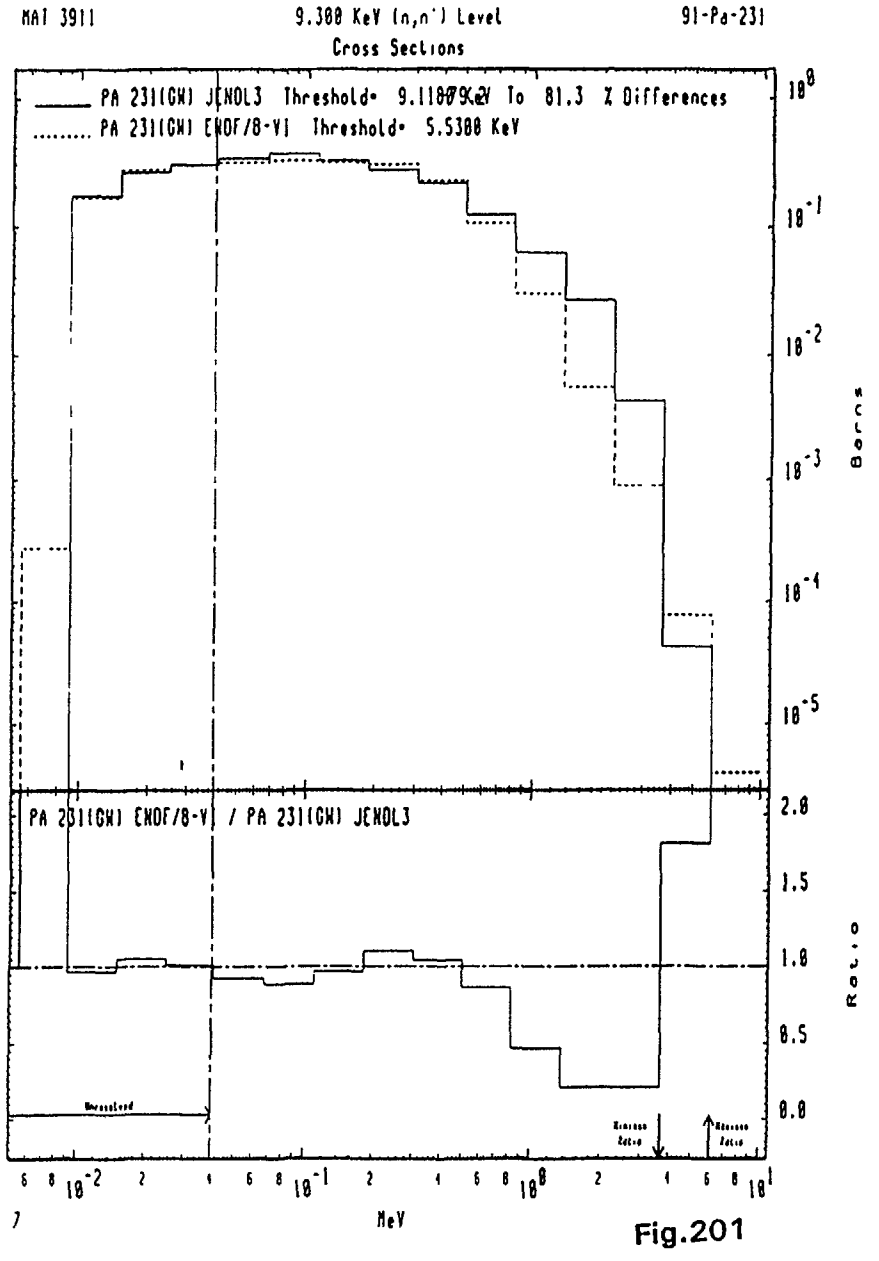

Fig.201

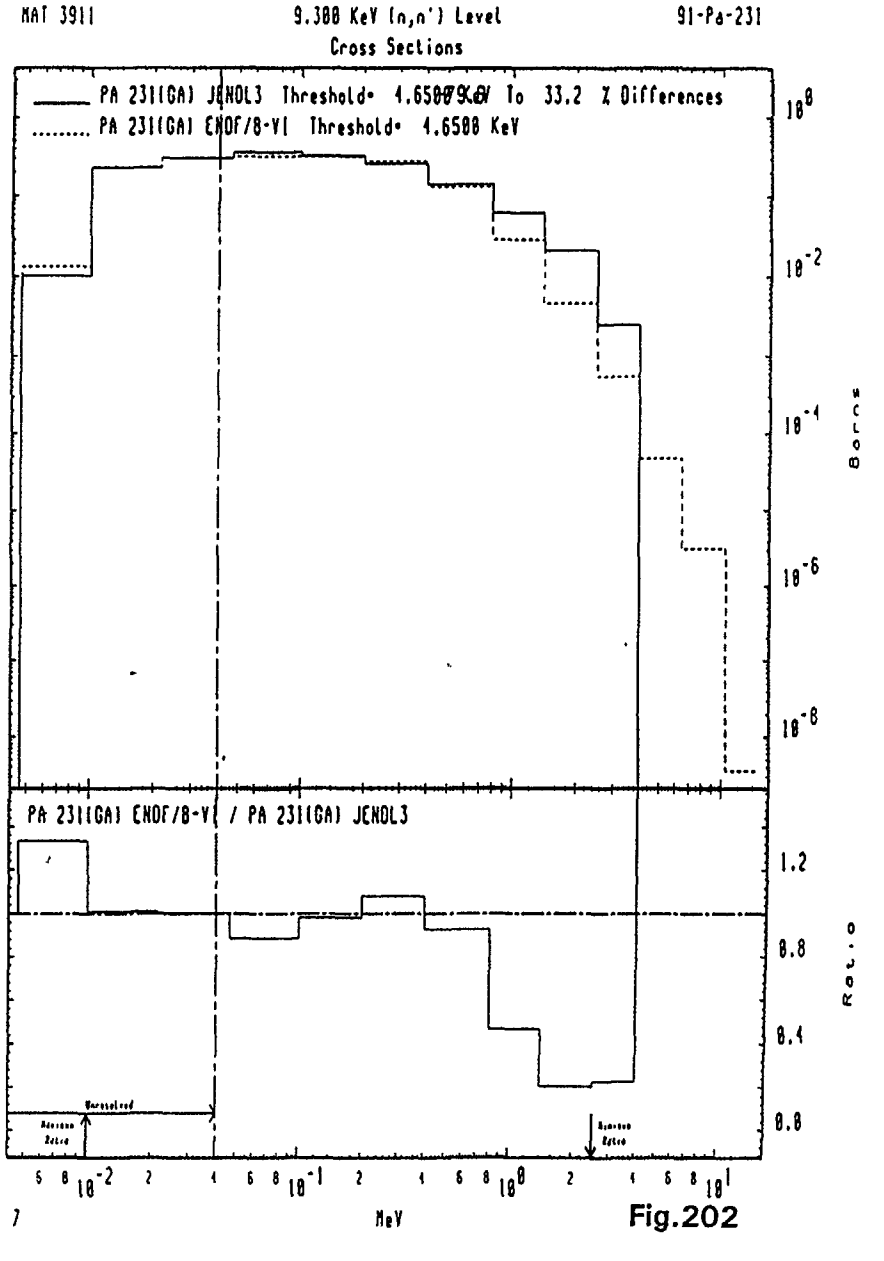

Fig.202

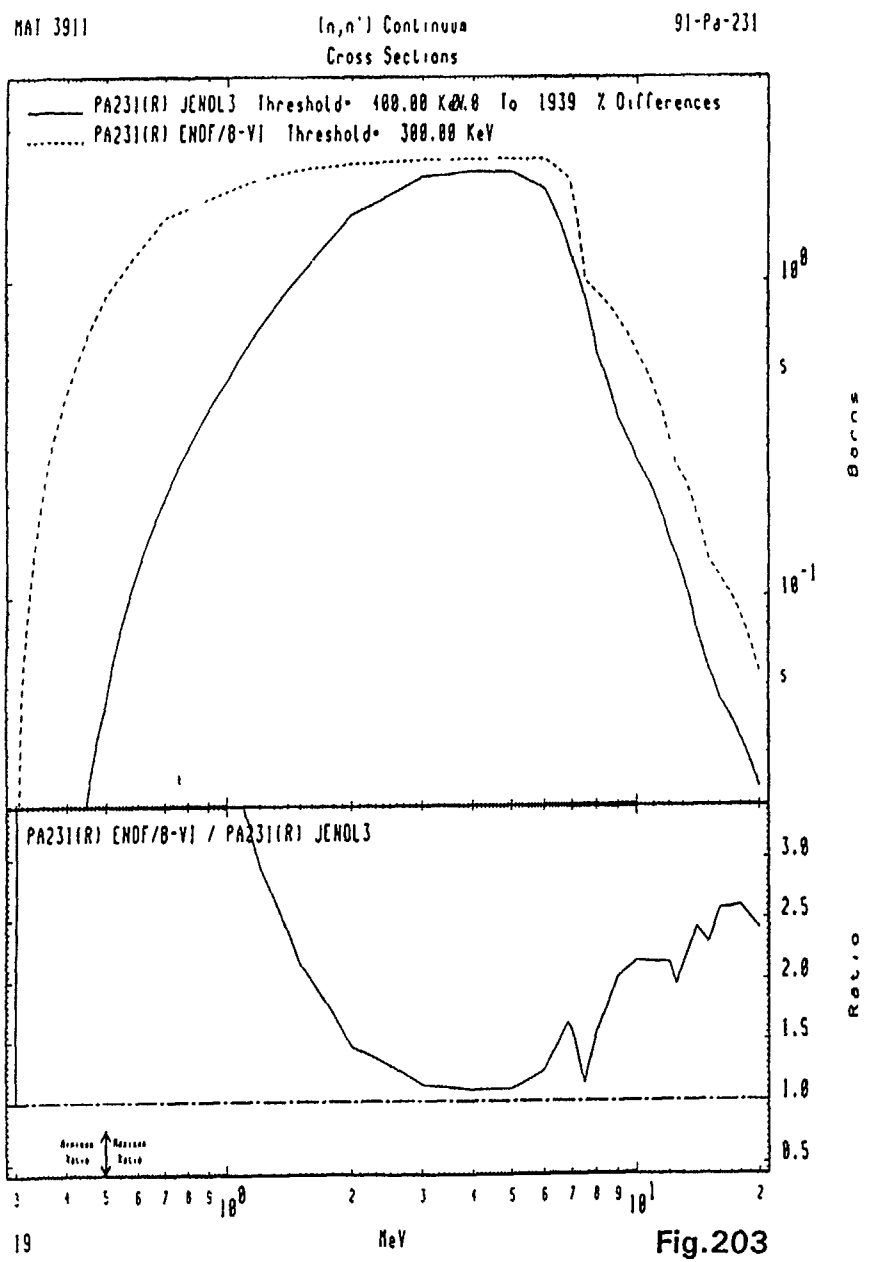

Fig.203

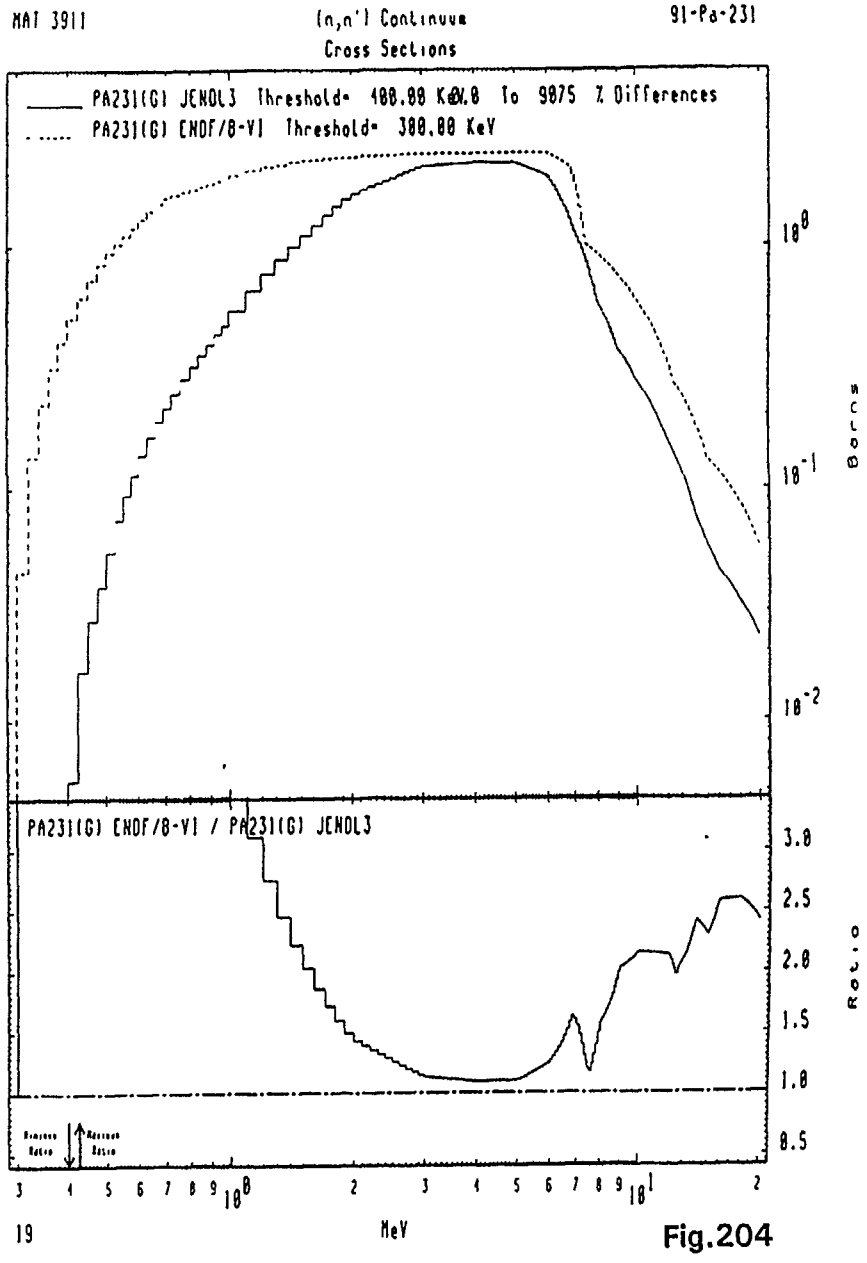

Fig.204

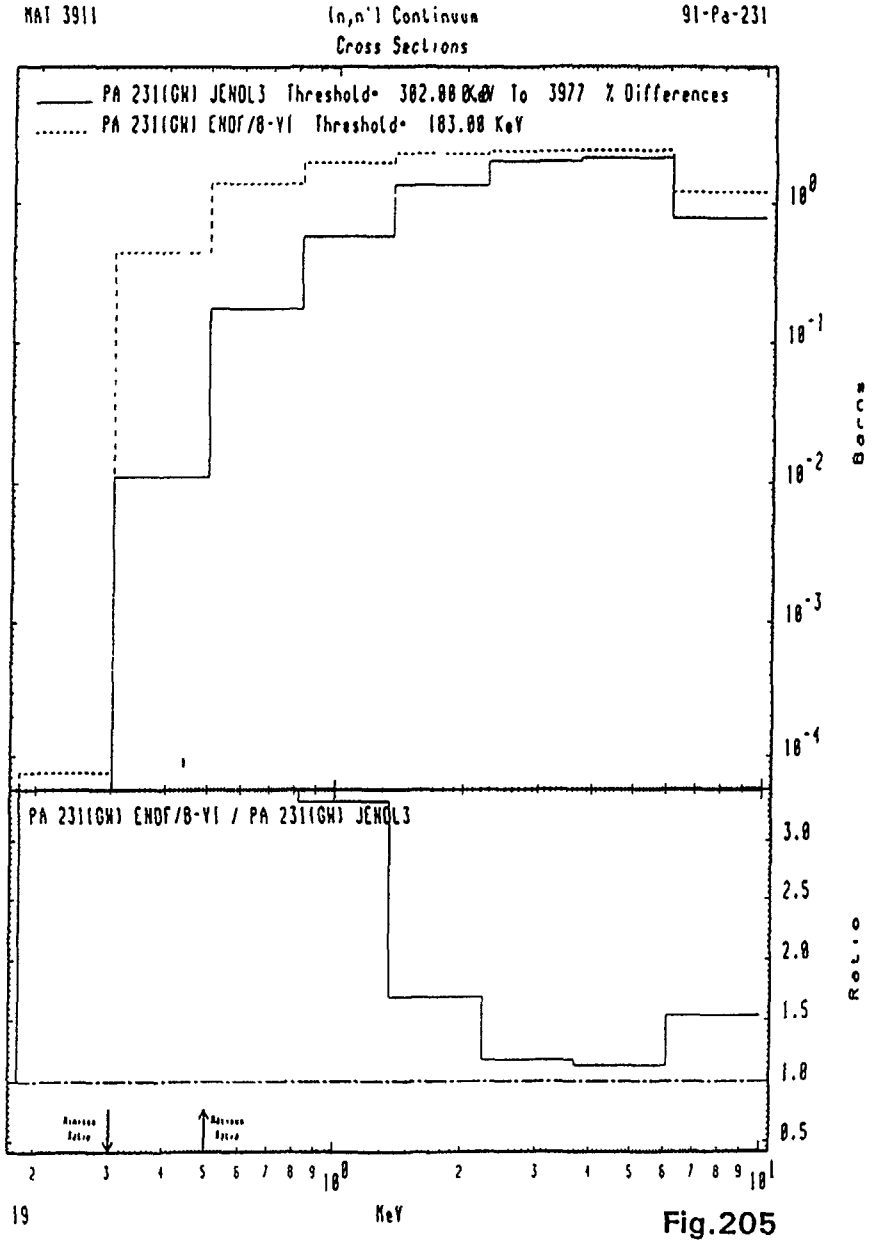

Fig.205

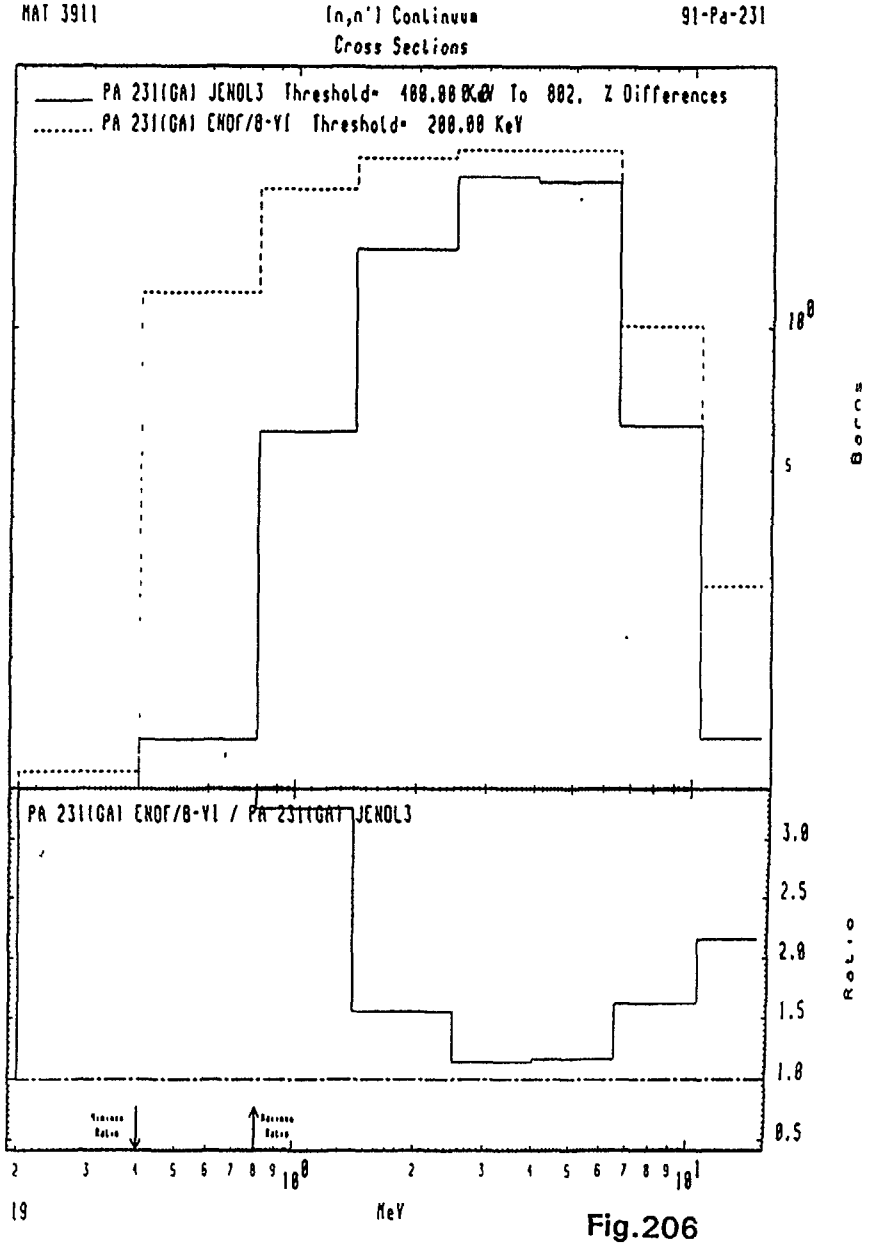

Fig.206

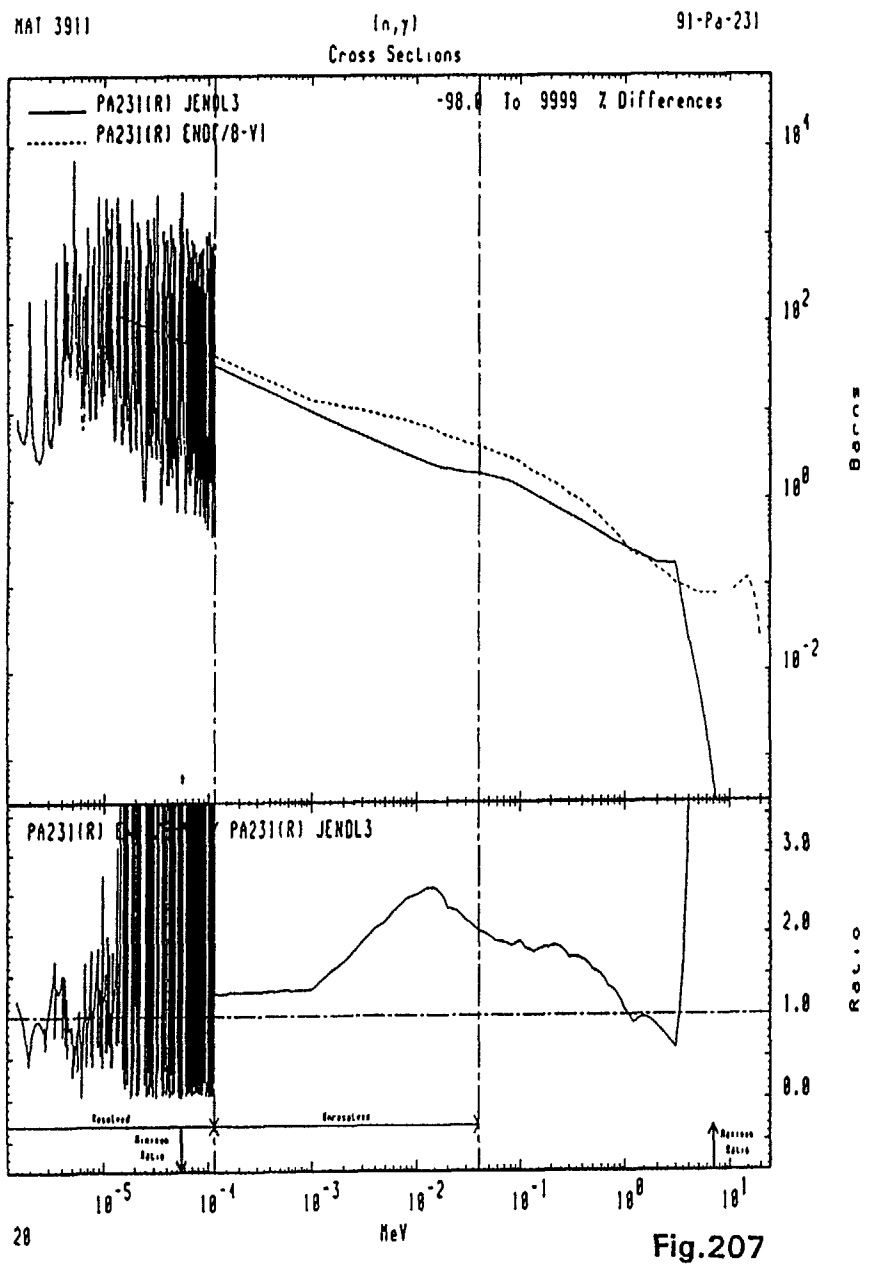

Fig.207

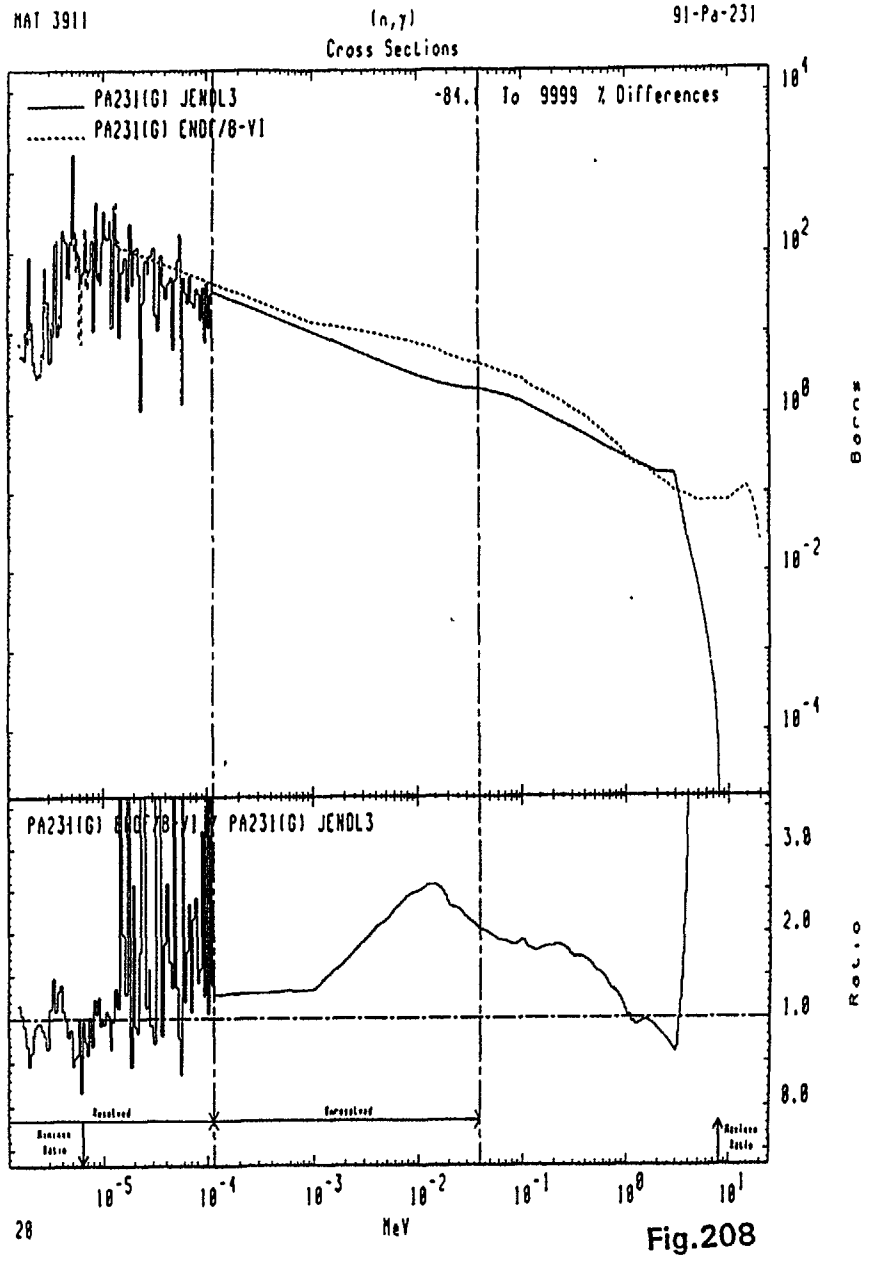

Fig.208

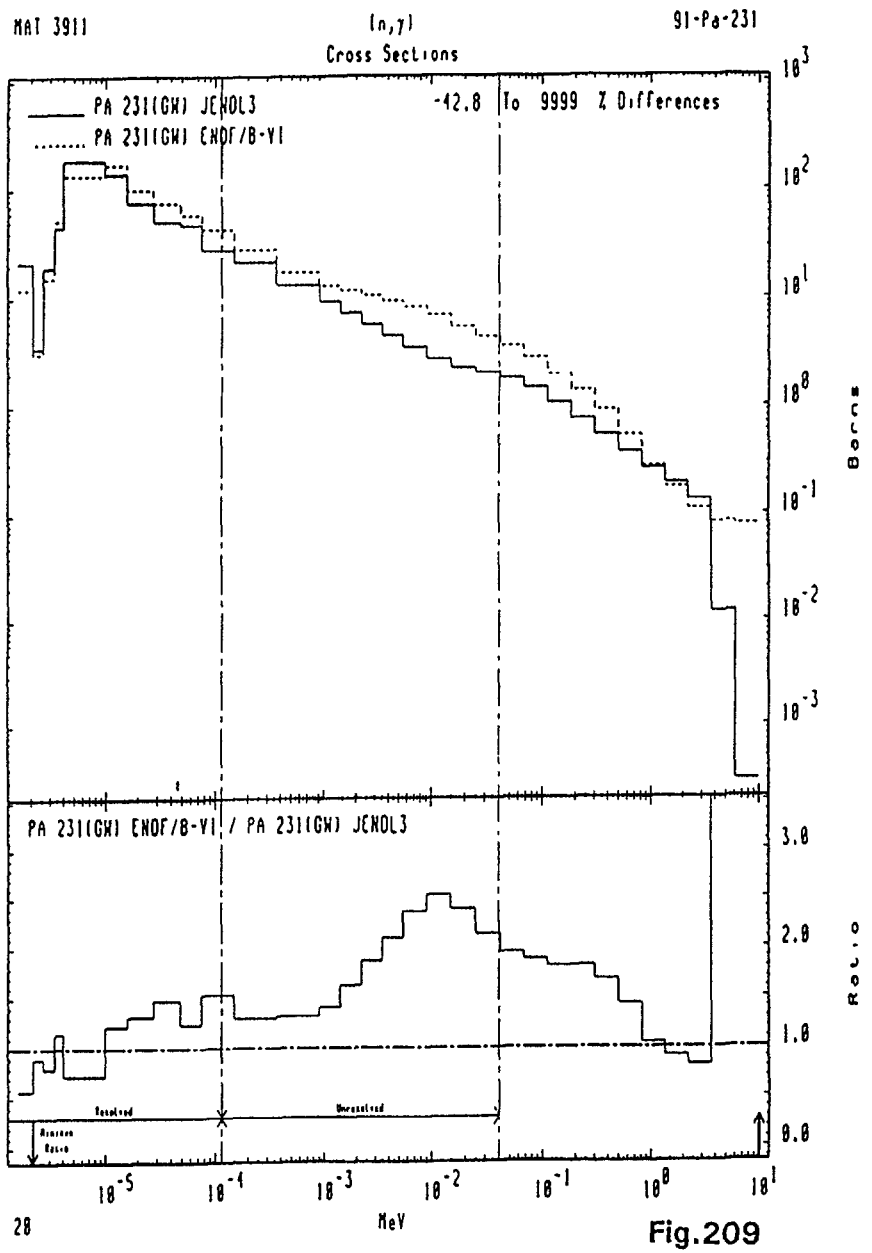

Fig.209

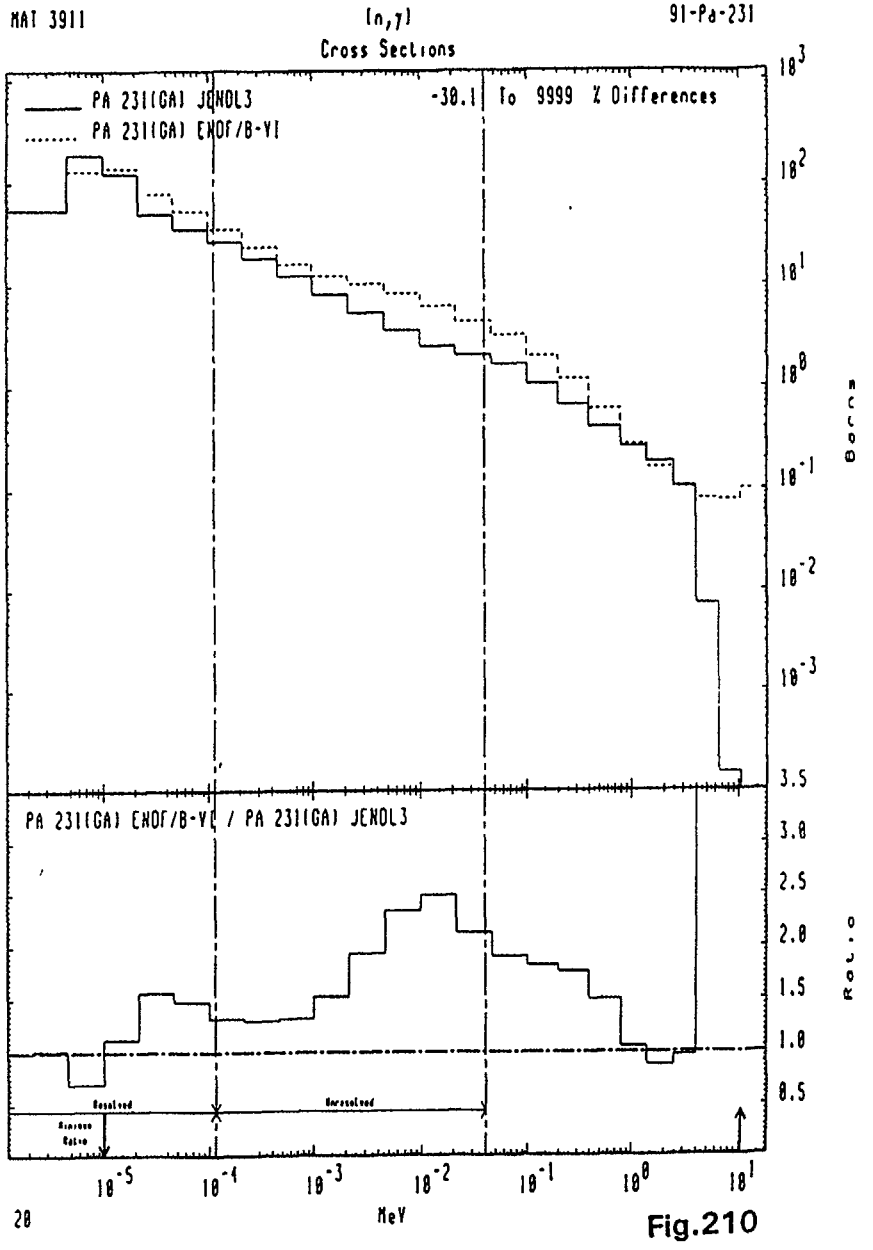

Fig.210

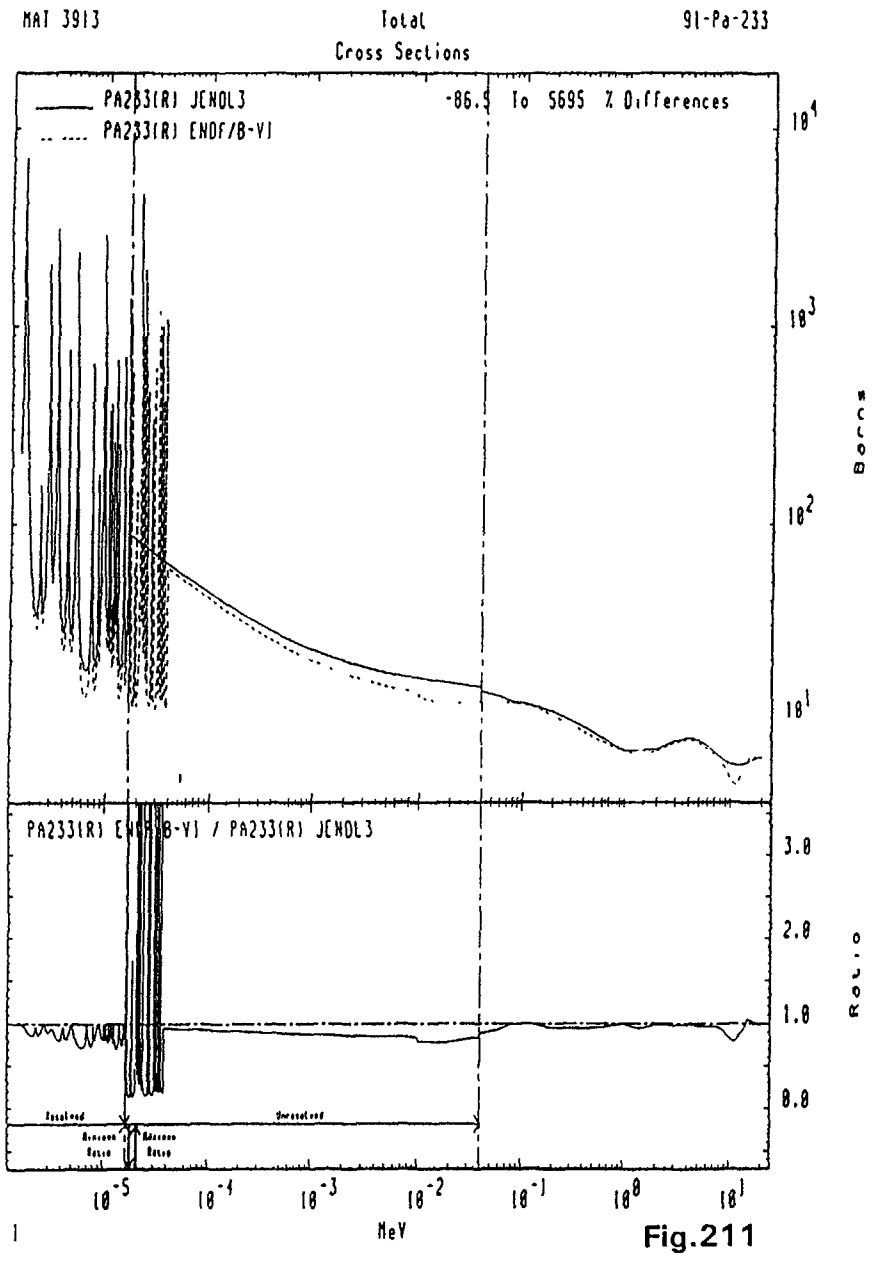

Fig.211

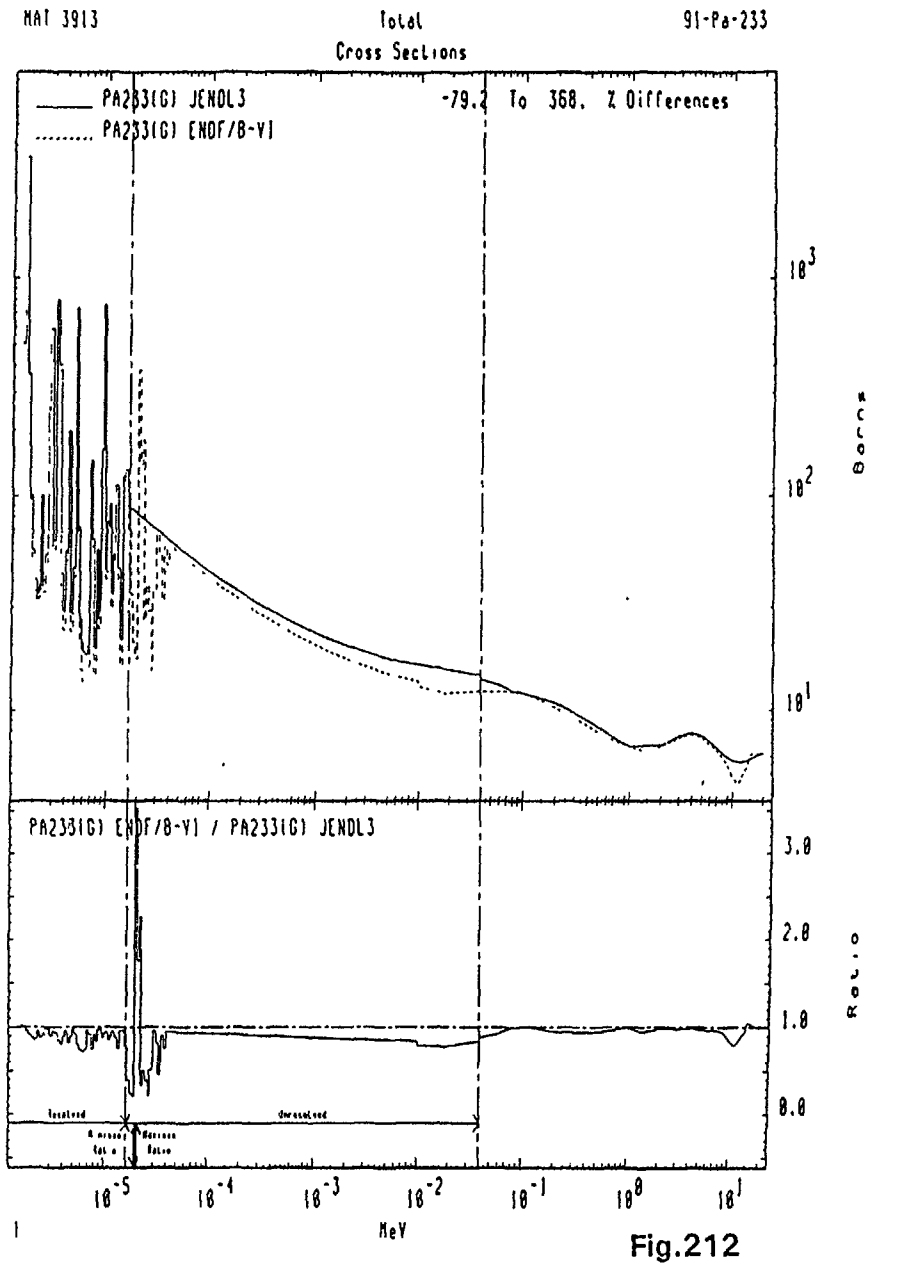

Fig.212

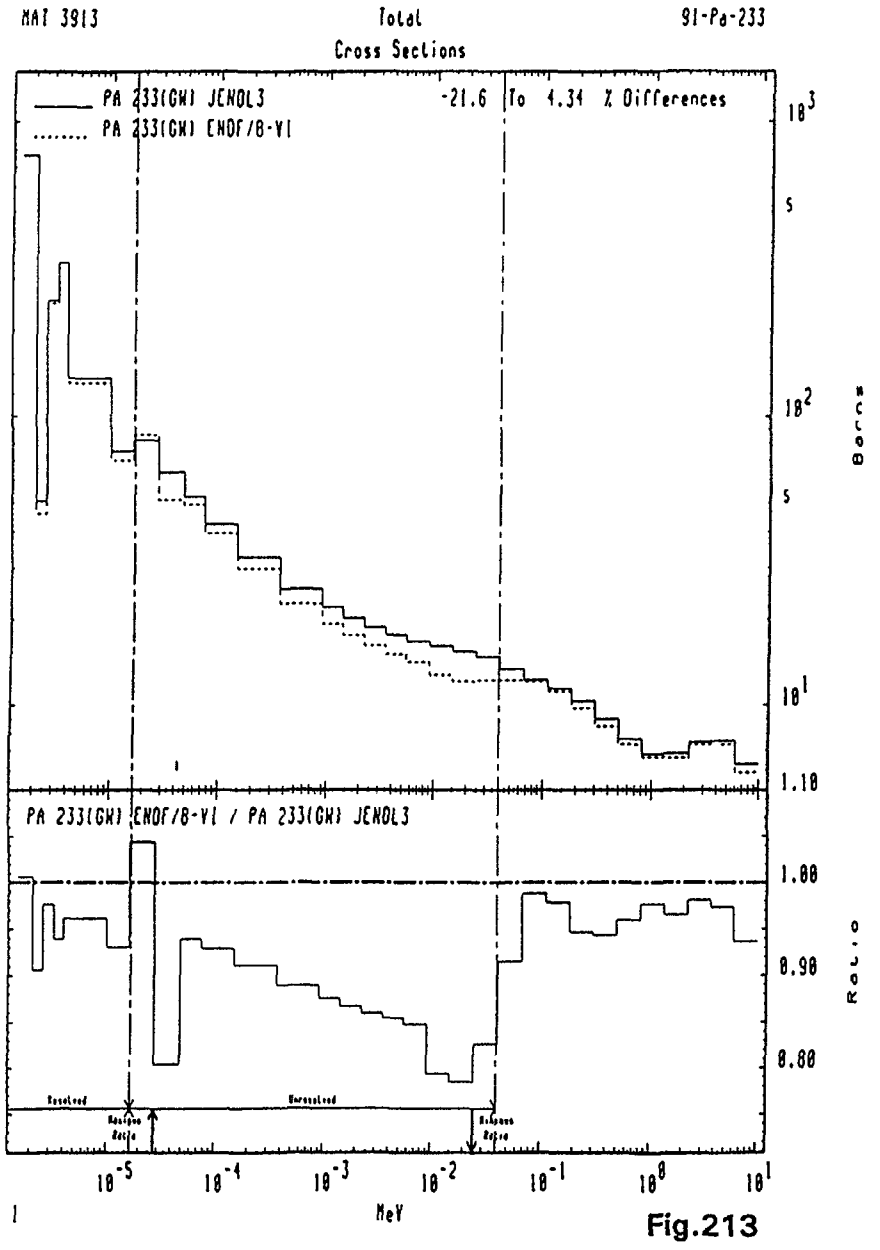

Fig.213

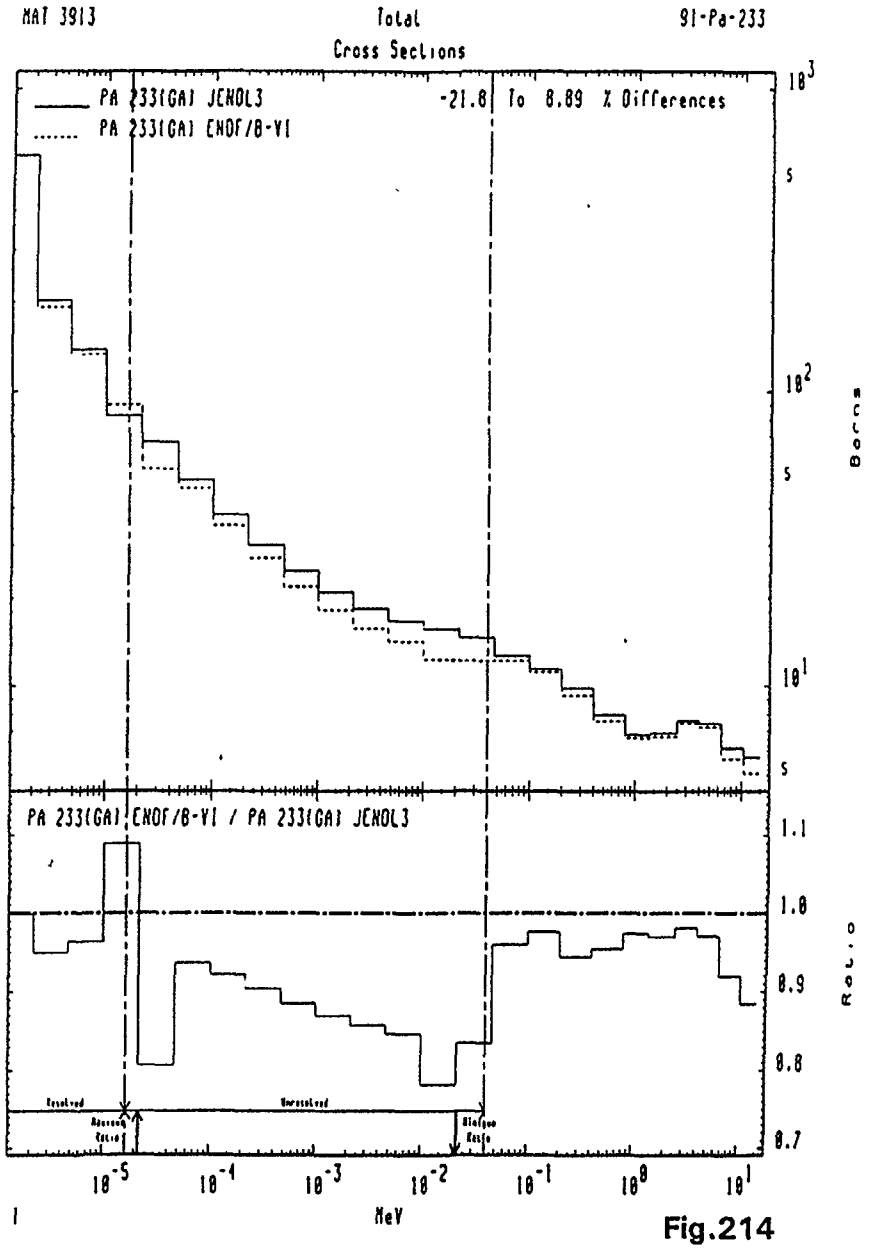

Fig.214

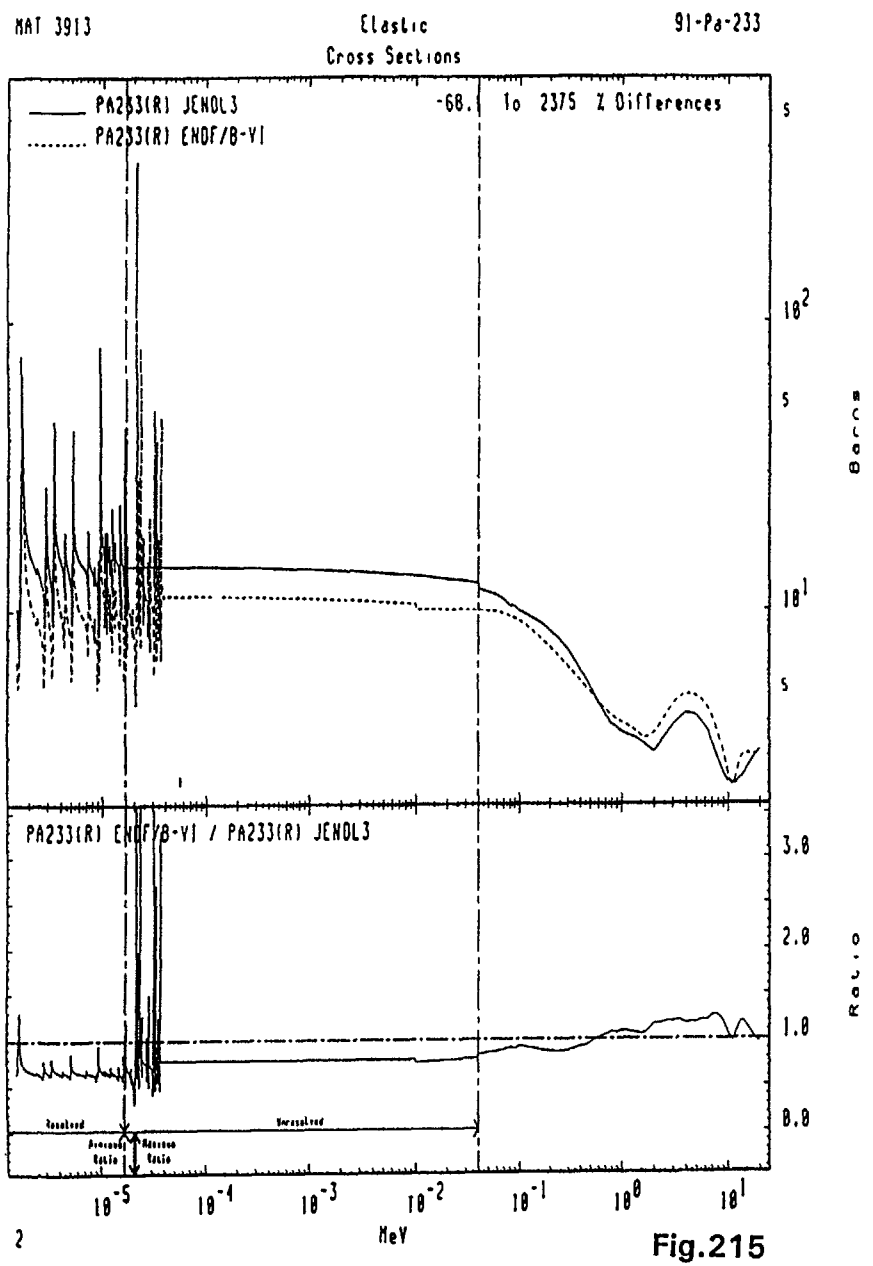

Fig.215

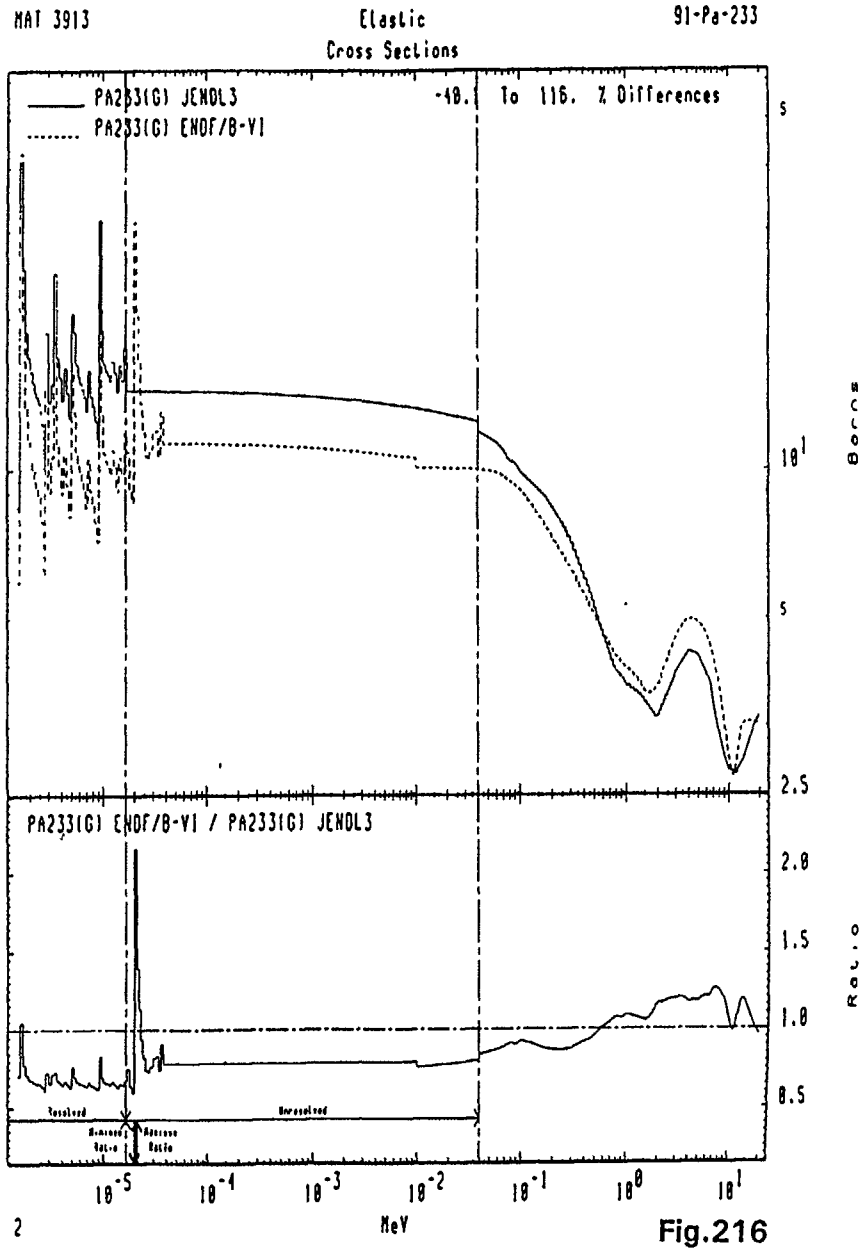

Fig.216

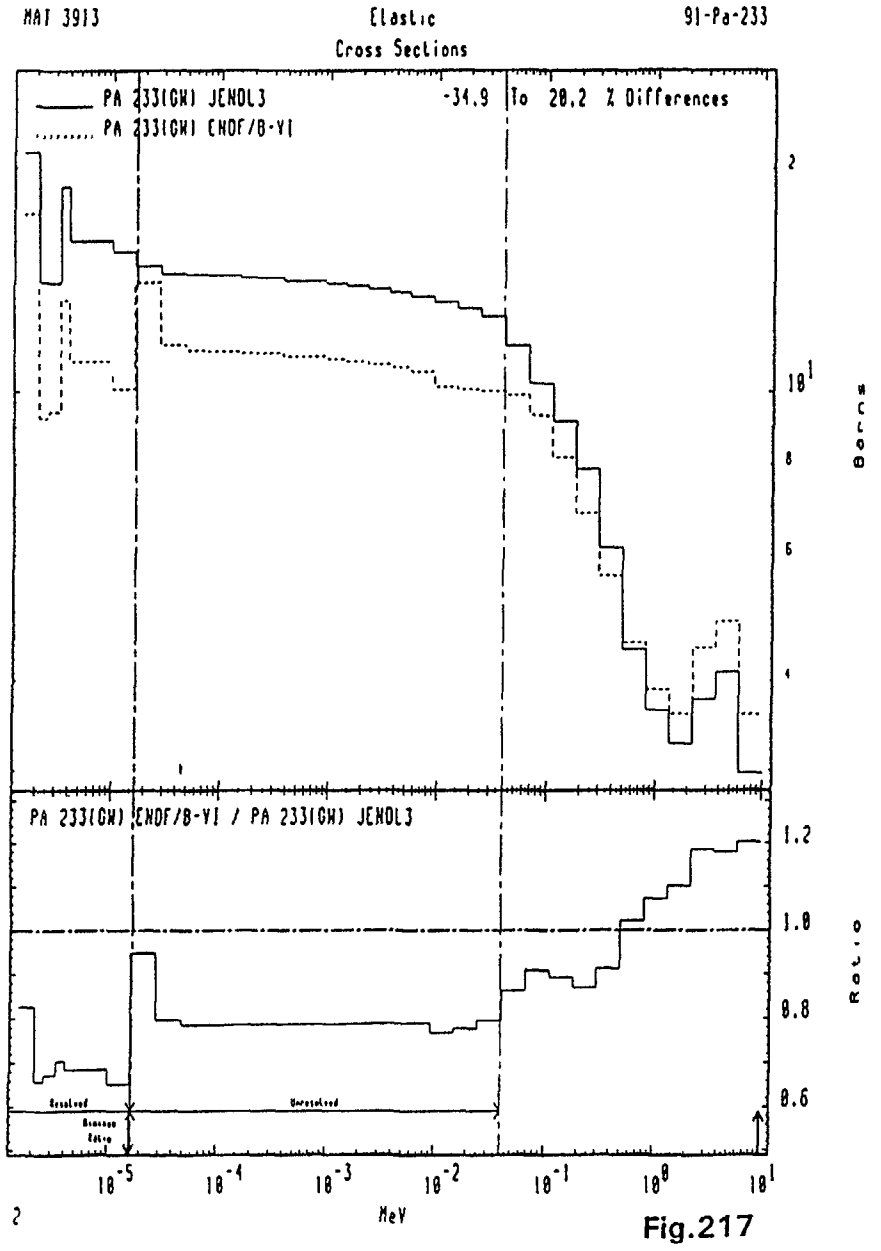

Fig.217

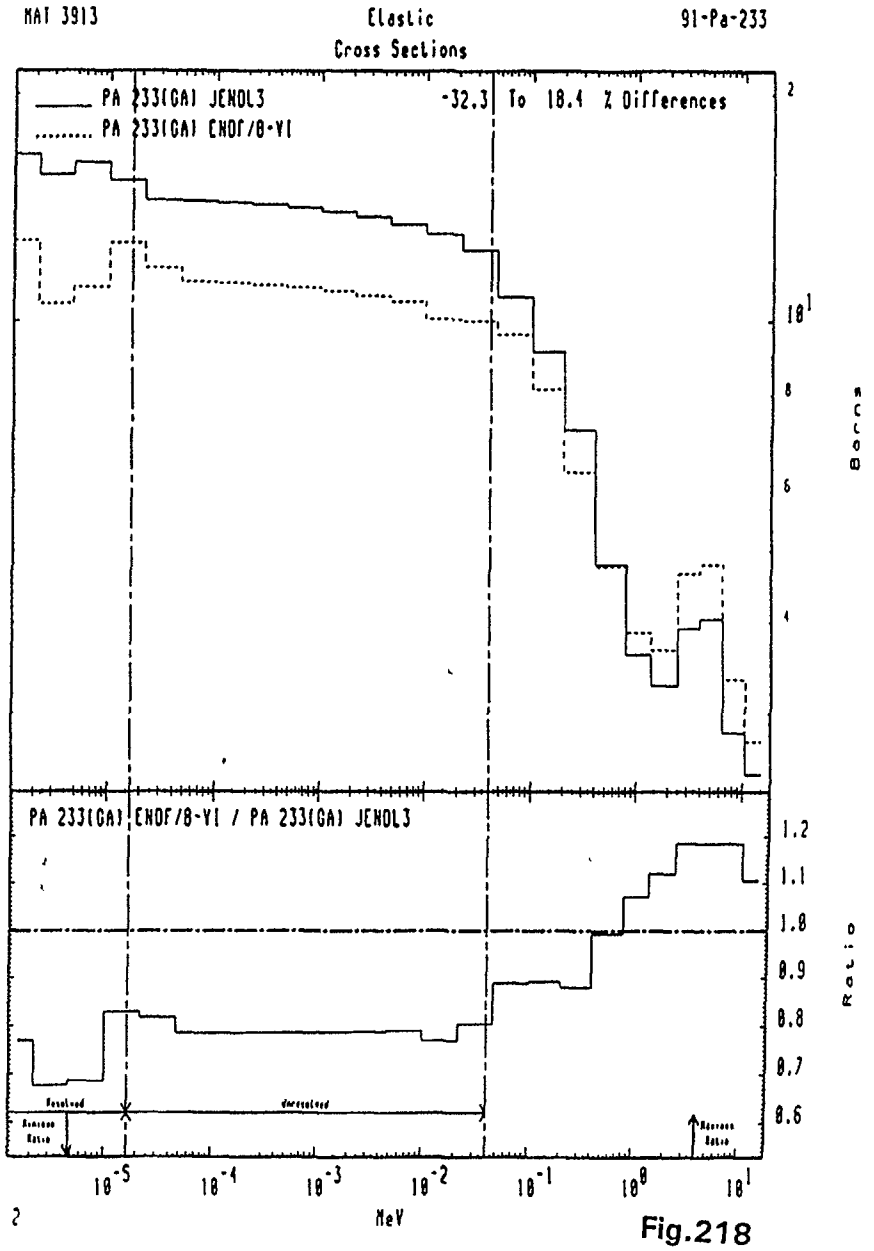

Fig.218

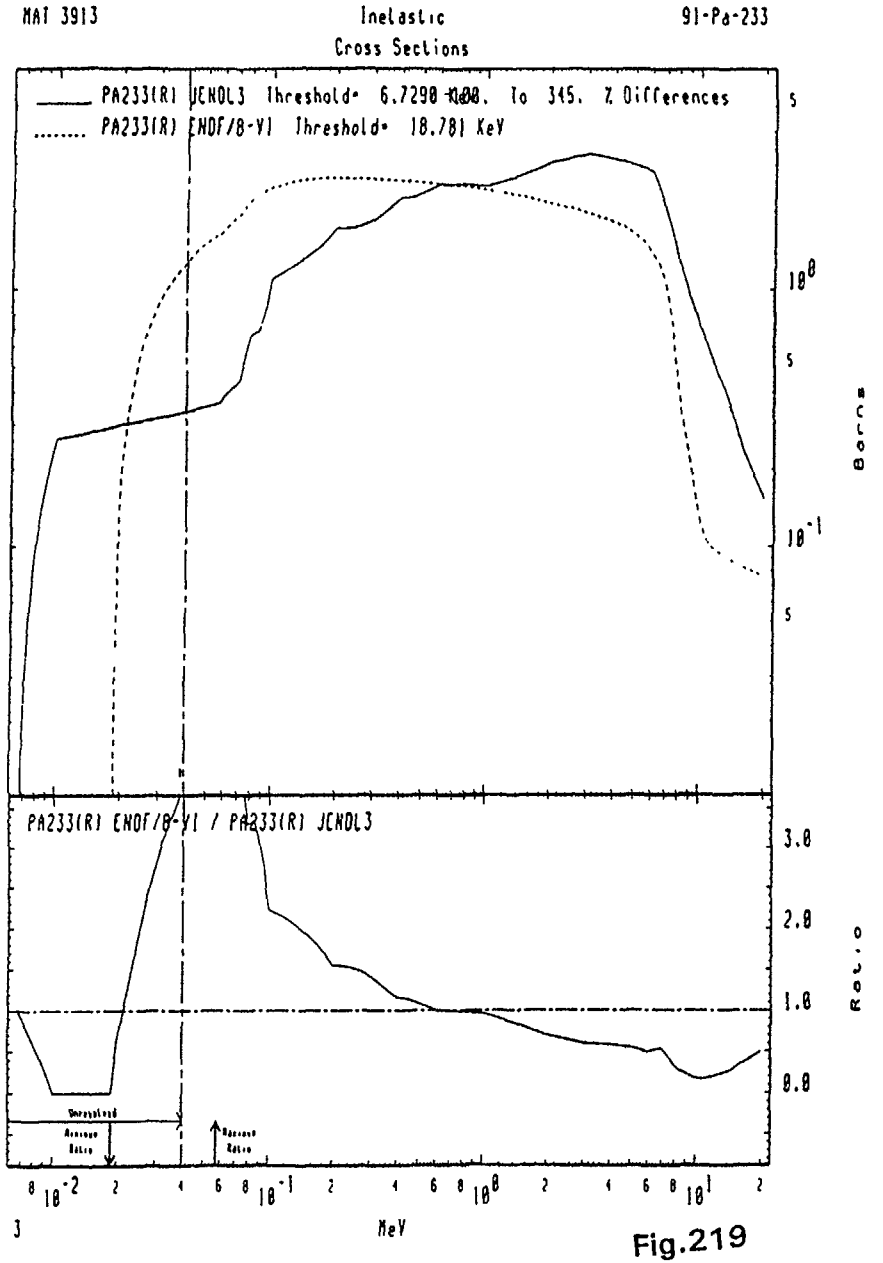

Fig.219

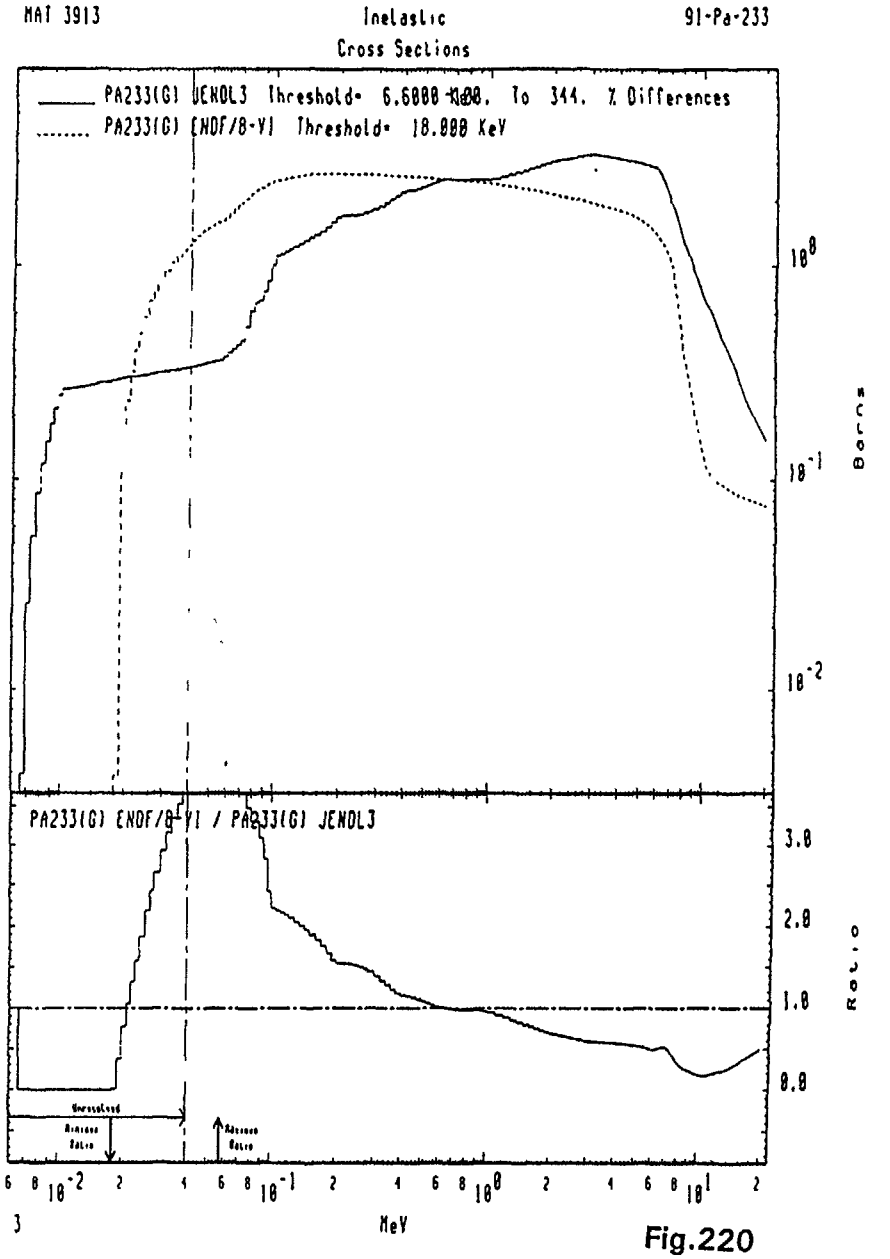

Fig.220

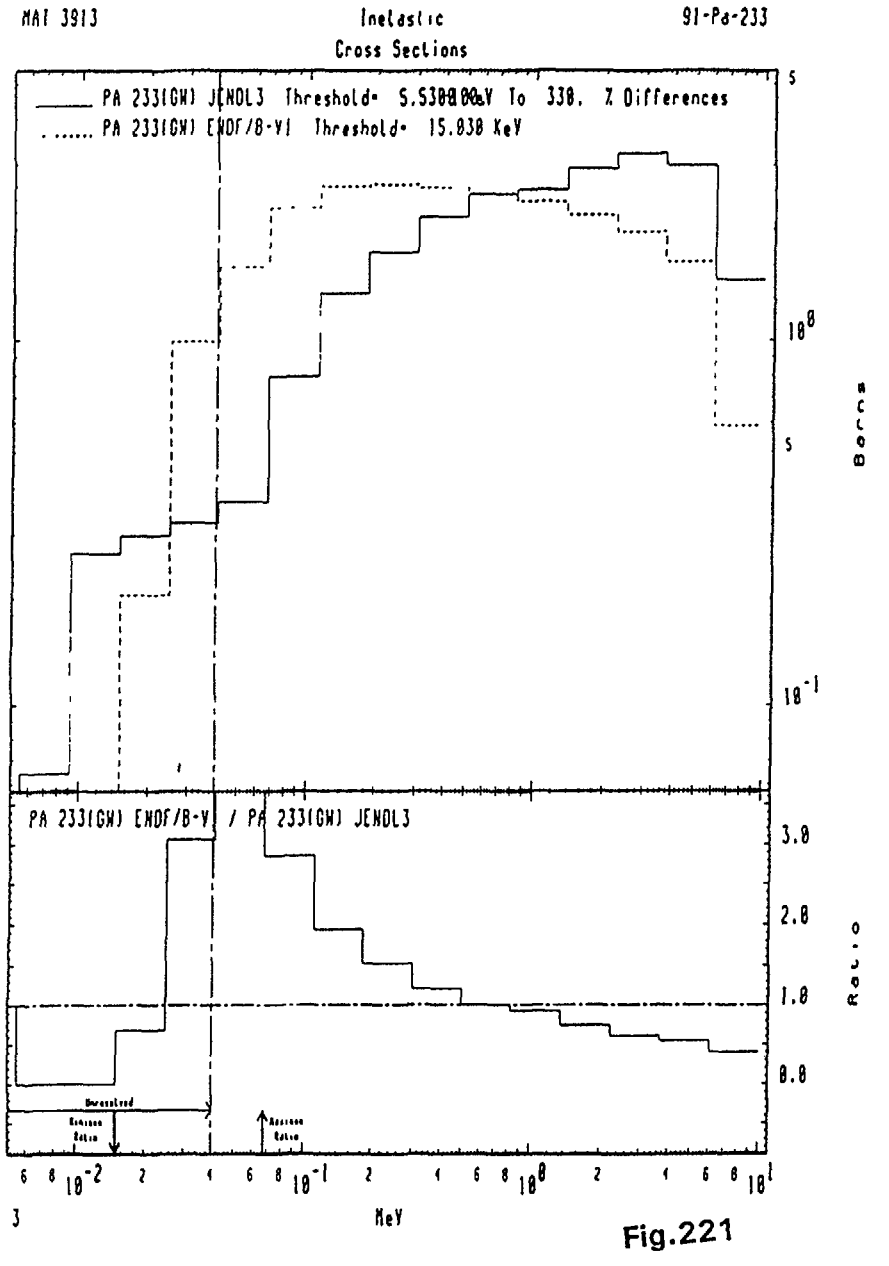

Fig.221

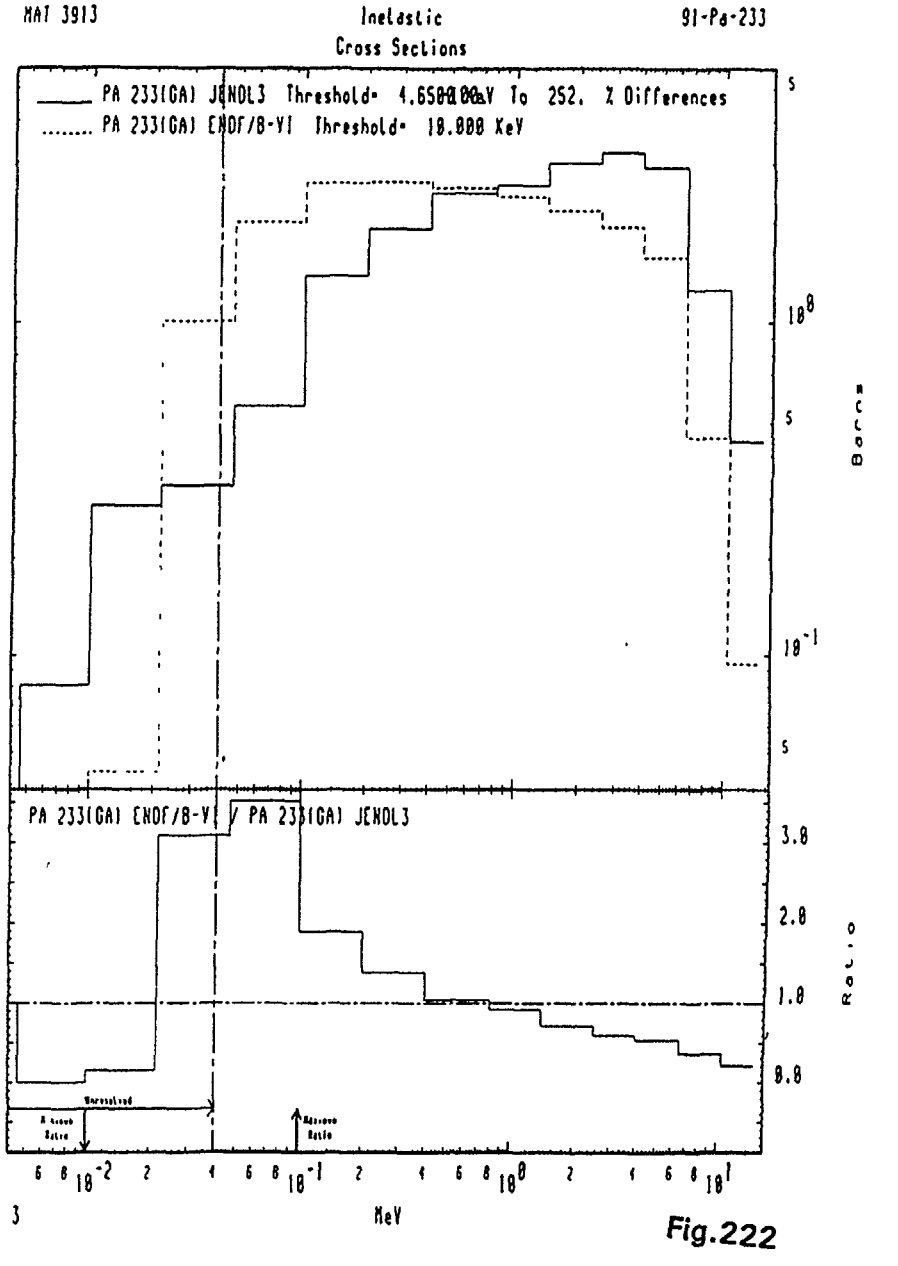

Fig.222

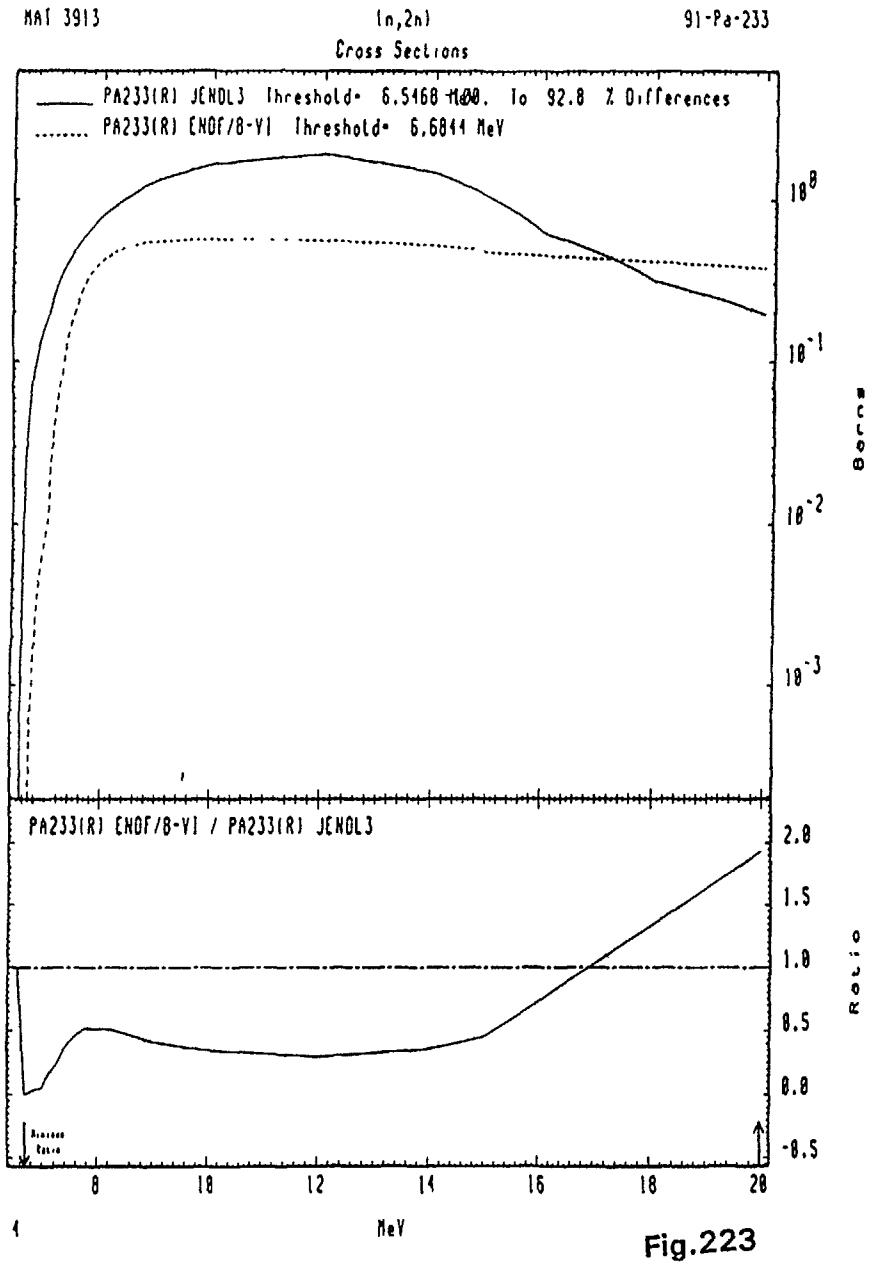

Fig.223

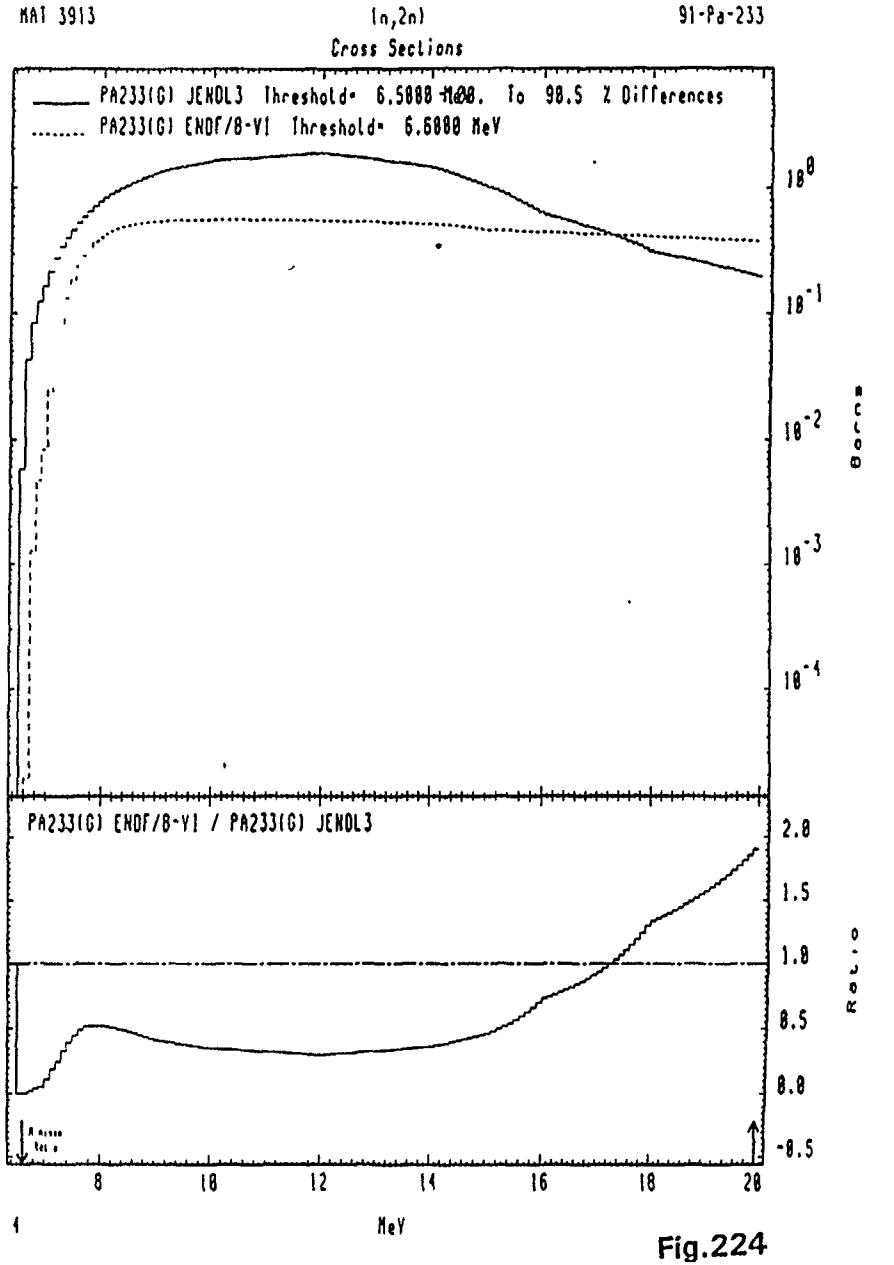

Fig.224

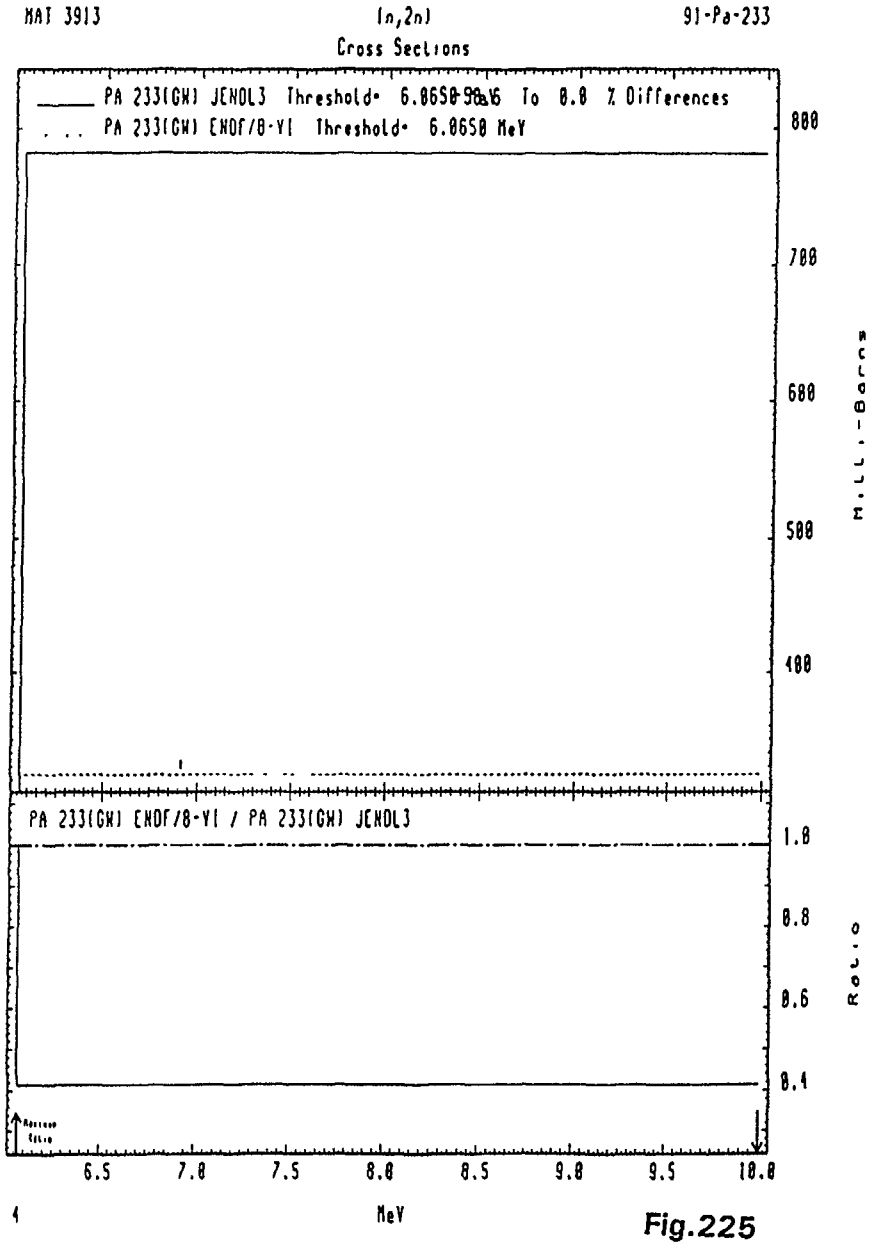

Fig.225

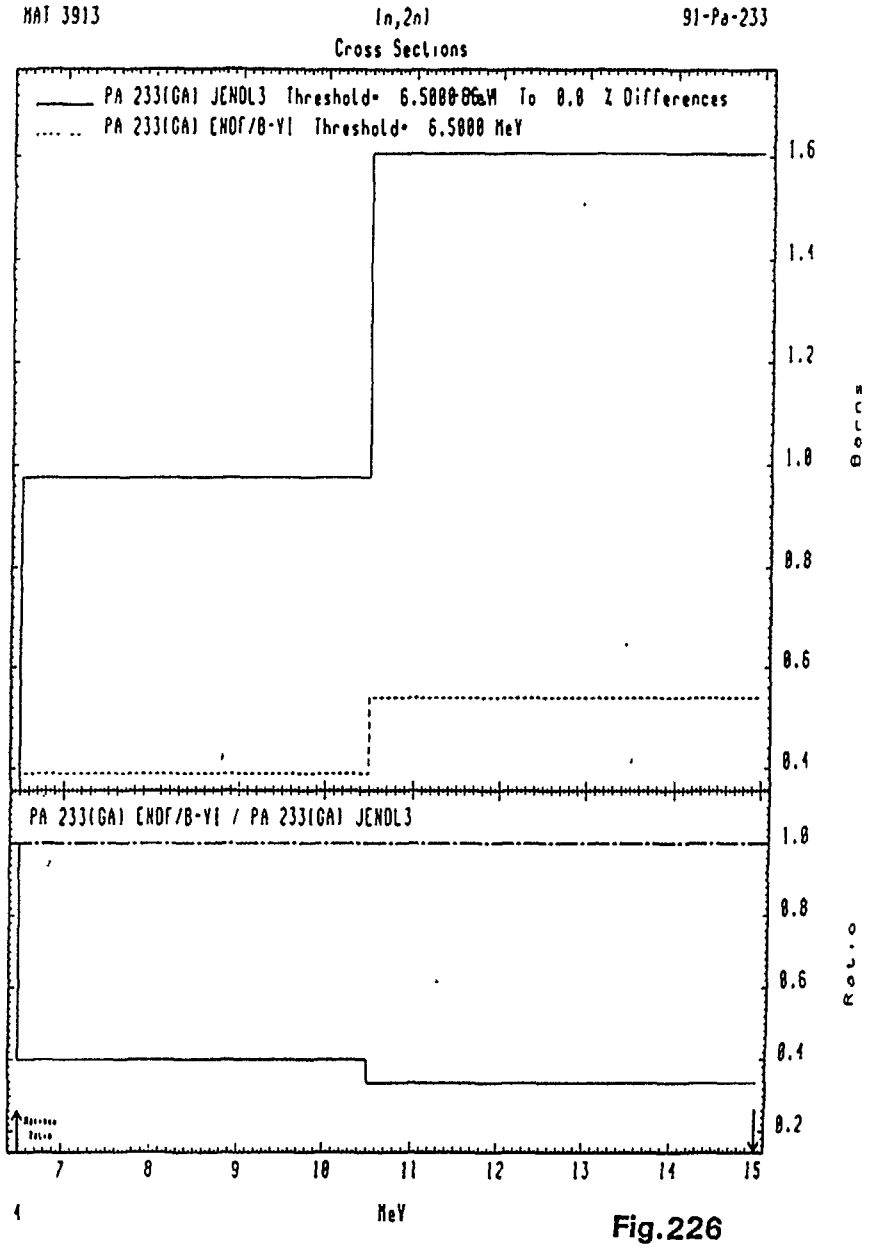

Fig.226

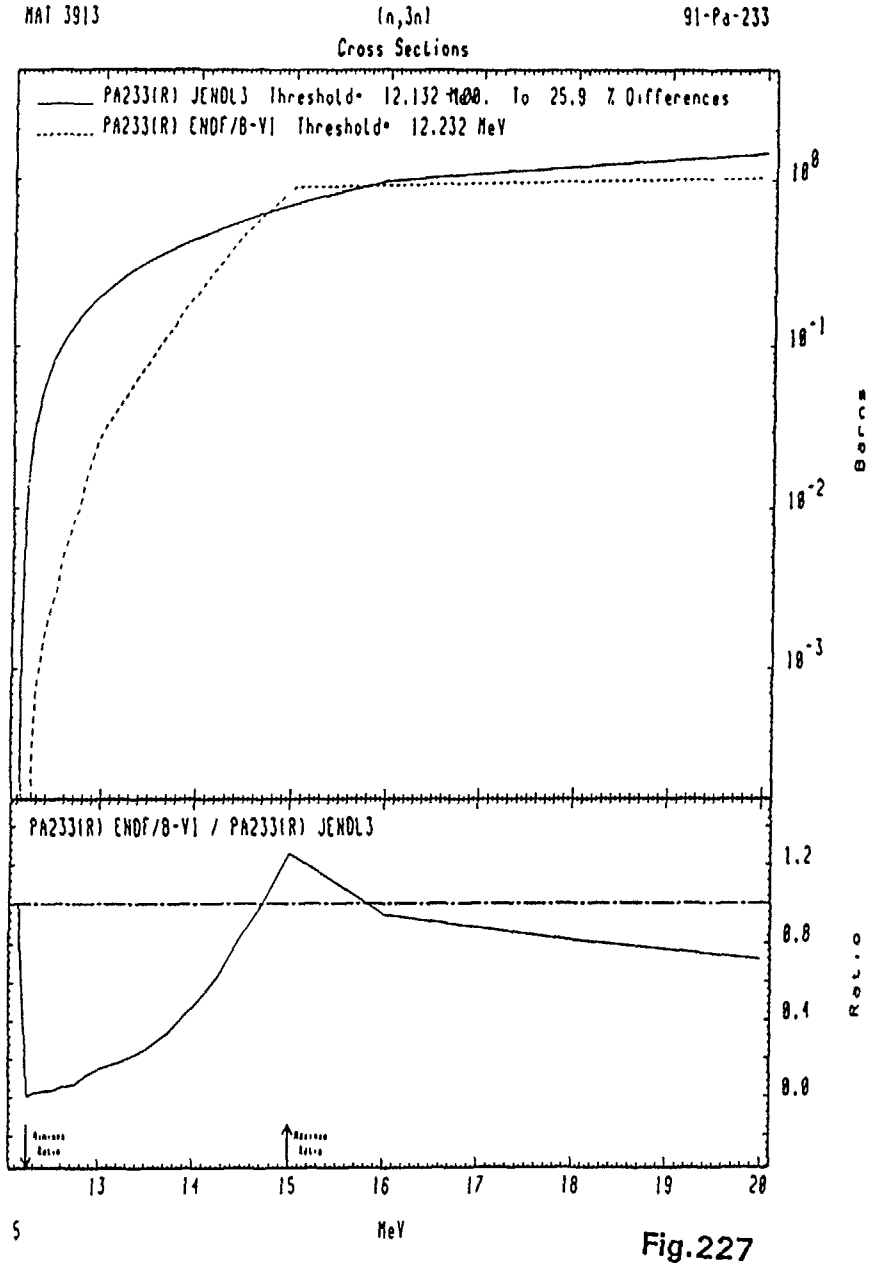

Fig.227

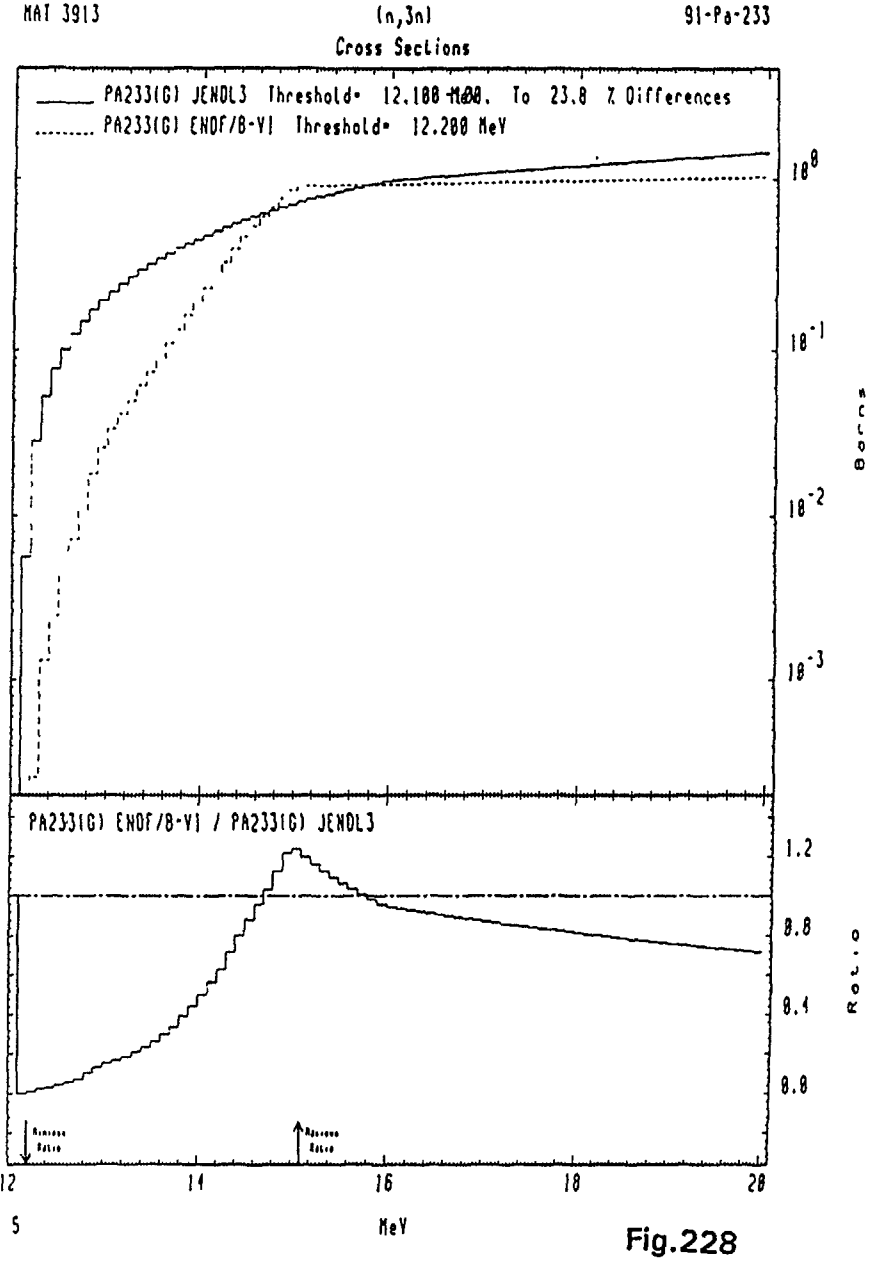

Fig.228

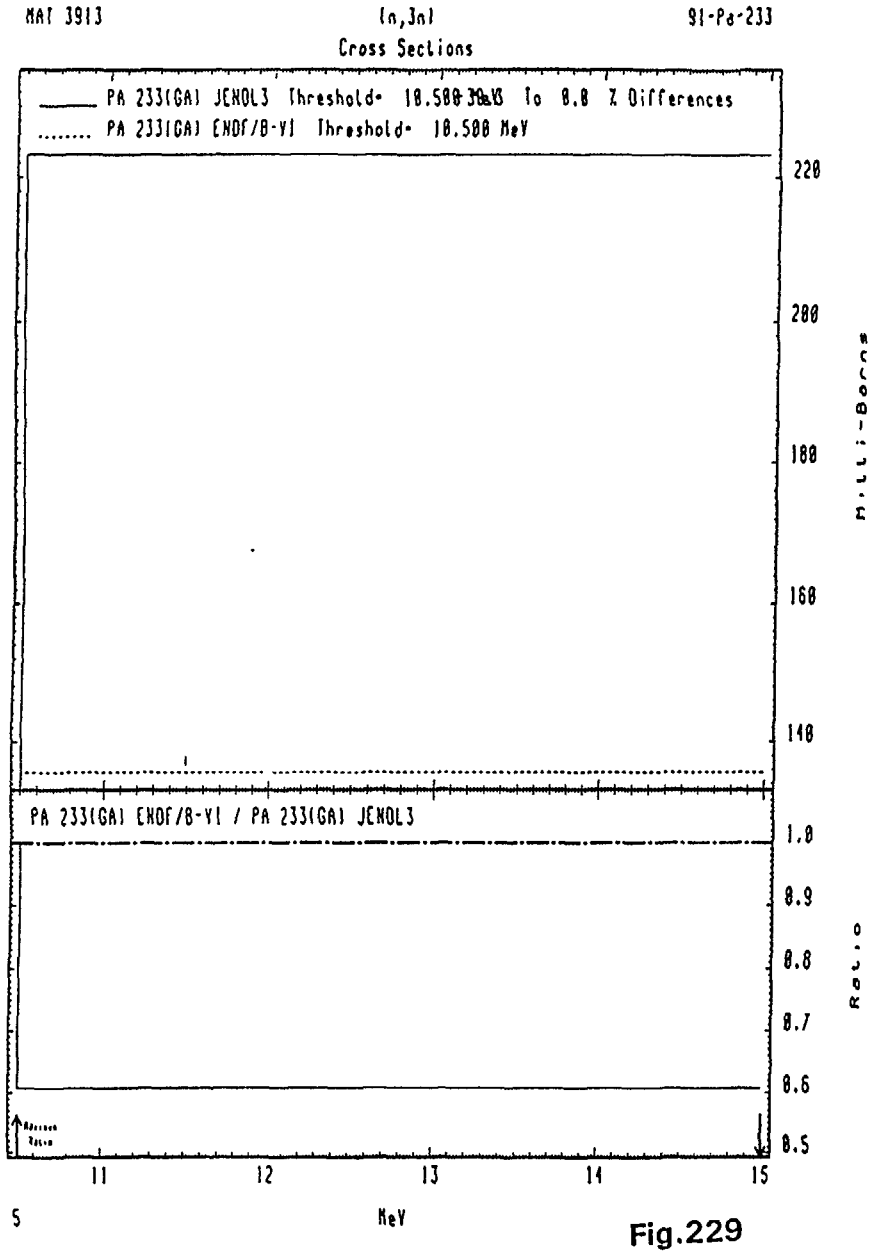

Fig.229

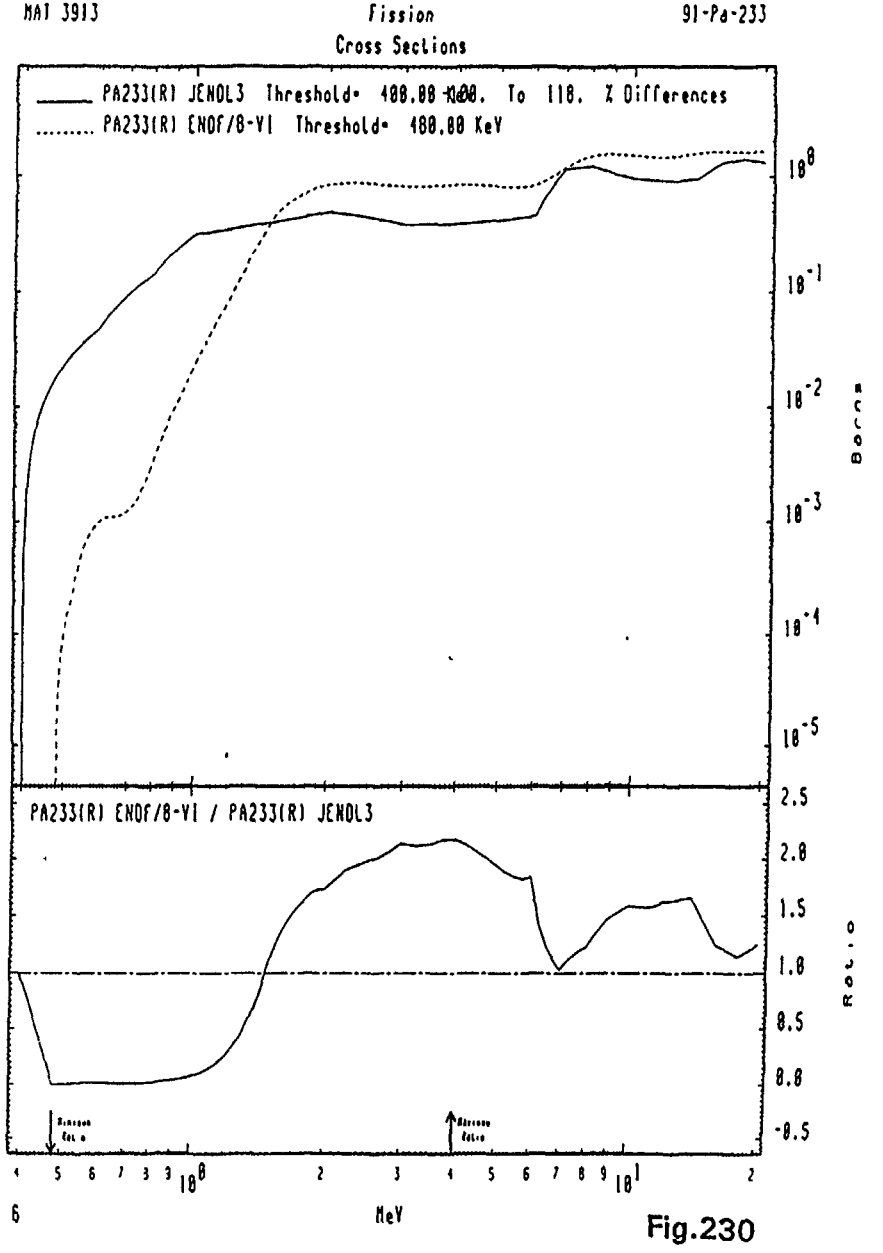

Fig.230

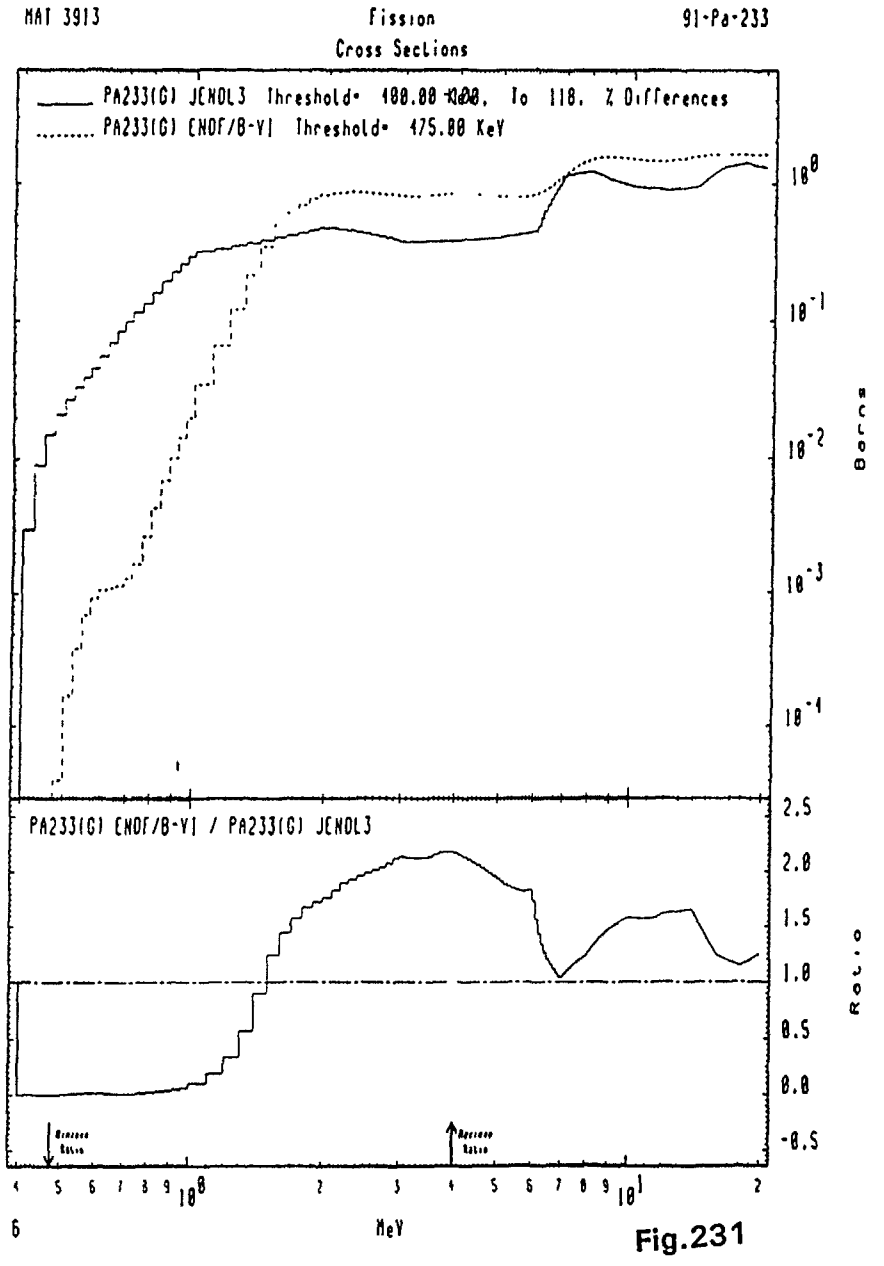

Fig.231

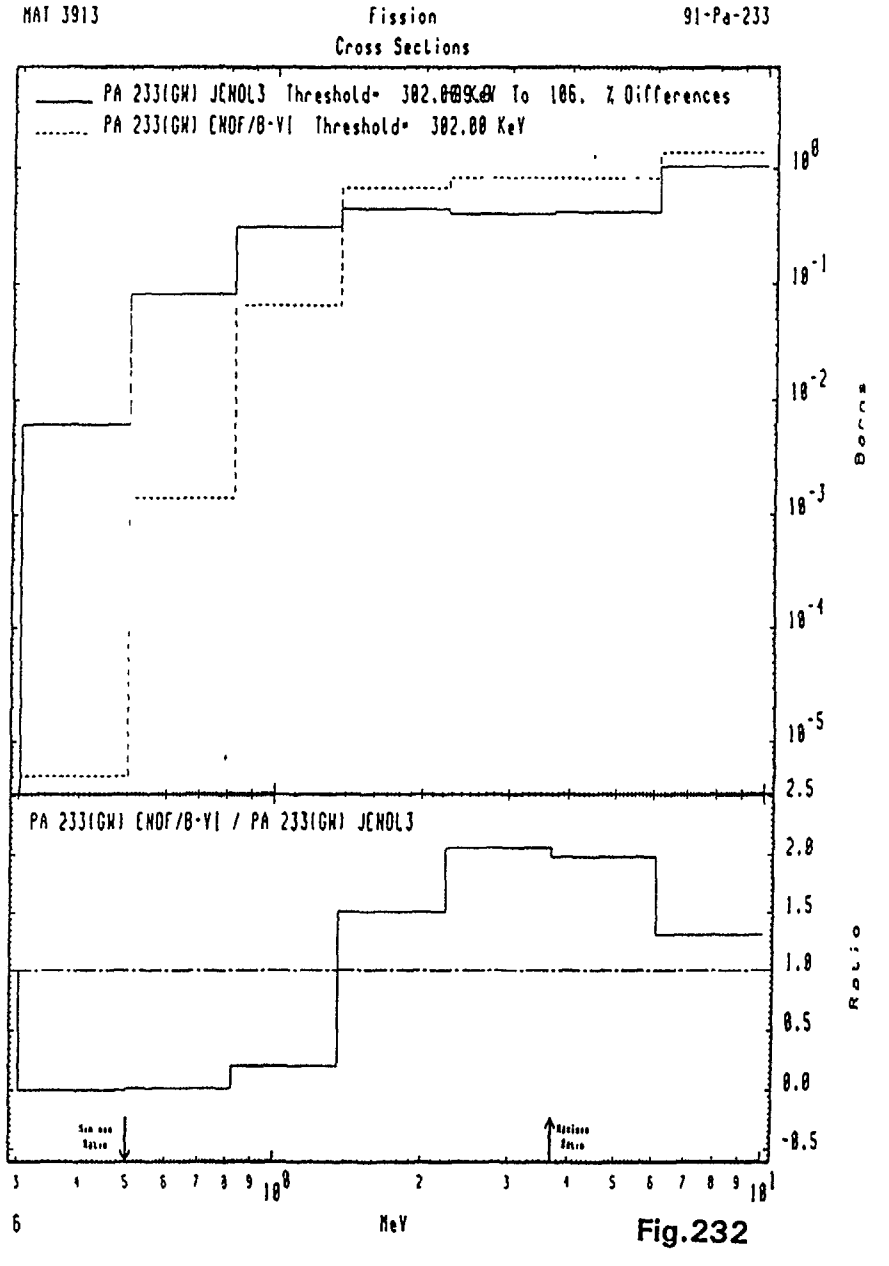

Fig.232

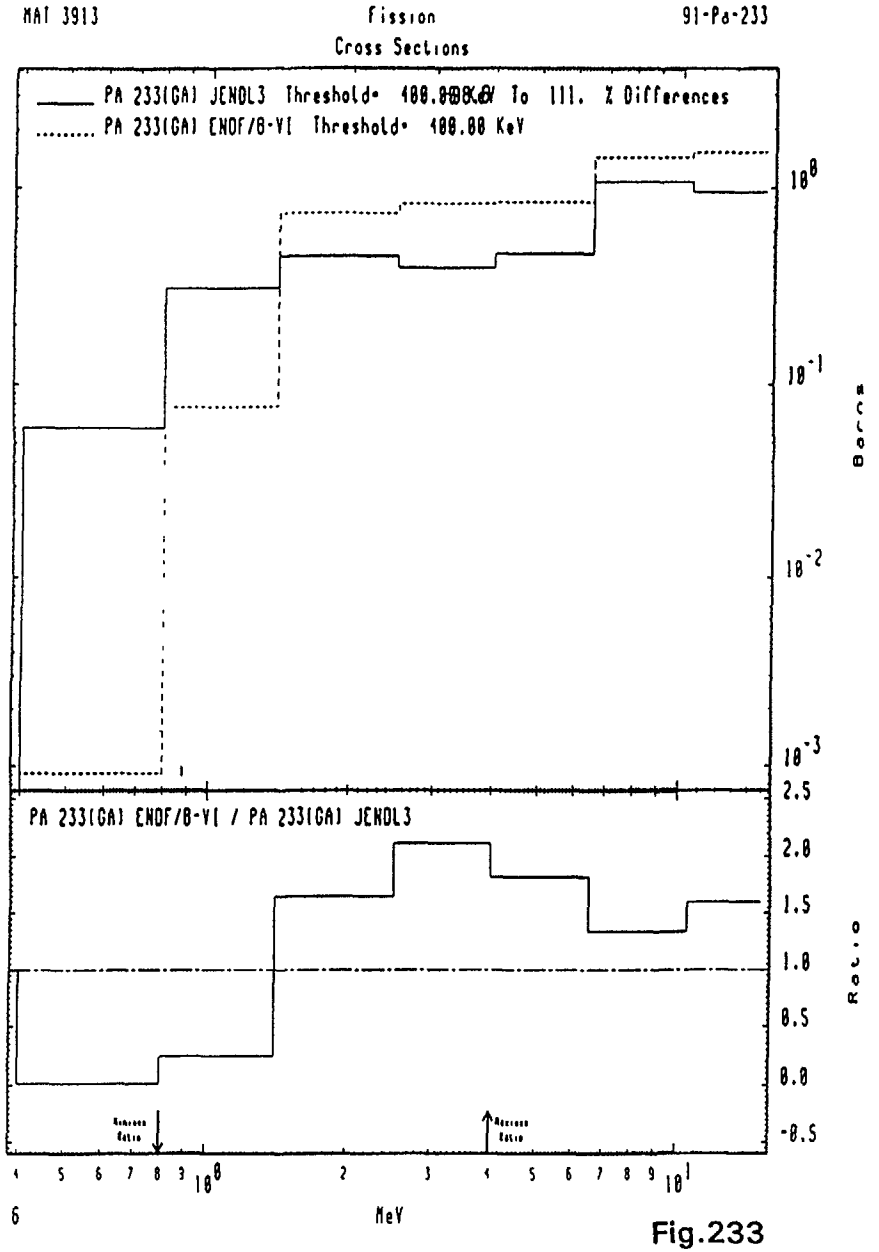

Fig.233

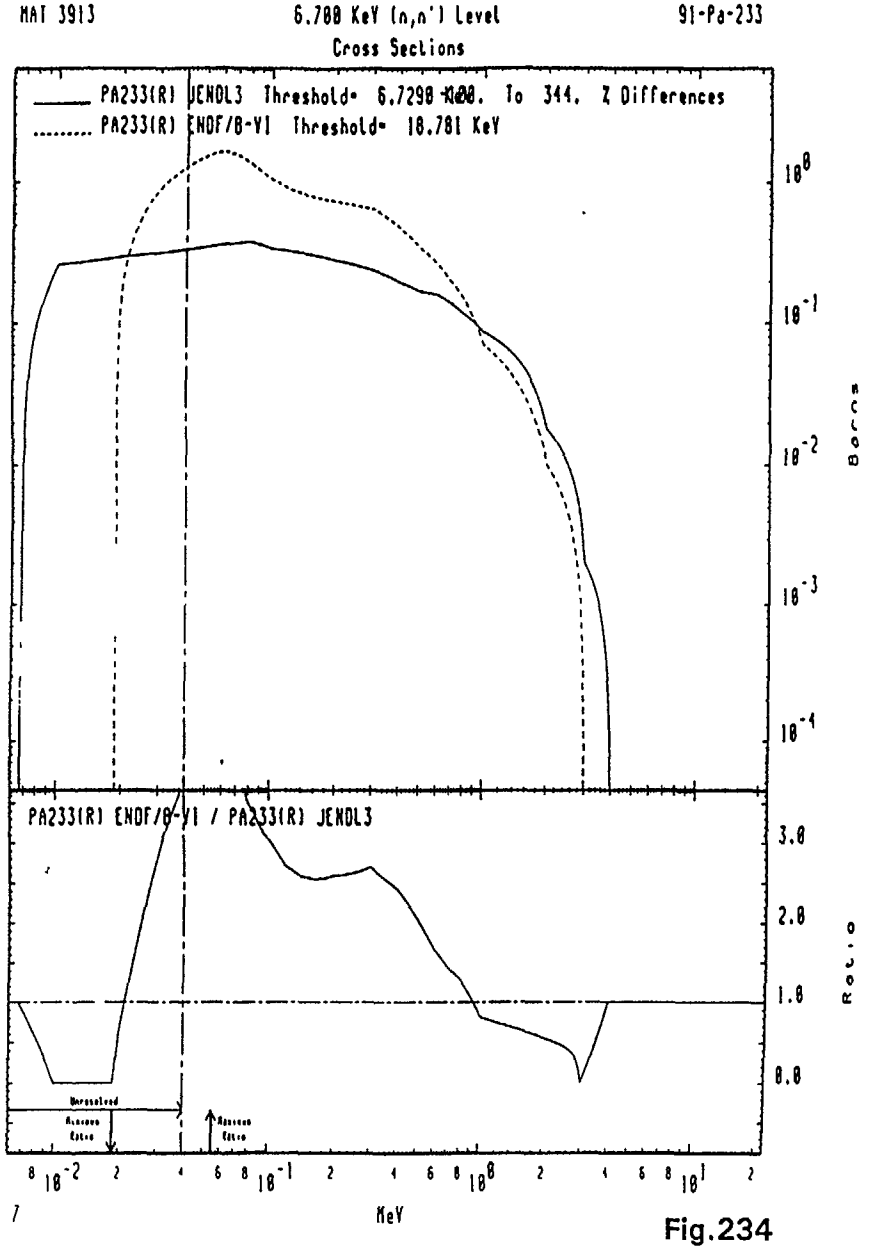

Fig.234

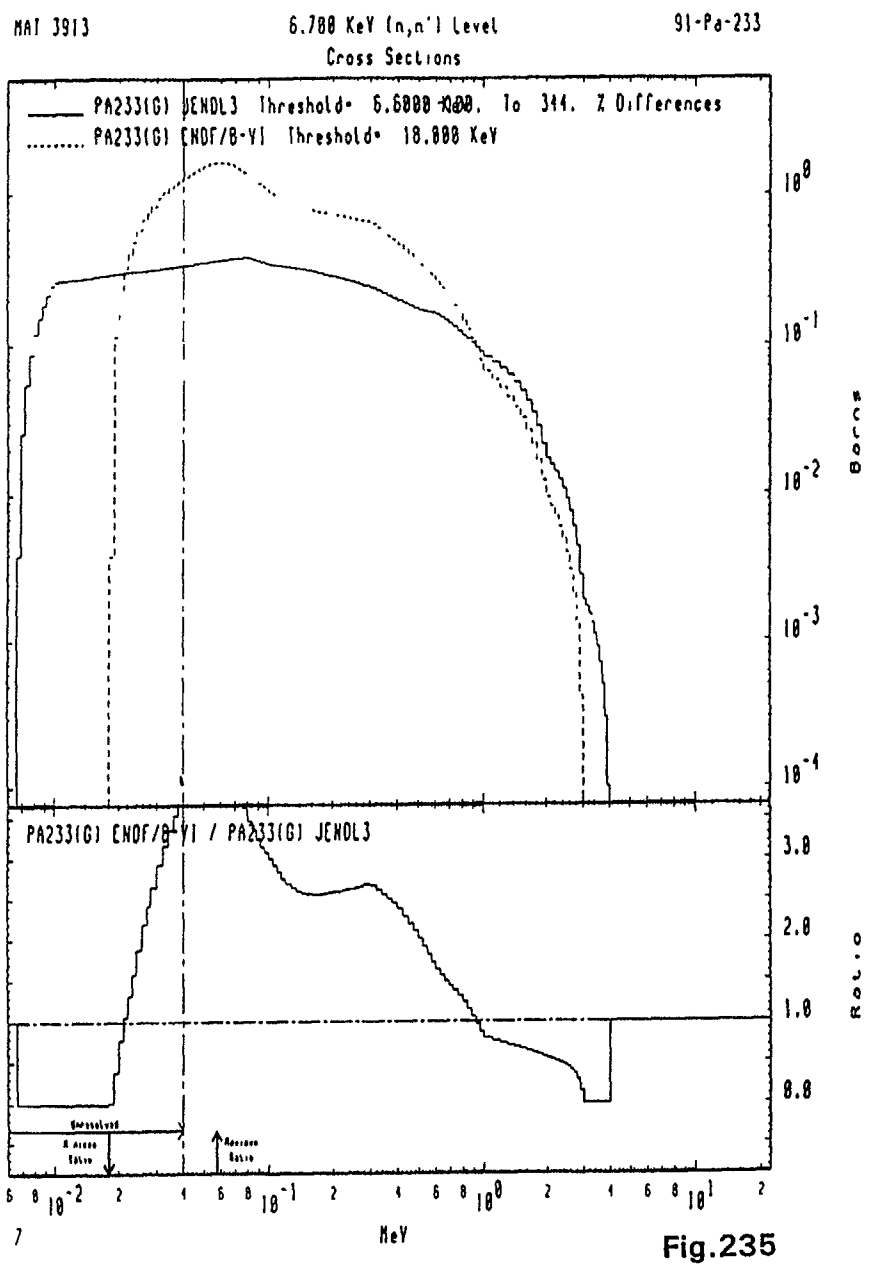

Fig.235

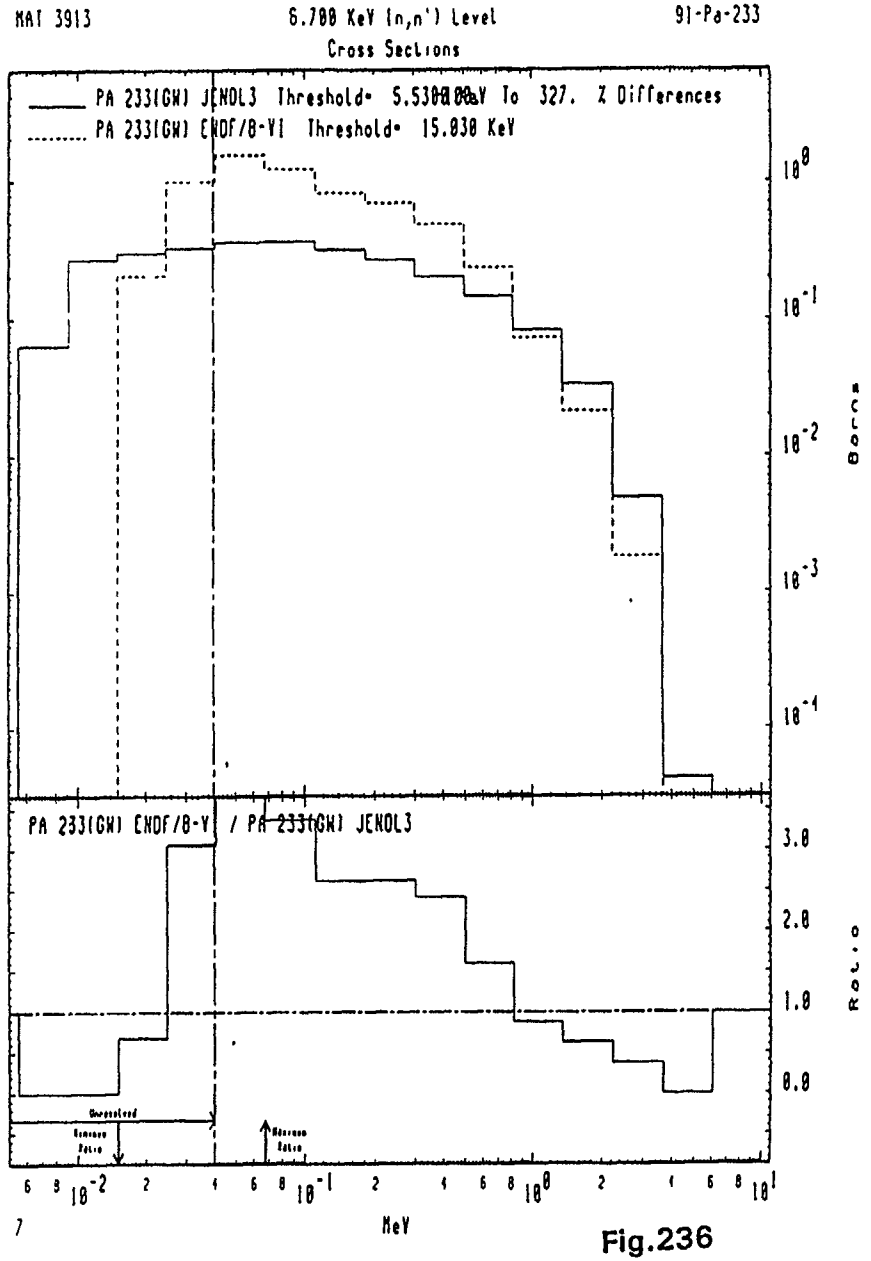

Fig.236

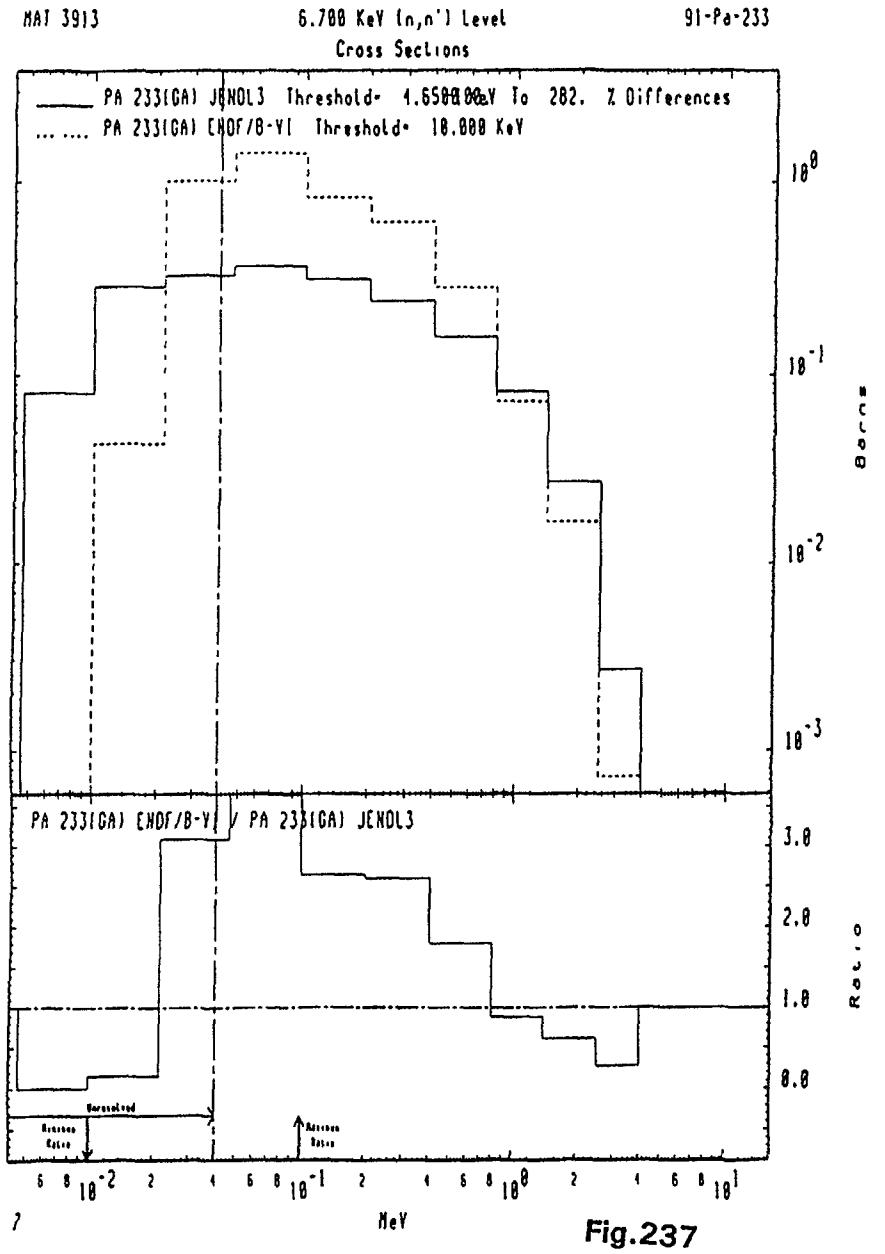

Fig.237

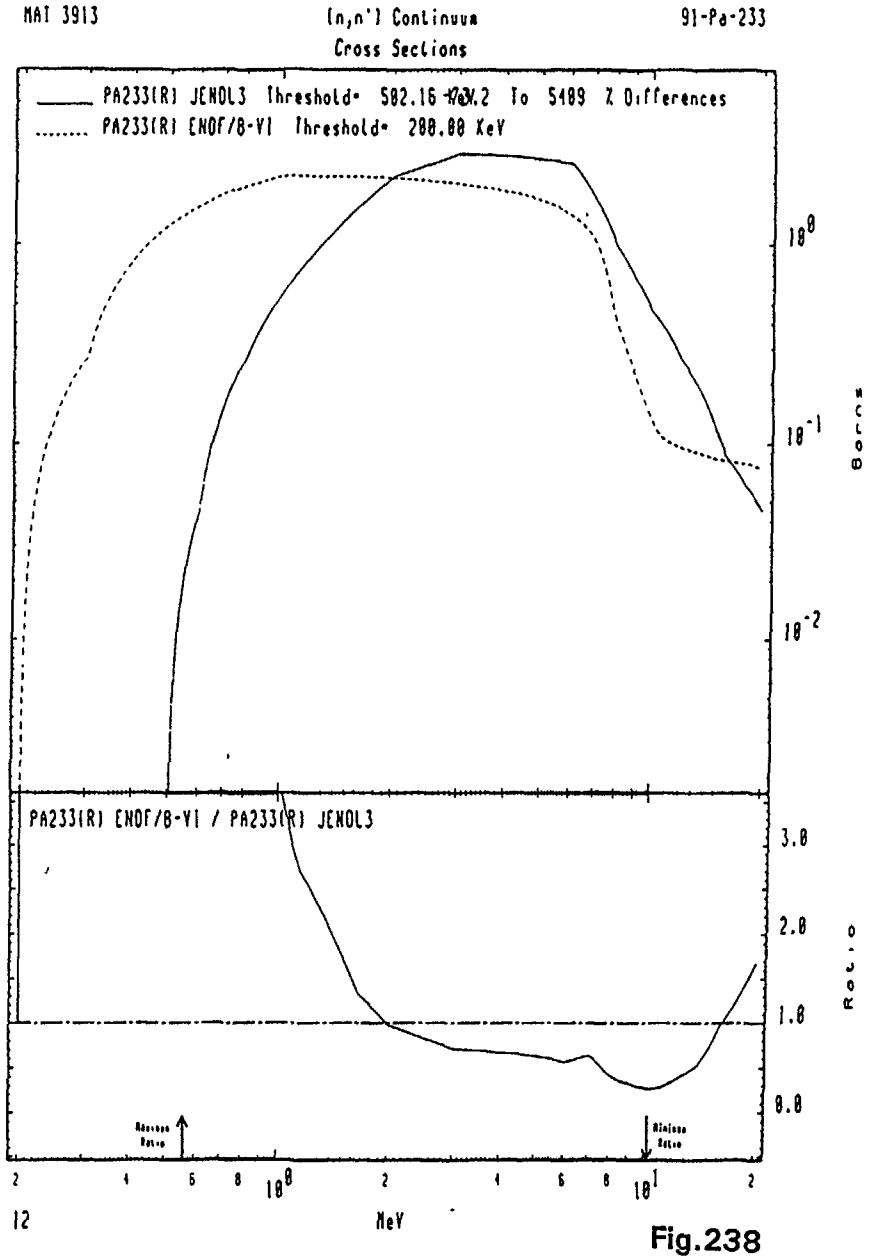

Fig.238

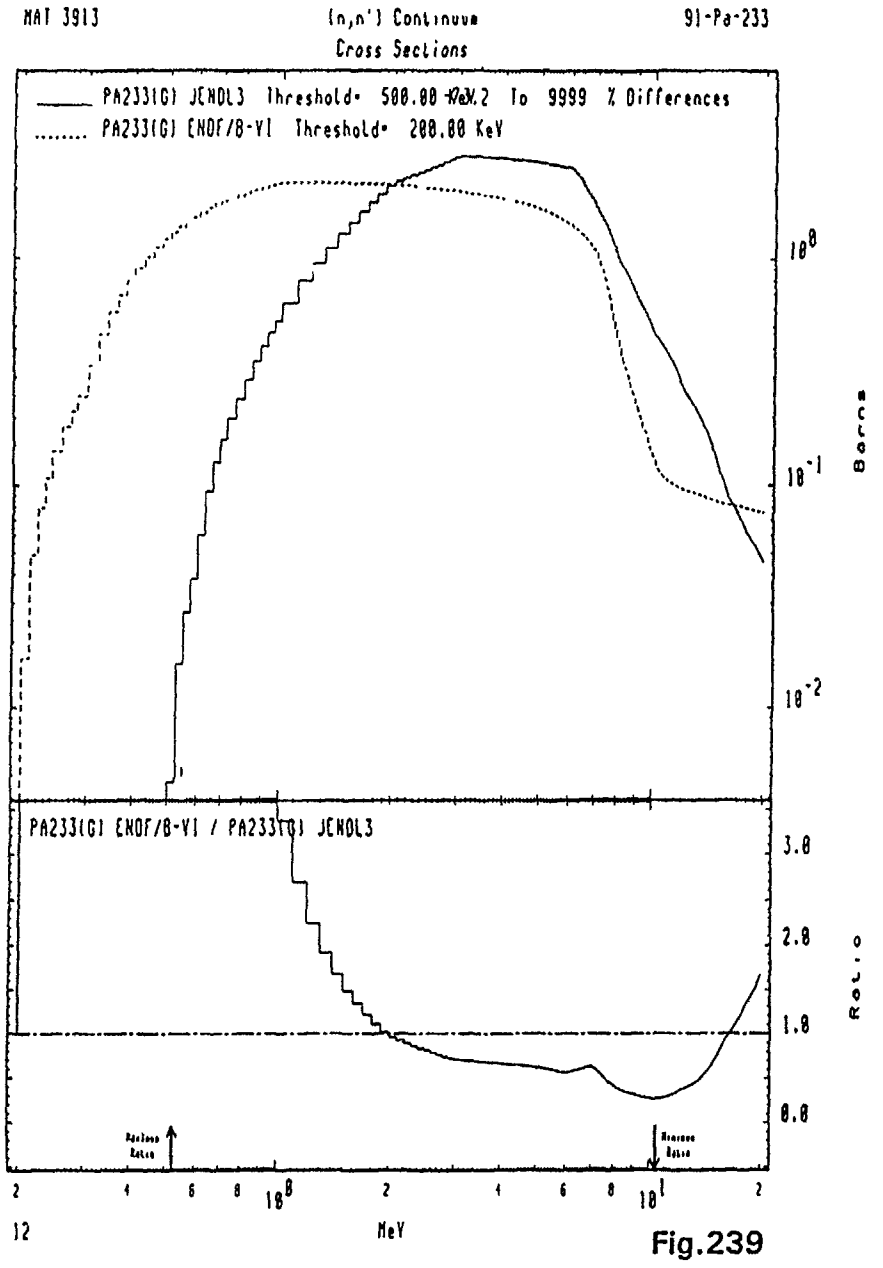

Fig.239

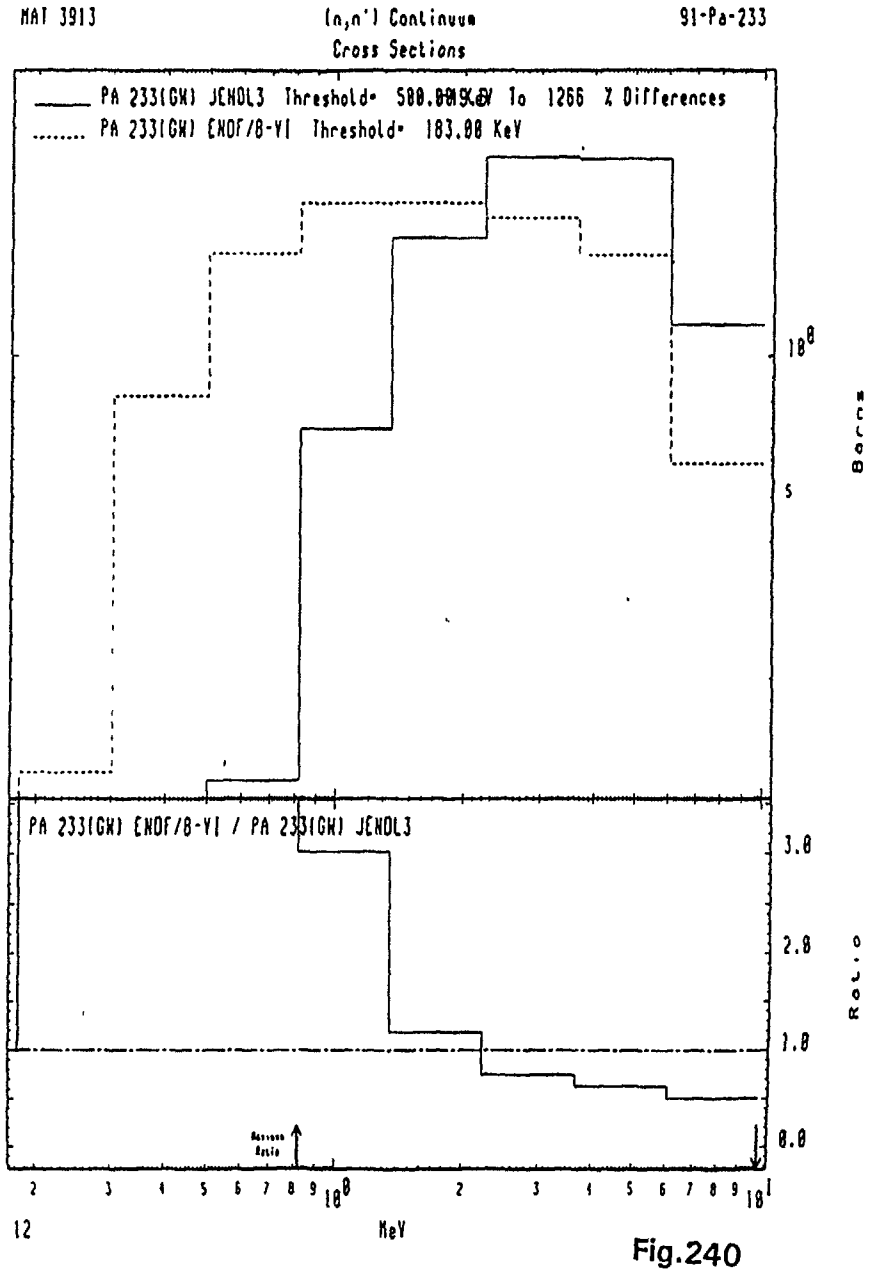

Fig.240

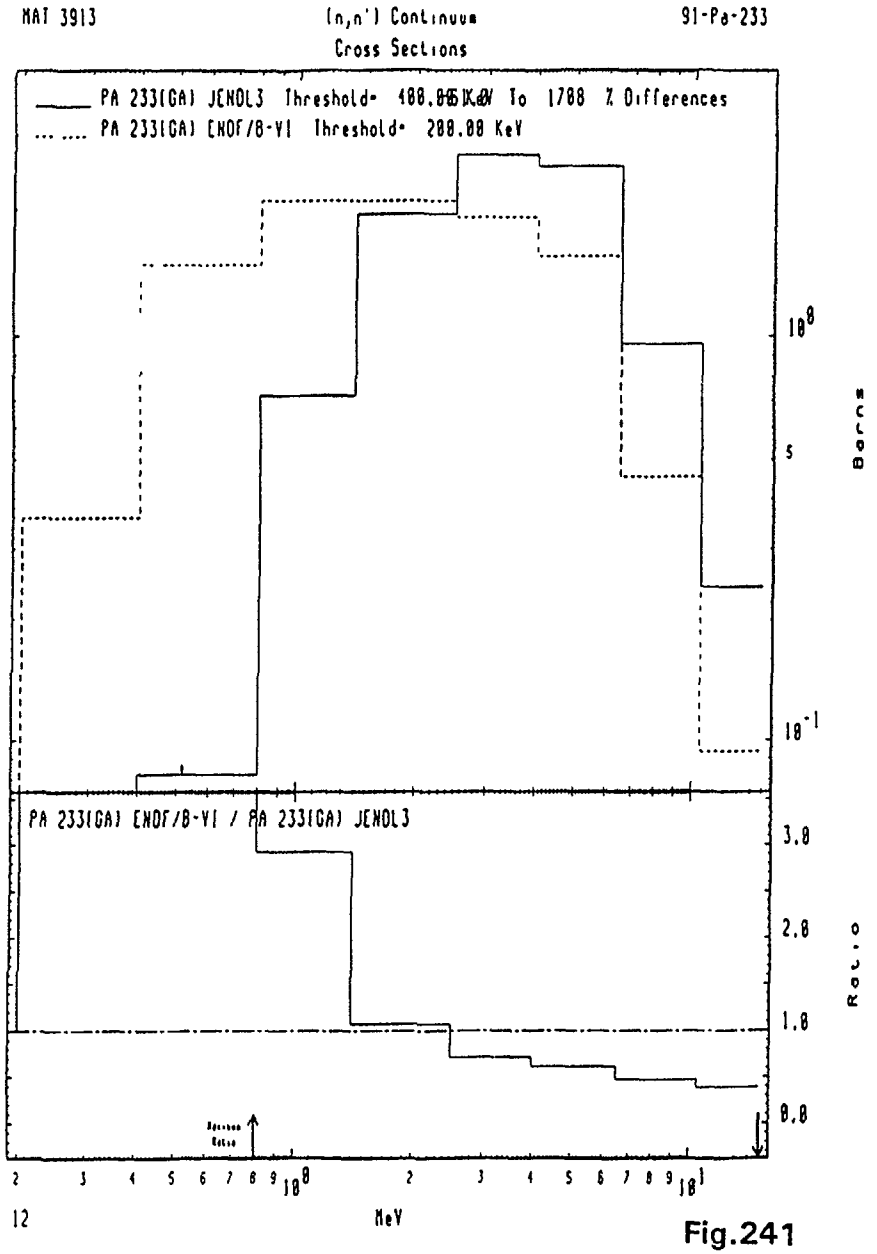

Fig.241

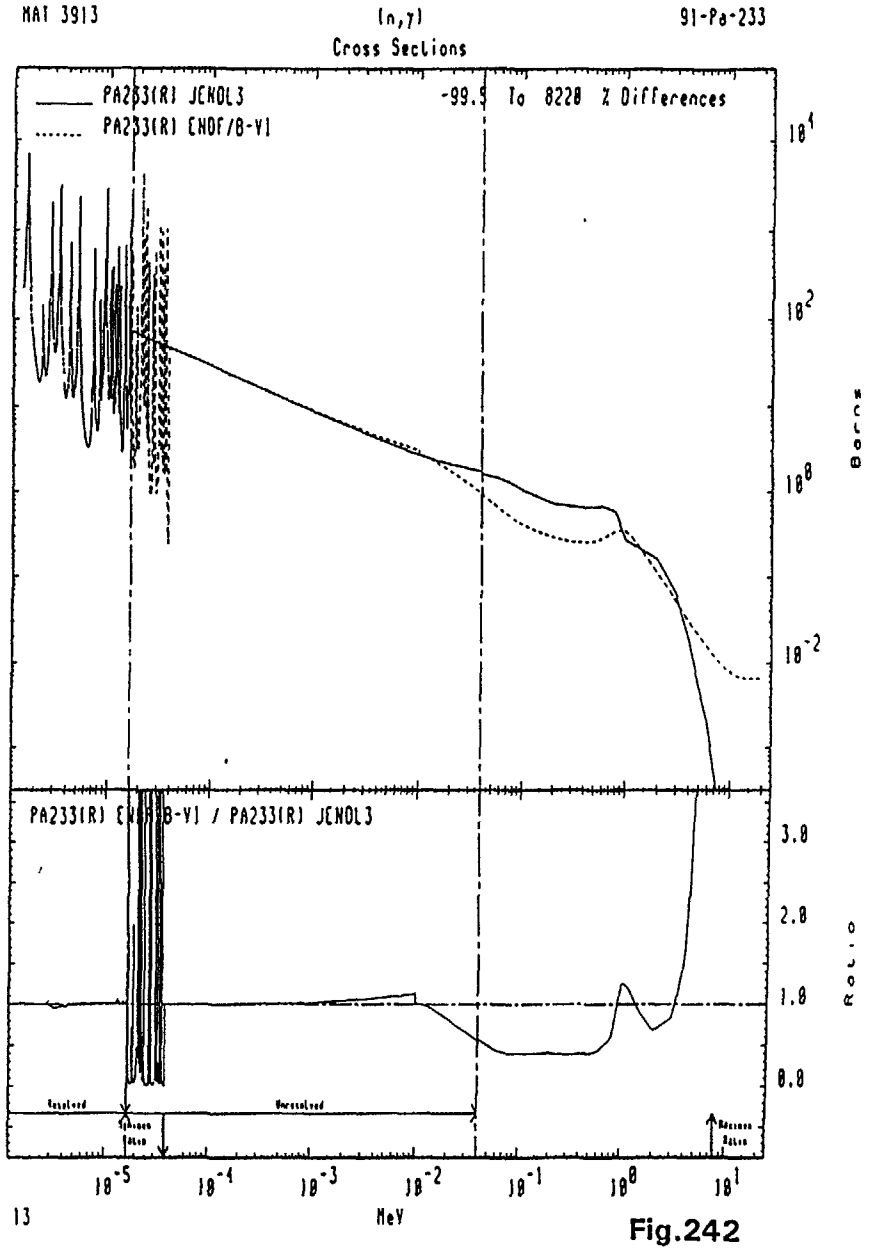

Fig.242

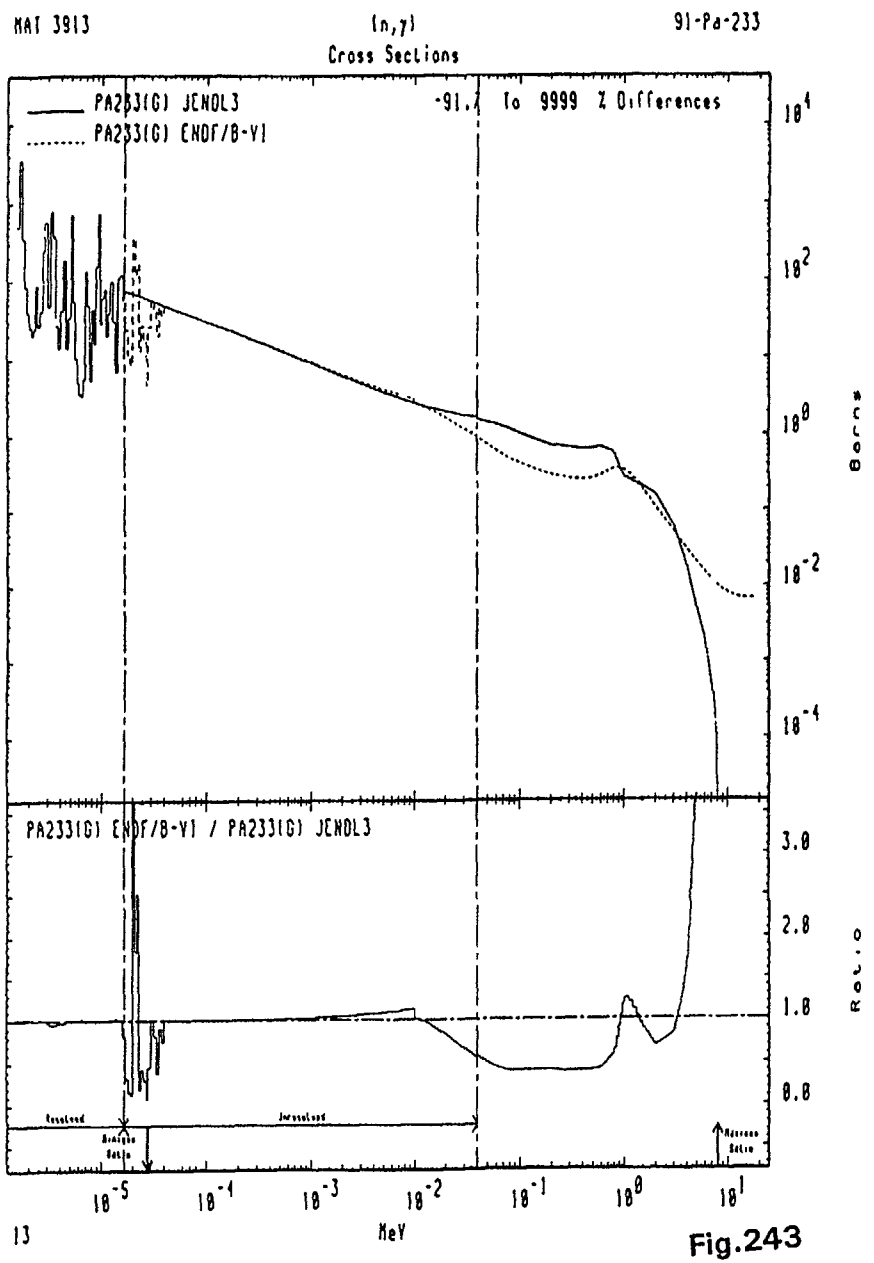

Fig.243

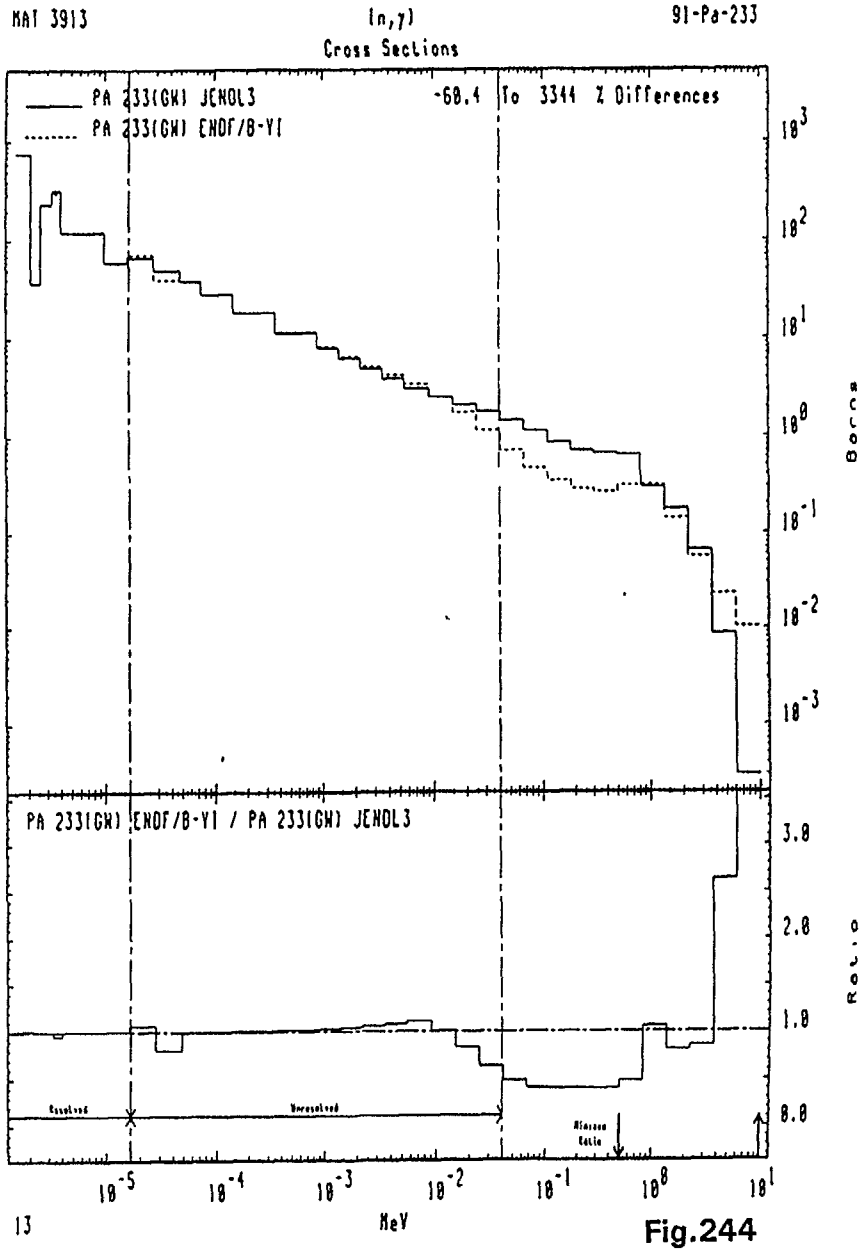

Fig.244

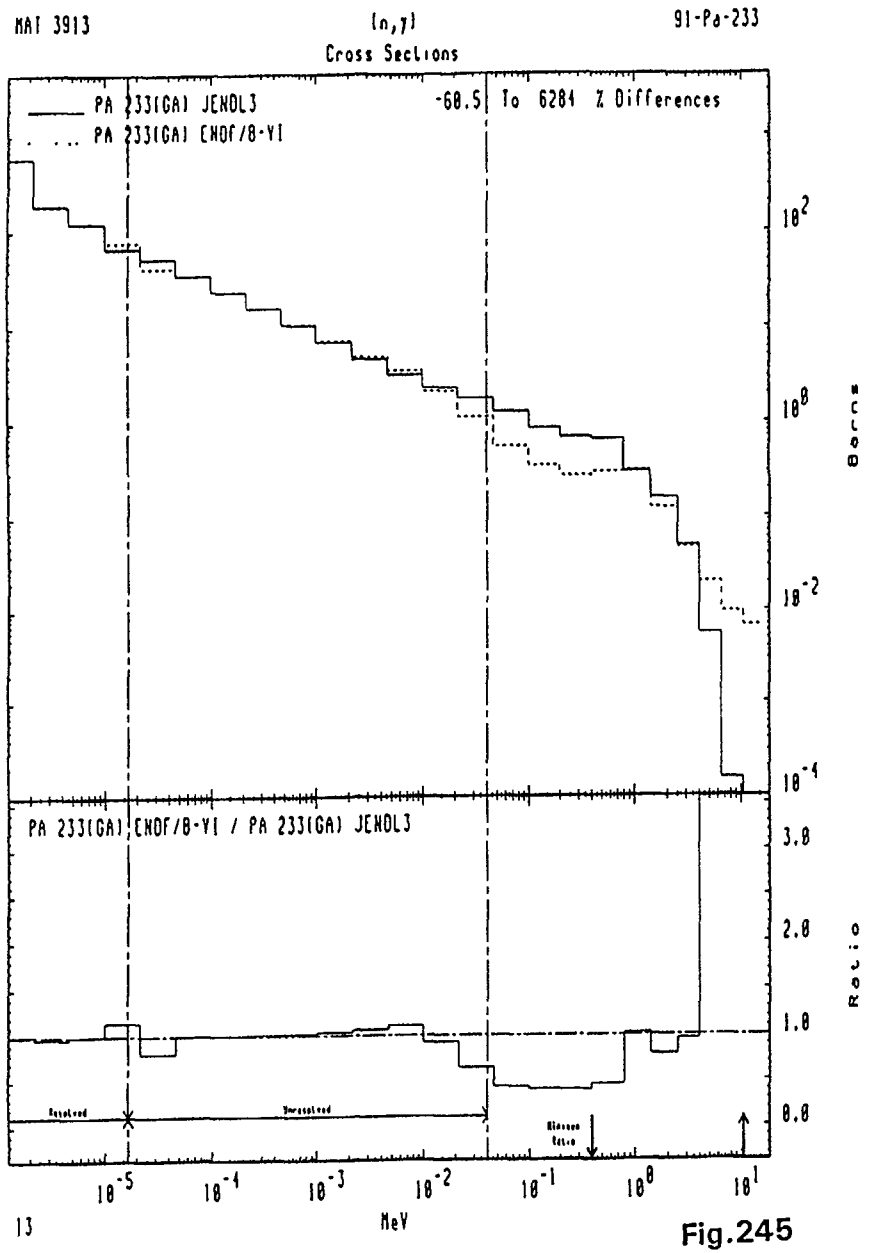
MAT 3913
(n,γ)
91-Pa-233
Cross Sections
PA 233(GA) JENDL3
PA 233(GA) ENDF/B-VI
-60.5 To 6284 % Differences
PA 233(GA) ENDF/B-VI / PA 233(GA) JENDL3
Barns
Ratio
MeV
13

Fig.245